UNIVERSITY OF MILANO-BICOCCA

Department of *Biotechnology and Biosciences*

PhD program in *Chemical, Geological and Enviromental Sciences*
XXX Cycle

PhD in CHEMICAL SCIENCES

New synthetic molecules active on human Toll-like receptor 4

Alberto Minotti

Reg. N° 709538

Tutor: Prof. Francesco Peri
Co-tutors: Prof. Alessandro Abbotto, Prof. Barbara La Ferla
Coordinator: Prof. Maria Luce Frezzotti

Academic Year 2016-2017

Table of contents

Abbreviations

Alphabetic order

ALI: acute lung injury

ALS: amyotrophic lateral sclerosis

ANS: 1-Anilinonaphthalene-8-Sulfonic Acid

APT: attached proton test

bis-ANS: 4,4'-Dianilino-1,1'-Binaphthyl-5,5'-Disulfonic Acid

BMMϕ: bone-marrow-derived murine macrophage

BSA: bovine serum albumine

CD14: cluster of differentiation antigen

CMC: critical micelle concentration

DAMP: danger (or damage) associated molecular pattern

DC: dendrytic cell

DCC: dicyclohexylcarbodiimide

DCM: dichloromethane

DIC: N,N'-Diisopropylcarbodiimide

DIPEA: N,N'-Diisopropylethylamine

DMAP: 4-dimethylaminopyridine

DMF: dimethylformamide

DMSO: dimethylsulphoxide

E. coli: Escherichia Coli

EC_{50}: half maximal effective concentration

EDC: N-(3-Dimethylaminopropyl)-N'-ethylcarbodiimide hydrochloride

ELISA: enzyme-linked immunosorbent assay

EVOO: extra virgin olive oil

FA: fatty acid

GLA: Gifu-lipid A

*h*CD14: *human* cluster of differentiation antigen

HEK: human embryonic kidney

*h*MD-2: *human* myeloid differentiation 2

HSQC: Heteronuclear Single Quantum Coherence

IBD: inflammatory bowel disease

IC_{50}: half maximal inhibitory concentration

Ig: immunoglobulin

IL-1β: interleukin-1β

IM: inner membrane

IFN: interferon

Kd: dissociation constant

Kdo: 3- deoxy-D-manno-oct-2-ulosonic acid

LBP: lipid Binding Protein

LOS: lipooligosaccharide

LPS: lipopolysaccharide

Lpt: lipopolysaccharide transport

LRR: leucine-rich repeat domain

mCPBA: meta-Chloroperoxybenzoic acid

MD-2: myeloid differentiation protein 2

MTT: thiazolyl blue tetrazolium bromide

NF-κB: nuclear factor kappa-light-chain-enhancer of activated B cells

NMO: N-Methylmorpholine-N-Oxide

OM: outer membrane

ON: overnight

PAMP: pathogen associated molecular pattern

PBA: polyclonal B cell

PBS: Phosphate Buffer Saline

PMP: para methoxyphenyl

PMB: para methoxybenzyl

pNPP: para-nitrophenilphosphate

PRR: pattern recognition receptor

Py: Piridine

R-LPS: Rough form of LPS

rt: room temperature

S-LPS: Smooth form of LPS

SEAP: secreted alkaline phosphatase

SPR: surface plasmon resonance

STD: saturation transfer difference

TBAF: tetra-*n*-butylammonium fluoride

TBS: tert-Butyldimethylsilyl

TPS: tert-Butyldiphenylsilyl

TEA: triethylamine

TFA: trifluoro acetic acid

THF: tetrahydrofuran

TIR: Toll/Interleukin-1 receptor

TLR: Toll-like receptor

TNF-α: tumor necrosis factor alpha

Tris: 2-hydroxymethyl-2-methyl-1,3-propaendiol

TsOH: *p*-Toluenesulfonic acid

WT: wild-type

Abstract

TLR4 is the innate immunity receptor which selectively recognizes LPS from the Gram-negative bacteria that eluded the physical and anatomical barriers of our organisms.

TLR4 responds to bacterial LPS and to different endogenous ligands in association with the protein adaptor MD-2 and triggers the immune and inflammatory responses.

The receptors LBP and CD14 are involved in the LPS recognition process and in the transfer of LPS from aggregates in solution to TLR4-MD-2 complex .

TLR4 has recently been related to many important pathologies still lacking specific pharmacological treatment: from diseases caused by bacterial infection such as sepsis and septic shock, to cancer and acute or chronic inflammatory diseases, atherosclerosis, allergies, asthma, cardiovascular disorder, diabetes.

Compounds able to block TLR4 activation (antagonists) are drug candidates against these pathologies, compounds active in stimulating TLR4 (agonists) may be used as antitumoral agents or vaccine adjuvants.

The chemical structure of lipid A (the biologically active part of LPS) has been simplified into synthetic glycolipids resembling lipid X, a biosynthetic precursor of lipid A (Figure I). These compounds retained part of the agonist or antagonist activity on TLR4.

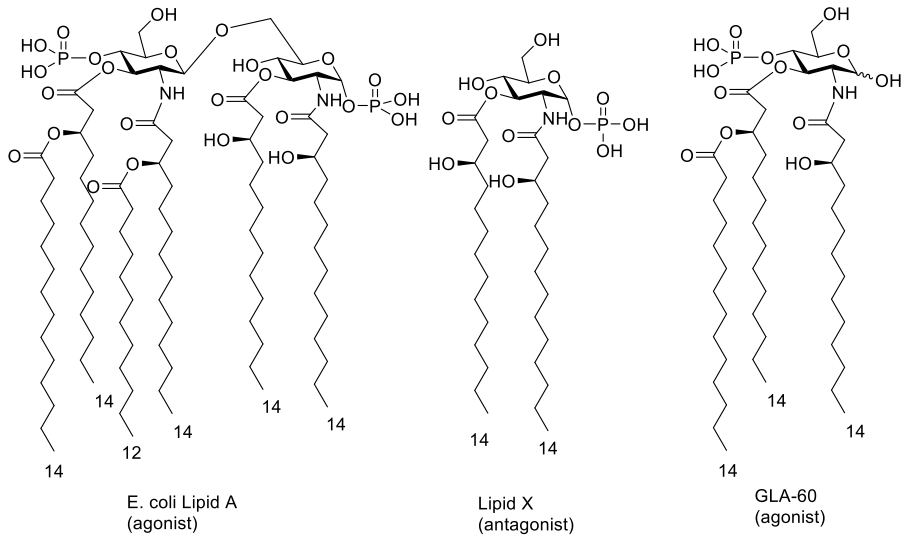

Figure I. *E. coli* Lipid A and monosaccharide molecular simplifications Lipid X, an antagonist, and GLA-60, an agonist

Of the 8 vaccine adjuvants currently approved or in clinical evaluation, 3 are monosaccharide derivatives of Lipid A partial structures. However, SAR and the switch from agonism to antagonism for monosaccharide TLR4 modulators have not been completely clarified yet, nor their activities have been clearly rationalized with respect to MD-2 binding.

With the aim of obtaining new monosaccharide-based TLR4 modulators (antagonists or agonists), to explore their SAR and to study their MD-2 binding properties, during this PhD thesis 9 new monosaccharide molecular simplifications of Lipid A have been designed and synthesized: FP7, FP11, FP111, AM158, AM173, AMX1, AM246248-d1, AM246248-d2 and AM241 (Figure II).

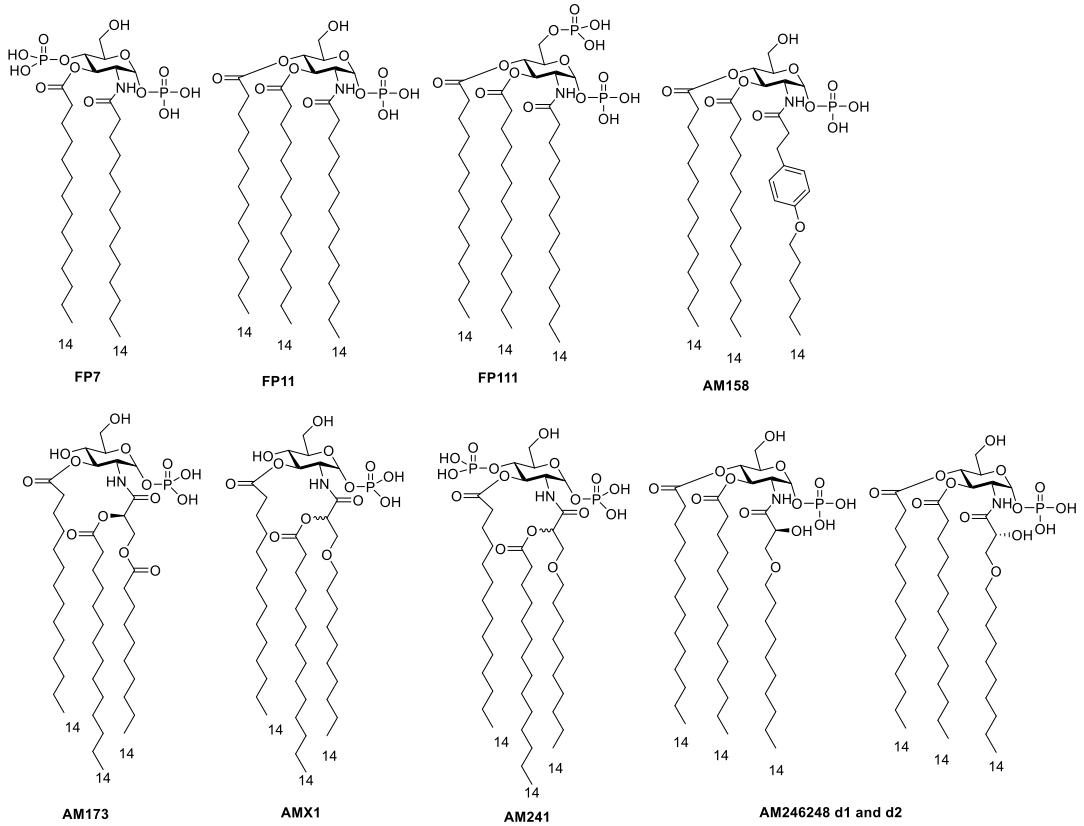

Figure II. FP7 and the 8 new Lipid A monosaccharide molecular simplifications successfully synthesized during this PhD thesis: FP11, FP111, AM158, AM173, AM246248-d1, AM246248-d2, AMX1 and AM241

This series of molecules has been designed by varying chain length and number as well as the number and position of phosphate groups, taking into account the already known SAR from the active (agonist or antagonist respectively) monosaccharides. New types of acyl chains have also been synthesized and inserted.

The ability of these compounds to activate or inhibit the TLR4/LPS signal was first tested in HEK-Blue™ cells. HEK-Blue™ cells are HEK-293 cells stably transfected with human TLR4, MD-2, and CD14 genes.

The compounds have shown strikingly different activities with respect to their structures. In particular an agonist was discovered, and its chemical structure, together with related variants, was patented.

In vitro binding assays between these synthetic compounds and MD-2 expressed in the yeast *P. pastoris* have been performed with the purpose of studying the correlation between biological activity and MD-2-binding properties.
These binding experiments comprise Surface Plasmon Resonance (SPR), Antibody-sandwich ELISA assay, Biotin-LPS displacement ELISA assay and fluorescent bis-ANS displacement assay.

Moreover, studies with FT-IR, FRET and SAXS techniques are currently being performed to understand which is the aggregates shape in solution of our active and inactive amphiphilic compounds.
Indeed the specific supramolecular aggregates shape of Lipid A disaccharides as well as that of monosaccharide Lipid A partial structures appears strictly related to their activity.

Finally, **AM30** (figure III), a new innovative TLR4 antagonist based on the scaffold of natural anti-inflammatory compound oleocanthal, was synthesized.
The very promising feature of this compound lays in the higher water-solubility (due to the lack of amphiphilicity) and the easier synthesis with respect to classical Lipid A-derived TLR4 antagonists.

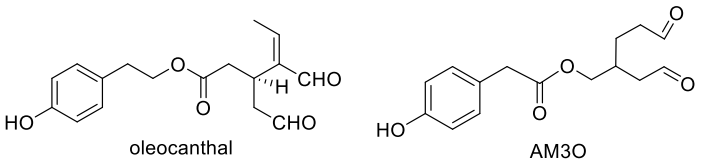

Figure III. Anti-inflammatory natural compound oleocanthal and compound **AM30**

Chapter I

Introduction

1. Immunity

The human immune system is a complex network of cells, biological processes and cell-forming tissues, whose aim is to protect the human body from various pathogens that might invade and damage it. This can be achieved by an efficient detection and rapid elimination of dangerous molecules or organisms, which requires an ability to distinguish harmless species from dangerous ones. This discrimination occurs at a molecular level and it involves specific cellular structures, such as Toll-like receptors (TLRs), antibodies and T cell receptors

Differently from invertebrates and plants, vertebrates possess a more articulate immune system, which can be subdivided into two separate systems: the adaptive immune system and the innate immune system.

1.1 Adaptive immunity

The adaptive immune system is the more evolved section of the immune system, mainly because it possesses the property of immunological memory.
This is the ability to memorise the specific structure of a detected pathogen, making future immune responses stronger and more efficient if the same pathogen re-enters our body.
As a consequence, adaptive components are characterized by high specificity, which explains why the adaptive immune system is our second line of defence and why it intervenes more slowly than the innate system.

1.2 Innate Immunity and PRRs

The **innate immune system** is our first line of defence when a pathogen enters our body and can be described as the ancient and fundamental section of the immune system.
Differently from the adaptive system, its mechanisms and nature do not vary depending on the ever-changing environment, mainly because this part of the immune system does not possess immunological memory. In fact, this ability would require high specificity, while innate components recognize a limited amount of antigens and are often not sensitive to slight variations in the antigen chemical structure.

The innate immune system employs defence mechanisms on two different levels.
Physiological and anatomical barriers are often the first structures that block and eliminate external pathogens. For example, skin provides a strong physical barrier and inhibits bacterial growth, the acid

environment of the stomach can kill several microorganisms and lysozymes in mucous secretions can cleave the bacterial cell wall.

On a cellular level specialised cells either produce cytotoxic substances, such as nitric oxides and lysosomal enzymes, or use phagocytosis to eliminate pathogens. The vast majority of these specialized components are **myeloid cells**, which include macrophages, neutrophils and eosinophils; however, some lymphoid cells (mainly NK cells – natural killer cells), which are generally used by the adaptive immune system, are involved in the innate immune response.

The strategy of the innate immune recognition is based on the detection of molecules characterized by particular molecular patterns, called **PAMPs** (Pathogen-Associated Molecular Patterns), which are normally found in bacteria and not in the host.

The recognition involves specific receptors called **Pattern-Recognition Receptors (PRRs).**

These PAMPs usually include combinations of sugars, lipid-bearing molecules, proteins and nucleic acid motifs. Examples of PAMPS are the lipoproteins, lipid A of LPS, peptidoglycan and the lipoteichoic acids.

The detection of such molecular patterns triggers a general activation of the immune system, which provides a general and normally effective response, thus allowing the elimination of the majority of dangerous microorganisms before the adaptive immune system is activated.

2. Toll-like Receptors - TLRs

Toll-like receptors (TLR*s*) represent a family of PRR and play a key role in the innate immune system. [1,2]

The TLRs belong to a cluster of molecules called the IL-1R/TLR super-family characterized by the presence of cytoplasmic Toll/IL-1R (TIR) domains. The three subgroups are: the IL-1R (which presents extracellular immunoglobulin domains), the adapter subgroup (cytoplasmic proteins without extracellular region) and the TLRs.

TLRs are type I transmembrane proteins with extracellular amino terminus and a carboxyl terminal intracellular domain.[3]

They are receptors that recognize structurally conserved molecules derived from microbes, consequently activating immune cell responses.[1,2]

Unlike other receptors, TLRs do not have an enzymatic activity. [3]

Their name "*Toll*" is related to the strong homology of these receptors to the ***Drosophila* fly receptor Toll**. Toll is as a maternal-effect gene of the Dorsal complementation that functions in a pathway that controls establishment of dorso-ventral polarity and thus dorso-ventral axis formation in fruitfly embryo.[4–8]

Drosphila Toll pathway controls not only dorsoventral patterning in embryos, but also the antifungal immune defence in adult fruitflies.[8]

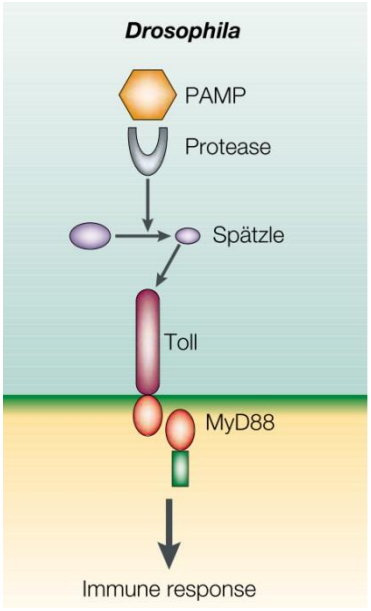

Figure 1. *Drosophila* Toll pathway (from Medzhitov 2001[2])

However *Drosophila* Toll does not function as a PRR, in that it does not seem to recognize pathogens directly. Instead, the processing of Spätzle, another Dorsal complementation gene, into a biologically active form is induced on infection and leads, in turn, to the activation of the Toll pathway (figure 1).

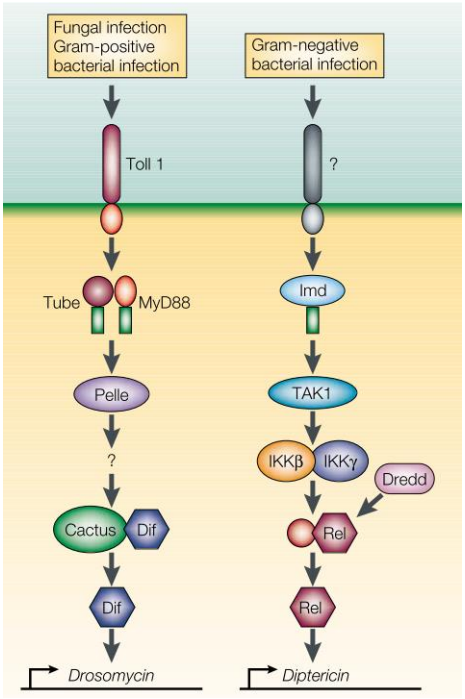

Figure 2. *Drosophila* Toll and imd pathways (from Medzhitov 2001[2])

Interestingly, the Toll pathway (figure 2) can also be activated in response to Gram-positive infection, indicating that several pattern-recognition molecules might function upstream.[9]
However, despite their profound defect in antifungal immunity, fruitflies harbouring mutations in Toll and the other components of the Toll pathway show normal resistance to infection by Gram-negative bacteria. [8]
Indeed resistance to Gram-negative infection is conferred by a distinct pathway, which was defined by a mutation in the imd (immune-deficient) gene.[10]
Imd mutants fail to induce the antibacterial peptide Diptericin and, therefore, have a profound defect in resistance to Gram-negative bacterial pathogens, although remaining essentially normal with regard to fungal and Gram-positive infection.

It was in search of a human homologue of the *Drosophila* Toll protein that the first mammalian TLR (TLR4, see next section) was discovered in 1997.[11]

TLR*s* were later discovered to be widespread and ubiquitous receptors in plants and animals, in which they have a key role in immune recognition.
Indeed, TLRs are present in vertebrates as well as in invertebrates, and they also represent the host defence against infection in plants.
It has been estimated that most mammalian species have between ten and fifteen types of Toll-like receptors and thirteen TLRs (named TLR1 to TLR13) have been identified both in humans[12] and mice.

From a structural point of view, all TLRs are characterized by two conserved regions: an extracellular leucine-rich repeat (LRR) domain and an intracellular Toll/IL-1 receptor (TIR) domain.
LRRs are found in a diverse set of proteins in which they are involved in ligand recognition and signal transduction. The characteristic feature of the LRRs is the consensus sequence motif, $L(X_2)LXL(X_2)NXL(X_2)L(X_7)L(X_2)$, in which X is any amino acid. The LRR region in the TLRs is separated from the transmembrane region by a so-called 'LRR carboxyl-terminal domain', which is characterized by the consensus motif $CXC(X_{23})C(X_{17})C$.
The TIR domain of Toll proteins is a conserved protein–protein interaction module, which is also found in a number of transmembrane and cytoplasmic proteins in animals and plants

TLRs recognize a bewildering range of microbial ligands, such as bacterial and fungal cell wall components, bacterial lipoproteins, highly conserved microbial proteins, and bacterial and viral nucleic acids. Moreover individual TLRs can recognize several, structurally unrelated ligands (figure 3).

The molecular basis of such diverse ligand binding is associated to conserved molecular patterns in microbial products (PAMPs) that signal the presence of infection, even if the direct interaction of TLRs to ligand as PRR often requires accessory proteins as mediators.

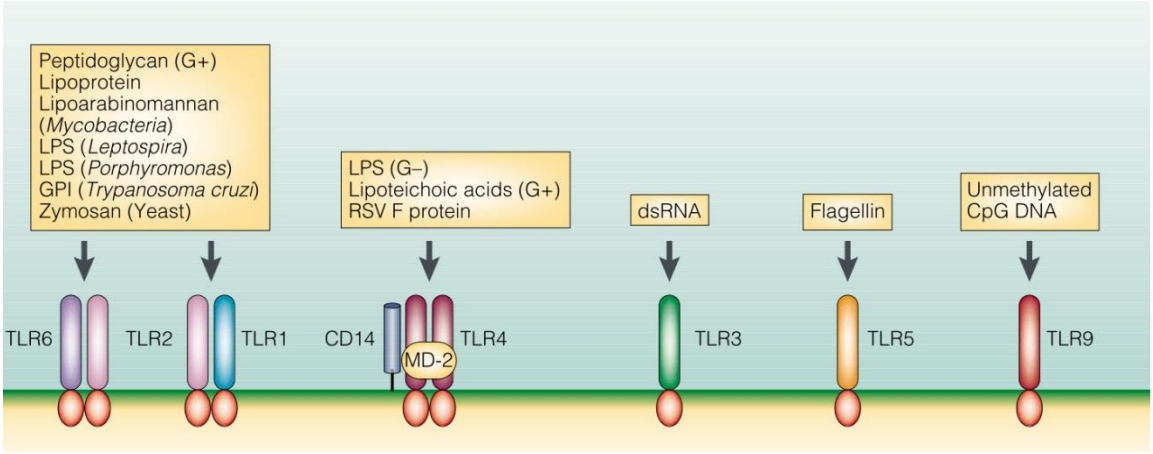

Figure 3. TLRs and their PAMPs (from Medzhitov 2001[2])

The recognition of microorganisms by TLRs initiates distinct signal transduction pathways as cascades of intracellular events that culminate in potent transcriptional responses promoting inflammation, activation of innate immune responses and priming of adaptive immune responses. Key to this central role in host defence is the expression of TLRs on antigen-presenting cells, especially macrophages and dendritic cells (DCs).

In addition to the induction of distinct signalling pathways, TLRs sample different compartments within cells. The cellular localization of these receptors has important consequences for ligand accessibility and can also affect downstream signalling events. Certain differences in subcellular localization are stable, whereas others are more dynamic.

The TLRs involved in the recognition of nucleic acids (TLR3, TLR7, TLR8 and TLR9) are localized within endolysosomal compartments, whereas other TLR family members (TLR1, TLR2, TLR4, TLR5 and TLR6) are found at the cell surface (figure 4).

The precise nature of the compartment where intracellular TLRs meet internalized ligands remains poorly defined, and it is likely that features of the compartment differ depending on the composition of the internalized cargo and the cell type under consideration. TLRs that are normally present at the surface can also enter the endocytic pathway following their activation. These receptors are rapidly recruited to phagosomes or endosomes containing microbial cargo.

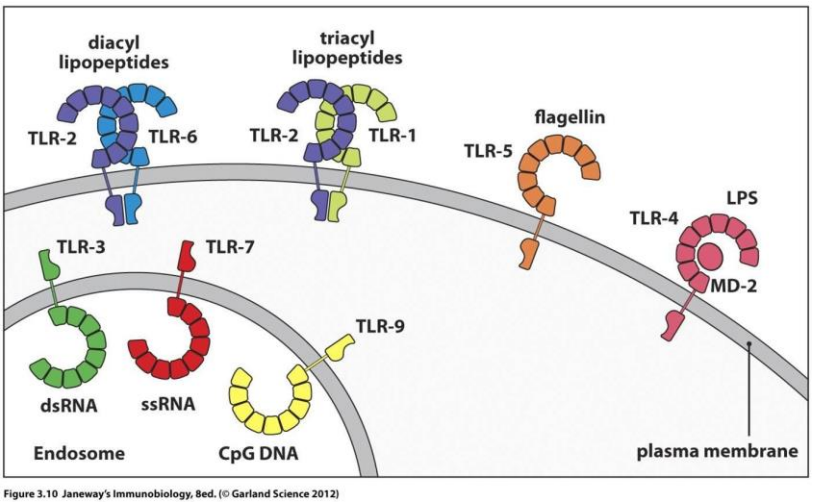

Figure 4. TLRs cellular localization

2.1 Toll-like Receptor 4 - TLR4

Toll-like receptor 4 was the first mammalian Toll to be characterized.[11]

It is expressed in a variety of cell types, most predominantly in the cells of the immune system, including monocytes, macrophages, dendritic cells, γ/δ Tcells,Th1 and Th2 α/β T cells, a small intestinal epithelial cell line and a B-cell line.[2,11]

The TLR4 gene is expressed most strongly in spleen (Sp) and peripheral blood leukocytes (PBL).

As the other TLRs, TLR4 plays a critical role in the recognition of PAMPs derived from microbial pathogens.

In particular TLR4 selectively recognizes bacterial endotoxin (E), Gram-negative bacterial lipo-oligosaccharides (LOS) and lipopolysaccharides (LPS).[13–15]

The discovery that TLR4 functions as the **signal-transducing receptor for LPS** was made in 1998 when C3H/HeJ strain of mice, which tolerates lethal doses of LPS and has altered inflammatory responses, was found to have a missense mutation in the conserved region of the TLR4 intracellular domain.[13]

Similar tolerance was observed in the C57BL/10ScCr mutant, which has a deletion of the entire tlr4 locus, and in TLR4-deficient mice.[13–15]

In addition, TLR4 recognizes a broad variety of substances from viruses and mycoplasma.

TLR4 is also activated by endogenous factors, generally known **as danger (or damage) associated molecular patterns (DAMPs)**.[16]

Typical DAMPs acting as TLR4 agonists are endogenous substances that are released as a consequence of injury and inflammation. They include β-defensin, high-mobility group protein 1 (HMGB1), heat shock proteins (HSPs), hyaluronic acid, heparin sulfate, substance P, and others. [16]

Moreover also environmental factors, e.g., ozone, atmosphere particulate matter, long-lived reactive oxygen intermediate, pentachlorophenol, ionizing radiation, and toluene seem to trigger TLR4.[16]

Despite the key role of TLR4, however, in all higher vertebrates no physiological role of TLR4 alone has been demonstrated.

Indeed transfection of TLR4 alone in unresponsive mice cell lines is not enough to confer LPS recognition.[17]

Cell activation induced by LPS through TLR4 is peculiar in the sense that it does not to bind the ligand directly to its ectodomain but requires the protein adaptor called Myeloid Differentiation Factor 2 (MD-2).

MD-2 binds to the ectodomain of TLR4 and is essential for LPS signalling. [18–21]

This was demonstrated by studying LPS responsiveness of stable transfectants expressing TLR4 alone or with MD-2 by measuring NF-κB activity. The stable transfectant line that expressed TLR4 alone did not respond to LPS while transfection of MD-2 conferred on the line strong NF-κB responses to either LPS or lipid A.[19]

This was also confirmed by the discovery of a lesion in one of the complementation groups in the gene for MD-2 (but not of TLR4) of CD14-transfected Chinese hamster ovary–K1 (CHO-K1) fibroblasts defective in responses to bacterial endotoxin. The non-responsive phenotype of this mutant was reversed by transfection with MD-2.[21]

From a structural point of view, TLR4 is a single-spanning transmembrane protein containing 841 amino acids with a molecular mass of 92 kDa and, as for many TLRs, it is composed of an extracellular leucine-rich repeat (LRR) domain, formed by 608 residues, a single transmembrane domain and an intracellular TIR (Toll/Interleukin-I Receptor) domain of 187 residues.[11,22]

The extracellular domain of human TLR4 is composed of a 608 residues divided in 21 tandemly repeated leucine-rich (LRR) motifs separated by a non LRR region. At the N-terminal end of the LRR domain there is a 31-amino-acid long N-flanking region that is also present in several other LRR-containing proteins, for example RP105, Decorin and Biglycan. The C-terminal end of the LRR domain is flanked by a cysteine-rich domain which is also present in *drosophila* Toll and some other transmembrane proteins.

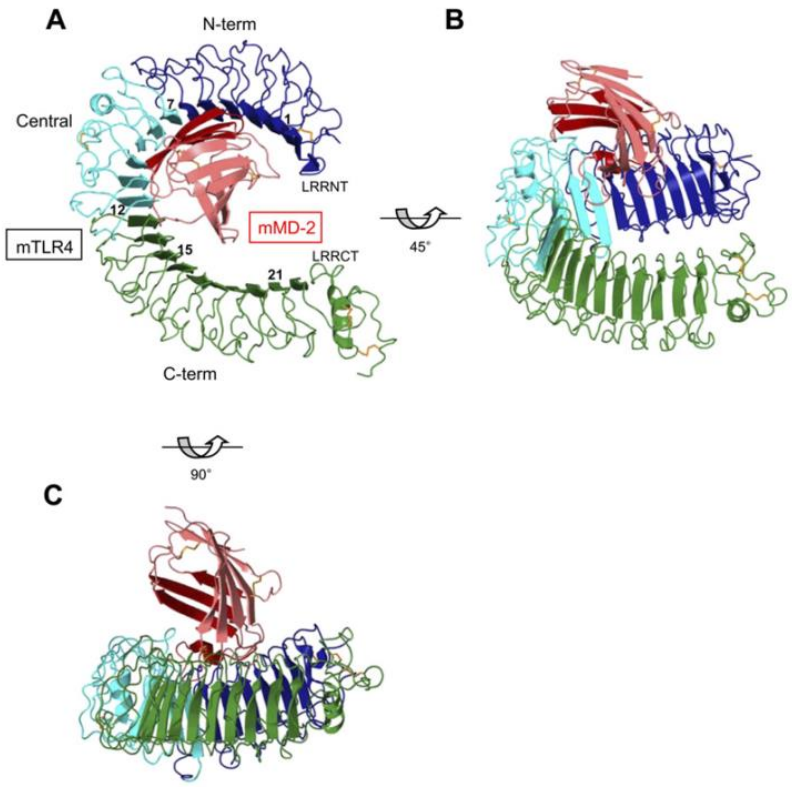

Figure 5. Crystal structure of mouse TLR4-MD-2 complex as studied by Kim et al.[22] Three different views. (from Kim et al. 2007[22])

The crystal structures of mouse and human TLR4 in complex with MD-2 have been first reported by Kim et al. in 2007[22] (figure 5) and later by Park et al. in 2009[23] (figure 6).

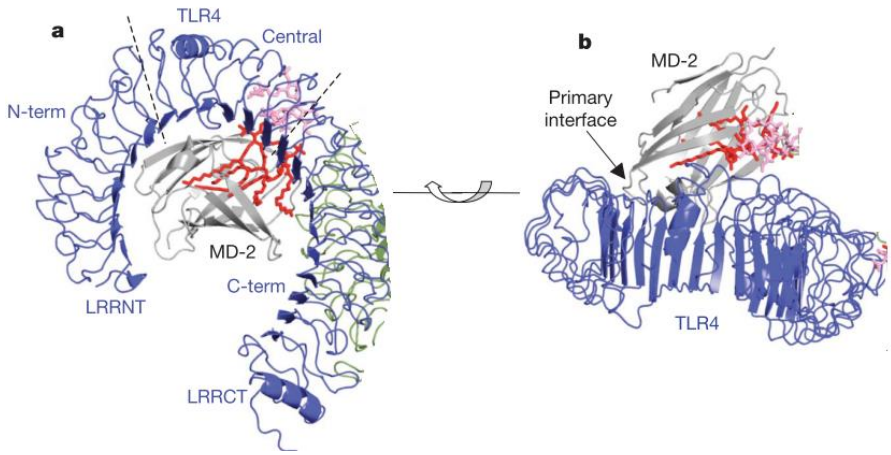

Figure 6. Crystal structure of human TLR4-MD-2 complex as studied by Park et al.[23] Two different views. (from Park et al. in 2009[23])

Human TLR4 has 62.4% sequence identity with mouse TLR4 and they have highly homologous structure. Indeed, the N- and C-terminal domains of the two TLR4 structures could be superimposed.

On the contrary, the central domains differ substantially more in structure than the N- and C-terminal domains as seen with crystal structures. However mouse and human central domains are 56% identical, and residues with clear structural roles are strictly conserved.[22]

3. Gram-positive bacteria and Gram-negative bacteria

As stated above, TLR4 main functional role is to recognize Gram-negative bacterial lipopolysaccharide (LPS), providing an effective response against bacteria that eluded the physical and anatomic barriers of the organism.

Among Gram-negative bacteria there are important commensal or human pathogenic species such as *Escherichia coli, Salmonella enterica, Neisseria meningitidis, Haemophilus influenzae, Bordetella pertussis, Pseudomonas aeruginosa, Helicobacter pylori, Klebsiella pneumoniae, Legionella pneumophila* and *Chlamydia trachomatis, N. gonorrhoeae, C. trachomatish.*
To date, the only group of Gram-negative wild-type bacteria known not to express LPS are diverse species of the genus Sphingomonas, the outer membranes of which have been recently shown to contain glycosphingolipids (GSL) instead of LPS.[24]

Bacteria are prokaryotic microorganisms representing the most common human pathogens.
All bacterial cells hold a cell envelope or membrane that protects the cytoplasm and it is composed by a wide variety of biological molecules involved in many cellular processes.
The cell envelope is made of several layers and it is possible to distinguish bacteria into two groups according to their differences in it: Gram-positives and Gram-negatives (the names are related to their different responses to the Gram staining protocol)(figure 7).

In the **Gram-negative bacteria** cell envelope, three principal layers can be distinguished: the outer membrane (OM), the periplasm, and the inner membrane (IM).
On the contrary **Gram-positive** cell envelope has no outer membrane.

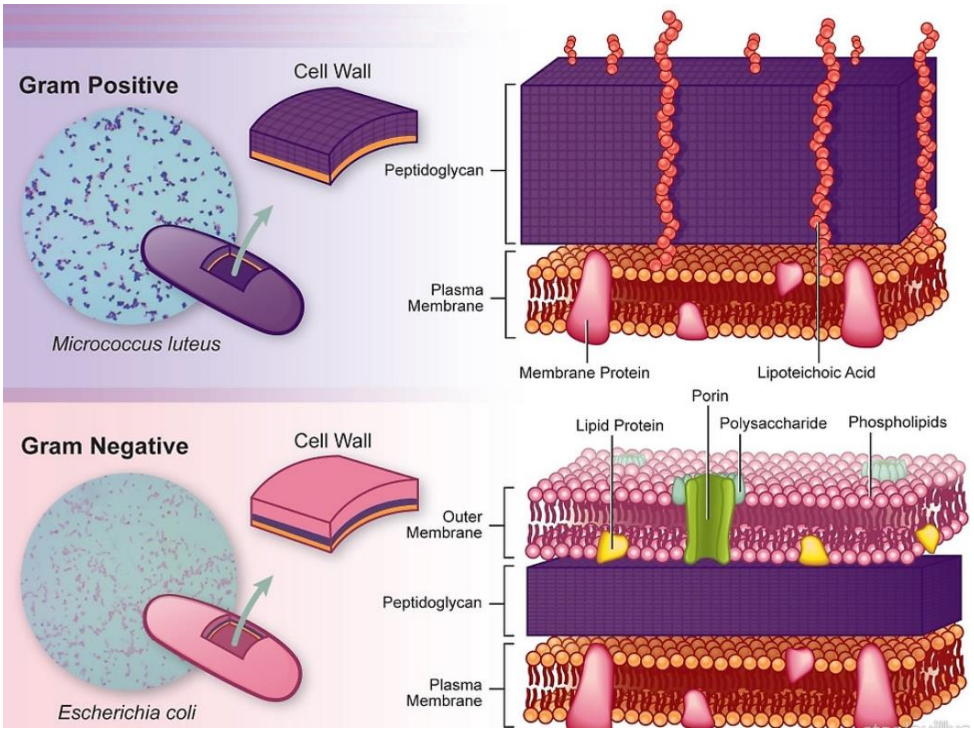

Figure 7. Gram-positive and gram-negative bacteria cell walls

This **Gram-negative bacteria** outer membrane is oriented towards the outside of the cell and shows a peculiar asymmetrical organization.

The inner leaflet is composed of glycerophospholipids and lipoproteins, while the outer leaflet is made of lipopolysaccharides (LPSs). In addition, the outer membrane contains several integral, trans-membrane and outer membrane proteins (figure 8).

The asymmetrical arrangement of the Gram-negative outer membrane confers various functions to the bacterium: proteins allow the diffusion of compounds across the outer membrane and the LPS component is capable of various chemical arrangements that can influence the bacterium's ability to elude host immune defenses.

On the contrary the Gram-negative bacteria inner membrane, which is in direct contact with the cytoplasm, consists of a phospholipid bilayer, mainly composed of phosphatidyl ethanolamine and phosphatidyl glycerol, decorated with several proteins.

The bilayer is arranged with polar heads oriented towards the extracellular face, in order to shield hydrophobic chains from the surrounding polar fluid. Since bacteria lack intracellular organelles that perform a number of essential cellular processes in eukaryotes, such as mitochondria and endoplasmic reticula, many of these functions are performed within the inner membrane in prokaryotic organisms.

The two-membrane system allows for the existence of the periplasm, an aqueous cellular compartment.

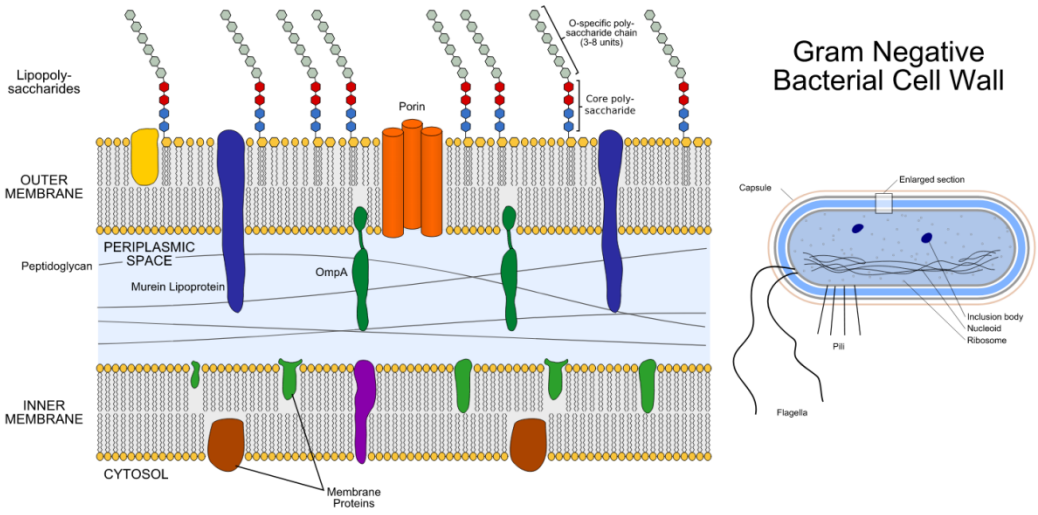

Figure 8. Gram-negative bacteria cell wall

The periplasm is more viscous than the cytoplasm and it is densely packed with proteins, such as environment-sensing proteins that determine the bacterial response to environmental signals. The periplasm plays an important role in the survival and activities of the bacterium, acting as a buffer between its interior and the external environment. In the periplasm, a slim peptidoglycan layer is present: peptidoglycan is a biopolymer made up of repeating units of the disaccharide N-acetyl-glucosamine and N-acetyl-muramic acid, joined with β-(1→4) linkages. The saccharide strands are cross-linked by tetrapeptide side chains. This polymer gives a strong contribution to the cell shape, thanks to its considerable rigidity.

The lack of the outer membrane and its protruding lipopolysaccharides, however, is not the only feature distinguishing **Gram-positive bacteria.**

The peptidoglycan of the two bacterial types differs with respect to thickness: the Gram-negative peptidoglycan is only a few nanometers thick, whereas the Gram-positive is characterized by a dense layer of 30–100 nm.

In addition, the peptide cross-links among glycan strands in peptidoglycan is different.

In fact, the amino acid sequence of the peptide cross-link is L-Alanine, D-Glutamic acid, Lysine (Gram-positive) or meso-2,6-diaminopimelic (DAP) acid (Gram-negative), D-Alanine. Furthermore, Gram-positive bacteria have peptide stems usually cross-linked through an inter-peptide bridge (generally made of glycines), whereas Gram-negative bacteria peptide stems are usually directly cross-linked.

The macromolecules constituting the cell envelope of virulent Gram-positive and Gram-negative bacterial strains are involved in mechanisms of adhesion, colonization and infection of the host.

In particular, peptidoglycan (PGN) for Gram-positive and lipopolysaccharides (LPS) for Gram-negative bacteria are also antigens, because conserved molecular patterns (PAMPs) are recognized by specific receptors of immune system cells.

3.1. LPS

Lipopolysaccharide (LPS) is an outer membrane constituent of all Gram-negative bacteria where it has indispensable barrier functions.[24]

LPS molecules (also named bacterial endotoxins) cover 75% of the external cell surface and confer to the outer membrane its characteristic asymmetry. They play an essential role in bacterial growth and survival due to their morphological, protective and adhesion functions.

The LPS layer of the outer membrane which is stabilized by associated divalent cations represents an effective permeability barrier of the bacterial cell towards external stress factors. Many agents which are selectively directed against Gram-negative bacteria, such as the group of polymyxin antibiotics, cationic proteins, and peptides or polyamines, and also chelators like ethylenediaminotriacetic acid (EDTA) or nitrilotriacetic acid (NTA), increase the permeability of the outer membrane by destabilizing the tight interactions of the LPS-cation-network on the bacterial surface. [24]

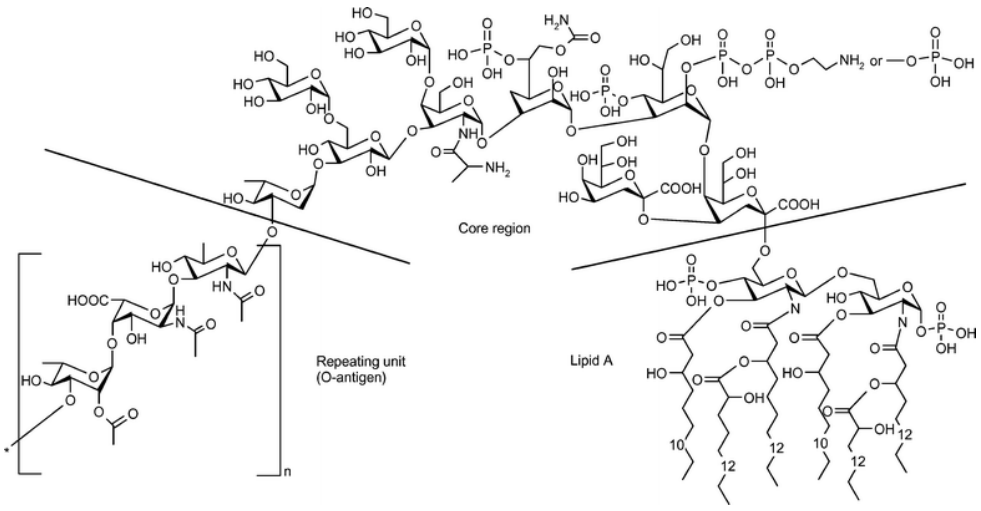

Figure 9. *E. coli* Lipopolysaccharide structure (LPS)

After the development of efficient purification procedures for LPS in the late 1940s and early 1950s, among which is the classical phenol-water method of Otto Westphal, Otto Lüderitz and Fritz Bister, the structures of the strongly immunostimulatory LPS derived from *E. coli* and S. enterica were first elucidated (figure 9).[24] Since that, within the last three decades, highly purified preparations of LPS from a large number of Gram-negative bacterial species have been characterized chemically, physically and biologically.[24]

Despite the great variability in structure (and in activity, as shown later) all forms of LPS possess a general structural architecture.

Their complex structures can indeed be divided into three domains (figure 10):

- membrane-anchoring glycolipid component with phosphoryl groups, called Lipid A
- polysaccharide or oligosaccharide portion covalently linked to this membrane anchor domain, called core
- polysaccharide or oligosaccharide O-specific (or O-antigen) terminal chain

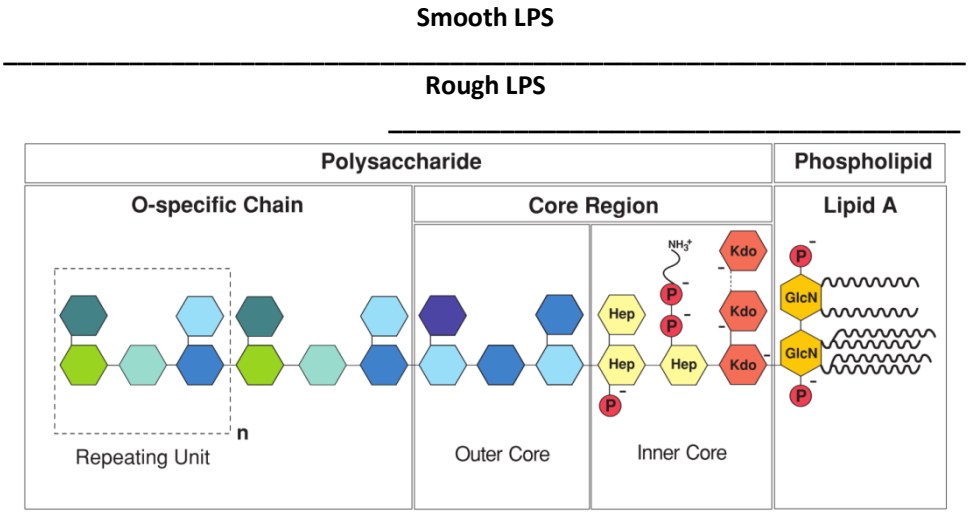

Figure 10. General structure of LPS from Alexander et al. [24]

Despite this general features some exception are present with many wild-type species of pathogenic Gram-negative bacteria colonizing especially the mucosal surfaces of the respiratory and urogenital tracts, such as *N. meningitidis, N. gonorrhoeae, H. influenzae, B. pertussis* or *C. trachomatis* have been identified lacking the O-specific chain in the LPS structure.

LPS forms lacking the O-specific chain are called **Rough-LPS** (R-LPS) to differentiate them from the **Smooth form of LPS** (S-LPS)(see next paragraphs).

LPS from these bacterial species have also been termed as low molecular weight LPS (LMW-LPS) or lipooligosaccharides (LOS).

Within this general classification, there is an enormous multiplicity of natural LPS structure variants that is primarily due to an extended diversity in the chemical composition of the polysaccharide region, but also due to considerable variations in the fine structure of lipid A.

It must be pointed out, however that only certain forms of LPS (characterized by rather similar chemical structures in the lipid A region) trigger strong immunostimulatory (agonistic) activities.
From this consideration it appears also clear that the use of the term "**bacterial endotoxin**" as synonym of LPS, although often used today, is incorrect.

Core region

The core region of LPS can be divided in two parts according to predominating monosaccharide compositions: an outer core region consisting of hexoses like D-glucose, D-galactose, D-glucosamine, N-acetyl glucosamine or N-acetyl galactosamine; an inner core region shows the least structural variability within the polysaccharide region and, in the case of most Gram-negative bacteria, consists of the characteristic monosaccharide units 3-deoxy-D-manno-octulosonic acid (dOclA) usually also termed '2-keto-3-deoxyoctulosonic acid' (**Kdo**) and L- or D-glycero-D-manno-heptose (L,D-Hep) often carrying additional anionic substituents like phosphate (P), diphosphate (PP) or diphosphoethanolamine (PPEtn) groups. According to the current state of knowledge, the sugar acid Kdo represents a characteristic and essential component of the inner core region of bacterial LPS [24] and is, therefore, considered as a diagnostic marker for LPS as well as a target for the development of new antibacterial agents aimed to inhibit the Kdo-related steps in the biosynthesis of LPS

O-specific terminal chain

This domain consists of up to 50 repeating oligosaccharide units formed of 2–8 monosaccharide moieties in a highly species- and strain-specific manner. [24]
Only few bacterial strains or species like *E. coli* O8 and O9, *K. pneumoniae* O3 and O5 as well as *L. pneumophila* have shown to contain homopolymeric O-chains.
In the vast majority of LPS structures, the O-specific chain is characterized by extremely high structure variability even within a given bacterial species which constitutes the chemical basis for the serological classification of individual wild-type bacterial strains according to the O- antigenic determinants.
The synthesis of the O-specific chain in enterobacteria is determined by the enzymes encoded by the wb* (or rfb) gene cluster.[25]
Bacterial mutants having a defect in the wb* locus or lacking it completely, synthesize LPS without O-specific chains. Based on the characteristic colony morphology, distinct from the smooth (S)-form of wild-type enterobacterial species these mutants have been historically termed as rough (R)-mutants leading to a corresponding general subclassification into **S- and R-forms of LPS**. Such mutants are able to grow and multiply *in vitro*, showing that the O-chain in principle is dispensable for bacterial viability. However, in tissues or body fluids, pathogenic enterobacteria can only persist and survive if they express an O-specific

chain which in this case protects the bacteria from the uptake by phagocytes and the attack of serum complement.

Smooth (S)-form LPS are commonly the preferred choice for whole animal studies, whereas Rough (R)-form LPS are primarily used in cellular *in vitro* activation studies.

Because of its importance for bacterial survival in vivo, the O-specific chain represents a suitable target for the development of new antibacterial strategies.

3.1.1 Lipid A

As first demonstrated by Galanos in 1975, Lipid A represents the immunostimulatory or 'endotoxic' principle of LPS. [24]

As the result of several highly detailed studies the complete chemical structure of the major type of lipid A derived from LPS of *E. coli* was successfully elucidated in 1983 (figure 11).

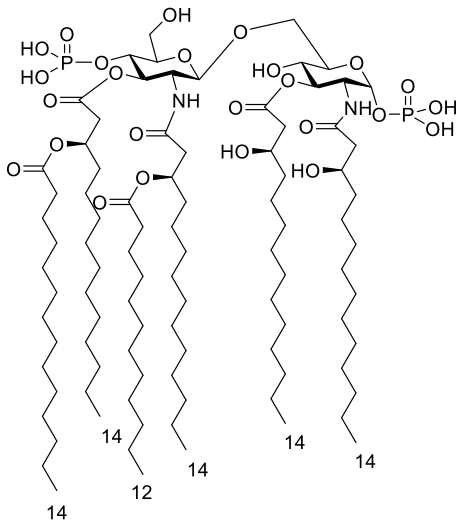

Figure 11. *E. coli* Lipid A

E. coli Lipid A consists of a central β(1→6)-linked D-glucosamine disaccharide unit carrying two phosphate groups, one at position 1 and α-oriented and one at position 4', and six acyl chains asymmetrically distributed.

Among these chains two (R)-3-hydroxymyristoyl residues were shown to be directly linked at the positions 2 and 3 via amide and ester linkages respectively, while on the distal glucosamine moiety, both of the primary (R)-3-hydroxyacyl chains at positions 2' and 3' were found to be further esterified with lauric and myristic acid, respectively, forming acyloxyacyl groups in both positions.

The primary hydroxyl function at position 6' is the only free position since it is the binding site of the polysaccharide region.

After *E. coli* LPS Lipid A structure elucidation, the lipid A structures of LPS derived from numerous Gram-negative bacterial species have been elucidated and characterized especially in terms of biological activities (figure 12).

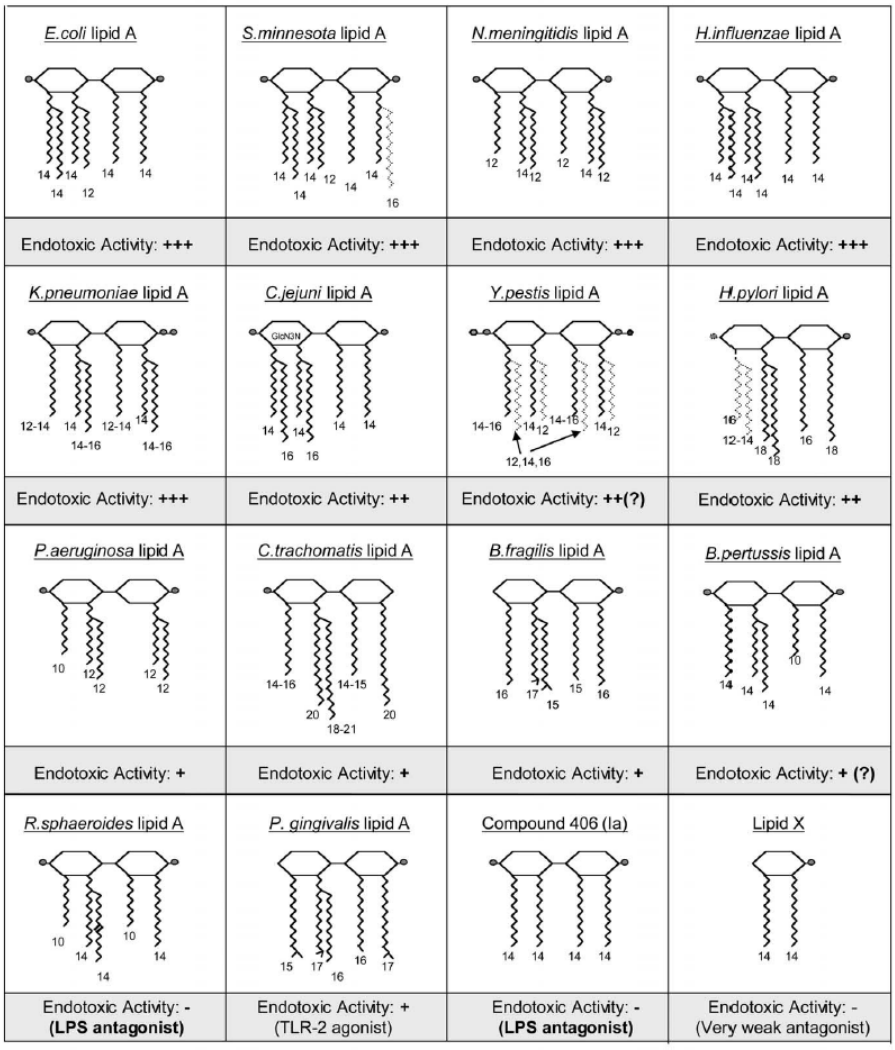

Figure 12. An image from a review of 2002 reporting the biological activities of extracted natural lipid As[26]

In general, preparations of natural lipid A derived from a single bacterial species have been shown to represent an intrinsically micro heterogeneous mixture of major and minor molecular species often requiring sophisticated purification protocols for the characterization of individual natural compounds.

In the vast majority of lipid A structures characterized to date, the backbone structure consists of a central β(1→6)-linked disaccharide unit that is composed of D-glucosamine (D-GlcN) or D-2,3-diamino-2,3-dideoxy-

glucose (D-GlcN3N; DAG) in either homodimeric or heterodimeric combination, which is phosphorylated in positions 1 and 4', and with different acyl chains in the position 2, 3, 2' and 3'.

Comparative studies of natural lipid A structures have revealed that besides the intact β(1→6)-linked disaccharide structure and the nature of the groups linked to positions 1 and 4', it is above all the acylation pattern that determines the immunostimulatory capacity of lipid A in a given eukaryotic organism.
A considerable diversity in the chemical structures of natural Lipid As has been shown to exist in the specific acylation pattern, i.e. the number (hexacyl, hepta-acyl, penta-acyl, tetra-acyl), position and chemical nature of the acyl residues linked to the central backbone, and this diversity reflects into biological activities.
In particular, by comparing all Lipid As, natural or synthetic, the classical hexa-acylated lipid A-species consisting of two (R)-3-hydroxyacyl and two (R)-3-acyloxyacyl residues limited in length of individual acyl chains to 12 or 14 carbons in either *E. coli*- or *N. meningitidis*-type distribution, in addition to at least one phosphate group in both positions 1 and 4' of the central disaccharide unit, still represents the most potent stimulatory or agonistic structures for activation of innate immunity in humans and other mammalian hosts.

The reasons for such structural requirements and for Lipid A key role in LPS biological effect can be understood only from the knowledge of the molecular details of the TLR4 LPS-recognition process.

4. TLR4 LPS-recognition process

As stated above TLR4 is able to sense and respond to bacterial LPS, however TLR4 does not bind LPS directly but it requires the adaptor protein Myeloid Differentiation Factor-2 (MD-2).[19]
In addition the recognition process of LPS involves other endotoxin-binding proteins, the LPS binding protein (LBP)[27–29] and the Cluster Differentiation antigen 14 (CD14).[30–33]
The complete recognition process of these four endotoxin-binding proteins can be explained in this way (figure 13):[34,35]

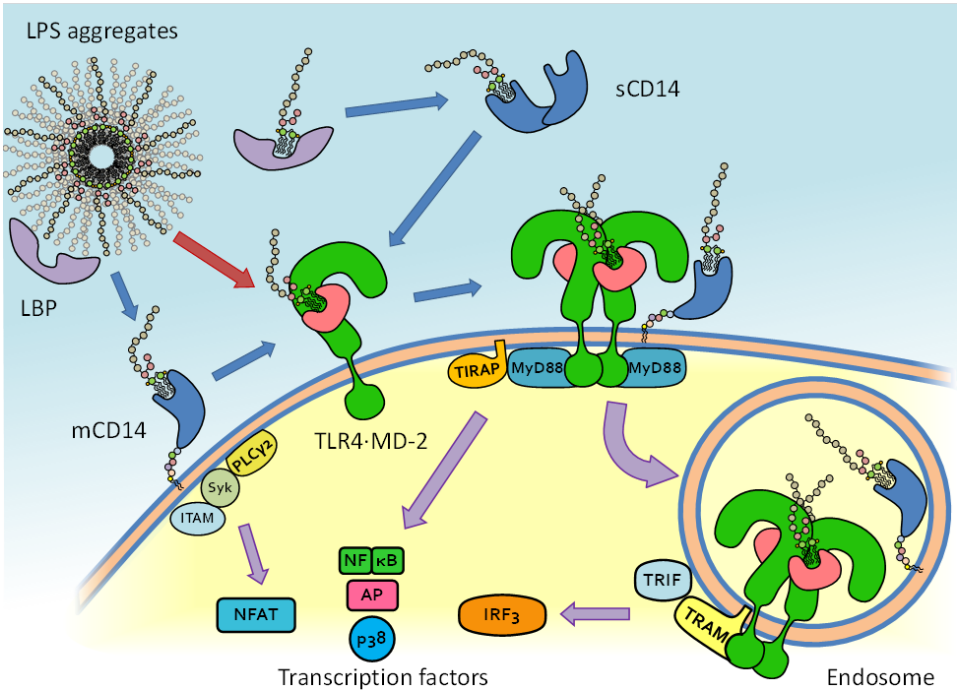

Figure 13. TLR4 recognition process (image by R. Cighetti)

1) The whole molecular process starts by LBP interaction with LPS aggregates in solution which catalyzes the extraction of monomeric LPS molecules from large aggregates. [29]

   Different contributions of electrostatic (contributed by patches of basic residues) and hydrophobic interactions (contributed by the hydrophobic binding pocket) support the flow of LPS from the bacterial membranes and aggregates to the LPS-sensing receptor.

2) In the second step CD14 forms a ternary complex with monomeric LPS and LBP in solution. CD14 protects the acyl chains of the lipid A from the solvent, and the complex is stable in solution in the monomeric form, while LBP preferentially interacts with LPS aggregates.[30]

   It is noteworthy to mention that only when in low concentrations LBP transfers the monomers of LPS to CD14. On the contrary, at high concentrations of LBP, as the ones found in the serum of septic patients, LBP inhibits the LPS signalling by shuttling the LPS to serum lipoproteins and by formation of aggregates with LPS. Therefore LBP serves as an inhibitor of the excessive response to LPS.

   However while the S-form of LPS is not able to induce any biological response without CD14, Lipid A and R-LPS are able to activate TLR4/MD-2 without CD14.[36]

   A role of albumin has been reported in the interaction of LPS with LBP and CD14.[37]

3) In the third step CD14 transfers LPS monomers to MD-2, the TLR4 co-receptor bound to its ectodomain, which interacts with LPS through both cationic residues and hydrophobic groups.[19,38]

4) Binding of lipid A to MD-2 causes the rearrangement of TLR4, leading to dimerization of the TLR4-MD-2 complex and the formation of the (LPS·MD-2·TLR4)2 complex[39]

5) the receptor dimerization leads to the recruitment of adapter proteins to the intracellular TIR domain of TLR4[40]

6) recruitment of adapter proteins initiates the intracellular signal cascade that culminates in the translocation of transcription factors to the nucleus and the biosynthesis of cytokines.

   Two distinct signal/transduction pathways are possible (figure 14)[41]: one is the MyD88 (Myeloid Differentiating primary response gene88)-dependent pathway, which leads to the activation of transcription factors Nuclear Factor Kappa B (NF-κB) and Activator Protein 1 (AP-1); the second is the TRAM-TRIF (two effectors) MyD88-independent pathway, which leads to the activation of the Interferon Regulating Factor 3 (IRF-3).

   MyD88-independent pathway is however only activated in presence of CD14.

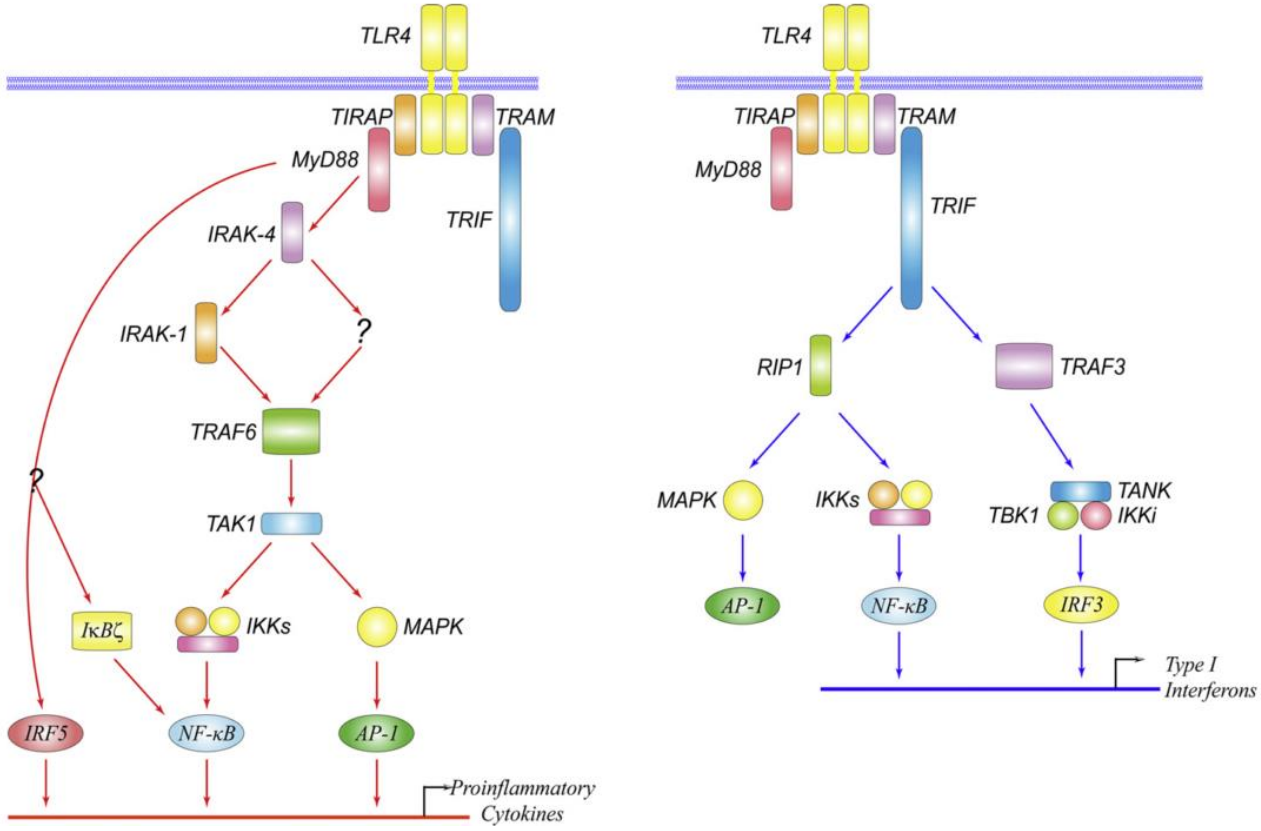

Figure 14. TLR4 intracellular signalling: MyD88-dependent pathway (left) and MyD88-independent pathway (right) from Lu et al. [41]

7) The activation of NF-κB, AP-1 or IRF-3 finally leads to the expression of several inflammatory mediators (cytokines, chemokines or co-stimulatory molecules).

However another pathway involving LPS internalization is possible and different studies have been conducted to elucidate this pathway.

Detmers and coworkers, along with Lichtman and coworkers, suggested that monomeric LPS is internalized in vesicles and uptake may be required for signaling.

Indeed, Detmers et al. in 1996 showed that the introduction of fluorescent LPS monomers into the plasma membranes of leukocytes is followed by rapid transport of LPS to an intracellular site and that agents such as wortmannin, a PI3K inhibitor that interrupts this traffic, block cellular responses to LPS.[42]

Thieblemont et al. showed that LPS transport is absent in peritoneal macrophages from mice with a genetic deficiency in responsiveness to LPS.[43]

The same group proved that cells sort agonist and antagonist LPS molecules differently. Biologically active LPS is transported from the plasma membrane to a defined intracellular site while antagonist *Rhodobacter spheroides* LPS (RsLPS) remains at the cell periphery.[44]

Also TLRs intracellular trafficking have been studied and while TLR4 was found to be localized to the Golgi in certain epithelial cells and to co-localize with LPS,[45] Latz et al. proved that LPS rapidly transfers to and from the Golgi apparatus with the TLR4/MD-2/CD14 complex in a process that is distinct from the initiation of signal transduction.[46]

Triantafilou et al. found in the same year that TLR4 is recruited in membrane microdomains (lipid rafts) following stimulation by LPS.[47]

Finally in 2008 Kagan et al. reported that LPS activates TLR4 in two sequential ways[48]: first it activates TLR4 from the plasma membrane after LPS encounter, then TLR4 is internalized into the endosomal network where the second signaling pathway is triggered.

The authors also proposed that TLR4 first induces two distinct signaling pathways with respect to the modality of TLR4 activation: TIRAP-MyD88 signaling is activated from the plasma membrane while TRAM-TRIF is activated from early endosomes.

4.1 Lipopolysaccharide-binding protein (LBP)

Lipopolysaccharide-binding protein (LBP) is a serum glycoprotein which belongs to the lipid transfer/LBP family comprising bactericidal/permeability-increasing protein (BPI), cholesteryl ester-binding protein (CETP) and phospholipid transfer protein (PLTP). [35]

The first discovery of LBP role in LPS recognition dates back to 1986 with the work of Tobias et al.[27] but it was only with later works that its role was clearly elucidated.[28–30,49]

LBP is a true pattern recognition molecule as it binds and transfers several different phospholipids

LBP is synthesized primarily by hepatocytes and released into the bloodstream after glycosylation.

Other sources of LBP include epithelial cells of the skin, the lung, the intestine, and human gingival tissues, as well as the small-muscle cells of the lung arteries, heart muscle cells, and renal cells.

LBP has a molecular weight of 58 and 60.5 kDa, wherein the difference in molecular mass reflects different degrees of glycosylation.

Human LBP consists of 452 amino acids and has the characteristic 25-amino acid signal sequence of secreted proteins.[29]

Its amino acid sequence reveals a sequence homology to bactericidal/permeability-increasing protein (BPI), cholesteryl ester transfer protein (CETP), and phospholipid transfer protein (PLTP) of 45%, 23%, and 25%, respectively. It has also suggested a similarity in the tertiary structure of these proteins.

The crystal structure of its homologue murine BPI has been determined by X-ray crystallography (figure 15), which allows the construction of a reliable tertiary structural model of LBP.[50]

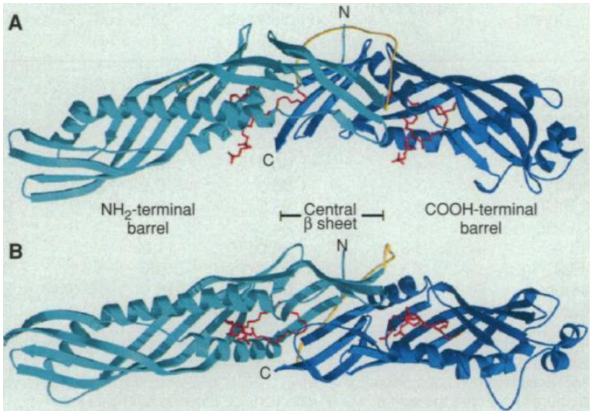

Figure 15. BPI crystal structure as determined by Beamer et al. in 1997[50] The NH_2-terminal domain is shown in light-blue, the CO_2H terminal domain is shown in blue and the two phopshatidylcholine molecules in red. The linker is yellow and the disulfide bond is shown as a ball-and-stick model. Two different views after 70° rotation. (from Beamer et al. 1997[50])

The tertiary structure of BPI contains two barrel domains arranged in a banana-like shape which are connected by a proline-rich linker. Each domain is composed of an antiparallel β-stranded layer twisted around the long α-helix. In the pocket between the helix and the β-strand, a phospholipid molecule has been co-crystallized in each domain.

From these observations, Beamer et al. in 1998 proposed a simulated three- dimensional model for LBP that is very similar to the structurally and functionally related BPI.[51]

Analogously with BPI, the three-dimensional LBP model showed that a cluster of cationic residues fully exposed at the N-terminal tip.

LBP has been studied to have a dual role: it extracts monomers of LPS from the bacterial membranes (LPS monomerization)[28] and it transfers LPS monomers to CD14. [33]

The cationic cluster of LBP represents LPS-binding domain of LBP as demonstrated by Lamping et al. with mutagenesis experiments.[52] LBP mutants with amino acid exchanges within the N-terminal region were expressed and tested. The double mutant glutamic acid 94/95 was completely lacking LPS binding, transfer, and cell-stimulatory activity, indicating that the integrity of amino acids Arginine-94 and Lysine-95 is required for LBP function. On the contrary the ability to facilitate binding of LPS aggregates to membrane-bound cluster of differentiation 14 (mCD14) at the cell surface was retained. These findings emphasize the distinction between binding of LPS aggregates to cells and the binding of LPS monomers to CD14—the former is not associated with cell stimulation and the latter leads to cell stimulation.
An indirect support for the role of the cationic residues of LBP in is provided by the activity of arginine- rich peptides, which can also stimulate monocyte activation. [53]

The role of these cationic residues is in principle that of destabilizing the LPS aggregates and consequently facilitating LPS binding and signalling.

However LBP has also a dual behaviour: if at low LPS concentrations, it enhances LPS signaling by extracting and transferring the LPS monomers to CD14, at high concentrations, on the opposite, it inhibits the LPS signaling by shuttling the LPS to the serum lipoproteins and by forming aggregates with LPS. Indeed, the increased secretion of LBP as a result of LPS stimulation serves as an inhibitor of excessive response to LPS in the serum of septic patients.[54]

The phospholipid-binding site of the N-terminal domain of LBP seems like a suitable site for binding of the lipid A moiety. However, the size of the binding pocket is by far too small to accommodate the acyl chains of the typical lipid A. Therefore, the location of the lipid A-binding site on LBP is not quite clear, since the distance between the cationic and hydrophobic site is also too large to allow the interaction of the lipid A molecule with both sites. Hydrophobic interactions play a certain role in this interaction since a detergent prevents LPS binding to the N-terminal domain of LBP.[55]

While the amino-terminal domain of LBP is fundamental for LPS binding, its C-terminal domain is required for the interaction with CD14 or the cell membrane. This has been demonstrated by a fusion protein of the N-terminal domain of the inactive BPI and the C-terminal domain of LBP, which mediates the same stimulation of monocytes as LBP.[56]

To explain the catalytic reaction mechanism for the transfer of LPS to sCD14, two models were proposed. The “binary complex” model proposes that the initial step in the transfer involves a bimolar reaction

between LBP and an LPS micelle. Following dissociation from the micelle with one molecule of LPS bound, LBP then binds to sCD14.[49]

The "ternary complex" model, on the other hand, suggests a simultaneous interaction among LBP, LPS micelles, and sCD14.[57]

From what stated above and in the previous section the roles of LBP can be summarized in this way:

- it catalyses the extraction of LPS monomers from LPS aggregates in solution
- it transfers LPS monomers to CD14
- it serves as an inhibitor of the excessive response to LPS (effect related to the intensity of LBP secretion)

4.2 Cluster Differentiation Antigen 14 (CD14)

CD14 is glycoprotein existing in two forms: a glycosylphosphatidylinositol (GPI)-anchored membrane form (mCD14), expressed on the surface of monocytes and granulocytes; a soluble form in the serum (sCD14).

It was discovered in 1989 by Wright et al.[28], that means ten years before the discovery of TLR4 as the critical "LPS receptor", being the first PRR to be described.

In their report, Wright et al. showed that CD14 binds complexes of LPS and LBP, and the blockade of CD14 with anti-CD14 antibodies prevents further binding of LPS-coated erythrocytes to macrophages. With the absence of a binding event, macrophages are unable to produce an LPS-induced inflammatory response. [28]

CD14 is another pattern recognition receptor which can bind anionic phospholipids similar to LBP and participates in the phospholipid transport.

CD14 is expressed by various cells such as cells of the myeloid lineage (monocytes, macrophages, PMNs), B cells, parenchymal cells of the liver, gingival fibroblasts, and microglial cells.

In addition to the fatty acids of lipid A, CD14 binds carbohydrate chains of LPS and peptidoglycan.

Since sCD14 lacks the glycosyl phosphatidylinositol (GPI) anchor, mCD14 and sCD14 have molecular masses of 53 and 48 kDa, respectively. To determine the amino acid composition of CD14, Ferrero and Goyert cloned the CD14 gene and revealed a transcript encoding a 356-amino acid protein. It was also found to have high leucine content (15.5%) and four putative N-glycosylation sites.[58]

Indeed CD14 is composed of 11 leucine-rich repeats and it has been crystallized as a dimer resembling the horseshoe fold of TLRs and other leucine-rich repeats (figure 16).[59]

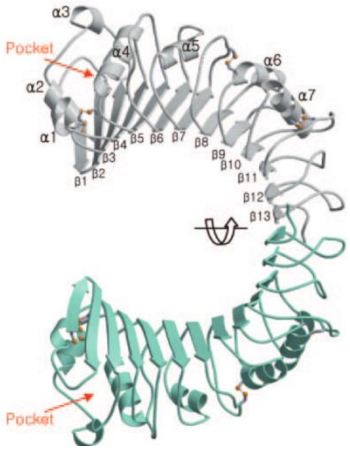

Figure 16. Overall structure of the mouse CD14 dimer. Two monomers of CD14 in the crystal are colored in gray and cyan. Disulfide bridges are shown in orange. (from Kim et al. 2005[59])

The structure of CD14 contains a β-sheet at the concave and helices with loops at the convex face. The amino-terminal segment forms a hydrophobic pocket between the first and second loop/helix at the convex face.

The main function of CD14 has long been considered to enhance local LPS concentration, in order to increase the sensitivity of the TLR4 complex with respect to the endotoxin.
However CD14 is not required for the MyD88-dependent activation of TLR4 by the rough chemotypes of LPS and at high concentration of LPS.[36]

The N-terminal part of CD14 has been identified to be the site involved with LPS binding.[60]
In particular the 820 $Å^3$ pocket formed by this segment with the charged cationic residues at the edge of it is thought to be the binding place since it is large enough to accommodate large part of the acyl chains of the lipid A of LPS.
By entering the pocket lipid A could be also protected from the enzymatic activity of acyloxyacyl hydrolase (AOAH).
The charged residues at the edge of CD-14 pocket could in turn explain CD14 preferential binding with anionic amphiphiles.
However it must be stated that the hydrophobic pocket of CD-14 is so large that CD14 is not able to discriminate between antagonistic and agonistic lipid A chemotypes.
This discrimination is in fact operated by MD-2, the other PRR involved in LPS recognition.

CD14 also plays a fundamental role in TLR4·MD-2 internalization after LPS binding as reported by Zanoni et al. in 2011 for microbe-induced endocytosis of TLR4.[61]

Summarizing the roles of CD-14:

- it forms a ternary complex with LPS and LBP
- it transfers LPS monomers to MD-2
- it is essential for TLR4 activation by the S-form of LPS
- it is essential to activate MyD88- independent pathway for both smooth and rough LPS chemotype
- it is essential for the activation of TLR4-MD-2 complex when LPS concentration is low
- it is NOT able to discriminate alone between active or inactive forms of LPS/Lipid As
- fundamental role in TLR4.MD-2 internalization after LPS binding

4.3 Myeloid Differentiation protein 2 (MD-2)

Myeloid Differentiation protein 2 (MD-2), also called Lymphocyte antigen 96 (LY96), or ESOP-1, has been identified for the first time by Shimazu et. al. in 1999 as a paralogue of MD-1, an RP105-associated protein.[19]

Its discovery has been an extremely relevant result since it was immediately identified as the missing ring sought for long between the already known CD-14 and the human Toll-like receptor 4.

Indeed they showed in a series of experiments that MD-2 is physically associated with the ectodomain of TLR4 and confers responsiveness to LPS.[19]

Moreover in 2001 Da Silva Correia determined that LPS binds directly to each of the three PRR already known to be LPS receptors.[62]

Using modified and radio-iodinated LPS, they showed that LPS is cross-linked specifically to TLR4 and MD-2 when co-expressed with CD14. Thus, maximal cellular activation by LPS must be a cascade of events that likely involves transferring of LPS by LBP to CD14 and then to TLR4-MD-2.

However, although CD14 and LBP enhance cellular activation, activation of TLR4 by LPS was found to absolutely require MD-2: no physiological role of TLR4 has been demonstrated in the absence of MD-2.[63]

Moreover, MD-2 is the only PRR involved in TLR4 activation able to discriminate between active or inactive LPS chemotypes.

MD-2 is a 20- to 25-kDa extracellular glycoprotein classified into the ML superfamily of lipid-binding proteins.

Human MD-2 contains 160 amino acid residues.

To identify the regions of functional importance on human and mouse MD-2, common analytical methods, namely, analysis of peptide fragments, mutation analysis, and computational modeling have been utilized.

The most relevant regions for LPS activity were found to be the 17-amino acid sequence at the N-terminus, 7 cysteine residues, and 2 N-glycosylation sites.[64] The cysteine residues have been predicted to form three disulfide bonds and a free cysteine residue at position 133 and proper disulfide formation was found to be essential for the biological activity of MD-2.

Mouse and human MD-2 have been crystallized, together with TLR4, in 2007 by Kim at al. [22] (figure 17).

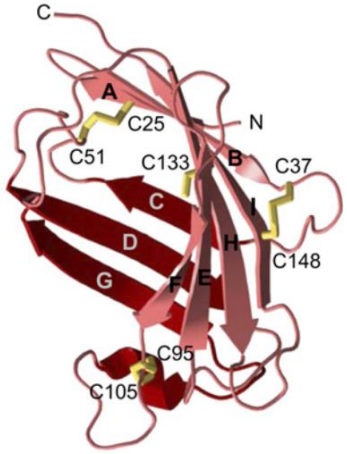

Figure 17. Crystal structure of mouse MD-2 as studied by Kim et al.[22] (from Kim et al. 2007[22])

Mouse and human MD-2 share 64% sequence identity. As expected, the two MD-2 structures show high structural homology.

MD-2 shares the β cup topology with the ML family of lipid-binding proteins.

Indeed MD-2 adopts a β cup fold with two antiparallel β sheets that contain three and six β strands, respectively. The β cup fold is different from the immuno globulin fold although both of them contain sandwiched antiparallel β. In the β cup fold, the two β sheets become separated on one side of the protein and the hydrophobic internal core is open for ligand binding.

Furthermore, the conserved disulfide bridge that connects the two β sheets in the immunoglobulin fold is absent from the β cup so that the two sheets can be separated, further permitting the formation of a large internal pocket.

This pocket proved to be of fundamental importance for LPS binding in crystal structures and for discriminating between active or inactive LPS chemotypes, which is a key feature of MD-2.

Indeed active or inactive LPS chemotypes bind differently to MD-2 and only the mode of binding of the former generate a response.

Moreover MD-2 ligand specificity differs between the species: human and mouse MD2 can bind the same ligands but these can determine opposite effects behaving as agonists in mice and as antagonists in humans.

The MD-2 pocket is narrow and deep with a total surface area of 1000 $Å^2$. The overall shape and chemical behavior of the pocket appear to be suitable for binding large flat molecules such as LPS that contain multiple hydrophobic acyl chains and negatively charged phosphate groups. The generous internal surface of the pocket is completely lined with hydrophobic residues, and the opening region of the pocket contains positively charged residues that facilitate the binding of LPS.
However compounds based on the structure of the lipid A, such as aminoalkyl glucosaminide phosphates, still bind to the same binding site of MD-2 as lipid A, showing that the recognition motif is primarily composed of the arrangement of the negative charges and the hydrophobic moiety, while the disaccharide backbone does not seem to be essential for the recognition.

X-ray structural analyses of variably acylated lipid A bound to human MD-2·TLR4 complex revealed strikingly different modes of binding of agonistic and antagonistic ligands.
In the case of tetra-acylated antagonists such as Eritoran (Kim et al., 2007[22]) and Lipid IVa (Ohto et al., 2007[65]), all four FA acyl chains are inserted into the hydrophobic binding pocket of hMD-2, while in the case of endotoxic *E. coli* lipid A only five FA chains are intercalated in the interior of the binding cavity, whereas the sixth acyl chain is exposed onto the surface of MD-2 and the whole molecule is turned by 180°.[23]
In the first two cases (antagonists) the ligand occupied the MD-2 binding pocket without triggering TLR4 dimerization, while in the case of Lipid A (agonist) the FA chain exposed on MD-2 surface constitutes, together with the patch of hydrophobic amino acids (Phe126 loop), the hydrophobic core interface for the interaction with the second TLR4*·MD-2*·LPS complex. Hydrophobic contacts of the exposed acyl chain of lipid A with the second TLR4*, along with intermolecular ionic interactions of the lipid A phosphates, promote the formation of the active $(LPS·MD\text{-}2·TLR4)_2$ complex.
These structural-activity relationships for different types of Lipid A total or partial structures will be discussed deeper in the section 7.1.

However, it must be pointed here that the protrusion of a fatty acyl chain out of the MD-2 pocket is not alone sufficient to drive potent TLR4 dimerization as demonstrated by the NMR studies of Gioannini and co-workers.[66]
For the second role of MD-2 to be exploited, indeed, that is to activate TLR4 dimerization, a conformation change in MD-2 Phe126 loop must occur due to ligand binding.
This conformational change will be then relayed to TLR4 enabling its dimerization.

Due to its discriminating role, MD-2 is used for docking studies in the rational design of TLR4 agonists and antagonists

Summarizing the roles of MD-2:

- it exists bound to the ectodomain of TLR4
- it binds LPS transferred by CD-14 or LBP itself
- it is essential for TLR4 activation by all TLR4 modulators
- it is the active unit able to discriminate between active or inactive forms of LPS/Lipid As through the binding interaction they generate with its pocket
- it has slightly conformational changes due to this binding that are relayed to TLR4
- this conformational changes induced in TLR4 activates its dimerization
- due to its discriminating role MD-2 is used for docking studies in the rational design of TLR4 agonists and antagonists

5. TLR4 related pathologies

The described activation of TLR4 pathway and the subsequent intracellular signalling, in response to bacterial endotoxins, result in the triggering of pro-inflammatory processes necessary for optimal host immune responses to invading Gram-negative bacteria.

However, excessively potent and deregulated TLR4 activation by PAMPS, like LPS, and its consequent signalling can lead to severe life-threatening syndromes.

Moreover in these syndromes the activation is also enhanced by the amounts of DAMPS released as a consequence of injury and inflammation.

A systematic review of the TLR literature shows that TLR4 is involved in many civilization disorders.

Activation of TLR4 indeed seems to be related the pathophysiology of many human diseases, including sepsis and septic shock, cancer, amyotrophic lateral sclerosis, atherosclerosis, allergies, asthma, cardiovascular disorder, diabetes, liver injury, ischemia/reperfusion injury, pulmonary disease, kidney disease, obesity, metabolic syndrome, inflammatory bowel disease, autoimmune disorders, neuroinflammatory disorders, schizophrenia, bipolar disorder, autism, clinical depression and chronic fatigue syndrome.[3,16]

5.1 TLR4 and Sepsis

Sepsis (Septicemia and blood poisoning are terms that referred to the microorganisms or their toxins in the blood and are no longer commonly used) is a systemic inflammatory response syndrome (SIRS) in response to an infectious process.

Most commonly, the infection is bacterial, but it may also be from fungi, viruses, or parasites.

When the immune system is over-activated by high levels of bacteria or their products in the bloodstream indeed the body's response to infection is so intense to cause injury to its own tissues and organs.
If the infection is even more intense the term **Severe sepsis** is used to refer to a condition in which poor organ function or insufficient blood flow arises.
Septic shock represents the most severe condition with persistent low blood pressure due to sepsis that does not improve after reasonable amounts of intravenous fluids are given.

Sepsis (and its two more severe conditions) is one of the major causes of death in the developed world causing millions of deaths globally each year and is the most common cause of death in people who have been hospitalized. The worldwide incidence of sepsis is estimated to be 18 million cases per year.
In the United States sepsis affects approximately 3 in 1,000 people, and severe sepsis contributes to more than 200,000 deaths per year. Sepsis occurs in 1–2% of all hospitalizations and accounts for as much as 25% of ICU bed utilization.
Due to it rarely being reported as a primary diagnosis (often being a complication of cancer or other illness), the incidence, mortality, and morbidity rates of sepsis are likely underestimated.
Disease severity partly determines the outcome. The risk of death from sepsis is as high as 30%, from severe sepsis as high as 50%, and from septic shock it is as high as 80%.

Sepsis usually is treated with intravenous fluids and antibiotics. Typically, antibiotics are given as soon as possible. Often, ongoing care is performed in an intensive care unit. If fluid replacement is not enough to maintain blood pressure, medications that raise blood pressure may be used.
Treatment is most likely to be effective if it is started early in the infection, but diagnosis of septic shock in its early stages is not straightforward, because the early symptoms of shock (fever, hypotension, and tachycardia) are nonspecific.
In addition, the transition from the early stages to multiple-organ failure can occur with frightening rapidity.
And even if bacteria are the microorganisms most frequently implicated in septic shock, many different species of Gram-positive and Gram-negative bacteria can cause shock and no single antibiotic is effective against all of these bacterial pathogens.
Moreover advances in the understanding of cell-signalling pathways that mediate the response to microbes have demonstrated that the concept of blocking endotoxin in order to prevent septic complications may be simplistic.[3]
All these reasons together have prompted scientists to the search of new paradigmas in the cure of sepsis.
One of these new approaches is the use of anti-inflammatory agents able to block the immune response that in sepsis is so deregulated and excessive to lead patients to organ damages or even death.

Numerous trials were conducted of agents that block the inflammatory cascade: corticosteroids, anti-endotoxin antibodies, tumor necrosis factor (TNF) antagonists, interleukin-1–receptor antagonists, and other agents.[67]

Currently, over 30 pharmaceutical products have been in the development stage to treat this condition, yet only few have reached the market. Many of these products that target specific inflammatory mediators have been unsuccessful because of the complex nature of sepsis.

Eli Lilly's Xigris® is one of the few drugs currently available on the market to treat sepsis. Xigris® is a recombinant human activated protein C that has anti-inflammatory, anti-thrombotic and pro-fibrinolytic properties to block the coagulation cascade which plays a critical role in the development of organ failure due to sepsis.[3,67]

In addition, simvastatin and atorvastatin had also shown to have some non-specific anti-inflammatory effects contributing to their clinical benefits in treating sepsis. However, statins are currently not been considered as a treatment for sepsis.

To find a more specific target, scientists have identified TLR4 as one of the candidates in blocking the innate immune system since its ligand LPS has been associated with sepsis and the high mortality rate seen in septic shock.

TLR4 up-regulation in non-immune cells after initial TLR mediated immune response may trigger secondary responses such as activation of endothelial cells that promotes the production of adhesion molecules, followed by macrophage infiltration and vascular permeability during infection (30). This cascade may result in a systemic septic syndrome including tissue perfusions, an imbalanced coagulation cascade and organ failure.

Amongst the most important TLR4 antagonists developed so far there are CRX-526, E5531, E5564 and TAK-242 but only E5564 (Eritoran) and TAK-242, have made far into the clinical phase.

However even if Eritoran passed clinical phase II trials in 2003, it didn't passed phase III due to a lack of statistically significant activity when tested on a panel of 2.000 septic patients.[68]

Research on new TLR4 antagonists for the cure of sepsis is still ongoing.

5.2 Other pathologies related to TLR4 activation and signaling

TLR4 and Atherosclerosis

Arteriosclerosis is an inflammatory and oxidative stress disorder of the blood vessels with involvement of TLRs either due to chronic infectious or sterile processes[16]

Activated cells are involved in its initiation and progression.

Guha and Mackman[69] have shown that activated TLR4 elicits the production of inflammatory cytokines and chemokines. Edfeldt et al. have also found that TLR4 is prominently expressed in endothelial cells of human atherosclerotic lesion, but poorly expressed in normal human arteries.[70]

In the early atherosclerotic lesion, LPS and other ligands can stimulate the TLR4 expression on macrophages. The activated receptors can then initiate the signalling cascade that induces the expression of inflammatory cytokines, proteases, and cytotoxic oxygen and nitrogen radicals. These entities further speed up the progression of the atherosclerotic lesion.

In advanced atherosclerotic lesion, LPS can induce the proliferation of vascular smooth muscle cells, as well as the expression of elastin-degrading enzyme via TLR4.[71]

Besides that, in response to chemokines, more smooth muscle cells will also migrate to the sites of the lesions.[72] These predominant changes cause the accumulation of cells, extra- cellular matrix components, thickening of the intima, as well as the deformity of the arterial wall. Furthermore, TLR4 signalling might also be involved in atherosclerotic plaque destabilization. Grenier and Grignon have demonstrated that LPS induces the expression of matrix metalloproteinase-9 (MMP-9) by TLR4 in macrophages; MMP-9 has been shown to degrade collagen fibrous cap, thus predisposing plaque to rupture.[73]

Sterile inflammation in atherosclerosis seems to occur through an unusual dimerization of TLR4 with TLR6.[16]

Amyotrophic lateral sclerosis (ALS)

Amyotrophic lateral sclerosis (ALS) is a rare adult-onset neurodegenerative disease characterized by selective motoneuron death in the spinal cord, brain stem and motor cortex. The etiology is still elusive and at present ALS is regarded as a multifactorial disease in which several susceptibility genes act in concert in a complex interaction with environmental factors.[74,75]

Altered immune system responses and the consequent activation of the neuroinflammatory cascade have been proposed among the pathological mechanisms.[76–78]

It has been demonstrated that in SOD1G93A mice the inflammatory monocytes that express a polarized macrophage phenotype (M1 signature) is probably recruited into the CNS by activated microglia.[79] In human ALS, the analogous monocytes expressing CD14+ CD16− also exhibit an ALS-specific microRNA inflammatory signature. These monocytes apparently undergo a migration into the CNS as their levels in the peripheral blood are significantly decreased in ALS patients with respect to other cells.[80]

At a molecular level, a prominent role in mediating inflammation and innate immunity responses is played by Toll-like receptors (TLRs).

TLR2, TLR4, and their co-receptor CD14, have been reportedly identified as the major molecular players in the neuroimmune dysregulations involved in ALS.[81,82] It has been recently demonstrated that mutant SOD1 (copper zinc superoxide dismutase 1), which is responsible for 20% of familial ALS and causes selective motoneuron death in mouse models, exhibits its neurotoxic effect in motoneuron-microglia cocultures by activating proinflammatory microglia through interaction with CD14 in concert with TLR2 and TLR4.[83,84] Expression of CD14 is increased in spinal cord of both mutant SOD1 mice and sporadic ALS patients[85,86] and the chronic stimulation of CD14/TLR pathway by LPS was found to exacerbate disease in ALS mice.[87]

TLR4 and one of its major endogenous ligands, high-mobility group box 1 (HMGB1) are specifically expressed by activated microglia and astrocytes and increase during disease progression in SOD1G93A mice.[88,89] Moreover, deletion of TLR4 significantly extends survival and transiently improves hind-limb grip strength in this ALS disease model.[89]

Thus, inhibition of TLR4 pathway may provide beneficial effects and represent a new putative target for neuroprotective strategies and a promising pharmacological approach in ALS

Indeed it has also been demonstrated that cyanobacteria-derived TLR4 antagonists exert anti-inflammatory and neuroprotective effects in LPS-treated spinal cord cultures, by inhibiting microglia morphological activation and release of proinflammatory cytokines, eventually counteracting motoneuron death.[90]

TLR4 and Asthma

Asthma is the most common chronic disease among children (WHO 2012).

Even if the etiology of asthma is still poorly understood, many epidemiological studies have reported adverse effects of ambient air pollution on respiratory health, and birth cohort studies have shown effects on the development of asthma in particular.[16,91]

The mechanisms behind the adverse effects of air pollution on the lungs have not been fully elucidated. It has been established that air pollutants induce an inflammatory response that is maintained by activation of pro-inflammatory molecules. This may induce lung damage due to generation of reactive oxygen species.[92]

Furthermore, it has been suggested that air pollutant particles may act as carriers of microbes and allergens, directing their deposition to sites in the airways they would not by themselves reach due to their aerodynamic properties.

Thus, innate immune responses appear involved in the response to microbial components associated with particulate matter from ambient air pollution.

This has been demonstrated by Becker et al whose work on airway wall and bronchoalveolar cells obtained from healthy subjects suggests that Toll-like receptors (TLR) 2 and 4 on human alveolar macrophages and, preferentially, TLR2 on bronchial epithelial cells are involved in responses to pollution particles, with only children with specific genotypes of TLR2 and TLR4 experiencing adverse effects of air pollution on asthma.[93,94]

Other supportive evidence for the involvement of TLRs in the airway inflammatory response has been provided by the observation that mice previously exposed to ozone developed asthma-like reactions after inhalation of lipopolysaccharide (LPS) accompanied by mobilization of TLR4 to the surface of inflammatory cells.[95]

Since there is a wide interindividual variability in responses to air pollution,[96] it is plausible that genetic factors contribute to this variability.

A linkage analysis with recombinant inbred strains of mice showed TLR4 to be a candidate gene contributing to the response to ozone-induced lung permeability and inflammation.[97]

Kerkhof et al.[91] in particular showed that single nucleotide polymorphisms (SNPs) in TLR4 and TLR2 contribute to the observed deleterious effects of air pollution on the development of asthma.

Gut-related pathologies

There is now also evidence that the TLR4 complex may play a role in a large number of diseases related to bacterial translocation of the gram-negative enterobacteria, with a gut-derived inflammatory pathway.[16]

Indeed through increased gut hyper-permeability, these gut commensals may translocate and activate the immunocyte TLR4 complex either in the blood stream or in the mesenteric lymph nodes.

This process, in turn, causes activation of intracellular signalling pathways, such as nuclear factor-κB(NF-κB), which increases the production of ROS/RNS and pro-inflammatory cytokines.

Therefore, this pathway may be associated with the onset of a number of inflammatory and oxidative and nitrosative stress (IO&NS) diseases or intensify and perpetuate the IO&NS pathways in these diseases.

Such diseases include clinical depression, chronic fatigue syndrome (CFS), IBD, rheumatoid arthritis, cardiovascular disorders, psoriasis, HIV infection, Parkinson's and Alzheimer's disease, multiple sclerosis, and chronic alcoholism. [16]

TLR4 and IBD

Inflammatory Bowel Disease Inflammatory bowel disease (IBD) is a medical condition that predominantly affects the gastrointestinal tract.

De Jager et al. showed that TLR4 and its signalling molecule TIRAP affect susceptibility to IBD.[98] Recent studies have shown that TLR4−/− and MyD88−/− knockout mice tend to be more prone to severe dextran sulfate sodium-induced colitis than their wild-type littermates.[99]

Interestingly, CRX-526 a TLR4 antagonist has been shown to prevent an inflammatory disease in the dextran sulfate sodium and mdr1a−/−/1b−/− deficient mice models.[100]

To explain these contradictory results it may be considered that constitutive signalling through TLR4 may result in the production of tissue protective factors such as IL-6 and TNF-α.[98] This is the scenario in the MyD88−/− knockout mice, while in the case of the CRX-526 selective down-regulation of one of the TLR-4/ LPS signalling pathways may happen.

6. TLR4-directed therapies

Since the majority of the pathologies depicted in the previous section still lack specific pharmacological treatment and they are all TLR4 related, targeting TLR4 pathway have attracted increasing interest in a wide range of possible clinical settings.

By inference, these compounds targeting the TLR4 pathway may be new “drugs” to treat TLR4-mediated inflammatory disorders.

In particular, since the activation of TLR4 by LPS is a complex process involving several steps and four PRR four different approaches are available for pharmacological interventions:[16]

1. neutralizing LPS through the use of cationic LPS sequestrants
2. inhibiting LPS interaction with LBP, CD-14;
3. targeting inflammation and ROS/RNS (not treated in this thesis)
4. TLR4 antagonists that compete with LPS for MD-2 binding
5. TLR agonists as adjuvants in vaccines

6.1 Neutralizing LPS: LPS sequestrants

Inactivation of LPS by the use of an agent that binds and sequesters it, thus abrogating its activity is a promising approach to fight sepsis as well as many more inflammatory diseases such as clinical depression or CFS related to increased bacterial translocation and in many infectious diseases mediated by LPS.[101]

A variety of cationic synthetic LPS-sequestering agents have been developed by David and co-workers and reviewed exhaustively by the same author.[102]
The amphiphilic nature of lipid A indeed enables it to interact with a variety of cationic hydrophobic ligands.

Various proteins such as LPS-binding protein (LBP), bactericidal/permeability-increasing protein (BPI), and Limulus anti-LPS factor (LALF) have a strong affinity for LPS and also display antimicrobial activity against Gram-negative bacteria. Synthetic peptides based on the putative LPS-binding domains of LBP, BPI, and LALF proteins, were especially designed and synthesized to target Gram-negative bacteria.
Cationic antimicrobial peptides with diverse structures bind LPS and suppress its ability to stimulate TLR4-dependent cytokine production.
Polymyxin B (PMB) is a membrane-active peptide antibiotic that binds to LPS and inhibits its toxicity *in vitro* and in animal models of endotoxemia.
Approved for clinical use in Japan in late 2000, PMB provides a clinically validated proof-of-concept of the therapeutic potential of sequestering circulating LPS.

A major goal over the past decade was to develop small-molecule analogues of PMB that would sequester LPS with similar potency and be non-toxic and safe, so to be used parenterally for the prophylaxis or therapy of Gram-negative sepsis.
To this end, various classes of synthetic cationic amphiphiles were developed including acyl and sulfonamido homospermines.

6.2 Inhibitors of LPS-LBP and LPS-CD14 interaction

Another strategy to block TLR4 signaling is inhibiting LPS-LBP and LPS-CD14 interaction by using LBP or CD-14 ligands that bind to a vicinal or identical binding site of LPS Lipid A or polysaccharide O-chain
Indeed although LPS is the most studied and characterized ligand, CD14 can interact also with other molecules.[101]

For example both LBP and CD14 can bind lipoteichoic acid (LTA) derived from the gram-positive bacterium *Bacillus subtilis*.

In addition, whole bacteria are recognized by CD14 in an LBP-dependent reaction but only after pre-incubation with serum.

Soluble peptidoglycans (PGN) are recognized by TLR2, and CD14 is important to enhance recognition.

In vitro studies provide evidence that the PGN binding interface on CD14 can overlap with the binding site of LPS polysaccharide O-chain, although the biological relevance of PGN binding to CD14-TLR2 is under debate. The LPS- and PGN- binding sites must overlap, at least in part, because PGN competes with LPS for binding to CD14.

A glycoconjugate preparation from *Treponema spirochetes* (Tm-Gp) inhibited the interaction of TLR4 ligands (lipid A, LPS, taxol) and TLR2 ligands (PGN) with LBP and CD14, acting as an antagonist of the corresponding TLR4 or TLR2-dependent pathways.

The synthetic cationic amphipiles developed by our group and named IAXO compounds[103] belong to this category.

6.3 TLR4 agonists as vaccine adjuvants

Another field in which Lipid A total and partial structures found application is the use as adjuvants in vaccines.

Activation of the immunoresponse without deleterious effect is indeed the purpose of a vaccine.

In particular, after the discovery of the natural role of TLR4 in controlling a large number of infectious diseases and its ability to utilize both the MyD88/Mal and TRIF/TRAM signalling pathways, significant interest has been given to the development of lipid A-like agonists targeting TLR4 for use as adjuvants in vaccine formulations.

Noteworthy TLR4 has been shown to play a non-redundant role in eliciting DC maturation, a vital component to adjuvant-mediated vaccine-antigen immunogenicity, since DCs play a significant role in priming naive T cells and initiating potent immune responses. [104]

A **vaccine** is a biological preparation that provides active acquired immunity to a particular disease.

Vaccines can be prophylactic, that means administered with the aim to prevent or ameliorate the effects of a future infection by a natural or "wild" pathogen, or therapeutic, with the aim of curing a particular pathology.

In general a vaccine consists of inactivated or attenuated microorganism or in by-product or components which are able to induce the immunoresponse but are in such a concentration not to generate deleterious effects.

One way to increase the efficacy of a vaccine or its safety is the use of adjuvants.

Adjuvants are molecules or compounds which improve the efficacy of vaccines by boosting the potency and longevity of the immune response to the administered antigens without causing increased toxicity.

Vaccination usually is done using a mild immunizing agent in combination with an adjuvant.

Early studies by Johnson et al. demonstrated that the LPS of Gram-negative bacterial cell wall was a potent adjuvant when delivered with protein antigens.[105]

However, administration of LPS or its biologically active component lipid A also caused systemic responses and these bacterial extracts were deemed too toxic to be used as adjuvants for human vaccines.

For this reason subsequent efforts have focused on research to chemically modify the LPS/Lipid A in an attempt to separate much of the toxicity associated with lipid A from its desired immune stimulatory activity.

The first attempt in this direction has been the one of Ribi et al. in the 1970s who succeeded in the chemical modification of LPS obtaining a mixture with a monophosphoryl hexacylated Lipid A, called 4'MPL, as the major component which showed greatly reduced pyrogenicity while maintaining immune stimulatory activity (see also section 7.1.2.2).[106]

This mixture was then further purified thus resulting in the clinical-grade version currently manufactured by GlaxoSmithKline (GSK) Biologicals, now referred to as **MPL**, used in the widespread vaccines FENDrix® (GSK Biologicals, Brentford, UK) for hepatitis B, and Cervarix® (GSK Biologicals) against HPV.

However, despite achieving significant success in the vaccine adjuvant pipeline, the use of MPL still faces several challenges.

The product purified from *S. minnesota* is in fact heterogeneous in its acylation state, containing a mixture of tetra-acyl, penta-acyl and hexa-acyl 3D-MPL which vary in terms of their potency on human cells.

Since these variances can affect the biological activity, a careful verification of the composition of MPL is thus imperative to maintain a consistent end product.

Indeed even if nowadays the most active component of MPL, hexacylated MPL, could be obtained as a pure compound from chemical synthesis, the MPL mixture obtained from LPS is still the one used in vaccines.

This decision of the manufacturing company was due to some drawbacks of its synthesis and in particular: the difficulty, the cost of the synthesis and its insufficient scalability.

The molecule **OM-174,** a diphosphoryl, triacyl, disaccharide lipid A derivative, developed by OM Pharma (Meyrin, Switzerland) and currently in phase I clinical evaluation for the treatment of cancer is obtained from of *E. coli* and it is not synthetic (section 7.1.2.7).

The third disaccharide currently in approved vaccines or clinical evaluation, that is ***E. coli* Lipid A** itself, is also a molecule extracted from the bacterium by the company WRAIR, and formulated as a liposome for the use against malaria. This molecule is currently in clinical phase II.

As discussed for MPL, despite the huge chemically synthesized panels of lipid A analogues no synthetic lipid A compound underwent clinical evaluation as vaccine adjuvants until recently because problems in manufacturing this class of drugs.

The only synthetic disaccharide currently in clinical evaluation is indeed PHAD^{TM} , also referred to as GLA (not to be confused with Gifu Lipid As also termed GLA, see above) or as "synthetic MPL", which like MPL is a monophosphoryl disaccharide but has all six chains of C14 length and asymmetrically distributed (4+2) as in *E. coli* Lipid A (section 7.1.2.4).

PHAD^{TM} has been developed by the USA Infectious Disease Research Institute (IDRI) in 2011 and then has been manufactured by Avanti Polar Lipids (USA).

This synthetic MPL was shown to be 10- to 100-fold more active than *S. minnesota* Re595-derived MPL on human monocyte-derived DCs. The difference in the activity has to be attributed to the lack of tetra-acylated and penta-acylated lipid A molecules that contaminate MPL derived from natural sources and are not present in synthetic MPL.

Early results from clinical trials using vaccines containing GLA formulations indicate excellent safety profiles that are accompanied by the enhancement of antigen-specific responses.[107] The GLA compound has been used in Phase I clinical studies for influenza and is in preclinical development as an adjuvant for vaccines against tuberculosis and leishmaniasis, schistosomaisis and hookworm.

Being so little the number of disaccharides that entered clinical evaluation and being so difficult and cost-demanding their synthesis, TLR4 agonists with a monosaccharide structure have been developed as vaccine adjuvants.

Of the 8 adjuvants currently in approved vaccines or in clinical evaluation, 3 are monosaccharide based molecules: RC-529, an aminoalkylglusosaminide, 4-phosphates (AGPs), ONO-4007 and PET Lipid A.

The activity and the chemical structures of RC-529 and ONO-4007 compounds will be presented in the section on Monosaccharide-based TLR4 modulators (section 7.1.3).

Summarizing all results obtained till now, it can be concluded that TLR4 agonists represent a safe and effective class of molecules that have demonstrated to possess interesting potential as vaccine adjuvants.

6.4 TLR4 and Cancer

Also the cure of **cancer** represents an important application of immunostimulants. Non-toxic TLR4 agonists are therefore potential candidates as anticancer agents.

Activation of macrophages and induction of cytokine secretion, particularly tumor necrosis factor (TNF), are indeed implicated in host defense against cancer, so immunostimulants have also been studied and clinically tested as antitumoral agents.[104,108]

Antitumor polysaccharides and bacteria-derived agents such as LPS have been shown to induce intratumoral TNF production corresponding to their individual antitumor activity. [109]

Different type of Lipid A total and partial structures have been tested for this application.

One example is ONO-4007 which entered phase I clinical trials (section 7.1.3.5).

Lipid A monosaccharide mimetic PET-Lipid A, thanks to the remarkable results shown, has already proceeded till phase III clinical trials in liposomal formulation for the treatment of cancer (section 7.1.4.1).

7. TLR4 modulators

7.1 Ligand-based rational drug design

The most commonly used and well-established approach for the synthesis of TLR4 modulators is the design of chemical modification of *E. coli* Lipid A structure, which is the biologically active part of the natural ligand of TLR4, LPS.

At the basis of this approach are the structure-activity relationships (SAR) of natural lipid A variants which provide a clear picture of structural requirements for TLR4 activity.

The crystal structural data of different ligand−MD-2 complexes are available, which have clarified some tricky points.

On the contrary the other ligands of TLR4, DAMPs, are rarely used for the design of TLR4 modulators.

This is due first of all to the high chemical diversity of DAMPs.[110]

Secondly, as stems for the first point, DAMPS have different modes of interaction with TLR4.

Moreover the role of accessory proteins CD14 and MD-2 is still controversial in the case of DAMP stimulation. For instance it has recently been proposed that while CD14 might be a universal adaptor for PAMPs and DAMPs, MD-2 would selectively recognize only exogenous PAMPs.

As stated in previous sections, *E. coli* Lipid A (also called compound 506) (figure 18) consists of a β(1→6)-linked D-glucosamine disaccharide unit carrying two phosphate groups, one at position C1 and α-oriented and one at position C4', and six acyl chains all of C14 length except the branch of the chain in C2. These chains have an asymmetrical (4 + 2) distribution: two linear chains in C2' and C3', and two branched chains in C2 and C3.

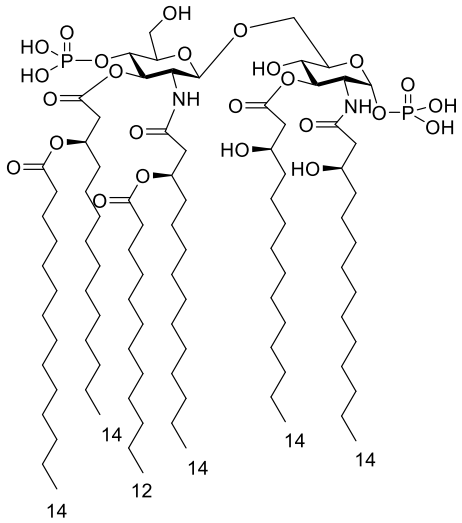

Figure 18. *E. coli* Lipid A

The first total synthesis of *E. coli* Lipid A was accomplished by Imoto et al. in 1985 and since that it has been gone under deep studies about its activity and binding.[111,112]

However the exact geometry of the Lipid A/MD-2 complex has been described only in 2009 through the crystallographic data published by Park et al.[23]

To understand the ligand specificity and receptor activation mechanism of the **hTLR4–MD-2–*E. coli*-LPS (Ra chemotype of *E. coli* LPS) complex**, Park and co-workers determined the crystal structure of this complex after dimerization at a 3.1 Å resolution by incubating the Ra chemotype of *E. coli* LPS with a partially de-glycosylated purified TLR4–MD-2 complex.

The crystal structure (figure 19) shows that the overall folding of TLR4 and MD-2is not disturbed by LPS binding or dimerization. TLR4 adopts the characteristic horseshoe-like shape of the LRR superfamily and MD-2 has a β-cup fold structure composed of two anti- parallel β sheets forming a large hydrophobic pocket for ligand binding. LPS binds to MD-2 cavity and directly mediates dimerization of the two TLR4–MD-2 complexes.

In this crystal structure the lipid A chains interact with the hydrophobic pocket of MD-2 with five carbon lipid chains completely buried inside the pocket, but the R2 chain (the lipid chain attached to the C2′ carbon of the glucosamine) is partially exposed to the MD-2 surface composing the core hydrophobic interface for

interaction with TLR4* (the asterisk indicates the second TLR4 and MD-2 molecules and their amino acid residues in the hetero-tetrameric complex to distinguish them from those of the primary TLR4 and MD-2 complex).

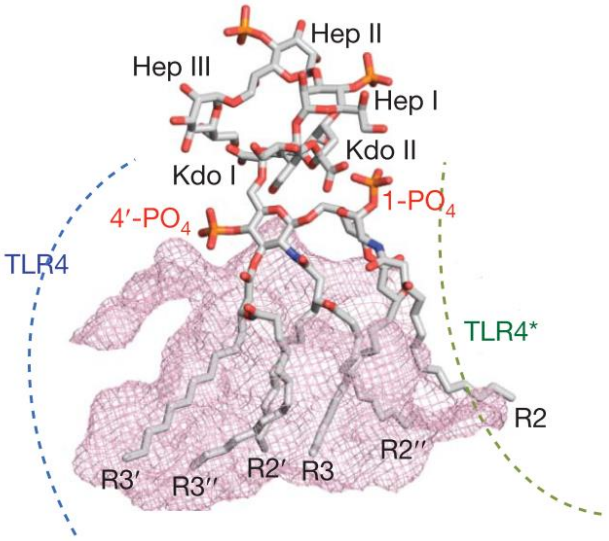

Figure 19. View of the crystallized complex between human MD-2 and Ra-LPS of *E. coli*. The molecular surface of the MD-2 pocket is drawn in mesh. The protrusion of the sixth acyl chain appears clearly.[23] (from Park et al. 2009[23])

The ester and amide groups connecting the lipids to the glucosamine backbone or to the other lipid chains are exposed to the surface of MD-2. They interact with hydrophilic side chains located on one of the β strands of the MD-2 pocket and on the surface of the two TLR4.

Finally the two phosphate groups of the lipid A bind to the TLR4–MD-2 complex by interacting with positively charged residues in the two TLR4 and MD-2 and making a hydrogen bond to S118 of MD-2.

Both hydrophobic and hydrophilic interactions contribute to the main dimerization interaction between MD-2/LPS and TLR4* that is fundamental for TLR4 activation (figure 20).

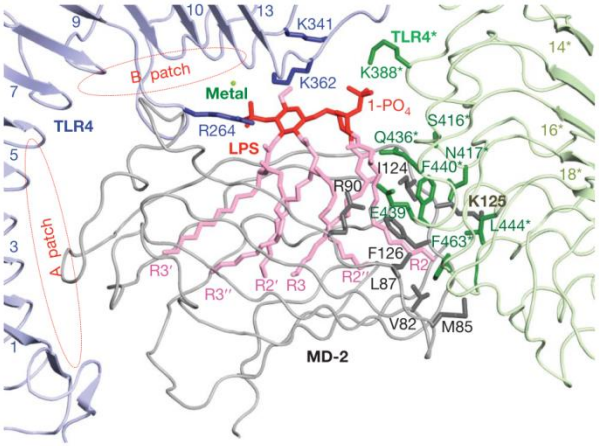

Figure 20. Overall shape of the TLR4 main dimerization interface. The inner core of LPS is omitted for clarity. The primary interface is classified into A and B patches, which are marked in red. K58, S118 and K122 of MD-2 are not shown for clarity. (Image from Park et al. 2009[23])

In particular the role of the sixth chain (R2) of the sugar appears crucial (figure 19).
The hydrophobic R2 lipid chain of LPS protruding outside the MD-2 pocket indeed interacts directly with a small hydrophobic patch on the C-terminal convex face of the horseshoe structure of TLR4* thus inducing the interaction with the second MD-2. TLR4 complex and the formation of the "m"-shaped 2:2:2 hTLR4/ MD-2/LPS complex. The close proximity of the C terminus of the extracellular domain in the complex induced by binding to LPS may allow for dimerization and signalling by the intracellular TIR domains.[113]
Also the 3-hydroxyl group of the R2 chain of LPS contributes by forming a hydrogen bond with TLR4*.
The hydrophobic residues of MD-2 supplement this core hydrophobic interface, while hydrophilic residues in the F126 loop and the R90 residue of MD-2 form hydrogen bonds and ionic interactions with TLR4* that surround and support the hydrophobic core of the dimerization interface.
Two phosphate groups, the 1-phosphate and 4'-phosphate of lipid A, also play an important role in TLR4 dimerization.
They both bind to a positively charged cluster of lysines and an arginine from TLR4, TLR4* and MD-2.
LPS binding and dimerization induce localized changes in the structure of the F126 loop of MD-2, and in the radius and bending angle of TLR4.

It is important to add here that recently published NMR studies indicate that protrusion of one of the six fatty acyl chains of endotoxin bound to MD-2 precedes interaction with TLR4 when endotoxin is bound to MD-2.[110]
Moreover, according to NMR data, the presence of a protruding fatty acyl chain is not necessarily a distinguishing feature of TLR4-activating LPS.MD-2 complexes and so is not sufficient for driving TLR4 dimerization.
In order to promote dimerization the ligand should induce also a conformation change in MD-2 Phe126 loop. This conformational change will be then relayed to TLR4 enabling its dimerization.

While lipid A from *E. coli* is considered the typical chemical structure associated with endotoxic properties, a variety of natural lipid A variants exist with modifications in the number and disposition of FA chains and with other covalent modifications that impact pathogenesis, bacterial physiology, and bacterial interactions with the host immune system.
As *E. coli* LPS, also these different LPS chemotypes (and their Lipid A portions) have been used as templates for the design and synthesis of TLR4 agonists and antagonists.
However only when Lipid As variants have been synthesized and obtained as a single molecular species, it has been possible to determine their activity unequivocally, excluding the effects of other components present in the natural extracts tested.

7.1.1 Role of aggregates shape in TLR4 activation

Since natural Lipid As and their synthetic analogues are amphiphilic molecules with long hydrophobic chains and polar phosphate heads, they are expected to form micelles in solution above their CMC.
LPS has been reported to form very stable supramolecular micellar aggregates in solution, with very low critical micelle concentration (CMC) values, estimated in the pM range.[114]
Since micelles or supramolecular aggregates may have different 3D shapes and these shapes may in turn influence the availability of the Lipid A or its interaction with TLR4, different studies have been performed through the years to determine the Lipid A aggregates shape.

A role of the molecular structure and its shape in solution in determining the aggregate shape of a micelle is expected.
However it was surprising to see that even small variation in the structure of Lipid A molecules, that means a change in the number or length or the type of chains or the number of anionic groups, can change the form of the aggregate itself from lamellar to cubic or to hexagonal.

It was even more relevant to discover that the already known correlations between molecular structure and activity of Lipid As insert themselves into specific correlations between aggregate shape and activity.[115,116]

In this way, by using conformational energy calculations and X-ray investigations, it has been found that *E. coli* Lipid A, with six acyl chains asymmetrically distributed and two phosphate groups, that generates the most powerful immunostimulation, has a pure non-lamellar structure, while lipid A samples such as *Rb. capsulatus* and *C. violaceum* as well as tetra- and pentaacyl lipid A from enterobacterial origin, that lack agonist activity and in some cases have antagonist activity adopt lamellar structures.[117]
Monophosphoryl lipid A and lipid A from *Campylobacter jejuni* which has intermediate activity assume mixed lamellar/cubic structures.

These correlations may be summarized as follow (figure 21):

- Lipid As assuming cubic (Q) or hexagonal II (H_{II}) aggregate structures in solution are highly active as agonists
- Lipid As giving rise to lamellar aggregates are unable in activating immunocompetent cells thou they can be active as LPS antagonists inhibiting cytokine production in response to LPS stimulus

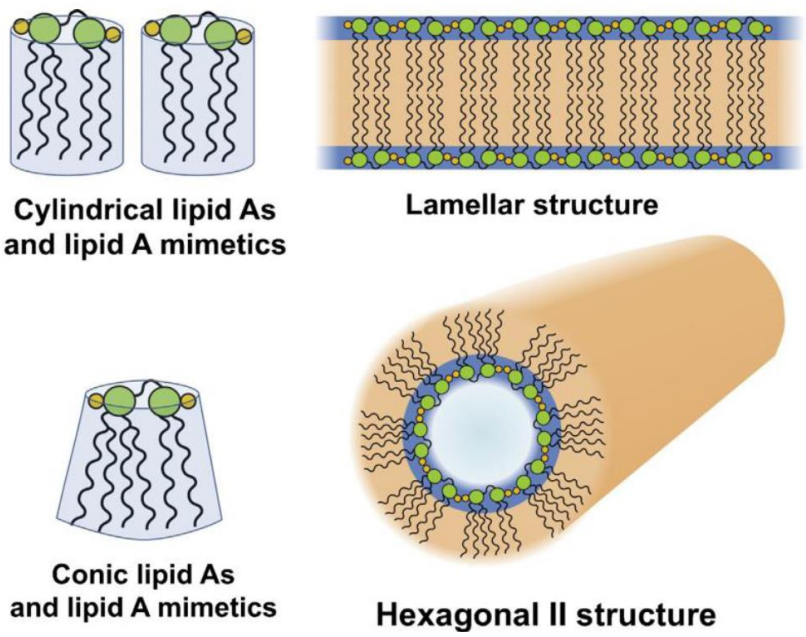

Figure 21. Relationship between lipid A chemical structures, molecular shape and 3D aggregate structures. (Image from Calabrese et al. 2014[34])

Defined **molecular shape** in solution have been correlated to the different type of aggregates.[34]

The minimum energy conformations of different types of lipid A are related to the angle formed between the diglucosamine backbone and FA chains (**tilt angle**), which are packed almost parallel to each other (figure 22).[117]

This angle can be determined through ATR spectroscopy using polarized light.

For *E. coli*-type lipid A, that forms non-lamellar aggregates, this angle was found >50°, thus giving a conical molecular shape.[118]

For species with lamellar aggregates, the tilt angle was <25° thus giving cylindrical shape. These species include Lipid IVa, and the penta-acylated and symmetrically (3 + 3) hexaacylated species of *Rhodobacter sphaeroides* and *Rhodobacter capsulatus*.

Species with an angle between 25° and 50°, as monophosphorylated lipid A, present an intermediate conformation.

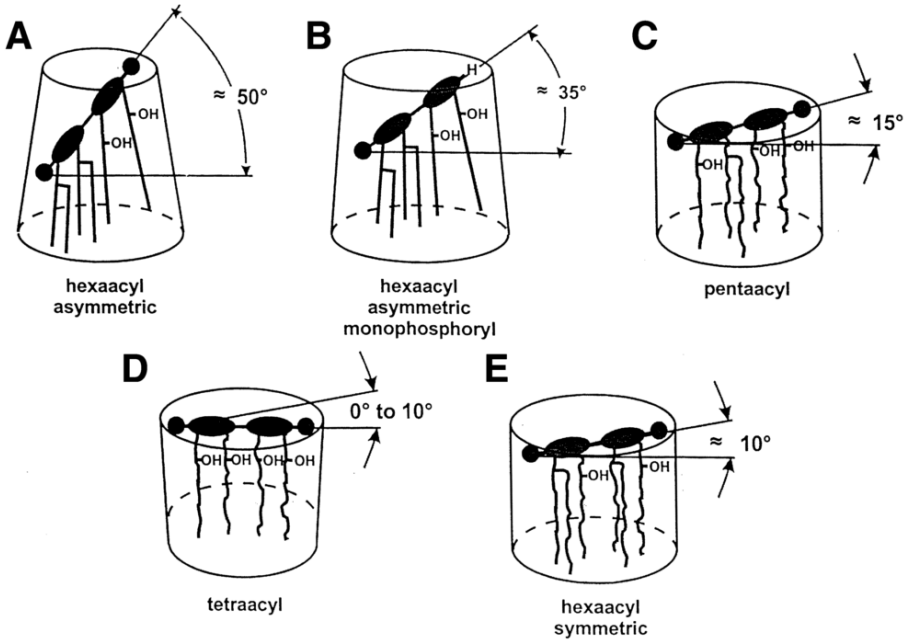

Figure 22. Tilt angle determined for endotoxically highly active E. Coli Lipid A (A), medium active monophosphoryl Lipid A (B), and of inactive, antagonistic pentacyl Lipid A (C), tetracyl Lipid A (D) and Lipid A from *C. Violaceum* (E). and pictures of molecular shapes as obtained from aggregate studies. (from Seydel et al. 2000[118])

This means that active molecules in solution assume conical shape, with hydrophobic chains distributed on a higher area with respect to the polar part of the molecule (the sugar core with phosphates). On the contrary these areas are similar for cylindrical inactive molecules.

Interestingly, the correlation between the structure of aggregates and the biological activity can be extended also to synthetic lipid A mimetics, even if the aggregates shape has been investigated just for a limited number of compounds including tri-acylated monosaccharides, GLA compounds and some phospholipids with a non-sugar backbone.

Summarizing what stated till now, molecular structure, molecular shape, aggregate shape and biological activity correlations can be expressed as follow:[117]

- those samples preferring pure non-lamellar (Q, H_{II}) structures (conical conformation) such as enterobacterial hexa-acyl lipid A have a high inclination angle and are highly active
- Lipid A samples adopting lamellar structures (having a cylindrical conformation) such as those from *Rb. capsulatus* and *C. violaceum* as well as tetra- and pentaacyl lipid A from enterobacterial origin are completely inactive, and were found to have a very low inclination angle of the membrane surface with respect to the acyl chain direction.
- Those assuming mixed lamellar/cubic structures (partly conical conformation such as Monophosphoryl lipid A and lipid A from *Campylobacter jejuni*) have intermediate activity and a higher inclination angle

- The inactive lipid A samples, which adopt lamellar structures, were found to act as efficient antagonists against biologically active LPS if a sufficiently high negative backbone charge is present
- Uncharged lipid A with lamellar structures such as lipid A from *Rhodomicrobium vannielii* and dephosphono hexa-acyl lipid A turned out neither to be agonistically nor antagonistically active
- monosaccharide monophosphoryl triacyl lipid A compounds (GLA) with an acyloxyacyl chain in the position 3 have a non-lamellar aggregate structure and exhibit bioactivity (but significantly lower than entire lipid A), whereas those compounds with the acyloxyacyl chain linked to position 2 are inactive

This role of aggregates shape in the interaction with the PRR of the TLR4 recognition has been studied for long in search of a rationalization.

However, even now that the TLR recognition process of Lipid As has been intensively studied, it has not been elucidated clearly whether the correlation of aggregates shape with activity is related to the binding with receptors upstream from TLR4, LBP or CD-14, or to unspecific intercalation into the cell membrane (hydrophobic interaction).

In the latter case the effect of such intercalation, which seems to happen to some extent, have been studied showing that active forms of aggregates induce activation of transmembrane ion channel like MaxiK, which in turn enhance the influx of potassium ions.[119–124]

These ions would in principle exert their effect on intracellular caspases which are important proteins of the so called non-canonical inflammasome.

Moreover the intercalation could exert an effect on the TLR4-MD-2 complex dimerization or its multi-dimerization (a process which is currently under study) by inhibiting or accelerating this process.

Another crucial information emerging from these studied is that the addition of substances like peptides, proteins and other agents, which strongly reduce the immunostimulatory activity of LPS, also cause a conversion of the non-lamellar cubic structure of lipid A into the lamellar one. This was found to be true for lysozyme, lactoferrin and polymyxin.

Moreover the addition of chlorpromazine (CPZ) to the antagonistic pentaacyl lipid A from *E. coli*, which led to the conversion from lamellar to inverted cubic aggregates also resulted in the switch of its activity to agonism.[125]

The discovery of the relevance of the role of aggregates shape in solution has however had a great impact in the field of TLR4 since it has given an explanation to such different biological activities (agonism or antagonism or inactivity) of Lipid As observed.

The correlations outlined have then been confirmed by the MD-2 binding-activity relationships studied with crystal structures of different Lipid As when MD-2 was discovered in 1999 by Shimazu et al.
On the contrary, in the field of monosaccharide molecular simplification of Lipid A, where still now little is known about MD-2 binding-activity relationships, it still constitutes a key explanation.
SAR correlations with aggregate shape of monosaccharide molecular simplifications of Lipid A and agonism will be discussed in section 7.3.

7.1.2 Disaccharide TLR4 modulators

Great synthetic efforts have been done through the years to obtain synthetic Lipid A analogues and Lipid A mimetics.
Several TLR4-active compounds have been synthesized starting from the lipid A structure varying:

- the number, the length, the position or the nature of FA chains
- the number of phosphate groups or replacing them with phosphate bio-isosteres
- the disaccharide scaffold, that was also reduced to a monosaccharide: the so called molecular simplification approach

These works allowed a better understanding of SAR and how the acyl chain number, chain length and phosphorylation state of lipid A alters the relationship between activity and toxicity.
A panoramic view of SAR has been first depicted by Rietschel in 1994.[126]

From now four terms will be used to describe the activity of such compounds.
The term LPS antagonist or LPS-immunostimulation blockers refers to the results in studies where for such compounds a direct interaction with the TLR4 complex was not yet demonstrated.
The term TLR4 antagonist will be generally used when talking about results in which a compound showed a direct interaction with the TLR4 complex.
It must indeed be remembered that even if now we know that TLR4 is unequivocally the LPS receptor, the role of TLR4 (and MD-2) in immunity has been defined clearly only in 1999.
The same distinction will be used for the term immunostimulants in spite of TLR agonists.

7.1.2.1. Hepta-acyl Lipid As

Early structural investigations of Re-LPS from *Salmonella enterica serovar minnesota* (*S. minnesota*) (mutant strain R595) revealed a major lipid A species that was hepta-acylated (figure 23).

This molecule is identical to *E. coli* Lipid A but it has an additional C16 (palmitoyl) residue esterified to the (R)-3-hydroxymyristoyl chain at position 2.

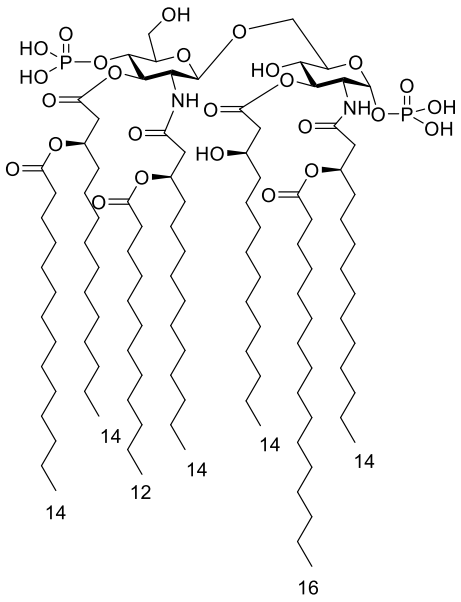

Figure 23. *S. minnesota* Lipid A

The corresponding synthetic hepta-acyl lipid A (termed compound 516) has been shown to display still profound, but significantly lower, immunostimulatory activities as compared to the highly active hexa-acylated *E. coli* lipid A.

From *S. minnesota* Lipid A the only currently disaccharide approved as adjuvant for vaccines, MPL, was obtained.

7.1.2.2 *S. minnesota* Monophosphoryl Lipid A (MPL)

In the 1970s a work with *Salmonella minnesota* by Ribi et al. was aimed at chemically modifying the LPS in an attempt to separate much of the toxicity associated with lipid A from its immune stimulatory activity.[104] Through the use of mild acid hydrolysis, the polysaccharide side chains, a phosphoryl group and one of the seven acyl chains of S. Minnesota LPS were removed, leaving a mixture of lipid A molecules that were devoid of polysaccharide with a single phosphate and had predominantly six fatty acid chains.
The resulting product, defined as **4´-MPL**, showed greatly reduced pyrogenicity while maintaining immune stimulatory activity. This mixture was then further purified and perfected thus resulting in the clinical-grade version currently manufactured by GlaxoSmithKline (GSK) Biologicals, now referred to as MPL

However, since the MPL preparation was a mixture of tetra-acyl, penta-acyl and hexa-acyl monophosphoryl Lipid A, it was only after the total synthesis of the pure major constituents of *S. minnesota* MPL in 1998 by Johnson et al. [127,128] that the most active component was identified.

This component (figure 24) resulted to be MPL hexacylated monophosphoryl disaccharide thus confirming previous studies showing that a β(1-6) diglucosamine moiety bearing six pendent fatty acids is prerequisite to the full expression of endotoxic activities.

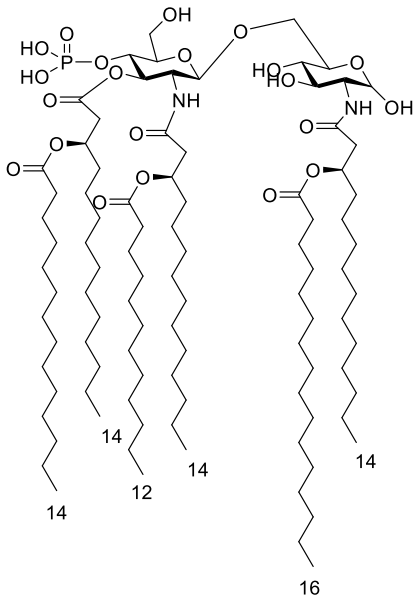

Figure 24. MPL (*S. minnesota* Monophosphoryl Lipid A)

Early clinical development of MPL focused on its use as an adjuvant for cancer therapy.

However despite some promising results in Phase II clinical trials (1993), further development was not continued.

In contrast to its limited use in therapeutic clinical trials, MPL has seen widespread use as an adjuvant in prophylactic vaccines with several having received regulatory approval and many more in the active development pipeline. The first approved vaccine products to include MPL are the GSK vaccines, FENDrix® (GSK Biologicals, Brentford, UK) for hepatitis B, and the Cervarix® vaccine (GSK Biologicals) against

HPV. The Cervarix vaccine has now been approved in many countries and has received US regulatory approval, making MPL the first defined adjuvant to be approved for widespread use in humans since aluminum salts.

7.1.2.3 Penta-acyl Lipid As: RsDPLA and RcDPLA

Rhodopseudomonas/Rhodobacter sphaeroides ATCC 17023 is a penta-acylated di-phosphoryl Lipid A (RsDPLA).

Initially purified by Takayama et al.[129] and chemically defined by Qureshi et al.[130–132], RsDPLA was tested for its immunostimulatory activity but it did not show LPS-agonistic activity toward neither human nor mouse macrophages.[133,134]

On the contrary RsDPLA showed strong LPS-antagonistic activity being able to block LPS-induced TNF-α production *in vivo*[133] and by monocytes/macrophages *in vitro.*[133,135]

Others groups have reported that RsDPLA blocks LPS-induced pre-B cell activation[136] and CD18 surface expression on human neutrophils.[137]

Since that RsDPLA has become one of the best characterized LPS antagonists.

Total synthesis of RsDPLA was accomplished in 1994 by Christ et al.[138] and it was tested confirming previous data.[139]

Similar to RsDPLA, also the penta-acylated di-phosphoryl Lipid A from Rhodobacter capsulatus has shown to have antagonistic properties by inhibiting cytokine production induced by LPS.[140]

7.1.2.4 Hexa-acyl Lipid A PHAD™

PHAD™ (figure 25), developed by the USA Infectious Disease Research Institute (IDRI) in 2011, is a monophosphoryl disaccharide with six acyl chains of C14 length in the same *E. coli* asymmetrical distribution (4+2).[104,141]

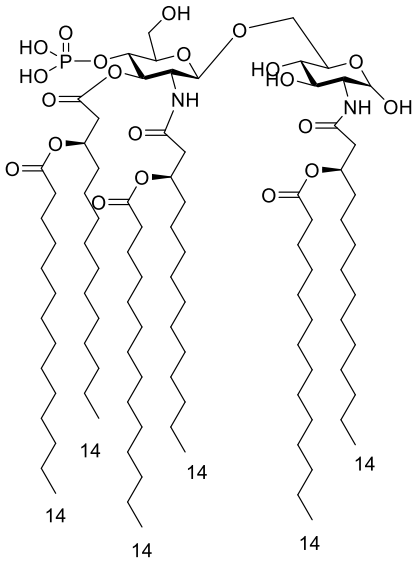

Figure 25. PHAD™

This synthetic lipid A was shown to be a powerful immunostimulator, 10- to 100-fold more active than S. minnesota Re595-derived MPL, on human monocyte-derived DCs with the increased activity attributed to the lack of tetra-acylated and penta-acylated lipid A moieties in the purified hexa-acylated material.[141]

Upon *in vivo* administration and when properly formulated, this synthetic molecule induces strong systemic innate responses and priming of antigen-specific Th1 cells.[141] Early results from clinical trials using vaccines containing GLA formulations indicate excellent safety profiles that are accompanied by the enhancement of antigen-specific responses.[107]

The GLA compound has been used in Phase I clinical studies for influenza and is in preclinical development as an adjuvant for vaccines against tuberculosis and leishmaniasis, schistosomaisis and hookworm.[104]

7.1.2.5 Lipid IVa (or compound 406)

Lipid IVa (also called precursor Ia or compound 406) (figure 26) is the tetra-acylated di-phosphoryl version of *E. coli* Lipid A and it actually corresponds to a biosynthetic precursor of Lipid A.

With respect to *E. coli* Lipid A, Lipid IVa lacks the two branched chains on C3' and C3 carbon chains.

Total synthesis of Lipid IVa was accomplished in 1984 by Imoto et al., even before the one of Lipid A, thus representing an historical milestone.[142,143]

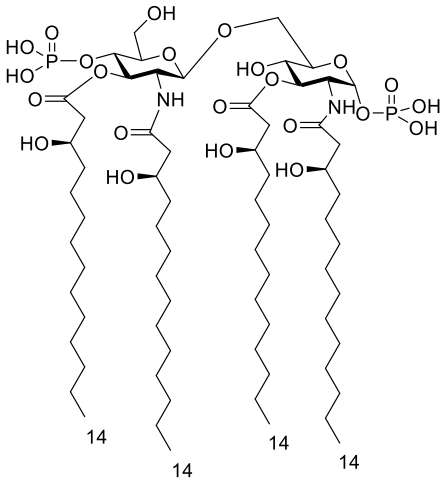

Figure 26. Lipid IVa

Interestingly, tetraacylated Lipid IVa acts as an antagonist on human but as an agonist on mouse TLR4.[34]

In order to better understand the interaction of Lipid IVa with MD-2, Ohto et al. in 2007 reported the crystal structures of human MD-2 and its complex with Lipid IVa.[65]

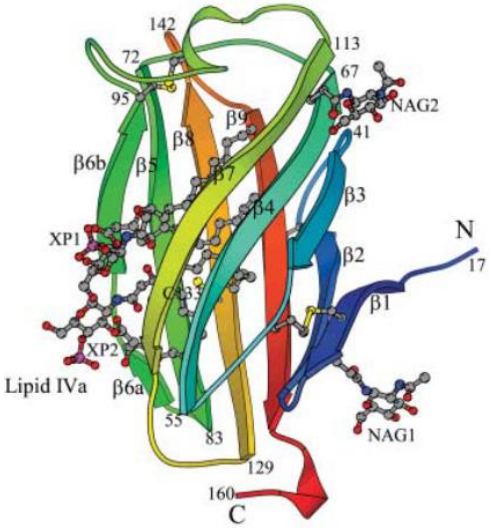

Figure 27.1 Stereo ribbon model of the crystallized complex between human MD-2 and Lipid IVa (from Ohto et al. 2007[65]). The N terminus is drawn in blue and the C terminus in red. The β strands are indicated with their labels, and some amino acid residue numbers are shown. Bound Lipid IVa is drawn as ball-and-stick models as well as cysteine residues. The entrance to the MD-2 cavity is lined by the β6b and β7 strands. Since polysaccharide moieties of MD-2 were trimmed off by endoglycosidase treatment, an N-acetylglucosamine (NAG) has remained at each glycosylation site. The two β sheets are inclined toward each other by about 45°.

In this crystal structure the two phosphate groups of Lipid IVa interacts with the positively charged lysine and arginine residues of hMD-2 while they do not form direct hydrogen bonds to MD-2 atoms.

The four fatty acid chains of Lipid IVa are all deeply confined in the cavity and are packed next to each other through van der Waals contacts.[65]

The crystal structure the MD-2 cavity appears unable to accommodate more than four acyl chains and made researchers thought that conformational changes enlarging the cavity are necessary to accommodate the six chains of lipid A.[65] However, the crystal structure of the TLR4–MD-2–LPS complex studied later by Park et al. in 2009.[23] has demonstrated that the size of the MD-2 cavity is unchanged with bound Lipid A.

Additional space for lipid binding is generated by displacing the glucosamine backbone of Lipid A upwards by 5Å

This may be the reason why LPS with five or less lipid chains are less active/inactive with respect to Lipid A: they should stay deeper in the pocket than Lipid A and so there should be substantial energetic penalties when the chains move back to the surface of MD-2 for dimerization with TLR4*.

In particular the crystal structure of the MD-2/lipid A complex published by Park in 2009 also showed that the R2 chains of hexaacylated agonists does not enter in the MD-2 cavity and forms an important binding interface with TLR4*.

Later on, in 2012 Ohto et al. completed their studies on Lipid IVa by preparing a mouse TLR4/MD-2 (mTLR4/MD-2) in complex with tetraacylated Lipid IVa and compared it to the crystal structure of mTLR4/ MD-2/Re-LPS (Re chemotype of *E. coli* LPS) and to the one of hTLR4/ MD-2/Ra-LPS (Ra chemotype of *E. coli* LPS) studied by Park, in order to clarify the different activity of Lipid IVa, but not of Lipid A, seen in mouse with respect to human.[113].

In both the mTLR4/MD-2/Re-LPS and mTLR4/MD-2/Lipid IVa complexes, mMD-2 underwent similar structural changes around the Phe126 loop as observed in the hTLR4/MD-2/LPS complex.

Re-LPS and Lipid IVa made many hydrophilic and hydrophobic interactions withmTLR4/MD-2, in a similar manner as with the hTLR4/ MD-2/Ra-LPS complex.

Surprisingly, although Lipid IVa lacks two acyl chains compared with hexaacylated LPS, Lipid IVa showed the same overall orientation as LPS, with phosphate atoms displacements of 1.3 and 2.6 Å in the 1-PO_4 and 4'-PO_4 groups, respectively, when superimposed with MD-2 molecules in mTLR4/MD-2/Lipid IVa and mTLR4/MD-2/Re-LPS.

However slight changes in the chains disposition take place.

While Lipid IVa chains R3, R2', and R3' occupy essentially the same space in the cavity, R3' acyl chain is more deeply buried inside the cavity with ∼11 Å from the cavity entrance to its tip end.

Moreover the R2 acyl chain of Lipid IVa folds back into the cavity, into the space occupied by the R2'' acyl chain of Re-LPS. As a result, R2 is partially exposed to the solvent, with its tip end extended to interact through van der Waals forces with the hydrophobic side chain of Phe438* on TLR4* as part of the

dimerization interface. The R2 acyl chain of Re-LPS in the mTLR4/MD-2/Re-LPS complex made a similar interaction, although all of the carbon atoms of the R2 acyl chain were involved in the interaction.

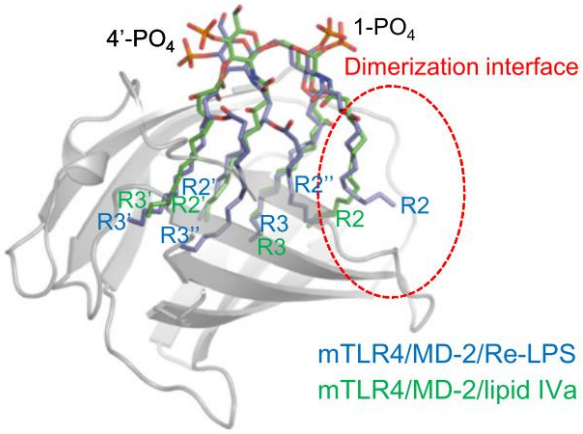

Figure 27.2 Structural comparison of the LPS ligand in the MD-2 cavity. Superposition of mTLR4/MD-2/Re-LPS (blue) and mTLR4/MD-2/lipid IVa (green) (from Ohto et al. 2007[113]).

Ohto et al. speculated that the favorable interaction induced by dimerization and thus by the interaction of the exposed R2 chain with the hydrophobic patch of TLR4*, should compensate the energetically unfavorable arrangement of Lipid IVa related to its acyl chain partially exposed to the protein surface and the hydrophobic cavity left partially unoccupied.

Differently from mMD-2, in the hMD-2/Lipid IVa crystal structure Lipid IVa orientation changes with respect to LPS.

This change appears related to both the different hydrophobicities of their dimerization interfaces as well as to the different electrostatic potential of the cavity entrance and thus to the different charged polar residues between human and mouse MD-2.

Indeed, while in mTLR4/MD-2 the two phosphate groups of Lipid IVa were surrounded by positively charged lysine and arginine residues, the mTLR4 residues, Arg266, Lys319, Arg337, Lys341, Lys367, and Arg434 of this group are not present in hTLR4. [65,113] Notably, Lys367 and Arg434 were located near the dimerization interface. Meng and coworkers reported that when these residues were replaced with their human counterparts, Glu369 and Gln436, the responsiveness of mTLR4/MD-2 to Lipid IVa was abolished.[144] Hence, these two residues play an important role in species specificity for Lipid IVa, possibly by augmenting the interaction with the 1-PO_4* group of Lipid IVa. These residues may modulate the electrostatic surface potentials to favor positioning of the negatively charged 1-PO4 group to be suitable for dimerization of mTLR4/MD-2/Lipid IVa. Meng and coworkers also reported that the mutation of Glu122 of mMD-2 to its human counterpart, Lys122, substantially reduced responsiveness to Lipid IVa.[144] Glu122 is located in the cavity entrance of MD-2. Mutation to the positively charged Lys residue would change the electrostatic potential of the cavity entrance and interaction with the charged phosphate group of Lipid IVa.

As a consequence of the overall orientation change, Lipid IVa was confined more deeply in the hydrophobic cavity of hMD-2 than it was in the mTLR4/MD-2/Lipid IVa complex.

In particular, while all six acyl chains of LPS align in the cavity of hMD-2 with identical conformation to mMD-2 (thus confirming again that the recognition mechanism of hexaacylated LPS is conserved between human and mouse TLR4/MD-2, both of which are potently activated by hexaacylated LPS), acyl chains of Lipid IVa are buried deeper in the pocket of hMD-2 and thus even R2 does not favour any dimerization.[65,113]

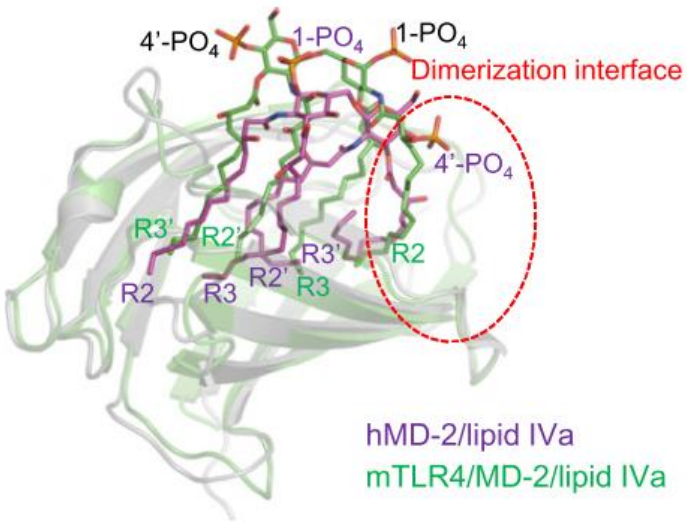

Figure 27.3 Structural comparison of the LPS ligand in the MD-2 cavity. Super- position of hMD-2/lipid IVa (magenta) and mTLR4/MD-2/lipid IVa (green) (from Ohto et al. 2007[113]).

These results together seem to confirm a central role of the charge distribution in proper positioning of Lipid As for the dimerization of TLR4/MD-2, and thus in determining their agonistic or antagonistic orientations, especially for a relatively weak agonist such as Lipid IVa.

7.1.2.6 Eritoran (or E5564)

Since both natural and synthetic RsDPLA showed a powerful antagonistic activity devoid of any stimulation, much chemical efforts have been devoted after its first biological results to the synthesis of its derivatives In this way Eritoran (or compound E5564) has been first synthesized by Christ et al. in 1999 (figure 28).[145]

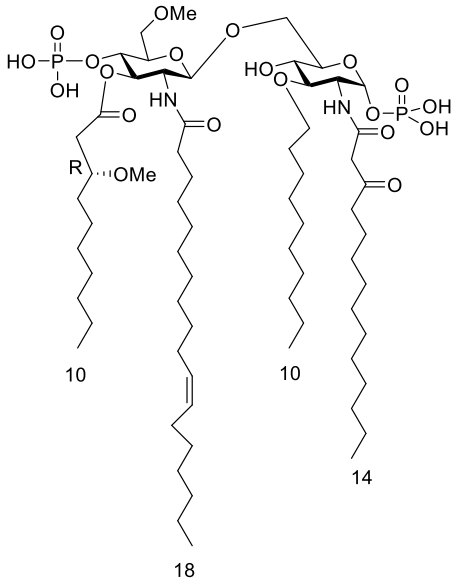

Figure 28. Eritoran

As Lipid IVa, Eritoran has a di-glucosamine scaffold with two phosphate groups and four acyl chains with one chain especially long: while chain in C2' is composed of 14 carbon atoms and the two chains in C3 and C3' are of 10 carbon atoms each, the R2' chain in C2' is of 18 carbon atoms and has one unsaturation.

Eritoran demonstrated an extremely powerful antagonistic activity both in human and in mouse *in vitro* as *in vivo* by blocking the induction of LPS-induced cytokines and LPS or bacterial-induced lethality in primed mice. It was devoid of agonistic activity when tested both *in vitro* and *in vivo*.[3]

Similar to E5531, another lipid A-like antagonist, E5564 associates with plasma lipoproteins, causing low concentrations of E5564 to be quantitatively inactivated in a dose- and time-dependent manner.[3] However, compared with E5531, E5564 is a more potent inhibitor of cytokine generation, and higher doses retain activity for a period of time likely sufficient to permit clinical application. [3]

These results indicate that E5564 is a potent LPS antagonist and lacks agonistic activity in human and animal model systems, making it a potentially effective therapeutic agent for treatment of disease states caused by sepsis.

For this reason Eritoran entered clinical trials for the treatment of sepsis.

Eritoran was significantly protective in animal models of sepsis and, in healthy volunteers, blocked the signs and symptoms of endotoxemia in a dose-dependent manner.[101]

However, despite the first encouraging results, the clinical phase III was discontinued in 2011, essentially because lack of statistically significant activity when tested on a panel of 2.000 septic patients[68]

The ability of Eritoran to act as TLR4 antagonists has been studied for long.[3]

E5564 blocked LPS/ sCD14-induced reporter activity in TLR4/MD-2-expressing HEK293, but not TLR2-mediated signalling by heat-killed *S. aureus*. These findings indicate that E5564 selectively inhibits LPS signalling via TLR4/MD-2.[146]

However, a limitation to this model system is that LPS requires the presence of sCD14 for cellular activation, making it difficult to determine whether E5564 blocks LPS binding to sCD14 or TLR4/MD-2. Results from experiments indicated that serum components did not affect the potency of E5564, indicating that they are not critical to E5564 antagonistic activity.[146]

Important information of the structure-activity relationships of E5564 have emerged from the crystal structure of its complex with mouse and human TLR4/MD-2 obtained with an Hybrid LRR Technique.[22]

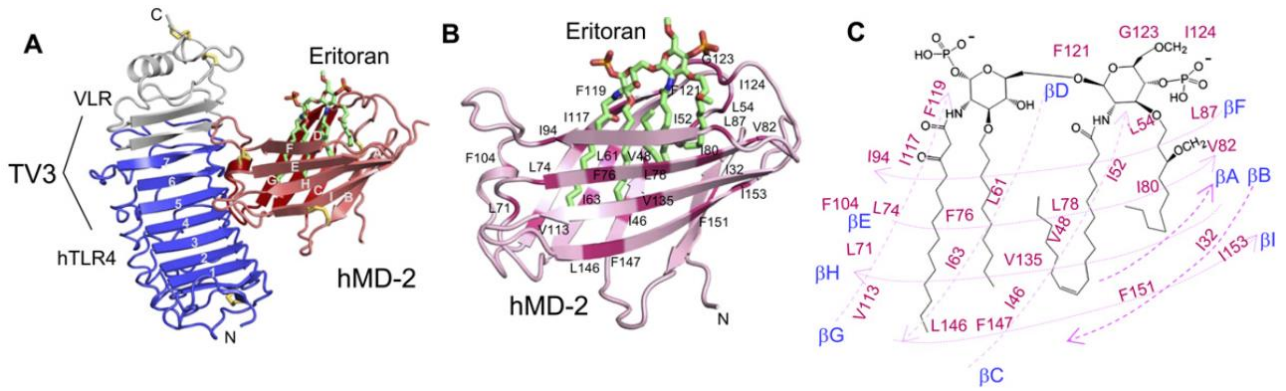

Figure 29. A) Overall structure of the crystallized TLR4(TV3 hybrid)-hMD-2-Eritoran complex; **B**) Close-up view of the crystallized human MD-2 and Eritoran complex; **C**) chemical structure of Eritoran with MD-2 residues interacting labeled. The β strands are shown schematically as broken arrows (from Kim et al. 2007[22])

The crystal structure on hTLR4/hMD-2 shows that Eritoran binds to the hydrophobic pocket in human MD-2, but without any direct interaction between Eritoran and TLR4.

In Ohto et al. and this MD-2 structures, Lipid IVa and Eritoran bind to the same area in MD-2.

In particular the presence of the long unsaturated chain in C2' appeared to have an important role in determining its powerful antagonistic activity.

Indeed, while the two phosphate groups form ionic bonds with positively charged residues located at the opening of the pocket as in the other Lipid As types, the four acyl chains of Eritoran fill the hydrophobic pocket and occupy almost 90% of the solvent-accessible volume of the pocket, leaving only a narrow groove near its opening.

This huge pocket filling appears related to the presence of R2' chains which, differently from R2 and R3 chains, but similarly to R3' chain, bends in the middle.

In addition the R2' acyl chain has a *cis* conformation so the chain makes a 180° turn at the *cis* double bond.

In this way R2' is able to occupy a larger space in the pocket, which is generally associated to a higher TLR4 antagonistic activity.

7.1.2.7 Tri-acyl disaccharide OM-174

In 2000 OM Pharma (Meyrin, Switzerland) purified from of *E. coli* a diphosphoryl, triacyl, disaccharide lipid A derivative called OM-174 (figure 30).[147]

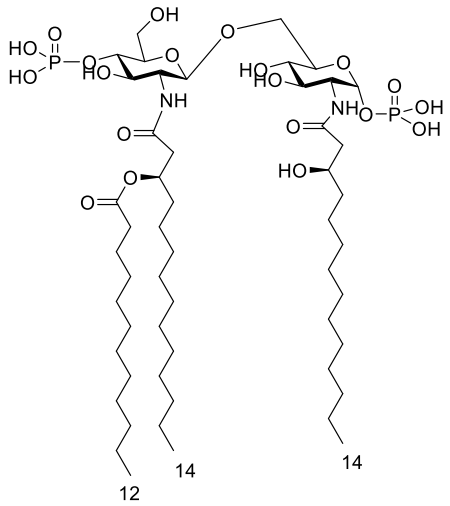

Figure 30. OM-174

Surprisingly despite the triacyl lipid A is more than 10^5-fold less active than hexa-acyl lipid A, it was only 10-fold less active in inducing IL-6 in human mononuclear cells, and equally active in inducing NO production in murine macrophages.

OM-174 as expected was found to differ from *E. coli* lipid A in many physicochemical characteristics, but it is still able to express cytokine-inducing activity probably due to its proved intercalation into the target cell membrane which happens in even in absence of LBP.

Indeed OM-174 exhibited a non-lamellar, but not inverted (H_I) structure.[117]

Since this compound was shown to be a candidate for an effective anticancer treatment it entered phase I clinical trials.[104]

7.1.3 Monosaccharide-based TLR4 modulators

The synthesis of natural lipid As or lipid A mimetics with a disaccharide structure is a complex process involving tens of synthetic steps. Moreover if a Lipid A analogue needs to be obtained, the two glycosylation steps must be stereocontrolled reactions with selective formation, respectively, of β-(1→6) glycosidic and 1-α-phosphate bonds as in natural Lipid As.

These are the reasons why an important trend in lipid A mimicry has been the design of simplified structures, with the aim to partially or totally preserve the lipid A biological activity while reducing the chemical complexity of the molecules, and improving in parallel synthetic affordability and solubility properties.[34]

7.1.3.1 Lipid X

The use of molecular simplification of Lipid A structures was inspired by the discovery in 1984 that Lipid X (or compound 401)(figure 31), a monosaccharide biosynthetic precursor of *E. coli* lipid A, analogues of its **reducing** sugar moiety, was able itself to generate an immunoresponse.[148]

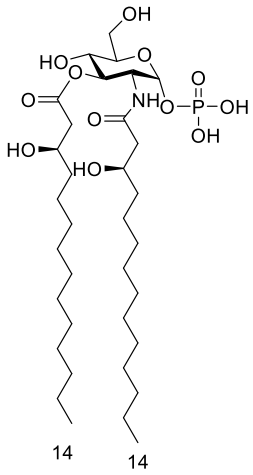

Figure 31. Lipid X

However the first synthetic Lipid X obtained by Kusumoto et al. in 1984[149] showed an apparent immunostimulatory activity in all tests performed till 1990 when Aschauer et al. found to be contaminated by small amounts of the immunostimulant N,O-acylated disaccharide-1-phosphate which can form during the last step of its synthesis.[150]

In 1991 finally Lam et al. purified the Lipid X by Kusumoto obtaining pure Lipid X which in the *in vitro* tests in mouse was devoid of the immunostimulatory properties of lipid A or endotoxin.

On the contrary, it behaved as a competitive inhibitor of lipopolysaccharide by blocking the activation of monocytes and macrophages by endotoxin and the priming of human neutrophils.
Same antagonistic activity was later confirmed on human cells.[151]

Because of its anti-endotoxic activity lipid X has been considered a simplified monosaccharide scaffold for the development of TLR4 agonists and antagonists.

7.1.3.2 Lipid X derivatives: SDZ-880.431

Starting from Lipid X structure different monosaccharide derivatives have been synthesized by changing the acyl chains (e.g. to an acetyl group or to a branched chain), the scaffold (from glucosamine to glucose) or the anionic groups.[151,152]

These derivatives of Lipid X were in general found to have reduced inhibitory activity or concentration dependent-mixed (blocking and priming) activity depending on the structural modification introduced.

On the contrary, SDZ-880.431 developed by Sandoz in 1987[152,153] (figure 32), which possesses just one additional phosphate in C4 with respect to Lipid X, showed the most potent antagonist activity with respect to all lipid X synthetic analogs synthesized and more potent than Lipid X itself, on both murine macrophages and human monocytes.[34,152,154]

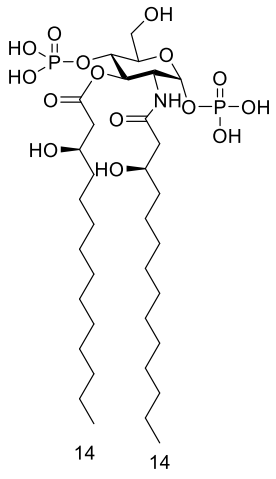

Figure 32. SDZ-880.431

7.1.3.3 Lipid X derivative SDZ MRL 953

Another important derivative of the reducing part of Lipid A is SDZ MRL 953 developed by Sandoz in 1991[155] (figure 33).

This compound differs from Lipid X for the insertion of a third linear acyl chain in C4.

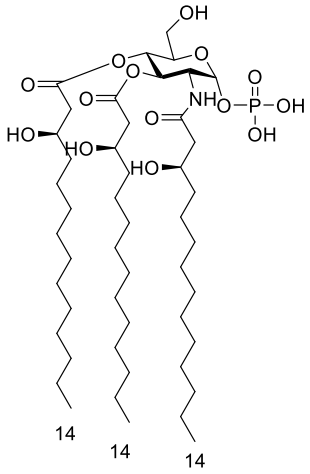

Figure 33. SDZ MRL 953

Differently from Lipid X, SDZ MRL 953 exerted no anti-endotoxin effect in the tests *in vitro*.

On the contrary it stimulated mouse macrophages to release high levels of granulocyte colony-stimulating factor (G-CSF) and low levels of proinflammatory cytokines such as interleukin-6, interleukin-8, TNF a (thus a cytokine profile being markedly different from the endotoxin-induced cytokine pattern) at relatively high concentrations (10^3 higher than Lipid A).

When tested *in vitro* in human cells, SDZ MRL 953 was able to induce the release of a comparable range of cytokines in human macrophages to LPS. Total amounts of cytokines induced were lower, and SDZ MRL 953 had to be used in 1 to $5x10^4$ times higher concentrations as LPS. Significant induction of TNF-α and IL-6 was first seen at 5 µg/ml, and, even by using these high levels of SDZ MRL, the amount of cytokines produced did not exceed 5 ng/ml. In concentrations up to 500 µg/ml, neither release of IL-1p nor of G-CSF by SDZ MRL 953 was noted.[156]

It was surprising to find another monosaccharide after GLA compounds able to induce immunostimulation in murine as in human like the much different disaccharides of Lipid As.

However monosaccharide GLA-60 was not considered a potential adjuvant for vaccine since it was still toxic in galactosamine-loaded mice at a dose of 1 µg per mouse and thus it did not exhibit an improved

therapeutic margin over LPS when their immunostimulatory activities are compared with either inherent or contaminating residual toxicities.

On the contrary SDZ MRL 953 was less toxic in in galactosamine-sensitized mice than LPS by a factor of 1.7 x 10^4 to >7.4 x 10^5. Thus, the therapeutic indices of SDZ MRL 953 were significantly improved over those of endotoxin and ranged from about S to >500, depending on the infection model and mode of administration.
Thus SDZ MRL 953 can be considered the first potential monosaccharide adjuvant discovered and the first compound showing the promising approach of monosaccharide molecular simplification in the clinical perspective.
Indeed SDZ entered in 1993 in clinical exploration for cytokine induction in the setting of chemotherapy-induced cytopenia[156].

Hyper-responsiveness towards LPS is the main reason leading to septic shock, but it has been studied that pretreatment with low doses of LPS can slow down the responsiveness. This effect has been termed adaptation (or endotoxin tolerance or desensitization) and relates to long-known *in vivo* effects in which animals became tolerant to endotoxin injections and survived lethal doses of LPS if they had previously received one or several low-dose injections of LPS.
Human cancer patients who repeatedly received endotoxin injections in an experimental treatment setting also showed the phenomenon
For this reason the preincubation effect of the synthetic lipid A analogue SDZ MRL 953 on human macrophages has been studied as well.[156]
Remarkably, the compound downregulated the production of TNF-α and IL-6, but upregulated the endotoxin-induced production of IL-1β and G-CSF.

Based on the known antitumor activity of endotoxins due to their immunostimulatory property, a phase I trial of SDZ MRL 953 in tumor patients first to evaluate its biologic response and safety of administration in humans was conducted in 1997.[157]
SDZ MRL 953 was at least 10^4 times less toxic as compared with endotoxin. This is consistent with findings in hypersensitized mice. Apparently, the improved tolerability of SDZ MRL 953, as compared with endotoxin, was related to its low activity, particularly for TNF-α and IL-1b induction.

Unfortunately, to my knowledge, after all so positive results, this study dated 1997 is the last scientific report available on compound SDZ MRL 953.

Little is known about SDZ MRL 953 mechanism of action even nowadays that all the TLR4 recognition process and related PRR have been elucidated.

In vitro studies suggest that SDZ MRL 953 may act independently of CD14,[158]

Unlike endotoxin, SDZ MRL 953 action on TNF-α release in human peripheral blood mononuclear cells could not be blocked by mono- clonal antibodies to CD14.

Taken together, these data seems to point towards a direct interaction with MD-2, but since MD-2 was not known at that time, no study was performed.

Noteworthy still nowadays no such study has been performed yet to our knowledge.

However, as stated above it was indeed very unexpected that also a monosaccharide could express an immunostimulatory activity that the more complex disaccharide structure can express only with the specific structural feature of six asymmetrically distributed chains.

The correlation between SAR for disaccharide and the ones for monosaccharide has been remarked by Matsuura in 1999.[159]

The aggregates shape of such amphiphilic compounds seems to be the key for their activity.

These studies and SAR will be discussed in the section 7.3.

7.1.3.4 Gifu Lipid As (GLA)

It was in the same years of Lipid X first synthesis that another Japanese group from Gifu University in Japan decided to work also on the synthesis of analogues of the non-reducing part of *E. coli* Lipid A in order to test their immunostimulating activities (Kiso and Matsuura et al., 1984[160,161]).

These compounds and the other analogues obtained after were named Gifu Lipid A (GLA) from the name of the university in which they have first been synthesized.

GLA (figure 34) mimic the non-reducing part of Lipid A and possess one phosphate group in C4 while different type of linear or branched chain have been inserted in C2 and C-3 in order to explore the structural requirements for immunostimulation or for blocking LPS activity.

These compounds have been tested on murine[162] and on human cells[159] and the results have been summarized in 1999 by Matsuura et al.[159]

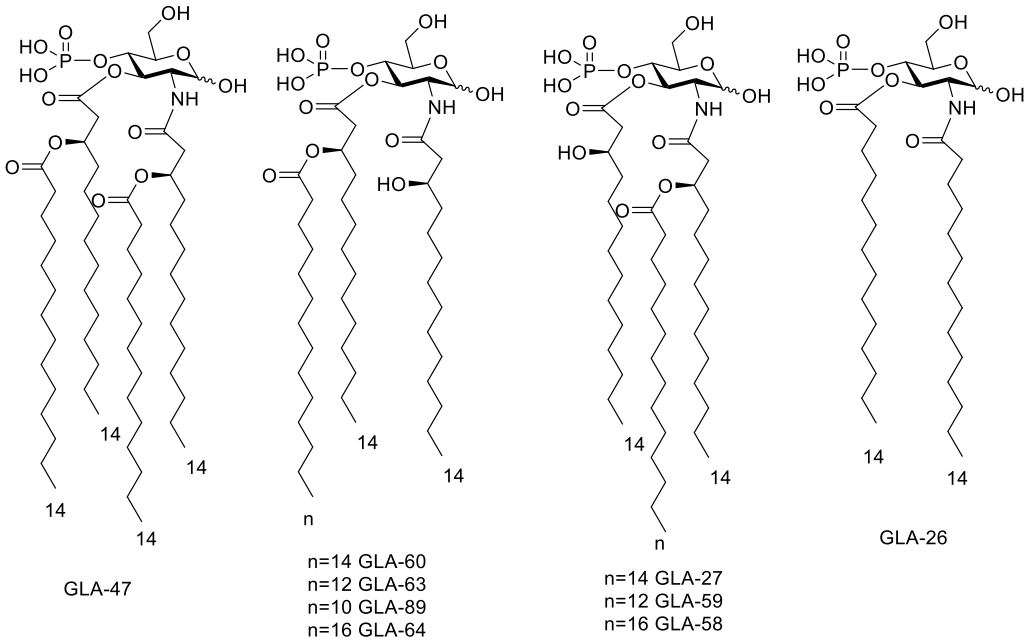

Figure 34. GLA compounds

In particular, while compounds having two chains, like GLA-26 or four acyl chains, like GLA-47 showed immunostimulatory activity only in murine, while they are LPS antagonist in human, compounds GLA-60, GLA-68 and GLA-63, with three acyl chains, that means one linear chain in C2 and one branched chain in C3 next the phosphate group, all of C-14 length, except the third C12 chain of GLA-63, have surprisingly demonstrated an agonistic activity also in human.

It was indeed very unexpected to see for the first time a monosaccharide expressing a pure immunostimulatory activity like the much complex disaccharides, and it was even more important to see the same pure immunostimulatory activity in human.

On contrary to these three pure agonists, the elongation to C16 or shortening to C10 of the third chain (the branch of the chain in C3) caused a switch from agonism to antagonism in human cells for GLA-64 and GLA-89.

The same effect was observed when the branched chain position was switched from C3 to C2 like in GLA-27 and GLA-59[163] .

Moreover when with both this switch and the elongation of the third chain are present, as in GLA-58, antagonistic activity was observed both in murine and in human.[159]

These data gave an important contribute to define much clearly the SAR for monosaccharide structures.

Since the majority of GLA compounds were synthesized in the ‘80s and 90’s, and nothing was known at that time about the role of TLR4-MD-2 complex, in search of a possible rationalization of such effects and a

correspondence with the effects of disaccharides, researchers focused on CD-14 and in particular on the aggregates shape of such molecules.

In 2002 a correlation was found: GLA that possess a non-lamellar aggregate shape are active as agonists both in human and murine while GLA having antagonistic activity in both or no activity generate lamellar aggregates. Finally those GLA possessing agonistic activity in murine and antagonistic activity in human have mixed aggregates shape .[163]

These observations are consistent with the relationship between aggregate structure and agonism/antagonism found for lipid A variants and previously presented.

Moreover it was found that the position of the branched chain also influences activity: if the acyloxyacyl (branched) chain is near the phosphate the compound generates a non-lamellar aggregate and exhibits bioactivity, whereas if the branched chain is farer the compound generates a lamellar inactive aggregate form.

After the discovery of TLR4 and MD-2 role in immunostimulation, scientists searched another rationalization of disaccharide Lipid As and monosaccharide Lipid A partial structures in their interaction with this receptor system.

With this aim, Tamai et al. in 2003 studied the dependence on TLR4 and other TLRs of the immunostimulation of these compounds.[164]

Tamai et al. measured the induction of proinflammatory factors by GLA compounds in human peripheral blood mononuclear cells (PMC) with or without addition of mouse monoclonal antibodies to human TLR2 and TLR4. In this way they found that only monoclonal antibodies to TLR4 block the response of active GLA. Thus their experiment clearly established for the first time a clear correlation between monosaccharide activity and TLR4 modulation.

However the GLA interaction with MD-2 has still to be characterized.

7.1.3.5 Monosaccharides with aromatic chains: ONO 4007

Acyl chains with an aromatic group have been used to develop monosaccharide analogues of the non-reducing part of Lipid A with the initial aim of obtaining immunostimulants as anticancer agents.

These compounds differ for the position of the phenyl-ring-containing chain (in C2 or C3, in the branched chain or in the main chain) and for the length of this chain. The position of the phenyl ring in the chain has been changed and naphthalene rings have been used (figure 35).

In general a sulfate group has been used instead of a phosphate except in 2 variants.

Different results of biological activities and toxicities were found with respect to type of structural modification.

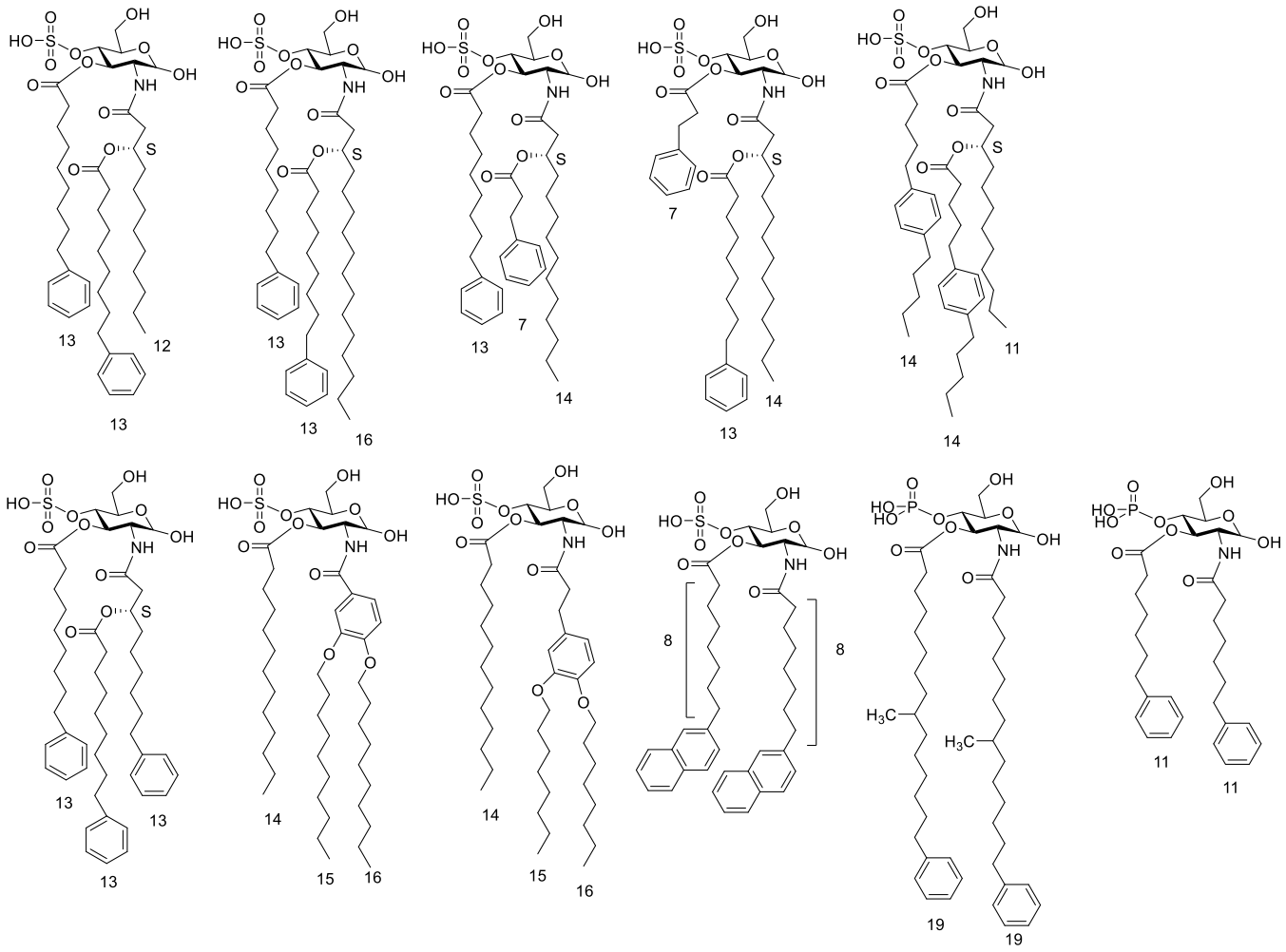

Figure 35. Lipid A partial structures with aromatic chains reported in literature

In 1987 ONO Pharmaceuticals developed a series of such compounds some of which showed enhancing activity of cellular immunity (e.g. mitogenic activity) to living tissue in murine and an inducing activity of TNF, IL-1 and IFN associated with low toxicity. [165]

On the contrary another series with a phosphate group developed in 1993 showed mitogenic activity only associated with toxicity.[166]

Finally in 1994 ONO Pharmaceuticals obtained a compound, called **ONO-4007** (figure 36), with an aromatic group at the end of two of its three chains and one sulfate in C4. This compound showed unique properties in this series: a greatly diminished toxicity against animals (less than 1/1000 that of natural Escherichia coli LPS); potent antitumor effects against implanted MethA sarcoma and MH-134 hepatoma in the murine system; water solubility, an advantageous property for therapeutic use.[109]

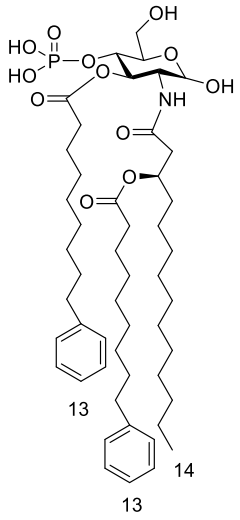

Figure 36. ONO 4007

These unique features made ONO-4007 a possible candidate among lipid A analogs for antitumor therapy and it entered phase I clinical study.[104]

ONO 4007 seemed to exhibit its antitumor effect by activating TIM in situ to produce intratumoral TNF and to be cytotoxic against MM46 mammary carcinoma tumor cells. [109]

On this basis, the effect of ONO-4007 administered *in vivo* on intratumoral TNF-α production was tested.

From the results obtained it appeared that ONO 4007 exerts its antitumor effect primarily by inducing high intratumoral TNF production and potentiating TIM to a strong tumoricidal state at least in the MM46-implanted tumor model system described.

Due to its immunostimulatory activity and its safe profile, ONO-4007 was also tested as adjuvant in vaccine. Nowadays ONO-4007 is in phase I clinical studies as adjuvants in vaccine against Leishmania.[104]

However, despite the extremely relevant results of ONO 4007, the effect of aromatic chains has been tested only on the few monosaccharide molecular simplifications of the non-reducing part Lipid A presented.

It has never been tested on di-sulfated/di-phosphorylated analogues nor on analogues of the reducing part of Lipid A.

Most importantly not even disaccharide Lipid A structures are reported with this feature to our knowledge.

7.1.4 Monosaccharides as disaccharide mimetics

Another approach to find new TLR4 modulators has been the synthesis of monosaccharide-derived compounds still mimicking the structure of Lipid A with a proper distance between two anionic groups.
This idea came from the consideration that one of the two glucosamines could be removed from the scaffold without affecting the biological activity. In particular it was speculated that the activity would be retained if the proper distance between acyl chains and phosphate groups are maintained.
This was later confirmed in 2002 by the TLR4 agonistic activity of the non-sugar lipid A mimetic ER112022.

Based on this mimicry strategy, both derivative of the reducing and non-reducing part of Lipid A with a proper linker carrying an anionic group and acyl chains as an analogue of the second sugar have been synthesized.

7.1.4.1 Aminoalkylglusosaminide 4-phosphates (AGPs): Corixa compounds (CRX), ethanolamine mimetics CRX-527, CRX-526, RC-529 and PET-Lipid A

In 1999 Johnson et al. from Ribi ImmunoChem synthesized a new class of monosaccharide molecules based on the **non-reducing part of Lipid A**, called aminoalkyl glucosaminide 4-phosphates (AGPs), that mimics the disaccharide scaffold.[167]
Since later Ribi Immunochem became Corixa Corp. (MT, USA) they were eventually called Corixa compounds or CRX.
AGPs are monosaccharide that still mimics Lipid As in the sense that the reducing sugar has been replaced by an acylated amino acid or other glycols (figure 37).
Thus AGPs still generally possess two anionic group (one phosphate on the sugar and one carboxylic group on the aglycon used as a stable bioisostere of the labile anomeric phosphate of lipid A) and six acyl chains.
The authors speculated that coupling a flexible N-acylated aglycon to the structurally more conserved non-reducing sugar of Lipid A would permit energetically favored close packing of the six fatty acyl chains in a hexagonal array that is crucial to obtain supramolecular aggregates with an immunostimulatory activity.

Serine has been used as the aglycon unit for the presence of three desired functional groups: an amino group to be acylated with a fatty acid chain, a carboxyl group as a bioisostere of lipid A C1 phosphate and a hydroxyl group for attachment to the monosaccharide.

Moreover serine-derived flavolipin and other naturally occurring N-(3-acyloxyacyl)amino acids were already known at that time for their immunostimulating activity.

However also aglycon chain without the carboxyl group and of different length, that means ethanolamine and other hydroxylalkylamines with or without a ramification in 2, have been synthesized and reported in the same paper.

Acyl chains of different length have been used to explore SAR in this type of molecules.

Compounds have been tested for their ability to induce nitric oxide synthase (iNOS) in murine macrophage and cytokine production in human peripheral monocytes, while toxicity was evaluated as the minimal pyrogenic dose (MPD) in a standard three-rabbit USP pyrogen test.
AGPs and hydroxylalkylamines were able to induce immunostimulation and their activity as well their toxicity showed striking chain-length dependence, and aglycon chain length-dependence for hydroxylalkylamines.
However while acyloxy ethanolamines showed good immunostimulation only associated with toxicity, AGPs like compound 3c (later called **CRX-527**) showed an extremely powerful immunostimulation with low toxicity.

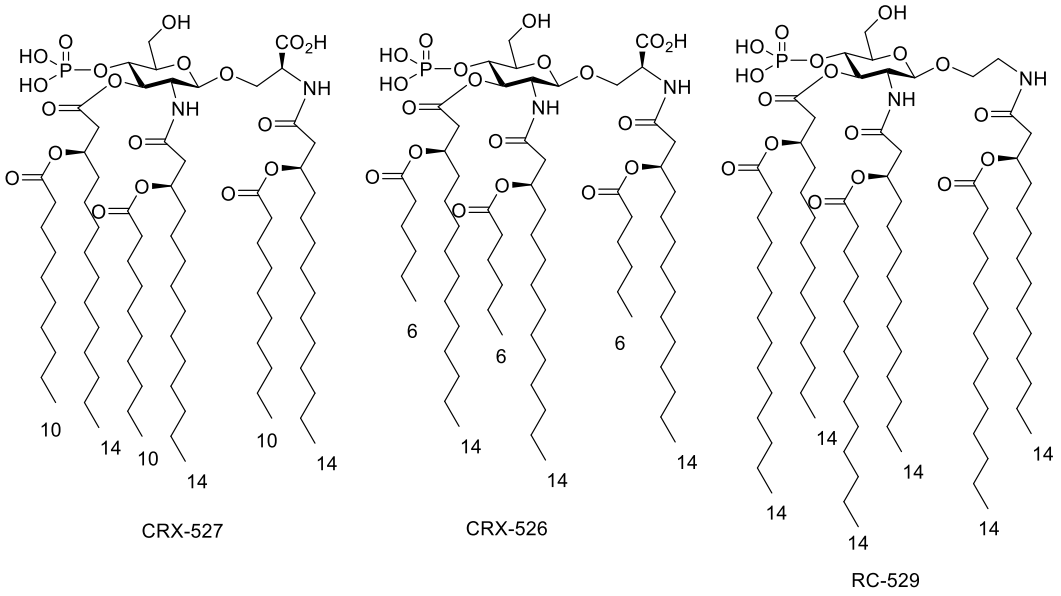

Figure 37. AGPs of the non-reducing part of Lipid A

These data show that the carboxyl group of serine-based AGPs is bioisosteric with the 1-phosphate moiety of lipid A but this second anionic group thus not fundamental for activity is important to express powerful immunostimulation as comparing Lipid A and MPL.

Also the ether version of the ester chains attached to AGPs was synthesized later showing similar results to their counterparts[168]. CRX-527 and its ether analogue were virtually indistinguishable with respect to their ability to induce cytokine production in human cell.

Such results indicated that the AGP motif can constitute a potent, low-toxicity biomimetic of lipid A and for such reason AGPs have been widely studied.

In contrast to CRX-527, compound **CRX-526** devoid of immunostimulating activity, was a potent LPS antagonist active in blocking the induction of pro-inflammatory cytokines induced by LPS both *in vivo* and *in vitro* (figure 37).[168]

Also variants of the acyloxy ethanolamine have been successively synthesized.
For example diethanolamines, that means there is an additional ethanol group on the acyloxy ethanolamines, have been obtained.
These compounds showed different immunostimulatory potency depending on the diethanolamine substituent on the free hydroxyl group when tested on human monocytic cell line THP-1, with compounds 1 bearing a carboxylic acid group and six FA chains exhibiting the greatest activity.[34,169]

Several members of this class of lipid A mimetics, including prototypical AGPs CRX-524, and CRX-527, **RC-529** (compound 3e in the Johnson paper of 1999[167]) (figure 37), have been shown to improve humoral and cell-mediated immune responses to a variety of different antigens in mice as well as enhance non-specific resistance in mice to viral and bacterial infections.[168]
To further demonstrate the prophylactic anti-infective effects with an AGP, CRX-527 was evaluated in a preclinical model for respiratory syncytial virus (RSV) and CRX-527 was found to effectively inhibit RSV replication in BALB/c mice when intranasally administered 24 hours prior to infection via the same route.
RC-529 was shown to induce antigen-specific serum and mucosal IgG and IgA antibodies and reduce nasal colonization in mouse intranasal challenge models for both Neisseria meningitidis and non-typeable Haemophilis influenzae (NTHi).
Since RC-529 demonstrated adjuvant profile similar to MPL, this AGP was further developed as a vaccine adjuvant, and the combination of RC-529 with aluminum hydroxide comprises the adjuvant formulation in the approved recombinant hepatitis B vaccine Supervax® produced by Crucell.[104]

With the same approach in 2006 Akamatsu et al. synthesized AGPs based on the **reducing part of Lipid** A in which the non-reducing end (3-phosphorylated glucosamine) was substituted with aspartic acid or phosphoserine containing D-or L-configurations at the α-position of the amino acids and acylated (figure 38).[170]

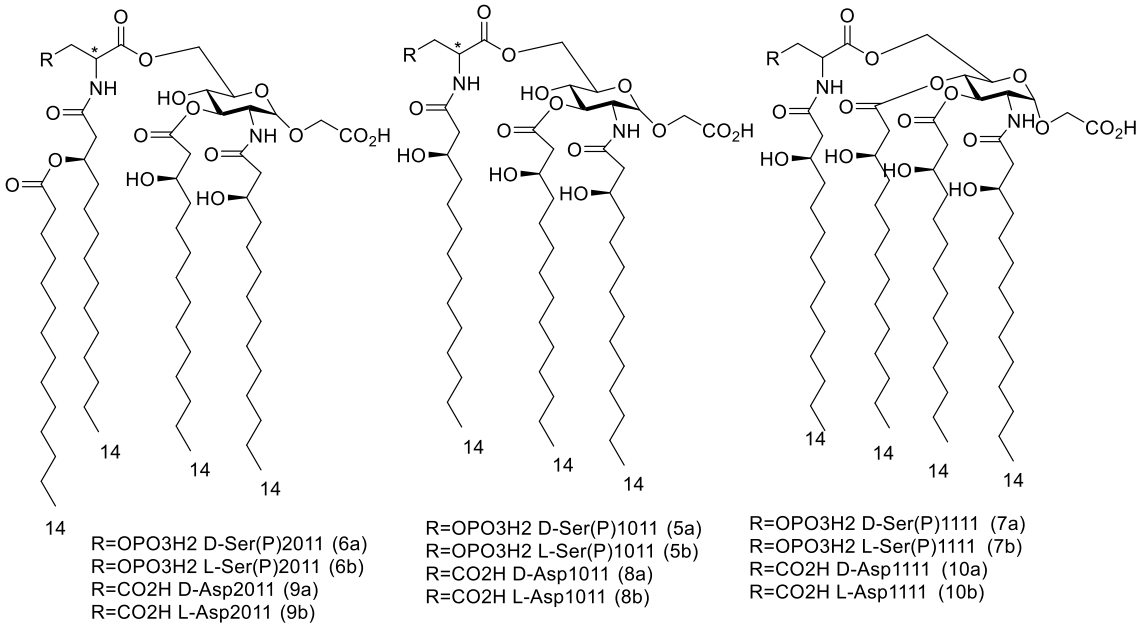

Figure 38. AGPs of the reducing part of Lipid A

Disaccharide mimetics with two anionic groups and three acyl- and four acyl- groups, four linear chains or one branched and two linear, have been synthesized.

These analogues were evaluated for induction of human cytokines and inhibitory activities against LPS.

All the phosphoserine analogues showed the antagonistic activity, with all these three acylation patterns.

Aspartic acid analogues showed varying results: the tri-acylated D-Asp1011 showed no LPS antagonistic effect and no immunostimulation; the tri-acylated L-Asp1011 on the contrary shows still no immunostimulation but has an LPS antagonistic effect; the branched tetra-acylated L-Asp2011 has a weak antagonistic effect and a weak agonistic activity; the branched tetra-acylated D-Asp2011 is a pure agonist 100-fold stronger than L-Asp2011; finally linear tetra-acylated D-Asp1111 and L-Asp1111 are pure antagonists.

By making comparisons between the structural modifications inserted, it appears that:

- the phosphoserine-containing analogues showed stronger inhibitory activities than the corresponding aspartic acid-containing analogues that feature the same acylation pattern

- The agonistic and antagonistic activities were switched by structural change between the phosphoryl group (e.g., D-Ser(P)2011, 6a) and the carboxylic group (D-Asp2011, 9a).
- the tetraacylated analogues showed stronger inhibitions than the triacylated analogues.

The results confirmed that the receptor protein of LPS/lipid A recognizes second acidic groups on amino acid residues, and also it confirmed that the volume and shape of the hydrophobic part consisted with acyl chains were recognized by the receptor.

A possible rationalization of AGPs and ethanolamines behaviour of course lies in their structural mimicry of Lipid A, which in turns is related to their ability to intercalate their acyl residues into the hydrophobic pocket of MD-2.

Two negatively charged groups as for lipid As are needed to interact with the positively charged lysine groups in the MD-2 binding site for maximal activity.

Moreover the AGPs experimental data suggests that the distance between ionizable groups, that is fixed for disaccharides, is a critical determinant for binding to MD-2

Also the aggregate shape of AGP reveals same correlations with Lipid As.

Biophysical characterization of MLA mimetic CRX- 527 shows that the individual molecules adopt a conical shape and non-lamellar, inverted hexagonal H_{II} aggregate structure in solution, which is consistent with its high agonist activity and in accord with data on other TLR4 agonists. In comparison, physicochemical analysis of CRX-526, a 6- carbon secondary acyl homolog of CRX-527, revealed that it forms lamellar aggregates in solution, which is characteristic of inactive or antagonistic molecules

Most importantly, while AGPs activation of TLR4 proceeded also in the absence of co-receptor CD-14 even if less efficiently, as demonstrated with TLR4/MD-2 HeLa cell transfectants with or without co- expression of CD14, the response to the most potent compound CRX-527 was strictly dependent on TLR4 and MD-2 but not CD14, suggesting that CRX-527 may be able engage both MyD88-independent (TRIF) (that requires CD-14) and MyD88 pathways in the absence of CD14.

Similar results were obtained in murine infectious disease models with these hybrid molecules.[171]

The CD-14 independence of AGPs activity is consistent with the same independence observed for SDZ MRL 953, another powerful monosaccharide agonist.

Another compound strictly related to AGPs is **PET-Lipid A** (figure 39) which has a propyl chain between the sugar-bound oxygen and the amine and two additional hydroxyalkyl groups in the middle of this chain.

This compound showed powerful immunostimulatory activity and for this reason it has been tested in different systems showing its more promising results in anticancer therapy entering phase III clinical trials.[104]

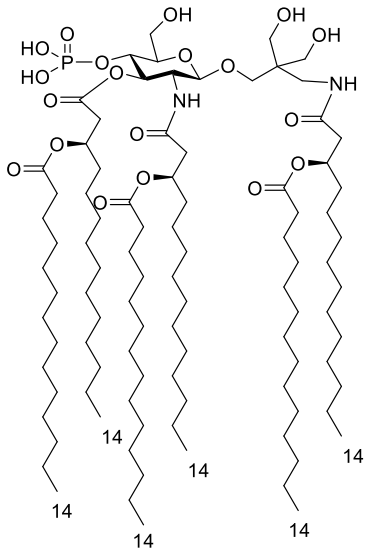

Figure 39. PET-Lipid A

7.1.5 Dimeric monosaccharide lipid A mimetics

Another approach in the synthesis of Lipid A mimetics has been the design of dimeric monosaccharide structure using a spacer of variable nature to link the monosaccharide units.

Molecular modeling and MD-2 docking suggest indeed that the use of a bridge between the two monosaccharides would ensure the conformational flexibility required to allow FA chains accommodation into hMD-2 binding cavity.

However no relevant results have yet come from this approach.

In 2011 Lewicky et al. reported for the first time the use of such dimeric monosaccharide framework as an alternative to the archetypical disaccharide framework of lipid A molecules.[172]

They linked two monophosphorylated di-acyl glucosamines through a (1→1') ethylene linker (figure 40).

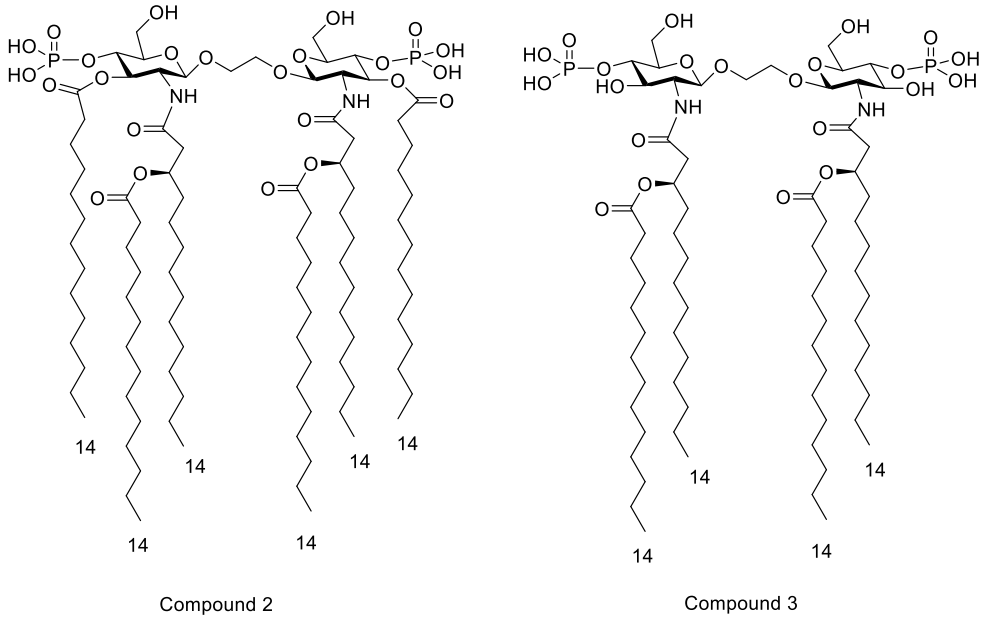

Figure 40. Dimeric compounds 2 and 3 from Lewicky et al. 2011.[172]

Preliminary biological studies indicated that such compounds were agonistically inactive in terms of stimulating ICAM-1 expression in human monocytic THP-1 cells.

Despite being also antagonistically inactive against LPS, yet these compounds exerted significant synergistic effect on LPS-induced ICAM-1 expression by THP-1 cells.

Two lipid A analogs (**compounds D1 and D7**) with a rotational symmetry were also designed and synthesized by our group in 2012 using a convergent strategy (figure 41).[173]

Two glucose monosaccharides are symmetrically linked through a (6→6') linker.

D1 has two sulfates as anionic group, D7 has two phosphates.

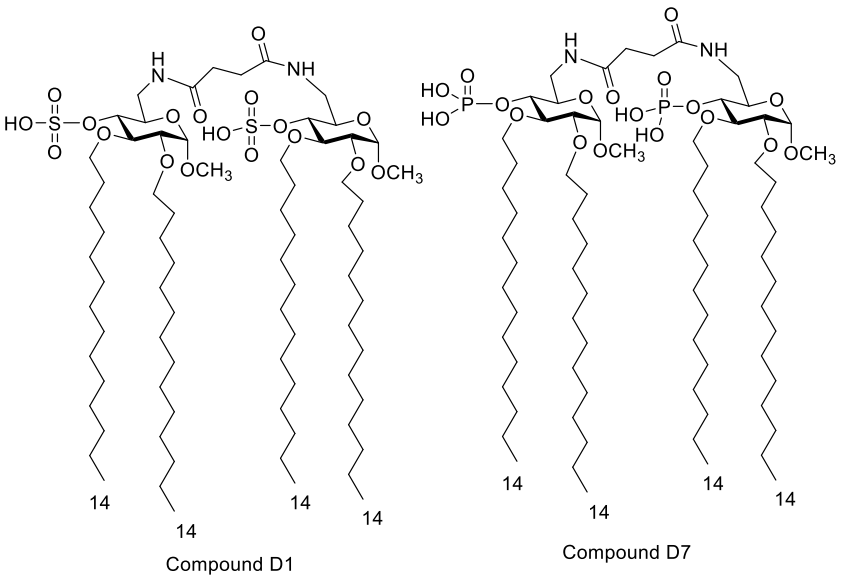

Figure 41. Our dimeric compounds D1 and D7. [173]

Unfortunately, diphosphate D7 was insoluble in water, precluding its biological characterization.
D1 was tested on HEK-Blue cells, a stably transfected line of HEK293 cells expressing human TLR4, which were supplemented with soluble LBP, hMD-2 and hCD14 and showed a dual activity: it behaved as a TLR4 antagonist when co-administered with LOS from Neisseria meningitidis, and as TLR4 agonist when administered alone. Further experiments showed that D1 inhibited the interaction of LOS with both CD14 and MD-2·TLR4, presumably occupying the same receptors binding sites.

7.2 SAR of disaccharide-based TLR4 agonists and antagonists

Summarizing what stated in the sections regarding TLR4 recognition process and its related PRR, and gathering all the useful information available for SAR for Lipid A derivatives, the biological activity of endotoxin (lipid A, LPS, and LOS) and synthetic TLR4 modulators appears determined by the still not clarified interplay of two different factors:

- The interaction of lipid A/LPS single molecules with MD-2;
- The 3D structure of lipid A/LPS aggregates, that very likely influences the first steps of LPS recognition process which involves LBP and CD14 proteins

TLR4 AGONISM

It must be pointed that immunostimulants in murine may be LPS antagonists in human, while usually an agonist in human is also an agonist in murine.
This species specific recognition has not been completely elucidated but it seems dependent upon hMD-2 and mMD-2 slight differences.

In particular in order to have an immunostimulatory effect, that is an **agonist** activation of the TLR4-MD-2 complex dimerization and its consequent intracellular signalling, both in human and in murine, for a disaccharide Lipid A derivatives three structural feature appears fundamental:

- the presence of six acyl chains in order to have a sixth acyl chain protruding outside the MD-2 pocket thus providing the hydrophobic surface necessary for the interaction with the second TLR4-MD-2 complex at dimerization.
  Moreover sixth acyl chains seem to generate a slight change in MD-2 conformation that is crucial to activate dimerization.
- the presence of two phosphate groups so to interact with the positive residues at the edge of the rim of the MD-2 pocket, with one phosphate still able to induce a much lower immunostimulation

- a conical shape of the molecule in solution, which give rise to non-lamellar (cubic or hexagonal II) supramolecular micellar aggregates.

  This shape is the one possessed by a compound with six acyl chains asymmetrically distributed and of particular length and two phosphate groups.

  A symmetrical distribution on the contrary seems not able to generate a conical shape.

Any structural variation to structure of *E. coli* Lipid A and in particular any changes with respect to the number of acyl chains, their length, their position and the number of phosphate groups resulted in a lower or absent activity, as already reported by Rietschel at al. in 1994[126] (figure 42).

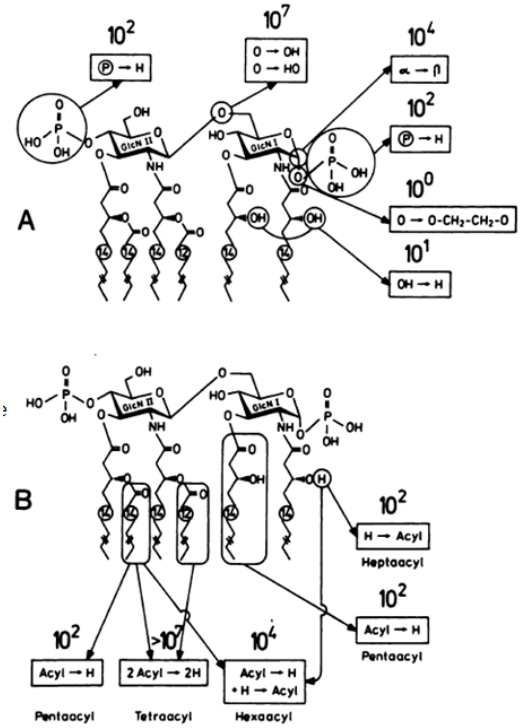

Figure 42. Schematic representation from Rietschel at al. 1994[126] of SAR for Lipid As. Shown are the chemical modifications with respect to *E. coli* Lipid A and the factor by which the structure generated is less active than it. **A**) Modifications to the hydrophilic regions **B**) modifications to the hydrophobic region

One of the very few exception to the first (and partially the third) feature is OM-174.

Very interestingly, the triacyl lipid A part structure OM-174 with a normal disaccharide backbone also exhibited a non-lamellar, but not inverted (HI) structure, connected with lower but not vanishing activity in the cytokine assay.[117]

TLR4 ANTAGONISM

On the other hand we have compounds that are able to block LPS immunostimulation, which means that are able to avoid LPS activation of TLR4 by acting as LPS **antagonists** on TLR4.

These compounds indeed interact with the MD-2 receptor of the TLR4-MD-2 complex but in a non-productive way.

However not all compounds lacking immunostimulation are TLR4 antagonists.

The structural features for antagonism cannot be described specifically as for agonism but they are surely related to two effects:

- the ability of the disaccharide to fill as much as possible the MD-2 pocket, which is necessary to hamper LPS interaction with MD-2 pocket.

  However the full capacity of the MD-2 pocket should not be reached.

  This may be the reason why LPS with five or four lipid chains are less active/inactive with respect to Lipid A: they should stay deeper in the pocket than Lipid A and so there should be substantial energetic penalties when the chains move back to the surface of MD-2 for dimerization with TLR4*.
- a cylindrical shape of the molecule in solution, which gives rise to lamellar supramolecular micellar aggregates. Of course not all lamellar aggregates give antagonism.

7.3 SAR of Monosaccharide-based TLR4 agonists and antagonists

As stated earlier it was surprising to see Lipid A monosaccharide partial structures still able to act as LPS antagonists and even more surprising as immunostimulants like their corresponding much complex disaccharide structures.

Since the majority of these compounds were synthesized in the ‘80s and 90’s, and nothing was known at that time about the role of TLR4-MD-2 complex, in search of a possible rationalization of such effects and a correspondence with the effects of disaccharides, researchers focused on CD-14 and in particular on the aggregates shape of such molecules.

TLR4 AGONISM

It was in this way that in 2002 a correlation was found: monosaccharides that still possess a non-lamellar aggregate shape are active as agonists both in human and murine while those having antagonistic activity in both or no activity generate lamellar aggregates. Finally monosaccharides possessing agonistic activity in murine and antagonistic activity in human have mixed aggregates shape.[163]

Moreover it was found that the position of the branched chain also influences activity: if the acyloxyacyl chain is near the phosphate the compound generates a non-lamellar aggregate and exhibits bioactivity, whereas if the acyloxyacyl chain is farer the compound generates a lamellar inactive aggregate form.

However, already in 1998, Funatogawa and Matsuura noted for the first time that the few Lipid A monosaccharide partial structures still able to express **immunostimulation** both in human and in murine as their much complex disaccharide counterparts were all possessing specific structural features and a specific correlation with the active disaccharide structures:[159,162]

- one phosphate/sulfate group in 1 or 4 position
- one glucosamine scaffold
- three chains, one branched and one linear (or three linear chains as in SDZ MRL 953) of C14-C12 length (and by looking at ONO 4007 structure now we can say that also aromatic ring insertion is possible)

Moreover

- the branched chain should be next to the phosphate or the compound will be inactive.[163]
  This feature emerged clearly by comparing monosaccharide 4-monophosphoryl triacyl lipid A compounds (GLA) with an acyloxyacyl chain in the position 3 or 2 and it was studied to be related to molecular shape and the corresponding aggregate form: the former are active and have a non-lamellar aggregate structure; the latter are inactive and a have lamellar aggregates.

Funatogawa and Matsuura proposed that these structural features correlate with the disaccharide structural features since 1 phosphate 1 glucosamine scaffold and 3 chains are exactly half of 2 phosphate 2 glucosamine scaffold and 6 chains, that is the distinguish feature of the most active types of Lipid As.

In 2003 Tamai et al. found a clear dependence of the activity of GLA compounds on TLR4 receptor activation.[164]

However, to my knowledge, still nowadays no detail is known about GLA interaction with MD-2 and the role of its structural features in this interaction.

A two-monosaccharide binding with respect to the one-disaccharide binding could happen.

If two tri-acylated molecules enter the MD-2 pocket maybe a sixth acyl chain could still protrude outside the pocket to permit dimerization.

The clarification of the interaction of monosaccharide agonist compounds with MD-2 at least with proofs of such interaction has been a main aim of my PhD project.

Active monosaccharide Lipid A partial structures, like SDZ-MRL-953, thanks to their lower immunostimulatory activity associated with no toxicity, could become extremely important compounds to be used as adjuvant in vaccines.

However the number of Lipid A monosaccharide available (that means variation in chain length but also in chain type) is very limited which also hampers SAR studies.

TLR4 ANTAGONISM

The same gap is present in the study of monosaccharide LPS antagonists, like CRX-526 and SDZ-880.431.
The structural features required for antagonism are not clearly defined as for disaccharide structure, in the sense that not all violation to agonism molecular and aggregate requirements are antagonist compounds.

As for monosaccharide agonists, the number of Lipid A monosaccharide antagonists is very limited which also hampers SAR studies.
An important part of the work in this direction has been done by our group during the last years thanks to the synthesis of Lipid X derivatives like our FP7 compound[174] (see section 1.1 of chapter II) and other variants and the related biological but most importantly MD-2 binding studies performed, which confirmed the role of MD-2 in these compounds activity.
It can be said that the fundamental feature for antagonism are:

- Two phosphate groups, to anchor to the MD-2 edges of the pocket
- two chains of C12-C14 length (C10 chains still possess low antagonistic effect, C16 no effect)
  despite a higher (three and four) number of chain (on a two phosphate monosaccharide) has been obtained at the end of the '80s but tested only (to my knowledge) for immunostimulatory activity and their ability to enhance nonspecific resistance to microbial or viral infections

In general however monosaccharides possess much lower antagonistic activity than antagonistic disaccharides and this is not a desirable feature differently from agonists.

As for agonists rationalization is still at the beginning.
Again, since with FP7 we demonstrated that MD-2 binding is involved, two monosaccharide-binding with respect to the one disaccharide-binding could happen.
If two molecules enter the MD-2 pocket maybe they will be able to fill the pocket with four chains as antagonist disaccharides Lipid IVa and Eritoran, thus hampering the binding of LPS to MD-2.

7.4 Non-sugar TLR4 modulators and natural TLR4-modulators

Different compounds that do not possess a sugar scaffold but still possess an effective disposition of hydrophobic and ionic groups have proved interesting LPS-like or LPS antagonistic activities correlated with MD-2 binding.

Some these structures have been designed to mimic Lipid As, like phospholipid dimers, others, have been tested after comparing their structural similarities to Lipid As, and have been found to act as TLR4 modulators like bis-ANS.
These compounds still permit to grasp important SAR.

TLR4 modulators totally unrelated to Lipid A structural features are present: like auranofin, JTT705, heme/hemin and its derivatives like coprohemin and thalidomide. [101]

Also different natural compounds as opioids like naloxone and naltrexone or taxane paclitaxel, cinnamaldehyde, isoliquiritigenin, 6-shogaol, caffeic acid ester and curcumin were found to be TLR4-active compounds. They are discussed in section 7.4.4.

7.4.1 Phospholipid dimers ER112022, ER111232, ER112066, E6020 and OM294

Based on the structure of lipid A, in 2002 Hawkins et al. hypothesized that a phospholipid dimer containing a total of six lipid chains, or three lipid chains per monomeric unit, and an stable diamine linker between the monomeric units, to mimic the glucosamines of the lipid A structure, would be sufficient to obtain biological activity.[175]
In this way compound **ER112022** (figure 43) was prepared and it was found to have agonistic lipid A-like activity in human whole blood, determined by the release of TNF-α.[175]
This finding prompted these researchers to generate additional dimeric molecules to investigate the structural requirements for biological activity *in vitro*. Further simplification provided the more active compounds **ER111232** with a shorter dimer linker, **ER112066** with saturated lipids, and **ER119327** with non-functionalized lipids.

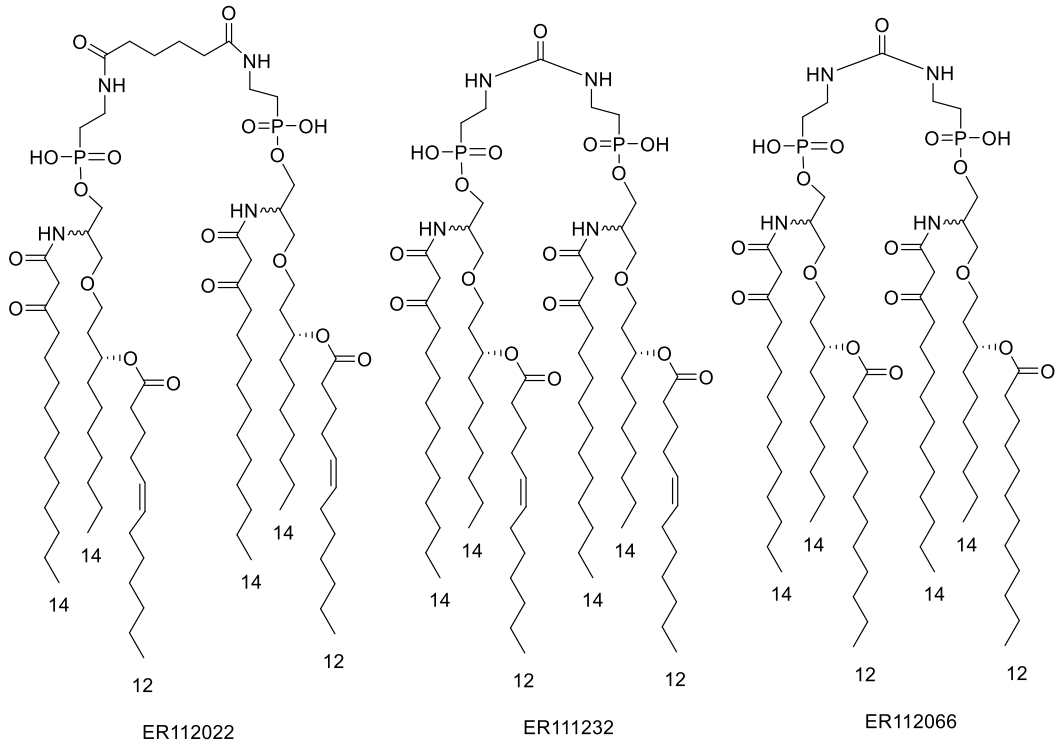

Figure 43. Phospholipid dimers ER112022, ER1112322, ER112066

The distance between the phosphates in ER111232 approximates the distance observed for the lipid moieties of lipid As when using simple modeling techniques.

To learn whether these synthetic agonists activate cells through the same or similar signaling mechanisms as LPS, they have been tested for their ability to induce NF-B activity in HEK293 cells stably expressing TLR4, MD-2, and an NF- B reporter gene (HEK-TLR4/MD-2/ELAM-luc).

These data indicated that TLR4 mediates the activation of signaling pathways to NF- B by the synthetic agonists.

This was also confirmed by the inhibitory effect on TNF-α release of these compounds in presence of TLR4 antagonist Eritoran.

The degree to which receptor interaction, measured in terms of cytokine stimulation, is sensitive to changes in the configuration of the backbone of these molecules is also of interest and parallels observations on synthetic lipid A analogs.

Moreover this study indicate that while the arrangement in space, chain length, and number of fatty acyl residues in lipid As appeared important for immunostimulant activity, the disaccharide scaffold seems not.

The all-R stereochemistry version of ER112066, developed by the same group, (Ishizaka and Hawkins, Eisai Chemical, Japan[176]) **E6020** (figure 44) is currently the most relevant compound of this class.

This compound demonstrated TLR4 agonist activity both in murine and human.

E6020 has been licensed to Sanofi Pasteur and is being developed as an adjuvant (preclinical phase) for use in vaccines with different application Trypanosoma cruzi, Meningococcus, Influenza and Cancer.[104]

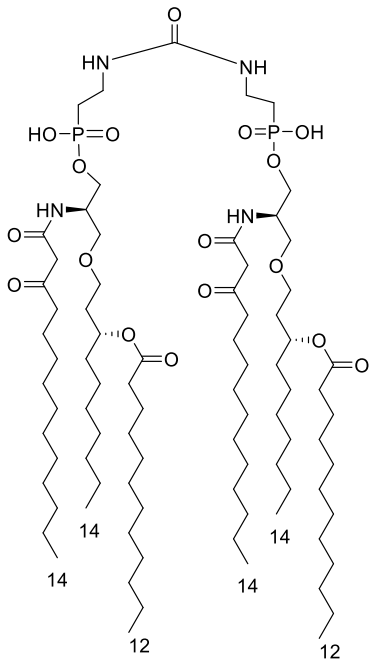

Figure 44. E6020

Inspired by ER112022, Martin et al. (OM Pharma) in 2006 developed triacylated diphosphorylated pseudopeptide backbones called **OM-294-DP** (DP=diphosphorylated) and **OM-294-MP** (figure 45) based on agonistic tri-acylated disaccharide OM-174 but carrying only the essential functionalities of the parent lipid A structure.[177]

This scaffold is a pseudo-dipeptide of orinithine (C terminal aminoacid) and homoserine or aspartic acid (N terminal aminoacid).

All possible stereochemical combinations of the aminoacids have been used and tested.

These compounds showed mixed immunological activities (agonistic/antagonistic), comparable to that of the parent lipid A, while being practically devoid of endotoxicity.

Indeed all OM-294-DP are powerful inducers of NO production, and these activities are comparable to the effect of the "parent" biological molecule OM-174, but aren't inducers of IL-6; moreover they act as strong LPS antagonist but only when LPS is added before the compounds.

OM-294-MP compounds show lower agonistic and antagonistic activities than OM-294-DP compounds.

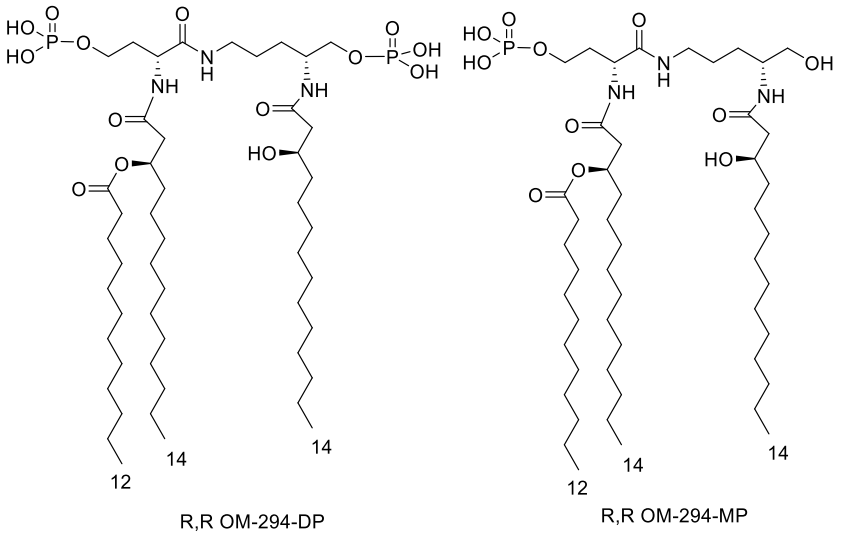

Figure 45. (R,R)- OM-294 DP and (R,R)- OM-294-MP

7.4.2 bis-ANS

bis-ANS (4,4'-Dianilino-1,1'-Binaphthyl-5,5'-Disulfonic Acid) (figure 46) has a hydrophobic binaphtyl core that keeps at 11Å distance two anionic sulfates so its structural pattern is similar to Lipid As. whose phosphates are at 13Å distance.

This distance matches the one between the basic clusters on the surface of MD-2 structural models.

For this reason bis-ANS was selected for a test in 2006 to prove the existence of a hydrophobic binding site in MD-2.[178]

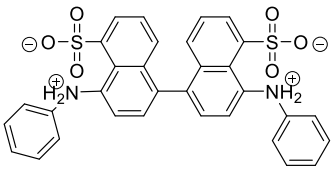

Figure 46. bis-ANS

Indeed this compound was found to bind functional MD-2 *in vitro* with high affinity.

The binding of this dye to a hydrophobic surface leads to an increase in its fluorescence intensity due to fluorescence resonance energy transfer (FRET).

A decrease in the bis-ANS fluorescence on addition of LPS shows that the binding site for bis-ANS overlaps with the binding site for LPS

As a consequence bis-ANS acted as weak LPS antagonist, inhibiting LPS signalling in HEK-TLR4 cells with SEAP gene reporter.

Weaker affinity and antagonistic activity of bis-ANS for MD-2 might be explained by the incomplete match of the two anilino-naphthalene rings of bis-ANS with the hydrophobic pocket, since those groups occupy a significantly smaller volume than acyl chains of the LPS, resulting in an insufficient expansion of the protein

7.4.3 TAK-242

Another very important compound is **TAK-242** (called (R)-(+)-5n in the original paper) (figure 47) developed by Takeda Pharmaceutical Company in 2005.[179]

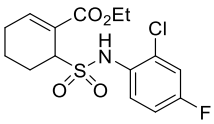

Figure 47. TAK-242

It was developed as a derivative of a lead compound discovered by an extensive screening of the Takeda chemical library in search of a new therapeutic agent for sepsis, using mouse macrophages stimulated with lipopolysaccharide (LPS).

It is a cyclohexene bearing a 2-chloro,4-fluorophenylsulfamoyl and ethyl ester group.

This compound selectively inhibits TLR4 signal and efficiently protects mice against LPS-induced lethality.

Because the high potency shown as antisepsis agent in animal models, TAK-242 was tested in clinic, and passed Phase I and II clinical trials. [101]

However in February 2010 Takeda announced after phase III the discontinuation of clinical development for TAK-242, because the compound failed to suppress cytokine levels in patients with severe sepsis and septic shock or respiratory failure.

Regarding the mode of action of TAK 242, it has been recently shown that TAK-242 binds directly to the Cys747 in the intracellular (ICD) domain of TLR4. As TAK-242 is a Michael acceptor, it has been proposed, but not experimentally proved, that this compound forms a covalent adduct with Cys.747.

It is still however unclear how TAK-242 inhibits TLR4 signalling after TLR4 binding. Upon binding to TLR4, TAK-242 could inhibit myristoylation and phosphorylation of the intracellular TRAM protein, which are covalent modifications essential for TLR4 signalling.

7.4.4 Natural compounds as TLR4 modulators

Plant secondary metabolism provides an endless source of chemically diverse bioactive and pharmacologically active compounds many of which have been used in traditional medicine for centuries without knowing the mechanism of action.

Regarding TLR4, recent studies have been devoted to the search of plant extracts as potential modulators of TLRs.

Interestingly, many herbs used in traditional Chinese medicine (TCM) and Ayurvedic medicine seem to be rich in molecules that interfere with TLR4 activation and signaling. These include green tea, Glycyrrhiza uralensis, better known as licorice, Magnolia officinalis, ginger (Zingiber officinalis), Salvia miltiorrhiza (red sage), and curcumin.[110]

Many efforts have thus been devoted to isolate the bioactive molecules contained in the active extracts.

It was in this way that a lot of natural TLR4 modulators have been discovered.

These include:

- Sulforaphane (SFN), identified from cruciferous vegetables such as broccoli or cabbages
- Curcumin, identified from the rhizomes of the plant Curcuma longa (turmeric)
- cinnamaldehyde, from the cinnamon bark of Cinnamomum trees
- Glycyrrhizin (GL), and chalcone isoliquiritigenin (ILG), identified from roots and rhizomes of Glycyrrhiza plants (licorice)
- Ginger, the rhizome of the herb Zingiber officinalis
- Caffeic acid phenethyl ester (CAPE), isolated as an active constituent of honeybee propolis
- (−)-epigallocatechin 3-gallate (EGCG), from green tea

Also the already known drugs of natural source Taxane paclitaxel, the anticancer drug derived from the Pacific yew tree, the anticancer macrocyclic lactone bryostatin (bryo-1) and opioids like morphine and naloxone were tested on TLR4 and found to be active as TLR4 modulators.

Despite the great structural differences of such compounds, all these molecules seem to share some common structural feature like the presence of phenolic rings.

Moreover cinnamaldehyde, isoliquiritigenin, 6-shogaol, and caffeic acid ester contain α,β-unsaturated carbonyl moieties and this feature that seems fundamental for their activity.

The main mechanism of action proposed for these compounds is indeed the disruption of TLR4.MD-2 heterodimer by formation of covalent bonds with solvent-exposed MD-2 and/or TLR4 cysteines through a Michael addition on the compound itself.

Also sulforaphane that contains a different electrophilic group, the isothiocyanato moiety, seems to forms covalent adducts with MD-2 exposed cysteine thiols, as observed by mass analysis.
On the contrary 1-dehydro-10-gingerdione (1D10G) and curcumin, despite the presence of an unsaturated carbonyl moiety in the latter, seem to inhibit the formation of TLR4 activated complex by interacting non-covalently with MD-2 and competing with endotoxin for MD-2 binding.

All the data on these compounds increase the interest in the identification of active natural compounds and the study of their mechanism of action in search of new chemical scaffolds for developing innovative non-toxic TLR4 modulators.
One of the advantages of such compounds is in principle their better water solubility and bioavailability with respect to lipid A analogues, that are characterized by low solubility in aqueous media due to their amphiphilic nature.

7.4.4.1 Olive oil constituents

Olive oil has long been associated with the many health benefits conferred with Mediterranean diet.[180]
As for other natural sources, olive oil has been inspected in search of the bioactive molecule responsible for its beneficial effect.
In this way the phenolic constituents of extra virgin olive oil (EVOO) were found to possess very interesting biological activities as anti-oxidant, anti-inflammatory and anti-thrombotic agents.[181]
In particular the most active anti-inflammatory phenolic compounds were found to be oleuropein[182], hydroxytyrosol[183] and oleocanthal[184,185](figure 48).

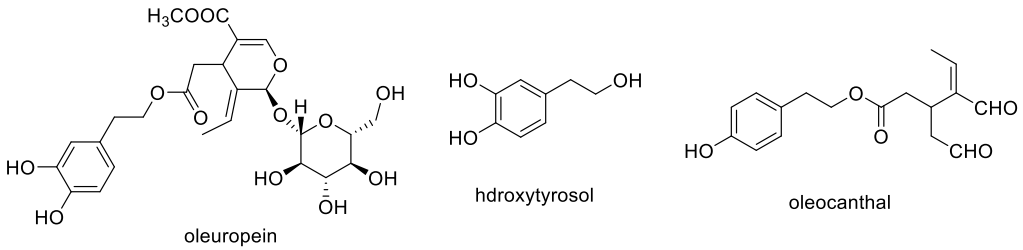

Figure 48. Oleuropein, hydroxytyrosol and oleocanthal.

Also some flavonoids and lignans contained in olive oil, such as apigenin, luteolin and pinoresinol (figure 49) have been associated with anti-inflammatory activity.[186,187]

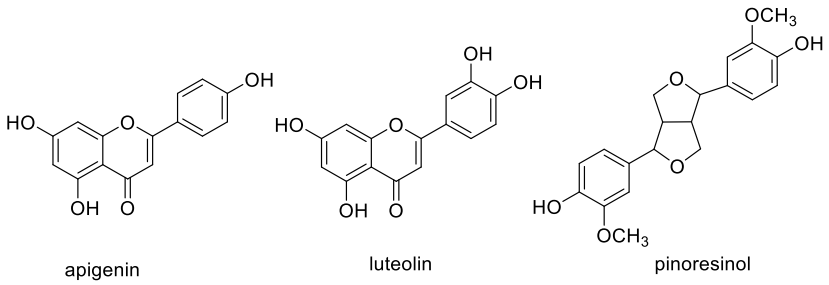

Figure 49. Apigenin, luteolin and pinoresinol

However, despite the anti-inflammatory effect of hydroxytyrosol and oleuropein aglycon appears very likely related to TLR4 antagonism, [188] the activity of the anti-inflammatory compounds of olive oil has not been directly correlated to the activity of TLR4 receptor system yet.

Our research group in the last years tried to fill this gap, investigating the activity of olive oil phenolic extracts and of some isolated phenolic constituents on TLR4 receptor system.

Moreover we have designed and developed different oleocanthal derivative to explore the potential of this class of compounds in search of new TLR4 modulators.

This work will be discussed in the Results and discussion section.

7.5 Non sugar cationic TLR modulators

Also the majority of cationic TLR4 modulators reported in the literature are based on non-saccharide structures however these compounds generally act as “LPS sequestrant” neutralizing its toxicity (antagonists) rather than interacting with the TLR4-MD-2 complex or they interact directly with LBP or CD14.[34]

For this reason they are in general LPS antagonists even if some compounds interacting with CD-14 behave as agonists.

Example includes[34] cationic decapeptide Polymyxin B (PMB)[189] and its Non-toxic derivatives, such as acyl[190] and sulfonamide homospermines[191], DOTAP[192] and diC14-amidine[193], calixarenes[194,195] and the antagonistic IAXO compounds developed by our group. [103]

Aim of the work

This PhD project concerns the design, the synthesis and the chemical and biological characterization of Lipid A partial structures as TLR4 antagonists or agonists.

TLR4 is the innate immunity receptor which selectively recognizes LPS from the Gram-negative bacteria that eluded the physical and anatomical barriers of our organisms.

Due to its ability to trigger inflammatory signal in response to bacterial and endogenous agonists, TLR4 has recently been related to many important pathologies still lacking specific pharmacological treatment: sepsis and septic shock, cancer, atherosclerosis, allergies, asthma, cardiovascular disorder, diabetes.

Compounds able to block TLR4 activation (antagonists) as drugs against these pathologies or able to generate an immunoresponse lower than LPS as adjuvants for vaccine could therefore be of great importance from the scientific and clinical perspectives.

Different efforts have been devoted in the past to this aim by different international groups, after the discovery that the part of LPS responsible for its activity was its disaccharide part Lipid A.
Several *E. Coli* Lipid A derivatives have been developed with variations in chain number, length and type or in the number of phosphate groups, and important SAR have emerged.
However since disaccharide Lipid A derivatives can be obtained only through complex synthesis, the current disaccharides in use in the clinics as adjuvants are still extracted from the natural source and not synthetic.

The difficulty and the cost of the synthesis of these disaccharides and its insufficient scalability are three main reasons why in the past chemists, after the discovery that also the partial structures of Lipid A were active as LPS antagonists or agonists, pointed towards the obtainment of monosaccharide molecular simplifications of Lipid A.

A huge part of the difficulty in this research field, as for disaccharide modulators, is however related to a still incomplete understanding of structure-activity requirements.

Since the key-role of MD-2 has been discovered, different crystal structures of MD-2 bound Lipid A derivatives have been characterized and they have given a visual rationalization to all the effects produced by the different structural changes in Lipid A derivatives.

Moreover the supramolecular aggregates shape of these disaccharides has been found to correlate with their activity, thus suggesting a role of aggregates which has not been rationalized yet.

Also monosaccharide active compounds, almost all developed in the '90s, have been studied as well for their aggregates shape and in 2003 Tamai et al. found a clear dependence of the activity of GLA compounds on TLR4 receptor activation.[164]

Due to the potential relevance of TLR4 modulators in the clinical perspective, the **first aim** of this project has been the design and synthesis of new TLR4 modulators as anti-inflammatory drugs or adjuvants candidates.
The compounds here presented have been designed as innovative derivatives and analogues of monosaccharide Lipid A partial structures which already proved active in the past as LPS antagonists or agonists.
The compounds of this work have been tested in human and murine cells for their ability to induce the production of pro-inflammatory cytokines and for their ability to block LPS immunostimulation.
Since toxicity would hamper any clinical application also the effect on the viability of cells has been tested.

The innovative structural modifications inserted in the compounds of the present work have been designed taking into account what was already known about SAR for agonism and antagonism for monosaccharide Lipid A partial structures.
A **second aim** of this project is the validation and the extension of such SAR available.
This in turn could permit to synthesize more active compounds.

As stated above MD-2 demonstrated its crucial role in TLR4 signaling activation and distinction of LPS or Lipid A active/inactive forms.
Moreover MD-2 binding has been characterized for synthetic disaccharide compounds giving an explanation to its ability to distinguish Lipid As.
However, to our knowledge, still nowadays no detail is known about the interaction of active monosaccharide molecular simplifications of Lipid A with MD-2 and the role of their structural features in this interaction.
The clarification of such aspects, at least with proofs of this interaction and of a correlation between activity/inactivity and interaction/non-interaction with MD-2, has been the **third aim** of my PhD project.

Finally since the aggregates shape is related to Lipid As activity and appears related also to monosaccharide molecular simplifications of Lipid A activity, the **fourth aim** of my work has been the study of the aggregates shape of our new molecules.

This objective relates in turn to a **fifth** one which is establishing, for the first time in literature, a correlation, but not the explanation, since they should be not directly linked, between MD-2 binding and aggregates shape for monosaccharide molecular simplifications of Lipid A.

Natural TLR4 Modulators

The design, the synthesis and the biological evaluation of an olive oil oleocanthal analogue as natural TLR4 modulator will also be presented in this thesis.
This work reflects a previous line of research of our group.
The molecule of oleocanthal has indeed very interesting biological properties and in particular it has been identified to be a very strong anti-inflammatory agent.[184]
However, as for other constituents of olive oil, oleocanthal has never been tested directly for its activity on the TLR4 system. From such studies the identification of a powerful TLR4 modulator or a scaffold to develop a new class of modulators could be obtained.

For these reasons in the last years our group tried to investigate oleocanthal mechanism of action to see if it targets TLR4.
However oleocanthal is not commercially available and despite its synthesis is already reported in literature, it is challenging and time-consuming, so the previous efforts of my co-workers didn't accomplish the goal.
Therefore we designed and synthesize analogues of oleocanthal by maintaining those structural features that are conserved between its already existing derivatives expressing strong anti-inflammatory effects.
These compounds have then been tested for the TLR4 antagonistic activity and the results are presented in the next chapter.

Chapter II

Results and Discussion

1. Monosaccharide molecular simplifications: antagonists

1.1 FP7

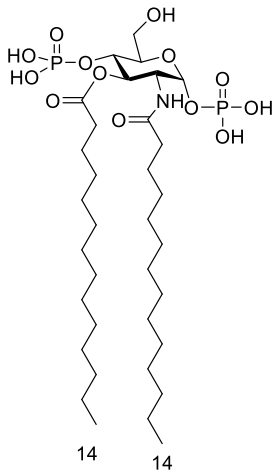

Figure 50. Compound FP7

The first target compound of my PhD project has been the antagonist monosaccharide molecular simplification of Lipid A called FP7 (figure 50).[196]

This compound has already been synthesized for the first time in 2014 by our group[196], however, since we were in need of higher amounts of this compound for a series of new experiments, I worked on the re-synthesis of FP7 trying to improve the yields by slightly varying the reaction conditions.

Indeed FP7 represents one of the leading compounds of our laboratory and the studies performed on it (and its derivatives) have been of crucial importance to understand SAR for antagonism of monosaccharide molecular simplifications of Lipid A.

Moreover extremely relevant studies on its activity on TLR4 and its binding to MD-2 have been performed thus clarifying details of Lipid A partial structures activities that have never been elucidated in literature before.

FP7 has been designed as an analogue of SDZ-880.431.

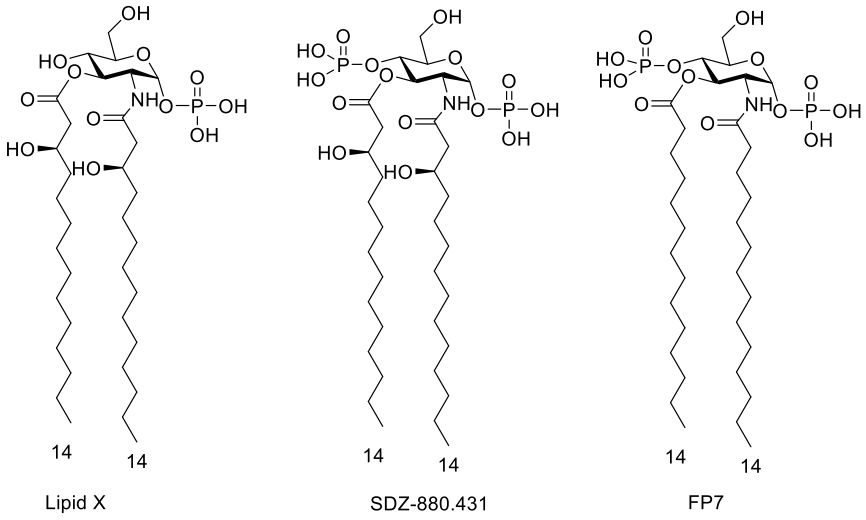

Figure 51. Lipid X, SDZ-880.431 and our compound FP7

SDZ-880.431 (figure 51) is a derivative of Lipid X, the reducing sugar of Lipid A, developed by Sandoz in 1987,[152,153] which possesses just one additional phosphate in C4 with respect to Lipid X.
This compound showed the most potent antagonist activity with respect to all lipid X synthetic analogs synthesized as well as Lipid X itself, on both murine macrophages and human monocytes.[34,152,154]

However this powerful antagonist, developed before the discovery of TLR4 and MD-2 role in immunostimulation, was never tested for its ability to bind MD-2.

Seen the promising results of SDZ-880.431, our group decided to design and synthesize FP7 as simplified version of SDZ-880.431 with myristic chains replacing the β-hydroxyl myristic chains, in search of a new potential TLR4 antagonist.
Moreover we were interested in studying the MD-2 interaction of such molecular simplification of Lipid A.

1.1.1 Previous biological characterization of FP7:[196]

FP7 inhibition of LPS-induced, TLR4-dependent NF-κB activation in HEK-blue cells

The abilities of FP7 and its two derivatives S1 and S2 (figure 52) to activate the TLR4 receptor system or to interfere with LPS-triggered TLR4 activation were first investigated in HEK-blue™ cells, that are HEK-293 cells transfected with human CD14 and MD-2.TLR4 genes.

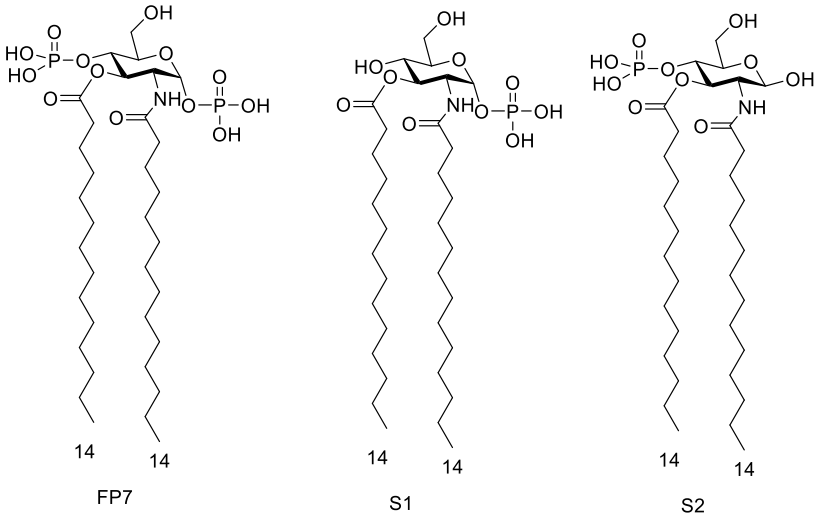

Figure 52. Compound FP7 and its derivative S1 and S2

All compounds showed no immunostimulation.

On the contrary, when cells were pretreated with increasing concentrations of the synthetic monosaccharides (from 0 to 50 µm) and then stimulated with *E. coli* LPS a powerful antagonistic activity was detected for FP7 (figure 53).

On the contrary compounds S1 and S2 were only weakly active in inhibiting LPS-stimulated TLR4 signaling.

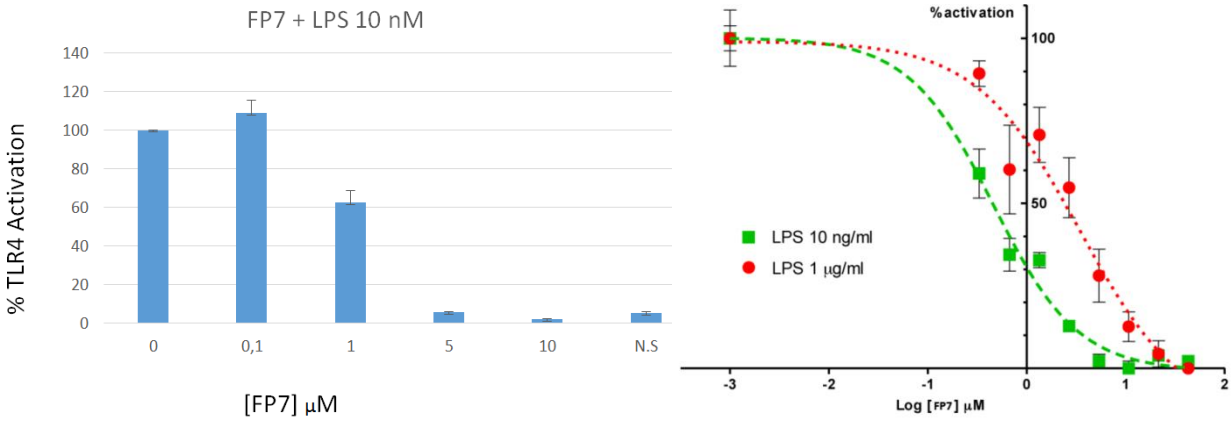

Figure 53. FP7 inhibition of LPS-induced, TLR4-dependent NF-κB activation in HEK-blue™ cells. HEK-blue™ cells (HEK-293 cells transfected with human CD14 and MD-2.TLR4) were treated with increasing concentrations of compounds (0-100 µM) and then stimulated with LPS. TLR4 activation is monitored as sAP production. The results are normalized to activation by LPS alone and expressed as the mean of percentage ± SD of 3 independent experiments. In the second graph data have been interpolated to a 4-parameter sigmoid logic equation to determine the IC_{50} values.

FP7 turned out to be more active as an antagonist at the low LPS concentration (10 ng/mL), with a calculated IC_{50} of 0.46 µm, whereas when LPS was more concentrated the IC_{50} was increased to 3.42 µm.

All compounds showed no or very limited toxicity up to the highest concentration tested (50 μm).

The same antagonistic effect for FP7 only was obtained on TNF-α production in bone-marrow-derived murine macrophages (BMMϕs) from wild-type and CD14-/- mice (figure 54).
FP7 showed a dose-dependent LPS antagonistic activity in wt. cells at the low LPS concentration and in CD14-/- at the high LPS concentration. The antagonist activity on both wt and CD14-defective cells suggests that FP7 competes with LPS in interaction both with CD14 and with the MD-2·TLR4 complex.

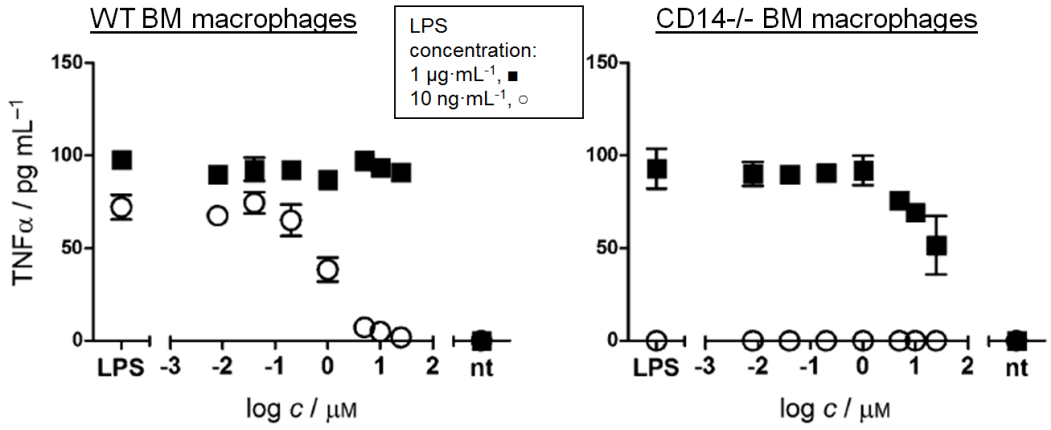

Figure 54. Effects of compounds FP7, S1 and S2 on LPS-induced TNF-α production by BM-derived macrophages. WT or CD14-/- BM macrophages were preincubated with synthetic compounds for 30 min and then treated either with a high LPS concentration (1 mg/mL,■) or a low one (10 ng/mL, ○). Readout was the TNF-α production after one night's incubation.

FP7 MD-2 binding

As stated in section 7.1.3.4, Tamai et al. found in 2003 the first clear proof of dependence of the activity of monosaccharide molecular simplifications of Lipid A (for GLA compounds) on TLR4 receptor activation.[164]

However the role of MD-2 in their activity has not been clarified yet to our knowledge.
Activation of TLR4 could in principle happen through other effects generated by the aggregates shape of such compounds, e.g. intercalation into the membrane and/or activation of potassium channels and thus caspases.[119–124] The correlation between the aggregate shapes of such compounds and their activity has indeed been proved even if not rationalized clearly.

To understand the role of MD-2 at least for antagonist Lipid A partial structures, the binding of FP7 and the inactive S1 and S2 to the MD-2 receptor in solution was investigated first by docking studies and then by means of NMR techniques.

The docked theoretical MD-2 binding energies for compounds S1 and S2 were significantly high, while reasonable lower –energy binding poses for FP7 were predicted.

Analysis of the docked binding poses in MD-2 showed the ability of FP7 to bind in two different fashions, with close predicted binding energies.

Most of the best docked solutions corresponded to binding poses with the two FA chains deeply confined inside the MD2 pocket, similarly to what had been seen with Lipid IVa.

Polar interactions of the phosphates with the charged residues at the rim of the pocket of MD-2 were also identified in some of the docked binding poses.

Docking calculations for FP7 into CD14 were also carried out and FP7 showed binding poses presenting both FA chains inside the pocket, with the polar phosphate groups and sugar placed at the entrance of the cavity, thus supporting the experimental evidence of CD14 binding properties for this compound.

Because of the tendency of FP7 to form stable aggregates at the concentrations required for NMR measurements (150–300 µm), it turned out to be impossible to detect ligand–protein interaction by saturation transfer difference (STD) experiments.

However, it was possible to record good-quality ^{1}H NMR spectra of FP7/MD-2 mixture

and selective attenuation of the signals corresponding to the fatty acid C14 chain protons of FP7 was observed upon addition of MD-2 to the monosaccharide sample solution.

These data suggest the existence of a major interaction of both FA chains of the sugar ligand with the hydrophobic binding cavity of MD-2, as also confirmed by docking calculations.

To our knowledge this is the first direct proof of the role of MD-2 in the antagonistic activity of monosaccharide molecular simplifications of Lipid A.

1.1.2 New results on FP7

Thanks to the batches of FP7 I prepared during the initial part of my thesis, different type of experiments in several types of cellular systems and applications have been performed.

Inhibition of LPS-induced activation of human monocytes and of LPS-induced maturation of DCs

Monocytes and DCs are essential cells for the regulation of innate immunity and inflammation. These innate immune cells reside in different tissues and fulfill various functions.

Monocytes that circulate in the peripheral blood play an important role in the detection of pathogens and danger signals by secreting cytokines and chemokines and are precursors of tissue-infiltrating DCs that are potent antigen-presenting cells during infection.

Monocytes recruited into inflamed tissues can differentiate to DCs or MΦ s depending on the local micro-environment.

Both monocytes and monocyte-derived dendritic cells DCs express TLR4 and stimulation of TLR4 by LPS induces the secretion of proinflammatory cytokines, although the nature of the cytokine response varies according to the cell type (figure 55).

For this reason the TLR4 antagonistic activity of FP7 was tested *in vitro* on human monocytes and monocyte-derived DCs. [197]

In these experiments FP7 almost completely blocked induction of IL-8, IL-6, and MIP-1β , 3 of the major cytokines secreted by monocytes stimulated with LPS (figure 55a).

TLR4 stimulation of DCs induces their phenotypic and functional maturation.

DCs can be stimulated to mature DCs by exogenous pathogen-derived molecules (as LPS) or endogenous danger signals released by cells that are stressed, infected, or necrotic. During the maturation process, DCs acquire enhanced abilities to present antigens resulting from enhanced capturing activity, increased expression of major histocompatibility complex (MHC) antigens, and induced expression of genes encoding co-stimulation molecules and cytokines. Mature DCs can migrate to lymph nodes where they present antigens and prime naïve T cells.

DCs stimulated by LPS showed a classic phenotype of human mature DC (mDC) with a strong induction of CD86 and CD40 expression and increased expression of HLA-DR, CD80, CD83 and CD54.

LPS-stimulated DCs secrete high levels of IL-8, IL-6, MIP-1β and TNFα , as well as IL-12 and IL-10 that are important indicators of their function. FP7 abrogated the enhanced expression of all these phenotypic markers triggered by LPS (figure 55b).

After DC differentiation, FP7 treatment also prevented LPS-induced secretion of IL-8, IL-6, MIP-1β , TNF-α , IL-12 p40, and IL-10 up to 100 ng/ml of LPS and inhibited cytokine secretion induced by 1000 ng/ml (figure 55c and 55d).

Thus, FP7 prevents LPS-induced maturation of DCs.

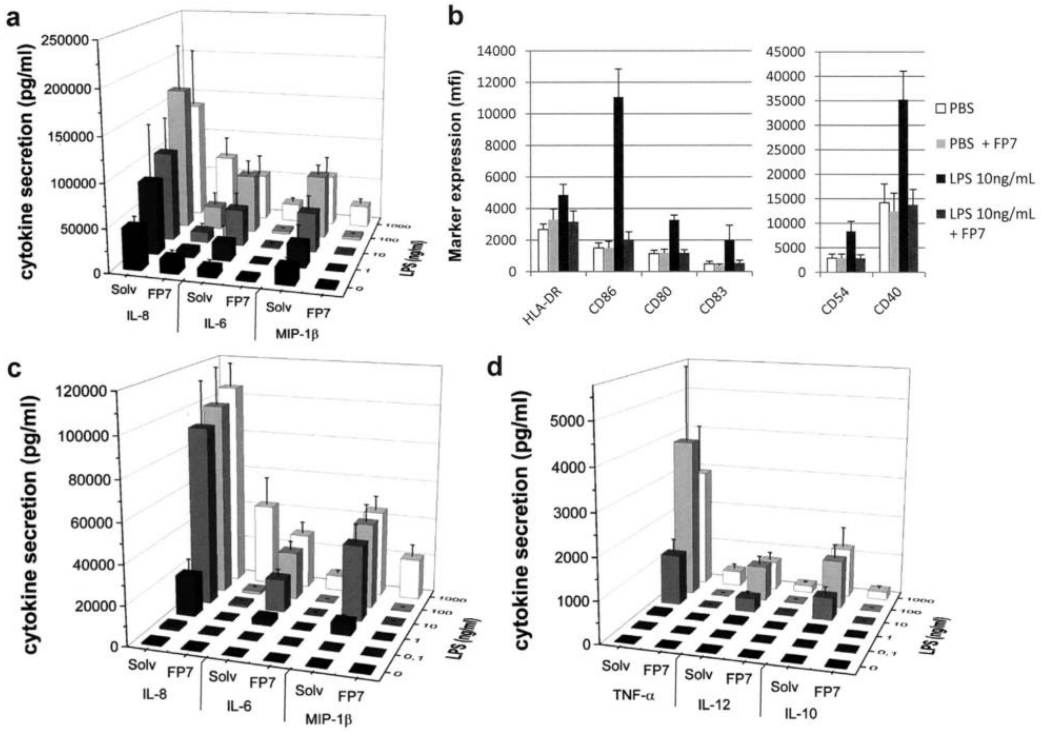

Figure 55. FP7 antagonizes LPS-induced human monocyte stimulation and DC maturation. (**a**) Monocytes were isolated from peripheral human blood, stimulated for 24 h with increasing amounts of LPS or the same volume of PBS as control, in the presence of 10 µ M FP7 or solvent (Solv). Data represents mean cytokine secretion in monocyte supernatants from 4 independent experiments; (**b–d**) DCs were differentiated from human peripheral blood monocytes for 6 days. DCs were stimulated for 24 h with increasing amounts of LPS or the same volume of PBS as control, in the presence of 10 µ M FP7 or solvent. Surface expression of DC maturation markers was monitored by flow cytometry and means ± SEM of fluorescence intensity are shown (b). Cytokine secretion was assayed in DC supernatants by Cytometric Bead Array (CBA). Data represents mean cytokine secretion from 6 independent experiments.

Dose-dependent inhibition of TLR4 signalling in monocytes and DCs

To evaluate the IC_{50} of FP7 on primary cells, monocytes and DCs were pre-treated with increasing doses of FP7 before stimulation with LPS.[197]

The results (figure 56) indicate that FP7 inhibits the secretion of proinflammatory cytokines both in monocytes and DCs in a dose-dependent manner. For monocytes, FP7 IC_{50} was 0.06 µ M for IL-6, 0.13 µ M for IL-8, and 0.07 µ M for MIP-1β secretion. For DCs, FP7 IC_{50} was 0.22 µ M for IL-6, 0.44 µ M for IL-8, and 0.32 µ M for MIP-1β secretion.

These results correlate with the previous data obtained with HEK-Blue™ -hTLR4 cells.[174] Monocyte and DC viability measurements showed that FP7 was not toxic at the maximal concentration of 10 µ M. This concentration of FP7 was thus used in further experiments.

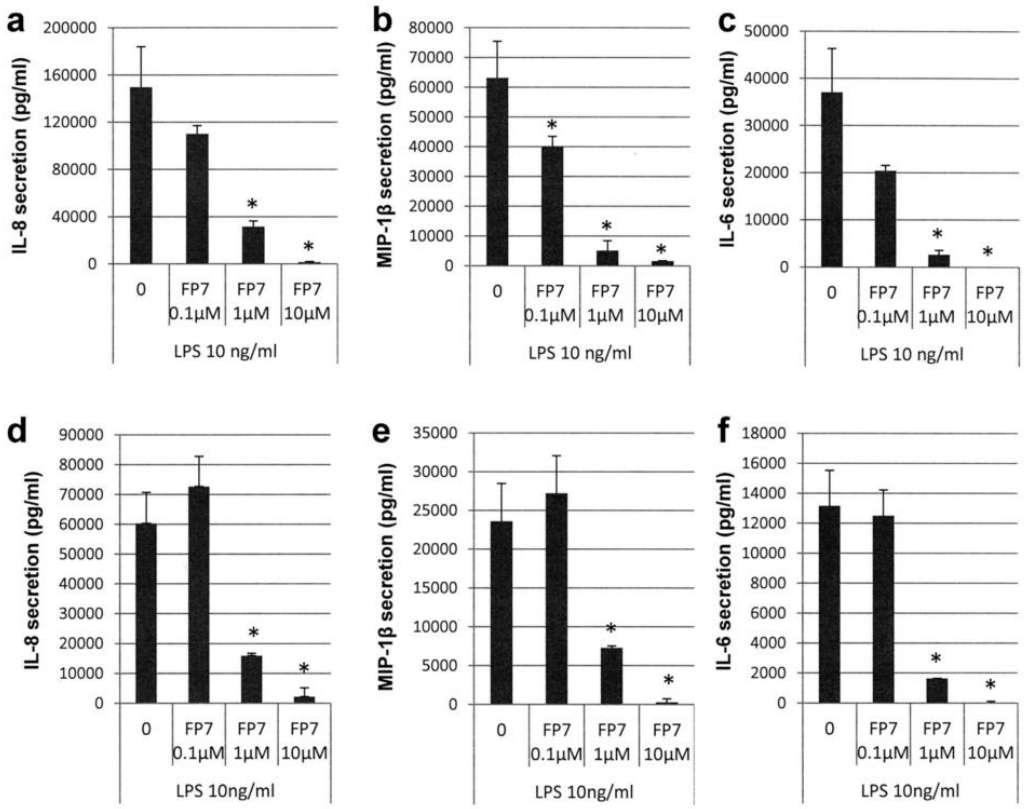

Figure 56. Dose-dependent inhibition of monocyte and DC activation by FP7. Human monocytes (a–c) or DCs (d–f) were stimulated for 24 h with 10 ng/ml LPS, in the absence or presence of increasing amounts FP7. IL-8, MIP-1β , and IL-6 were assayed in supernatants of a representative experiment. *P < 0.05 compared to LPS-stimulated cells.

Assay on selective inhibition of TLR4 signalling in monocytes and DCs

The selectivity of FP7 for TLR4 had not been investigated previously. Indeed TLR4 and TLR2 receptors share the capacity to be activated by lipid ligands.

To determine clearly its selectivity, HEK293 cells co-expressing human TLR4 with MD2 and CD14 (HEK293/hTLR4-MD2-CD14), or TLR1 and TLR2 (HEK293/hTLR1-TLR2), or TLR2 and TLR6 (HEK293/hTLR2-TLR6) were treated respectively with with ultrapure LPS (the TLR4 ligand) or Pam3CSK4 (Pam3) (a TLR1/2 ligand or peptidoglycan (PGN) (a TLR2/6 ligand)[197] (Endotoxin-free ligand Pam3CSK4 (Pam3), peptidoglycan (PGN), and TLR3 ligand double-stranded RNA poly(I:C) (pIC) failed to stimulate TLR4-expressing cells)(figure 57).[197]

FP7 strongly antagonized the stimulation of DCs by TLR4 ligand, whereas it did not affect the stimulation by TLR1/2, TLR2/6, or TLR3 ligands.

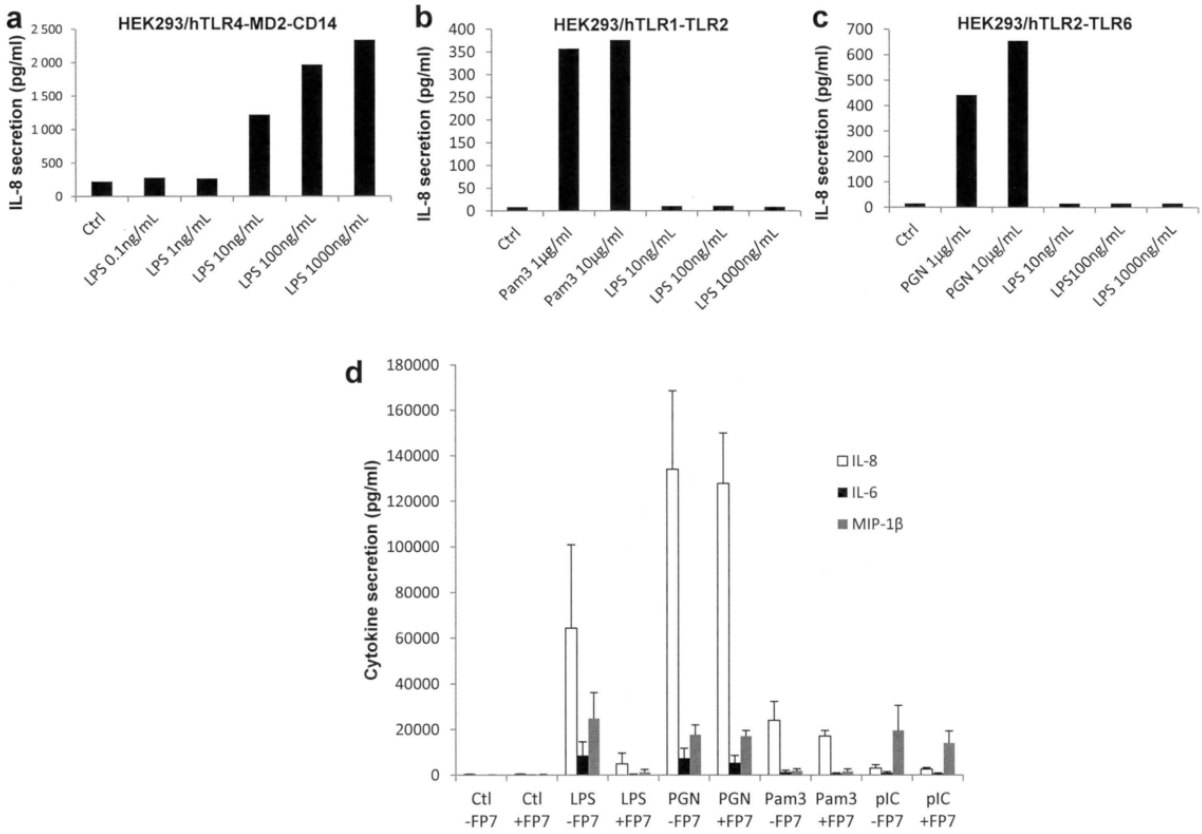

Figure 57. FP7 selectively antagonizes TLR4. (**a–c**) HEK293/hTLR4-MD2-CD14, HEK293/hTLR1-TLR2, HEK293/hTLR2-TLR6 cells were treated 24 h with ultrapure LPS, peptidoglycan (PGN), or Pam3CSK4 (Pam3). Supernatants were collected and IL-8 secreted in response to TLR stimulation was assayed. (**d**) DCs were stimulated for 24 h with 10 ng/ml ultrapure LPS or 10 µ g/ml PGN, PAM3, or pIC in the absence or presence of 10 µ M FP7. Control cells (Ctl) received PBS instead of TLR ligand. Cytokine secretion was assayed in DC supernatants means ± SEM from 3 independent experiments are shown.

Activity on influenza-induced lethality.

Previous studies reported that influenza-induced lethality due to acute lung injury (ALI) was secondary to the cytokine storm triggered by the stimulation of TLR4 by host-derived DAMPs including OxPAPC and HMGB1, which are both TLR4 agonists [198,199].

Interestingly, the TLR4 antagonist Eritoran protected mice from lethal influenza infection and blunted ALI [199,200]. The mechanism of action of Eritoran is suspected to be based on the inhibition of TLR4 activation by endogenous DAMPs produced in the late phase of viral infection.

Although treatment of bacterial sepsis with TLR4 antagonists may be limited to selected patients, there is a large potential of development for TLR4-oriented therapeutics to target sterile or microbially-induced inflammation.

For these reasons the activity of antagonist FP7 *in vivo* during a lethal influenza challenge has been tested (figure 58).[197]

WT mice were infected with mouse-adapted influenza strain PR8 and treated with vehicle (saline; NT), or FP7 for 5 consecutive days starting on day 2 post-influenza challenge (days 2–6).

Treatment of PR8-infected mice with FP7 resulted in significant protection ($P < 0.01$). *In vivo* FP7 strongly reduced influenza infection-induced lethality (figure 58a).

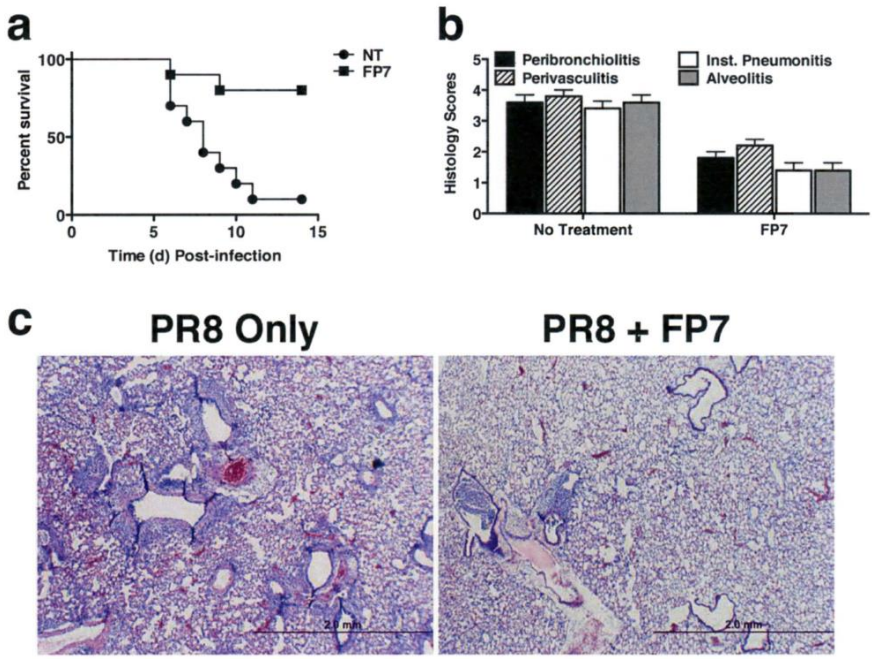

Figure 58. FP7 treatment protects mice from lethal influenza challenge. C57BL/6 J mice were infected with mouse-adapted influenza, strain PR8 (~7500 TCID50, i.n.; ~LD90). Two days later, mice received vehicle (saline; i.v.), or FP7 (200 μ g/mouse; i.v.) once daily from days 2 to 6 post-infection. (**a**) Mice were monitored daily for survival for 14 days (5 mice/treatment group) (a). (**b**) On day 7 post-infection, another group of 5 mice per treatment were euthanized and lungs were extracted and stained for histopathology and examined for tissue damage, necrosis, apoptosis, and inflammatory cellular infiltration. Mean histopathology scores for each group were determined blindly as previously described38 (n = 5 mice/treatment group). (**c**) Representative H&E-stained lung sections are shown.

Haematoxylin and eosin-stained lung tissue sections were analyzed and scored blindly for peribronchiolitis, interstitial pneumonia, perivasculitis, and alveolitis.

FP7 significantly improved the histopathology scores of infected lungs (figure 58b).

FP7 prevented excessive inflammation and lung tissue damage induced by influenza infection (figure 58b,c)

Influenza induces expression of cytokines, i.e., TNFα , IL-1β and IFN-β and chemokines such as KC (murine IL-8) and the accumulation of oxidized products of phospholipids in infected lungs or circulating HMGB1, both of which are inhibited by Eritoran therapy.[199,200]

FP7 led to a significant reduction in influenza-induced gene expression for TNF-α , IL-1β , IFN-β , KC, IL-6, and RANTES (data not shown). These data were confirmed and extended by measuring cytokine protein levels and HMGB1 levels in lung homogenates from mice that were PR8-infected and treated with vehicle only or with FP7.

Given the inhibitory effect of FP7 on the level of cytokines and HMGB1 induced by PR8 infection, it can be reasonably assumed that the benefit of FP7 treatment of influenza virus–infected mice is linked to its ability to inhibit TLR4 signalling by DAMPs like HMGB1 and the subsequent TLR4-dependent cytokine storm.

LPS-mediated motoneuron death inhibition

Increasing evidence indicates that inflammatory responses could play a critical role in the pathogenesis of motor neuron injury in amyotrophic lateral sclerosis (ALS). Recent findings have underlined the role of Toll-like receptors (TLRs) and the involvement of both the innate and adaptive immune responses in ALS pathogenesis. In particular, abnormal TLR4 signaling in pro-inflammatory microglia cells has been related to motoneuron degeneration leading to ALS.

For this reason the effect of FP7 on *in vitro* ALS models has been investigated.[201]

FP7 showed a high efficacy in reducing motoneuron death, since it significantly counteracted the LPS neurotoxicity down to 100 nM (figure 59).

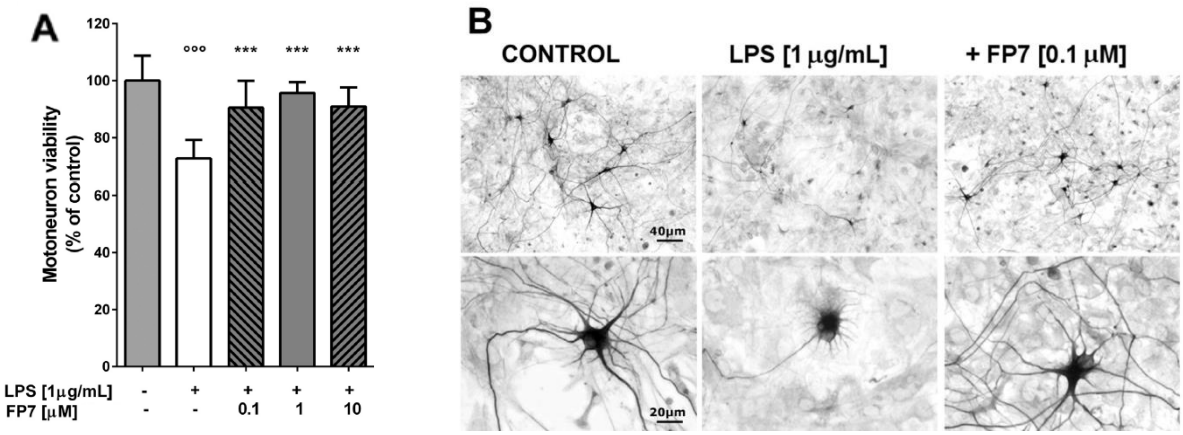

Figure 59. Motoneuron death in cocultures stimulated by LPS: protective effects of FP7. Motoneuron death induced by LPS (alone or in co-treatment with FP7) was assessed in motoneuron/glia cocultures after 24 h of exposure. (**A**) Bars represent mean percentage ± standard deviation of motoneuron death in the different treatment condition compared to control. Data from at least three independent experiments were analyzed. ◦◦◦$p < 0.001$ vs control; ***$p < 0.001$ vs LPS. One-way ANOVA and Tukey's test. (**B**) Low- (upper line) or high- (lower line) magnified representative pictures of SMI32-positive motoneurons maintained in control conditions or treated with LPS alone or in combination with 0.1 μM FP7.

Effects on cytokine and nitric oxide release induced by LPS in spinal cord cultures

In order to identify possible mechanisms underlying the neuroprotective effects of FP7 against LPS toxicity, two inflammatory events known to be elicited by LPS exposure have been investigated: microglia activation and nitric oxide release in motoneuron/glia cocultures.

To study microglia activation, changes in pro-inflammatory cytokine release were assessed in purified microglia cultures. LPS treatment induced increase in IL-1β and TNF-α release in culture medium. Co-treatment with FP7 significantly prevented the LPS-mediated IL-1β release, while no significant effects were observed on TNF-α release (figure 60).

On the contrary, FP7 (tested at the protective concentrations observed in motoneuron death assessment) was not effective on NO release induced by LPS.

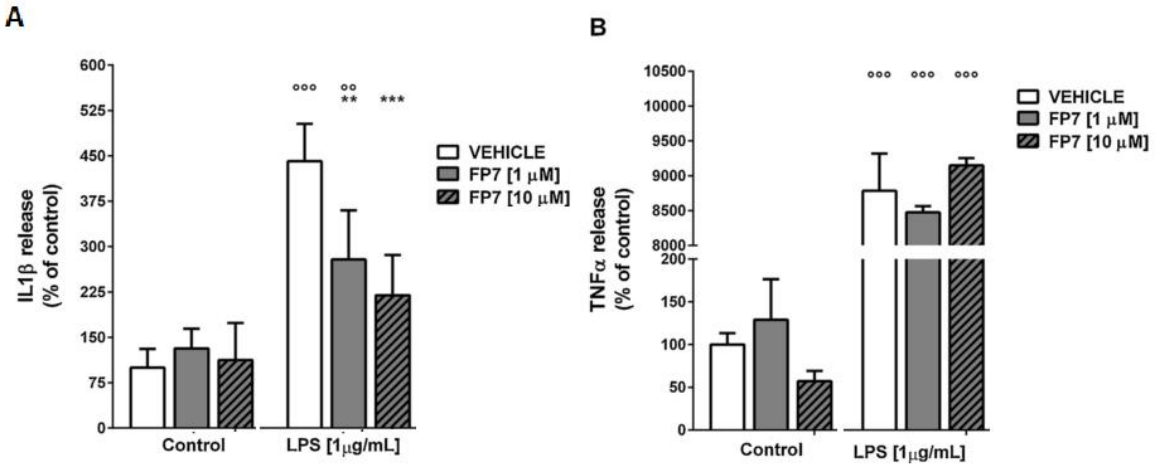

Figure 60. FP7 reduced the IL-1β release by LPS-activated microglia. Purified microglia culture were treated with LPS, 1 or 10 μM FP7, or cotreated with LPS + FP7. IL-1β (**A**) or TNF-α (**B**) concentrations in culture medium was assessed after 24 h by ELISA assay. Bars represent the mean percentage ± standard deviation of cytokine concentrations in medium, normalized to control. Data from at least three independent experiments were analyzed. ◦◦◦p < 0.001 vs control; **p < 0.01, ***p < 0.001 vs LPS. Two-way ANOVA and Bonferroni's test.

Effect on the SOD1mut glia-driven motoneuron death

Microglia carrying the SOD1G93A mutation, typical of familial ALS, are toxic for motoneurons.

In the experiments performed when wild-type motoneurons were cocultured with SOD1mut glia instead of NTg glia, increase in motoneuron death was observed (figure 61).

This neurotoxic effect was prevented when 0.1–1 μM FP7 was added into the medium on the day after coculture establishment, thus confirming again the protective effect of this compound.

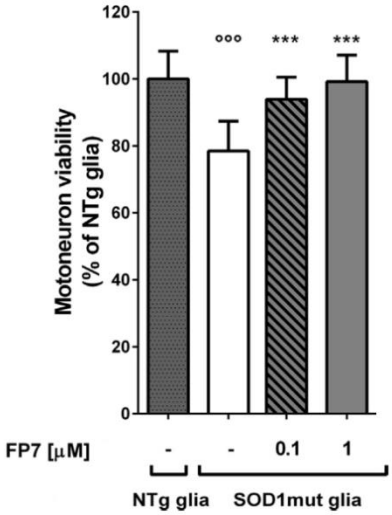

Fig. 61. Motoneuron death induced by SOD1mut glia is counteracted by FP7. Motoneuron death assessed in motoneurons/glia cocultures with wild type or SOD1mut glia after 24 h. Bars represent mean ± standard deviation of the percentage of motoneuron death compared to untreated wild-type motoneuron/glia cocultures (control). Data from at least three independent experiments were analyzed. ◦◦◦$p < 0.001$ vs control; ***$p < 0.001$, vs untreated motoneuron/SOD1mut glia cocultures. One-way ANOVA and Tukey's test.

2. Monosaccharide molecular simplifications: agonists

Agonists of the TLR4 receptor, that means molecule able to induce an immunoresponse as LPS, are molecules of great pharmacological interest.

Indeed, an agonist with no toxicity could be used as an adjuvant in vaccines for an extended range of applications.

Different monosaccharide molecular simplifications of Lipid A are able to induce such an effect and since they are characterized by shorter and less costly synthetic routes, they represent an interesting alternative to classical disaccharide compounds (like MPL and Lipid A) from the clinical and pharmaceutical perspectives.

However SAR for monosaccharide molecular simplifications of Lipid A have not been clearly elucidated, nor the role of their structural features in activating the MD-2-TLR4 receptor system, that is known to be the one activated by LPS and its Lipid A parts.

For all these two reason the **first line of research** of my PhD project has been the design and synthesis of new TLR4 agonists.

2.1 FP11

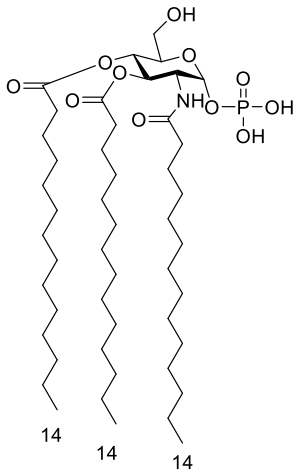

Figure 62. FP11

Aim and Rational design

As stated in section 7.3 of the previous chapter, in 1998, Funatogawa and Matsuura noted for the first time that the few Lipid A monosaccharide partial structures still able to express **immunostimulation** both in human and in murine as their much complex disaccharide counterparts were all possessing specific structural features and a specific correlation with the active disaccharide structures:[159,162]

- one phosphate/sulfate group in 1 or 4 position
- one glucosamine scaffold
- three chains, one branched and one linear (or three linear chains) of C14-C12 length

Funatogawa and Matsuura proposed that these structural features correlate with the disaccharide structural features since 1 phosphate 1 glucosamine scaffold and 3 chains are exactly half of 2 phosphate 2 glucosamine scaffold and 6 chains, that is the distinguish feature of the most active types of Lipid As.

However, being this a totally new line of research of our group, and being the number of monosaccharide molecular simplifications of Lipid A possessing these feature limited, the starting point of my project has been the validation of this rule with our biological studies.

To address this target a new compound that does not distinguish too much from an agonist compound already synthesized and tested in literature, that is respectful of the 1-1-3 rule, have been developed in my PhD project.

Thus validation of the rule and patenting a new compound could be addressed with one target.

The agonist compound selected from literature is the patented SDZ MRL 953,[155] whose synthesis is not described anywhere (figure 63).

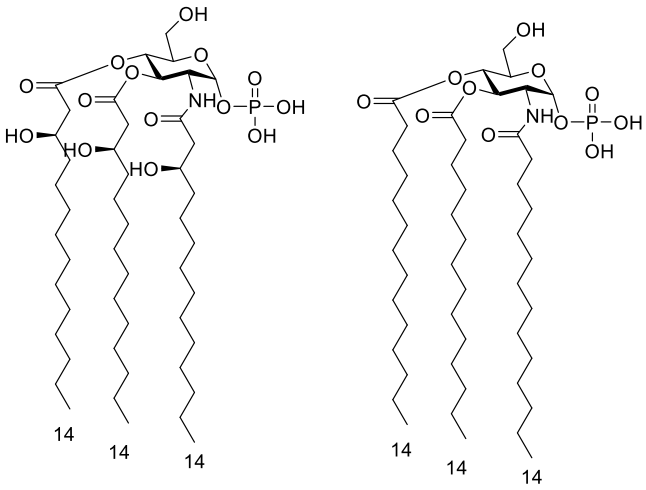

Figure 63. SDZ MRL 953 and FP11

SDZ MRL 953 was developed by Sandoz in 1991 as a Lipid X derivative with an additional chain in C3.

The extremely interesting results that SDZ MRL 953 showed *in vitro* (both in human and murine) as *in vivo* (in murine and guinea pig and in human) are described in section 7.1.3.3 of the previous chapter.

For these results SDZ MRL 953 was selected for a phase I trial in tumor patients in 1997.[157]

Unfortunately, to my knowledge, after all so positive results, this has been the last scientific paper on SDZ MRL 953.

The compound designed in my project differs from SDZ MRL 953 being a simplified version of it with myristic chains replacing the β-hydroxy myristic chains, and we called it FP11 (figure 63).

Synthetic route

The synthetic route designed to obtain FP11 is depicted in scheme 1.

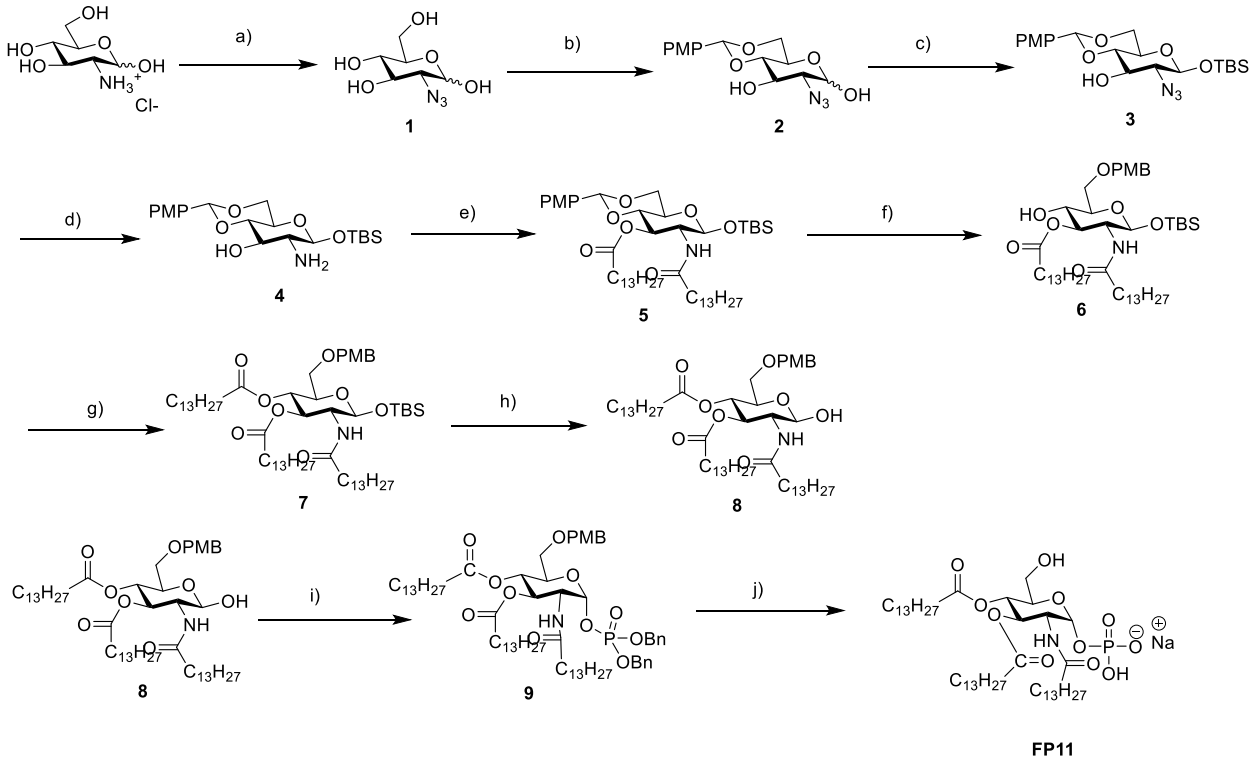

Scheme 1. Reagents and conditions: (a) $CuSO_4$, TEA, Py:H_2O, 0°C, 30 min then TfN_3, Py, 0°C-->rt, O.N., quant.; (b) p-$MeOPhCH(OMe)_2$, CSA, DMF dry, 40 °C, 8h, 68%; (c) TBSCl, imidazole, CH_2Cl_2 dry, rt, 1.5 h, 62%; (d) PPh_3, THF/H_2O, 60°C, 2h, quant.; (e) myristic acid, EDC, DMAP, CH_2Cl_2 dry, rt, O.N., 73%; (f) $NaCNBH_3$, 4 Å MS, THF dry, rt, 1h., then HCl 1M in dioxane, 0°C-->rt, 45 min, 85%; (g) myristic acid, DCC, DMAP, CH_2Cl_2 dry, rt, 1h, 98%; (h) TBAF (1M in THF), AcOH, THF dry, -15°C-->rt, 30 min, 87%; (i) $(BnO)_2PNiPr_2$, imidazolium triflate, CH_2Cl_2 dry, rt, 30 min, then m-CPBA, 0°C-->rt, O.N., 55%; (j) I) H_2, Pd/C, MeOH dry/CH_2Cl_2 dry, rt, O.N., II) Et_3N, III) resin IR 120 H^+ , IV) resin IR 120 Na^+, 82%;

The synthesis of this compound needs glucosamine as starting molecule.

However, since a glucosamine presents several nucleophilic substituents linked to its sugar ring, an efficient synthetic pathway must consist in a series of selective protection and deprotection steps.

The synthesis of FP11 was designed as follows:

- In the first step the amino group in the glucosamine is converted to an azide through a diazo-transfer reaction
- The two hydroxyls on C-4 and C-6 are protected in the second step with ADMA (p-anisaldehyde dimethyl acetal) by formation of a cyclic acetal and CSA (camphorsulphonic acid) is introduced to favour this protection reaction as a catalyst. Its presence allows the conversion of ADMA into a more reactive carbocation, which can be attacked by the hydroxyl groups of compound **2** to give compound **3**.
- The hydroxyl on C-1 is protected by using tert-butyldimethylsilyl chloride as a silylating agent. The reaction is carried out at -10° C to avoid the possible protection of the hydroxyl on C-3, rather than the desired one.

- The azide on C-2 is reduced back to an amine through the Staudinger reduction
- Compound **4** is acylated at C-2 and C-3 with two myristic acid chains using EDC (1-Ethyl-3-(3-dimethylaminopropyl) carbodiimide) and DMAP (4 – N,N –dimethylaminopyridine).
- As the hydroxyl on C-4 needs to be acylated with the third chain, it is deprotected through the reduction of C-7 of compound 5. $NaCNBH_3$ is used as a reducing agent however HCl is needed to complete the reaction. HCl indeed acidifies the solution, so that sodium cyanoborohydryde is more effective.

  This reaction is tricky and must be continuously monitored by TLC to avoid the concomitant undesired deprotection of C-1 and thus the drastic reduction in yield.
- The third acylation, in C-3, with myristic acid is conducted similar to before (EDC and DMAP)
- The trimethylsilyl group on C-1, is removed with TBAF and AcOH to give compound **8.**
- $(BnO)_2PN(i\text{-}Pr)_2$ (Dibenzyl-N,N–diisopropylphosphoramidite), a monoamide of a phosphite diester, is employed together with imidazolium triflate to add one phosphite group to compound **8** on C-1 (with α-stereoselection). In the second step of this reaction mCPBA (meta-Chloroperoxybenzoic acid), a strong oxidising agent, is used to oxidise phosphite to phosphate.
- In order to obtain compound FP11, hydrogenation catalysed by palladium on activated charcoal is applied to intermediate **9** to remove the benzyl protecting group of the phosphates and the p-methoxybenzyl ether (PMB) substituent on C-6. Once the reaction has taken place, triethylamine is added to form the triethylammonium salt of the product.

  However, since the sodium salt has been seen for other similar compounds to be more soluble, an acid Ion exchange resin and an IR 120 Na^+ resin are employed to give the final product in its sodium salt form.

This strategy thus allows the progressive linking of the three acyl chains and the phosphate group.

Following this synthetic route compound FP11 has been obtained in high purity as confirmed by NMR and mass analysis.

2.2 FP111

Aim and Rational design

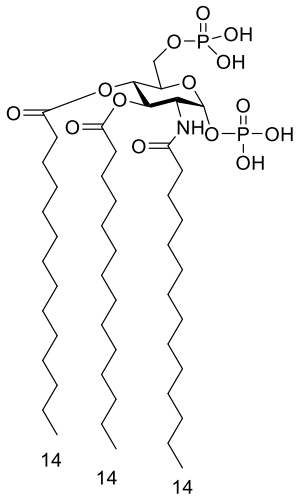

Figure 64. FP111

In order to validate the agonism rule and at the same time explore the effect of new structural features we also synthesized a derivative of FP11, possessing a second phosphate group in C6 (figure 64).

The insertion of another phosphate changes the ratio 1:1:3 seen for agonists structural features, thus in principle no agonism should be observed.

However the addition of phosphate in C6 is a chemical modification rarely explored in literature.
Only 2 monosaccharide molecular simplifications of lipid A are reported with this feature: the triacylated GLAs with two phosphate groups in 4 and 6 GLA 36, GLA 42 (also the 6-monophosphorylated corresponding monosaccharide GLA 35 and GLA 41 have been synthesized and tested). [202]

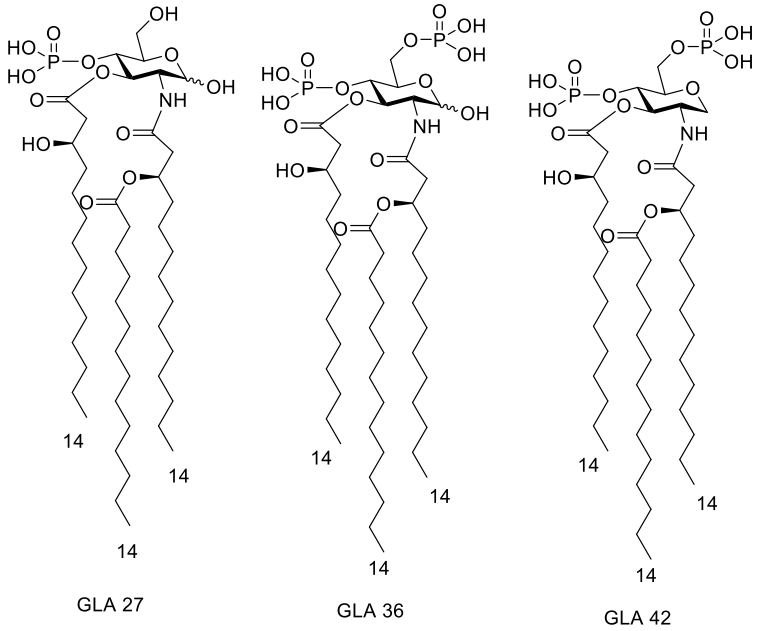

Figure 65. GLA 27, GLA 36 and GLA 42.

Those two compounds showed no Interferon-Inducing Activity nor TNF-Inducing Activity with respect to the murine immunostimulant GLA 27 as expected from Matsuura rule.[202]

However they also reported that GLA 35 and GLA 42 were still able to activate the Limulus ambeocyte lysate gelation.

Moreover a polyclonal B cell activation (PBA) almost identical to that of GLA 27 and a just somewhat weaker mitogenic activity than GLA-27 were observed for GLA-36 (and GLA-35).[203]

On the other hand nothing is known about the TLR4 antagonistic activity of such compounds developed and tested in the '80s, and they still possess two phosphate groups as the active antagonist SDZ-880.431, even if to a different distance, so possibly an new antagonists could be obtained.

Synthetic route

The synthetic route designed and followed to obtain FP111 starts from intermediate **8** of FP11 synthesis (scheme 2).

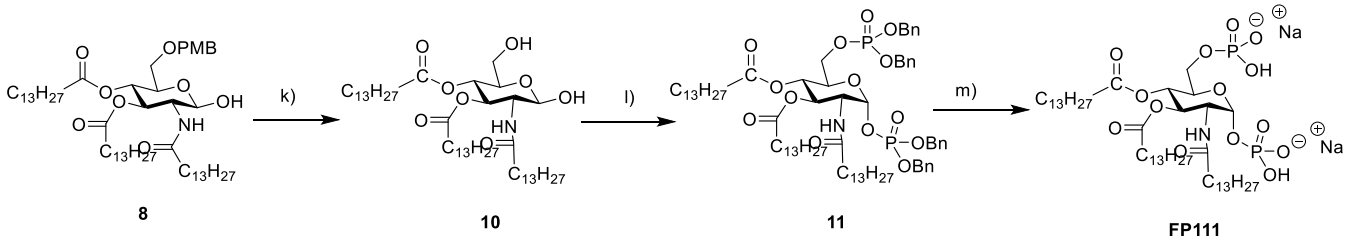

Scheme 2. Reagents and conditions: (k) H_2, Pd/C, MeOH dry/CH_2Cl_2 dry, rt, O.N., 96%; (l) $(BnO)_2PNiPr_2$, imidazolium triflate, CH_2Cl_2 dry, rt, 1 h 30 min, then m-CPBA, 0°C-->rt, O.N., 44%; (m) I) H_2, Pd/C, MeOH dry/CH_2Cl_2 dry, rt, O.N., II) Et_3N, III) resin IR 120 H^+ , IV) resin IR 120 Na^+, 68%.

With a hydrogenation reaction compound **10**, with both C-1 and C-6 free hydroxyls, is obtained so that the following phosphorylation reaction will functionalize both these groups.

Finally, another hydrogenation reaction results in deprotection of the hydroxyl groups on the phosphate giving compound FP111 as its sodium salt.

2.2.1 FP11 and FP111 NF-κB induction

Monosaccharides FP11 and 111 were tested for their ability to activate the TLR4 receptor system in HEK-Blue™ cells using LPS as positive control.

HEK-Blue™ cells are used by our group, as by others in literature, for the initial screening of the activity of our molecules.
If positive results arise (in agonism or antagonism), following experiments are then performed on monocytes and macrophages (as for FP7) which are much more realistic systems.

HEK-Blue™ cells are indeed HEK-293 cells stably transfected with human TLR4, MD-2, and CD14 genes.
Moreover HEK-Blue™ cells stably express a gene reporter which codifies for a secreted alkaline phosphatase (SEAP). This gene is placed under the control of a promoter inducible by several transcription factors such as NF-κB and AP-1 whose production is induced by TLR4 activation. This reporter gene allows monitoring the activation of TLR4 signal pathway by agonists via a colorimetric assay.
If LPS/agonists binding activates TLR4 dimerization and thus its intracellular signaling and the production of transcription factor NF-κB, SEAP is in turn secreted.
By adding a substrate of SEAP, to the cell culture media, as para-nitrophenilphosphate (pNPP) an enzymatic reaction takes place with the formation of p-nitrophenol, characterized by a strong absorbance at 405 nm.
The intensity of absorbance measured permits to quantify the degree of TLR4 activation.

In the HEK-Blue™ hTLR4 cells assay, (figure 66) compound FP11 was able to stimulate TLR4-dependent sAP production in a dose-dependent way at concentrations higher than 5 μM, with a 30% activation with respect to LPS at concentrations 10^3 times higher than LPS.
The EC_{50} calculated is 12.35 μM.

Differently from FP11, compound FP111 was completely inactive at the concentrations tested.
This first test represents a clear confirmation of the rule of agonism stated above and its shows that the addition of phosphate in C6 removes agonistic activity, at least in this model.
Thus this test has been used as the solid base for the start of a totally new line of research of our group based on agonistic monosaccharide molecular simplifications of Lipid A.

Moreover since the activation of the immunoresponse is much lower than LPS, the new and patentable compound FP11 represents a promising candidate to be used as adjuvant in vaccines.

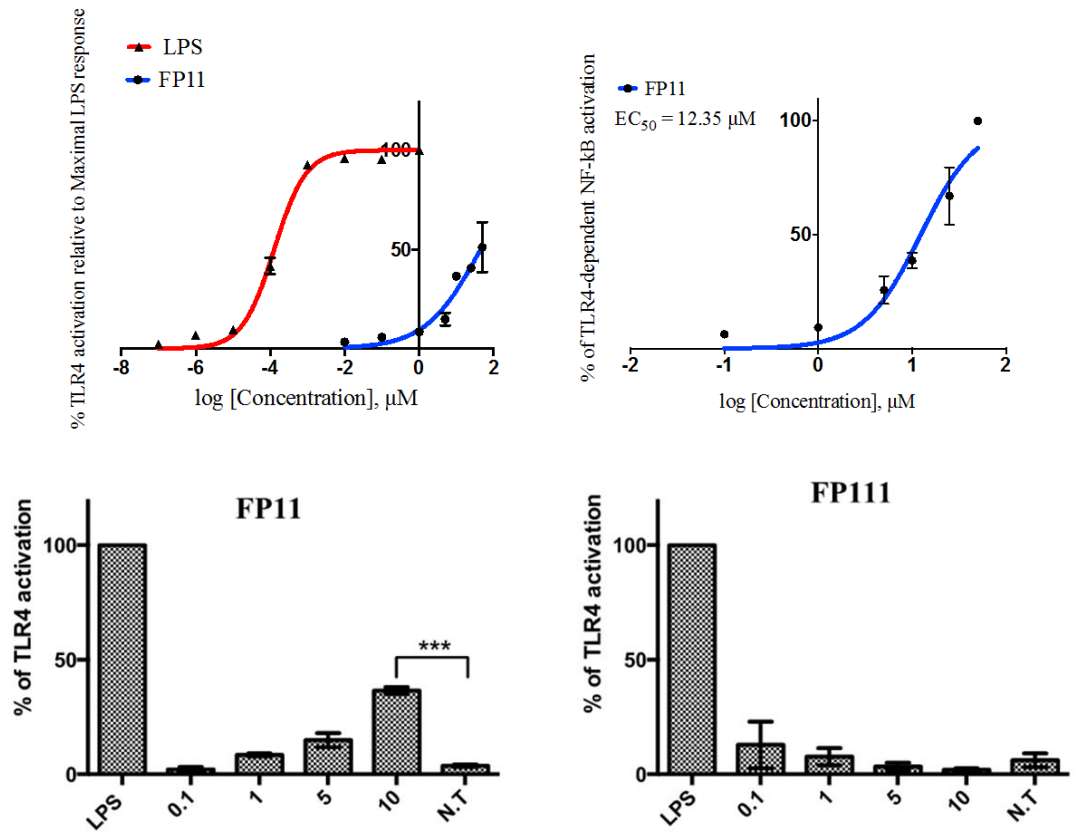

Figure 66. HEK-Blue™ hTLR4 cells assay of FP11 and FP111. HEK-blue™ cells (HEK-293 cells transfected with human CD14 and MD-2.TLR4) were treated with increasing concentrations of compounds (0-10 µM) and incubated for 16-18 hours. TLR4 activation is monitored as sAP production. The results are normalized to maximal activation by LPS alone and expressed as the mean of percentage ± SD of 3 independent experiments. Data have then been interpolated to a 4-parameter sigmoid logic equation to determine the EC_{50} values.

Both FP11 and FP111 were also tested for their ability to inhibit LPS activation of the TLR4 complex in HEK-Blue™ cells pre-incubated with LPS.

None of the compounds showed any antagonistic activity, thus confirming a pure agonistic activity for FP11.

Another main aim of my PhD project, apart from SAR studies and the discovery of new TLR4 modulators, as stated before, was the clarification of the role of TLR4 and MD-2 in the immunostimulation of monosaccharide molecular simplifications of Lipid A.

Thus, to be sure that the biological effect expressed by FP11 was due to the interaction with TLR4, compounds FP11 and FP111 were tested on a HEK-Blue™ Null2 cell line (figure 67).

This cell line expresses the same gene reporter than HEK-Blue™ hTLR4 cells (SEAP), but it doesn't express any of the receptors involved in endotoxins recognition (TLR4, MD-2, CD14).

Both the compounds tested were unable to activate the production of transcription factors NF-κB e AP-1.

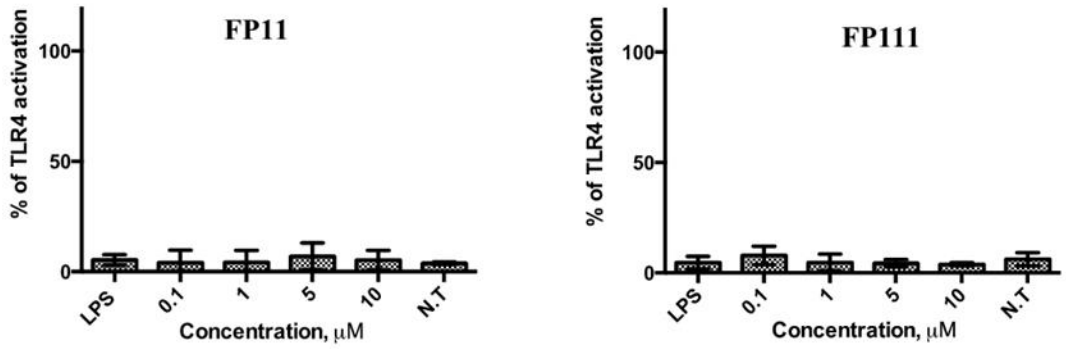

Figure 67. HEK-Blue™ Null2 cells assay of FP11 and FP111. HEK-Blue™ Null2 cells (HEK-293 cells expressing the same gene reporter than HEK-Blue™ hTLR4 cells (SEAP), but it none of the receptors involved in endotoxins recognition (TLR4, MD-2, CD14)) were treated with increasing concentrations of compounds (0-10 μM) and incubated for 16-18 hours. TLR4 activation is monitored as sAP production. The results are normalized to maximal activation by LPS alone and have been interpolated to a 4-parameter sigmoid logic equation to determine the IC_{50} values. Data are expressed as the mean of percentage ± SD of 3 independent experiments.

These data clearly demonstrate that the immunostimulatory effect of FP11 is related to the activation of the TLR4 receptor system.

This is the same confirmation that was obtained for GLAs agonists in 2003.[164]

However these data, as the ones on GLAs, still don't clarify whether there is a direct interaction of agonist monosaccharide molecular simplifications of Lipid A with MD-2 or not, which was another main aim of my PhD project.

2.2.2 FP11 and FP111 MD-2 binding assays

Thanks to the purified MD-2 batches (expressed in the yeast *P. pastoris*) obtained in these years by the work of our group, different MD-2 binding assays have been performed with the purpose to understand such aspect.

One technique to acquire this information is the obtainment of purified crystal structure of the complex between MD-2 and the ligand/synthetic TLR4 modulator. This has already been done on different Lipid A derivatives as reported in sections 7.1, 7.1.2.5 and 7.1.2.6 of the previous chapter.

However different other powerful and well-established techniques are also available.

The binding experiments performed on FP11 and FP111 are Surface Plasmon Resonance (SPR), Antibody-sandwich ELISA assay, Biotin-LPS displacement ELISA assay and fluorescent bis-ANS displacement assay.

Surface plasmon resonance (SPR) analysis

One important technique that could be used to evaluate MD-2 binding of a compound is Surface Plasmon resonance (SPR).[204]

Since the development almost a decade ago of the first biosensor based on surface Plasmon resonance (SPR), the use of SPR has increased steadily.

Surface Plasmon resonance (SPR) is a powerful optical technique widely used and established for monitoring the affinity and selectivity of biomolecular interactions in real-time and without molecular labelling.[204]

SPR allows for analysis of association and dissociation rate constants and modeling of biomolecular interaction kinetics, as well as for equilibrium binding analysis and ligand specificity studies.

In SPR one of the two molecules whose interaction is under study (most frequently a protein) is immobilised onto the sensor surface, a thin metal film usually of gold and its binding partner (the analyte) is injected in aqueous solution (sample buffer) through the flow cell, also under continuous flow.

A beam of polarized light is directed toward the sensor surface during all the experiment and the angle of minimum intensity reflected light is detected. The thin film must be under total internal reflection conditions and in most cases, gold is used because it gives a SPR signal at convenient combinations of reflectance angle and wavelength. In addition, gold is chemically inert to solutions and solutes typically used in biochemical contexts

Since the binding of the analyte to the ligand causes an increase in the mass adsorbed on the thin film,

the reflection angle of polarized light (refractive index) changes as molecules bind (increase in refractive index) and dissociate (decrease in refractive index)(figure 68).

After an analysis cycle is completed, regeneration solution is passed over the sensor chip, removing bound analyte, preparing for the next analysis cycle.

K_D values are then calculated by global fitting of the equilibrium binding responses from various concentrations of analytes using a Langmuir binding model.

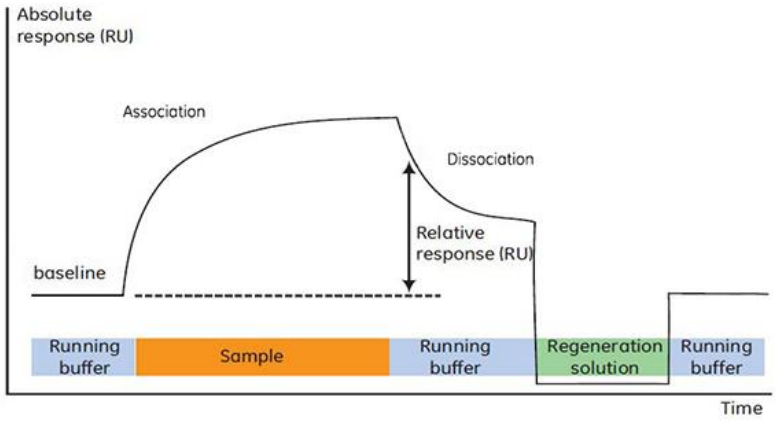

Figure 68. The SPR technique

Although there are several SPR based systems, by far the most widely used one is the BIAcore, produced by BIAcore AB.

SPR has already been used in literature to evaluate binding to MD-2 of different natural compounds, such as curcumin and chalcones, and their synthetic derivatives.[205–207]

During his secondment in the National Institute of Chemistry (KI) of Lubiana, one of my co-workers studied the ability of FP11 and FP111 to bind MD-2 through SPR analyses.
SPR results on our purified receptor MD-2 showed that FP11 binds directly MD-2. A K_D value of 6.5 µM has been estimated (figure 69).

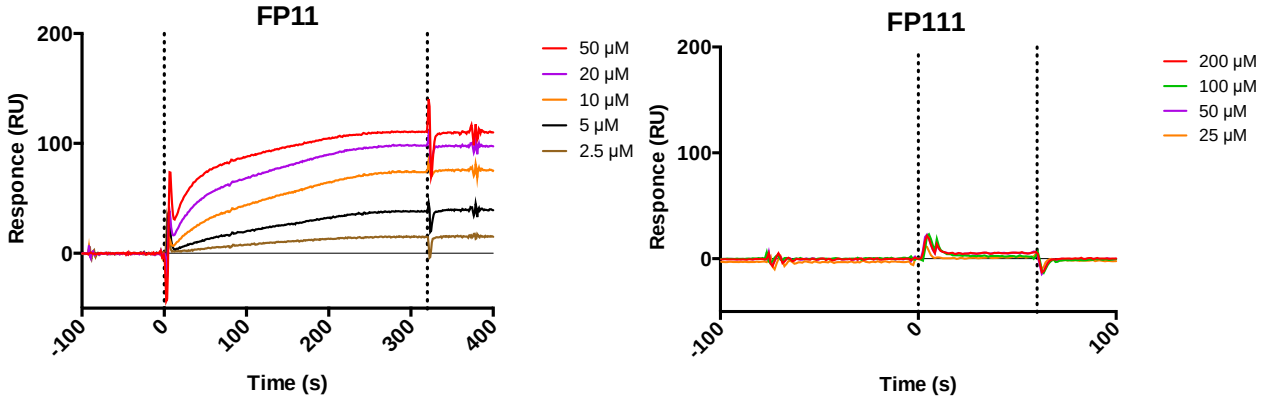

Figure 69. SPR measurements of FP11 and FP111 binding to MD-2. 0.5 µM MD-2 was immobilized onto the sensor chip previously activated with 1-minute pulse of 10 mM NiSO4. First flow cell was used as a reference surface to control non-specific binding. Both flow cells were injected with the analyte at a flow rate of 10 µL/min at 25 °C in increasing concentrations. The data were analyzed with Biacore Evaluation software.

On the contrary FP111 did not show any binding interaction with MD-2.
These experiments confirm that the immunostimulatory effect of FP11, that is its ability to activate TLR4 receptor, is associated with its ability to bind MD-2.

To our knowledge this is the first data in literature correlating agonist monosaccharide molecular simplifications of Lipid A activities to MD-2 binding and the lack of activity to the lack of binding.

Antibody-sandwich ELISA assay

To confirm the results of SPR, an Antibody-sandwich ELISA assay has been performed on our compounds.
In this experiment the ability of our compounds to hamper the binding to MD-2 of an anti-MD-2 antibody is investigated.
9B4 monoclonal anti-MD-2 antibody binds specifically an epitope near the hydrophobic pocket of MD-2. However when LPS is bound to MD-2, this epitope is no more available for such interaction, so no antibody

binding can be detected.[208]

This important information was first exploited in an ELISA assay to determine taxanes binding to hMD-2 (paclitaxel and docetaxel are two LPS antagonists in human) in competition with 9B4 monoclonal anti-MD-2 antibody.[209]

In this colorimetric assay polyclonal anti-hMD-2 antibody was coated on a plate and MD-2 was added.
The binding immobilizes MD-2 on the plate.
Then the compounds to be tested were added followed by antibody 9B4 and goat anti-mouse IgG conjugated with Horse Radish Peroxidase (HRP) which binds 9B4.
Finally ABTS (= 2,2'-azino-bis(3-ethylbenzothiazoline-6-sulphonic acid), a water-soluble HRP substrate that yields a measurable green end product upon reaction with peroxidase, was added.
Detection at 420 nm permits to monitor ABTS colorimetric reaction.
If 9B4 binding to MD-2 is hampered because the ligand binds to MD-2 and its binding site overlaps with the one of LPS, HRP does not remain anchored to the plate after washing so no colorimetric reaction of ABTS is detected at the end.

This first experiment detected a decreased binding to hMD-2 of 9B4 monoclonal anti-hMD-2 antibody in the presence of paclitaxel and docetaxel but not with the inactive roxithromycin, used as a control, thus confirming that LPS antagonism of these taxanes is related to MD-2 binding in a site that overlaps with the one of LPS.[209]

In our experiment compound FP11 induced a decrease in the binding of 9B4 antibody to MD-2 up to 95% at a FP11 concentration of FP11 20 µM (figure 70).
Again FP111 was not able to produce any effect at the concentrations tested.

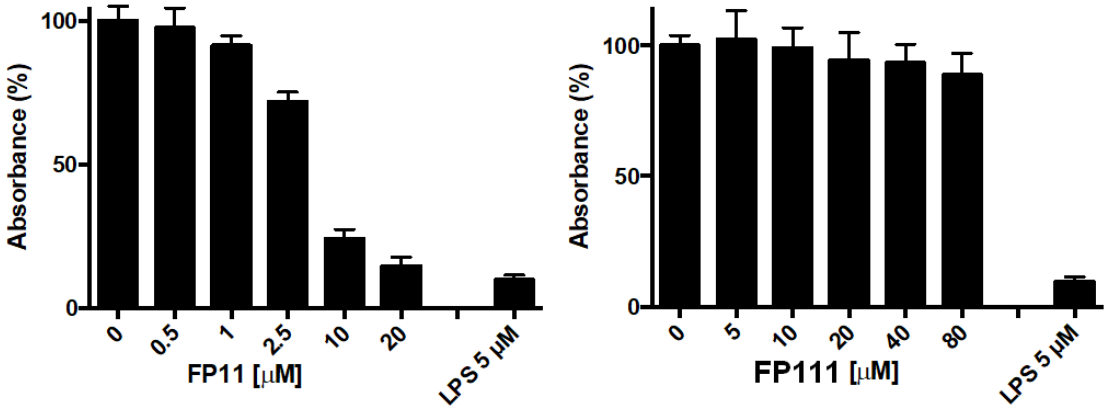

Figure 70. Antibody-sandwich ELISA assay of compounds FP11 and FP111. A microtiter plate was coated with chicken polyclonal anti-hMD-2 antibodies, and 1 µM of MD-2 with tested compounds was added and incubated for 2 hours. 0,1 µg/mL mouse anti-MD-2 MAb (9B4) e 0.1 µg/mL goat anti-mouse IgG conjugated with HRP in PBS were added, followed by addition of 100 µL of ABTS. Detection of absorbance at 420 nm is reported.

Biotin-LPS displacement ELISA assay

Also ligand displacement assays have been performed as non-direct confirmation of MD-2 binding of agonist monosaccharide FP11.

As for SPR, these experiments have already been used in literature to evaluate TLR4 modulators binding to MD-2.[205–207]

An ELISA assay has been used also to determine the ability of the compounds to be tested to displace biotininated-LPS from MD-2 pocket.

Commercially available biotininated LPS is added to the plate coated with MD-2 before adding the compounds. A protein (streptavidin) that strongly binds biotin is successively added. This protein is already bound to HRP so the addition of HRP substrate ABTS produces a detectable colorimetric reaction. The absorbance detected at 420 nm decreases if biotininated LPS is displaced by increasing concentrations of the tested compounds.

FP11 demonstrated the ability to displace biotininated-LPS from the hydrophobic pocket of MD-2 in a dose-dependent fashion with 55% displacement at a 160 µM concentration (figure 71).

FP111 in turn was not able to displace biotininated-LPS even at the highest concentration tested, i.e. 160 µM.

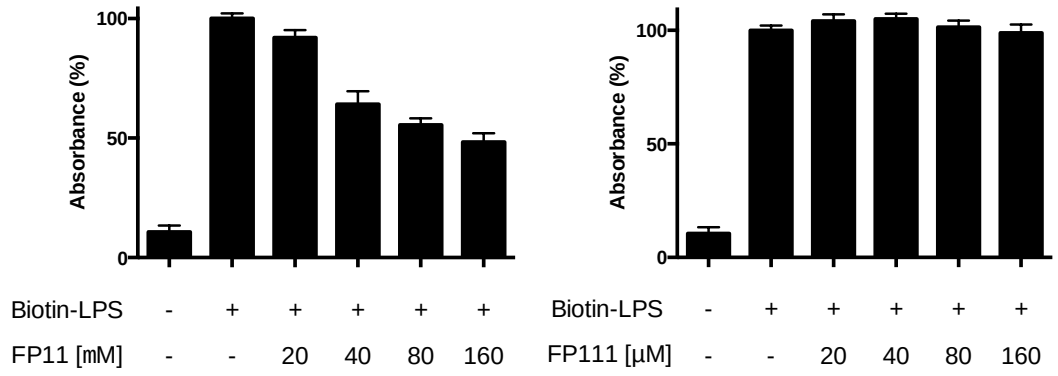

Figure 71. Biotin-LPS displacement ELISA assay of compounds FP11 and FP111. A microtiter plate was coated with chicken polyclonal anti-MD-2 antibodies, and 1 µM of MD-2 with biotin-labeled LPS was added and incubated for 2 hours. After washing, the compounds were added at different concentration and incubated per 1.5 hours. HRP-conjugated streptavidin in PBS was finally added, followed by 100 µL of ABTS. Detection of absorbance at 420 nm is reported.

bis-ANS displacement assay

bis-ANS is a fluorescent compound which was found to be able to bind MD-2 *in vitro* with high affinity thus acting as an LPS antagonist. [178]

The binding of this dye to MD-2 pocket leads to an increase in its fluorescence intensity due to the fluorescence resonance energy transfer (FRET).
Thus the ability of a compound to displace bis-ANS could be determined by fluorescence spectroscopy.

In our experiments FP11 causes a concentration-dependent decrease of bis-ANS fluorescence pointing towards a competitive binding of FP11 to MD-2 (figure 72).
Again FP111 is not able to induce any decrease in the fluorescence of bis-ANS compound at the concentrations tested.

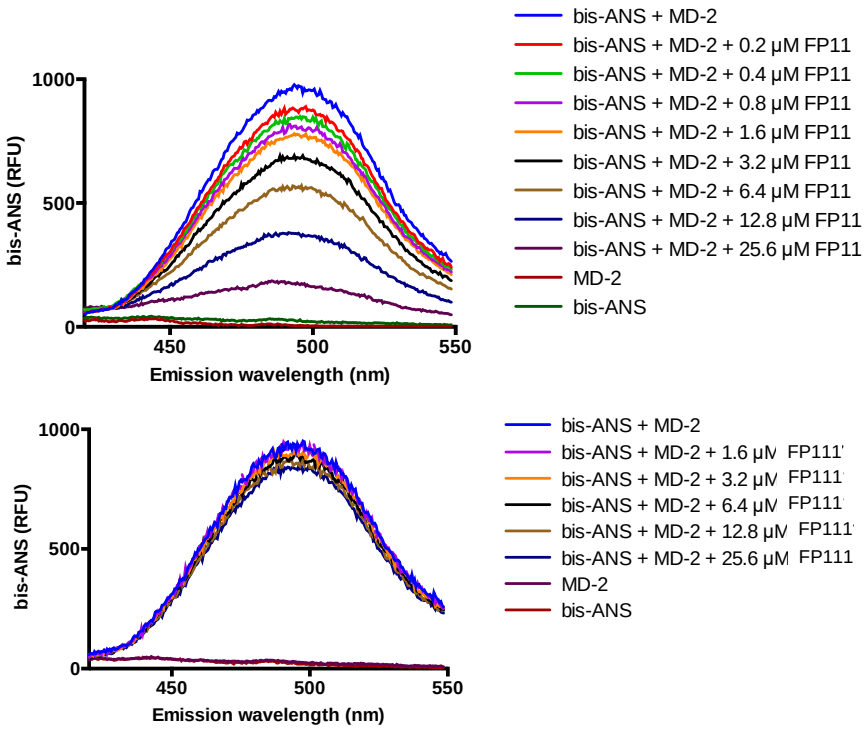

Figure 72. bis-ANS displacement assay of compounds FP11 and FP111. MD-2 protein (200 nM) and bis-ANS (200 nM) were mixed e incubated until reaching stable relative fluorescence units (RFUs) emitted at 420–550 nm under excitation at 385 nm. Compounds, at different concentrations, were then added, followed by relative fluorescence unit (RFU) measurement at 420–550 nm.

2.2.3 FP11 cytotoxicity

The cytotoxicities of the active FP11 has been tested by an MTT vitality assay.

The MTT assay is a colorimetric assay for assessing cells metabolic activity and thus cells viability by which the cytotoxicity (loss of viable cells) or cytostatic activity (shift from proliferation to quiescence) of a potential medicinal agents and toxic materials could be deduced.

NAD(P)H-dependent cellular oxidoreductase enzymes may, under defined conditions, reflect the number of viable cells present and these enzymes are capable of reducing the tetrazolium dye MTT 3-(4,5-dimethylthiazol-2-yl)-2,5-diphenyltetrazolium bromide to its insoluble formazan, which has a purple color.

For these reason MTT is added to the cells pre-incubated with the compound and the concentration of formazan has been determined by measuring absorbance at 570 nm.

HEK-Blue™ hTLR4 cells have been treated with the highest concentration of FP11 used in the previous test (25 e 50 µM).

MTT assay shows that FP11 is not toxic at these concentrations (figure 73).

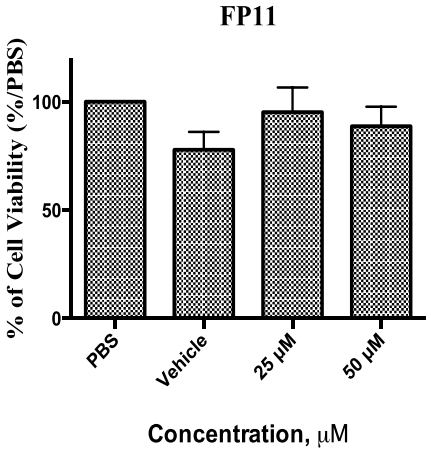

Figure 73. Viability assay (MTT) on compound FP11 (0-50 µM) in HEK-Blue cells. DMSO is used as negative control. The results are normalized on the positive control (cells treated with PBS) and expressed as the mean of percentage ± SD of 3 independent experiments.

2.3 AM158

Aim and Rational design

ONO 4007 (figure 74) is one of the few monosaccharide molecular simplifications of Lipid A currently under clinical studies as adjuvants in vaccine.

It is actually in phase I clinical studies as adjuvants in vaccine against Leishmania.(see section 7.1.3.5 of chapter I)

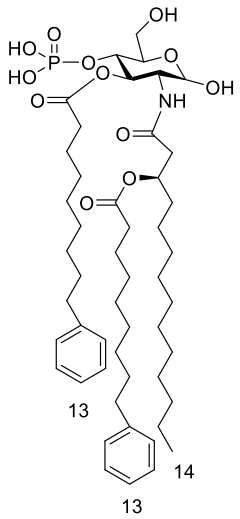

Figure 74. ONO 4007

ONO 4007 is still respectful of the agonism rule 1:1:3 stated above, but it also presents the interesting feature of aromatic rings inserted in two of its three chains.

ONO 4007 represents the most active compounds of a class of monosaccharide molecular simplifications of the non-reducing part Lipid A possessing this feature (figure 75).

In the monosaccharide compounds of this class present in literature (almost all synthesized in the '80s and '90s) the presence of the phenyl ring has demonstrated different effects on the biological activities depending on the position of the phenyl-ring-containing chain (C2 or C3, branched chain or main chain) and the length of this chain.

Also the position of the ring in the chain has been changed in one derivative and in two others the phenyl ring has been used as core from which two chains departs.

Finally also naphthalene rings have been used.

In general a sulfate group has been used instead of a phosphate except in 2 variants. (see section 7.1.3.5 of the previous chapter)

For example in 1987 ONO Pharmaceuticals developed a series of such compounds some of which showed enhancing activity of cellular immunity (e.g. mitogenic activity) to living tissue in murine and an inducing activity of TNF, IL-1 and IFN associated with low toxicity. [165]

On the contrary another series with a phosphate group developed in 1993 showed mitogenic activity only associated with toxicity.[166]

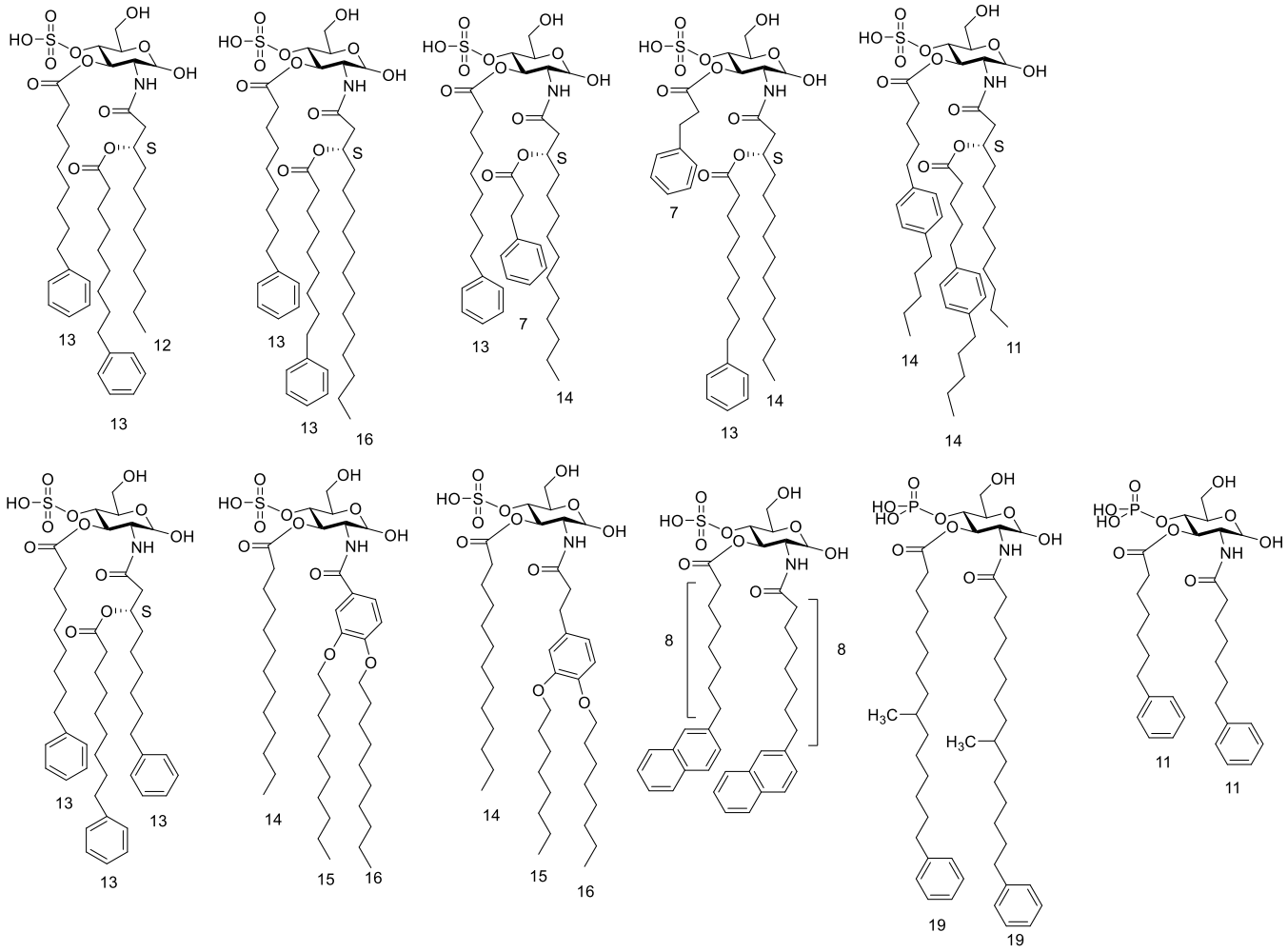

Figure 75. Lipid A partial structures with aromatic chains reported in literature

However, despite the extremely relevant results of ONO 4007, the effect of aromatic chains has been tested only on these few monosaccharide molecular simplifications of the non-reducing part Lipid A and it has never been tested on di-sulfated/di-phosphorylated analogues and most importantly not even on disaccharide Lipid A structures to our knowledge.

Moreover no such analogues of the reducing part of Lipid A have been synthesized.

To investigate with a one-at-a-time-variation approach the effect of aromatic rings on TLR4 activity and MD-2 binding, we decided thus to start from the FP11 compound just developed, to design a novel class of derivatives of the reducing part of Lipid A with aromatic rings at different position in the chain.

Since no aromatic-chains analogues of the reducing part of Lipid A are present this path offers also the possibility to discover new patentable active compounds.

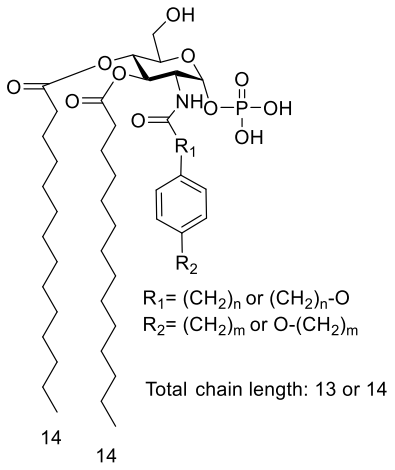

Figure 76. The novel class of FP11 derivatives designed

The compounds designed still possess the features required for agonism while the aromatic-ring-containing chain has been placed near the phosphate group both to mimic ONO-4007 as well as to put the increased spatial requirement of the aromatic ring near the phosphate group as for the active GLA compounds (figure 76).

This in turn was related to active aggregates shapes (see sections 7.1.1 and 7.3 of the previous chapter).

The first representative compound of this class we designed is compound AM158 (figure 77).

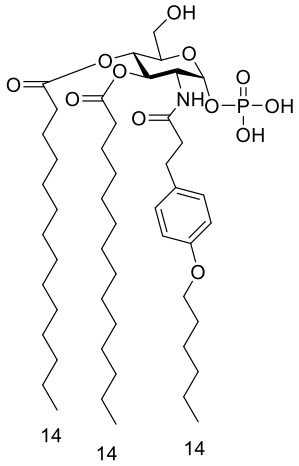

Figure 77. AM158

AM158 is identical to FP11 while it possesses an O-alkyl aromatic chain attached at two carbon distance at C-2 position of the sugar.

In this structure the aromatic ring is somehow higher than in the middle of the chain so being not too close, nor too distant from the sugar core.

Such ring could in this way be used to attach additional chains in a branched GLA-like future compound.

An example of such chain is depicted in figure 78.

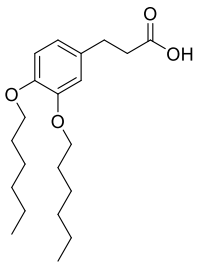

Figure 78. Example of a branched aromatic chain

Synthetic route

The synthetic route designed and followed to obtain AM158 starts from intermediate 8 of FP11 synthesis however the aromatic chain needs to be synthesized.

Scheme 3 shows the path designed and followed for the obtainment of chain A.
Commercially available ethyl 3-(4-hydroxyphenyl)propanoate has been selected as starting reactant to provide the core with the desired features.
An initial Williamson reaction is followed by basic cleavage of the ester to obtain the free acid needed for conjugation to the sugar.

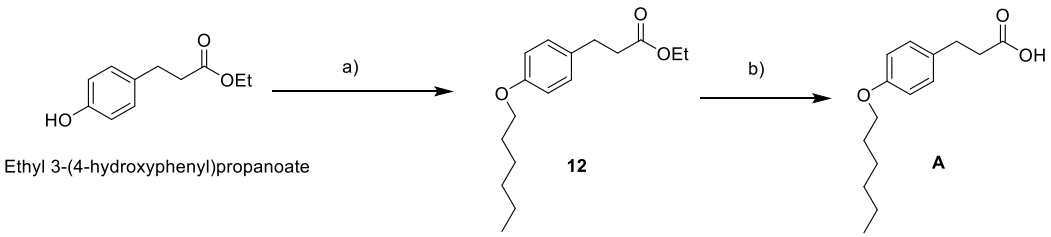

Scheme 3. Reagents and conditions: (a) K_2CO_3, Hexyl bromide, DMF dry, 80°C, 18h, 81%; (b) NaOH aq., MeOH, 2h, 65°C, 96%;

The synthesis of the sugar from the conjugation step on is depicted in scheme 4.

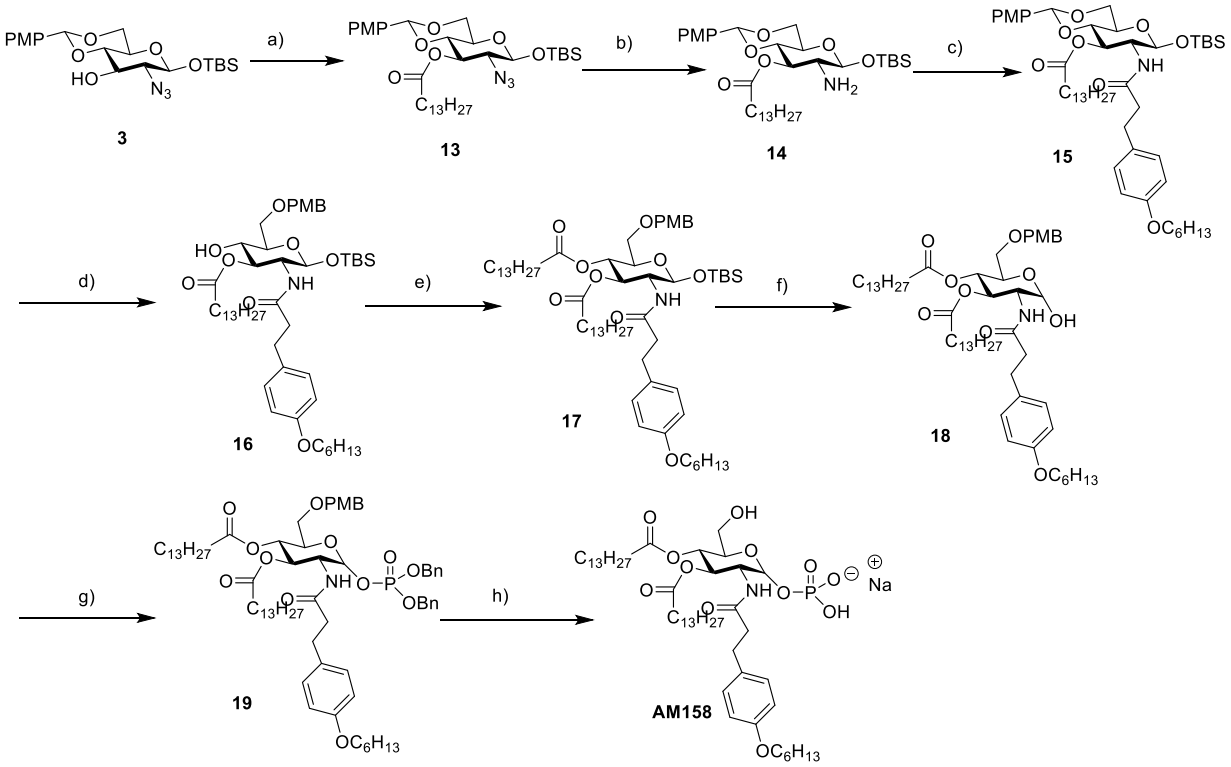

Scheme 4. Reagents and conditions: (a) myristic acid, EDC, DMAP, CH_2Cl_2 dry, rt, O.N., 71%; (b) PPh_3, THF/H_2O, 60°C, O.N., quant.; (c) chain A, DCC, DMAP, CH_2Cl_2 dry, rt, O.N., 70%; (d) $NaCNBH_3$, 4 Å MS, THF dry, rt, 2h, then HCl 1M in dioxane, 0°C-->rt, 20 min, 47%; (e) myristic acid, DCC, DMAP, CH_2Cl_2 dry, rt, 1h, 97%; (f) TBAF (1M in THF), AcOH, THF dry, -15°C-->rt, 2h, 63%; (g) $(BnO)_2PNiPr_2$, imidazolium triflate, CH_2Cl_2 dry, rt, 1h, then m-CPBA, 0°C-->rt, 2h, 59%; (h) I) H_2, Pd/C, MeOH dry/CH_2Cl_2 dry, rt, O.N., II) Et_3N, III) resin IR 120 H^+ , IV) resin IR 120 Na^+, 83%;

Intermediate **3** of FP11 has been selected as the starting point since the amine group in 2 is still protected as azide thus permitting the insertion of two different chains between C-2 and C-3 as desired.

Compound **3** has been initially alkylated with myristic acid, then, after the Staudinger reaction to release the free amine, it has been conjugated to chain A giving intermediate **15**.

Steps d to h are similar to the corresponding steps of FP11 synthesis.

Again, as in FP11 and FP111 synthesis high attention must be put on the acetal opening step, to avoid the concomitant undesired deprotection of C-1 (or even complete PMB removal) and thus the drastic reduction in yield.

2.3.1 AM158 NF-κB induction

Monosaccharide AM158 was tested for its ability to activate the TLR4 receptor system in HEK-Blue™ cells using LPS as positive control.

Unfortunately, in our experiment AM158 failed to express any immunostimulatory activity at the concentrations tested (figure 79).

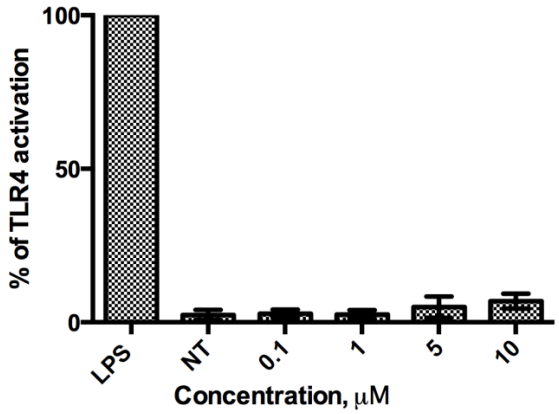

Figure 79. HEK-Blue™ hTLR4 cells assay of AM158. HEK-blue™ cells (HEK-293 cells transfected with human CD14 and MD-2.TLR4) were treated with increasing concentrations of compounds (0-10 μM) and incubated for 16-18 hours. TLR4 activation is monitored as sAP production. The results are normalized to maximal activation by LPS alone and expressed as the mean of percentage ± SD of 3 independent experiments.

Also no antagonistic effect on LPS stimulation has been detected.

Such negative result of its biological activity clearly demonstrates the huge importance of the position of the phenyl ring inside the chain to express immunostimulation.

Future C-2 derivatives will clarify this point, with the specular version of ONO 4007 (but with just one aromatic ring) being the priority.
If not even the specular version of ONO 4007 will show any activity, the presence of the second ring of ONO 4007 should be taken into account for a crucial effect on activity.

3. Monosaccharide molecular simplifications: innovative glycerol chains

Aim and Rational design

Despite the huge number of disaccharide Lipid A structures designed and synthesized in literature, chemical innovation on the type of chains used is still limited.
This offers new possibility in terms of biological activities, structural variation and moreover it opens the way to new patentable drugs/adjuvants.
However the synthesis of disaccharide Lipid A structures possessing also complex chains would make their synthesis even longer and more difficult. Moreover the pattern of chains distribution is crucial.

This somehow hampers the exploration of arrays of new chains for these compounds, except for theoretical docking studies.

Fortunately, the common linear as well the branched chains present in disaccharide are still able to confer an immunomodulating ability to monosaccharide molecular simplifications of Lipid As, while small variation in chains length remove activity as for disaccharide structures.
For this reason, again monosaccharide molecular simplifications of Lipid As present an extremely promising field.
New chain-types can be inserted in these compounds with fewer efforts and in this way two aims in one could be reached: new active monosaccharide molecular simplifications of Lipid As could be obtained and in addition the chains found to confer an immunomodulating ability to monosaccharide could be then inserted into disaccharide compounds to obtain new active and patentable compounds.

For this reason a **second line of research of my PhD project** has been the exploration of the effect of a new type of chains.
The type of chain I have selected for this study is the simple glycerol molecule.
This molecule has been selected for the presence of three hydroxy groups available for conjugation/chemical modification, two of which can be used to attach alkyl chains or other functional groups of interest, while the third can be oxidised to acid for conjugation to the sugar.
For the same reason amino acids have been selected to be conjugated to the sugar core in AGP/CRX molecules as well as functionalized diethanolamines in PET-Lipid A.
Moreover literature presents different type of protection reactions on glycerol to react chemoselectively just one of the three hydroxy groups at a time.
Finally glycerol protected structures (as acetals) are commercially available in their enantiomerically pure forms which permits to obtain enantiomerically pure final compounds.

The first attempt to use such chains in Lipid A partial structures would be of course in the sense of mimicking the linear and branched chains already proved active in Lipid A compounds.
With this strategy three different mimetic chains have been designed in my PhD project (figure 80).

However four main differences will distinguish all these mimetics from the original chains.

- If the secondary hydroxy group of glycerol is left free, it will be at a higher position in the chain with respect to the β-hydroxy group of the corresponding original alkyl chain

- The same is true for any branched chain based on glycerol. The ramification starts from a higher position. The effect of such changes has never been studied for normal alkyl chains. Just one monosaccharide derivative has an α-Oh hydroxy group but the biological activity of this compound is not reported.[210]
- for the same the correct configuration (R or S) of the chains to express biological activity must be verified since it could be different from the R configuration of active Lipid As
- An oxygen atom is present in the main chain and its polarity may affect the insertion of the chain in MD-2 pocket
- the same is true for the additional carbonyl group present in the main chain of the ester-ester derivative

The effect of such differences may be crucial.

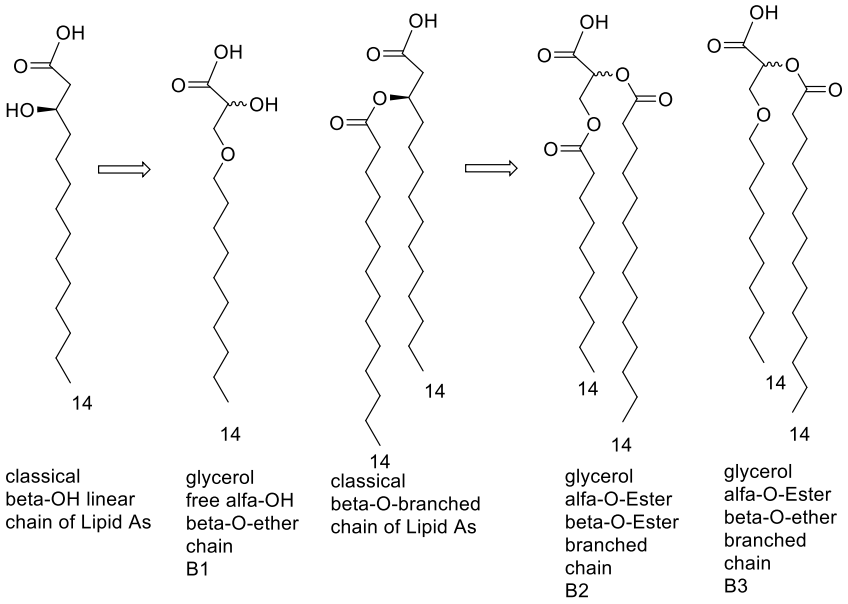

Figure 80. The new glycerol-based chains designed compared to the classical Lipid A chains they try to mimic

3.1 Chain B2

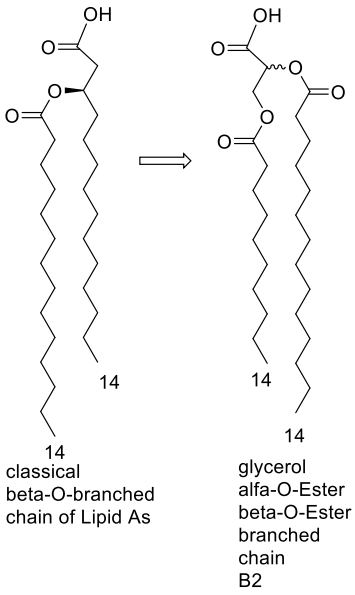

Figure 81. Chain B2 and the classical Lipid A chain it tries to mimic

The synthetic pathway designed and followed to obtain chain B1 (figure 81) is reported in scheme 5.

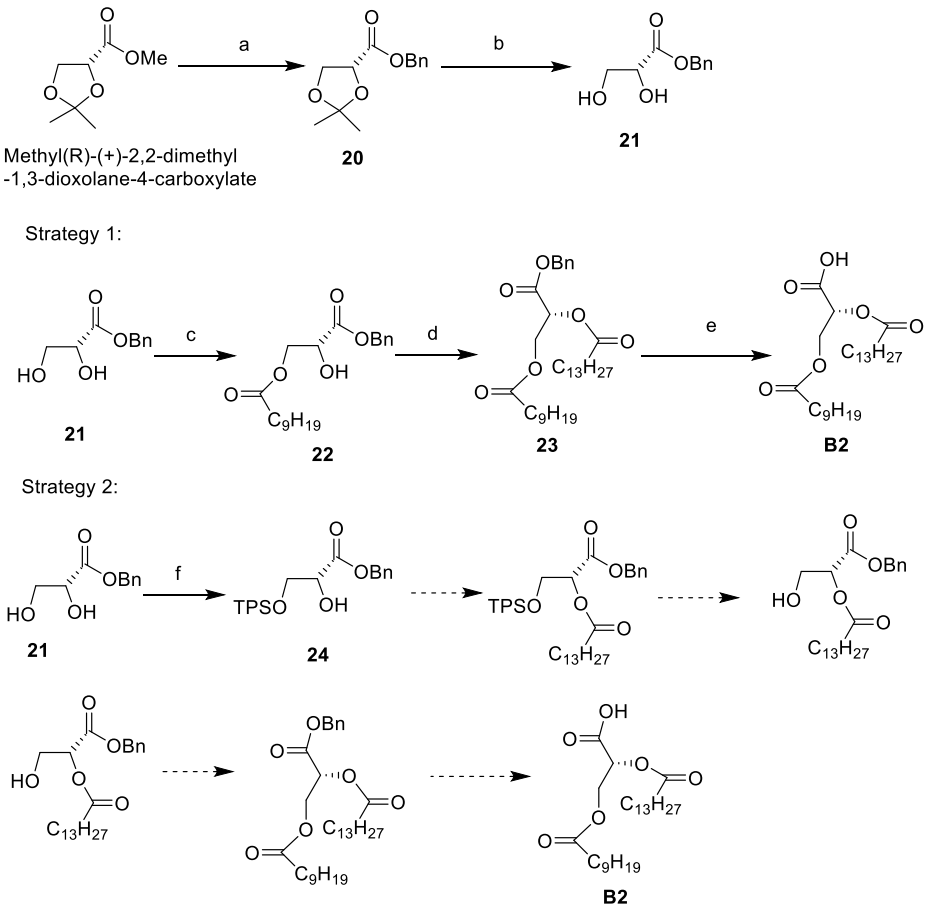

Scheme 5. Reagents and conditions: (a) Bu_2SnO, BnOH, 120° C, 2h, 81%; (b) HCl aq, THF, rt, O.N., 50%; (c) decanoic acid, DCC, DMAP, CH_2Cl_2 dry, 4°C, O.N., 61%; (d) myristic acid, DCC, DMAP, CH_2Cl_2 dry, rt, O.N., 92%; (e) H_2, Pd/C, MeOH dry/CH_2Cl_2 dry, rt, 3h, quant; (f) tert-Butyl(chloro)diphenylsilane, imidazole, CH_2Cl_2 dry, -20°C, O.N., 91%;

2,3-O-acetal protected glycerol with an ester in 1 was used as the starting molecule so to have two positions with different reactivity already protected and the third easily convertible into the acid needed for conjugation to the sugar.

Moreover the commercially available R enantiomer of Methyl-2,2-dimethyl-1,3-dioxolane-4-carboxylate was used so to obtain an enantiomerically pure final product with R configuration that means with the same configuration than classical β-OH and β-O-branched chains of active Lipid As.
However it must be remembered, as stated above, that the stereocenter here is in α position to the carbonyl and not in β so the chain with the other stereochemistry will be also synthesized and tested in the future using the same synthetic route and the commercially available Methyl-(S)-2,2-dimethyl-1,3-dioxolane-4-carboxylate.

In the first step tin-catalyzed transesterification was employed to turn the ester into a benzyl ester whose aromatic protective group will be easily removable at the end of the synthesis through hydrogenation.

In the second step the acid cleavage of the acetal is accomplished even if with a 50% yields, mainly due to ester acid hydrolysis.

The opening of the acetal set free two of the three hydroxyls of glycerol.
From this point two strategies are possible and both exploit the different reactivity and steric hindrance of the two hydroxyl groups.
In the first strategy this difference has been used to conjugate directly one of the two chains on the primary hydroxyl group in β with yields up to 61%. This has been possible by using DCC and low temperatures.
The second strategy on the contrary is based on an initial protection step by using still low temperatures but also the very hindered tert-butyl diphenyl silyl group. In this way only the primary hydroxyl group has reacted in our trial and with very high yield (91%).
However from this intermediate four other steps are needed to reach the final chain B2 while with the first approach just a second acylation and a final hydrogenation step give the final compound.

3.2 AM173

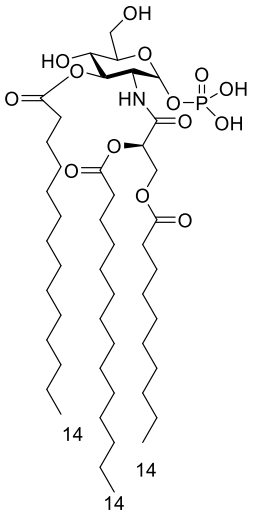

Figure 82. AM173

Aim and Rational design

The first sugar we designed containing this innovative type of glycerol-based chain is AM173 (figure 82). AM173 is still a derivative of the reducing part of Lipid A, as FP11, and is still respectful of the agonism rules above stated and verified.

However, differently from FP11 it has one branched chain and one linear chain as GLA compounds.

In particular it can be considered a mimetic of agonist compound GLA-60, or, better, a mimetic of its "specular" version, that is agonist compound 8 reported in Van Dervort et al. paper of 1992 (figure 83).[151]

In all these three compounds the branched chain is next to the phosphate as reported in agonism rules, since a branched chain far from the phosphate results in no immunostimulatory activitty.[163]

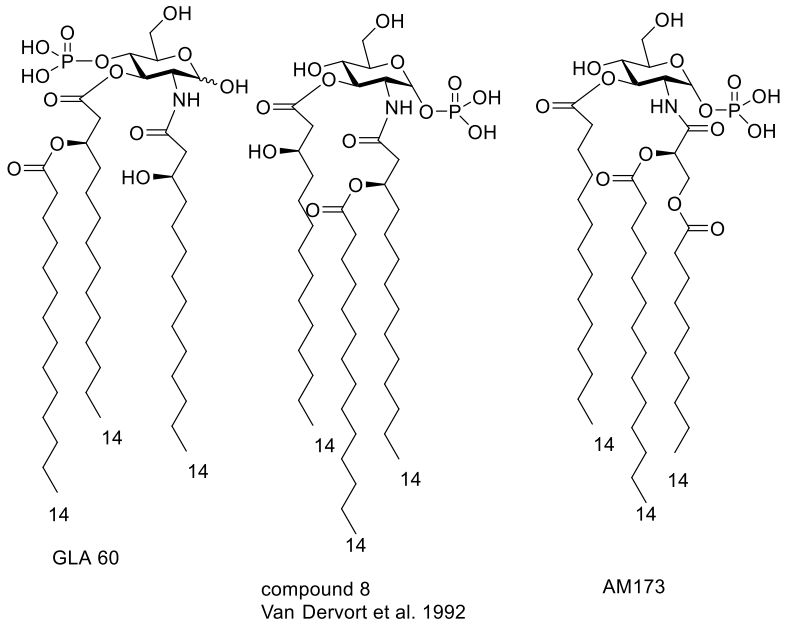

Figure 83. GLA 60, compound 8 of Van Dervort et al. 1992[151] and AM173

Synthetic route

The synthetic route designed and followed to obtain AM173 (scheme 6) starts from intermediate **14** of AM158 synthesis and chain B2 synthesized as reported above.

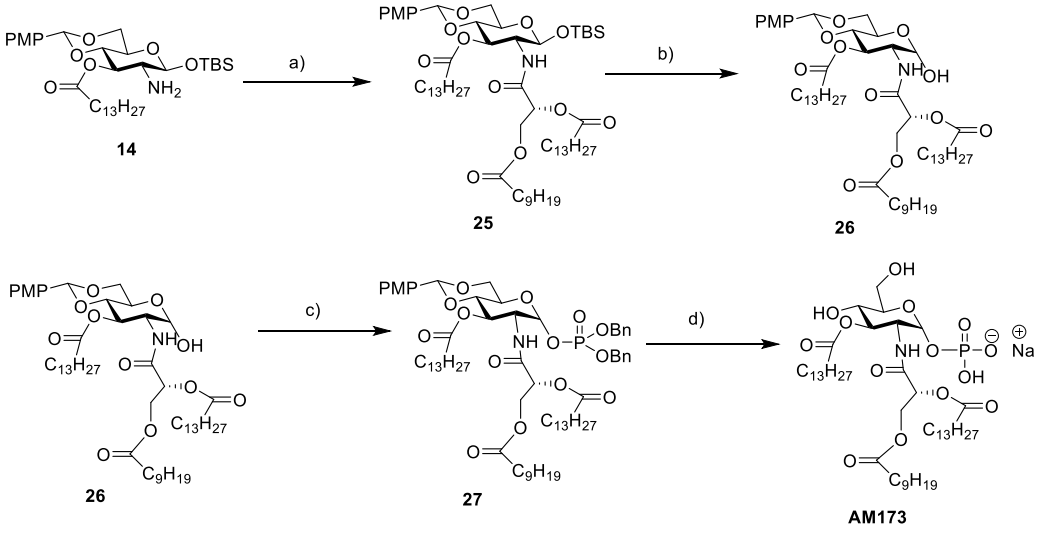

Scheme 6. Reagents and conditions: (a) chain B2, DCC, DMAP, CH_2Cl_2 dry, rt, O.N., 66%; (b) TBAF (1M in THF), AcOH, THF dry, -15°C-->rt, 2h, 83%; (c) $(BnO)_2PNiPr_2$, imidazolium triflate, CH_2Cl_2 dry, rt, 1h, then m-CPBA, 0°C-->rt, 2h, 39%; (d) I) H_2, Pd/C, MeOH dry/CH_2Cl_2 dry, rt, O.N., II) Et_3N, III) resin IR 120 H^+ , IV) resin IR 120 Na^+, quant.;

In the first step the chain and the sugar are reacted together with the proper condensing agent so to insert the branched chain in the desired position 2 of the sugar.

Next steps are similar to FP11 synthesis.

3.2.1 AM173 NF-κB induction

The newly synthesized monosaccharide AM173 based on the innovative glycerol chain B2 was tested for its ability to activate the TLR4 receptor system in HEK-Blue™ cells using LPS as positive control.

In our experiment AM173 failed to express any immunostimulatory activity at the concentrations tested (figure 84).

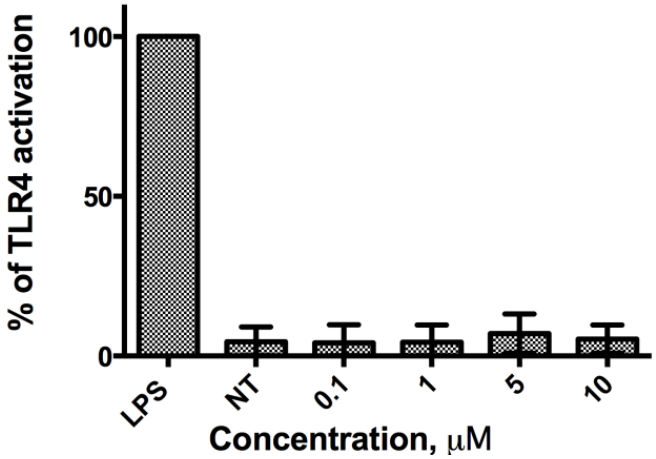

Figure 84. HEK-Blue™ hTLR4 cells assay of AM173. HEK-blue™ cells (HEK-293 cells transfected with human CD14 and MD-2.TLR4) were treated with increasing concentrations of compounds (0-10 μM) and incubated for 16-18 hours. TLR4 activation is monitored as sAP production. The results are normalized to maximal activation by LPS alone and expressed as the mean of percentage ± SD of 3 independent experiments.

Also no antagonistic effect on LPS stimulation has been detected.

Such negative result is clearly related to one or more structural features present in this new type of chain with respect to the classical one.

As stated above the new features of chain B2 are:

- the ramification starts from a higher position: the effect of such changes has never been studied for normal alkyl chains. Just one monosaccharide derivative has an α-Oh hydroxy group but the biological activity of this compound is not reported.[210]
- there is an additional carbonyl group in the main chain
- there is an additional oxygen atom in the main chain

However it is also possible that the diastereoisomer of AM173 containing the same chain but with S configuration, that means opposite to the configuration of classical chains of active Lipid As, will still be active.

All these features may in turn exert their effect on the entrance and binding into MD-2 pocket and/or on aggregates shape of such compound.

To clarify this point, two other chains have been synthesized, named B1 and B3.

3.3 Chains B1 and B3

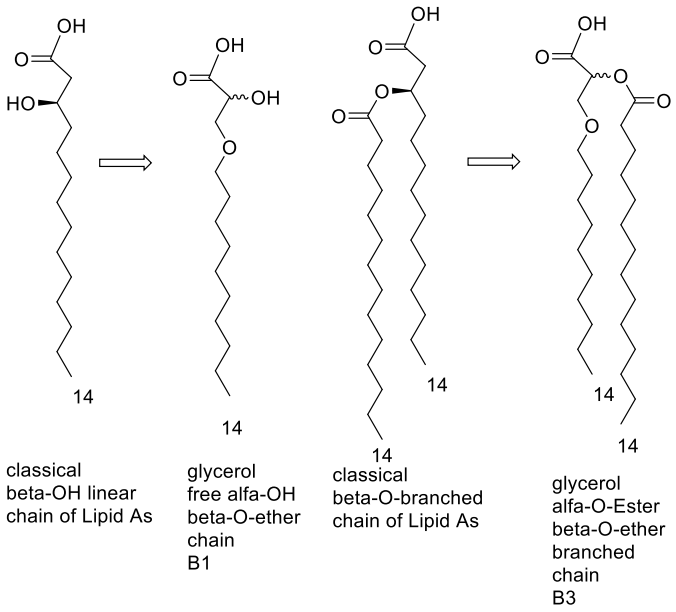

Figure 85. Chains B1 and B3 and the classical Lipid A chains they try to mimic

Aim and Rational design

The rationale behind the design of chains B1 and B3 (figure 85) lies in the removal of one or more features present in chain B2 that may constitute the reason of its inactivity.

Indeed chain B3 has all the features of chain B2 but since an ether functionality replaces the ester linkage of the main chain of B3, no additional carbonyl group is present with respect to classical Lipid As chains.

Chain B1 on the contrary is a linear chain with an ether group and a free hydroxyl group, so here also the possible effect of the higher position of the ramification is removed.

Of course this chain must be used on an FP11-like compound with three linear chains, so to respect the 1:1:3 rule, if an agonist compound is desired.

Moreover since only the S enantiomer of chain B2 has been tested, this time we decided to synthesize a racemic mixture of R and S enantiomers of B3 and B1 even if the presence of an additional stereocenter in the sugar will generate two diastereoisomers.
The mixture of the two diastereoisomers (or the two separate diastereoisomers obtained, if their separation is feasible at some step of the synthesis; despite the determination of the exact diastereoisomer will not be possible then) can be tested as initial screening, then if the mixture expresses activity, enantiomerically pure chains will be used to synthesize and test separately the two diastereoisomers.

Synthetic route

For the synthesis of chains B1 and B3 and we decided to start from the 2,3-O-acetal protected glycerol with free OH in 1 (DL-1,2-Isopropylideneglycerol) so to avoid any problem arising from the use of the base in the Williamson reaction on the ester present in the starting compound of the previous chain.
This compound can be easily obtained through a protection step with acetone on glycerol.

The full synthetic scheme of chain B1 and B3 is reported in scheme 7.
As stated above, the use of the racemic mixture of starting acetal-protected glycerol (despite the two pure enantiomers are commercially available) is reported.

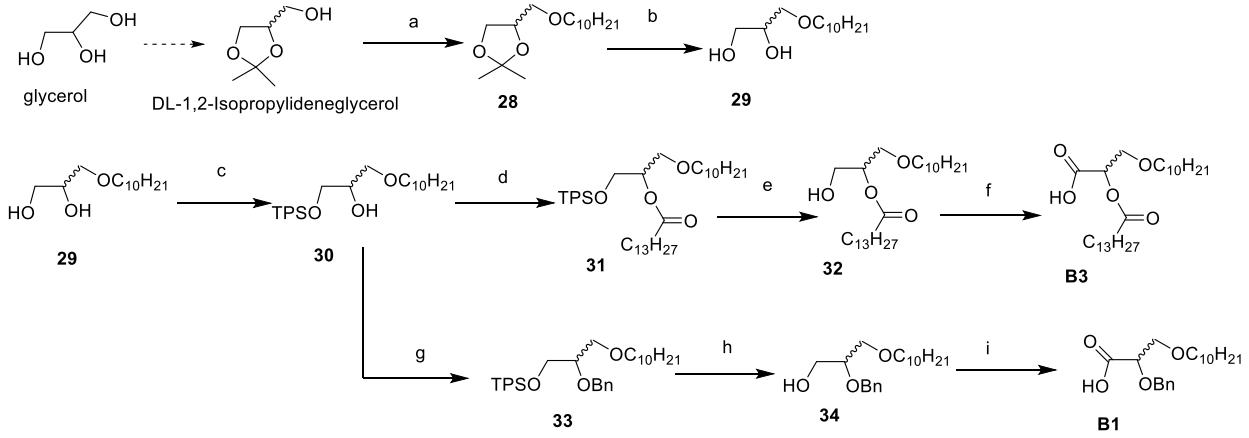

Scheme 7. Reagents and conditions: (a) Bromodecane, NaH, DMF dry, 0°C-->rt, O.N., quant.; (b) HCl aq, MeOH, rt, 40 min, quant.; (c) tert-Butyl(chloro)diphenylsilane, imidazole, CH_2Cl_2 dry, -20°C, O.N., 88%; (d) myristic acid, DCC, DMAP, CH_2Cl_2 dry, rt, 5h, 86%; (e) TBAF (1M in THF), AcOH, THF dry, -15°C-->rt, O.N., 52%; (f) I) Dess-Martin periodinane, $NaHCO_3$, DCM dry, rt, 1 h 30 min; II) NaClO aq. 5%, NaH_2PO_4, CH_3CN, rt, 21h, 80%; (g) BnBr, NaH, DMF dry, 0°C-->rt, O.N., 81%; (h) TBAF (1M in THF), AcOH, THF dry, -15°C-->rt, O.N., 70%; (i) PDC, DMF dry, rt, 2 days, 62%;

After the first Williamson reaction to add the proper alkyl chain and acetal opening to release free the hydroxyl groups, the same silyl protective group with high selectivity of B2 synthesis has been used.

At this step the synthesis of the two chains split: to obtain B1 the secondary hydroxyl of glycerol is protected with a benzyl group. This protection group will be removed only in the final step of the related sugar synthesis through an easy hydrogenation step.

On the contrary, to obtain chain B3 the secondary hydroxyl of glycerol is acylated.

The final steps of B1 and B3 chains are then identical: deprotection of primary hydroxyl group and oxidation directly to carboxylic acid with PDC or, more safely, oxidation to aldehyde at first, with Dess-Martin periodinane, followed by oxidation to acid with NaClO aq.

3.4 AMX1

Aim and Rational design

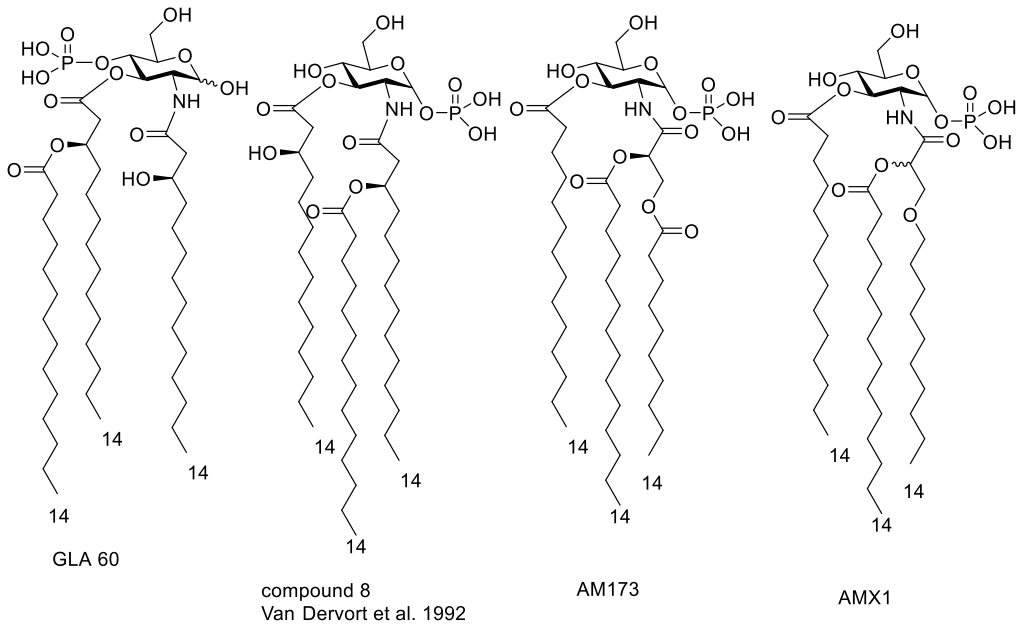

Figure 86. GLA 60, compound 8 of Van Dervort et al. 1992[151], AM173 and AMX1

Racemic chain B3 has been used in the trial to synthesize the corresponding analogue of AM173, AMX1, in a mixture of the two diastereoisomers (figure 86).

The choice of using racemic mixture of the glycerol chains has been explained in the previous sections.

Synthetic route

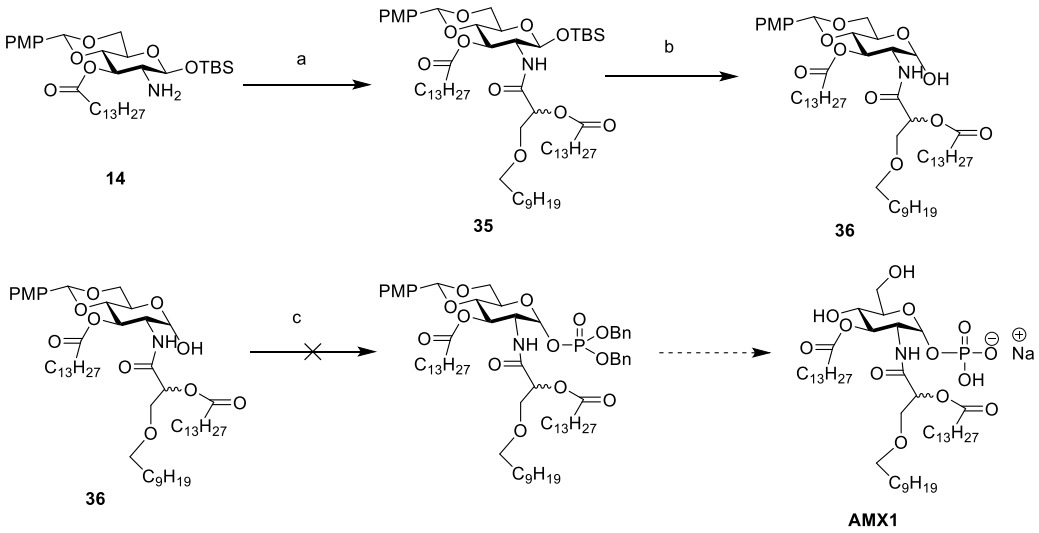

Scheme 8. Reagents and conditions: (a) chain B3, DCC, DMAP, CH_2Cl_2 dry, rt, O.N., 36%; (b) TBAF (1M in THF), AcOH, THF dry, -15°C-->rt, O.N., 29%; (c) $(BnO)_2PNiPr_2$, imidazolium triflate, CH_2Cl_2 dry, rt, 4 h 30 min, then m-CPBA, 0°C-->rt, O.N., FAIL;

Synthesis of AMX1 (scheme 8) starts again from intermediate **14** of AM158 synthesis and the following steps are identical to those performed for AM173 synthesis.

No diastereoisomers separation has been attempted during this synthesis.

Unfortunately the phosphorylation step didn't permit to obtain the final product. On the contrary the acetal opening of the sugar happened.

Probably the acidity of mCPBA affected the stability of the acetal, despite all the other successful reactions we performed on similar compounds have been left overnight and with the same equivalents of reactant.

For this reason, this reaction will be performed again in a short time by using fewer equivalents of mCPBA and a shorter reaction time.

By looking back at our previous experience, it would be quite awkward to obtain a similar result, so in principle our next compound to be tested will be soon at hand.

3.5 AM246248

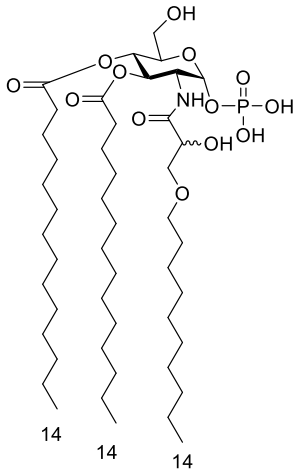

Figure 87. AM246248

Aim and Rational design

Compound AM246248 has been designed as an analogue of FP11 and SDZ MRL 953 to test the effect of chain B1 on activity (figure 88).

We decided at first to insert just one racemic B1 chain in the compound as initial test.

The effect of the insertion of additional chains however is expected to be similar by looking at SDZ MRL 953 derivatives.

Moreover since we decided to use racemic chains, the insertion of just one racemic B1 chain will produce two diastereoisomers, while the insertion of two and three racemic chains will produce much more diastereoisomers and the advantage of using the racemic mixture for avoiding parallel reactions would be overwhelmed by the disadvantage of synthetic purification and the huge decrease in yields.

Once the correct active enantiomer (or both) is determined, than three enantiomerically pure B1 chains could be inserted only in C2, or at the same time in C2, C3 and C4, following the same synthetic pathway of FP11 without diastereoisomers formation.

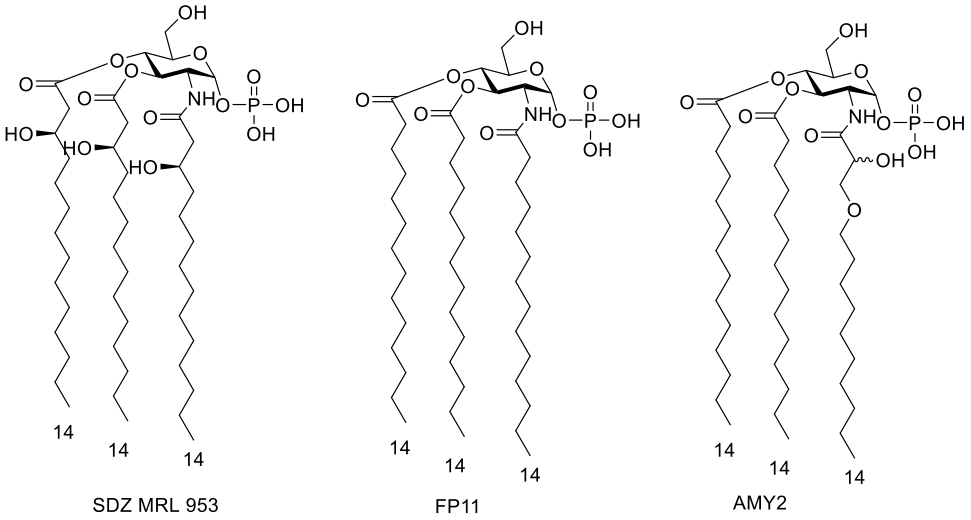

Figure 88. SDZ MRL 953, FP11 and AM246248

Synthetic route

We designed the synthetic route of AM246248 similar to FP11 (scheme 9).

However we decided to start from intermediate **4** of FP11 instead of intermediate **14** of AM158 synthesis, that means the first alkylation has been performed with chain B1.

This decision aims at removing some steric hindrance from the sugar to be functionalized that may negatively influence the reactivity of the acylation with the bulky benzyl group.

In this way it will be also possible to determine the effect of the presence of a chain already attached in C3 on the C2 acylation with a chain β-alkoxy-functionalized, in search of a better yield than the one obtained during AMX1 synthesis (compound **38**, yield 36%) or even better than the one of AM173 synthesis (compound 28, yield 66%).

Double acylation on the free OH in C3 is indeed expected to be minimal with proper reaction conditions.

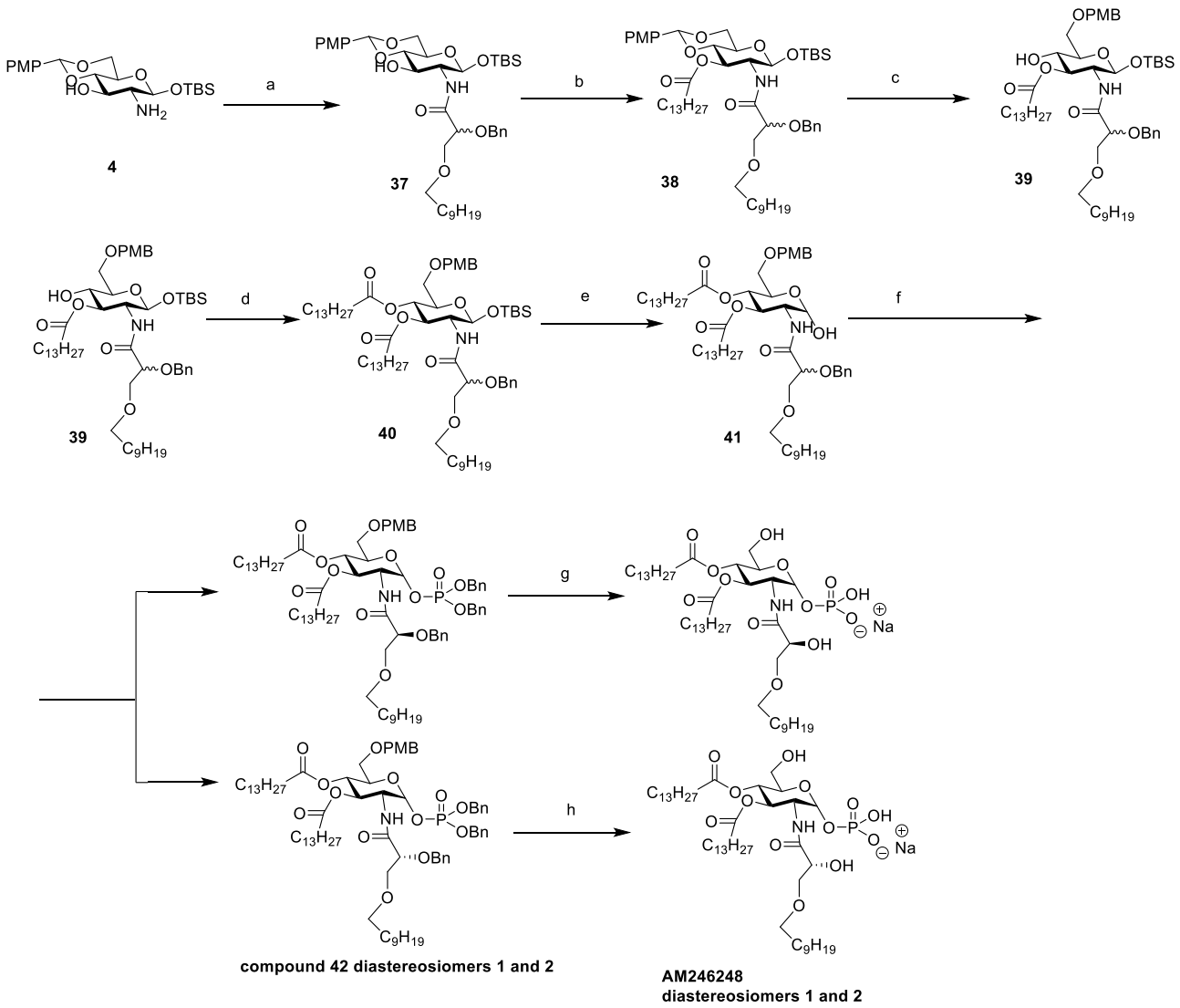

Scheme 9. Reagents and conditions: (a) chain B1, DCC, DMAP, CH_2Cl_2 dry, rt, O.N., 44%; (b) myristic acid, EDC, DMAP, CH_2Cl_2 dry, rt, O.N., 74%; (c) $NaCNBH_3$, 4 Å MS, THF dry, rt, 1h., then HCl 1M in dioxane, 50 min, 83%; (d) myristic acid, DCC, DMAP, CH_2Cl_2 dry, rt, 1h, 93%; (e) TBAF (1M in THF), AcOH, THF dry, -15°C-->rt, 1h, quant: (f) $(BnO)_2PNiPr_2$, imidazolium triflate, CH_2Cl_2 dry, rt, 2 h 45 min, then mCPBA, 0°C-->rt, 2h, 61%; (g/h) I) H_2, Pd/C, MeOH dry/CH_2Cl_2 dry, rt, O.N., II) Et_3N, III) resin IR 120 H^+, IV) resin IR 120 Na^+, 50-70%;

Even if the yield of this first acylation step resulted lower than the AM173 second acylation, the first trial of this reaction shows an improvement with respect to AMX1 synthesis.

However this may also be related to the different steric hindrance of the two β-alkoxy substituents of the chains.

Again, as in FP11, FP111 and AM158 synthesis high attention must be put on the acetal opening step, to avoid the concomitant undesired deprotection of C-1 (or even complete PMB removal) and thus the drastic reduction in yield.

The couples of diastereoisomers of different intermediates of this synthesis have been efficiently separated and characterized even if it is not possible to say which diastereoisomer is which without starting from the enantiomerically pure chain. However since for the initial screening it is the mixture of the two diastereoisomers that is needed, the following steps have been always carried on the diastereoisomeric mixture except for the hydrogenation reaction.

Indeed the two diastereoisomers of compound **42** have been put to react separately.
With this strategy both diastereoisomers of compound AM246248 have been successfully obtained.

Biological experiments to test the ability of AM246248 to induce immunostimulation through the TLR4 receptor system in HEK-Blue™ cells will be performed in the next months.

3.6 AM241

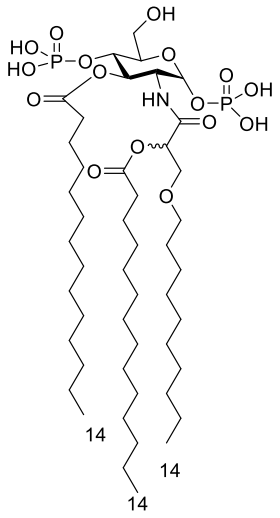

Figure 89. AM241

Aim and Rational design

After the synthesis of analogues of agonistic monosaccharide molecular simplifications of Lipid A,
we decided to use these innovative glycerol chains also on diphosphorylated monosaccharide in search of new antagonists but also to explore SAR for antagonism.

As stated in section 7.3 of the previous chapter, the number of diphosphorylated monosaccharide molecular simplifications of Lipid A is limited to Lipid X, our compound FP7 and few others.
One of these molecules is GLA 70 (or compound 15) of Ogawa et. al paper of 1987 (figure 90).[211]
This compound is interesting in the sense that it possesses three chains and two phosphate groups in 1 and 4.

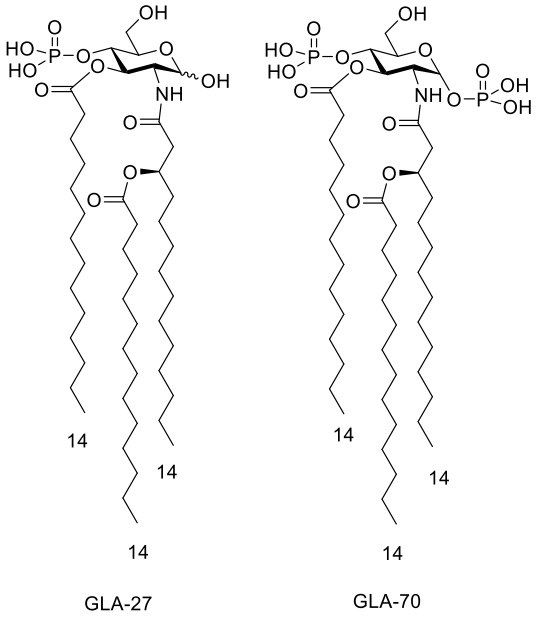

Figure 90. GLA-27 and GLA-70[211]

Even if we have confirmed MD-2 binding of FP11, that means a tri-acylated mono-phosphate monosaccharide molecular simplifications of Lipid A, we still don't know how is possible that still a part of the disaccharide Lipid A is still able to express an immunostimulatory activity.

By looking at crystal structures of *E. coli* Lipid A and at the rule 1-1-3 of Funatogawa and Matsuura, it seems possible that two molecules of FP11 enter MD2 pocket so that still a sixth acyl chain protrude.

The same is possible for the agonistic compound GLA-60 and GLA-27 with still one phosphate and three chains, despite the latter is agonist only in murine.

However when a second phosphate group is introduced, as in compound GLA-70[212], a derivative of GLA-27, immunostimulatory activity decreases a lot also in mouse[212] thus suggesting a negative effect of the second anionic group, and only its protective activity against vaccinia virus is similar to GLA-27.

GLA 70 has been studied for its mitogenic activity, tumor-necrosis factor (TNF)-inducing activity, macrophage-activating activity, IFN-inducing activity, antiviral activity against vaccinia virus and its nonspecific protective activity against P. aeruginosa infection, which are all tests for immunostimulation.

On the contrary its antagonistic activity against LPS has never been tested.

The "specular" version of GLA 70, that means with the branched chain in 3, has never been synthesized

The lack of studies on the antagonist activity of GLA 70, that means the lack of antagonistic studies on monosaccharide molecular simplifications of Lipid A with two phosphates and three acyl chains is another relevant piece of information missing to understand SAR for Lipid A partial structures for antagonism.

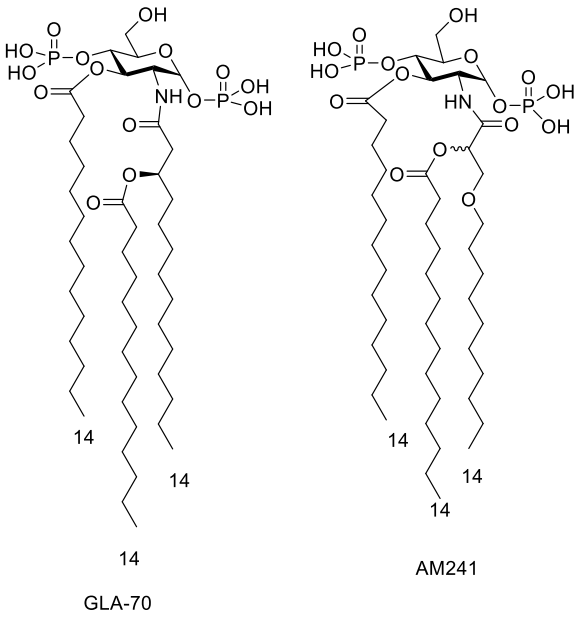

Figure 91. GLA-70 and AM241

For this reason another target at which I decided to aim with my work is compound AM241 (figure 91). AM241 is an analogue of GLA 70 possessing the innovative branched glycerol chain B3. This chain (and its position) makes it comparable to the already synthesized compound whose interesting features we want to explore while is makes AM241 at the same time new and patentable.

A principle already expressed and already exploited with our other compounds.

Synthetic route

The synthesis of AM241 (scheme 10) can easily start from the already synthesized intermediate **36** of AMX1 synthesis.

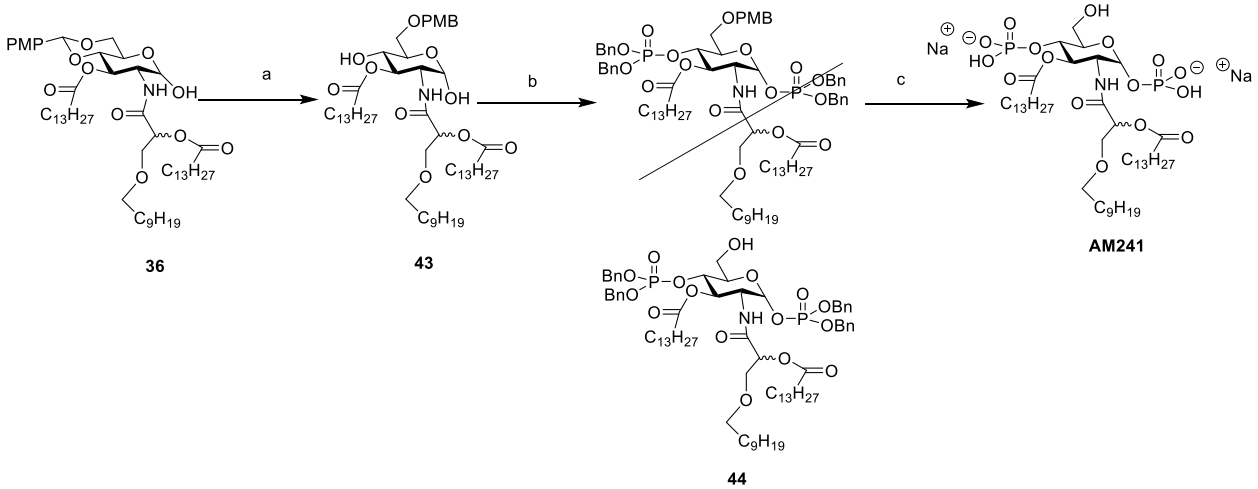

Scheme 10. Reagents and conditions: (a) $NaCNBH_3$, 4 Å MS, THF dry, rt, 1h., then HCl 1M in dioxane, 50 min, 60%; (b) $(BnO)_2PNiPr_2$, imidazolium triflate, CH_2Cl_2 dry, rt, 4 h 30 min, then m-CPBA, 0°C-->rt, O.N., 47%; (c) I) H_2, Pd/C, MeOH dry/CH_2Cl_2 dry, rt, O.N., II) Et_3N, III) resin IR 120 H^+ , IV) resin IR 120 Na^+, 87%;

The following three steps are the opening of the acetal, the phosphorylation and the final hydrogenation which permitted to obtain the final compound.
It must be precised that here, again as in AMX1 synthesis, but still differently from all other trials of this reaction on many sugar compounds, the use of mCPBA resulted in the cleavage of PMB. However, since the cleavage happened during the oxidation step, the complete phosphorylation in 4 and 1 without any phosphorylation of position 6 was clearly assessed by NMR.

As for AMX1 no diastereoisomers separation has been attempted during this synthesis.

Biological experiments to test the ability of AM241 to block LPS stimulation of the TLR4 receptor system in HEK-Blue™ cells will be performed in the next months.

4. Natural compounds derivatives as TLR4 modulators: oleocanthal derivatives

Olive oil constituents are well-known for their anti-inflammatory activity.
However, despite the anti-inflammatory effect of hydroxytyrosol and oleuropein aglycon appears very likely related to TLR4 antagonism,[188] the activity of the anti-inflammatory compounds of olive oil has not been directly correlated to the activity of TLR4 receptor system yet.
Our research group in the last years tried to fill this gap, investigating the activity of olive oil phenolic extracts and of some isolated phenolic constituents on TLR4 receptor system.
In particular, several compounds belonging to the principal classes of phenolics contained in extra virgin olive oil were tested: phenolic acids, phenehtyl alcohols, lignans, flavonoids and secoiridoids. The majority of these molecules are commercially available.

The compounds containing carboxylic acids, generally derivatives of cinnamic acid (2-hydroxycinnamic acid, 4-hydroxy-3-methoxycinnamic acid, caffeic acid, rosmarinic acid, trimethoxycinnamic acid), were not able to inhibit TLR4 activation by LPS, as well as the lignan pinoresinol.
Surprisingly, also the strong anti-inflammatory phenols tyrosol and hydroxytyrosol were inactive in inhibiting LPS-stimulated TLR4 signal.
Among the phenolic compounds screened for biological activity on TLR4 receptor system, oleuropein showed a moderate dose-dependent TLR4 antagonism, not associated with cell toxicity, as assessed by cell viability test.

The best inhibitors of LPS-induced TLR4 activation were found to be the flavonoids apigenin and luteolin with IC_{50} values of 15.7 and 14.3 μM respectively. These molecules also proved not to be toxic for HEK-293 cells.

These results are very interesting because they pointed out for the first time that the anti-inflammatory activity of phenolic extracts from EVOO can be correlated to their activity as modulators of the TLR4 receptor system.

However, among olive oil constituents, it has not been possible to study the activity of the powerful anti-inflammatory agent oleocanthal[184] (figure 92) since it is not commercially available.

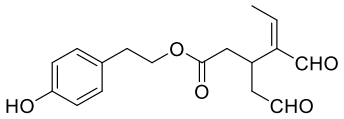

Figure 92. Oleocanthal

From such studies the identification of a powerful TLR4 modulator or a scaffold to develop a new class of modulators could be obtained.

For this reasons our research group in the last years tried to reproduce the synthesis of this compound already reported in literature.[213]

Unfortunately due to the difficulty of the synthesis previous efforts of the researchers of my group didn't accomplish the goal.

For this reason we have designed and developed different oleocanthal derivative to explore the potential of this class of compounds in search of new TLR4 modulators.

Rational design behind our oleocanthal derivatives

Previous works on the synthesis and biological characterization of oleocanthal derivatives with anti-inflammatory activity outlined some important SAR.[184] First of all, the phenolic portion seems to be fundamental in retaining the anti-inflammatory activity, while bearing one or two phenolic OH in different positions. However, we demonstrated that molecules like tyrosol and hydroxytyrosol, presenting only the phenolic portion, were not capable of inhibiting the activation of the TLR4 pathway.

Consequently, in our mimetics of oleocanthal the di-aldehyde portion was maintained and structural variations focused on the direction of the ester bond and the length of the linker between the phenolic portion and the di-aldehyde function, together with the variation of the distance between the two aldehyde groups.

On the contrary the double bond present in α to one of the two aldehydes has been removed because it doesn't seem to be fundamental for activity and because its removal makes the synthesis of oleocanthal derivatives much easier.

We designed 8 analogues of oleocanthal.

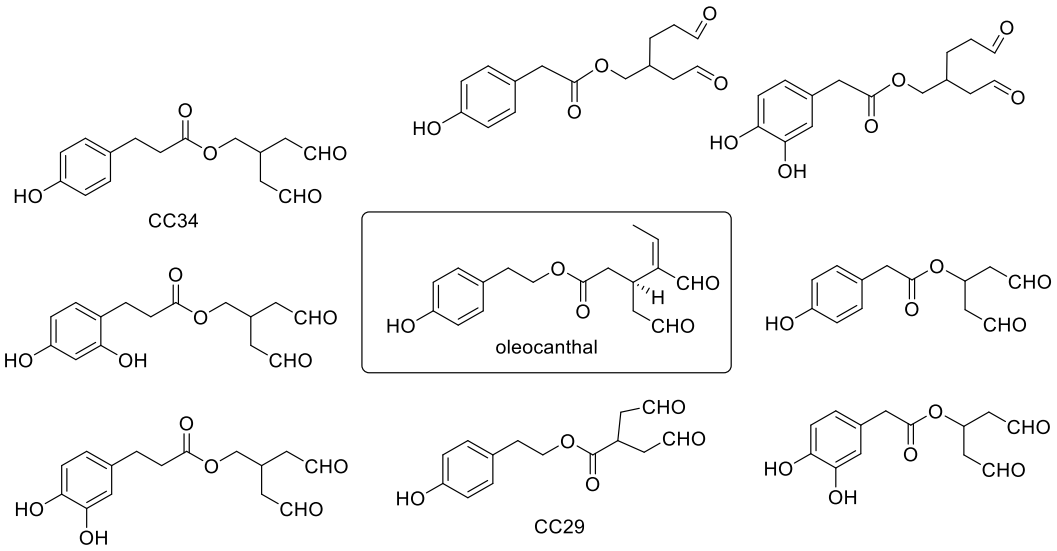

Figure 93. The designed derivatives of oleocanthal

The work of my co-workers focused in the last years on CC34 and CC29.

Unfortunately, the isolation of the pure final product CC29 was impossible because it probably underwent fast rearrangements, affording a mixture of products.

The molecular mechanism of these rearrangements is under study and a hypotesis is shown in scheme 11.

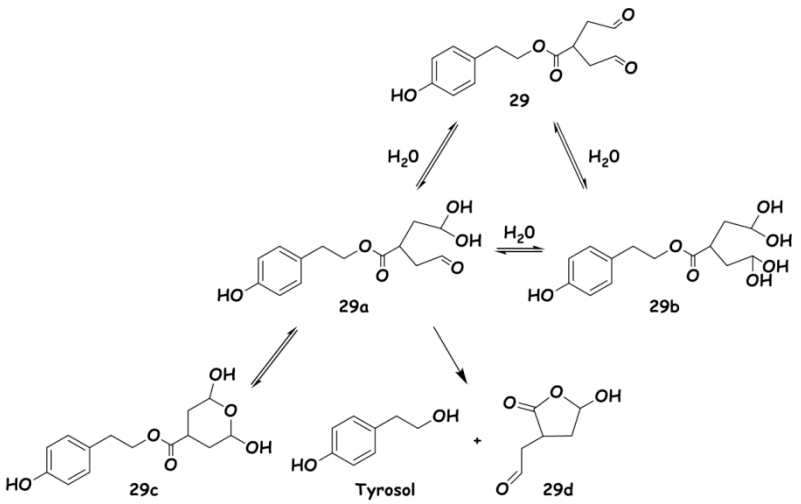

Scheme 11. Rearrangement hypotheses for molecule CC29.

On the contrary compound CC34 was successfully obtained and tested.

As in the case of compound CC29, compound CC34 is in equilibrium with the hydrated forms of aldehydes, however the rearrangements that causes the instability of compound CC29 do not occur so fast for CC34. Only after two months some degradation was observed.

It has been proposed that this doesn't happen because compound CC34 would pass through the formation of a disfavoured seven-atom ring (see scheme 11 for the mechanism).

As for FP7, the ability of CC34 to interfere with LPS-triggered TLR4 activation was first investigated in HEK-blue™ cells (figure 94).

Compound CC34 significantly inhibited TLR4-depending sAP production showing a good dose-dependent TLR4 antagonism with an IC_{50} of 50-75 µM.

Moreover, compound CC34 was tested for its toxicity on cells and it showed no toxicity at the concentrations used for HEK-Blue™ assay.

Consequently, compound CC34 presented very promising characteristics: it is a chemically stable, water-soluble, not toxic, good TLR4 antagonist.

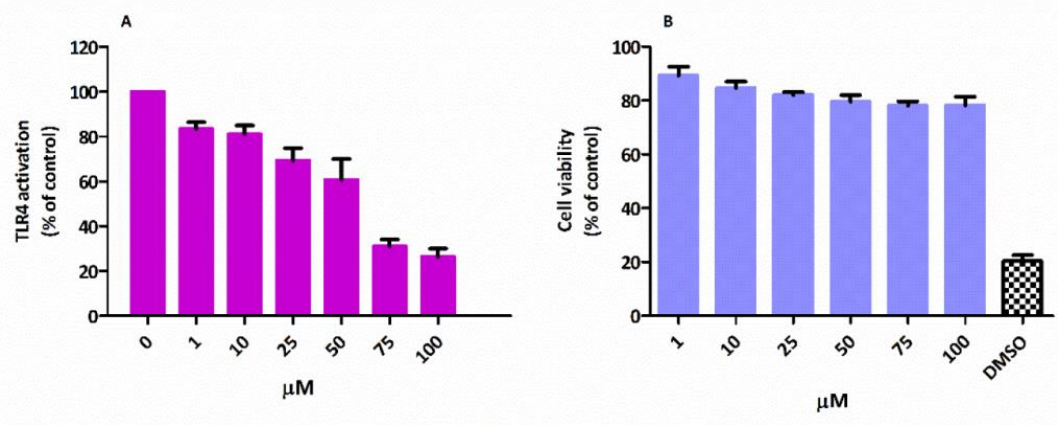

Figure 94. A) Dose-dependent inhibition of LPS-stimulated TLR4 activation by compound 34. HEK-Blue™ cells were treated with increasing concentrations of compounds (0-100 µM) and then stimulated with LPS. TLR4 activation is monitored as sAP production. The results are normalized to activation by LPS alone and expressed as the mean of percentage ± SD of 3 independent experiments. B) Viability assay (MTT) on compound CC34 (0-100 µM) in HEK-Blue cells. DMSO is used as negative control. The results are normalized on the positive control (cells treated with PBS) and expressed as the mean of percentage ± SD of 3 independent experiments.

4.1 AM30

Following this line of research, during my PhD thesis I have also worked on the synthesis of another derivative of this class of potential TLR4 modulators: compound AM30 (figure 95).

This compound has an inverted direction of the ester bond with respect to oleocanthal while the length of the carbon chain between the phenolic portion and the ester has been decreased to 1 carbon atom.

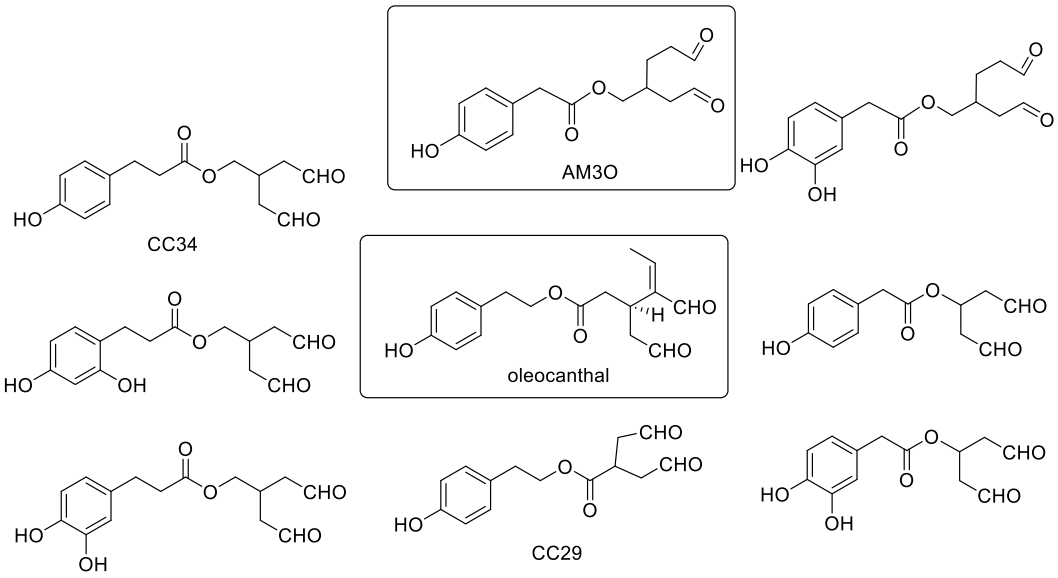

Figure 95. The designed derivatives of oleocanthal and AM30

The retrosynthetic approach that has been designed to reach such final compound involves the disconnection between the carbonyl of the ester and its O-alkyl group.

However the two aldehyde group must be somehow protected during the synthesis. For this reason a double bond oxidizable to a diol has been designed as precursor of the di-aldehyde function.

Also the OH group of the phenol must be protected.

Thus the two identified partners for the full synthesis of AM30 are the commercially available 4-hydroxyphenylacetic acid and 3-cyclohexene-1-methanol.

The synthetic pathway designed and followed to obtain AM30 is depicted in <u>scheme 12.</u>

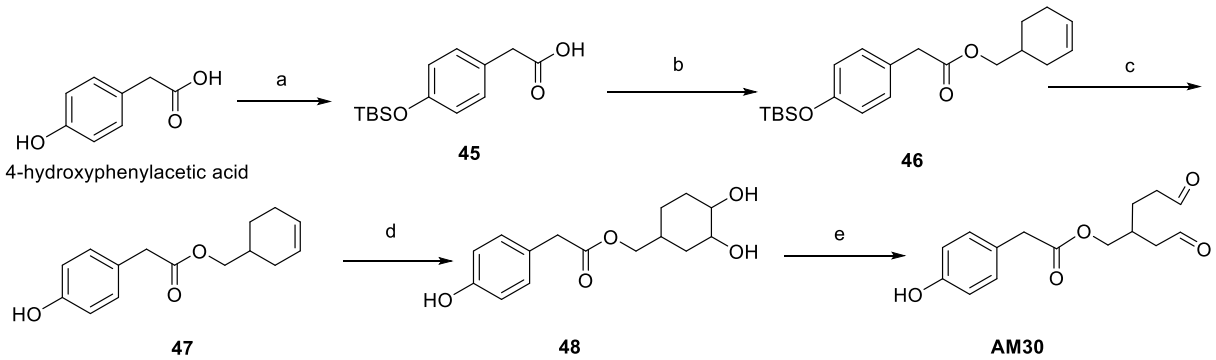

Scheme 12. Reagents and conditions: (a) TBDMSCl, imidazole, DMF dry, rt, O.N., then NaOH aq., 76%; (b) cyclohexen-1- methanol, DCC, DMAP, CH_2Cl_2 dry, rt, O.N., 61%; (c) TBAF, AcOH, CH_2Cl_2 dry, 0°C-->rt, O.N., quant; (d) OsO_4 (2,5% wt in t-BuOH), NMO, acetone/PBS 9:1, rt, 3 h, then $NaHSO_3$, rt, 1h, 52%) e) Amberlite-$IO4^-$, CH_3CN/H_2O 10:1, 3 h 30 min, quant.;

After the conjugation with DCC between protected 4-hydroxyphenylacetic acid and 3-cyclohexene-1-methanol and removal of the silyl group, the olefin of ciclohexene is converted to a cis-vicinal diol through Upjohn dihydroxylation, in which OsO4 and NMO (4-methylmorpholine 4-oxide) are used (figure 96).

The hydroxylation process is strongly favored by the catalytic cycloaddition of OsO_4 to the olefin, in which the osmium (VIII) species is oxidized to the osmium (IV) species. NMO is employed to oxidize osmium (IV), so that osmium tetroxide is formed again and the catalytic reaction can carry on.

During work-up $NaHSO_3$ is introduced to stop this catalytic cycle by reducing osmium.

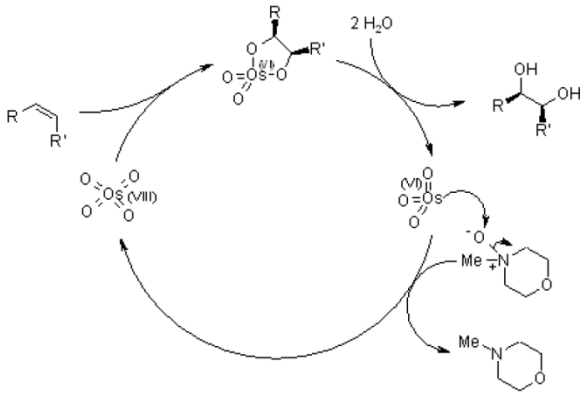

Figure 96. The catalytic OsO_4-NMO cycle used in step d

In the final step periodate is employed as an oxidizing agent (oxidation mechanism in figure 97); however, $NaIO_4$ (sodium periodate) would not be convenient as a medium to introduce this ion, because it would be more difficult to remove once the oxidation has taken place. In fact, compound AM30 is likely to be soluble in water and would be too unstable to undergo a column purification procedure, due to the possible formation of its hydrated form. Therefore, Amberlite, an easily removable ion exchange resin, is used as a more suitable periodate-carrying medium. In this way the diol hydroxyls are oxidized to two aldehydic groups.

Mechanism involves the formation of a cyclic intermediate, known as periodate ester, which then leads to the formation of the formyl groups and the cleavage of the C-C bond. After the reaction has occurred, Amberlite is easily filtered out and the pure final product is obtained.

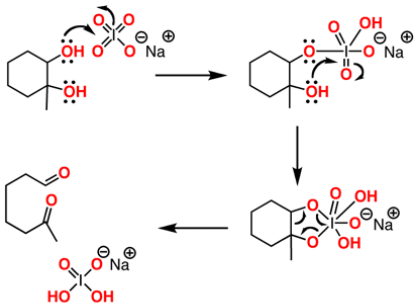

Figure 97. Oxidative cleavage by $NaIO_4$

This product proved to be stable for less than 2 months.

However in this time lapse all the biological experiments needed to determine its activity have been performed.

4.1.1 AM30 inhibition of LPS-induced, TLR4-dependent NF-κB activation in HEK-blue cells

The ability of compound AM30 to inhibit LPS-triggered TLR4 activation in HEK– Blue™ was analysed (figure 98).

As its parent oleocanthal derivative CC34, compound AM30 proved to be a TLR4 antagonist with an IC_{50} of 70-100 µM.

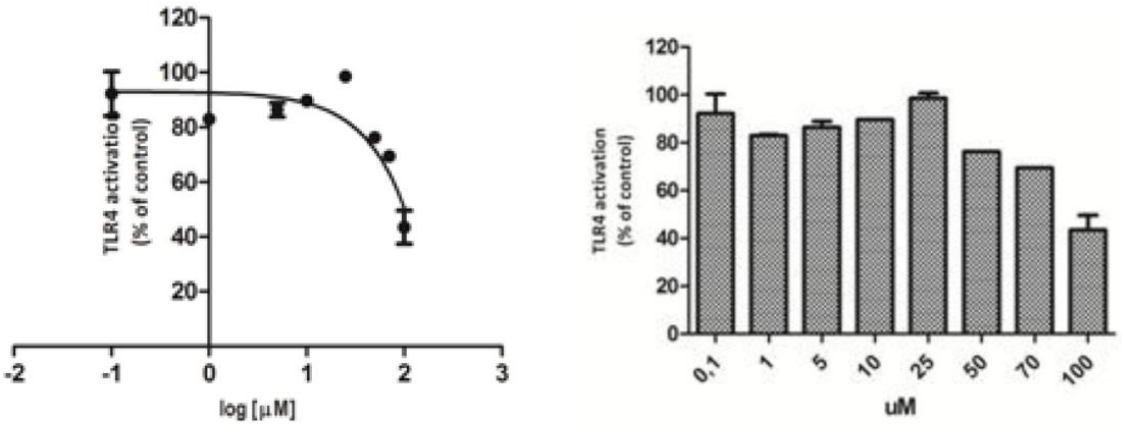

Figure 98. AM30 inhibition of LPS-induced, TLR4-dependent NF-κB activation in HEK-blue™ cells. HEK-blue™ cells were treated with increasing concentrations of compounds (0-100 µM) and then stimulated with LPS. TLR4 activation is monitored as sAP production. The results are normalized to activation by LPS alone and expressed as the mean of percentage ± SD of 3 independent experiments.

This value is still much higherer than the best inhibitors of LPS-induced TLR4 activation found in olive oil (flavonoids apigenin and luteolin, with IC50 values of 15.7 and 14.3 µM respectively) however it is only slightly higher than CC34 (IC_{50} = 50-75 µM).

4.1.2 AM30 cytotoxicity

An MTT test was also performed to verify the compound's toxicity: the results show that the molecule is not toxic up to the highest concentration tested (figure 99).

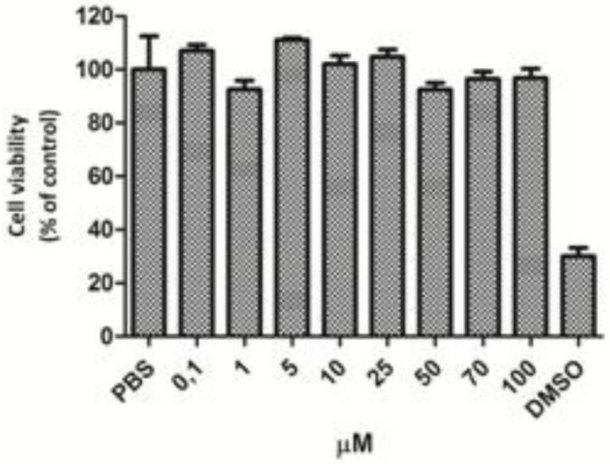

Figure 99. Viability assay (MTT) of compound AM30 (0-100 μM) in HEK-Blue cells. DMSO is used as negative control. The results are normalized on the positive control (cells treated with PBS) and expressed as the mean of percentage ± SD of 3 independent experiments.

In conclusion both oleocanthal derivatives, compound CC34 and AM20, proved to be TLR4 antagonist thus pointing for an antagonistic effect of oleocanthal itself.

The synthesis and the tests of the other derivatives will clarify SAR for this class of compounds whose very promising feature lies in the higher water-solubility (due to the lack of *amphiphilicity*) and the easier synthesis with respect to classical Lipid A-derived TLR4 antagonists

Conclusions

Eight new Lipid A monosaccharide molecular simplifications have been designed and successfully synthesized during this PhD thesis: FP7, FP11, FP111, AM158, AM173, AM246248-d1, AM246248-d2 and AM241 (figure 100).

An additional derivative, AMX1 is one easy step from its obtainment.

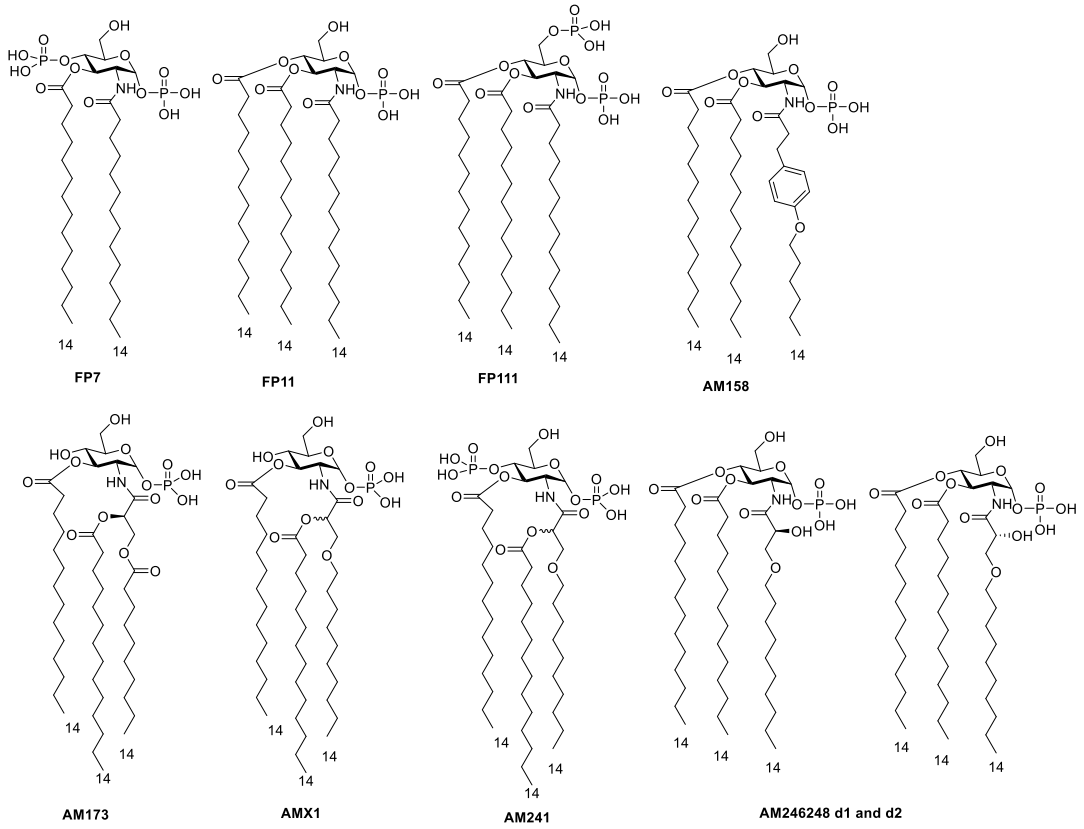

Figure 100. FP7 and the 8 new Lipid A monosaccharide molecular simplifications successfully synthesized during this PhD thesis: FP11, FP111, AM158, AM173, AM246248-d1, AM246248-d2, AMX1 (see note) and AM241

Between these compounds, **FP11**, synthesized according to the rules of agonism depicted by Funatogawa and Matsuura (one phosphate, one glucosamine and three acyl chains), expressed a powerful pure agonistic activity *in vitro* thus confirming this structure-activity rule.

In the HEK-Blue^{TM} hTLR4 cells assay, compound FP11 showed a dose-dependent activation of TLR4 signal resulting in the secretion of NF-κB and AP-1 at concentrations higher than 5 µM.

30% activation with respect to LPS was reached at concentration 10^3 times higher than LPS and the **EC_{50}** is 12.35 µM.

Such lower immunostimulatory activity than bacterial LPS is an extremely important feature of this compound, since it makes FP11 a promising candidate to be used as adjuvant in vaccines.

For this reason a patent regarding the potential application of such non-toxic compound as adjuvant for vaccines has already been filed.

Moreover the *in vivo* evaluation of FP11 on mouse is being performed by the Italian company Lofarma during these months.

Since another main aim of my PhD project, apart from SAR studies and the discovery of new TLR4 modulators, was the clarification of the role of TLR4 and MD-2 in the immunostimulation of monosaccharide molecular simplifications of Lipid A, the ability of FP11 to interact with TLR4 and MD-2 has also been studied with different *in vitro* binding assays.

A comparative test on HEK-Blue™ Null2 cell line, a cell line that expresses the same gene reporter than HEK-Blue™ hTLR4 cells (SEAP), but it doesn't express any of the receptors (TLR4, MD-2, CD14) involved in endotoxins recognition, was also performed.

FP11 showed to be unable to activate the production of transcription factors NF-κB e AP-1 in this cell system, thus this data clearly demonstrates that the immunostimulatory effect of FP11 is related to the activation of the TLR4 receptor system. This is the same confirmation that was obtained for GLAs agonists in 2003.[164]

Regarding interaction with MD-2, SPR results on our purified receptor MD-2 show that FP11 binds directly MD-2. A K_D value of 6.5 μM has been estimated.

The same result was confirmed with all other binding experiments performed: an antibody-sandwich ELISA assay, a biotin-LPS displacement ELISA assay and a bis-ANS displacement assay.

Thus it appears clear that FP11 immunostimulatory activity is related both to TLR4 activation, as demonstrated by the test on HEK-Blue™ cells, and to MD-2 binding.

Indeed, for the inactive (nor antagonist) compound **FP111** no MD-2 binding was observed in all these experiments.

This is a very relevant information being the first data to our knowledge confirming that monosaccharide agonistic activity is still related to MD-2 binding and not only a generic effect related to activation of the TLR4 system. Indeed such activation could have been the result of aggregates intercalation in the membrane and/or interaction with transmembrane ion channels, even if such activation pathways have not been determined clearly in literature.[119–124]

The main rationalization of the LPS-blocking or the immunostimulating ability of monosaccharide compounds obtained in the past was the correlation of their molecular structures to aggregates shapes similar to those observed for active Lipid As, despite for GLA the key role of TLR4 was proved.

To complete our study and to correlate it to the ones done in the past, we have also ongoing studies with FT-IR, FRET and SAXS techniques by the group of Prof. A. Schromm (one of the first researchers working on the biophysical characterizations of the aggregates of Lipid As) in Germany to understand which is the aggregate shape of our active and inactive compounds.

Of the other seven compounds, **FP7** was a TLR4 antagonist already developed by our group in 2014.
However, thanks to the new batches prepared, different type of experiments in several types of cellular systems and application have been performed.
The TLR4 antagonistic activity of FP7 has been characterized on human monocytes and DCs, that are essential cells for the regulation of innate immunity and inflammation.
Our results indicate that FP7 inhibits TLR4-mediated monocyte and DC activation.
Moreover the antagonistic activity of FP7 has been tested *in vivo* on influenza-induced cytokine gene expression *in vivo*. [197] Indeed recent studies suggest that influenza-induced lethality and acute lung injury are due to the TLR4-stimulating effects of DAMPs such as OxPAPC and HMGB1, which are both TLR4 agonists.
FP7 not only strongly reduced influenza infection-induced lethality, but also significantly improved the histopathology scores of infected lungs. FP7 prevented excessive inflammation and lung tissue damage and improved the survival rate in this model. Given the inhibitory effect of FP7 on the level of cytokines and HMGB1 induced by PR8 infection seen *in vitro*, it can be reasonably assumed that the benefit of FP7 treatment of influenza virus–infected mice is linked to its ability to inhibit TLR4 signalling by DAMPs like HMGB1 and the subsequent TLR4-dependent cytokine storm.
Increasing evidence indicates that inflammatory responses could play a critical role in the pathogenesis of motor neuron injury in amyotrophic lateral sclerosis (ALS). Recent findings have underlined the role of Toll-like receptors (TLRs) and the involvement of both the innate and adaptive immune responses in ALS pathogenesis. In particular, abnormal TLR4 signaling in pro-inflammatory microglia cells has been related to motoneuron degeneration leading to ALS.
For this reason the effect of FP7 on *in vitro* ALS models has also been investigated.[201]
In these experiments FP7 efficiently protected motoneurons from LPS-induced lethality in spinal cord cultures, and inhibited the interleukine-1β production by LPS-stimulated microglia.

Between the other compounds, **AM158** is the first member of our designed series of analogues of ONO 4007, an agonistic compound currently in clinical studies as adjuvant for vaccines.
AM158 possesses one phosphate group and three acyl chains like FP11 but with an aromatic group in its C-2 chain as ONO4007, even if at a different distance from the carbonyl group.

Unfortunately, in our experiment AM158 failed to express any immunostimulatory activity (nor antagonistic effect) at the concentrations tested.

Such negative result of its biological activity clearly demonstrates the huge importance of the position of the phenyl ring inside the chain to express immunostimulation.

AM173, AMX1, AM246248-d1, AM246248-d2 and AM241 are five innovative monosaccharide compounds based on three new type of acyl chains derived from glycerol.

We have been designed these chains to mimic the classical acyl chains (linear or branched) present in Lipid As.

Despite **AM173** showed no activity both in agonism and antagonism, in our experiments, the biological studies on the other four compounds not yet performed could reveal new TLR4 modulators as well as provide new important pieces of knowledge to the SAR for TLR4 modulation.

Moreover if these new chains will be found to confer an immunomodulating ability (or antagonistic activity) to monosaccharide compounds then they could be in principle inserted also into disaccharide compounds to obtain new active and patentable compounds.

Finally, **AM30**, a new TLR4 modulator based on the scaffold of natural anti-inflammatory compound oleocanthal, is presented (figure 101).

The very promising feature of this compound lays in the higher water-solubility (due to the lack of amphiphilicity) and the easier synthesis with respect to classical Lipid A-derived TLR4 antagonists

AM30 showed an interesting (despite not powerful) antagonistic activity on HEK-Blue^{TM} cells with an IC_{50} of 70-100 µM.

This result, combined with the positive physiochemical features of AM30, and together with the activity demonstrated by CC34, the other oleocanthal derivative we have synthesised, demonstrates the potential of compounds based on the oleocanthal scaffold.

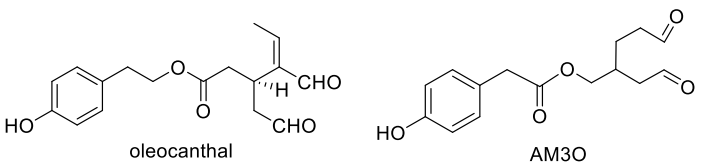

Figure 101. Anti-inflammatory natural compound oleocanthal and compound **AM30**

In summary this work describes an active patented TLR4 agonist with potential as adjuvant for vaccines, an active non-amphiphilic TLR4 antagonist based on a natural compound, and four potential TLR4 modulators. This series of compounds, with the biological experiments performed, has permitted (and will permit) to explore SAR for monosaccharide TLR4 modulators both for agonism and antagonism and to study the relationship between MD-2 binding and activity for monosaccharide molecular simplifications of Lipid A. Moreover biophysical studies on the aggregates shape of these compounds are currently being performed.

With the target molecules obtained, the biological experiments performed, the goals achieved and the still open perspectives, this PhD thesis presents itself as an unique work in the sense that through biological, biophysical and binding experiments and the current knowledge of TLR4 recognition process, it correlates monosaccharide agonistic activity to MD-2 binding and at the same time aims at correlating their activity to the shape of the supramolecular aggregates they form.

Chapter III

Materials and methods

1. Chemistry

All the commercially available reagents were used without further purification unless indicated otherwise All solvents were anhydrous grade unless indicated otherwise. When dry conditions were required, the reactions were carried out in oven-dried glassware under a slight pressure of argon.

Reaction were magnetically stirred and monitored by Thin-Layer Chromatography (TLC) on Silica Gel 60 F254 plates (Merck).

Detection of spots was performed through UV detection (254 nm) or using developing solutions: a molybdate solution [aqueous H_2SO_4 (5%) with $(NH_4)_6Mo_4O_7 \cdot 4H_2O$ (4%) and 0.2% $Ce(SO_4)_2$] or a H_2SO_4 solution [H_2O (45%) and EtOH (45%) with aqueous H_2SO_4 (10%)], followed by heating the TLC plate at 120°C.

Flash column chromatography was performed on silica gel 230–400 mesh (Merck).

The petroleum ether used as eluent in chromatography had boiling range of 40–60°C.

^{1}H and ^{13}C NMR spectra were recorded on a Varian 400 MHz MERCURY instrument. Chemical shifts are reported in ppm downfield from TMS as internal standard.

Mass spectra were recorded on ESI-MS triple quadrupole (model API2000 QTrap™, Applied Biosystems).

All molecules synthesized for the first time during this PhD project were characterized using ^{1}H NMR, 2D-COSY NMR and ^{13}C APT NMR or 2D-HSQC NMR spectroscopy for 1H and 13C chemical shifts.

All final molecules were additionally characterized by MS spectrometry for m/z values.

NMR spectra are reported in the Supporting Information.

Synthetic procedures and characterizations

FP7 Synthesis

FP7 and all its intermediates were obtained according to published procedures. [196]

FP11 Synthesis

Compounds 1-5 are common intermediates of FP7 synthesis so their synthesis and characterization is not reported here.

Compound 6

1-O-tert-butyldimethylsilyl-2-deoxy-6-O-(4-methoxybenzyl)-3-O-tetradecanoyl-2-tetradecanoylamino- β *-D-glucopyranoside.*

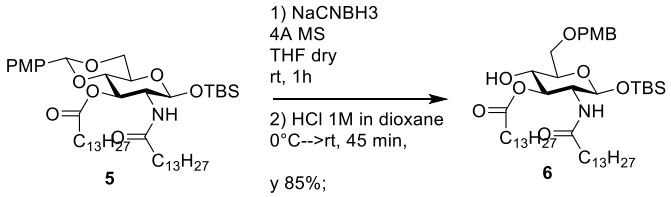

Compound **5** (320 mg, 0.38 mmol) was dissolved in dry THF (19 mL) and 4Å molecular sieves (1.15 g) and $NaCNBH_3$ (157 mg, 18.38 mmol) were added. The reaction was stirred at r.t. for 1h, then it was cooled in an ice bath and HCl (1M in dioxane) was added dropwise till bubbling ceases. The solution was left stirring 45 min at rt (monitoring the reaction by TLC) and then it was neutralized by adding saturated $NaHCO_3$ solution. Three extractions with DCM were performed and the organic phase was further washed with brine and then dried over anhydrous Na_2SO_4, filtered and the solvents were evaporated *in vacuo*.
The crude product was purified with flash chromatography (petroleum ether–EtOAc 8:2) to give compound 6 as a red oil (273 mg, 85%).

^{1}H NMR (400 MHz, $CDCl_3$, 25 °C, TMS) δ 7.23 (d, $^3J_{H,H}$= 8.6 Hz, 2H; 2x H-*ortho* PMB), 6.85 (t, $^3J_{H,H}$= 8.7 Hz, 2H: 2x H-*meta* PMB), 5.81 (d, $^3J_{H,H}$= 9.3 Hz, 1H; NH), 5.04 (dd, $^3J_{H,H}$= 10.7, 9.2 Hz, 1H; H-3), 4.67 (d, $^3J_{H,H}$= 8.1 Hz, 1H, H-1) 4.54 – 4.42 (m, 2H; CH_2-Ph) 3.94 (m, 1H; H-2), 3.78 (s, 4H; OMe, H-5), 3.70 (dd, $^3J_{H,H}$= 10.8, 5.3 Hz, 1H, H-6a), 3.54 (m, 2H, H-4, H-6b), 2.38 – 2.24 (t, $^3J_{H,H}$= 7.8 Hz, 2H, CH_2α-chain1), 2.15 – 1.98 (m, 2H, CH_2α-chain2),1.64 – 1.44 (m, 4H CH_2β-chains1,2), 1.19 (m, 40H, 20x CH_2), 0.96 – 0.70 (m, 15H, 2xCH_3 chains1,2 ,tBu-Si), 0.03 (s, 3H; CH_3-Si), 0.00 (s, 3H; CH_3-Si).

13C NMR (101 MHz, CDCl3, 25 °C, TMS) δ 174.88, 172.79, 159.29, 129.66, 129.30, 113.80, 96.53, 75.26, 73.71, 73.42, 71.25, 70.57, 55.46, 55.23, 36.98, 34.28, 31.93, 29.72, 29.68, 29.55, 29.47, 29.38, 29.36, 29.14, 25.57, 24.97, 22.69, 17.88, 14.13.

Compound 7

1-O-tert-butyldimethylsilyl-2-deoxy-6-O-(4-methoxybenzyl)- 4-O-tetradecanoyl 3-O-tetradecanoyl-2-tetradecanoylamino- β *-D-glucopyranoside*.

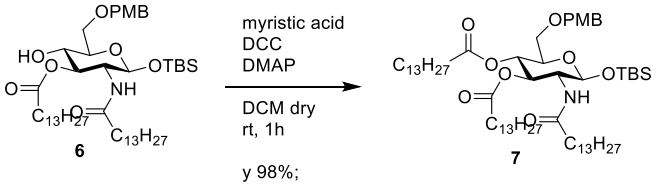

Myristic acid (144 mg, 0.63 mmol) was dissolved in dry CH_2Cl_2 (3 mL) and DCC (195 mg, 0.95 mmol) was added. After 30 min compound 6 (263 mg, 0.32 mmol) dissolved in CH_2Cl_2 dry (2 mL) and DMAP (39 mg, 0.32 mmol) were added and the mixture was stirred at room temperature for 1 h. The precipitate is removed by filtration and the solvents were evaporated *in vacuo*. The crude product was purified with flash chromatography (petroleum ether–EtOAc 9:1) to give compound 7 as a white solid (323 mg, 98%).

^{1}H NMR (400 MHz, $CDCl_3$, 25 °C, TMS) δ 7.23 (d, $^3J_{H,H}$= 8.4 Hz, 1H, 2x H-*ortho* PMB), 6.85 (d, $^3J_{H,H}$= 8.4 Hz, 1H, 2x H-*meta* PMB), 5.30 (d, 1H, NH), 5.15 (t, $^3J_{H,H}$= 10.2 Hz, 1H, H-3), 5.03 (t, $^3J_{H,H}$= 9.6 Hz, 1H, H-4), 4.77 (d, $^3J_{H,H}$= 8.1 Hz, 1H, H-1), 4.45 (s, 2H, CH_2-Ph), 3.96 – 3.85 (m, 1H, H-2), 3.79 (s, 3H, OCH_3), 3.66 – 3.58 (m, 1H, H-5), 3.51 (m, 2H, H-6a, H-6b), 2.23 (t, $^3J_{H,H}$= 7.8 Hz, 2H, CH_2α-chain1), 2.14 (t, $^3J_{H,H}$= 7.6 Hz, 2H, CH_2α-

chain2), 2.10 – 2.02 (m, 2H, CH_2α-chain3),1.63 – 1.43 (m, 6H, CH_2β-chains1,2,3), 1.24 (m, 60H, 30xCH_2), 0.94 – 0.79 (m, 15H, 2xCH_3-chains1,2 ,tBu-Si), 0.12 (s, 3H; CH_3-Si), 0.08 (s, 3H; CH_3-Si).

^{13}C NMR (101 MHz, $CDCl_3$, 25 °C, TMS) δ 173.89, 172.59, 172.26, 159.14, 129.98, 129.27, 113.67, 96.37, 73.50, 73.19, 72.31, 69.33, 69.27, 56.26, 55.23, 36.91, 34.18, 34.11, 32.78, 31.92, 29.67, 29.50, 29.36, 29.32, 29.14, 26.40, 25.58, 24.94, 24.79, 22.69, 17.88, 14.12, -4.02, -5.23

Compound 8

2-deoxy-6-O-(4-methoxybenzyl)- 4-O-tetradecanoyl 3-O-tetradecanoyl-2-tetradecanoylamino- β -D-glucopyranoside.

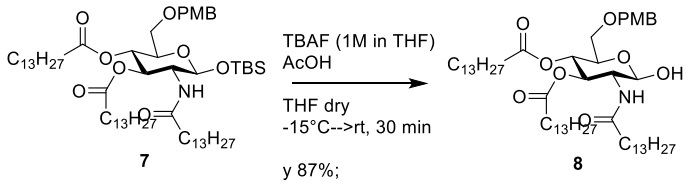

7 8

Compound 7 (323 mg, 0.31 mmol) was dissolved in dry THF (15 mL), cooled to -15 °C and a solution of TBAF (107 mg, 0.34 mmol) and AcOH (22 µL, 0.39 mmol) in THF (340 µL) was added. The reaction was stirred at -15° C for 10 min, then it was allowed to warm till rt and it was left stirring at rt for 30 min. The solution was diluted with water and extracted with CH_2Cl_2. The organic layer was dried over anhydrous Na_2SO_4, filtered and the solvents were evaporated *in vacuo*. The crude product was purified with flash chromatography (petroleum ether–EtOAc 7:3) to give compound 8 as a red oil (250 mg, 87%).

^{1}H NMR (400 MHz, $CDCl_3$, 25 °C, TMS) δ 7.24 (d, $^3J_{H,H}$= 8.7 Hz, 1H, 2x H-*ortho* PMB), 6.85 (d, $^3J_{H,H}$= 8.6 Hz, 1H, 2x H-*meta* PMB), 5.71 (d, $^3J_{H,H}$= 9.5 Hz, 1H, H-1), 5.34 – 5.23 (m, 2H, NH, H-3), 5.07 (t, $^3J_{H,H}$= 9.9 Hz, 1H, H-4), 4.45 (s, 2H, CH_2-PMP), 4.32 – 4.24 (m, 1H, H-2), 4.19 – 4.11 (m, 1H, H-5), 3.79 (s, 3H, OCH_3), 3.55 – 3.38 (m, 1H, H-6a, H-6b), 3.02 – 2.84 (bs, 1H, OH), 2.22 (t, $^3J_{H,H}$= 7.6 Hz, 2H, CH_2α-chain1), 2.18 – 2.05 (m, 4H, CH_2α-chain2,3), 1.68 – 1.41 (m, 6H, CH_2β-chains1,2,3), 1.24 (m, 60H, 30xCH_2), 0.88 (t, $^3J_{H,H}$= 6.7 Hz, 9H, 3x CH_3-chains1,2)

^{13}C NMR (101 MHz, $CDCl_3$, 25 °C, TMS) δ 174.18, 173.02, 172.22, 159.29, 129.58, 113.73, 91.68, 73.18, 70.50, 68.85, 68.73, 55.22, 52.09, 36.73, 34.22, 34.11, 31.92, 29.68, 29.37, 29.28, 29.17, 25.59, 24.91, 22.69, 14.13.

Compound 9

1,4-bis(O-dibenzylphosphoryl)-2-deoxy-6-O-(4-methoxybenzyl)- 4-O-tetradecanoyl 3-O-tetradecanoyl-2-tetradecanoylamino- α -D-glucopyranoside.

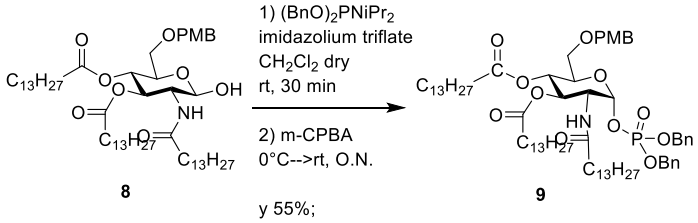

8 9

Compound **8** (100 mg, 0.11 mmol) was dissolved in dry CH_2Cl_2 (1.8 mL), then imidazolium triflate (83 mg, 0.32 mmol) and dibenzyl *N*,*N*-diisopropyl phosphoramidite (108 µl, 0.32 mmol) were added and the reaction was stirred at r.t. for 30 min. The solution was then cooled in an ice bath and *m*CPBA (93 mg, 0.54 mmol) was added. The reaction was stirred at rt overnight, then the mixture was diluted with CH_2Cl_2, washed with a saturated solution of $NaHCO_3$ and brine. The organic layer was dried over anhydrous Na_2SO_4,

filtered and the solvents were evaporated *in vacuo*. The crude product was purified with flash chromatography (petroleum ether–EtOAc 8:2) affording compound 9 as a brown solid (70 mg, 55%).

^{1}H NMR (400 MHz, $CDCl_3$, 25 °C, TMS) δ: 7.42 – 7.27 (m, 10H, 2x BnO-P) 7.17 (d, $^3J_{H,H}$= 8.5 Hz, 2H, 2x H-*ortho* PMB) 6.80 (d, $^3J_{H,H}$= 8.4 Hz, 2H, 2x H-*meta* PMB) 5.71 (dd, $^3J_{H,P}$= 5.7, $^3J_{H,H}$= 3.3 Hz, 1H, H-1) 5.57 (d, $^3J_{H,H}$= 9.1 Hz, 1H, NH) 5.24 – 5.14 (m, 2H, H-3, H-4) 5.11 – 4.95 (m, 4H, 2x CH_2(Ph)-O-P) 4.45 – 4.23 (m, 3H; CH_2-Ph PMB, H-2) 4.05 (m, 1H, H-5) 3.76 (s, 3H, OCH_3) 3.38 (d, $^3J_{H,H}$= 3.4 Hz, 2H, H6a, H6b) 2.21 (t, $^3J_{H,H}$= 7.6 Hz, 2H, CH_2α-chain1) 2.14 (t, $^3J_{H,H}$= 7.5 Hz, 2H, CH_2α-chain2) 1.85 (m, 2H, CH_2α-chain3) 1.50 (m, 4H, CH_2β-chains1,2) 1.46 – 1.36 (m, 2H, CH_2β-chain3) 1.27 (m, 60H, 30xCH_2 chains) 0.88 (t, $^3J_{H,H}$= 6.6 Hz, 9H, 3x CH_3 chains)

^{13}C NMR (101 MHz, $CDCl_3$, 25 °C, TMS) δ 184.72, 174.06, 171.63, 139.76, 129.49, 128.71, 127.97, 113.65, 92.90, 75.02, 73.14, 71.00, 69.92, 69.78, 69.68, 69.29, 69.23, 67.79, 67.75, 55.18, 36.29, 34.14, 31.92, 29.67, 29.51, 29.16, 25.36, 24.84, 22.69, 14.13.

FP11

1-O-Phosphoryl -2-deoxy-4-O-tetradecanoyl 3-O-tetradecanoyl-2-tetradecanoylamino- α -D-glucopyranoside (sodium salt)

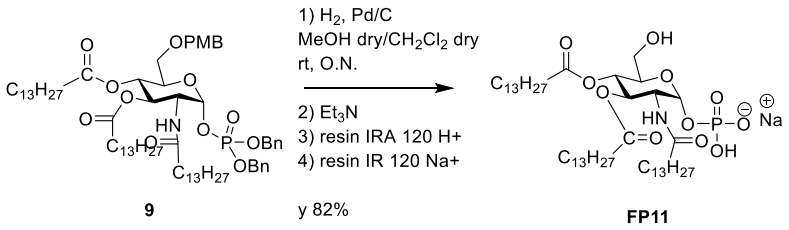

Compound 9 (25 mg, 0.021 mmol) was dissolved in dry CH_2Cl_2/MeOH 1:2 (1.3 mL), and Pd on activated charcoal was then added in catalytic amounts. The reaction mixture was stirred at rt under H_2 atmosphere overnight. Triethylamine (80 µL) was then added to the reaction mixture, and the suspension was filtered with a syringe filter. The triethylammonium salt was dissolved in dry CH_2Cl_2/MeOH 1:2 (3 mL) and treated first with an Amberlite IRA 120 H^+ exchange resin and then with an IR 120 Na^+ exchange resin to remove triethylamine and to form the sodium salt, giving compound FP11 as a white solid (16 mg, 82%).

^{1}H NMR (400 MHz, CD_3OD, 25 °C, TMS) δ: 5.47 (dd, $^3J_{H,P}$= 6.7, $^3J_{H,H}$= 3.2 Hz, 1H; H-1), 5.34 (t, $^3J_{H,H}$= 10.0 Hz, 1H, H-3), 5.09 (t, $^3J_{H,H}$= 9.9 Hz, 1H, H-4) 4.28 (dd, $^3J_{H,H}$= 10.8, 2.5 Hz, 1H, H-2), 4.14 – 4.06 (m, 1H, H-5), 3,66 (m, 1H, H-6a) 3,56 (m, 1H, H-6b) 2.39 – 2.10 (m, 6H, 3x CH_2α-chains) 1.55 (s, 6H, 3x CH_2β-chains) 1.29 (m, 60H, 30xCH_2 chains) 0.89 (t, $^3J_{H,H}$= 6.6 Hz, 9H, 3x CH_3-chains)

^{13}C NMR (101 MHz, $CDCl_3$, 25 °C, TMS) δ 174.72, 172.78, 131.63, 109.99, 92.22, 73.52, 72.09, 66.78, 62.07, 59.75, 48.57, 38.68, 34.14, 33.96, 32.77, 31.96, 29.88, 29.80, 29.71, 29.67, 29.43, 29.29, 24.89, 22.72, 14.14, 1.03.

ESI-MS: $[M]^-$ m/z = 888.6; found: m/z = 888.7

FP111 Synthesis

Compounds 1-8 are common intermediates of FP11 synthesis.

Compound 10
2-deoxy-4-O-tetradecanoyl 3-O-tetradecanoyl-2-tetradecanoylamino-β-D-glucopyranoside

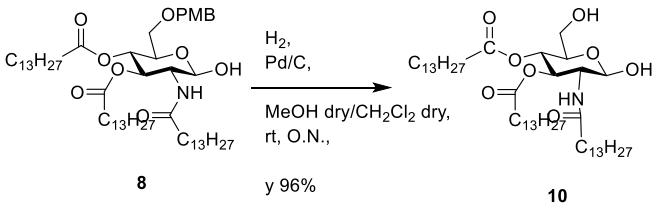

Compound 8 (120 mg, 0.129 mmol) was dissolved in dry CH_2Cl_2/MeOH 1:2 (8 mL), and Pd on activated charcoal was then added in catalytic amounts. The reaction mixture was stirred at rt under H_2 atmosphere overnight. Solvents were evaporated *in vacuo* giving compound 10 as a white solid (100 mg, 96%).

^{1}H NMR (400 MHz, $CDCl_3$, 25 °C, TMS) δ 6.09 (d, $^3J_{H,P}$= 9.1 Hz, 1H, H-1) 5.34 (t, $^3J_{H,H}$= 10.1 Hz, 1H, H-3) 5.02 (t, $^3J_{H,H}$= 9.7 Hz, 1H, H-4) 4.21 (t, $^3J_{H,H}$= 9.1 Hz, 1H, H-2) 4.04 (m, 1H, H-5) 3.67 (m, 1H, H-6a) 3.56 (m, 1H, H-6b) 2,25 (m, 4H, CH_2α-chains1,2) 2,11 (m, 4H, CH_2α-chain3) 1.52 (m, 6H, CH_2β-chains1,2,3) 1.23 (m, 60H, 30xCH_2) 0.86 (t, $^3J_{H,H}$= 6.6 Hz, 9H, CH_3-chains1,2,3)

^{13}C NMR (101 MHz, $CDCl_3$, 25 °C, TMS) δ 174.15, 173.64, 173.17, 91.41, 70.32, 69.68, 68.48, 61.15, 52.46, 36.70, 34.14, 31.93, 29.71, 29.38, 29.29, 25.62, 24.94, 22.69, 14.12, 1.01

Compound 11
1,6-bis(O-dibenzylphosphoryl)-2-deoxy- 4-O-tetradecanoyl 3-O-tetradecanoyl-2-tetradecanoylamino- α -D-glucopyranoside

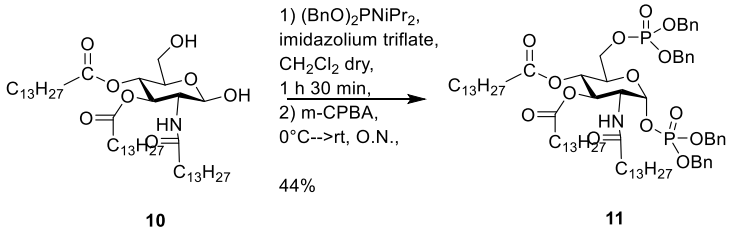

Compound 10 (50 mg, 0.062 mmol) was dissolved in dry CH_2Cl_2 (1.0 mL), then imidazolium triflate (72 mg, 0.28 mmol) and dibenzyl *N*,*N*-diisopropyl phosphoramidite (91 µl, 0.27 mmol) were added and the reaction was stirred at r.t. for 1,5 h. The solution was then cooled in an ice bath and *m*CPBA (85 mg, 0.49 mmol) was added. The reaction was stirred at rt overnight, and then the mixture was diluted with CH_2Cl_2, washed with a saturated solution of $NaHCO_3$ and brine. The organic layer was dried over anhydrous Na_2SO_4, filtered and the solvents were evaporated *in vacuo*. The crude product was purified with flash chromatography (petroleum ether–EtOAc 8:2) affording compound 11 as a brown solid (36 mg, 44%).

^{1}H NMR (400 MHz, CDCl3, 25 °C, TMS) δ 7.44 – 7.21 (m, 20H, 4xBnO-P) 5.64 (dd, 3JH,P= 6.0, $^3J_{H,H}$= 3.3 Hz, 1H, H-1β) 5.61 (d, $^3J_{H,H}$= 9.3 Hz, 1H, NH) 5.20 – 5.10 (m, 2H, H-3, H-5) 5.10 – 4.96 (m, 9H, 4x CH_2(Ph)-O-P, H-4) 4.33 (t, $^3J_{H,H}$= 9.8 Hz, 1H, H-2) 3.92 (m, 2H, H-6a, H-6b) 2,20 (m, 4H, CH_2α-chains1,2) 1.95 – 1.77 (m, 2H, CH_2α-chain3) 1.49 (m, 4H, CH_2β-chains1,2) 1.47 – 1.36 (m, 2H, CH_2β-chain3) 1.27 (m, 60H, 30xCH_2) 0.88 (t, $^3J_{H,H}$= 6.6 Hz, 9H, CH_3-chains1,2,3)

^{13}C NMR (101 MHz, CDCl3, 25 °C, TMS) δ 173.95, 171.72, 151.63, 128.53, 128.03, 127.89, 105.03, 70.17, 69.72, 69.39, 66.68, 51.60, 36.30, 33.98, 31.92, 29.71, 29.67, 29.37, 29.16, 25.40, 24.86, 22.69, 14.13.

FP111

1,6-bis(O-Phosphoryl) -2-deoxy-4-O-tetradecanoyl 3-O-tetradecanoyl-2-tetradecanoylamino- α -D-glucopyranoside (sodium salt)

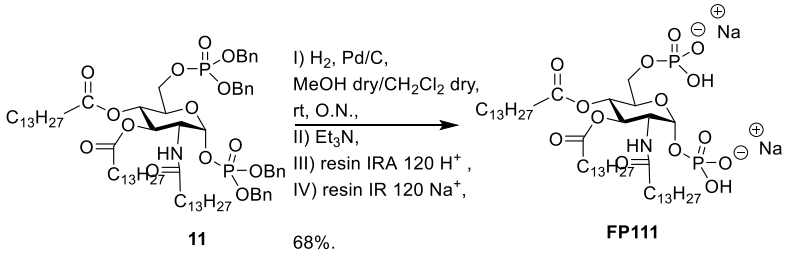

Compound 11 (33 mg, 0.028 mmol) was dissolved in dry CH_2Cl_2/MeOH 1:2 (1.3 mL), and Pd on activated charcoal was then added in catalytic amounts. The reaction mixture was stirred at rt under H_2 atmosphere overnight. Triethylamine (80 µL) was then added to the reaction mixture, and the suspension was filtered with a syringe filter. The triethylammonium salt was dissolved in dry CH_2Cl_2/MeOH 1:2 (3 mL) and treated first with an Amberlite IRA 120 H^+ exchange resin and then with an IR 120 Na^+ exchange resin to remove triethylamine and to form the sodium salt, giving compound FP111 as a white solid (20 mg, 68%).

^{1}H NMR (400 MHz, CD_3OD, 25 °C, TMS) δ 5.53 (dd, $^3J_{H,P}$= 6.3, $^3J_{H,H}$= 3.2 Hz, 1H, H-1) 5.32 (t, $^3J_{H,H}$= 10.8 Hz, 1H, H-3) 5.14 (t, $^3J_{H,H}$= 9.8 Hz, 1H, H-4) 4.32 (dt, $^3J_{H,H}$= 10.9, 3.1 Hz, 1H, H-2) 4.28 – 4.21 (m, 1H, H-5) 4.12 – 3.97 (m, 2H, H-6a, H-6b) 2.48 – 2.06 (m, 6H, CH_2α-chains1,2,3) 1.71 – 1.47 (m, 6H, CH_2β-chains1,2,3) 1.29 (s, 60H, 30xCH_2) 0.90 (t, $^3J_{H,H}$= 6.6 Hz, 9H, CH_3-chains1,2,3)

^{13}C NMR (101 MHz, CD_3OD, 25 °C, TMS) δ 175.10, 172.94, 172.29, 127.68, 70.49, 69.36, 68.31, 51.52, 47.85, 35.57, 33.46, 31.70, 29.45, 29.12, 28.85, 25.62, 24.50, 22.36, 13.06, -5.54.

ESI-MS: $[M]^-$ m/z = 968.6; found: m/z = 968.7

AM158 Synthesis

Chain A:

Compound 12
Ethyl 3-(4-hexyloxyphenyl)propanoate

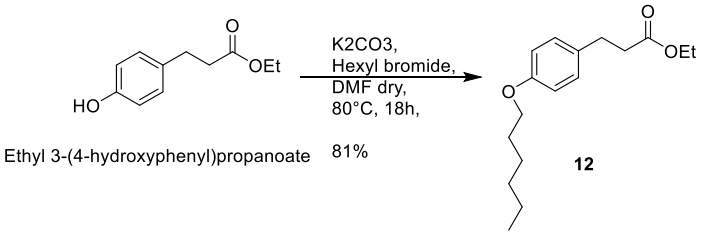

Ethyl 3-(4-hidroxyphenyl)propanoate (250 mg, 1.29 mmol) was dissolved in dry DMF (13 mL) and K_2CO_3 (356 mg, 2.57 mmol) was added. The reaction was stirred at r.t. for 1h, then Hexyl bromide was added dropwise. Solution is brought to reflux and left stirring O.N.
The solvent was evaporated *in vacuo*, then EtOAc is added and the mixture was washed with water and brine. The organic layer was dried over anhydrous Na_2SO_4, filtered and the solvents were evaporated *in vacuo*. The crude product was purified with flash chromatography (petroleum ether–EtOAc 9.6:0.4) affording compound 12 (290 mg, 81%).

^{1}H NMR (400 MHz, $CDCl_3$, 25 °C, TMS) δ 7.10 (d, $^3J_{H,H}$= 8.6 Hz, 2H, 2x H-*meta* Ph), 6.81 (d, $^3J_{H,H}$= 8.6 Hz, 2H, 2x H-*ortho* Ph), 4.12 (q, $^3J_{H,H}$= 7.2 Hz, 2H, OCH_2 ester), 3.92 (t, $^3J_{H,H}$= 6.6 Hz, 2H, OCH_2 ether), 2.88 (t, $^3J_{H,H}$= 7.8 Hz, 2H, CH_2-β), 2.58 (t, $^3J_{H,H}$= 7.8 Hz, 2H, CH_2-α), 1.83 – 1.66 (m, 2H, CH_2 in 2 ether), 1.50 – 1.39 (m, 2H, CH_2 in 3 ether), 1.35 – 1.29 (m, 4H, 2XCH_2 ether), 1.23 (t, $^3J_{H,H}$= 7.1 Hz, 3H, CH_3 ester), 0.95 – 0.81 (m, 3H, CH_3 ether)

Chain A
3-(4-hexyloxyphenyl)propionic acid

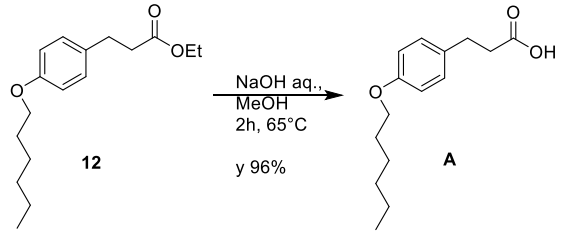

Compound 12 (290 mg, 1.04 mmol) was dissolved in MeOH (2,5 mL) and NaOH aq. 4M (640 µL, 2.76 mmol) was added dropwise. The resulting suspension was heated to 65°C and left stirring for 2h.
Methanol was evaporated *in vacuo*, then the suspension is diluted with water till all precipitates dissolves. HCl aq. 1M is finally added till pH1 and the white precipitate formed is filtered to give desired compound A without any additional purification (250 mg, 96%).

^{1}H NMR (400 MHz, $CDCl_3$, 25 °C, TMS) δ 7.11 (d, $^3J_{H,H}$= 8.6 Hz, 2H, 2x H-*meta* Ph), 6.83 (d, $^3J_{H,H}$= 8.6 Hz, 2H, 2x H-*ortho* Ph), 3.92 (t, $^3J_{H,H}$= 6.6 Hz, 2H, OCH_2 ether), 2.90 (t, $^3J_{H,H}$= 7.8 Hz, 2H, CH2-β), 2.65 (t, $^3J_{H,H}$= 7.8 Hz, 2H, CH_2-α), 1.83 – 1.66 (m, 2H, CH_2 in 2 ether), 1.50 – 1.39 (m, 2H, CH_2 in 3 ether), 1.35 – 1.29 (m, 4H, 2x CH_2 ether), 0.95 – 0.81 (m, 3H, CH_3 ether)

Scaffold:

Compounds 1-3 are common intermediates of FP11 synthesis.

Compound 13
1-O-tert-butyldimethylsilyl-2-azido-2-deoxy-4,6-O-(4-methoxybenzylidene)-3-O-tetradecanoyl-β-D glucopyranoside

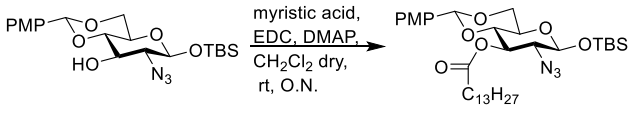

3 — 71% — 13

Myristic acid (2.3 g, 10.1 mmol) was dissolved in dry CH_2Cl_2 (40 mL) and EDC (3.2 g, 16.8 mmol) was added. After 30 min compound 3 (1.47 g, 3.35 mmol) dissolved in dry CH_2Cl_2 (15 mL) was added, followed by DMAP (410 mg, 3.35 mmol) and the mixture was stirred at room temperature overnight. The reaction mixture was diluted with CH_2Cl_2 and washed with saturated NaHCO3 solution and brine. The organic layer was dried over anhydrous Na_2SO_4, filtered and the solvents were evaporated *in vacuo*. The crude product was purified with flash chromatography (petroleum ether–EtOAc 9:1) to give compound 13 as a yellow oil (1,550 g, 71%).

^{1}H NMR (400 MHz, $CDCl_3$, 25 °C, TMS) δ 7.33 (d, $^3J_{H,H}$= 8.5 Hz, 2H, 2x H-*ortho* PMP),6.82 (d, $^3J_{H,H}$= 8.5 Hz, 2x H-*meta* PMP), 5.43 (s, 1H; CH-Ph), 5.11 (t, $^3J_{H,H}$= 9.8 Hz, 1H; H-3), 4.70 (d, $^3J_{H,H}$= 7.6 Hz, 1H; H-1), 4.27 (dd, $^3J_{H,H}$= 10.5, 4.9 Hz, 1H; H-5), 3.79 (s, 3H, OCH_3), 3.81-3.76 (m, 1H, H-6a), 3.61 (t, $^3J_{H,H}$= 9.5 Hz, 1H; H-4), 3.46 (m, 1H, H-6b), 3.39 (dd, $^3J_{H,H}$= 10.1, 7.6 Hz, 1H, H-2), 2.36 (t, $^3J_{H,H}$= 7.4 Hz, 1H; CH_2α-chain1) 1.62 (m, 2H, CH_2β-chain1) 1.27 (m, 20H, 10x CH_2) 0.93 (s, 9H; t-Bu) 0.86 (t, $^3J_{H,H}$= 6.6 Hz, 3H, CH_3-chain1) 0.16 (s, 6H, 2x CH_3-Si)

^{13}C NMR (101 MHz, CDCl3, 25 °C, TMS) δ 172.52, 160.04, 129.29, 127.39, 113.47, 101.37, 97.62, 78.70, 70.63, 68.40, 67.24, 66.55, 60.35, 55.17, 34.25, 31.92, 29.64, 29.36, 28.92, 25.50, 25.04, 22.69, 21.01, 17.89, 14.13, -4.43, -5.25.

Compound 14
1-O-tert-butyldimethylsilyl-2-amino-2-deoxy-4,6-O-(4-methoxybenzylidene)-3-O-tetradecanoyl- β -D-glucopyranoside

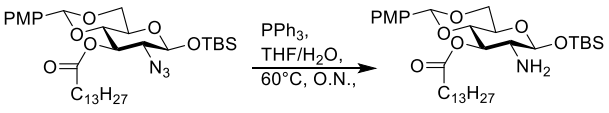

13 — quant. — 14

Compound 13 (413 mg, 0.64 mmol) was dissolved in THF (3.5 mL) then H_2O (459 µL, 25.50 mmol) and PPh_3 (1.8 g, 6.86 mmol) was added and the reaction was stirred at 60° C overnight. The solvents were evaporated *in vacuo* and the crude product was purified with flash chromatography (petroleum ether–EtOAc 8:2) to give compound 14 as a colorless oil (378 mg, quant.).

^{1}H NMR (400 MHz, $CDCl_3$, 25 °C, TMS) δ 7.33 (d, $^3J_{H,H}$= 8.5 Hz, 2H, 2x H-*ortho* PMP),6.82 (d, $^3J_{H,H}$= 8.5 Hz, 2x H-*meta* PMP), 5.40 (s, 1H; CH-Ph PMP), 5.08 (t, $^3J_{H,H}$= 9.7 Hz, 1H; H-3), 4.54 (d, $^3J_{H,H}$= 7.5 Hz, 1H, H-1), 4.21 (dd, $^3J_{H,H}$= 10.5, 4.9 Hz, 1H; H-5), 3.72 (s, 3H, OCH_3), 3.76-3.70 (m, 1H, H-6a), 3.59 (t, $^3J_{H,H}$= 9.4 Hz, 1H; H-4), 3.45 (td, $^3J_{H,H}$= 9.7, 4.8 Hz, 1H; H-6b), 2.84 – 2.71 (m, 1H; H-2) 2.36 (t, $^3J_{H,H}$= 7.4 Hz, 2H; CH_2α-chain1) 1.62

(m, 2H, CH_2β-chain1) 1.27 (m, 20H, 10x CH_2) 0.93 (s, 9H; t-Bu) 0.86 (t, $^3J_{H,H}$= 6.6 Hz, 3H, CH_3-chain1) 0.16 (s, 6H, 2XCH_3-Si)

^{13}C NMR (101 MHz, CDCl3, 25 °C, TMS) δ: 173.30, 159.93, 129.65, 127.38, 113.40, 101.25, 99.89, 79.24, 76.88, 73.27, 68.59, 66.72, 58.98, 55.08, 34.34, 31.92, 25.69, 25.13, 22.68, 22.66, 17.93, 14.13, -1.58, -5.18.

Compound 15

*1-O-tert-butyldimethylsilyl-2-deoxy-4,6-O-(4-methoxybenzylidene)-3-O-tetradecanoyl-2-[3-(4-hexyloxyphenyl)propionoyl]-amino-*β*-D-glucopyranoside*

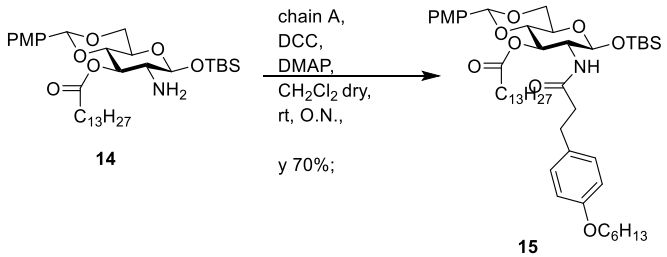

Compound A (121 mg, 0.48 mmol) was dissolved in dry CH_2Cl_2 (4 mL) and DCC (149 mg, 0.72 mmol) was added. After 30 min compound 14 (150 mg, 0.24 mmol) and DMAP (29 mg, 0.24 mmol) were added and the mixture was stirred at room temperature for 1 night. The precipitate is removed by filtration and the solvents were evaporated *in vacuo*. The crude product was purified with flash chromatography (petroleum ether–EtOAc 8.5:1.5) to give compound 15 as a yellow oil (144 mg, 70%).

^{1}H NMR (400 MHz, $CDCl_3$, 25 °C, TMS) δ 7.34 (d, $^3J_{H,H}$= 8.5 Hz, 2H, 2x H-*ortho* PMP), 7.01 (d, $^3J_{H,H}$= 8.5 Hz, 2H, 2x H-*meta* Ph chain A), 6.83 (d, $^3J_{H,H}$= 8.6 Hz, 2H, 2x H-*ortho* Ph chain A), 6.75 (d, $^3J_{H,H}$= 8.5 Hz, 2x H-*meta* PMP), 6.19 (d, $^3J_{H,H}$= 9.7 Hz, 1H; N-H) 5.45 (s, 1H; CH-Ph PMP), 5.21 (t, $^3J_{H,H}$= 10.0 Hz, 1H; H-3), 4.66 (d, $^3J_{H,H}$= 7.9 Hz, 1H, H-1), 4.19 (dd, $^3J_{H,H}$= 10.5, 4.9 Hz, 1H, H-5), 4.12 (m, 1H, H-2), 3.89 (m, 2H, OCH_2 ether), 3.77 (s, 3H, OCH_3), 3.78-3.70 (m, 2H, H-6a, H-4), 3.46 (td, $^3J_{H,H}$= 9.7, 4.8 Hz, 1H; H-6b), 2.80 (t, $^3J_{H,H}$= 7.8 Hz, 2H, CH_2-β chain A), 2.37 (t, $^3J_{H,H}$= 7.8 Hz, 2H, CH_2-α chain A), 2.26 (m, 2H; CH_2α chain 1) 1.62 (m, 4H, CH_2β-chain1, CH_2 in 2 ether chain A) 1.27 (m, 20H, 10x CH_2) 0.87 (s, 15H; t-Bu, CH_3-chain1, CH_3-chain A) 0.02 (s, 3H, CH_3-Si) 0.00 (s, 3H, CH_3-Si)

^{13}C NMR (101 MHz, $CDCl_3$, 25 °C, TMS) δ 174.50, 171.84, 159.96, 157.52, 153.84, 132.60, 129.57, 129.39, 127.31, 114.44, 113.45, 101.20, 97.22, 78.76, 72.00, 67.92, 66.40, 56.10, 55.17, 49.79, 38.76, 37.72, 34.26, 32.54, 31.92, 31.61, 30.89, 30.63, 29.72, 29.67, 29.37, 29.29, 29.02, 26.21, 25.75, 25.52, 25.47, 25.11, 24.72, 22.69, 22.61, 17.79, 14.13, 14.05, -4.16, -5.39..

Compound 16

*1-O-tert-butyldimethylsilyl-2-deoxy-6-O-(4-methoxybenzyl)-3-O-tetradecanoyl-2-[3-(4-hexyloxyphenyl) propionoyl]-amino-*β*-D-glucopyranoside*

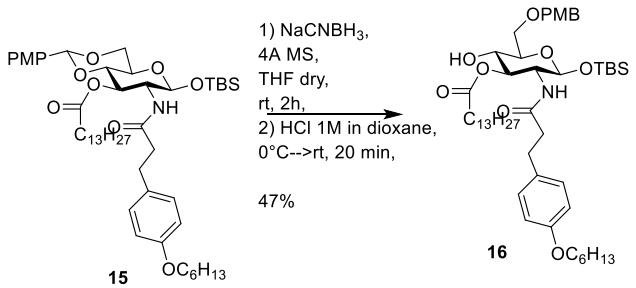

Compound 15 (144 mg, 0.17 mmol) was dissolved in dry THF (8.5 mL) and 4Å molecular sieves (518 mg) and $NaCNBH_3$ (69 mg, 1.09 mmol) were added. The reaction was stirred at r.t. for 2h, then it was cooled in an

ice bath and HCl (1M in dioxane) was added dropwise till bubbling ceases. The solution was left stirring 20 min at rt (monitoring the reaction by TLC) and then it was neutralized by adding saturated $NaHCO_3$ solution. Three extractions with DCM were performed and the organic phase was further washed with brine and then dried over anhydrous Na_2SO_4, filtered and the solvents were evaporated *in vacuo*.
The crude product was purified with flash chromatography (petroleum ether–EtOAc 8:2) to give compound 16 as a yellow oil (68 mg, 47%).

^{1}H NMR (400 MHz, $CDCl_3$, 25 °C, TMS) δ 7.24 (d, $^3J_{H,H}$= 8.5 Hz, 2H, 2x H-*ortho* PMB), 7.05 (d, $^3J_{H,H}$= 8.5 Hz, 2H, 2x H-*meta* Ph chain A), 6.87 (d, $^3J_{H,H}$= 8.6 Hz, 2H, 2x H-*ortho* Ph chain A), 6.77 (d, $^3J_{H,H}$= 8.5 Hz, 2x H-*meta* PMB), 5.77 (d, $^3J_{H,H}$= 9.7 Hz, 1H; N-H) 5.02 (dd, $^3J_{H,H}$= 10.9, 9.0 Hz, 1H; H-3), 4.68 (d, $^3J_{H,H}$= 7.9 Hz, 1H, H-1), 4.55 – 4.43 (m, 2H, CH_2-Ph PMB) 4.00 – 3.92 (m, 1H, H-2), 3.89 (t, $^3J_{H,H}$= 6.7 Hz, 2H, OCH_2 ether), 3.80 (s, 3H, OCH_3), 3.78-3.70 (m, 2H, H-6a, H-4), 3.54 (dt, $^3J_{H,H}$= 9.8, 4.9 Hz, 1H; H-6b) 2.80 (t, $^3J_{H,H}$= 7.8 Hz, 2H, CH_2-β chain A), 2.37 (t, $^3J_{H,H}$= 7.8 Hz, 2H, CH_2-α chain A), 2.26 (m, 2H; CH_2α chain 1) 1.62 (m, 4H, CH_2β-chain1, CH_2 in 2 ether chain A) 1.27 (m, 26H; 10x CH_2, 3x CH_2 ether) 0.87 (s, 15H; t-Bu, CH_3-chain1, CH_3-chain A) 0.02 (s, 3H, CH_3-Si) 0.00 (s, 3H, CH_3-Si)

^{13}C NMR (101 MHz, $CDCl_3$, 25 °C, TMS) δ 174.97, 171.89, 159.31, 157.54, 132.61, 129.63, 129.33, 129.07, 114.46, 113.83, 96.53, 75.17, 73.73, 73.45, 71.25, 70.56, 67.95, 55.62, 55.26, 38.79, 34.27, 31.93, 31.61, 30.67, 29.71, 29.67, 29.50, 29.38, 29.31, 29.28, 29.11, 25.75, 25.57, 25.01, 22.70, 22.62, 17.89, 14.14, 14.05, -4.09, -5.28.

Compound 17
1-O-tert-butyldimethylsilyl-2-deoxy-6-O-(4-methoxybenzyl)- 4-O-tetradecanoyl 3-O-tetradecanoyl-2-[3-(4-hexyloxyphenyl)propionoyl]-amino-β-D-glucopyranoside

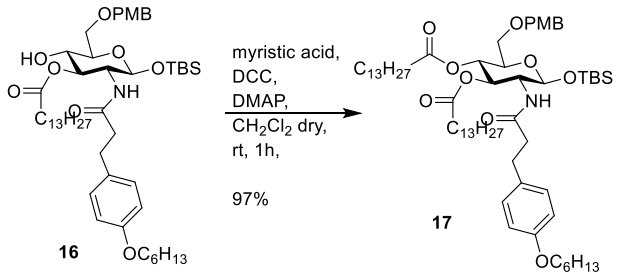

Myristic acid (54 mg, 0.24 mmol) was dissolved in dry CH_2Cl_2 (1 mL) and DCC (49 mg, 0.24 mmol) was added. After 30 min compound 16 (68 mg, 0.079 mmol) dissolved in CH_2Cl_2 dry (1.5 mL) and DMAP (10 mg, 0.079 mmol) were added and the mixture was stirred at room temperature for 1 h. The precipitate is removed by filtration and the solvents were evaporated *in vacuo*. The crude product was purified with flash chromatography (petroleum ether–EtOAc 9:1) to give compound 17 as a yellow oil (82 mg, 97%).

^{1}H NMR (400 MHz, $CDCl_3$, 25 °C, TMS) δ 7.24 (d, $^3J_{H,H}$= 8.5 Hz, 2H, 2x H-*ortho* PMB), 7.05 (d, $^3J_{H,H}$= 8.5 Hz, 2H, 2x H-*meta* Ph chain A), 6.87 (d, $^3J_{H,H}$= 8.6 Hz, 2H, 2x H-*ortho* Ph chain A), 6.77 (d, $^3J_{H,H}$= 8.5 Hz, 2x H-*meta* PMB), 5.55 (d, $^3J_{H,H}$= 9.3 Hz, 1H; N-H), 5.15 (t, $^3J_{H,H}$ = 10.0 Hz, 1H; H-3), 5.03 (t, $^3J_{H,H}$= 9.6 Hz, 1H, H-4), 4.76 (d, $^3J_{H,H}$= 7.9 Hz, 1H, H-1), 4.43 (s, 2H, CH_2-Ph PMB), 3.99 – 3.82 (m, 3H, H-2, OCH_2 ether), 3.80 (s, 3H, OCH_3), 3.70 – 3.57 (m, 1H, H-5), 3.56 – 3.43 (m, 2H; H-6a, H-6b), 2.81 (t, $^3J_{H,H}$= 8.1 Hz, 2H, CH_2-β chain A), 2.48 – 2.25 (m, 4H, CH_2-α chain A, CH_2α chain 1) 2.20 – 2.10 (m, 2H, CH_2α-chain3), 1.74 (m, 2H, CH_2 in 2 ether chain A) 1.46 (m, 4H, CH_2β chain 1, CH_2β chain 3) 1.27 (m, 46H, 20x CH_2, 3x CH_2 ether) 0.87 (s, 15H; t-Bu, CH_3-chain1, CH_3-chain A) 0.02 (s, 3H, CH_3-Si) 0.00 (s, 3H, CH_3-Si)

^{13}C NMR (101 MHz, $CDCl_3$, 25 °C, TMS) δ 173.93, 172.26, 171.68, 169.64, 159.14, 157.56, 132.53, 129.97, 129.28, 129.11, 114.48, 113.67, 96.31, 73.50, 73.20, 72.24, 69.30, 69.22, 67.96, 56.38, 55.23, 49.61, 38.74,

36.02, 35.29, 34.91, 34.12, 32.79, 31.93, 31.60, 30.89, 30.52, 29.71, 29.66, 29.57, 29.51, 29.47, 29.38, 29.27, 29.20, 29.15, 28.86, 26.41, 25.74, 25.58, 25.46, 25.32, 24.97, 24.79, 24.22, 22.70, 22.62, 17.89, 14.14, -4.02, -5.26.

Compound 18

2-deoxy-6-O-(4-methoxybenzyl)- 4-O-tetradecanoyl 3-O-tetradecanoyl-2-[3-(4-hexyloxyphenyl)propionoyl]-amino- α -D-glucopyranoside

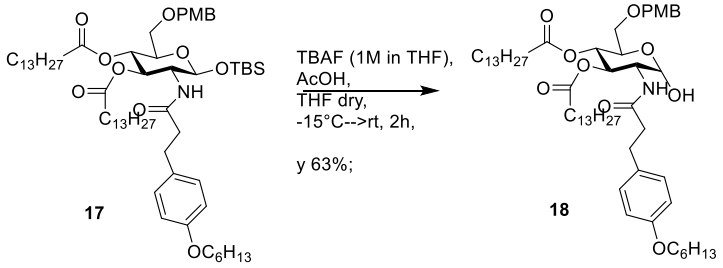

Compound 17 (75 mg, 0.07 mmol) was dissolved in dry THF (15 mL), cooled to -15 °C and a solution of TBAF (24 mg, 0.08 mmol) and AcOH (5 µl, 0.09 mmol) in THF (77 µL) was added. The reaction was stirred at -15° C for 10 min, then it was allowed to warm till rt and it was left stirring at rt for 2h. The solution was diluted with water and extracted with CH_2Cl_2. The organic layer was dried over anhydrous Na_2SO_4, filtered and the solvents were evaporated *in vacuo*. The crude product was purified with flash chromatography (petroleum ether–EtOAc 6:4) to give compound 18 as a white solid (42 mg, 63%).

^{1}H NMR (400 MHz, $CDCl_3$, 25 °C, TMS) δ 7.22 (d, $^3J_{H,H}$= 8.5 Hz, 2H, 2x H-*ortho* PMB), 7.06 (d, $^3J_{H,H}$= 8.5 Hz, 2H, 2x H-*meta* Ph chain A), 6.87 (d, $^3J_{H,H}$= 8.6 Hz, 2H, 2x H-*ortho* Ph chain A), 6.77 (d, $^3J_{H,H}$= 8.5 Hz, 2x H-*meta* PMB), 5.55 (d, $^3J_{H,H}$= 9.3 Hz, 1H; N-H), 5.24 (t, $^3J_{H,H}$= 10.2 Hz, 1H; H-3), 5.13 (d, $^3J_{H,H}$= 3.6 Hz, 1H; H-1), 5.03 (t, $^3J_{H,H}$= 9.8 Hz, 1H, H-4), 4.50 – 4.38 (m, 2H, CH_2-Ph PMB), 4.24 (td, $^3J_{H,H}$= 10.1, 3.5 Hz, 1H, H-2), 4.12 (m, 1H, H-5), 3.89 (t, $^3J_{H,H}$= 6.6 Hz, 2H, OCH_2 ether), 3.78 (s, 3H, OCH_3), 3.50 – 3.34 (m, 2H; H-6a, H-6b), 2.81 (t, $^3J_{H,H}$= 8.1 Hz, 2H, CH_2-β chain A), 2.38 (m, 2H, CH_2α chain A), 2.16 (m, 2H; CH_2α chain 1, CH_2α-chain3), 1.74 (m, 2H, CH_2 in 2 ether chain A) 1.46 (m, 4H, CH_2β chain 1, CH_2β chain 3) 1.27 (m, 46H, 20x CH_2, 3x CH_2 ether) 0.95 – 0.77 (m, 9H; CH_3-chain1, CH_3-chain A, CH_3 ether of chain A)

^{13}C NMR (101 MHz, $CDCl_3$, 25 °C, TMS) δ 177.94, 174.21, 172.22, 172.18, 159.27, 157.57, 132.34, 129.60, 129.42, 129.22, 114.43, 113.71, 91.52, 73.10, 70.48, 68.70, 68.60, 68.00, 55.20, 52.18, 38.51, 34.16, 34.09, 33.98, 33.71, 31.93, 31.60, 30.64, 29.71, 29.67, 29.51, 29.47, 29.37, 29.32, 29.28, 29.26, 29.16, 25.72, 25.51, 24.92, 24.86, 22.70, 22.61, 14.13, 14.05.

Compound 19

1-O-dibenzylphosphoryl-2-deoxy-6-O-(4-methoxybenzyl)- 4-O-tetradecanoyl 3-O-tetradecanoyl-2-[3-(4-hexyloxyphenyl)propionoyl]- amino- α -D-glucopyranoside

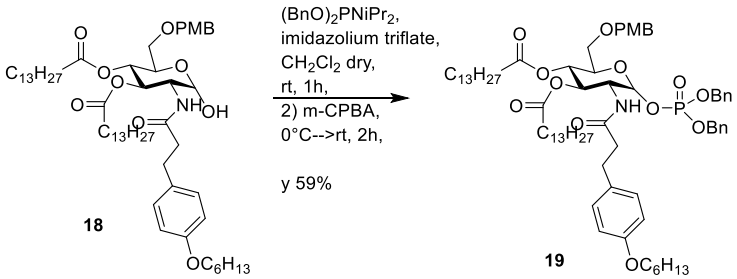

Compound 18 (40 mg, 0.042 mmol) was dissolved in dry CH_2Cl_2 (0.7 mL), then imidazolium triflate (33 mg, 0.126 mmol) and dibenzyl *N*,*N*-diisopropyl phosphoramidite (42 µl, 0.126 mmol) were added and the reaction was stirred at r.t. for 1h. The solution was then cooled in an ice bath and *m*CPBA (36 mg, 0.210 mmol) was added. The reaction was stirred at rt 2h, then the mixture was diluted with CH_2Cl_2, washed with a saturated solution of $NaHCO_3$ and brine. The organic layer was dried over anhydrous Na_2SO_4, filtered and the solvents were evaporated *in vacuo*. The crude product was purified with flash chromatography (petroleum ether–EtOAc 7:3) affording compound 19 as a colorless oil (30 mg, 59%).

^{1}H NMR (400 MHz, $CDCl_3$, 25 °C, TMS) δ 7.41 – 7.22 (m, 10H, 2xBnO-P), 7.22 (d, $^3J_{H,H}$= 8.5 Hz, 2H, 2x H-*ortho* PMB), 7.06 (d, $^3J_{H,H}$= 8.5 Hz, 2H, 2x H-*meta* Ph chain A), 6.87 (d, $^3J_{H,H}$= 8.6 Hz, 2H, 2x H-*ortho* Ph chain A), 6.77 (d, $^3J_{H,H}$= 8.5 Hz, 2x H-*meta* PMB), 5.72 (dd, $^3J_{H,P}$= 5.9, $^3J_{H,H}$= 3.3 Hz, 1H, H-1), 5.61 (d, $^3J_{H,H}$= 9.0 Hz, 1H; N-H), 5.24 – 5.12 (m, 2H; H-3, H-4), 5.09 – 4.94 (m, 4H, 2XCH_2(Ph)-O-P), 4.49 – 4.24 (m, 3H, CH_2-Ph PMB, H-2), 4.04 (dt, $^3J_{H,H}$= 10.0, 3.6 Hz, 1H; H-5), 3.89 (t, $^3J_{H,H}$= 6.6 Hz, 2H; OCH_2 ether), 3.78 (s, 3H, OCH_3), 3.40 – 3.36 (m, 2H; H-6a, H-6b), 2.69 (t, $^3J_{H,H}$= 8.1 Hz, 2H, CH_2-β chain A), 2.20 – 2.03 (m, 6H,CH_2-α chain A, CH_2α chain 1, CH_2α-chain3), 1.75 (m, 2H, CH_2 in 2 ether of chain A) 1.47 (m, 4H, CH_2β chain 1, CH_2β chain 3) 1.27 (m, 46H, 20x CH_2, 3x CH_2 ether) 0.95 – 0.77 (m, 9H; CH_3-chain1, CH_3-chain A, CH_3 ether of chain A)

^{13}C NMR (101 MHz, $CDCl_3$, 25 °C, TMS) δ 185.92, 172.12, 171.57, 159.19, 157.51, 149.39, 141.75, 139.35, 129.54, 129.50, 129.08, 128.73, 128.71, 128.66, 128.55, 128.50, 128.06, 127.97, 127.94, 116.98, 114.37, 113.65, 73.15, 69.70, 69.23, 67.69, 65.07, 55.19, 50.63, 34.07, 31.94, 29.72, 29.68, 29.52, 29.39, 29.31, 25.75, 24.90, 22.71, 14.15

AM158

1-O-Phosphoryl -2-deoxy-4-O-tetradecanoyl 3-O-tetradecanoyl-2-[3-(4-hexyloxyphenyl)propionoyl]- amino-α -D-glucopyranoside

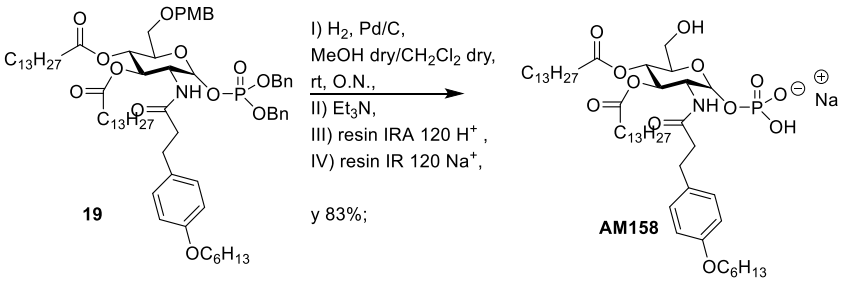

Compound 19 (30 mg, 0.025 mmol) was dissolved in dry CH_2Cl_2/MeOH 1:2 (1.3 mL), and Pd on activated charcoal was then added in catalytic amounts. The reaction mixture was stirred at rt under H_2 atmosphere overnight. Triethylamine (80 µL) was then added to the reaction mixture, and the suspension was filtered with a syringe filter. The triethylammonium salt was dissolved in dry CH_2Cl_2/MeOH 1:2 (3 mL) and treated first with an Amberlite IRA 120 H^+ exchange resin and then with an IR 120 Na^+ exchange resin to remove triethylamine and to form the sodium salt, giving compound AM158 as a white solid (22 mg, 83%).

^{1}H NMR (400 MHz, CD_3OD, 25 °C, TMS) δ 7.10 (d, $^3J_{H,H}$= 8.5 Hz, 2H, 2x H-*meta* Ph chain A), 6.78 (d, $^3J_{H,H}$= 8.6 Hz, 2H, 2x H-*ortho* Ph chain A), 5.55 (dd, $^3J_{H,P}$= 5.9, $^3J_{H,H}$= 3.3 Hz, 1H, H-1), 5.33 (dd, $^3J_{H,H}$= 10.8, 9.4 Hz, 1H; H-3), 5.09 (t, $^3J_{H,H}$= 9.8 Hz, 1H; H-4), 4.27 (m, 1H, H-2) 4.13 – 4.03 (m, 1H; H-5), 3.91 (t, $^3J_{H,H}$= 6.5 Hz, 2H; OCH_2 ether), 3.66 – 3.60 (m, 1H; H-6a) 3.52 (dd, $^3J_{H,H}$= 12.3, 4.7 Hz, 1H; H-6b), 2.83 – 2.72 (m, 2H, CH_2-β chain A), 2.47 (t, $^3J_{H,H}$= 7.5 Hz, 2H, CH_2-α chain A) 2.36 – 2.18 (m, 2H, CH_2α chain 1) 2.10 (t, $^3J_{H,H}$= 7.4 Hz, 2H, CH_2α-chain3), 1.75 (m, 2H, CH_2 in 2 ether of chain A) 1.49 (m, 4H, CH_2β chain 1, CH_2β chain 3) 1.27 (m, 46H, 20x CH_2, 3x CH_2 ether) 0.98 – 0.77 (m, 9H; CH_3-chain1, CH_3-chain A, CH_3 ether of chain A)

^{13}C NMR (101 MHz, CD_3OD, 25 °C, TMS) δ 187.70, 172.44, 128.74, 114.01, 96.59, 70.74, 67.49, 60.35, 44.78, 44.12, 37.38, 33.55, 29.47, 29.14, 25.54, 24.55, 22.38, 13.10, 7.73, 3.04, -5.54.

ESI-MS: $[M]^-$ m/z = 910.6; found: m/z = 910.6

Chain B2 Synthesis

Compound 20

Benzyl(R)-(+)-2,2-dimethyl-1,3-dioxolane-4-carboxylate **CAS 55032-17-2**

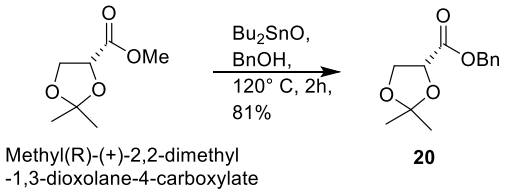

Methyl(R)-(+)-2,2-dimethyl-1,3-dioxolane-4-carboxylate (340 mg, 2.12 mmol) was dissolved in BnOH (2.96 mL, 28.7 mmol) and Bu2SnO (53 mg, 0.21 mmol) was added. The reaction was stirred at 120° C for 2h. The reaction was quenched by the addition of 10 mL of a saturated NaHCO3 solution and extracted (3x) with EtOAc. The organic layer was dried over anhydrous Na_2SO_4, filtered and the solvents were evaporated *in vacuo*. The crude product was purified with flash chromatography (petroleum ether–EtOAc 96:4) to give compound 20 as brown oil (405 mg, 81%).

^{1}H NMR (400 MHz, $CDCl_3$, 25 °C, TMS) δ 7.42 – 7.27 (m, 5H, Ph), 5.28 – 5.12 (m, 2H, CH_2-Ph), 4.62 (dd, $^3J_{H,H}$= 7.2, 5.0 Hz, 1H; CHα), 4.24 (dd, $^3J_{H,H}$= 8.6, 7.3 Hz, 1H, CHaβ), 4.11 (dd, $^3J_{H,H}$= 8.7, 5.1 Hz, 1H, CHbβ), 1.49 (s, 3H, CH_3), 1.40 (s, 3H, CH_3)

^{13}C NMR (101 MHz, $CDCl_3$, 25 °C, TMS) δ 171.04, 135.28, 128.61, 128.34, 111.40, 74.11, 67.26, 66.74, 25.86, 25.55, -1.60.

Compound 21

Benzyl(R)-(+)-2,3-dihydroxy propanoate **CAS 55032-35-4**

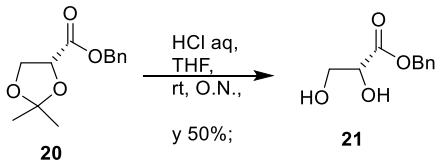

Compound 20 (430 mg, 1.82 mmol) was dissolved in THF (4.5 mL) and HCl 1M aq. (7.3 mL, 7.27 mmol) was slowly added. The mixture was stirred at room temperature overnight. The reaction was quenched by the addition of saturated NaHCO3 solution. THF was evaporated *in vacuo* and the aqueous phase obtained was extracted with EtOAc (3x). The organic layer was dried over anhydrous Na_2SO_4, filtered and the solvents were evaporated *in vacuo*. The crude product was purified with flash chromatography (DCM:MeOH 96:4) to give compound 21 as a red oil (180 mg, 50%).

^{1}H NMR (400 MHz, $CDCl_3$, 25 °C, TMS) δ 7.42 – 7.27 (m, 5H, Ph), 5.24 – 5.12 (m, 2H, CH_2-Ph), 4.31 (s, 1H, CHα), 3.95 – 3.79 (m, 2H, CH_2-β), 3.68 (s, 1H; OH)

^{13}C NMR (101 MHz, $CDCl_3$, 25 °C, TMS) δ 172.91, 135.08, 128.65, 128.28, 127.03, 71.97, 67.51, 65.14, 64.10, -1.60.

Compound 22

Benzyl(R)-(+)-2-hydroxy-3-O-decanoyl propanoate

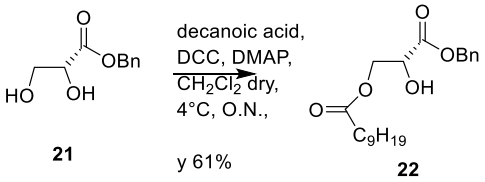

Compound 21 (180 mg, 0.92 mmol) and decanoic acid (158 mg, 0.92 mmol) were dissolved in dry CH_2Cl_2 (9.2 mL) and at 0°C DCC (360 mg, 1.74 mmol) and DMAP (34 mg, 0.27 mmol) were added and the mixture was stirred at 0°C overnight. The precipitate is removed by filtration and the solvents were evaporated *in vacuo*. The crude product was purified with flash chromatography (petroleum ether–EtOAc 9:1) to give compound 22 as a red oil (196 mg, 61%).

^{1}H NMR (400 MHz, $CDCl_3$, 25 °C, TMS) δ 7.42 – 7.27 (m, 5H, Ph), 5.28 – 5.14 (m, 2H, CH_2-Ph), 4.46 – 4.35 (m, 1H, CHα glycerol), 4.38 – 4.34 (m, 2H, CH_2-β glycerol), 3.16 (s, 1H; OH), 2.29 – 2.11 (m, 2H, CH_2α decanoyl), 1.54 (m, 1H, CH_2-β decanoyl), 1.25 (s, 12H, 6x CH_2 decanoyl), 0.87 (t, $^3J_{H,H}$= 6.7 Hz, 3H, CH_3)

^{13}C NMR (101 MHz, $CDCl_3$, 25 °C, TMS) δ 173.52, 172.00, 134.83, 128.68, 128.66, 128.45, 69.42, 67.81, 65.23, 33.89, 31.85, 29.40, 29.26, 29.23, 29.06, 24.75, 22.66, 14.12, -1.60.

Compound 23

Benzyl(R)-(+)-2-O-tetradecanoyl -3-O-decanoyl propanoate

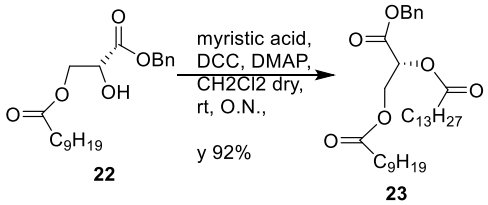

Compound 22 (110 mg, 0.31 mmol) and myristic acid (108 mg, 0.47 mmol) were dissolved in dry CH_2Cl_2 (3.1 mL) and at rt DCC (84 mg, 0.41 mmol) and DMAP (12 mg, 0.09 mmol) were added. The mixture was stirred at rt for 3h. The precipitate is removed by filtration and the solvents were evaporated *in vacuo*. The crude product was purified with flash chromatography (petroleum ether–EtOAc 97:3) to give compound 23 as a red oil (163 mg, 93%).

^{1}H NMR (400 MHz, $CDCl_3$, 25 °C, TMS) δ 7.39 – 7.28 (m, 5H, Ph), 5.36 (dd, $^3J_{H,H}$= 5.0, 3.6 Hz, 1H, CHα glycerol), 5.19 (q, $^3J_{H,H}$= 12.2 Hz, 2H, CH_2-Ph), 4.52 – 4.38 (m, 2H, CH_2-β glycerol), 2.48 – 2.33 (m, 2H, CH_2α myristoyl), 2.30 – 2.05 (m, 2H, CH_2α decanoyl), 1.70 – 1.57 (m, 2H, CH_2β myristoyl), 1.54 (m, 1H, CH_2β decanoyl), 1.25 (s, 32H, 16x CH_2), 0.87 (t, $^3J_{H,H}$= 6.7 Hz, 6H, 2xCH_3)

^{13}C NMR (101 MHz, $CDCl_3$, 25 °C, TMS) δ 173.12, 172.84, 167.20, 134.98, 128.58, 128.50, 128.28, 70.12, 67.42, 62.40, 33.88, 33.83, 31.92, 31.86, 29.69, 29.66, 29.62, 29.46, 29.43, 29.36, 29.28, 29.25, 29.05, 29.03, 24.76, 24.74, 22.70, 22.67, 14.13, 14.11.

Compound B2

(R)-(+)-2-O-tetradecanoyl-3-O-decanoyl propanoic acid

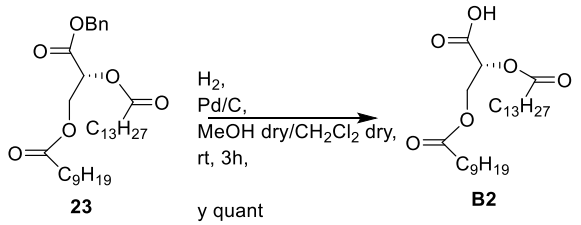

Compound 23 (163 mg, 0.29 mmol) was dissolved in dry CH_2Cl_2/MeOH 1:2 (1.5 mL), and Pd on activated charcoal was then added in catalytic amounts. The reaction mixture was stirred at rt under H_2 atmosphere for 3h. The reaction mixture was filtered over Celite and the filtrate was dried *in vacuo* giving compound B2 as a yellow solid (136 mg, y quant.).

^{1}H NMR (400 MHz, $CDCl_3$, 25 °C, TMS) δ 5.34 (t, $^3J_{H,H}$= 4.2 Hz, 1H, CHα glycerol), 4.54 (m, 1H; CHaβ glycerol), 4.42 (m, 1H; CHbβ glycerol), 2.39 (m, 2H; CH_2α myristoyl), 2.32 (m, 2H; CH_2α decanoyl), 1.61 (m, 4H; CH_2β myristoyl, CH_2-β decanoyl), 1.25 (s, 32H, 16x CH_2), 0.87 (t, $^3J_{H,H}$= 6.7 Hz, 6H, 2x CH_3)

^{13}C NMR (101 MHz, $CDCl_3$, 25 °C, TMS) δ 173.40, 172.93, 69.83, 62.29, 33.94, 33.76, 31.91, 31.86, 29.75, 29.69, 29.66, 29.63, 29.48, 29.43, 29.36, 29.26, 29.03, 24.79, 24.69, 22.68, 22.66, 14.11, 14.09.

AM173 Synthesis

Compounds 1,2,3 are common intermediates of FP11 **and compounds 13, 14** are common intermediates of AM158.

Compound 25

1-O-tert-butyldimethylsilyl-2-deoxy-4,6-O-(4-methoxybenzylidene)-3-O-tetradecanoyl-2-[(R)-3-(decanoyloxy)-2-(tetradecanoyloxy)propanoyl]- amino- β -D-glucopyranoside

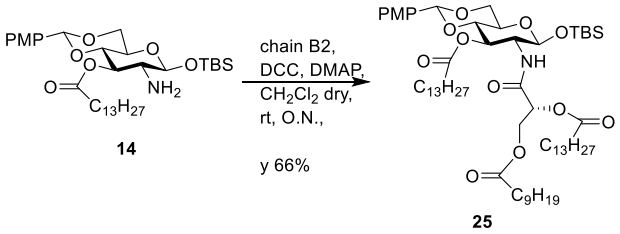

Compound B2 (123 mg, 0.26 mmol) was dissolved in dry CH_2Cl_2 (2.5 mL) and DCC (134 mg, 0.65 mmol) was added. After 30 min compound 14 (135 mg, 0.22 mmol) dissolved in CH_2Cl_2 dry (1.5 mL) and DMAP (27 mg, 0.22 mmol) were added and the mixture was stirred at room temperature overnight. The precipitate is removed by filtration and the solvents were evaporated *in vacuo*. The crude product was purified with flash chromatography (petroleum ether–EtOAc 9:1) to give compound 25 as a yellow oil (155 mg, 66%).

^{1}H NMR (400 MHz, $CDCl_3$, 25 °C, TMS) δ 7.34 (d, $^3J_{H,H}$= 8.3 Hz, 2H; 2x H-*ortho* PMP), 6.85 (d, $^3J_{H,H}$= 8.4 Hz, 2H; 2x H-*meta* PMP), 5.45 (s, 1H, CH-Ph PMP), 5.36 (dd, $^3J_{H,H}$= 6.6, 3.2 Hz, 1H, CHα glycerol), 5.20 (t, $^3J_{H,H}$= 10.0 Hz, 1H; H-3), 4.72 (d, $^3J_{H,H}$= 8.0 Hz, 1H; H-1), 4.59 (dd, $^3J_{H,H}$= 12.1, 3.2 Hz, 1H, CHaβ glycerol) 4.25 (dd, $^3J_{H,H}$= 10.6, 5.0 Hz, 1H; H-5), 4.18 (dd, $^3J_{H,H}$= 12.1, 6.7 Hz, 1H; CHbβ glycerol), 4.14 – 4.02 (m, 1H; H-2), 3.78 (m, 4H; OCH_3 PMP, H-6a), 3.69 (t, $^3J_{H,H}$= 9.5 Hz, 1H; H-4), 3.53 – 3.41 (m, 1H; H-6b), 2.38 (t, $^3J_{H,H}$= 7.6 Hz, 1H, 2H; CH_2α-chain1), 2.35 – 2.19 (m, 4H; CH_2α myristoyl glycerol, CH_2α decanoyl glycerol), 1.70 – 1.48 (m, 6H; CH_2β-chain1, CH_2β myristoyl glycerol, CH_2-β decanoyl glycerol), 1.27 (m, 52H, 26x CH_2) 0.94 – 0.77 (m, 18H; t-Bu, 3x CH_3 chains) 0.07 (s, 3H, CH_3-Si) 0.05 (s, 3H, CH_3-Si)

^{13}C NMR (101 MHz, $CDCl_3$, 25 °C, TMS) δ 173.99, 173.19, 172.05, 166.94, 129.41, 127.37, 113.48, 101.30, 97.13, 87.90, 78.60, 75.02, 71.33, 71.12, 68.52, 66.67, 62.70, 56.37, 55.20, 34.26, 33.97, 31.92, 29.74, 25.41, 24.96, 24.71, 22.68, 17.75, 14.12, -1.59, -4.18, -5.33.

Compound 26

2-deoxy-4,6-O-(4-methoxybenzylidene)-3-O-tetradecanoyl-2-[(R)-3-(decanoyloxy)-2-(tetradecanoyloxy) propanoyl]-amino-α-D-glucopyranoside

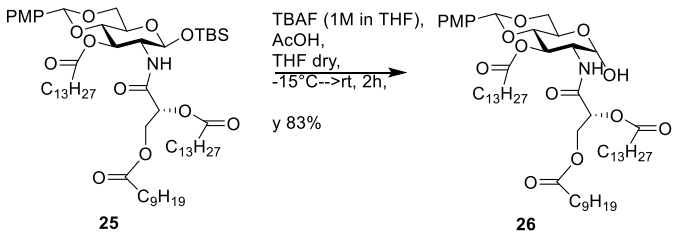

Compound 25 (140 mg, 0.13 mmol) was dissolved in dry THF (6.5 mL), cooled to -15 °C and a solution of TBAF (49 mg, 0.16 mmol) and AcOH (10 µl, 0.18 mmol) in THF (156 µL) was added. The reaction was stirred at -15° C for 10 min, then it was allowed to warm till rt and it was left stirring at rt for 2h. The solution was diluted with water and extracted with CH_2Cl_2. The organic layer was dried over anhydrous Na2SO4, filtered and the solvents were evaporated *in vacuo*. The crude product was purified with flash chromatography (petroleum ether–EtOAc 7:3) to give compound 26 as a yellow solid (104 mg, 83%).

^{1}H NMR (400 MHz, $CDCl_3$, 25 °C, TMS) δ
δ 7.34 (d, $^{3}J_{H,H}$= 8.3 Hz, 2H; 2x H-*ortho* PMP), 6.85 (d, $^{3}J_{H,H}$= 8.4 Hz, 2H; 2x H-*meta* PMP), 6.68 (d, $^{3}J_{H,H}$= 8.8 Hz, 1H; NH), 5.48 (s, 1H; CH-Ph PMP), 5.42 – 5.33 (m, 2H; H-3, CHα glycerol), 5.30 – 5.26 (m, 2H, H-1), 4.54 (dd, $^{3}J_{H,H}$= 12.0, 3.2 Hz, 2H, CHaβ glycerol), 4.28 – 4.17 (m, 2H; CHbβ glycerol, H-2), 4.16 – 4.04 (m, 1H; H-5), 3.78 (s, 3H; OCH_3), 3.77 – 3.56 (m, 3H; H-6a, H-4, H-6b), 2.51-2.40 (m, 2H; CH_2α-chain1), 2.40 – 2.26 (m, 4H; CH_2α myristoyl glycerol, CH_2α decanoyl glycerol), 1.70 – 1.48 (m, 6H; CH_2β-chain1, CH_2β myristoyl glycerol, CH_2-β decanoyl glycerol), 1.27 (m, 52H, 26x CH_2) 0.87 (t, $^{3}J_{H,H}$= 6.6 Hz, 9H; 3x CH_3 chains)

^{13}C NMR (101 MHz, $CDCl_3$, 25 °C, TMS) δ 174.21, 173.30, 172.43, 167.28, 160.04, 129.46, 127.41, 113.50, 101.44, 91.89, 78.99, 71.26, 69.32, 68.79, 62.82, 62.61, 55.22, 53.06, 34.27, 33.99, 33.87, 31.93, 31.88, 29.67, 29.54, 29.47, 29.38, 29.33, 24.97, 24.79, 24.76, 22.69, 14.13.

Compound 27
1-O-dibenzylphosphoryl-2-deoxy-4,6-O-(4-methoxybenzylidene)-3-O-tetradecanoyl-2-[(R)-3-(decanoyloxy)-2-(tetradecanoyloxy)propanoyl]amino-α-D-glucopyranoside

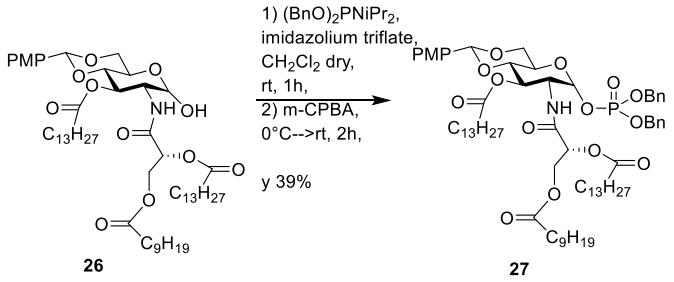

Compound 26 (100 mg, 0.10 mmol) was dissolved in dry CH_2Cl_2 (1.7 mL), then imidazolium triflate (81 mg, 0.31 mmol) and dibenzyl *N*,*N*-diisopropyl phosphoramidite (105 µl, 0.31 mmol) were added and the reaction was stirred at r.t. for 1h. The solution was then cooled in an ice bath and *m*CPBA (90 mg, 0.52 mmol) was added. The reaction was stirred at rt for 2h, then the mixture was diluted with CH_2Cl_2, washed with a saturated solution of $NaHCO_3$ and brine. The organic layer was dried over anhydrous Na_2SO_4, filtered and the solvents were evaporated *in vacuo*. The crude product was purified with flash chromatography (petroleum ether–EtOAc 8:2 to petroleum ether–EtOAc 7.5:2.5) affording compound 27 as a brown solid (55 mg, 39%).

^{1}H NMR (400 MHz, $CDCl_3$, 25 °C, TMS) δ 7.35 (m, 12H; 2xBnO-P, 2x H-*ortho* PMP), 6.88 (d, $^{3}J_{H,H}$= 8.4 Hz, 2H; 2x H-*meta* PMP), 6.72 (d, $^{3}J_{H,H}$= 8.4 Hz, 1H, NH), 5.73 (dd, $^{3}J_{H,P}$= 6.1, $^{3}J_{H,H}$= 3.4 Hz, 1H; H-1), 5.45 (s, 1H, CH-Ph PMP), 5.33 – 5.21 (m, 2H; H-3, CHα glycerol), 5.04 (t, $^{3}J_{H,H}$= 8.1 Hz, 4H, 2x CH_2(Ph)-O-P), 4.48 (dd, $^{3}J_{H,H}$= 12.2, 3.2 Hz, 2H, CHaβ glycerol), 4.34 – 4.23 (m, 1H; H-2), 4.19 (dd, $^{3}J_{H,H}$= 12.1, 6.2 Hz, 2H; CHbβ glycerol), 4.06 (dd, $^{3}J_{H,H}$= 10.3, 4.9 Hz, 1H, H-5), 4.02 – 3.87 (m, 1H, H-6a), 3.80 (s, 3H; OCH_3), 3.74 – 3.60 (m, 2H; H-4, H-6b), 2.47-2.40 (m, 2H; CH_2α-chain1), 2.40 – 2.18 (m, 4H; CH_2α myristoyl glycerol, CH_2α decanoyl glycerol), 1.70 – 1.48 (m, 6H; CH_2β-chain1, CH2β myristoyl glycerol, CH_2-β decanoyl glycerol), 1.25 (m, 52H, 26x CH_2) 0.87 (t, $^{3}J_{H,H}$= 6.6 Hz, 9H; 3x CH_3 chains)

^{13}C NMR (101 MHz, $CDCl_3$, 25 °C, TMS) δ 174.20, 173.10, 172.27, 167.47, 160.14, 141.63, 129.19, 128.84, 128.71, 128.07, 128.05, 127.44, 114.29, 113.54, 101.55, 95.88, 78.16, 70.93, 69.91, 69.86, 68.70, 68.20, 64.60, 62.47, 55.59, 55.26, 34.17, 33.88, 33.81, 31.93, 31.88, 29.73, 29.69, 29.54, 29.47, 29.38, 29.34, 29.14, 29.04, 24.91, 24.78, 24.64, 22.70, 14.13.

AM173

1-O-Phosphoryl -2-deoxy-3-O-tetradecanoyl-2-[[(R)-3-(decanoyloxy)-2-(tetradecanoyloxy)propanoyl]amino-α-D-glucopyranoside (sodium salt)

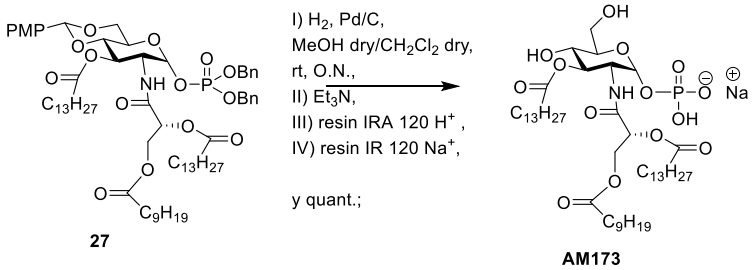

Compound 27 (31 mg, 0.025 mmol) was dissolved in dry CH_2Cl_2/MeOH 1:2 (1.5 mL), and Pd on activated charcoal was then added in catalytic amounts. The reaction mixture was stirred at rt under H_2 atmosphere overnight. Triethylamine (80 µL) was then added to the reaction mixture, and the suspension was filtered with a syringe filter. The triethylammonium salt was dissolved in dry CH_2Cl_2/MeOH 1:2 (3 mL) and treated first with an Amberlite IRA 120 H^+ exchange resin and then with an IR 120 Na^+ exchange resin to remove triethylamine and to form the sodium salt, giving compound AM173 as a white solid (24 mg, y quant.).

^{1}H NMR (400 MHz, CD_3OD, 25 °C, TMS) δ 5.52 (dd, $^3J_{H,P}$= 6.9, $^3J_{H,H}$= 3.4 Hz, 1H; H-1), 5.23 (dd, $^3J_{H,H}$= 6.5, 3.1 Hz, 1H; CHα glycerol), 5.18 (t, $^3J_{H,H}$= 10.0 Hz, 1H; H-3), 4.43 (dd, $^3J_{H,H}$= 12.1, 2.9 Hz, 1H; CHaβ glycerol), 4.27 (dd, $^3J_{H,H}$= 12.0, 6.5 Hz, 1H; CHbβ glycerol), 4.11 (dt, $^3J_{H,H}$= 11.0, 3.0 Hz, 1H; H-2), 3.89 – 3.83 (m, 1H; H-5), 3.83 – 3.66 (m, 2; H-6a, H-6b), 3.68 – 3.58 (m, 1H; H-4), 2.42 – 2.32 (m, 4H; CH_2α-chain1, CH_2α myristoyl glycerol) 2.26 (m, 1H; CH_2α decanoyl glycerol), 1.70 – 1.48 (m, 6H; CH_2β-chain1, CH_2β myristoyl glycerol, CH_2β decanoyl glycerol), 1.26 (m, 52H, 26x CH_2) 0.87 (t, $^3J_{H,H}$= 6.6 Hz, 9H; 3x CH_3 chains)

^{13}C NMR (101 MHz, CD_3OD, 25 °C, TMS) δ 174.18, 173.20, 172.27, 168.28, 94.38, 73.68, 72.46, 71.15, 67.58, 62.34, 60.52, 52.18, 33.64, 33.27, 31.71, 29.53, 29.48, 29.14, 28.84, 24.44, 22.36, 13.07.

ESI-MS: $[M]^-$ m/z = 920.6; found: m/z = 920.6

Chain B3 Synthesis

Compound 28
DL-4-((decyloxy)methyl)-2,2-dimethyl-1,3-dioxolane

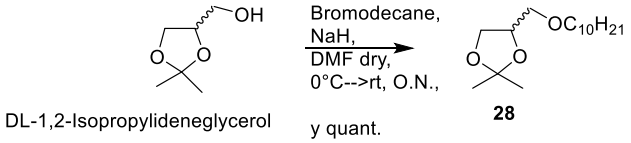

DL-1,2-Isopropylideneglycerol (5.35 mL, 37.83 mmol) was dissolved in dry DMF (6.5 mL), cooled to 0°C and NaH (60% dispersion in mineral oil) (3.0 g, 75.67 mmol) was added in 2 portions waiting 10 minutes between each. The resulting suspension was stirred at 0° C for 20 min, then it was allowed to warm till rt and Bromodecane was added. The reaction was stirred at rt overnight then it was quenched by adding methanol at 0°C and the solution was left stirring at 0°C for 30 min.
The solvents were evaporated *in vacuo* to give a white solid which was dissolved in EtOAc and the solution was washed with water and brine. The organic layer was dried over anhydrous Na2SO4, filtered and the solvents were evaporated *in vacuo*. The crude product was purified with flash chromatography (petroleum ether–EtOAc 95:5) to give compound 28 as a red liquid (10,29 g, quant).

^{1}H NMR (400 MHz, $CDCl_3$, 25 °C, TMS) δ 4.27 – 4.16 (m, 1H, CH-O), 4.01 (dd, $^{3}J_{H,H}$= 8.3, 6.3 Hz, 1H; CHa of acetal CH_2), 3.68 (dd, $^{3}J_{H,H}$= 8.2, 6.4 Hz, 1H; CHb of acetal CH_2), 3.51 – 3.31 (m, 4H, CH_2-O- decyl, CH_2 in 1 of decyl) 1.59 – 1.45 (m, 2H; CH_2 in 2 of decyl), 1.38 (s, 3H; CH_3 acetal), 1.32 (s, 3H; CH_3 acetal), 1.32 (s, 12H, 6x CH_2 decyl), 0.83 (t, $^{3}J_{H,H}$= 6.6 Hz, 3H; CH_3 decyl)

Compound 29
DL-3-(decyloxy)propane-1,2-diol

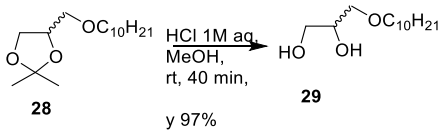

Compound 28 (10.2 g, 37.44 mmol) was dissolved in MeOH (93 mL) and HCl 1M aq. (150 mL, 149.77 mmol) was slowly added at rt.. The mixture was stirred at room temperature for 40 min. MeOH was evaporated *in vacuo* to give a white syrup which was purified with flash chromatography (DCM:MeOH 95:5) to give compound 29 as a brown oil (8.4 g, 97%).

^{1}H NMR (400 MHz, $CDCl_3$, 25 °C, TMS) δ 3.89 – 3.75 (m, 1H; CH-OH), 3.66 (dd, $^{3}J_{H,H}$= 11.6, 3.5 Hz, 1H; CHa-OH), 3.57 (dd, $^{3}J_{H,H}$= 11.5, 5.8 Hz, 1H; CHb-OH), 3.48 – 3.36 (m, 4H; CH_2-O-decyl, CH_2 in 1 of decyl), 1.66 – 1.48 (m, 2H; CH_2 in 1 of decyl), 1.34 (s, 7x CH_2), 0.84 (t, $^{3}J_{H,H}$= 6.5 Hz, 3H; CH_3)

^{13}C NMR (101 MHz, $CDCl_3$, 25 °C, TMS) 72.24, 71.79, 70.66, 64.10, 31.87, 29.52, 29.31, 26.03, 22.66, 14.10, -1.59, -1.60.

Compound 30

DL-1-((tert-butyldiphenylsilyl)oxy)-3-(decyloxy)propan-2-ol

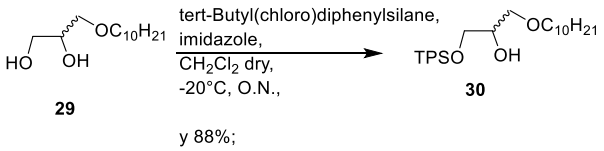

Compound 29 (8.4 g, 36.15 mmol) and imidazole (3.2 g, 46.99 mmol) were dissolved in dry CH_2Cl_2 (27 mL) and at -20°C TPSCl (10.34 mL, 39.77 mmol) was added. The reaction mixture was stirred at -20°C overnight. The solvent was removed *in vacuo*, and the crude was dissolved in EtOAc and washed first with HCl 1M and then with a saturated solution of $NaHCO_3$ and brine.

The organic phase was dried with Na_2SO_4, and then filtered and concentrated *in vacuo*. The residue was purified by silica gel column chromatography (petroleum ether–EtOAc 9:1) to give compound 30 as a purple oil (14.9 g, 88%).

^{1}H NMR (400 MHz, $CDCl_3$, 25 °C, TMS) δ 7.79 – 7.66 (m, 4H; 4x H-*ortho* TPS), 7.51 – 7.29 (m, 6H; 4x H-*meta*, 2x H-*para* TPS), 3.97 – 3.84 (m, 1H; CH-OH), 3.75 (d, $^3J_{H,H}$= 5.4 Hz, 2H; CH_2-OSi), 3.61 – 3.47 (m, 2H; CH_2-O-decyl) 3.46 (t, $^3J_{H,H}$= 6.7 Hz, 2H; CH_2 in 1 of decyl), 1.64 – 1.49 (m, 2H; CH_2 in 1 of decyl), 1.28 (s, 14H; 7x CH_2), 1.09 (s, 9H; t-Bu), 0.91 (m, 3H; CH_3 decyl)

^{13}C NMR (101 MHz, $CDCl_3$, 25 °C, TMS) δ 135.80, 135.56, 134.85, 133.24, 133.22, 129.76, 129.46, 127.74, 127.61, 71.65, 71.49, 70.74, 64.81, 60.38, 31.94, 29.68, 29.65, 29.62, 29.55, 29.38, 26.85, 26.60, 26.15, 22.73, 22.65, 20.99, 20.49, 19.27, 14.20, 14.16, 11.47, -1.60.

Compound 31

DL-1-((tert-butyldiphenylsilyl)oxy)-3-(decyloxy)propan-2-yl tetradecanoate

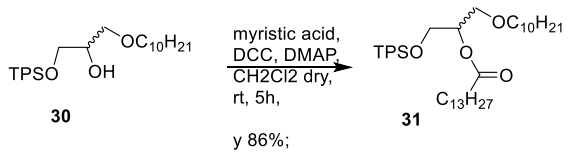

Myristic acid (3.46 g, 15.15 mmol) was dissolved in dry CH_2Cl_2 (50 mL) and DCC (2.04 g, 9.87 mmol) was added. After 30 min compound 30 (3.1 g, 6.58 mmol) dissolved in CH_2Cl_2 dry (16 mL) and DMAP (402 mg, 3.29 mmol) were added and the mixture was stirred at room temperature for 5 h. The precipitate is removed by filtration and the solvents were evaporated *in vacuo*. The crude product was purified with flash chromatography (petroleum ether–EtOAc 98:2) to give compound 31 as an orange oil (3.86 g, 86%).

^{1}H NMR (400 MHz, $CDCl_3$, 25 °C, TMS) δ 7.79 – 7.66 (m, 4H; 4x H-*ortho* TPS), 7.51 – 7.29 (m, 6H; 4x H-*meta*, 2x H-*para* TPS), 5.22 – 5.11 (m, 1H, CH-O-myristoyl), 3.84 (d, $^3J_{H,H}$= 5.0 Hz, 2H; CH_2-OSi), 3.69 – 3.57 (m, 2H; CH_2-O-decyl), 3.53 – 3.34 (m, 2H; CH_2 in 1 of decyl), 2.39 – 2.21 (m, 2H, CH_2α of myristoyl), 1.66 (m, 2H; CH_2β of myristoyl) 1.57 (m, 2H; CH_2 in 2 of decyl), 1.31 (m, 34H, 17x CH_2), 1.09 (s, 9H; t-Bu), 0.91 (t, $^3J_{H,H}$= 6.6 Hz, 6H; 2x CH_3)

^{13}C NMR (101 MHz, $CDCl_3$, 25 °C, TMS) δ 173.20, 135.60, 135.54, 133.35, 133.30, 129.69, 129.68, 127.68, 127.67, 72.72, 71.57, 68.91, 62.62, 34.47, 34.38, 31.97, 31.95, 29.73, 29.71, 29.68, 29.64, 29.55, 29.51, 29.41, 29.40, 29.36, 29.32, 29.18, 26.74, 26.13, 25.02, 22.73, 19.25, 14.27, 14.15.

Compound 32

DL-1-(decyloxy)-3-hydroxypropan-2-yl tetradecanoate

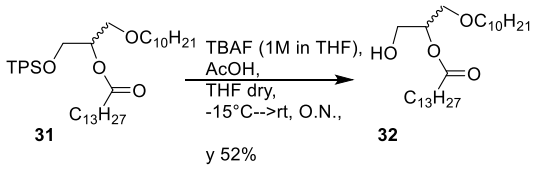

Compound 31 (3.7 g, 5.43 mmol) was dissolved in dry THF (270 mL), cooled to -15 °C and a solution of TBAF (1.88 g, 5.97 mmol) and AcOH (390 µl, 6.84 mmol) in THF (5.9 mL) was added. The reaction was stirred at -15° C for 30 min, then it was allowed to warm till rt and it was left stirring at rt overnight. The solution was reduced in volume to 5 mL, then it was diluted with CH_2Cl_2 and washed with water. The organic layer was dried over anhydrous Na_2SO_4, filtered and the solvents were evaporated *in vacuo*. The crude product was purified with flash chromatography (petroleum ether–EtOAc 9:1) to give compound 32 (1.25 g, 52%).

^{1}H NMR (400 MHz, $CDCl_3$, 25 °C, TMS) δ 5.05 – 4.95 (m, 1H, CH-O-myristoyl), 3.82 (d, $^3J_{H,H}$= 4.5 Hz, 2H; CH_2-OH), 3.69 – 3.55 (m, 2H; CH_2-O-decyl), 3.50 – 3.39 (m, 2H; CH_2 in 1 of decyl), 2.50 – 2.37 (m, 2H, CH_2α of myristoyl), 1.68 – 1.57 (m, 2H; CH_2β of myristoyl) 1.57 (m, 2H; CH_2 in 2 of decyl), 1.28 (m, 34H, 17xCH_2), 0.88 (t, $^3J_{H,H}$= 6.6 Hz, 6H; 2xCH_3)

^{13}C NMR (101 MHz, $CDCl_3$, 25 °C, TMS) δ 173.71, 72.83, 71.84, 71.73, 69.88, 68.79, 65.38, 62.75, 34.37, 34.15, 31.91, 31.89, 29.68, 29.65, 29.61, 29.60, 29.57, 29.53, 29.47, 29.45, 29.36, 29.33, 29.28, 29.12, 29.09, 26.03, 24.96, 24.91, 22.68, 14.10.

Compound B3

DL-3-(decyloxy)-2-(tetradecanoyloxy)propanoic acid

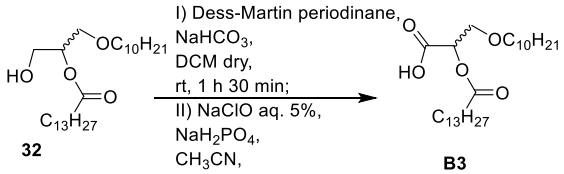

Step I) Dess-Martin periodinane (972 mg, 2.29 mmol) was dissolved in dry DCM (2 mL) and $NaHCO_3$ (664 mg, 7.90 mmol) was added at rt. The reaction was stirred at rt for 10 min, then a solution of compound 32 (700 mg, 1.58 mmol) in dry DCM (2 mL) was added and the mixture was stirred at rt for 1 h and 30 min. The reaction was quenched at 0°C by a saturated solution of $Na_2S_2O_3$ and extracted with DCM. The organic layer was washed with brine and then dried over anhydrous Na_2SO_4, filtered and the solvents were evaporated *in vacuo* to give a light orange oil (1,350 g). The crude product was used directly for step II.

Step II) The crude of step I was dissolved in dry CH_3CN (2.5 mL) and NaH_2PO_4 (1.06 g, 8.86 mmol) was added at rt followed by NaClO 5% aq. solution (13 ml, 8.70 mmol). The mixture was stirred at rt for 21 h and then it was quenched by adding NH_4Cl saturated solution.

Three extractions were performed with CH_2Cl_2 and the organic layer was further washed with brine. The organic layer was dried over anhydrous Na_2SO_4, filtered and the solvents were evaporated *in vacuo*. The obtainment of the product B3 was assessed by NMR (580 mg, 80%).

^{1}H NMR (400 MHz, $CDCl_3$, 25 °C, TMS) δ 5.28 – 5.20 (m, 1H, CH-O-myristoyl), 3.87 (dd, $^3J_{H,H}$= 11.1, 5.5 Hz, 2H; CHa-O-decyl), 3.77 (dt, $^3J_{H,H}$= 11.1, 3.5 Hz, 2H; CHb-O-decyl), 3.56 – 3.36 (m, 2H, CH_2 in 1 of decyl), 2.50

– 2.37 (m, 2H, $CH_2\alpha$ of myristoyl), 1.68 – 1.57 (m, 2H; $CH_2\beta$ of myristoyl) 1.57 (m, 2H; CH_2 in 2 of decyl), 1.28 (m, 34H, 17x CH_2), 0.88 (t, $^3J_{H,H}$= 6.6 Hz, 6H; 2xCH_3)

^{13}C NMR (101 MHz, $CDCl_3$, 25 °C, TMS) δ 173.16, 172.74, 74.83, 74.83, 72.31, 72.03, 71.32, 71.32, 69.25, 68.39, 66.71, 33.90, 33.88, 33.81, 31.92, 31.90, 29.69, 29.66, 29.64, 29.62, 29.59, 29.55, 29.52, 29.47, 29.45, 29.41, 29.36, 29.33, 29.26, 29.24, 29.07, 29.04, 25.98, 25.92, 24.86, 24.85, 24.76, 24.64, 22.69, 14.13.

Chain B1 Synthesis

Compound 33
DL-(2-(benzyloxy)-3-(decyloxy)propoxy)(tert-butyl)diphenylsilane

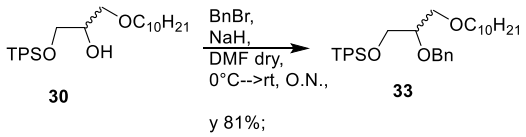

Compound 30 (8.10 g, 17.21 mmol) was dissolved in dry DMF (54 mL), cooled to 0°C and NaH (60% dispersion in mineral oil) (1.72 g, 43.02 mmol) was added in 3 portions waiting 10 minutes between each. The resulting suspension was allowed to warm till rt and it was stirred at rt for 20 min, then Benzyl bromide (6.9 mL, 58.50 mmol) was added. The reaction was stirred at rt overnight then it was quenched by adding methanol at 0°C and the solution was left stirring at 0°C for 30 min.
The solvents were evaporated *in vacuo* to give a yellow oil which was dissolved in EtOAc and the solution was washed with water and brine. The organic layer was dried over anhydrous Na_2SO_4, filtered and the solvents were evaporated *in vacuo*. The crude product was purified with flash chromatography (petroleum ether–EtOAc 99:1) to give compound 33 as a yellow oil (7.80 g, 81%).

^{1}H NMR (400 MHz, $CDCl_3$, 25 °C, TMS) δ 7.79 – 7.66 (m, 4H; 4x H-*ortho* TPS), 7.50 – 7.22 (m, 11H; 4x H-*meta* TPS, 2x H-*para* TPS, 5X H Bn), 4.76 – 4.64 (m, 2H; CH_2-Ph), 3.86 – 3.79 (m, 2H; CH_2-OSi), 3.79 – 3.69 (m, 2H; CH-O-Bn), 3.68 (dd, $^3J_{H,H}$= 10.2, 4.4 Hz, 1H; CHa- O-decyl), 3.61 (dd, $^3J_{H,H}$= 10.2, 5.7 Hz, 1H; CHb- O-decyl), 3.47 (t, $^3J_{H,H}$= 6.7 Hz, 2H; CH_2 in 1 of decyl), 1.67 – 1.55 (m, 2H; CH_2 in 2 of decyl), 1.33 (s, 14H; 7x CH_2), 1.09 (s, 9H; t-Bu), 0.91 (m, 3H; CH_3 decyl)

^{13}C NMR (101 MHz, $CDCl_3$, 25 °C, TMS) δ 138.88, 138.29, 136.00, 135.67, 133.56, 129.66, 128.44, 128.28, 127.82, 127.68, 127.43, 78.79, 72.14, 71.71, 70.80, 63.70, 31.97, 29.70, 29.41, 26.86, 26.22, 22.76, 19.28, 14.21, 5.75, -1.60.

Compound 34
DL-2-(benzyloxy)-3-(decyloxy)propan-1-ol

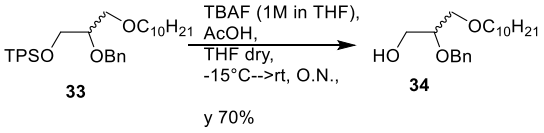

Compound 33 (9.10 g, 16.22 mmol) was dissolved in dry THF (810 mL), cooled to -15 °C and a solution of TBAF (5.63 g, 17.85 mmol) and AcOH (1.2 mL, 20.44 mmol) in THF (18 mL) was added. The reaction was stirred at -15° C for 30 min, then it was allowed to warm till rt and it was left stirring at rt overnight. The solution was reduced in volume to 5 mL, then it was diluted with CH_2Cl_2 and washed with water. The organic layer was dried over anhydrous Na_2SO_4, filtered and the solvents were evaporated *in vacuo*. The crude product was purified with flash chromatography (petroleum ether–EtOAc 9:1) to give compound 34 (3.60 g, 70%).

^{1}H NMR (400 MHz, $CDCl_3$, 25 °C, TMS) δ 7.40 – 7.21 (m, 5H; 5X H Bn), 4.72 (d, $^3J_{H,H}$= 11.8 Hz, 1H; CHa-Ph), 4.63 (d, $^3J_{H,H}$= 11.8 Hz, 1H; CHb-Ph), 3.76 (m, 2H; CH-O-Bn), 3.66 (m, 2H; CH_2-OH) 3.60 (dd, $^3J_{H,H}$= 10.0, 4.6 Hz, 1H; CHa- O-decyl), 3.54 (dd, $^3J_{H,H}$= 9.9, 5.2 Hz, 1H; CHb- O-decyl), 3.44 (td, $^3J_{H,H}$= 6.7, 1.6 Hz, 2H; CH_2 in 1 of decyl), 2.26 (s, 1H; OH), 1.64 – 1.53 (m, 2H; CH_2 in 2 of decyl), 1.28 (s, 14H; 7xCH_2), 0.88 (t, $^3J_{H,H}$= 6.7 Hz, 3H; CH_3 decyl)

^{13}C NMR (101 MHz, $CDCl_3$, 25 °C, TMS) δ 138.28, 128.46, 127.81, 127.79, 77.75, 77.36, 77.04, 76.72, 72.07, 71.88, 71.11, 63.05, 31.91, 29.63, 29.61, 29.58, 29.47, 29.34, 26.11, 22.70, 14.15.

Compound B1

DL-2-(benzyloxy)-3-(decyloxy)propanoic acid

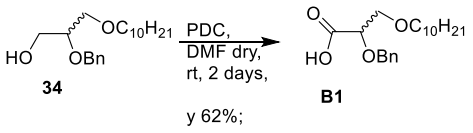

Compound 34 (40 mg, 0.124 mmol) was dissolved in dry DMF (530 µL) and PDC (196 mg, 0.520 mmol) was added. The reaction was stirred at rt for 2 days, then it was cooled to 0°C and celite was added to adsorb extra PDC left. Water and Et_2O were added to dilute the suspension which was stirred for 45 min at rt. celite was filtered off and washed with Et_2O. Then if a black color persist in the filtrate new celite is added again and filtration is repeated till no PDC remains. Solvents were evaporated *in vacuo* and the crude product was purified with flash chromatography (EtOAc 100%) to give compound B1 as a brown solid (27 mg, 62%).

^{1}H NMR (400 MHz, $CDCl_3$, 25 °C, TMS) δ 7.40 – 7.21 (m, 5H; 5X H Bn), 4.79 (d, $^{3}J_{H,H}$= 11.8 Hz, 1H; CHa-Ph), 4.63 (d, $^{3}J_{H,H}$= 11.8 Hz, 1H; CHb-Ph), 4.16 (t, $^{3}J_{H,H}$= 4.2 Hz, 1H; CH-O-Bn), 3.84 – 3.69 (m, 2H; CH_2- O-decyl), 3.60 – 3.36 (m, 2H; CH_2 in 1 of decyl), 1.62 (m, 2H; CH_2 in 2 of decyl), 1.28 (s, 14H; 7x CH_2), 0.88 (t, $^{3}J_{H,H}$= 6.7 Hz, 3H; CH_3 decyl)

^{13}C NMR (101 MHz, $CDCl_3$, 25 °C, TMS) δ 167.23, 136.75, 128.54, 128.18, 128.13, 77.35, 77.18, 77.03, 76.71, 72.78, 72.06, 70.79, 31.90, 29.60, 29.58, 29.43, 29.34, 25.98, 22.69, 14.14.

ESI-MS: $[M]^-$ m/z = 335,2; found: m/z = 335,2

AMX1 Partial Synthesis

Compounds 1,2,3 are common intermediates of FP11 **and compounds 13, 14** are common intermediates of AM158.

Compound 35

1-O-tert-butyldimethylsilyl-2-deoxy-4,6-O-(4-methoxybenzylidene)-3-O-tetradecanoyl-2-[DL-3-(decyloxy)-2-(tetradecanoyloxy)propanoyl]- amino- β -D-glucopyranoside

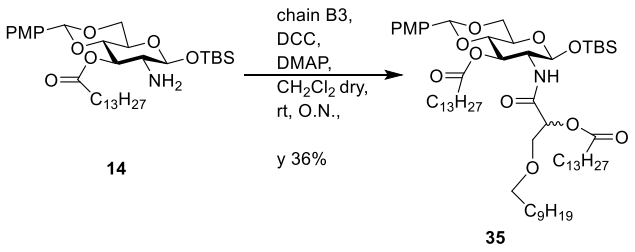

Compound B3 (602 mg, 1.31 mmol) was dissolved in dry CH_2Cl_2 (8 mL) and DCC (544 mg, 2.64 mmol) was added. After 30 min compound 14 (410 mg, 0.66 mmol) dissolved in CH_2Cl_2 dry (3 mL) and DMAP (81 mg, 0.66 mmol) were added and the mixture was stirred at room temperature overnight. The precipitate is removed by filtration and the solvents were evaporated *in vacuo*. The crude product was purified with flash chromatography (petroleum ether–EtOAc 9:1) to give compound 35 as a yellow oil (250 mg, 36%).

diastereoisomeric mixture 1:1

^{1}H NMR (400 MHz, $CDCl_3$, 25 °C, TMS) δ 7.34 (d, $^3J_{H,H}$= 6.7 Hz, 2H; 2x H-*ortho* PMP), 6.85 (d, $^3J_{H,H}$= 7.0 Hz, 2H; 2x H-*meta* PMP), 6.37 – 6.24 (m, 1H; NH diastereoisomer 1, NH diastereoisomer 2) 5.46 (s, 1H, CH-Ph PMP), 5.36 (dd, $^3J_{H,H}$= 6.4, 3.9 Hz, 0.5H; CHα glycerol diastereoisomer 1), 5.31 (dd, $^3J_{H,H}$= 7.2, 5.0 Hz, 0.5H; CHα glycerol diastereoisomer 2), 5.23 – 5.12 (m, 1H; H-3 diastereoisomer 1, H-3 diastereoisomer 2), 4.79 (d, $^3J_{H,H}$= 7.8 Hz, 0.5H; H-1 diastereoisomer1) 4.74 (d, $^3J_{H,H}$= 8.0 Hz, 0.5H; H-1 diastereoisomer2), 4.28 (dd, $^3J_{H,H}$= 10.5, 4.8 Hz, 1H; H-5), 4.09 – 3.92 (m, 1H; H-2), 3.79 (s, 3H; OCH_3 PMP), 3.75 – 3.56 (m, 4H; H-6a, H-4, CH_2-O-decyl), 3.56 – 3.36 (m, 3H, CH_2 in 1 of decyl, H-6b), 2.51 – 2.18 (m, 4H, CH_2α-chain1, CH2α myristoyl glycerol), 1.80 – 1.44 (m, 6H; CH_2β-chain1, CH_2β myristoyl glycerol, CH_2 in 2 of decyl), 1.27 (m, 52H, 27x CH_2) 1.00 – 0.81 (m, 18H; t-Bu, 3x CH_3 chains) 0.08 (m, 6H, 2x CH_3-Si)

diastereoisomeric mixture 1:1

^{13}C NMR (101 MHz, $CDCl_3$, 25 °C, TMS) δ 174.17, 172.22, 167.90, 160.06, 152.87, 127.41, 113.49, 101.33, 97.26, 78.48, 72.10, 71.98, 71.50, 70.92, 69.92, 68.56, 66.76, 55.21, 50.20, 41.40, 34.13, 33.83, 32.67, 31.92, 30.81, 29.67, 29.37, 26.01, 25.57, 25.45, 24.70, 24.67, 22.69, 17.79, 14.12, 7.98, -4.20, -5.32.

Compound 36

2-deoxy-4,6-O-(4-methoxybenzylidene)-3-O-tetradecanoyl-2-[DL-3-(decyloxy)-2-(tetradecanoyloxy) propanoyl]-amino-α-D-glucopyranoside

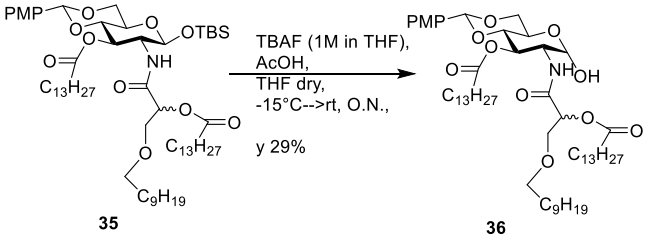

35 36

Compound 35 (140 mg, 0.13 mmol) was dissolved in dry THF (6.5 mL), cooled to -15 °C and a solution of TBAF (50 mg, 0.16 mmol) and AcOH (11 µl, 0.18 mmol) in THF (158 µL) was added. The reaction was stirred at -15° C for 10 min, then it was allowed to warm till rt and it was left stirring at rt o. The solution was diluted with water and extracted with CH_2Cl_2. The organic layer was dried over anhydrous Na_2SO4, filtered and the solvents were evaporated *in vacuo*. The crude product was purified with flash chromatography (petroleum ether–EtOAc 8:2) to give compound 36 as a yellow solid (36 mg, 29%).

diastereoisomeric mixture

^{1}H NMR (400 MHz, $CDCl_3$, 25 °C, TMS) δ

δ 7.34 (d, $^3J_{H,H}$= 6.7 Hz, 2H; 2x H-*ortho* PMP), 6.85 (d, $^3J_{H,H}$= 7.0 Hz, 2H; 2x H-*meta* PMP), 6.76 (d, $^3J_{H,H}$= 8.8 Hz, 0.5H, NH diastereoisomer 1) 6.69 (d, $^3J_{H,H}$= 8.8 Hz, 0.5H, NH diastereoisomer 2), 5.49 (s, 1H, CH-Ph PMP), 5.45 – 5.22 (m, 3H; CHα glycerol diastereoisomer 1, CHα glycerol diastereoisomer 2, H-3 diastereoisomer 1, H-3 diastereoisomer 2, H-1 diastereoisomer1, H-1 diastereoisomer2), 4.43 – 4.34 (m, 1H; H-5), 4.31 – 4.17 (m, 1H; H-2 diastereoisomer 1, H-2 diastereoisomer2), 4.17 – 4.05 (m, 1H; H-6a), 3.79 (s, 3H; OCH_3 PMP), 3.77 – 3.57 (m, 4H; H-6a, H-4, CH_2-O-decyl), 3.56 – 3.36 (m, 3H, CH_2 in 1 of decyl, H-6b), 2.49 – 2.36 (m, 2H; CH_2α-chain1), 2.34 – 2.27 (m, 2H; CH_2α myristoyl glycerol), 1.69 – 1.51 (m, 6H; CH_2β-chain1, CH_2β myristoyl glycerol, CH_2 in 2 of decyl), 1.27 (m, 52H, 27x CH_2) 1.00 – 0.81 (m, 9H; 3x CH_3 chains)

diastereoisomeric mixture

^{13}C NMR (101 MHz, $CDCl_3$, 25 °C, TMS) δ 175.33, 172.79, 168.42, 164.60, 160.04, 132.02, 129.90, 129.50, 127.43, 114.30, 113.50, 101.45, 72.51, 71.73, 71.57, 69.65, 68.82, 62.89, 55.59, 55.25, 31.93, 29.72, 29.68, 29.62, 29.55, 29.52, 29.46, 29.42, 29.38, 29.36, 29.13, 25.97, 24.85, 24.83, 22.70, 14.14, 14.13.

AM241 Synthesis

Compound 44

1,4-bis(O-dibenzylphosphoryl)-2-deoxy-4,6-O-(4-methoxybenzyl)-3-O-tetradecanoyl-2-[DL-3-(decyloxy)-2-(tetradecanoyloxy)propanoyl]amino-α-D-glucopyranoside

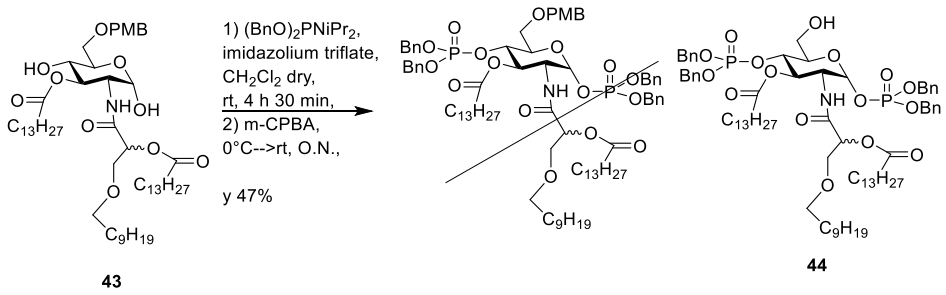

43 44

Compound 43 (30 mg, 0.032 mmol) was dissolved in dry CH_2Cl_2 (600 µL), then imidazolium triflate (25 mg, 0.095 mmol) and dibenzyl *N*,*N*-diisopropyl phosphoramidite (32 µl, 0.095 mmol) were added and the reaction was stirred at r.t. for 4h. The solution was then cooled in an ice bath and *m*CPBA (27 mg, 0.158 mmol) was added. The reaction was stirred at rt overnight, then the mixture was diluted with CH_2Cl_2, washed with a saturated solution of $NaHCO_3$ and brine. The organic layer was dried over anhydrous Na_2SO_4, filtered and the solvents were evaporated *in vacuo*. The crude product was purified with flash chromatography (petroleum ether–EtOAc 8:2 to petroleum ether–EtOAc 7.5:2.5) affording compound 44 as a brown solid (20 mg, 47%).

diastereoisomeric mixture 1:1

^{1}H NMR (400 MHz, $CDCl_3$, 25 °C, TMS) δ 7.38 – 7.18 (m, 20H; 4x BnO-P), 6.69 (d, $^3J_{H,H}$= 8.2 Hz, 0.5H; NH diastereoisomer 1), 6.63 (d, $^3J_{H,H}$= 8.6 Hz, 0.5H; NH diastereoisomer 2), 5.71 (dd, $^3J_{H,P}$= 6.0, $^3J_{H,H}$= 3.4 Hz, 0.5H; H-1 diastereoisomer1) 5.67 (dd, $^3J_{H,P}$= 5.9, $^3J_{H,H}$= 3.4 Hz, 0.5H; H-1 diastereoisomer2), 5.34 – 5.26 (m, 1H; H-3 diastereoisomer 1, H-3 diastereoisomer 2), 5.26 – 5.15 (m, 1H; CHα glycerol diastereoisomer 1, CHα glycerol diastereoisomer 2), 5.09 – 4.81 (m, 8H; 4x CH_2-Ph), 4.60 – 4.43 (m, 1H; H-4 diastereoisomer 1, H-4 diastereoisomer 2), 4.20-4.10 (m, 3H; H-2, H-6a, H-6b), 3.91 (m, 1H; H-5), 3.74 – 3.56 (m, 2H; CH_2-O-decyl), 3.45 – 3.27 (m, 2H; CH_2 in 1 of decyl), 2.47 – 2.27 (m, 2H; CH_2α-chain1), 2.22 – 2.08 (m, 2H; CH_2α myristoyl glycerol), 1.66 – 1.53 (m, 2H; CH_2β-chain1), 1.53 – 1.41 (m, 4H; CH_2β myristoyl glycerol, CH_2 in 2 of decyl), 1.27 (m, 52H, 27x CH_2) 1.00 – 0.81 (m, 6H; 2x CH_3 chains)

diastereoisomeric mixture 1:1

^{13}C NMR (101 MHz, $CDCl_3$, 25 °C, TMS) δ 174.39, 172.47, 168.38, 128.57, 127.96, 127.88, 113.82, 71.87, 71.58, 69.90, 69.83, 69.39, 52.15, 36.13, 33.96, 31.93, 29.72, 29.68, 29.11, 25.95, 24.44,

Compound 241

1,4-bis(O-Phosphoryl)-2-deoxy-4,6-O-(4-methoxybenzyl)-3-O-tetradecanoyl-2-[DL-3-(decyloxy)-2-(tetradecanoyloxy)propanoyl]amino-α-D-glucopyranoside (sodium salt)

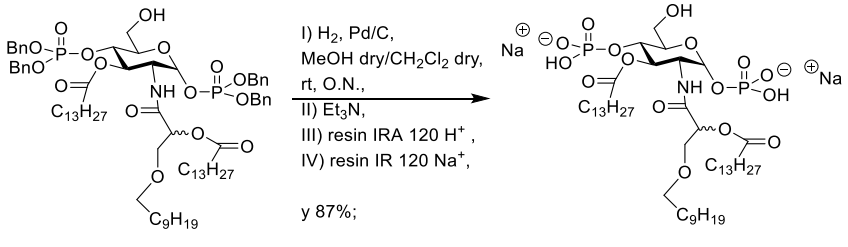

44 AM241

Compound 44 (20 mg, 0.015 mmol) was dissolved in dry CH_2Cl_2/MeOH 1:2 (1.0 mL), and Pd on activated charcoal was then added in catalytic amounts. The reaction mixture was stirred at rt under H_2 atmosphere overnight. Triethylamine (50 µL) was then added to the reaction mixture, and the suspension was filtered with a syringe filter. The triethylammonium salt was dissolved in dry CH_2Cl_2/MeOH 1:2 (3 mL) and treated first with an Amberlite IRA 120 H^+ exchange resin and then with an IR 120 Na^+ exchange resin to remove triethylamine and to form the sodium salt, giving compound AM241 as a white solid (13 mg, 87%).

diastereoisomeric mixture 1:1
^{1}H NMR (400 MHz, CD_3OD, 25 °C, TMS) δ 5.51 (m, 1H; H-1 diastereoisomer1, H-1 diastereoisomer2), 5.41 – 5.30 (m, 1H; H-3 diastereoisomer1, H-3 diastereoisomer2), 5.30 – 5.21 (m, 0.4H; CHα glycerol diastereoisomer 1) 5.23 – 5.15 (m, 0.6H; CHβ glycerol diastereoisomer 2), 4.53 – 4.39 (m, 1H, H-4 diastereoisomer2, H-4 diastereoisomer2), 4.29 – 4.14 (m, 3H; H-2, H-6a, H-6b), 3.78 – 3.63 (m, 2H; CH_2-O-decyl) 3.56 – 3.40 (m, 2H; CH_2 in 1 of decyl), 2.47 – 2.27 (m, 4H; CH_2α-chain1, CH_2α myristoyl glycerol), 1.66 –1.41 (m, 6H; CH_2β-chain1, CH_2β myristoyl glycerol, CH_2 in 2 of decyl), 1.27 (m, 52H, 27x CH_2) 1.00 – 0.81 (m, 6H; 2x CH_3 chains)

diastereoisomeric mixture 1.1
^{13}C NMR (101 MHz, CD_3OD, 25 °C, TMS) δ 174.01, 172.51, 169.17, 94.03, 72.58, 72.46, 71.88, 71.15, 70.86, 70.31, 69.90, 69.50, 63.97, 33.36, 31.74, 31.71, 29.51, 29.44, 29.14, 29.05, 25.81, 24.55, 22.38, 22.35, 13.05.

ESI-MS: $[M]^-$ m/z = 986.5; found: m/z = 986.6

AM246248 Synthesis

Compounds 1-4 are common intermediates of FP11 synthesis.

Compound 37
1-O-tert-butyldimethylsilyl-2-deoxy-4,6-O-(4-methoxybenzylidene)-2-[DL-2-(benzyloxy)-3(decyloxy) propanoyl] amino- β *-D-glucopyranoside*

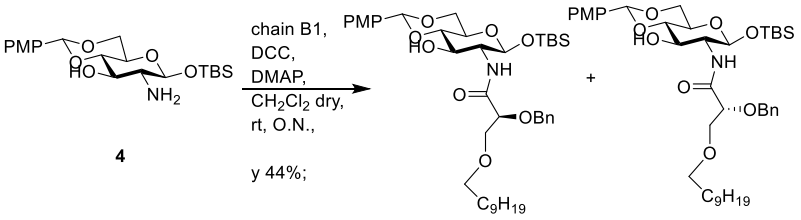

37
diastereoisomers 1 and 2

Compound B1 (706 mg, 2.02 mmol) was dissolved in dry CH_2Cl_2 (15 mL) and EDC (727 mg, 3.79 mmol) was added. After 30 min compound 4 (488 mg, 1.19 mmol) dissolved in CH_2Cl_2 dry (5.0 mL) and DMAP (145 mg, 1.19 mmol) were added and the mixture was stirred at room temperature overnight. The reaction mixture was diluted with CH_2Cl_2 and washed with saturated $NaHCO_3$ solution and brine. The organic layer was dried over anhydrous Na_2SO_4, filtered and the solvents were evaporated *in vacuo*. The crude product was purified with flash chromatography (petroleum ether–EtOAc 7:3) and even the separation of the two diastereoisomers of compound 37 was accomplished (diastereoisomer 1 at higher Rf: yellow oil, 170 mg; diastereoisomer 2 at lower Rf: orange oil, 152 mg. Mixed fractions of the two diastereoisomers: 63 mg. Total product: 385 mg, yield: 44%).
N.B.: it is not possible to say which diastereoisomer is which at this step

diastereoisomer 1 at higher Rf
^{1}H NMR (400 MHz, $CDCl_3$, 25 °C, TMS) δ 7.44 (d, $^3J_{H,H}$= 8.2 Hz, 2H; 2x H-*ortho* PMP), 7.40 – 7.21 (m, 5H; 5X H Bn glycerol), 7.05 (d, $^3J_{H,H}$= 6.3 Hz, 1H; NH), 6.89 (d, $^3J_{H,H}$= 8.2 Hz, 2H; 2x H-*meta* PMP), 5.52 (s, 1H; CH-Ph PMP), 5.06 (d, $^3J_{H,H}$= 7.8 Hz, 1H; H-1), 4.75 – 4.62 (m, 2H; CH_2-Ph), 4.28 (dd, $^3J_{H,H}$= 10.5, 4.7 Hz, 1H; H-5), 4.19 (t, $^3J_{H,H}$= 9.5 Hz, 1H; H-3), 4.07 (m, 1H; CH-O-Bn glycerol), 3.78 (s, 3H; OCH_3 PMP), 3.77 – 3.69 (m, 3H; H-6a, CH_2- O-decyl), 3.63 – 3.54 (m, 1H; H-4), 3.52 (dd, $^3J_{H,H}$= 9.5, 4.5 Hz, 1H; H-6b), 3.46 (t, $^3J_{H,H}$= 7.0 Hz, 2H; CH_2 in 1 of decyl), 3.38 – 3.29 (m, 1H; H-2) 1.57 (m, 2H; CH_2 in 2 of decyl), 1.28 (s, 14H; 7x CH_2), 0.91 (m, 12H; CH_3 decyl, t-Bu-Si), 0.13 (s, 3H, CH_3-Si) 0.10 (s, 3H, CH_3-Si)

diastereoisomer 2 at lower Rf
^{1}H NMR (400 MHz, $CDCl_3$, 25 °C, TMS) δ 7.44 (d, $^3J_{H,H}$= 8.2 Hz, 2H; 2x H-*ortho* PMP), 7.40 – 7.21 (m, 5H; 5X H Bn glycerol), 6.96 (d, $^3J_{H,H}$= 7.0 Hz, 1H; NH), 6.89 (d, $^3J_{H,H}$= 8.2 Hz, 2H; 2x H-*meta* PMP), 5.52 (s, 1H; CH-Ph PMP), 4.81 (d, $^3J_{H,H}$= 7.9 Hz, 1H; H-1), 4.75 – 4.62 (m, 2H; CH_2-Ph), 4.28 (dd, $^3J_{H,H}$= 10.4, 4.9 Hz, 1H; H-5), 4.07 (t, $^3J_{H,H}$= 3.3 Hz, 1H; CH-O-Bn glycerol), 3.94 (t, $^3J_{H,H}$= 9.4 Hz, 1H; H-3), 3.78 (s, 3H; OCH_3 PMP), 3.77 – 3.69 (m, 3H; H-6a, CH_2- O-decyl), 3.68 (m, 1H; H-6b), 3.63 – 3.54 (m, 1H; H-4), 3.49-3.43 (m, 2H; CH_2 in 1 of decyl, H-2), 1.57 (m, 2H; CH_2 in 2 of decyl), 1.28 (s, 14H; 7x CH_2), 0.91 (m, 12H; CH_3 decyl, t-Bu-Si), 0.13 (s, 3H, CH_3-Si) 0.10 (s, 3H, CH_3-Si)

diastereoisomer 1 at higher Rf
^{13}C NMR (101 MHz, $CDCl_3$, 25 °C, TMS) δ 171.44, 160.12, 137.06, 129.74, 128.59, 128.06, 127.74, 113.57, 101.80, 96.34, 95.62, 81.32, 79.46, 79.15, 72.91, 72.66, 71.93, 71.85, 71.50, 70.23, 68.56, 66.50, 61.31, 60.27, 55.26, 31.92, 29.64, 29.34, 25.98, 25.65, 22.70, 17.89, 14.17, -4.09, -5.14.

diastereoisomer 2 at lower Rf
^{13}C NMR (101 MHz, $CDCl_3$, 25 °C, TMS) δ 171.44, 160.12, 137.06, 129.74, 128.59, 128.06, 127.74, 113.57, 101.80, 96.34, 95.62, 81.32, 79.46, 79.15, 72.91, 72.66, 71.93, 71.85, 71.50, 70.23, 68.56, 66.50, 61.31, 60.27, 55.26, 31.92, 29.64, 29.34, 25.98, 25.65, 22.70, 17.89, 14.17, -4.09, -5.14.

Compound 38

1-O-tert-butyldimethylsilyl-2-deoxy-4,6-O-(4-methoxybenzylidene)-3-O-tetradecanoyl-2-[DL-2-(benzyloxy)-3(decyloxy)propanoyl] amino- β *-D-glucopyranoside*

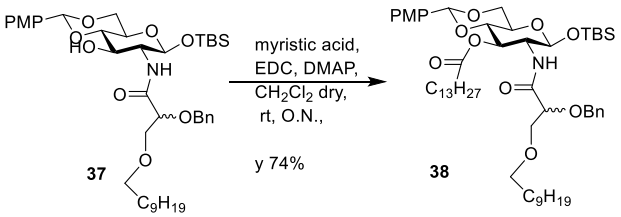

Myristic acid (148 mg, 0.65 mmol) was dissolved in dry CH_2Cl_2 (2.5 mL) and EDC (166 mg, 0.87 mmol) was added. After 30 min the diastereoisomeric mixture of compound 37 (158 mg, 0.22 mmol) dissolved in dry CH_2Cl_2 (1.5 mL) was added, followed by DMAP (26 mg, 0.22 mmol) and the mixture was stirred at room temperature overnight. The reaction mixture was diluted with CH_2Cl_2 and washed with saturated $NaHCO_3$ solution and brine. The organic layer was dried over anhydrous Na_2SO_4, filtered and the solvents were evaporated *in vacuo*. The crude product was purified with flash chromatography (petroleum ether–EtOAc 8:2) to give the diastereoisomeric mixture of compound 38 as a yellow oil (150 mg, 74%).

diastereoisomeric mixture 1:1
^{1}H NMR (400 MHz, $CDCl_3$, 25 °C, TMS) δ 7.42 – 7.32 (m, 7H; 2x H-*ortho* PMP, 5X H Bn glycerol), 6.89 – 6.84 (m, 3H; NH, 2x H-*meta* PMP), 5.45 (s, 0.5H; CH-Ph PMP diastereoisomer1), 5.44 (s, 0.5H; CH-Ph PMP diastereoisomer2), 5.34 (t, $^3J_{H,H}$= 9.9 Hz, 0.5H; H-3 diastereoisomer1), 5.27 (t, $^3J_{H,H}$= 9.9 Hz, 0.5H; H-3 diastereoisomer2), 4.88 (d, $^3J_{H,H}$= 7.9 Hz, 0.5H; H-1 diastereoisomer1), 4.83 (d, $^3J_{H,H}$= 7.9 Hz, 0.5H; H-1 diastereoisomer2), 4.76 – 4.61 (m, 2H: CH_2-Ph), 4.27 (dd, $^3J_{H,H}$= 10.6, 4.9 Hz, 1H; H-5), 4.17 – 4.06 (m, 1H; CH-O-Bn glycerol), 4.03 – 3.96 (m, 0.5H; H-2 diastereoisomer1), 3.95 – 3.87 (m, 0.5H; H-2 diastereoisomer2), 3.85 – 3.77 (m, 5H; OCH_3 PMP, CH_2- O-decyl), 3.67 (t, $^3J_{H,H}$= 9.4 Hz, 1H; H-4), 3.61 – 3.55 (m, 1H; H-6a), 3.55 – 3.45 (m, 1H; H-6b), 3.45 – 3.36 (m, 2H; CH_2 in 1 of decyl), 2.38 – 2.22 (m, 2H; CH_2α myristoyl), 1.57 (m, 4H; CH_2 in 2 of decyl, CH_2β myristoyl), 1.28 (s, 34H; 17x CH_2), 0.91 (m, 15H; CH_3 myristoyl, CH_3 decyl, t-Bu-Si), 0.13 (s, 3H, CH_3-Si) 0.10 (s, 3H, CH_3-Si)

diastereoisomeric mixture 1:1
^{13}C NMR (101 MHz, $CDCl_3$, 25 °C, TMS) δ 173.34, 170.04, 160.03, 137.44, 129.51, 128.44, 127.84, 127.46, 113.49, 101.33, 96.99, 96.67, 79.40, 78.91, 73.45, 73.11, 72.93, 72.52, 72.52, 71.44, 71.06, 68.57, 68.57, 66.46, 60.39, 56.66, 56.38, 55.22, 34.26, 31.93, 29.66, 29.38, 29.04, 26.14, 25.63, 25.09, 22.70, 17.85, 14.14, -3.99, -5.04.

Compound 39

1-O-tert-butyldimethylsilyl-2-deoxy-6-O-(4-methoxybenzyl)-3-O-tetradecanoyl-2-[DL-2-(benzyloxy)-3(decyloxy)propanoyl]amino- β *-D-glucopyranoside.*

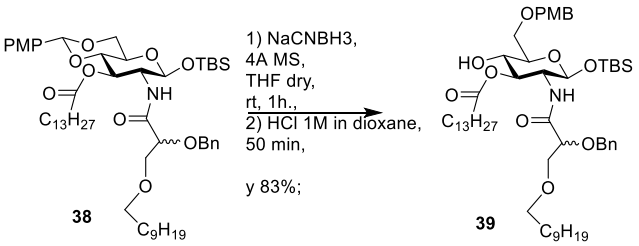

Compound 38 (120 mg, 0.13 mmol) was dissolved in dry THF (6.4 mL) and 4Å molecular sieves (430 mg) were added. After 10 min of stirring at rt, $NaCNBH_3$ (120 mg, 1.91 mmol) was finally added.
The reaction was stirred at r.t. for 1h, then it was cooled in an ice bath and HCl (1M in dioxane) was added dropwise till bubbling ceases. The solution was left stirring 50 min at rt (monitoring the reaction by TLC) and then it was neutralized by adding saturated $NaHCO_3$ solution.
Three extractions with DCM were performed and the organic phase was further washed with brine and then dried over anhydrous Na_2SO_4, filtered and the solvents were evaporated *in vacuo*.
The crude product was purified with flash chromatography (petroleum ether–EtOAc 7:3) to give the diastereoisomeric mixture of compound 39 as a yellow oil (100 mg, 83%).

diastereoisomeric mixture 1:1
^{1}H NMR (400 MHz, $CDCl_3$, 25 °C, TMS) δ 7.44 – 7.29 (m, 5H; 5X H Bn glycerol), 7.24 (d, $^3J_{H,H}$= 8.6 Hz, 2H; 2x H-*ortho* PMB), 6.87 (d, $^3J_{H,H}$= 8.5 Hz, 2H; 2x H-*meta* PMB), 6.79 (d, $^3J_{H,H}$= 9.3 Hz, 0.5H; NH diastereoisomer1), 6.74 (d, $^3J_{H,H}$= 9.5 Hz, 0.5H; NH diastereoisomer2), 5.10 (t, $^3J_{H,H}$= 9.8 Hz, 0.5H; H-3 diastereoisomer1), 5.02 (t, $^3J_{H,H}$= 9.9 Hz, 0.5H; H-3 diastereoisomer2), 4.81 (d, $^3J_{H,H}$= 7.8 Hz, 0.5H; H-1 diastereoisomer1), 4.75 (d, $^3J_{H,H}$= 7.9 Hz, 0.5H; H-1 diastereoisomer2), 4.72 – 4.60 (m, 2H; CH_2-Ph glycerol), 4.56 – 4.43 (m, 2H; CH_2-Ph PMB), 4.13 – 4.00 (m, 2H; H-5, CH-O-Bn glycerol), 3.80 (s, 4H; OCH_3, H-2), 3.76 – 3.65 (m, 3H; CH_2- O-decyl, H-4), 3.61 – 3.47 (m, 2H; H-6a, H-6b), 3.44 – 3.35 (m, 2H; CH_2 in 1 of decyl), 2.38 – 2.22 (m, 2H; CH_2α myristoyl), 1.57 (m, 4H; CH_2 in 2 of decyl, CH_2β myristoyl), 1.28 (s, 34H; 17x CH_2), 0.91 (m, 15H; CH_3 myristoyl, CH_3 decyl, t-Bu-Si), 0.13 (s, 3H, CH_3-Si) 0.10 (s, 3H, CH_3-Si)

diastereoisomeric mixture 1:1
^{13}C NMR (101 MHz, $CDCl_3$, 25 °C, TMS) δ 174.30, 169.99, 159.28, 137.33, 129.73, 129.32, 128.44, 127.82, 113.81, 96.28, 95.95, 79.48, 79.44, 74.95, 74.81, 74.10, 73.98, 73.41, 73.34, 73.00, 72.90, 72.47, 71.58, 71.44, 71.22, 71.16, 70.27, 70.25, 34.28, 34.20, 31.93, 29.70, 29.66, 29.66, 29.60, 29.51, 29.48, 29.37, 29.37, 29.35, 29.29, 29.20, 29.16, 29.16, 26.10, 25.67, 24.99, 24.88, 22.70, 17.89, 14.14, -1.60, -3.94, -5.09.

Compound 40

1-O-tert-butyldimethylsilyl-2-deoxy-6-O-(4-methoxybenzyl)-4-O-tetradecanoyl 3-O-tetradecanoyl-2-[DL-2-(benzyloxy)-3(decyloxy)propanoyl]amino- β *-D-glucopyranoside*

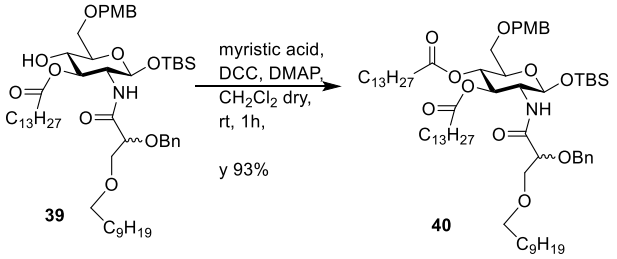

Myristic acid (44 mg, 0.19 mmol) was dissolved in dry CH_2Cl_2 (1 mL) and DCC (39 mg, 0.19 mmol) was added. After 30 min compound 39 (60 mg, 0.063 mmol) dissolved in CH_2Cl_2 dry (0.5 mL) and DMAP (8 mg, 0.063 mmol) were added and the mixture was stirred at room temperature for 1 h. The precipitate is removed by filtration and the solvents were evaporated *in vacuo*. The crude product was purified with flash chromatography (petroleum ether–EtOAc 9:1) to give compound 40 as a red solid (68 mg, 93%).

diastereoisomeric mixture 1:1

^{1}H NMR (400 MHz, $CDCl_3$, 25 °C, TMS) δ 7.41 – 7.29 (m, 5H; 5X H Bn glycerol), 7.23 (d, $^3J_{H,H}$= 8.2 Hz, 2H; 2x H-*ortho* PMB), 6.86 (d, $^3J_{H,H}$= 8.0 Hz, 2H; 2x H-*meta* PMB), 6.79 (d, $^3J_{H,H}$= 9.2 Hz, 0.5H; NH diastereoisomer1), 6.73 (d, $^3J_{H,H}$= 9.3 Hz, 0.5H; NH diastereoisomer2), 5.31 (t, $^3J_{H,H}$= 10.0 Hz, 0.5H; H-3 diastereoisomer1), 5.21 (t, $^3J_{H,H}$= 10.0 Hz, 0.5H; H-3 diastereoisomer2), 5.03 (t, $^3J_{H,H}$= 9.6 Hz, 1H, H-4 diastereoisomer1, H-4 diastereoisomer2), 4.92 (d, $^3J_{H,H}$= 7.8 Hz, 0.5H; H-1 diastereoisomer1), 4.83 (d, $^3J_{H,H}$= 7.8 Hz, 0.5H; H-1 diastereoisomer2), 4.74 – 4.58 (m, 2H; CH_2-Ph glycerol), 4.50 – 4.40 (m, 2H; CH_2-Ph PMB), 4.15 – 4.01 (m, 2H; H-5, CH-O-Bn glycerol), 3.92 – 3.72 (m, 4H; OCH_3, H-2), 3.71 – 3.48 (m, 4H; H-6a, CH_2- O-decyl, H-6b), 3.44 – 3.35 (m, 2H; CH_2 in 1 of decyl), 2.32 – 2.13 (m, 4H; CH_2α myristoyl1, CH_2α myristoyl2), 1.67 – 1.46 (m, 6H; CH_2 in 2 of decyl, 2x CH_2β myristoyl), 1.28 (s, 54H; 27x CH_2), 0.91 (m, 18H; 2x CH_3 myristoyl, CH_3 decyl, t-Bu-Si), 0.13 (s, 3H, CH_3-Si) 0.10 (s, 3H, CH_3-Si)

diastereoisomeric mixture 1:1

^{13}C NMR (101 MHz, $CDCl_3$, 25 °C, TMS) δ 173.94, 173.24, 172.34, 169.99, 159.14, 137.31, 129.95, 129.28, 128.44, 127.81, 113.66, 96.07, 95.66, 79.41, 73.31, 73.15, 72.92, 72.37, 71.94, 71.44, 69.40, 69.22, 60.14, 56.54, 56.09, 55.22, 40.85, 34.39, 34.10, 31.93, 30.89, 29.68, 26.13, 25.67, 24.99, 22.70, 17.89, 14.13, -4.04, -5.12.

Compound 41

2-deoxy-6-O-(4-methoxybenzyl)-4-O-tetradecanoyl 3-O-tetradecanoyl-2-[DL-2-(benzyloxy)-3(decyloxy)propanoyl]amino-α-D-glucopyranoside

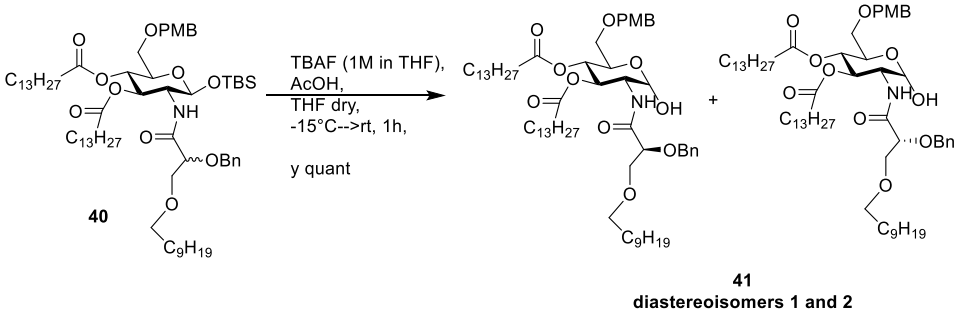

Compound 40 (66 mg, 0.057 mmol) was dissolved in dry THF (2.8 mL), cooled to -15 °C and a solution of TBAF (22 mg, 0.068 mmol) and AcOH (5 µL, 0.08 mmol) in THF (70 uL) was added. The reaction was stirred

at -15° C for 10 min, then it was allowed to warm till rt and it was left stirring at rt for 1h. The solution was diluted with water and extracted with CH_2Cl_2. The organic layer was dried over anhydrous Na_2SO_4, filtered and the solvents were evaporated *in vacuo*. The crude product was purified with flash chromatography (petroleum ether–EtOAc 8:2 to petroleum ether–EtOAc 7.5:2.5) and even the separation of the two diastereoisomers of compound 41 was accomplished (diastereoisomer 1 at higher Rf: yellow oil, 32 mg; diastereoisomer 2 at lower Rf: yellow oil, 26 mg. Total product: 58 mg, yield: quant).
N.B.: it is not possible to say which diastereoisomer is which at this step

diastereoisomer 1 at higher Rf
^{1}H NMR (400 MHz, $CDCl_3$, 25 °C, TMS) δ 7.39 – 7.26 (m, 5H; 5X H Bn glycerol), 7.22 (d, $^3J_{H,H}$= 8.2 Hz, 2H; 2x H-*ortho* PMB), 7.06 (d, $^3J_{H,H}$= 9.5 Hz, 1H; N-H), 6.85 (d, $^3J_{H,H}$= 8.2 Hz, 2H; 2x H-*meta* PMB), 5.38 (t, $^3J_{H,H}$= 10.1 Hz, 1H; H-3), 5.21 (d, $^3J_{H,H}$= 3.5 Hz, 1H; H-1), 5.08 (t, $^3J_{H,H}$= 9.9 Hz, 1H; H-4), 4.66 (d, $^3J_{H,H}$= 11.7 Hz, 1H; CHa-Ph glycerol), 4.51 (d, $^3J_{H,H}$= 11.7 Hz, 1H; CHb-Ph glycerol), 4.50 – 4.40 (m, 2H; CH_2-Ph PMB), 4.26 (td, $^3J_{H,H}$= 10.1, 3.4 Hz, 1H; H-2), 4.23 – 4.13 (m, 1H; H-5), 3.92 (dd, $^3J_{H,H}$= 5.4, 2.5 Hz, 1H; CH-O-Bn glycerol), 3.78 (s, 3H; OCH_3), 3.76 – 3.60 (m, 3H; H-6a, CH_2- O-decyl), 3.47 – 3.33 (m, 3H; H-6b, CH_2 in 1 of decyl), 2.21 (t, $^3J_{H,H}$= 7.6 Hz, 2H; CH_2α myristoyl1), 2.14 (t, $^3J_{H,H}$= 7.7 Hz, 2H; CH_2α myristoyl2), 1.67 – 1.46 (m, 6H; CH_2 in 2 of decyl, 2x CH_2β myristoyl), 1.28 (s, 54H; 27x CH_2), 0.91 (m, 9H; 2x CH_3 myristoyl, CH_3 decyl)

diastereoisomer 2 at lower Rf
^{1}H NMR (400 MHz, $CDCl_3$, 25 °C, TMS) δ 7.39 – 7.26 (m, 5H; 5X H Bn glycerol), 7.22 (d, $^3J_{H,H}$= 8.2 Hz, 2H; 2x H-*ortho* PMB), 6.98 (d, $^3J_{H,H}$= 9.4 Hz, 1H; N-H), 6.85 (d, $^3J_{H,H}$= 8.2 Hz, 2H; 2x H-*meta* PMB), 5.31 (t, $^3J_{H,H}$= 10.1 Hz, 1H; H-3), 5.13 (d, $^3J_{H,H}$= 3.5 Hz, 1H; H-1), 5.02 (t, $^3J_{H,H}$= 9.9 Hz, 1H; H-4), 4.68 (d, $^3J_{H,H}$= 11.7 Hz, 1H; CHa-Ph glycerol), 4.62 (d, $^3J_{H,H}$= 11.7 Hz, 1H; CHb-Ph glycerol), 4.43 (m, 2H; CH_2-Ph PMB), 4.24 (td, $^3J_{H,H}$= 10.1, 3.4 Hz, 1H; H-2), 4.20 – 4.13 (m, 1H; H-5), 4.03 (dd, $^3J_{H,H}$= 7.2, 2.7 Hz, 1H; CH-O-Bn glycerol), 3.78 (s, 3H; OCH_3), 3.67 (dd, $^3J_{H,H}$= 10.7, 2.7 Hz, 1H; H-6a), 3.51 (dd, $^3J_{H,H}$= 10.7, 7.2 Hz, 1H; H-6b), 3.49 – 3.34 (m, 4H; CH_2- O-decyl, CH_2 in 1 of decyl), 2.19 (t, $^3J_{H,H}$= 7.6 Hz, 2H; CH_2α myristoyl1), 2.12 (t, $^3J_{H,H}$= 7.7 Hz, 2H; CH_2α myristoyl2), 1.67 – 1.46 (m, 6H; CH_2 in 2 of decyl, 2x CH_2β myristoyl), 1.28 (s, 54H; 27x CH_2), 0.91 (m, 9H; 2x CH_3 myristoyl, CH_3 decyl)

diastereoisomer 1 at higher Rf
^{13}C NMR (101 MHz, $CDCl_3$, 25 °C, TMS) δ 173.63, 172.24, 170.36, 159.24, 136.94, 129.59, 129.53, 128.49, 128.17, 113.69, 78.83, 73.14, 72.85, 71.80, 71.57, 70.56, 68.89, 68.72, 68.47, 55.22, 51.98, 34.22, 31.93, 29.70, 29.67, 29.51, 29.50, 29.37, 29.29, 29.20, 29.18, 25.96, 24.91, 22.70, 14.14

diastereoisomer 2 at lower Rf
^{13}C NMR (101 MHz, $CDCl_3$, 25 °C, TMS) δ 173.42, 172.25, 170.34, 137.29, 129.60, 129.45, 128.43, 128.03, 113.70, 79.68, 73.23, 73.13, 72.05, 71.71, 70.31, 68.80, 68.49, 55.21, 51.64, 34.12, 31.93, 29.70, 29.37, 26.06, 24.86, 22.70, 14.14.

Compound 42

1-O-dibenzylphosphoryl-2-deoxy-6-O-(4-methoxybenzyl)-4-O-tetradecanoyl 3-O-tetradecanoyl-2-[DL-2-(benzyloxy)-3(decyloxy)propanoyl]amino-α-D-glucopyranoside

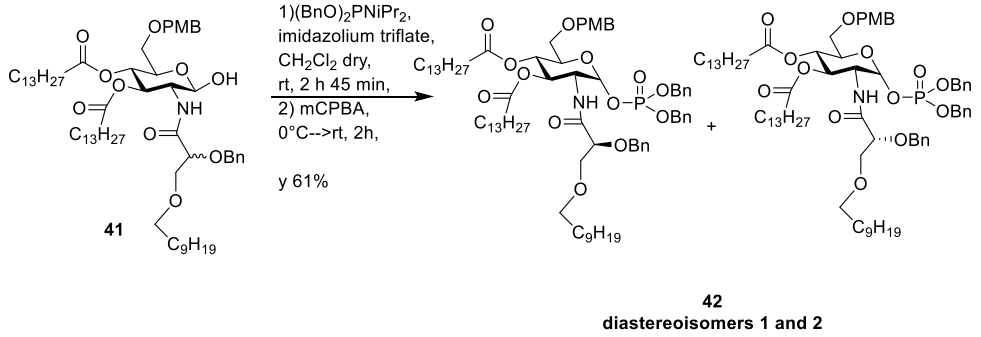

The diastereoisomeric mixture of compound 41 (45 mg, 0.043 mmol) was dissolved in dry CH_2Cl_2 (0.7 mL), then imidazolium triflate (34 mg, 0.127 mmol) and dibenzyl *N*,*N*-diisopropyl phosphoramidite (44 µl, 0.127 mmol) were added and the reaction was stirred at r.t. for 2h and 45 min. The solution was then cooled in an ice bath and *m*CPBA (37 mg, 0.216 mmol) was added. The reaction was stirred at rt 2h, then the mixture was diluted with CH_2Cl_2, washed with a saturated solution of $NaHCO_3$ and brine. The organic layer was dried over anhydrous Na_2SO_4, filtered and the solvents were evaporated *in vacuo*. The crude product was purified with flash chromatography (petroleum ether–EtOAc 7:3) and even the separation of the two diastereoisomers of compound 42 was accomplished (diastereoisomer 1 at higher Rf: orange oil, 22 mg; diastereoisomer 2 at lower Rf: red oil, 13 mg. Total product: 35 mg, yield: 61%).
N.B.: it is not possible to say which diastereoisomer is which at this step

diastereoisomer 1 at higher Rf
^{1}H NMR (400 MHz, $CDCl_3$, 25 °C, TMS) δ 7.40 – 7.12 (m, 17H; 5X H Bn glycerol, 2x BnO-P, 2x H-*meta* PMB), 7.05 (d, $^3J_{H,H}$= 9.4 Hz, 1H; NH), 6.80 (d, $^3J_{H,H}$= 8.2 Hz, 2H; 2x H-*ortho* PMB), 5.74 (dd, $^3J_{H,P}$= 5.9, $^3J_{H,H}$= 2.8 Hz, 1H; H-1), 5.31 (t, $^3J_{H,H}$= 10.1 Hz, 1H; H-3), 5.24 (t, $^3J_{H,H}$= 9.8 Hz, 1H; H-4), 5.05 – 4.86 (m, 4H; 2x CH_2(Ph)-O-P), 4.63 (d, $^3J_{H,H}$= 11.7 Hz, 1H; CHa-Ph glycerol), 4.53 (d, $^3J_{H,H}$= 11.7 Hz, 1H; CHb-Ph glycerol), 4.44 – 4.30 (m, 3H; CH_2-Ph PMB, H-5), 4.10 – 4.03 (m, 1H; H-2), 4.01 – 3.95 (m, 1H; CH-O-Bn glycerol), 3.81 – 3.69 (m, 4H; OCH_3, H-6a), 3.54 (dd, $^3J_{H,H}$= 10.7, 6.9 Hz, H-6b), 3.41 – 3.26 (m, 4H; CH_2- O-decyl, CH_2 in 1 of decyl), 2.19 (t, $^3J_{H,H}$= 7.6 Hz, 2H; CH_2α myristoyl1), 2.12 (t, $^3J_{H,H}$= 7.7 Hz, 2H; CH_2α myristoyl2), 1.67 – 1.46 (m, 6H; CH_2 in 2 of decyl, 2x CH_2β myristoyl), 1.28 (s, 54H; 27x CH_2), 0.91 (m, 9H; 2x CH_3 myristoyl, CH_3 decyl)

diastereoisomer 2 at lower Rf
^{1}H NMR (400 MHz, $CDCl_3$, 25 °C, TMS) δ 7.40 – 7.12 (m, 17H; 5x H Bn glycerol, 2x BnO-P, 2x H-*meta* PMB), 6.99 (d, $^3J_{H,H}$= 9.4 Hz, 1H; NH), 6.80 (d, $^3J_{H,H}$= 8.2 Hz, 2H; 2x H-*ortho* PMB), 5.82 (dd, $^3J_{H,P}$= 5.8, $^3J_{H,H}$= 3.3 Hz, 1H; H-1), 5.31 – 5.16 (m, 2H; H-3, H-4), 5.05 – 4.86 (m, 4H; 2x CH_2(Ph)-O-P), 4.57 (d, $^3J_{H,H}$= 11.7 Hz, 1H; CHa-Ph glycerol), 4.50 (d, $^3J_{H,H}$= 11.7 Hz, 1H; CHb-Ph glycerol), 4.44 – 4.28 (m, 3H; CH_2-Ph PMB, H-5), 4.08 – 4.03 (m, 1H; H-2), 3.97 – 3.89 (m, 1H; CH-O-Bn glycerol), 3.76 (m, 3H; OCH_3), 3.63 (dd, $^3J_{H,H}$= 10.7, 2.6 Hz, 1H; H-6a), 3.50 (dd, $^3J_{H,H}$= 10.6, 6.7 Hz, 1H; H-6b), 3.40 – 3.30 (m, 4H; CH_2- O-decyl, CH_2 in 1 of decyl), 2.19 (t, $^3J_{H,H}$= 7.6 Hz, 2H; CH_2α myristoyl1), 2.12 (t, $^3J_{H,H}$= 7.7 Hz, 2H; CH_2α myristoyl2), 1.67 – 1.46 (m, 6H; CH_2 in 2 of decyl, 2x CH_2β myristoyl), 1.28 (s, 54H; 27x CH_2), 0.91 (m, 9H; 2x CH_3 myristoyl, CH_3 decyl)

diastereoisomer 1 at higher Rf
^{13}C NMR (101 MHz, $CDCl_3$, 25 °C, TMS) δ 173.63, 171.92, 170.32, 159.17, 137.02, 129.52, 128.49, 128.45, 128.19, 127.99, 127.82, 126.97, 113.64, 78.93, 73.12, 72.08, 71.56, 70.89, 70.00, 69.64, 69.46, 67.77, 55.17, 51.53, 34.17, 34.08, 31.93, 29.67, 29.49, 29.37, 29.18, 26.04, 24.91, 24.84, 22.70, 14.14, -11.60.

diastereoisomer 2 at lower Rf

^{13}C NMR (101 MHz, $CDCl_3$, 25 °C, TMS) δ 173.63, 171.92, 170.32, 159.17, 137.02, 129.52, 128.49, 128.45, 128.19, 127.99, 127.82, 126.97, 113.64, 78.93, 73.12, 72.08, 71.56, 70.89, 70.00, 69.64, 69.46, 67.77, 55.17, 51.53, 34.17, 34.08, 31.93, 29.67, 29.49, 29.37, 29.18, 26.04, 24.91, 24.84, 22.70, 14.14, -11.60.

Compound AM246248

1-O-phosphoryl-2-deoxy-4-O-tetradecanoyl 3-O-tetradecanoyl-2-[DL-2-(hydroxy)-3(decyloxy)propanoyl]amino-β-D-glucopyranoside (sodium salt)

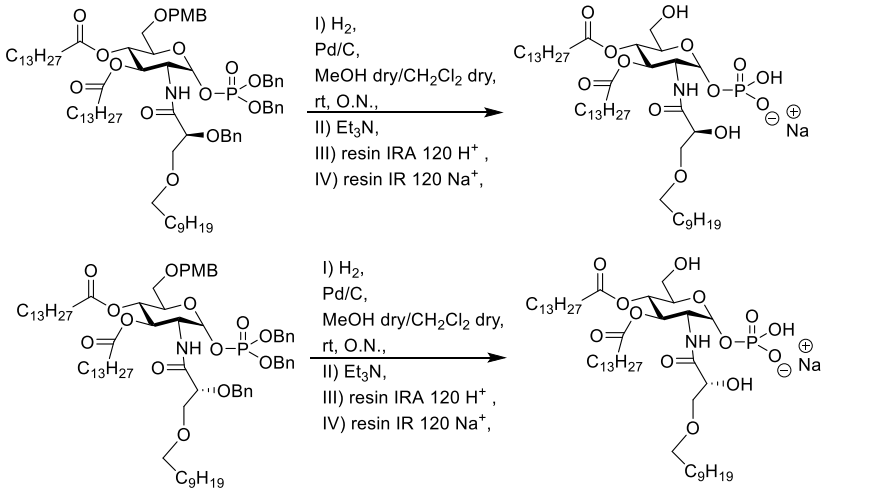

compound 42 diastereoisomers 1 and 2

AM246248 diastereoisomers 1 and 2

The two diastereoisomers of compound 42 have been put to react separately:

1) Compound 42 diastereoisomer 1 (at higher Rf) (4 mg, 0.003 mmol) was dissolved in dry CH_2Cl_2/MeOH 1:2 (0.6 mL), and Pd on activated charcoal was then added in catalytic amounts. The reaction mixture was stirred at rt under H_2 atmosphere overnight. Triethylamine (30 µL) was then added to the reaction mixture, and the suspension was filtered with a syringe filter. The triethylammonium salt was dissolved in dry CH_2Cl_2/MeOH 1:2 (2 mL) and treated first with an Amberlite IRA 120 H^+ exchange resin and then with an IR 120 Na^+ exchange resin to remove triethylamine and to form the sodium salt, giving compound AM246248 diastereoisomer 1 as a white solid (2 mg, 70%).
2) Compound 42 diastereoisomer 2 (at lower Rf) (13 mg, 0.003 mmol) was dissolved in dry CH_2Cl_2/MeOH 1:2 (0.6 mL), and Pd on activated charcoal was then added in catalytic amounts. The reaction mixture was stirred at rt under H_2 atmosphere overnight. Triethylamine (40 µL) was then added to the reaction mixture, and the suspension was filtered with a syringe filter. The triethylammonium salt was dissolved in dry CH_2Cl_2/MeOH 1:2 (2 mL) and treated first with an Amberlite IRA 120 H^+ exchange resin and then with an IR 120 Na^+ exchange resin to remove triethylamine and to form the sodium salt, giving compound AM246248 diastereoisomer 2 as a white solid (4.5 mg, 53%).

N.B.: it is not possible to say which diastereoisomer is which at this step

diastereoisomer 1

^{1}H NMR (400 MHz, CD_3OD, 25 °C, TMS) δ: 5.52 (dd, $^3J_{H,P}$= 7.3, $^3J_{H,H}$= 3.4 Hz, 1H; H-1), 5.38 (t, $^3J_{H,H}$= 9.3 Hz, 1H; H-3), 5.34 (m, 1H; NH), 5.13 (t, $^3J_{H,H}$= 9.8 Hz, 1H; H-4), 4.23 (d, $^3J_{H,H}$= 10.7 Hz, 1H; H-2), 4.16 (dd, $^3J_{H,H}$= 6.0, 2.9 Hz, 1H; H-5), 4.12 (m, 1H; CH-OH glycerol), 4.01 (d, $^3J_{H,H}$= 5.7 Hz, 0.8H; OH glycerol), 3.69 – 3.51 (m, 4H; CH_2- O-decyl, H-6a, H-6b), 3.50 – 3.40 (m, 2H; CH_2 in 1 of decyl), 2.38 – 2.19 (m, 4H; 2x CH_2α myristoyl), 1.67 – 1.46 (m, 6H; CH_2 in 2 of decyl, 2x CH_2β myristoyl), 1.28 (s, 54H; 27x CH_2), 0.91 (m, 9H; 2x CH_3 myristoyl, CH_3 decyl)

diastereoisomer 2
^{1}H NMR (400 MHz, CD_3OD, 25 °C, TMS) δ: 5.54 – 5.48 (dd, $^{3}J_{H,P}$= 7.3, $^{3}J_{H,H}$= 3.4 Hz, 1H; H-1), 5.41 – 5.27 (m, 2H; H-3, NH), 5.14 (t, $^{3}J_{H,H}$= 9.9 Hz, 1H; H-4), 4.32 – 4.22 (m, 1H; H-2), 4.18 – 4.06 (m, 2H; H-5, CH-OH glycerol), 4.01 (d, $^{3}J_{H,H}$= 5.6 Hz, 0.8H; OH glycerol), 3.71 – 3.59 (m, 3H; CH_2- O-decyl, H-6a) 3.57 – 3.44 (m, 3H; H-6b, CH_2 in 1 of decyl), 2.38 – 2.21 (m, 4H; 2x $CH_2\alpha$ myristoyl) 1.67 – 1.46 (m, 6H; CH_2 in 2 of decyl, 2x $CH_2\beta$ myristoyl), 1.29 (s, 54H; 27x CH_2), 0.91 (m, 9H; 2x CH_3 myristoyl, CH_3 decyl)

AM30 Synthesis

Compound 45

2-(4-((tert-butyldimethylsilyl)oxy)phenyl)acetic acid

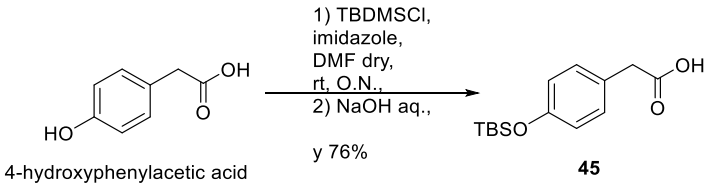

4-hydroxyphenylacetic acid — **45**

4–hydroxylphenylacetic acid (600 mg , 3.93 mmol) was dissolved in dry DMF (11 mL) and imidazole (1.07 g, 15.74) and TBDMSCl (1.48 g, 9.84 mmol) were added to the solution at r.t. The reaction mixture was stirred at r.t. overnight. The solvents were evaporated *in vacuo* and the crude was dissolved in Et_2O and washed with brine. The organic layer was dried over anhydrous Na_2SO_4, filtered and the solvents were evaporated *in vacuo*. The crude was dissolved in THF (1.5 mL) and MeOH (4 mL) and NaOH 1M aq. (1 M, 1.3 mL) was added dropwise. The reaction mixture was stirred for 20 min. Solvents were evaporated and the crude was dissolved with Et_2O and brine and a solution of HCl was added dropwise until pH=6 was reached. Then, the organic phase was extracted, dried with anhydrous sodium sulfate and evaporated *in vacuo*. Compound 45 (800 mg, 76%) was obtained without further purifications.

^{1}H NMR (400 MHz, $CDCl_3$, 25 °C, TMS) δ 7.13 (d, $^3J_{H,H}$= 8.4 Hz, 2H; 2x H-*ortho* Ph), 6.79 (d, $^3J_{H,H}$= 8.5 Hz, 2H; 2x H-*meta* Ph), 3.57 (s, 2H; CH_2), 0.97 (s, 9H; tBu-Si), 0.18 (s, 6H; 2x CH_3-Si)

^{13}C NMR (101 MHz, $CDCl_3$, 25 °C, TMS) δ 154.84, 130.39, 130.35, 126.19, 120.13, 40.60, 30.33, 25.69, 18.20, -4.40, -4.41.

Compound 46

cyclohex-3-en-1-ylmethyl 2-(4-((tert-butyldimethylsilyl)oxy)phenyl)acetate

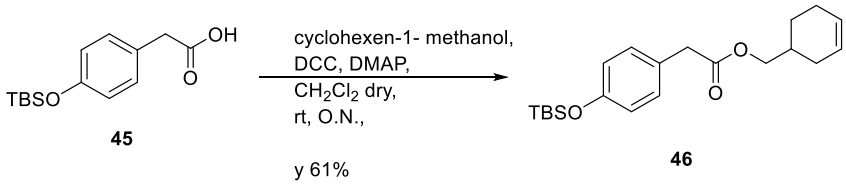

45 — **46**

Compound 45 (800 mg, 3.0 mmol) was dissolved in dry CH_2Cl_2 (19 mL) and DCC was added (732 mg, 3.55 mmol). The reaction mixture was stirred at rt for 30 min, then, 1-cycloesen-4-olo (316 µL, 2.73 mmol) and DMAP (cat) were added. The reaction was stirred rt overnight. After filtration, the solvents were evaporated *in vacuo* and the crude was purified on flash chromatography (petroleum ether–EtOAc 99:1), affording compound 46 (600 mg, 61%).

^{1}H NMR (400 MHz, $CDCl_3$, 25 °C, TMS) δ 7.13 (d, $^3J_{H,H}$= 8.4 Hz, 2H; 2x H-*ortho* Ph), 6.79 (d, $^3J_{H,H}$= 8.5 Hz, 2H; 2x H-*meta* Ph), 5.72 – 5.55 (m, 2H; 2x CH=C), 3.97 (d, $^3J_{H,H}$= 6.6 Hz, 1H; CH_2-O), 3.54 (s, 2H; CH_2-Ph), 2.11 – 1.99 (m, 2H; CH_2-C=C), 1.97 – 1.84 (m, 1H; CH), 1.79 – 1.62 (m, 2H, CH_2-C=C), 1.35 – 1.17 (m, 2H, CH_2-C-C=C), 0.97 (s, 9H; tBu-Si), 0.17 (s, 6H; 2x CH_3-Si)

^{13}C NMR (101 MHz, $CDCl_3$, 25 °C, TMS) δ 171.88, 154.65, 130.20, 126.96, 126.91, 126.91, 125.48, 120.09, 68.96, 40.67, 33.00, 28.08, 25.69, 25.20, 24.40, 18.19, -4.44.

Compound 47

cyclohex-3-en-1-ylmethyl 2-(4-hydroxyphenyl)acetate

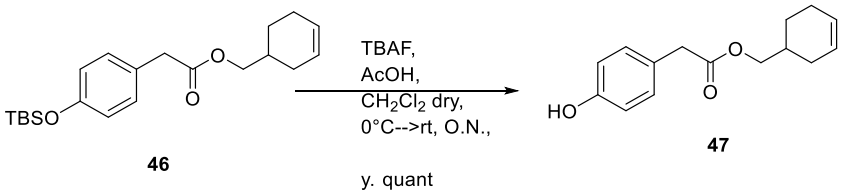

Compound 46 (200 mg, 0.55 mmol) was dissolved in dry CH_2Cl_2 (12 mL). Then reaction mixture was cooled to 0°C and a solution of TBAF (612 mg, 1.94 mmol) and AcOH (127 µL, 2.22 mmol) in CH_2Cl_2 (2 mL) was added dropwise. The reaction was stirred at rt overnight. The reaction mixture was washed with $NaHCO_3$ sat. solution and the organic phase was dried over anhydrous Na_2SO_4, filtered and the solvents were evaporated *in vacuo*. The crude was purified by flash chromatography (petroleum ether–EtOAc 9:1), affording compound 47 (136 mg, quant.)

^{1}H NMR (400 MHz, $CDCl_3$, 25 °C, TMS) δ 7.13 (d, $^3J_{H,H}$= 8.3 Hz, 2H; 2x H-*ortho* Ph), 6.76 (d, $^3J_{H,H}$= 8.4 Hz, 2H; 2x H-*meta* Ph), 5.72 – 5.55 (m, 2H; 2x CH=C), 3.97 (d, $^3J_{H,H}$= 6.6 Hz, 1H; CH_2-O), 3.54 (s, 2H; CH_2-Ph), 2.11 – 1.99 (m, 2H; CH_2-C=C), 1.97 – 1.84 (m, 1H; CH), 1.79 – 1.62 (m, 2H, CH_2-C=C), 1.35 – 1.17 (m, 2H, CH_2-C-C=C)

^{13}C NMR (101 MHz, $CDCl_3$, 25 °C, TMS) δ 173.23, 155.17, 130.38, 127.04, 125.44, 115.60, 69.47, 40.58, 32.94, 28.05, 25.19, 24.37.

Compound 48

(3,4-dihydroxycyclohexyl)methyl 2-(4-hydroxyphenyl)acetate

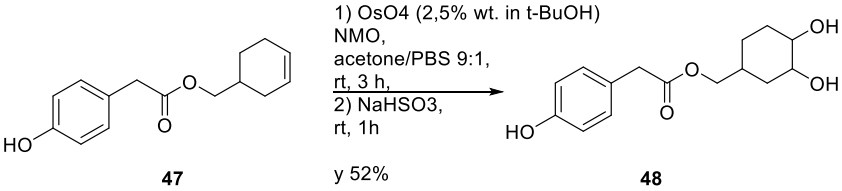

Compound 47 (136 mg, 0.55 mmol) was dissolved in a mixture of acetone/PBS buffer (pH=7.4) 9:1 (3.2 mL) and NMO (129 mg, 1.10 mmol) and OsO_4 2,5% wt. in *t*-BuOH (242 µL, 0.019 mmol) were added. The reaction was stirred RT for 3 h then the reaction was quenched by adding a solution of NaH_SO_3 (100 mg in 1.0 mL of water) and stirred for 1h. The solution was concentred *in vacuo*, diluted with CH_2Cl_2 and washed with brine. The organic phase was dried over anhydrous Na_2SO_4, filtered and the solvents were evaporated *in vacuo*. The crude was purified by flash chromatography (petroleum ether–EtOAc 3:7), affording compound 48 (80 mg, 52%).

^{1}H NMR (400 MHz, CD_3OD, 25 °C, TMS) δ 7.07 (d, $^3J_{H,H}$= 8.3 Hz, 2H; 2x H-*ortho* Ph), 6.72 (d, $^3J_{H,H}$= 8.4 Hz, 2H; 2x H-*meta* Ph), 3.96 – 3.83 (m, 3H; CH_2-O, CH-OH), 3.58 – 3.42 (m, 3H; CH_2-Ph, CH-OH), 1.90 – 1.76 (m, 1H, CH), 1.75 – 1.54 (m, 2H; CH_2-C-OH), 1.97 – 1.84 (m, 1H; CH), 1.51 – 1.19 (m, 4H; CH_2-C-OH, CH_2-C-C-OH)

^{13}C NMR (101 MHz, CD_3OD, 25 °C, TMS) δ 172.64, 129.93, 125.00, 114.83, 71.28, 70.89, 68.70, 68.58, 39.78, 35.54, 33.78, 30.79, 30.03, 29.65, 26.92, 26.72, 21.71, -5.53.

Compound AM30

5-oxo-2-(2-oxoethyl)pentyl 2-(4-hydroxyphenyl)acetate

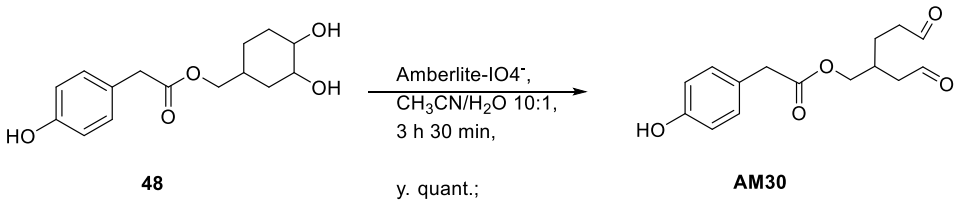

48 **AM30**

Compound 48 (60 mg, 0.21 mmol) was dissolved in CH_3CN/H_2O 10:1 (1.8 mL) and a freshly-prepared Amberlite-$IO4^-$ resin (268 mg, 0.43 mmol IO_4-) was added. The reaction was stirred at rt for 3 h 30 min. The resin was filtered off and the resin was washed with CH_3CN and Et_2O. The solvents were evaporated *in vacuo* to give compound AM30 as white powder (60 mg, quant.).

^{1}H NMR (400 MHz, DMSO-d_6, 25 °C, TMS) δ 9.59 (s, 1H; CHO), 9.30 (s, 1H; CHO), 7.01 (d, $^3J_{H,H}$= 8.2 Hz, 2H; 2x H-*ortho* Ph), 6.67 (d, $^3J_{H,H}$= 8.3 Hz, 2H; 2x H-*meta* Ph), 4.06 – 3.77 (m, 2H, CH_2-O) 3.48 (s, 2H; CH_2-Ph), 2.45 – 2.28 (m, 4H; 2x CH_2α to aldehyde), 2.25 – 2.14 (m, 1H; CH), 1.58 – 1.38 (m, CH_2β to aldehyde)

^{13}C NMR (101 MHz, DMSO-d_6, 25 °C, TMS) δ 203.35, 202.97, 172.65, 156.02, 130.87, 129.48, 115.50, 66.20, 45.41, 35.87, 31.82, 29.89, 23.36.

2. Biology

HEK-blue™ assay for agonism or antagonism

HEK-Blue-TLR4 cells (InvivoGen) were cultured according to manufacturer's instructions. Briefly, cells were cultured in DMEM high glucose medium supplemented with 10% fetal bovine serum (FBS), 2 mM glutamine, 1x Normocin (InvivoGen) and 1x HEK-Blue Selection (InvivoGen). Cells were detached by the use of a cell scraper and the cell concentration was estimated using Trypan Blue (Sigma Aldrich). The cells were diluted in DMEM high glucose medium, supplemented as described before and seeded in multiwell plate at a density of $2x10^4$ cells per well in 200 µL. After overnight incubation (37°C, 5% CO2, 95% humidity), supernatant was removed, cell monolayers were washed with warm PBS without Ca^{2+} and Mg^{2+} and treated with compounds (from 0 to 10-200 µM) dissolved in DMSO-ethanol (1:1).

When antagonistic activity was studied, the cells were stimulated 30 min after the compounds administration, with 10 ng/ml of LPS from *E. coli* O55:B5 (Sigma Aldrich) and incubated overnight at 37°C, 5% CO2 and 95% humidity. As a control, the cells were treated with or without LPS (10 ng/ml) alone.

After the night, the SEAP-containing supernatants were collected and 50µL of each sample was added to 100 µL PBS, pH 8, 0.84 mM para-Nitrophenylphosphate (pNPP) for a final concentration of 0.8 mM pNPP. Plates were incubated for 2-4 h in the dark at RT and then the plate reading was assessed by using a spectrophotometer at 405 nm (LT 4000, Labtech). The results were normalized with positive control (LPS alone) and expressed as the mean of percentage ± SD of 3 independent experiments. Data have then been interpolated to a 4-parameter sigmoid logic equation to determine the IC_{50} or EC_{50} values.

MTT cell viability assay

HEK-Blue cells were seeded in 100 µL DMEM without Phenol Red at a density of 2x104 cells per well. After overnight incubation, 10 µL compounds (from 0 to 200 µM) were added and the plates were incubated overnight at 37 °C, 5% CO_2, 95% humidity. DMSO and PBS were included as controls. Then 10 µl of MTT solution (5 mg/mL in PBS) were added to each well. After 3 h incubation (37 °C, 5% CO2, 95% humidity), HCl 0.1 N in isopropanol was added (100 µl/well) to dissolve formazan crystals. Formazan concentration in the wells was determined measuring the absorbance at 570 nm (LT 4000, Labtech). The results were normalized with untreated control (PBS) and expressed as the mean of percentage ± SD of 3 independent experiments.

3. MD-2 binding experiments

Antibody-sandwich ELISA assay

The method of antibody-sandwich ELISA for the detection of the binding of compounds to MD-2 was modified from a previous study.[208] A microtiter plate was coated overnight at 4 °C with 100 µL/well of 5 µg/mL of chicken polyclonal anti-MD-2 antibodies, diluted in 50 mM Na2CO3 buffer, pH 9.6 e blocked with 1% BSA in PBS. After washing, 1 µM MD-2 with tested compounds was added and incubated per 2 hours. 0.1 µg/mL mouse anti-MD-2 MAb (9B4) e 0.1 µg/mL goat anti-mouse IgG conjugated with HRP in PBS were added, followed by detection at 420 nm After the addition of 100 µL of ABTS (Sigma). Chicken anti-MD-2 polyclonal antibodies were prepared against recombinant MD-2 by GenTel (Madison, WI, USA), monoclonal mouse anti-MD-2 9B4 antibodies were from eBioscience (San Diego, CA, USA), and secondary goat anti-mouse IgG conjugated with horseradish peroxidase were from Santa Cruz Biotechnology (Santa Cruz, CA, USA).

bis-ANS displacement - fluorescence spectroscopy assay

Fluorescence was measured on Perkin Elmer fluorimeter LS 55 (Perkin Elmer, UK). All measurements were done at 20 °C in a 5 x 5 mm quartz glass cuvette (Hellma Suprasil, Müllheim, Germany). MD-2 protein (200 nM) e 1,1'-Bis(anilino)-4,4'-bis (naphthalene)−8,8' disulfonate (bis-ANS, 200 nM) were mixed e incubated until reaching stable relative fluorescence units (RFUs) emitted at 420–550 nm under excitation at 385 nm. Compounds, at different concentrations, were then added, followed by relative fluorescence unit (RFU) measurement at 420–550 nm.

Biotin-LPS displacement assay

The ability of the compounds to displace LPS from MD-2 hydrophobic pocket was determined by ELISA assay. A microtiter plate was coated overnight at 4 °C with 100 µL/well of 5 µg/mL of chicken polyclonal anti-MD-2 antibodies, diluted in 50 mM Na_2CO_3 buffer, pH 9.6 and blocked with 1% BSA in PBS. After washing, 1 µM of MD-2 with biotin-labeled LPS was added e incubated per 2 hours. After washing, the compounds were added at different concentration and incubated per 1.5 hours. After washing, 0.5 µg/mL HRP-conjugated streptavidin (Sigma) in PBS was added, followed by detection at 420 nm After the addition of 100 µL ABTS (Sigma). Chicken anti-MD-2 polyclonal antibodies were prepared against recombinant MD-2 by GenTel (Madison, WI, USA).

Surface plasmon resonance (SPR) analysis

The binding affinity of the compounds to recombinant MD-2 was determined using a Biacore X100 with an NTA sensor chip (Biacore, GE Healthcare, Uppsala, Sweden). Briefly, 0.5 µM MD-2 (in 50 mM TRIS, 150 mM NaCl, 0.5% Tween 20, pH 7.5) was immobilized onto the sensor chip previously activated with 1-minute pulse of 10 mM $NiSO_4$. First flow cell was used as a reference surface to control non-specific binding. Both flow cells were injected with the analyte (in PBS, 5% DMSO, 5% EtOH, pH 7.5) at a flow rate of 10 µL/min at 25 °C in increasing concentrations. The data were analyzed with Biacore Evaluation software. K_D values were calculated by global fitting of the equilibrium binding responses from various concentrations of analytes using a 1:1 Langmuir binding model.

Chapter IV

Supporting information

NMR spectra of synthetic compounds

The complete characterizations of the synthetic compounds obtained during this PhD project are reported in Chapter “Materials and Methods”, together with complete lists of ^{1}H and ^{13}C chemical shifts.
In this section, ^{1}H NMR and APT NMR spectra are reported for new molecules, while ^{1}H NMR spectra are reported for known compounds.

FP11 Synthesis: ^{1}H NMR and ^{13}C APT NMR spectra

Compound 6. ^{1}H NMR and ^{13}C APT NMR spectra in $CDCl_3$

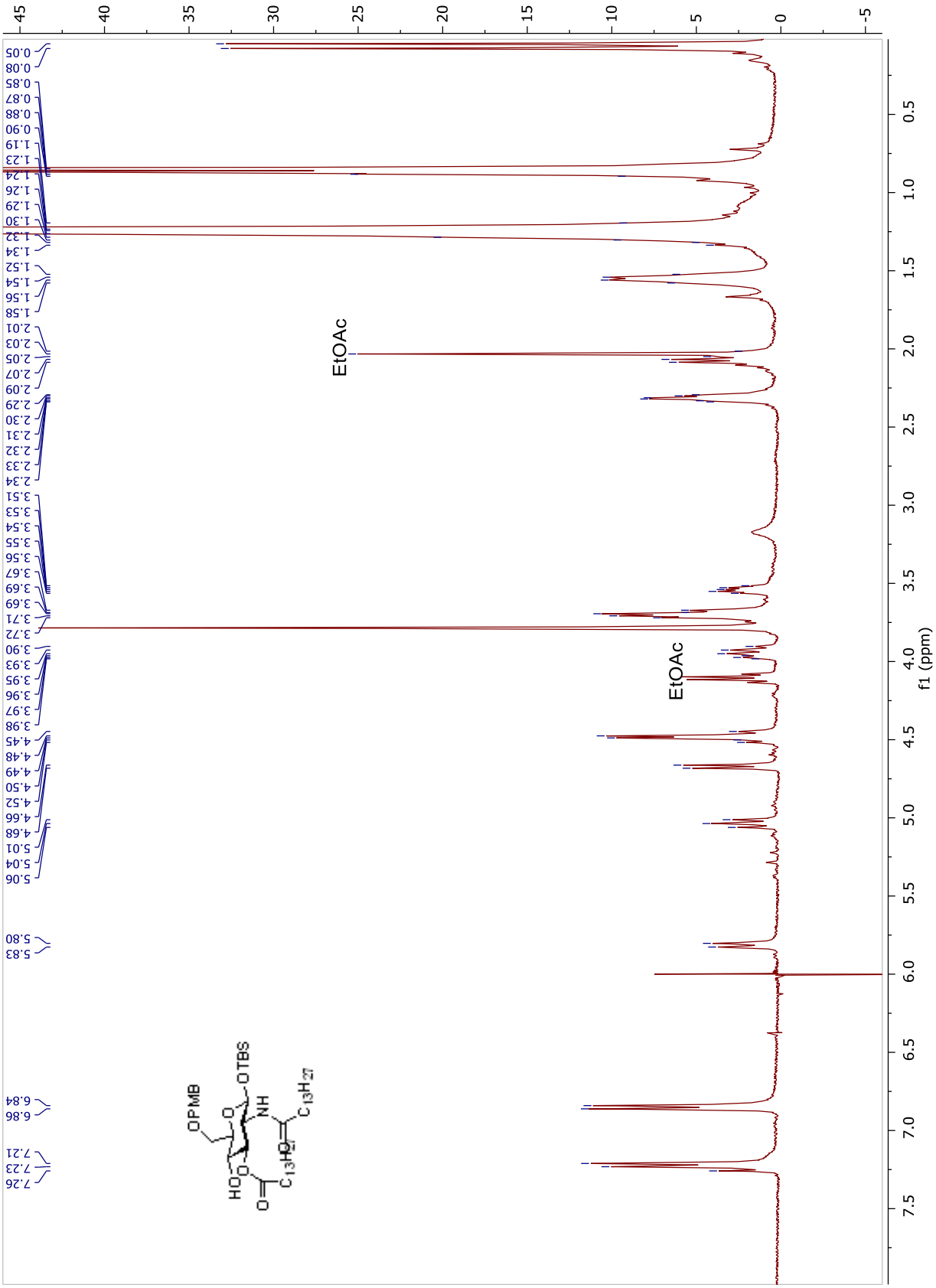

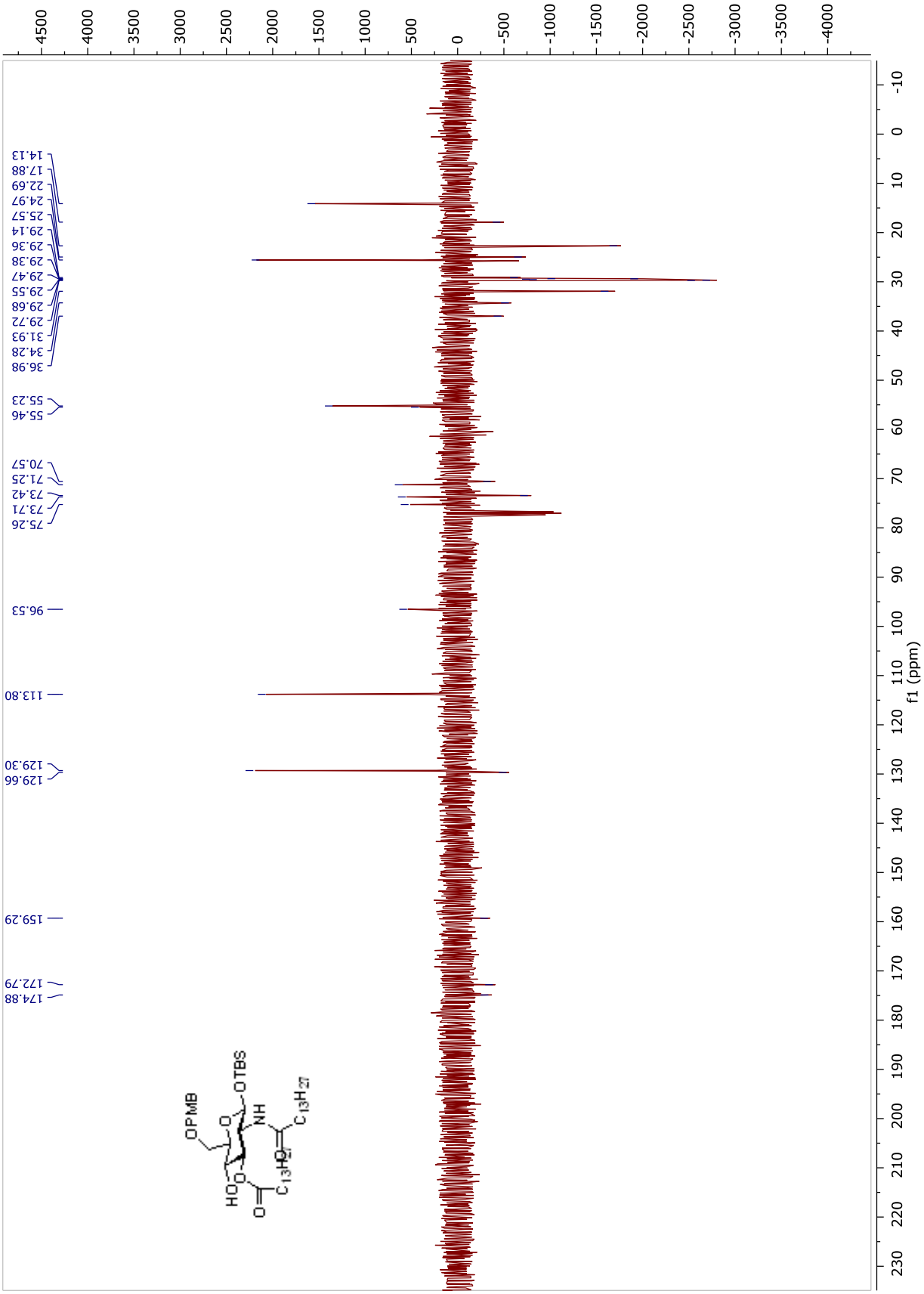
14.13
17.88
22.69
24.97
25.57
29.14
29.36
29.38
29.47
29.55
29.68
29.72
31.93
34.28
36.98
55.23
55.46
70.57
71.25
73.42
73.71
75.26
96.53
113.80
129.30
129.66
159.29
172.79
174.88
OPMB
OTBS
NH
HO
O
f1 (ppm)

Compound 7. ^{1}H NMR and ^{13}C APT NMR spectra in $CDCl_3$

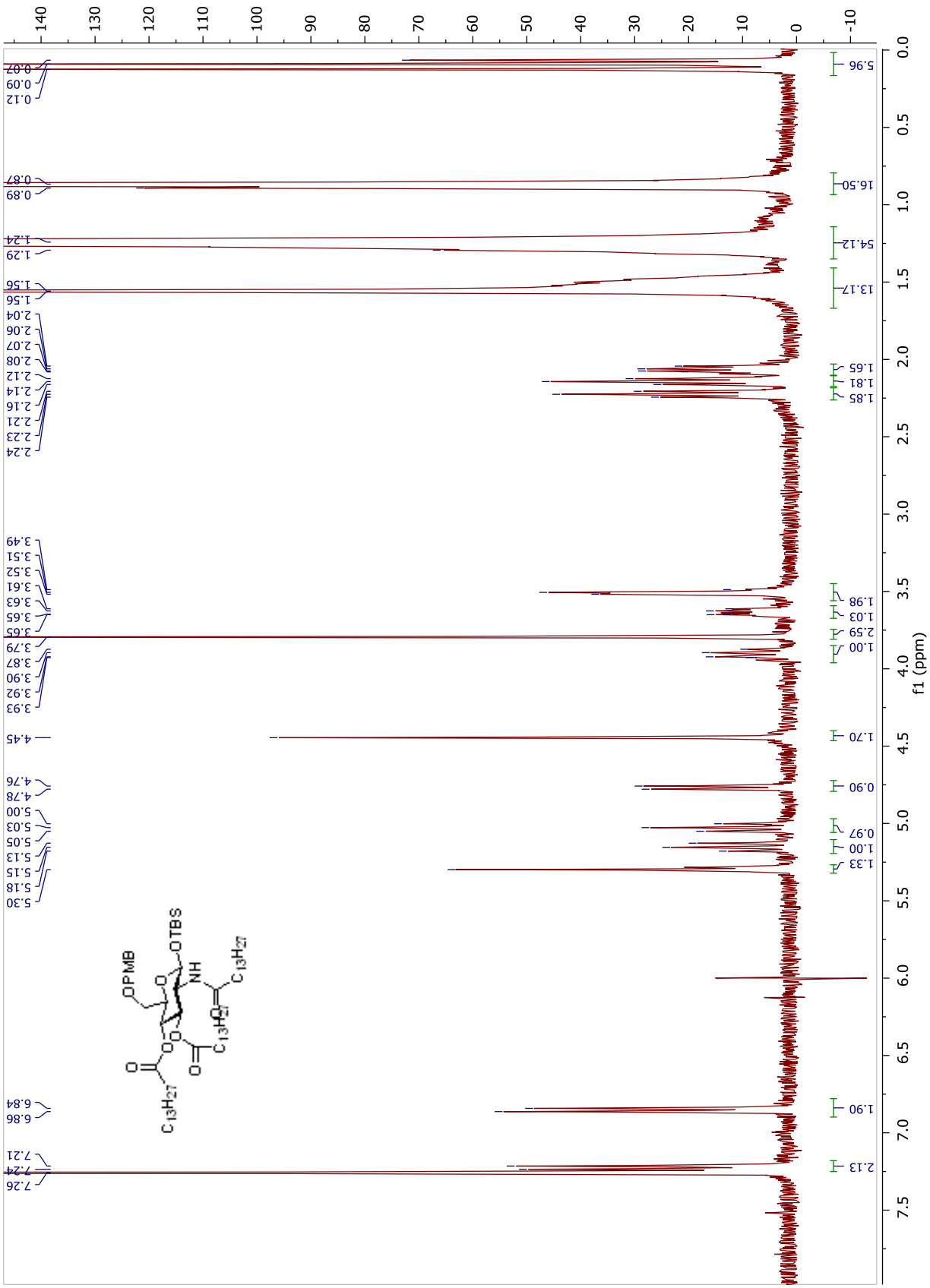

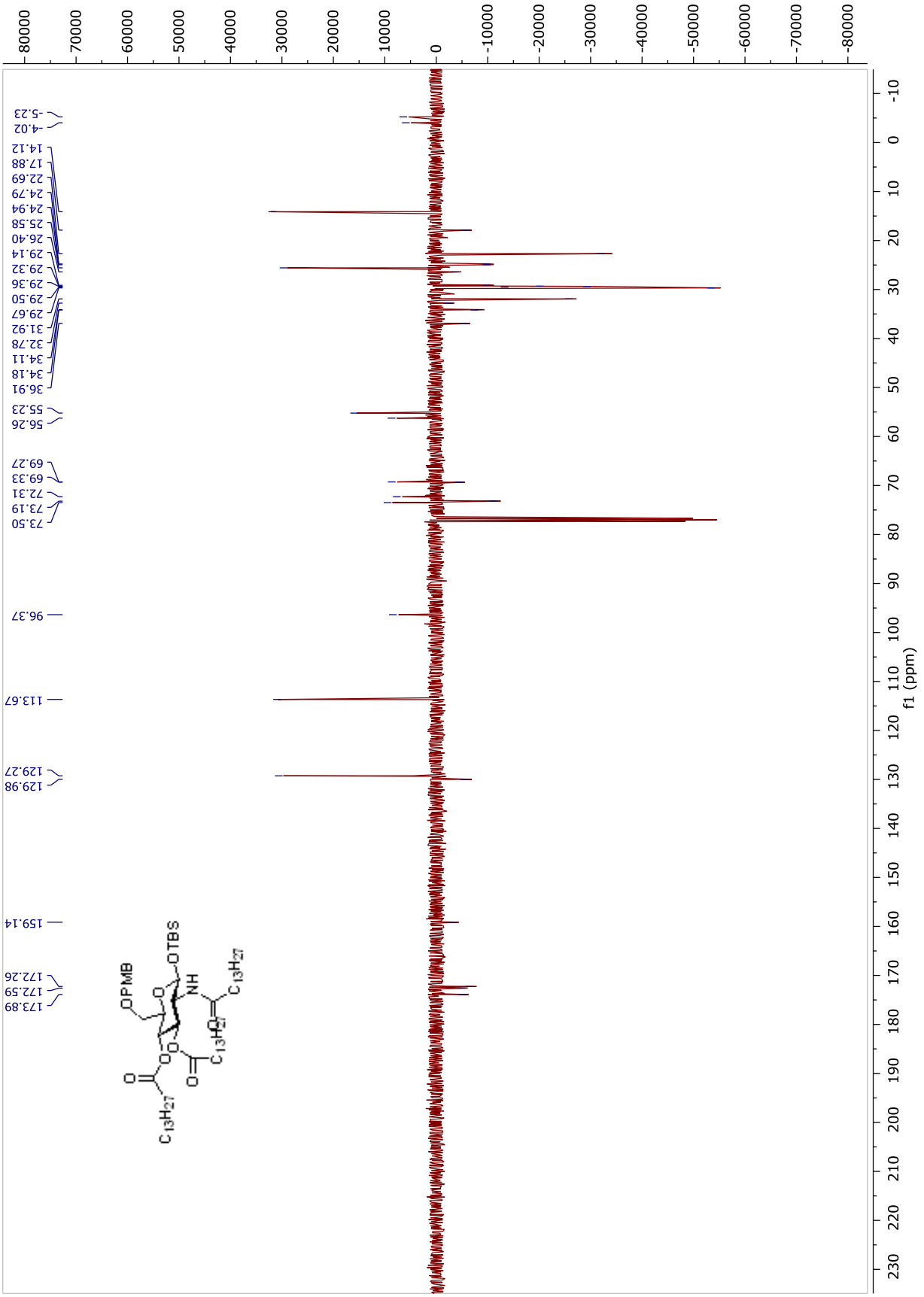
-5.23
-4.02
14.12
17.88
22.69
24.79
24.94
25.58
26.40
29.14
29.32
29.36
29.50
29.67
31.92
32.78
34.11
34.18
36.91
55.23
56.26
69.27
69.33
72.31
73.19
73.50
96.37
113.67
129.27
129.98
159.14
172.26
172.59
173.89
OPMB
OTBS
NH
f1 (ppm)

Compound 8. ^{1}H NMR and ^{13}C APT NMR spectra in $CDCl_3$

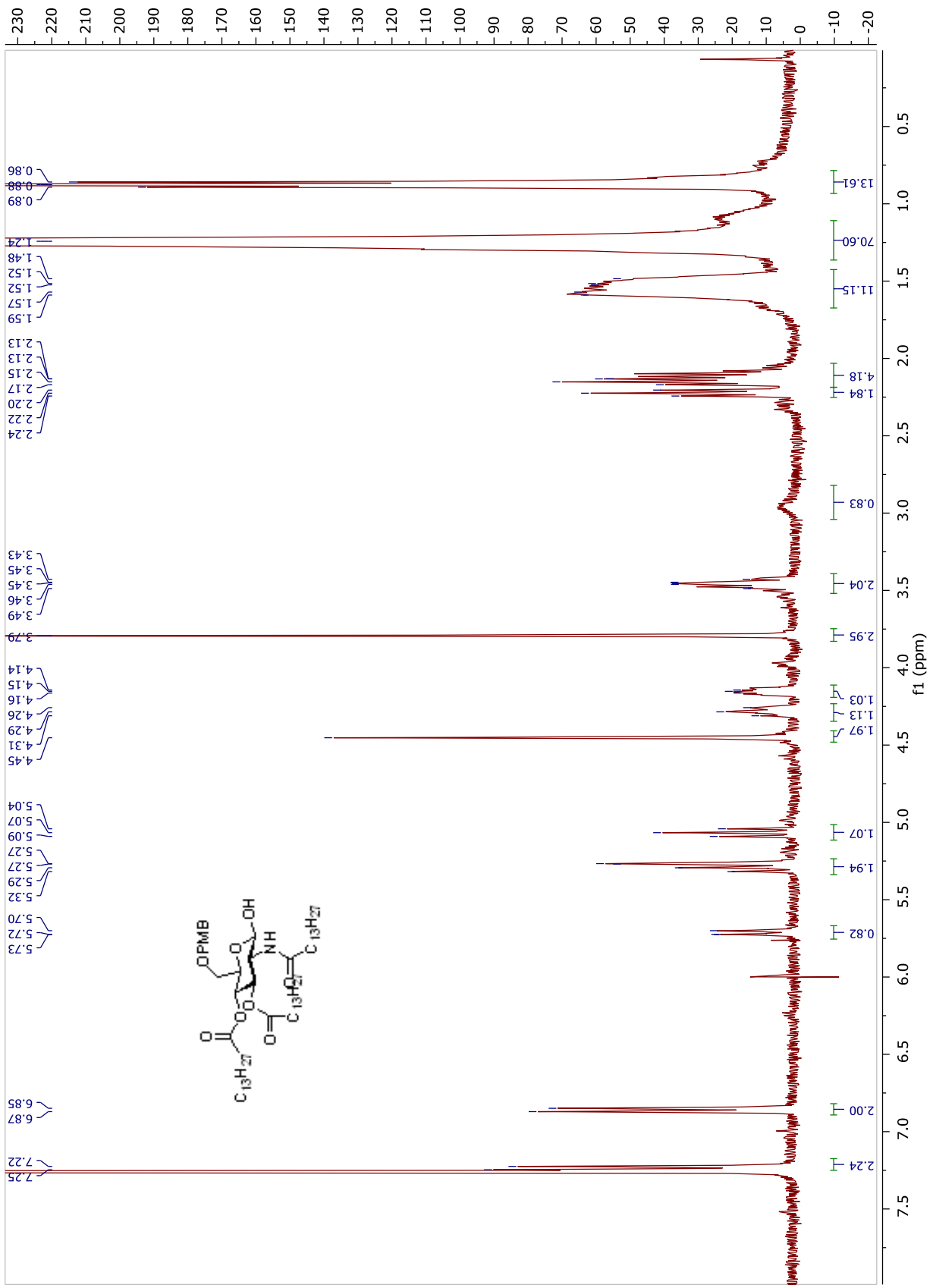

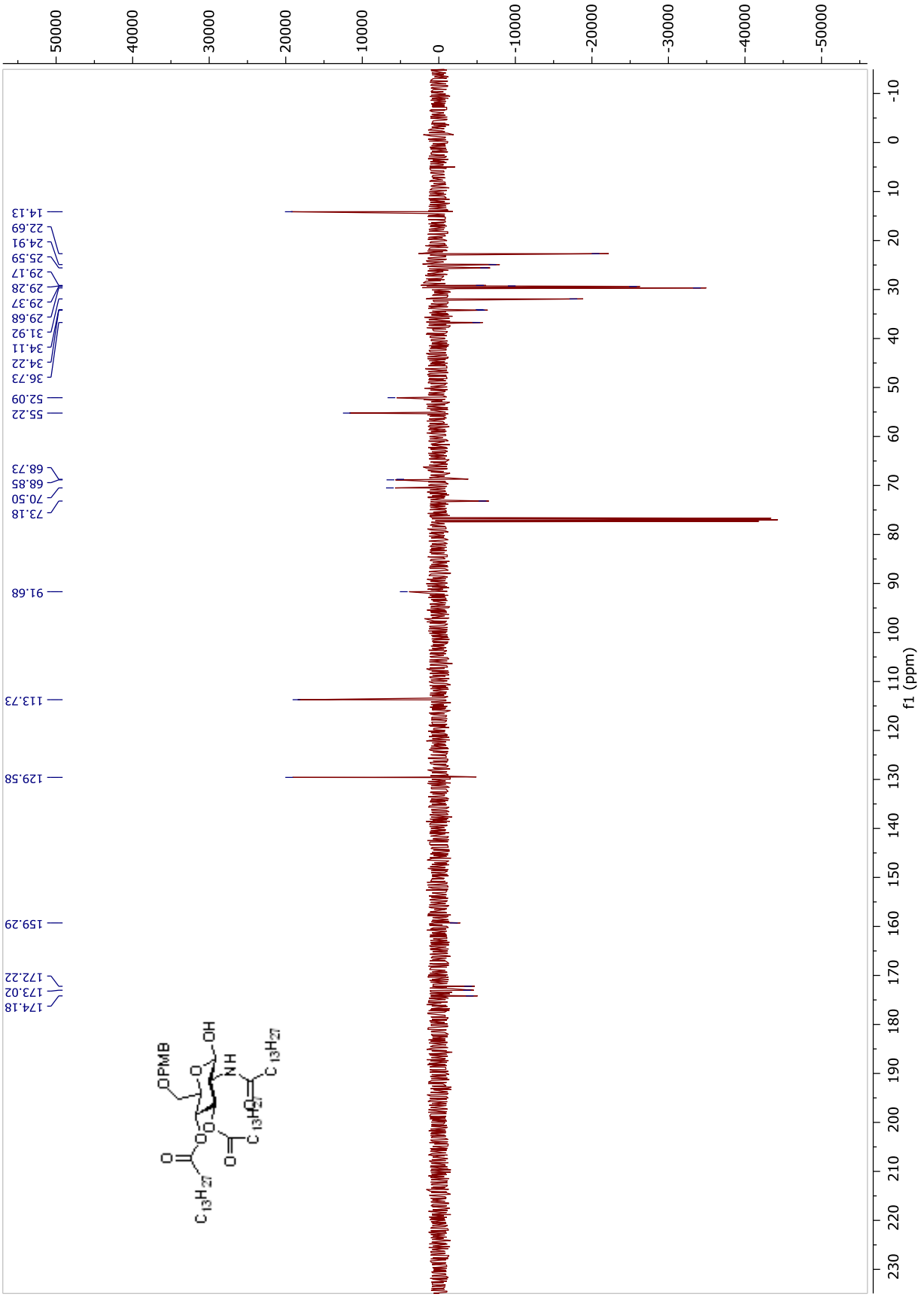
50000
40000
30000
20000
10000
0
-10000
-20000
-30000
-40000
-50000
14.13
22.69
24.91
25.59
29.17
29.28
29.37
29.68
31.92
34.11
34.22
36.73
52.09
55.22
68.73
68.85
70.50
73.18
91.68
113.73
129.58
159.29
172.22
173.02
174.18
-10
0
10
20
30
40
50
60
70
80
90
100
110
120
130
140
150
160
170
180
190
200
210
220
230
f1 (ppm)
OPMB
O
OH
NH
O
O
O
O
O
C13H27
C13H27
C13H27

Compound 9. ^{1}H NMR and ^{13}C APT NMR spectra in $CDCl_3$

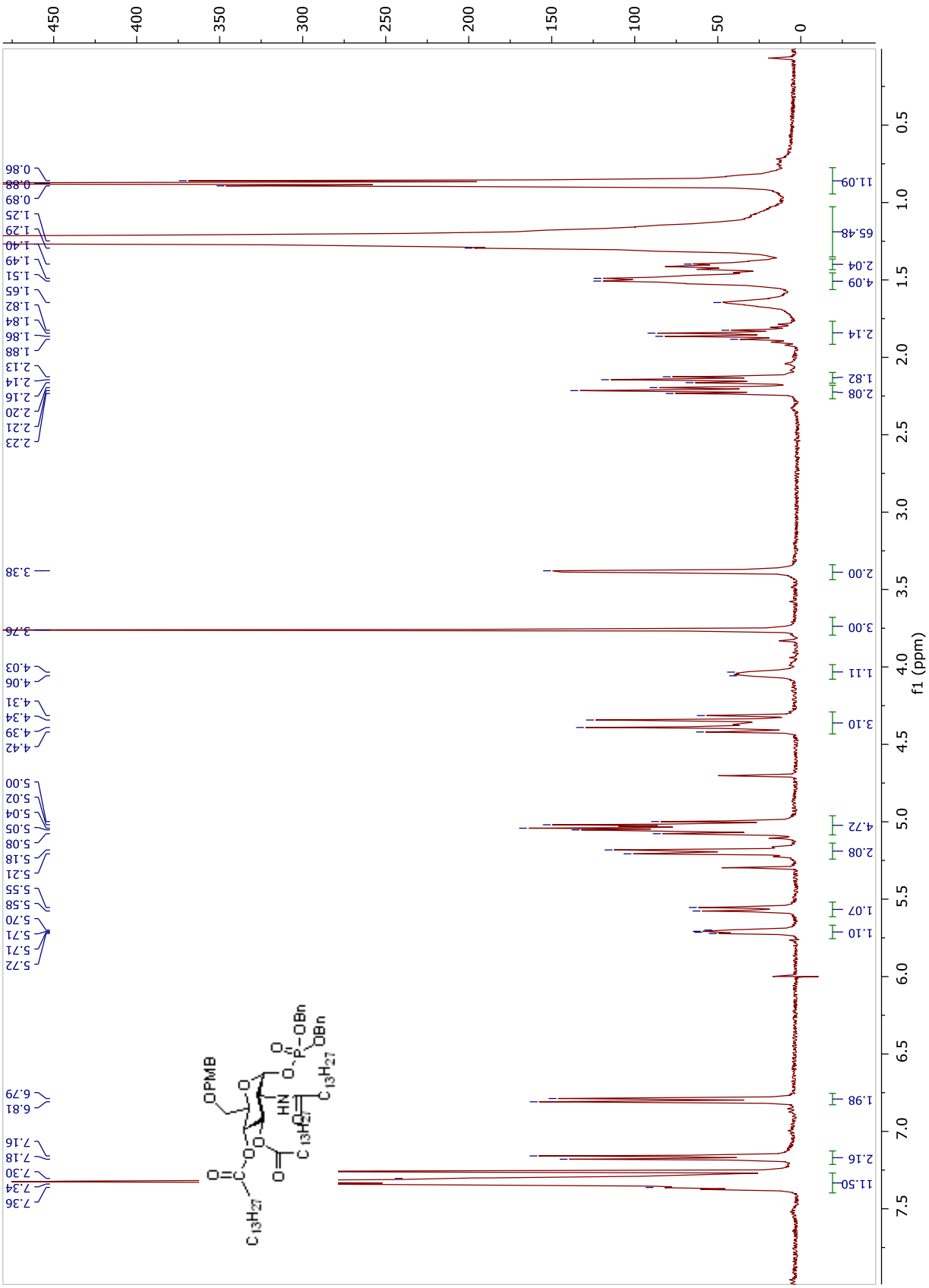

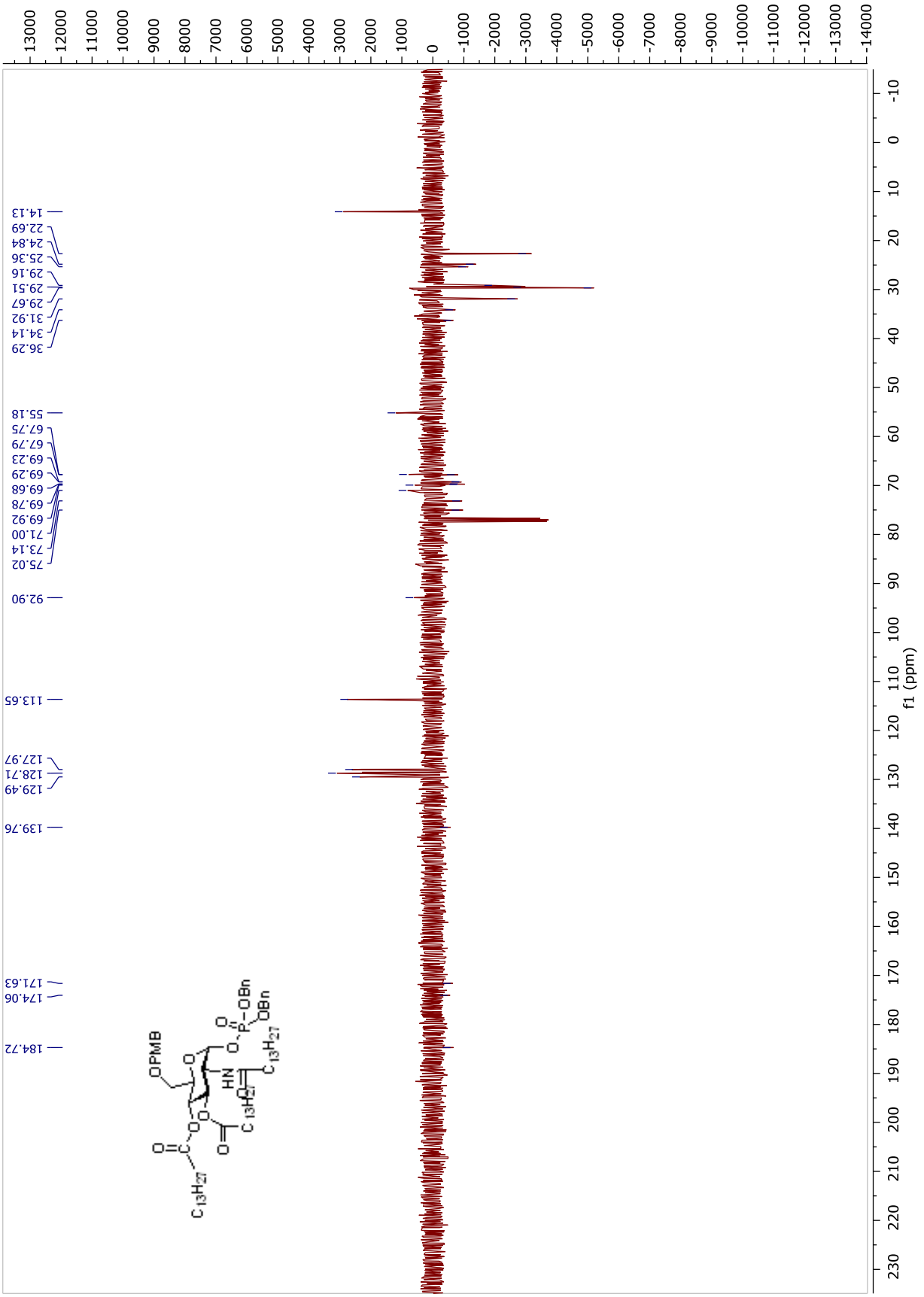
14.13
22.69
24.84
25.36
29.16
29.51
29.67
31.92
34.14
36.29
55.18
67.75
67.79
69.23
69.29
69.68
69.78
69.92
71.00
73.14
75.02
92.90
113.65
127.97
128.71
129.49
139.76
171.63
174.06
184.72
OPMB
HN
OBn
OBn
f1 (ppm)

Compound FP11. ^{1}H NMR spectrum in CD_3OD and ^{13}C APT NMR spectrum in $CDCl_3$

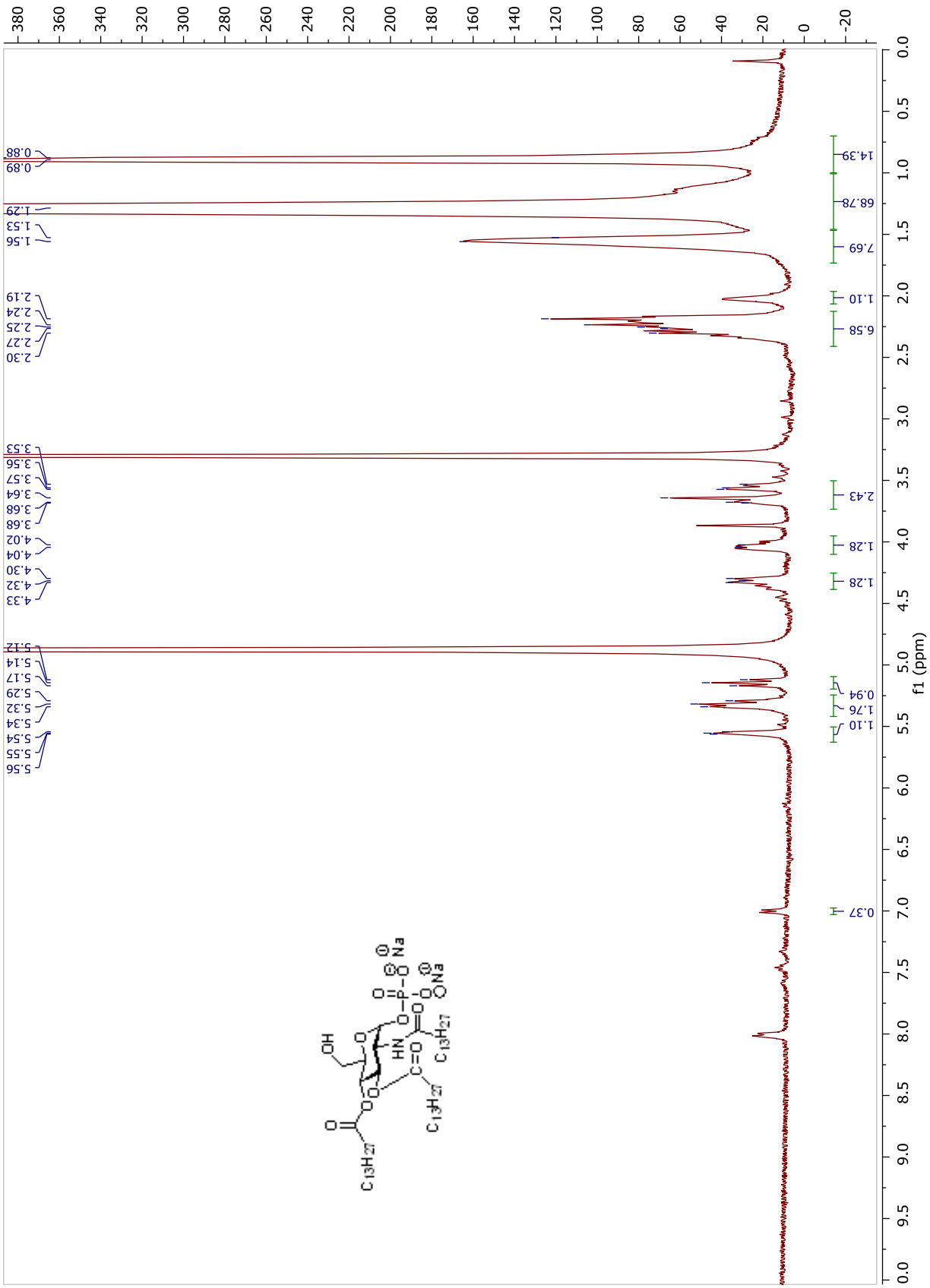

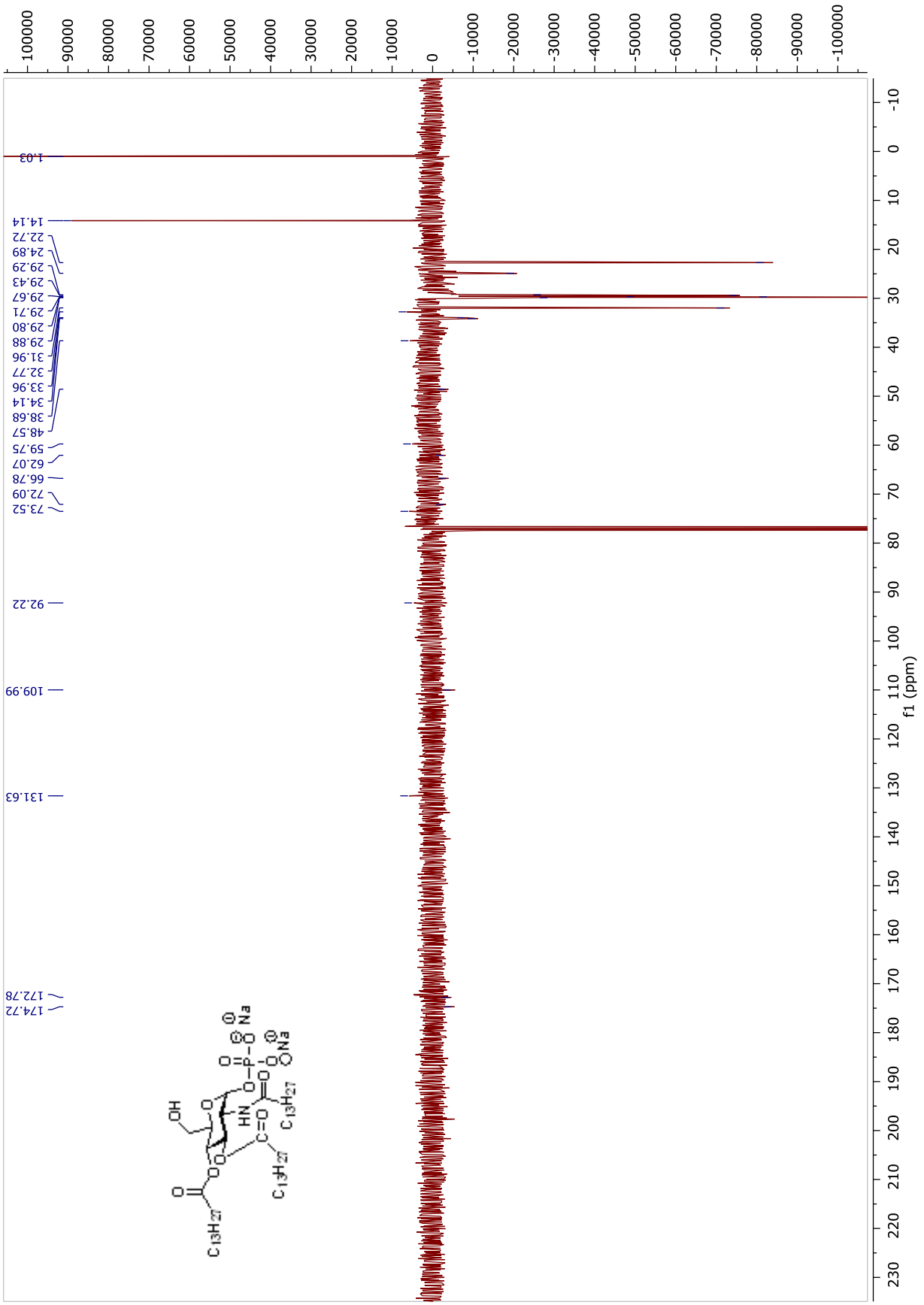
f1 (ppm)
1.03
14.14
22.72
24.89
29.29
29.43
29.67
29.71
29.80
29.88
31.96
32.77
33.96
34.14
38.68
48.57
59.75
62.07
66.78
72.09
73.52
92.22
109.99
131.63
172.78
174.72

FP111 Synthesis: ^{1}H NMR and ^{13}C-APT NMR spectra

Compound 10. ^{1}H NMR and ^{13}C APT NMR spectra in $CDCl_3$

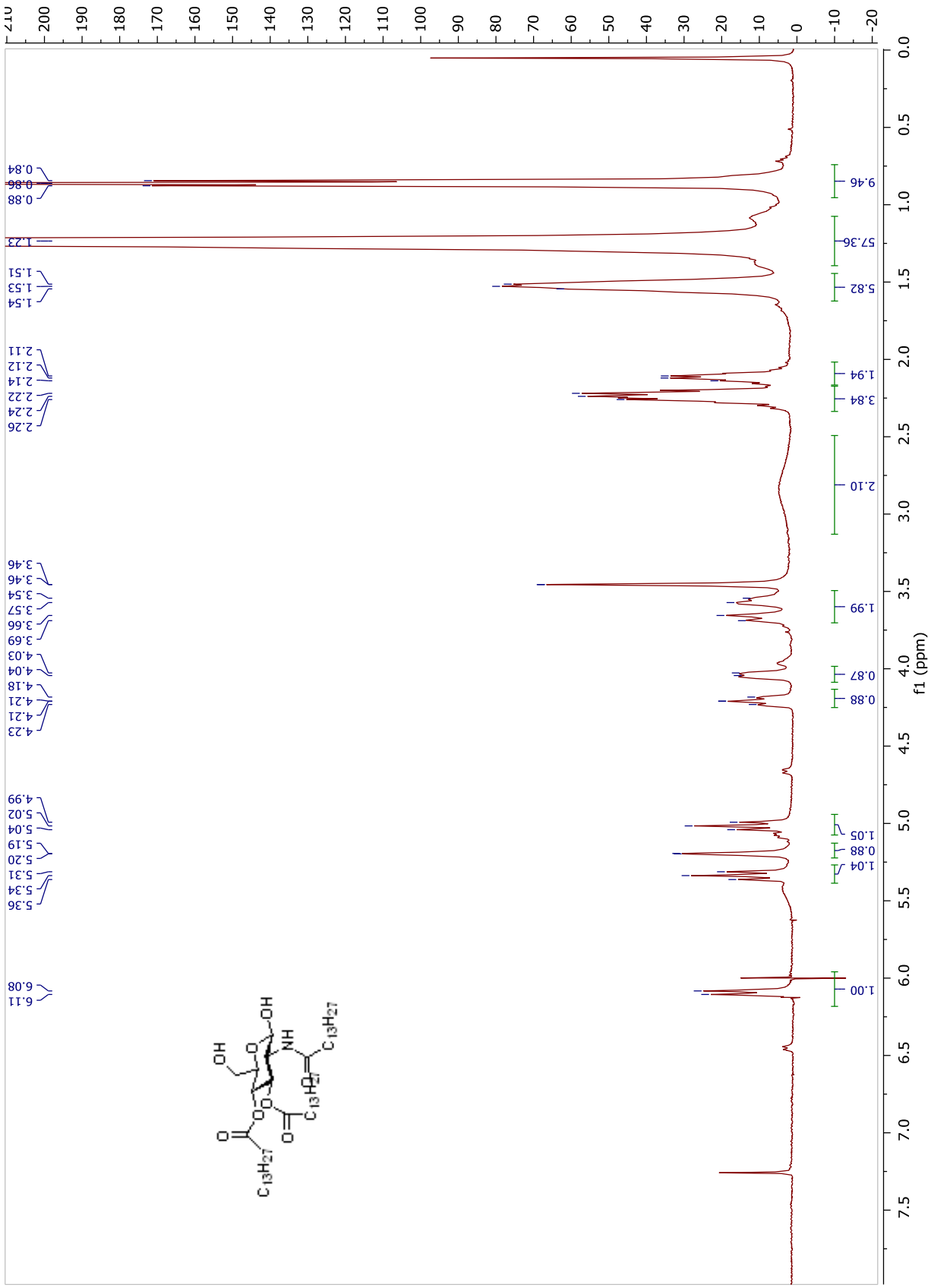

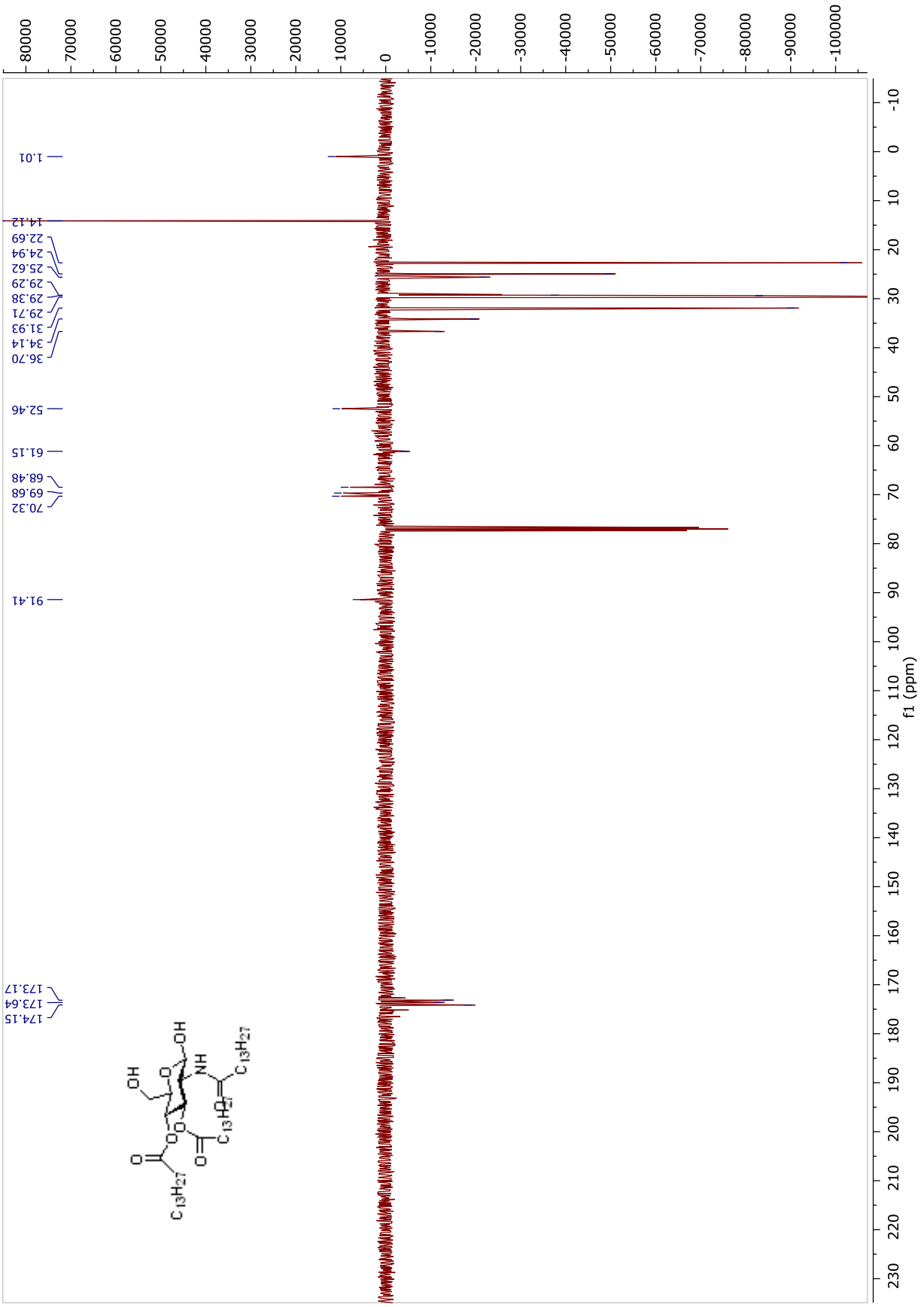
1.01
14.12
22.69
24.94
25.62
29.29
29.38
29.71
31.93
34.14
36.70
52.46
61.15
68.48
69.68
70.32
91.41
173.17
173.64
174.15
f1 (ppm)

Compound 11. ^{1}H NMR and ^{13}C APT NMR spectra in $CDCl_3$

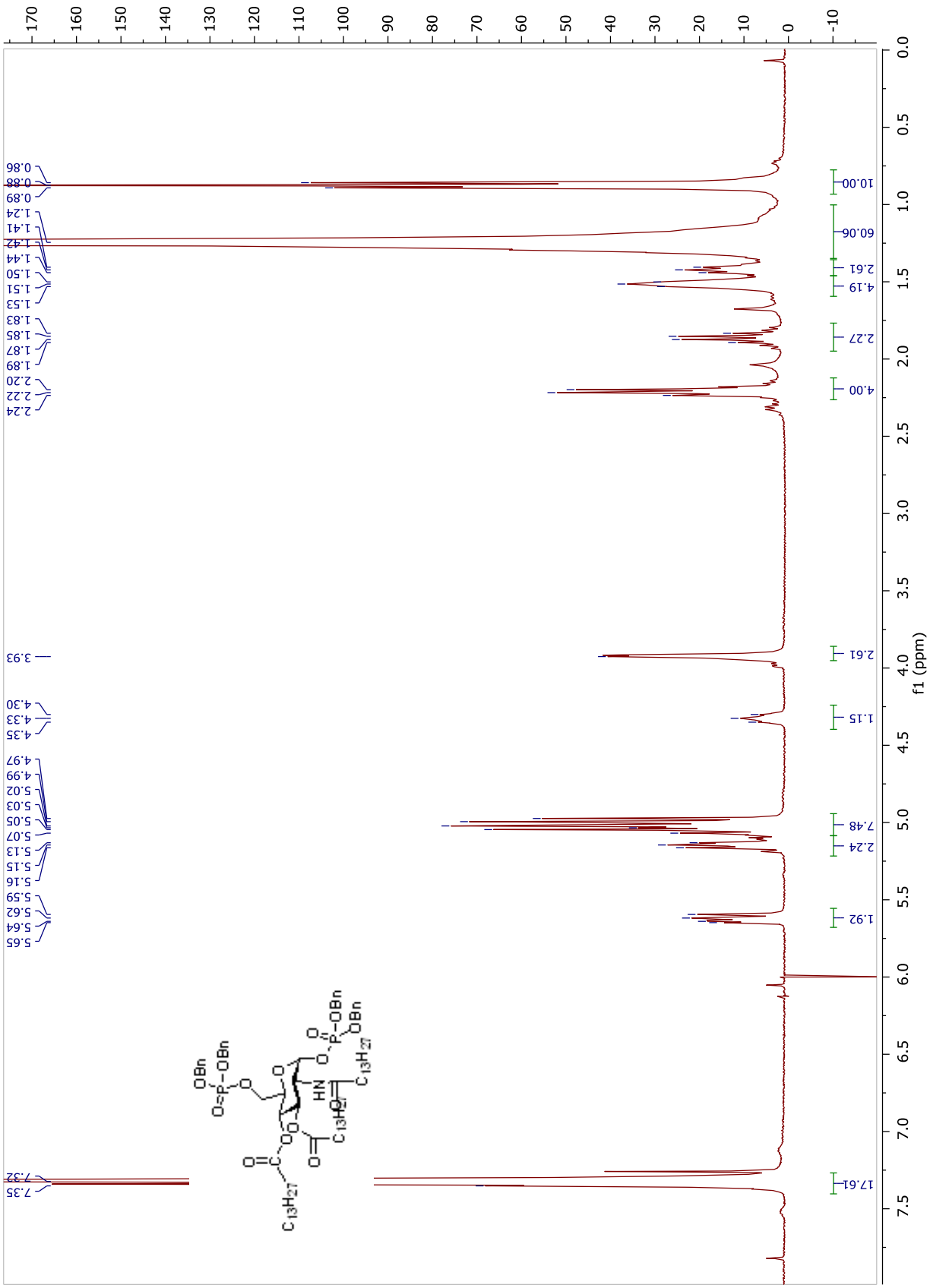

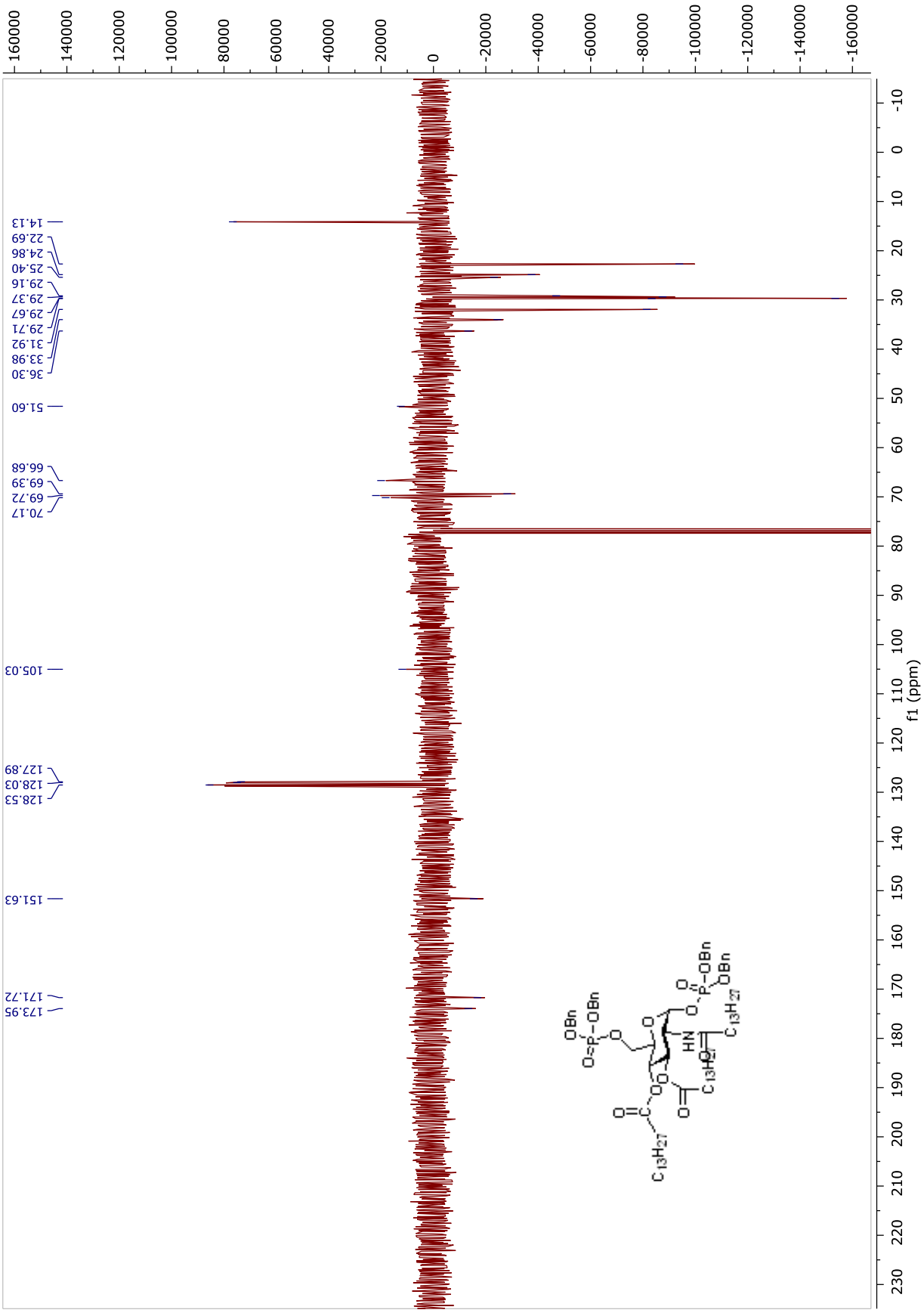
14.13
22.69
24.86
25.40
29.16
29.37
29.67
29.71
31.92
33.98
36.30
51.60
66.68
69.39
69.72
70.17
105.03
127.89
128.03
128.53
151.63
171.72
173.95
f1 (ppm)

Compound FP111. ^{1}H NMR and ^{13}C APT NMR spectra in CD_3OD

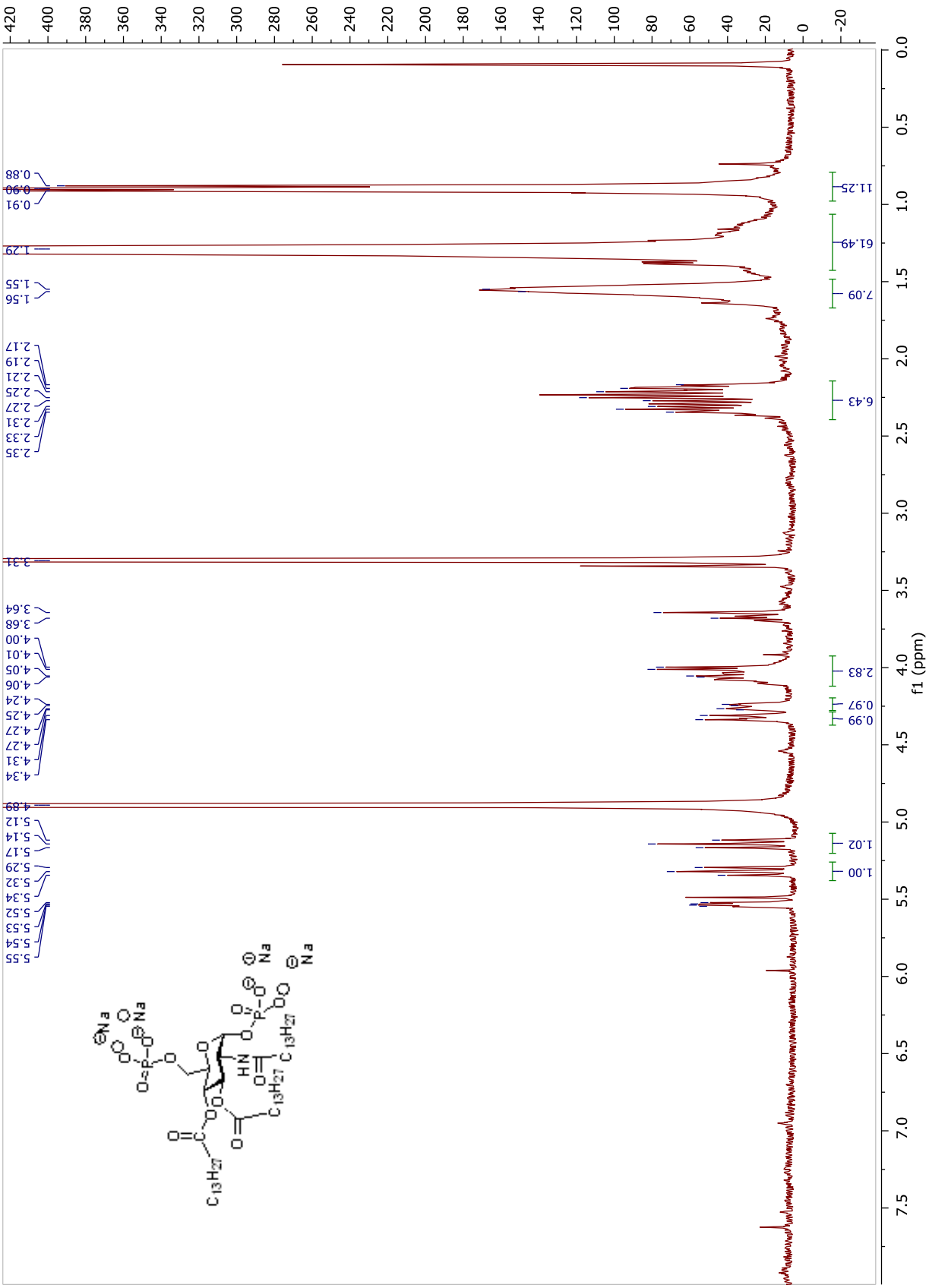

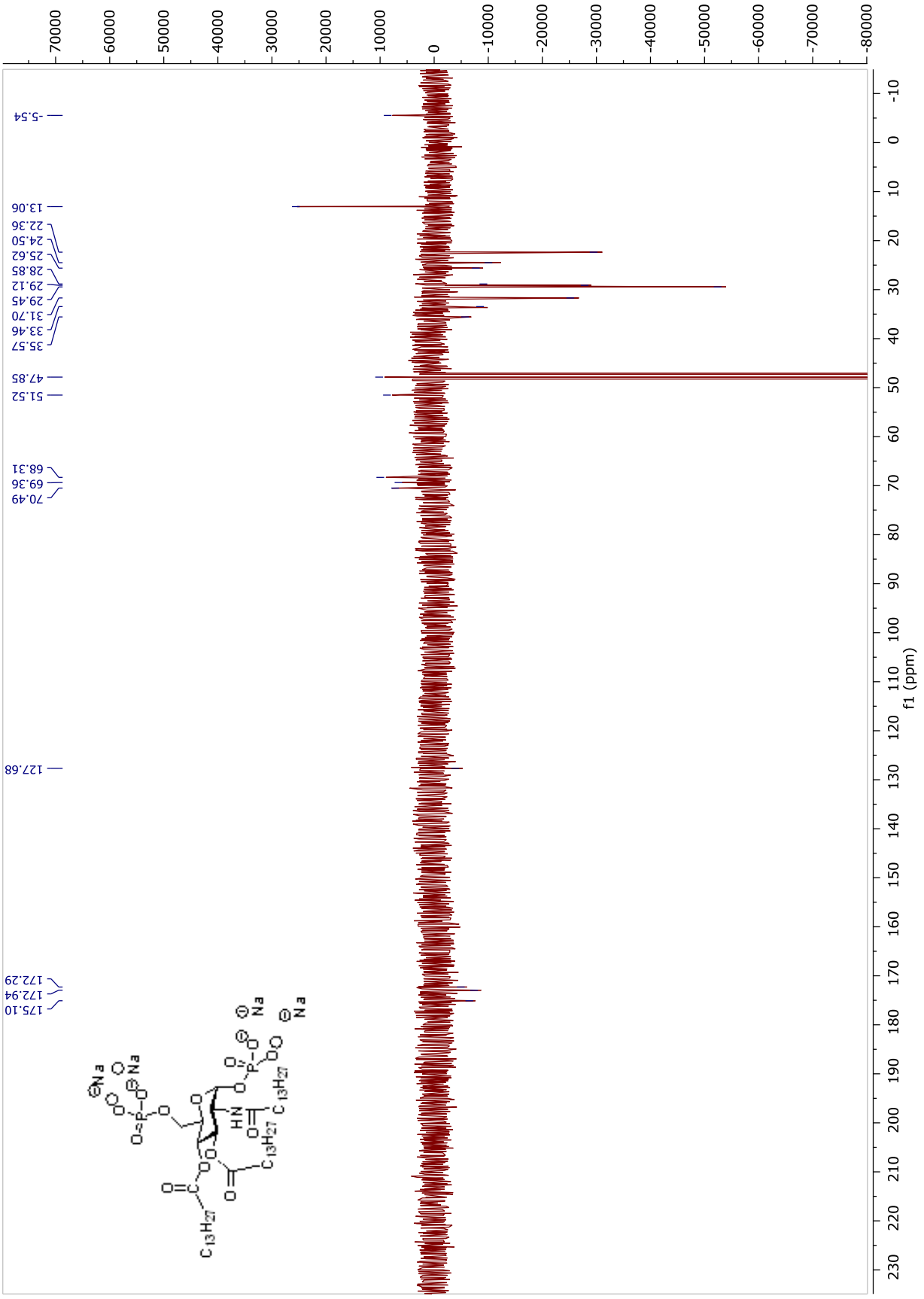
-5.54
13.06
22.36
24.50
25.62
28.85
29.12
29.45
31.70
33.46
35.57
47.85
51.52
68.31
69.36
70.49
127.68
172.29
172.94
175.10
f1 (ppm)

Chain A Synthesis: ^{1}H NMR and ^{13}C-APT NMR spectra

Compound 12. ^{1}H NMR spectrum in $CDCl_3$

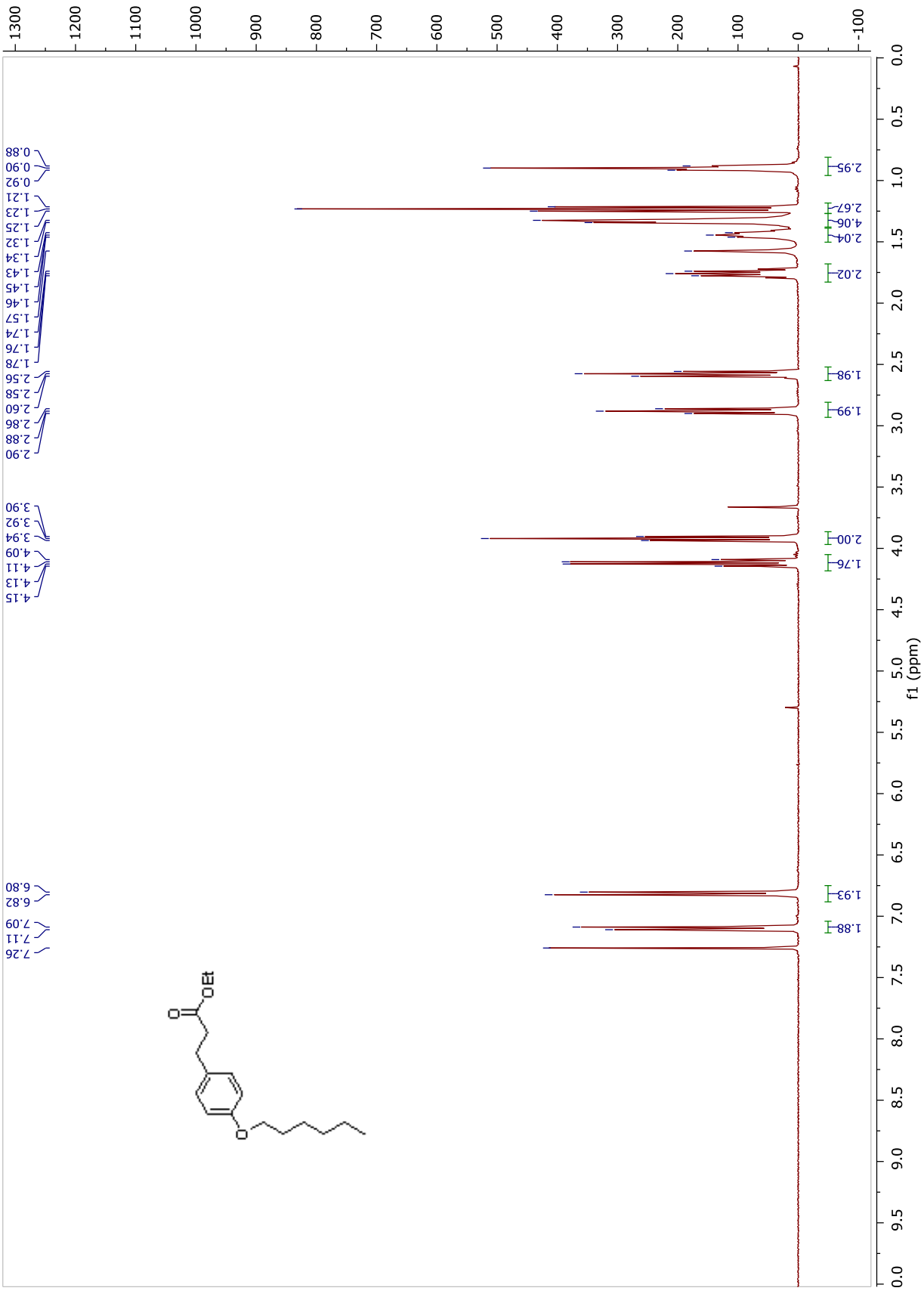

Compound A. ^{1}H NMR spectrum in $CDCl_3$

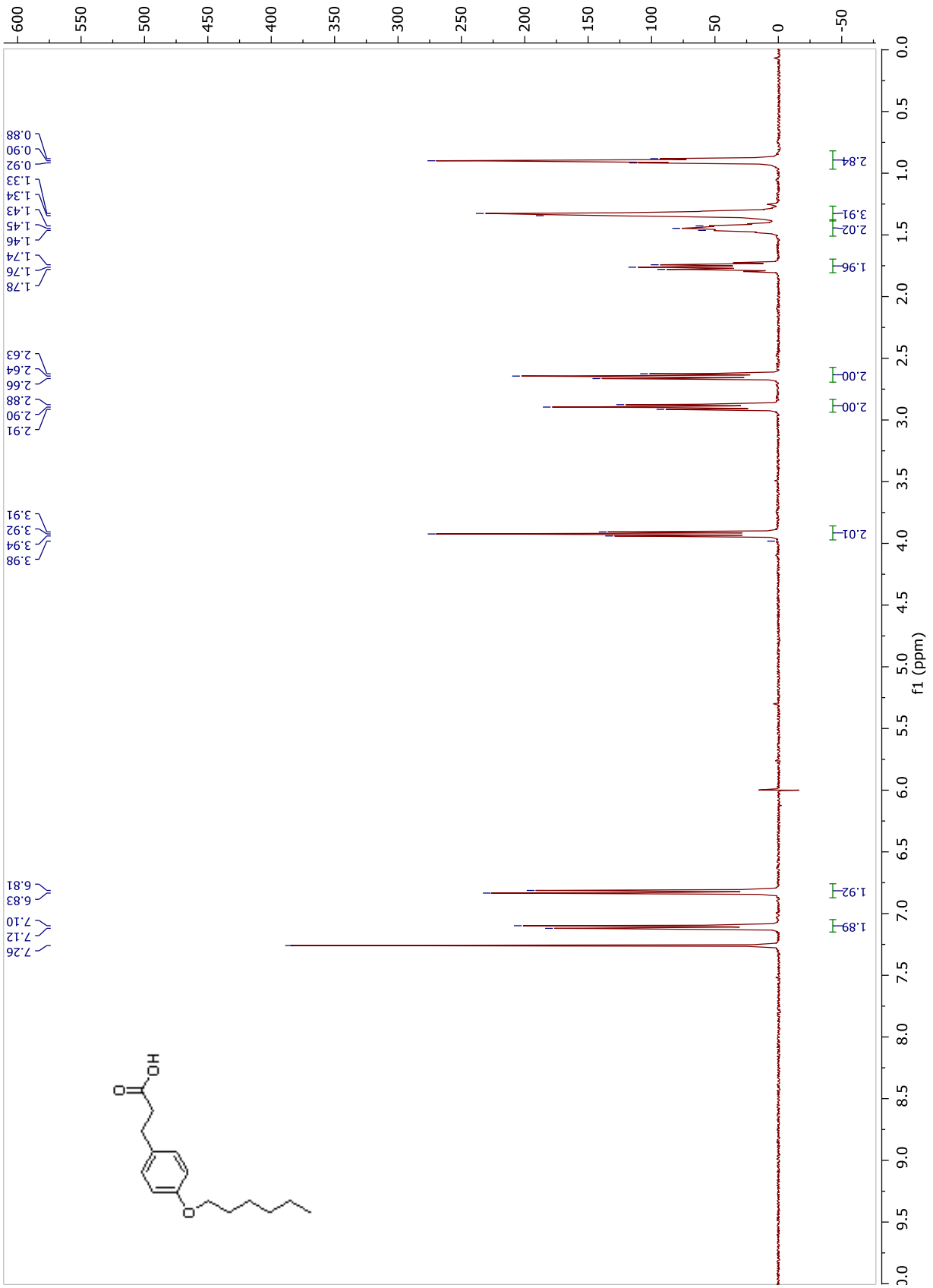

AM158 Synthesis: ^{1}H NMR and ^{13}C-APT NMR spectra

Compound 13. ^{1}H NMR and ^{13}C APT NMR spectra in $CDCl_3$

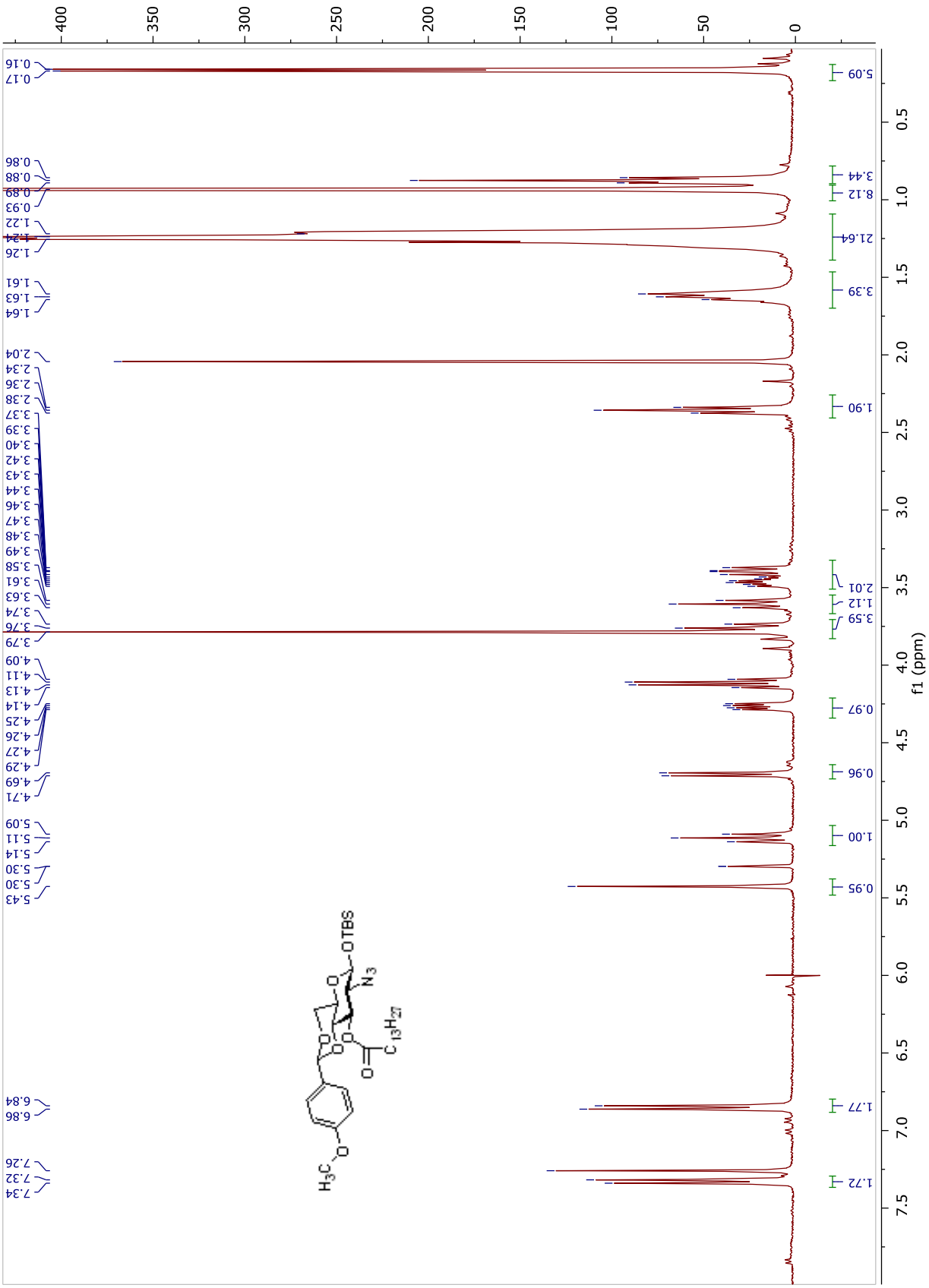

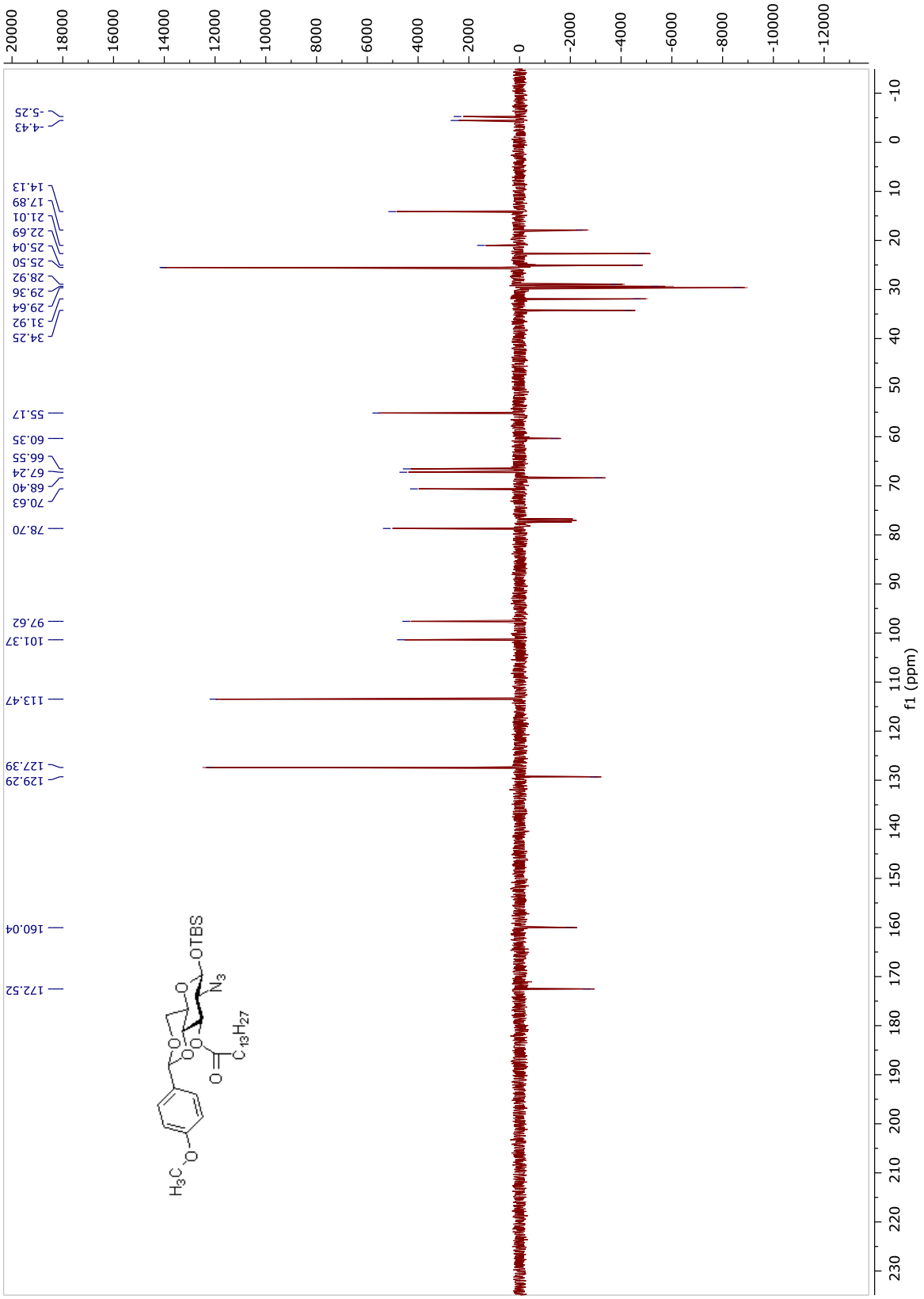
-5.25
-4.43
14.13
17.89
21.01
22.69
25.04
25.50
28.92
29.36
29.64
31.92
34.25
55.17
60.35
66.55
67.24
68.40
70.63
78.70
97.62
101.37
113.47
127.39
129.29
160.04
172.52
OTBS
N3
C13H27
H3C
f1 (ppm)

Compound 14. ^{1}H NMR and ^{13}C APT NMR spectra in $CDCl_3$

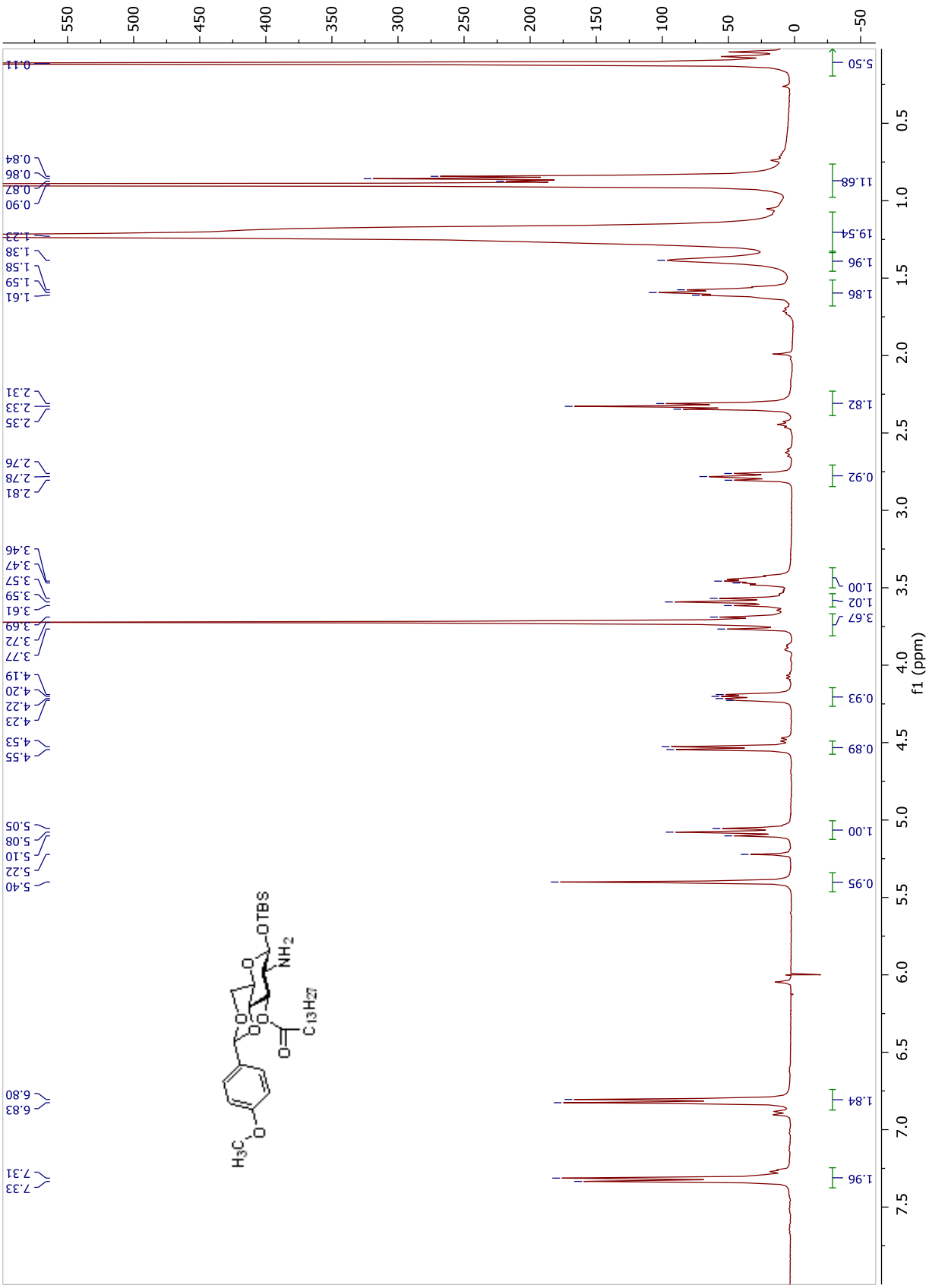

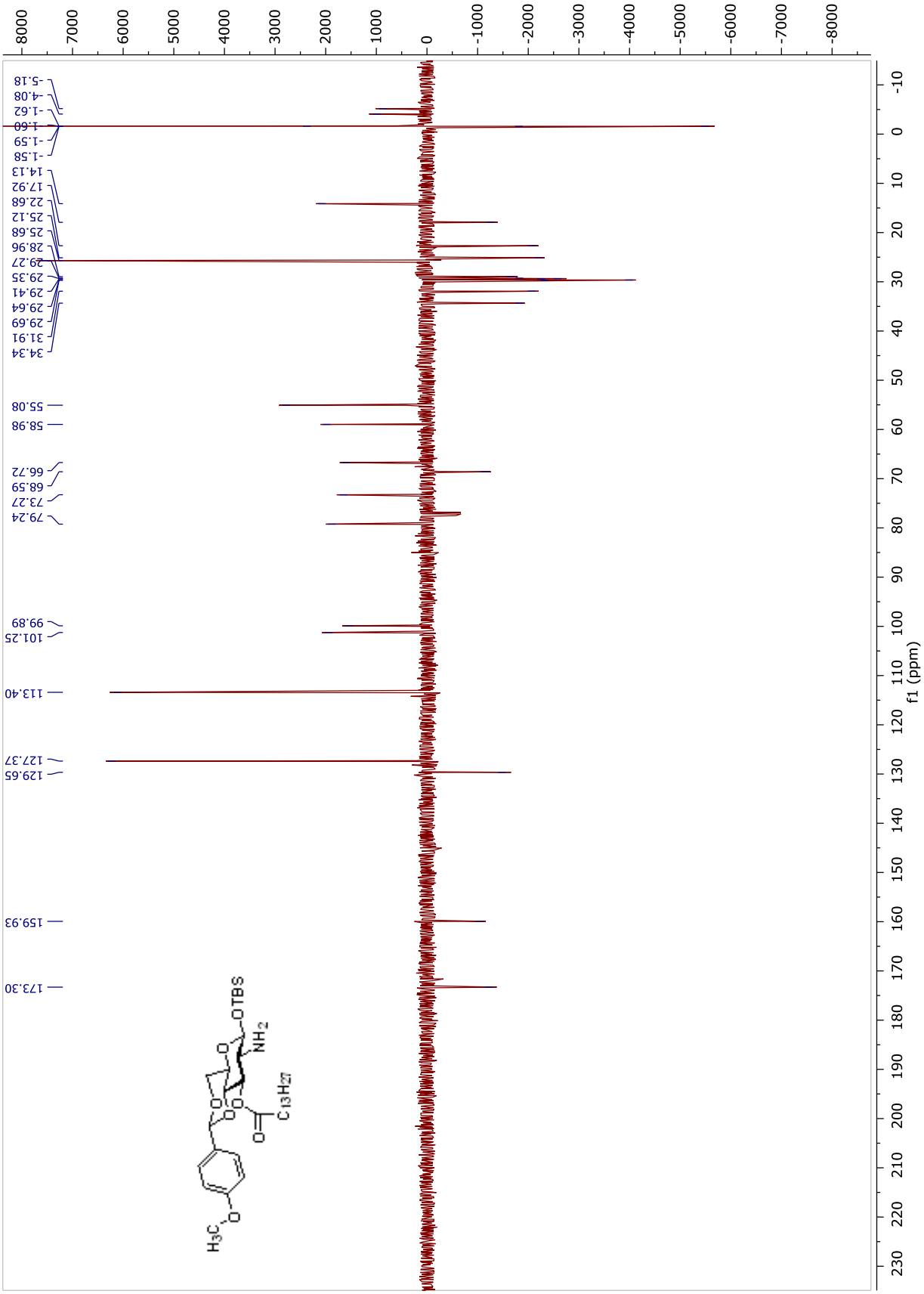
-5.18
-4.08
-1.62
1.60
-1.59
-1.58
14.13
17.92
22.68
25.12
25.68
28.96
29.27
29.35
29.41
29.64
29.69
31.91
34.34
55.08
58.98
66.72
68.59
73.27
79.24
99.89
101.25
113.40
127.37
129.65
159.93
173.30
OTBS
NH2
C13H27
H3C
f1 (ppm)

Compound 15. ^{1}H NMR and ^{13}C APT NMR spectra in $CDCl_3$

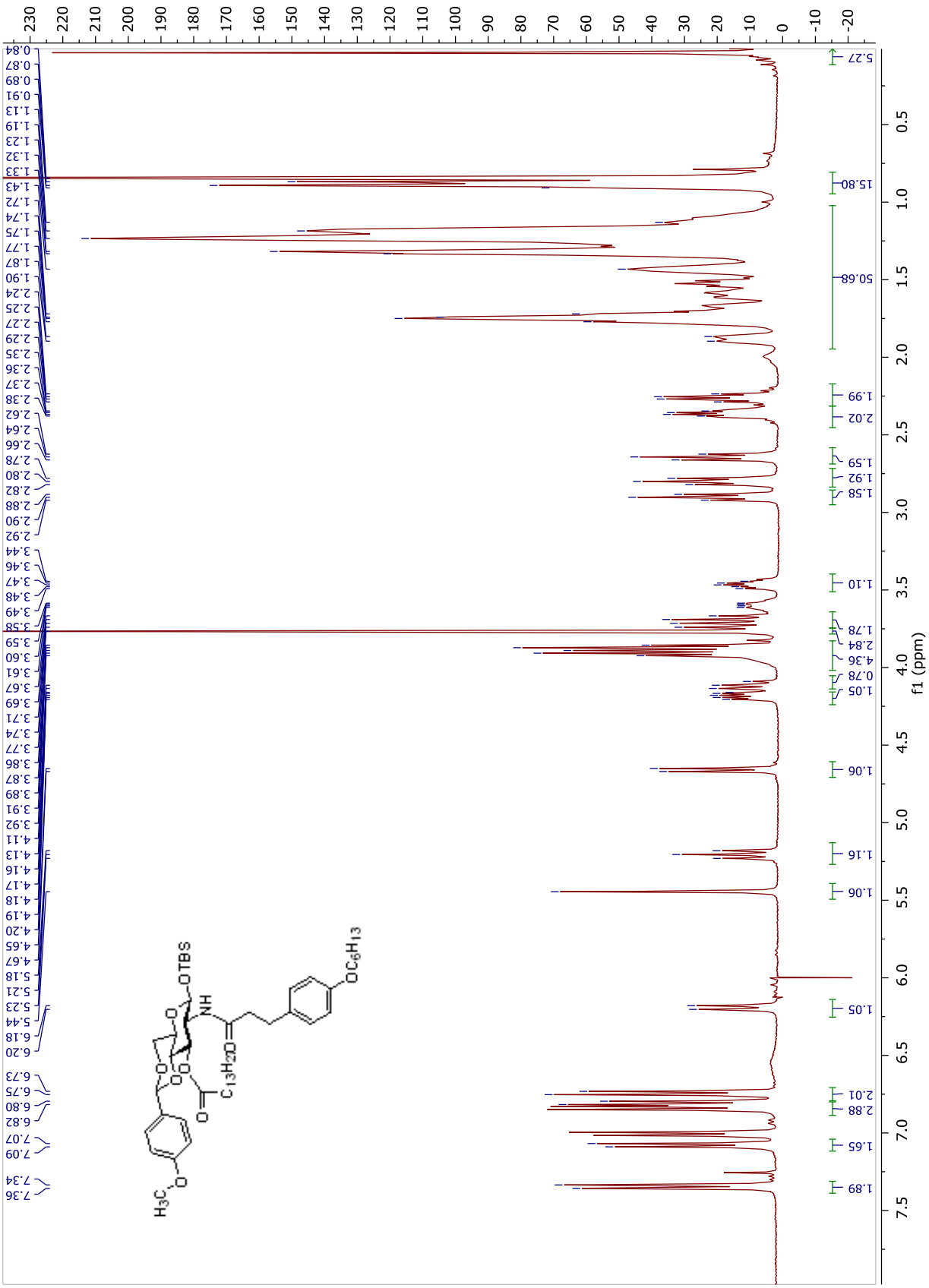

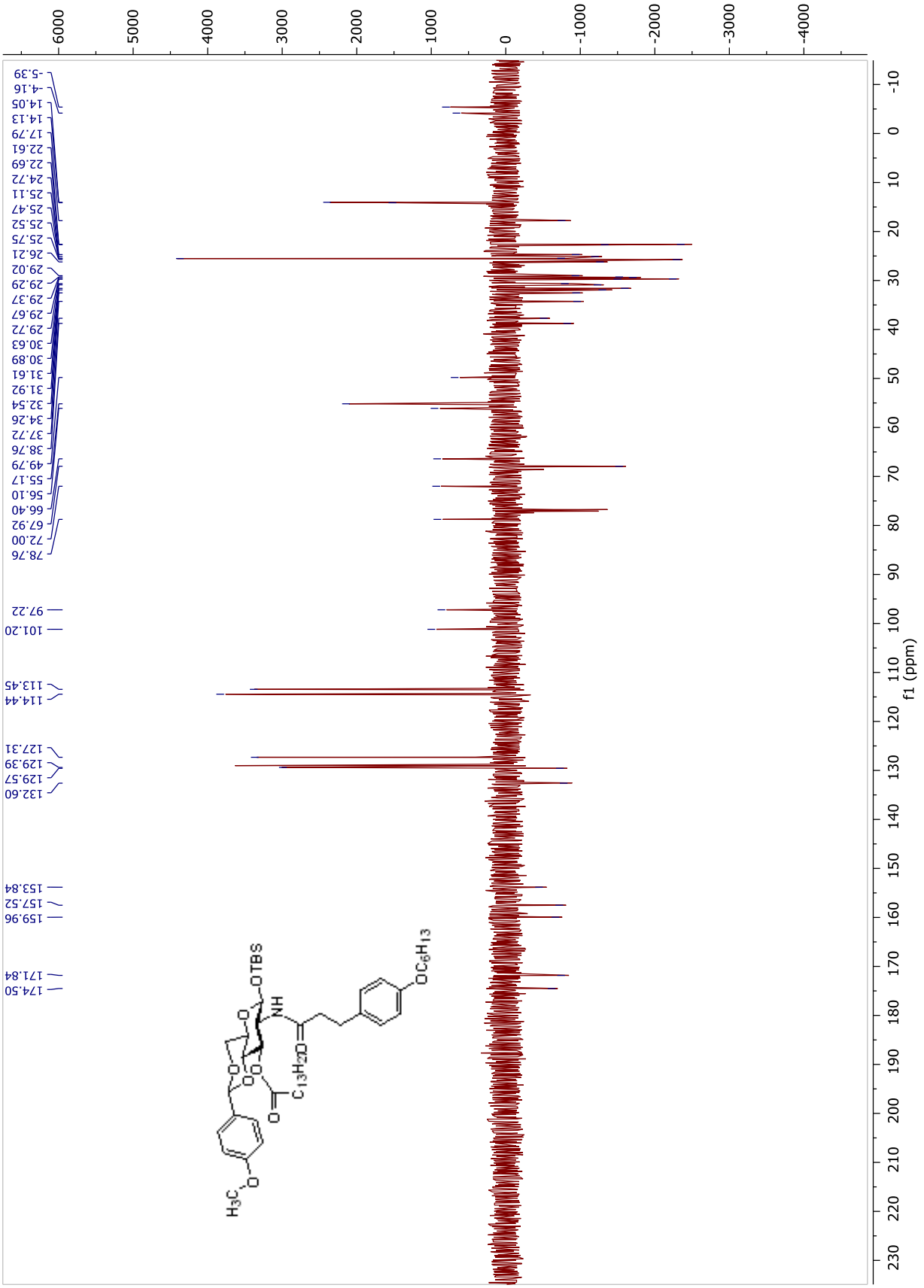
-5.39
-4.16
14.05
14.13
17.79
22.61
22.69
24.72
25.11
25.47
25.52
25.75
26.21
29.02
29.29
29.37
29.67
29.72
30.63
30.89
31.61
31.92
32.54
34.26
37.72
38.76
49.79
55.17
56.10
66.40
67.92
72.00
78.76
97.22
101.20
113.45
114.44
127.31
129.39
129.57
132.60
153.84
157.52
159.96
171.84
174.50
OTBS
NH
OC6H13
C13H27
O
H3C
f1 (ppm)

Compound 16. ^{1}H NMR and ^{13}C APT NMR spectra in $CDCl_3$

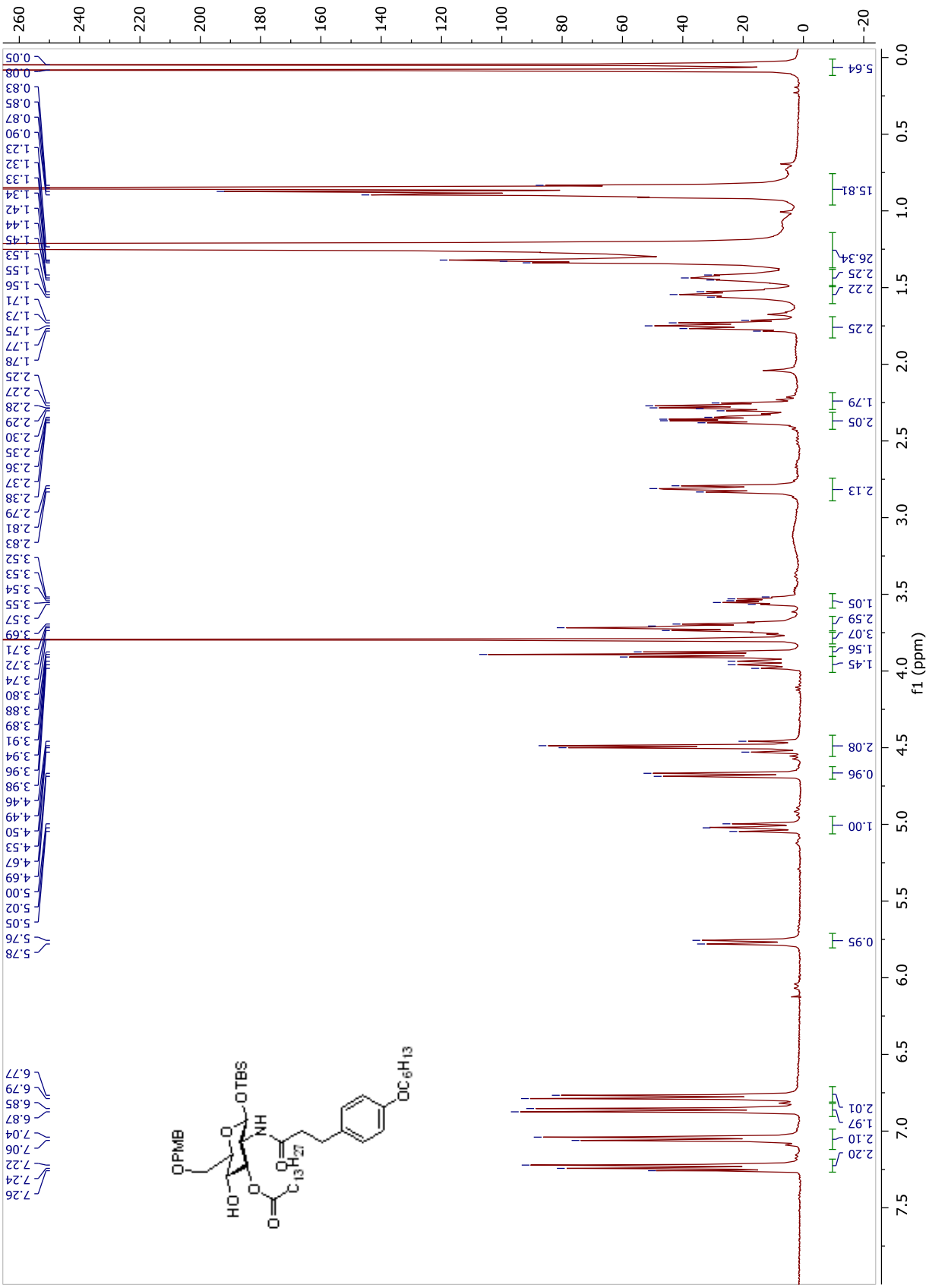

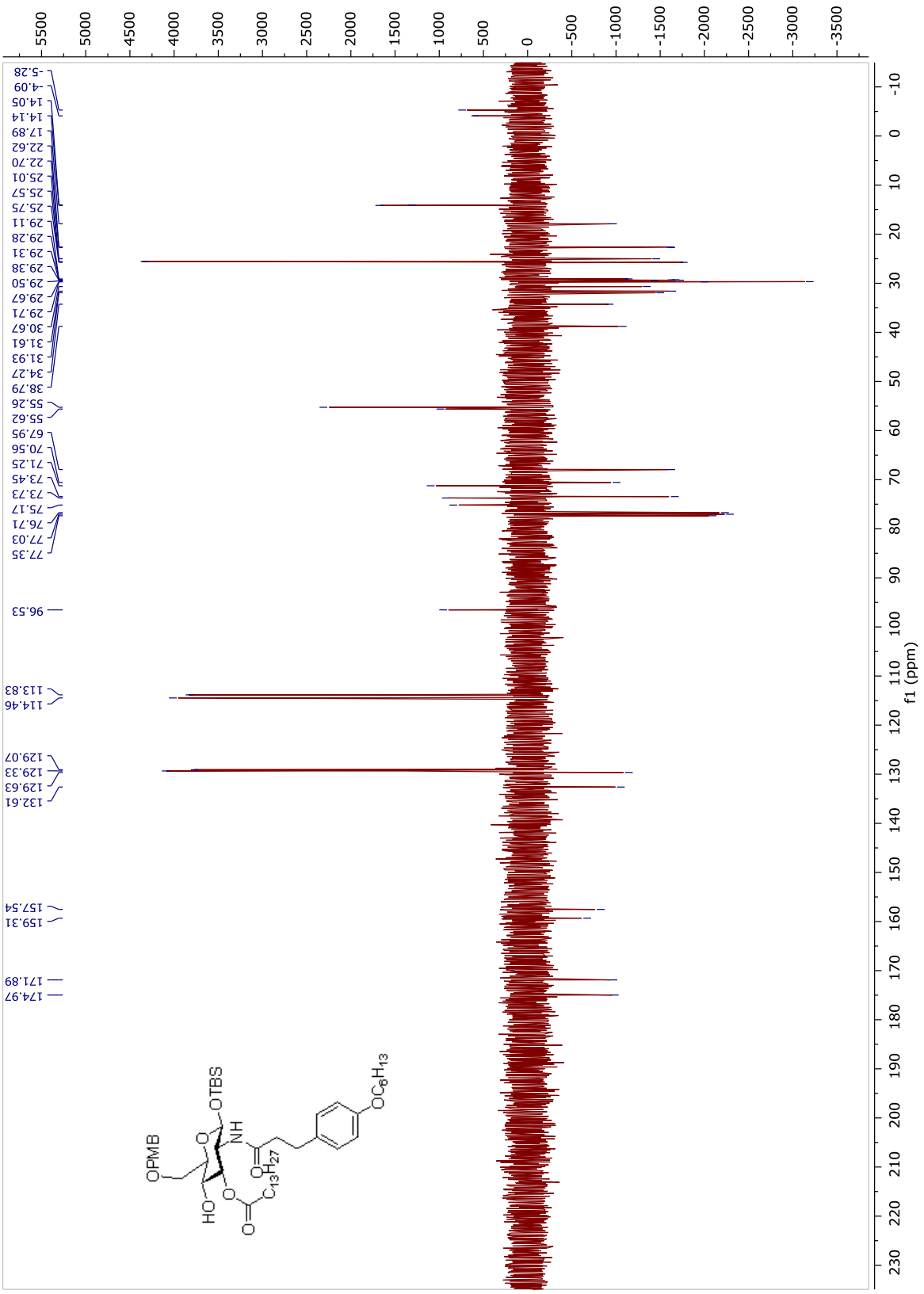
-5.28
-4.09
14.05
14.14
17.89
22.62
22.70
25.01
25.57
25.75
29.11
29.28
29.31
29.38
29.50
29.67
29.71
30.67
31.61
31.93
34.27
38.79
55.26
55.62
67.95
70.56
71.25
73.45
73.73
75.17
76.71
77.03
77.35
96.53
113.83
114.46
129.07
129.33
129.63
132.61
157.54
159.31
171.89
174.97
OPMB
HO
O
OTBS
NH
O
O
O
$C_{13}H_{27}$
OC_6H_{13}
f1 (ppm)

Compound 17. ^{1}H NMR and ^{13}C APT NMR spectra in $CDCl_3$

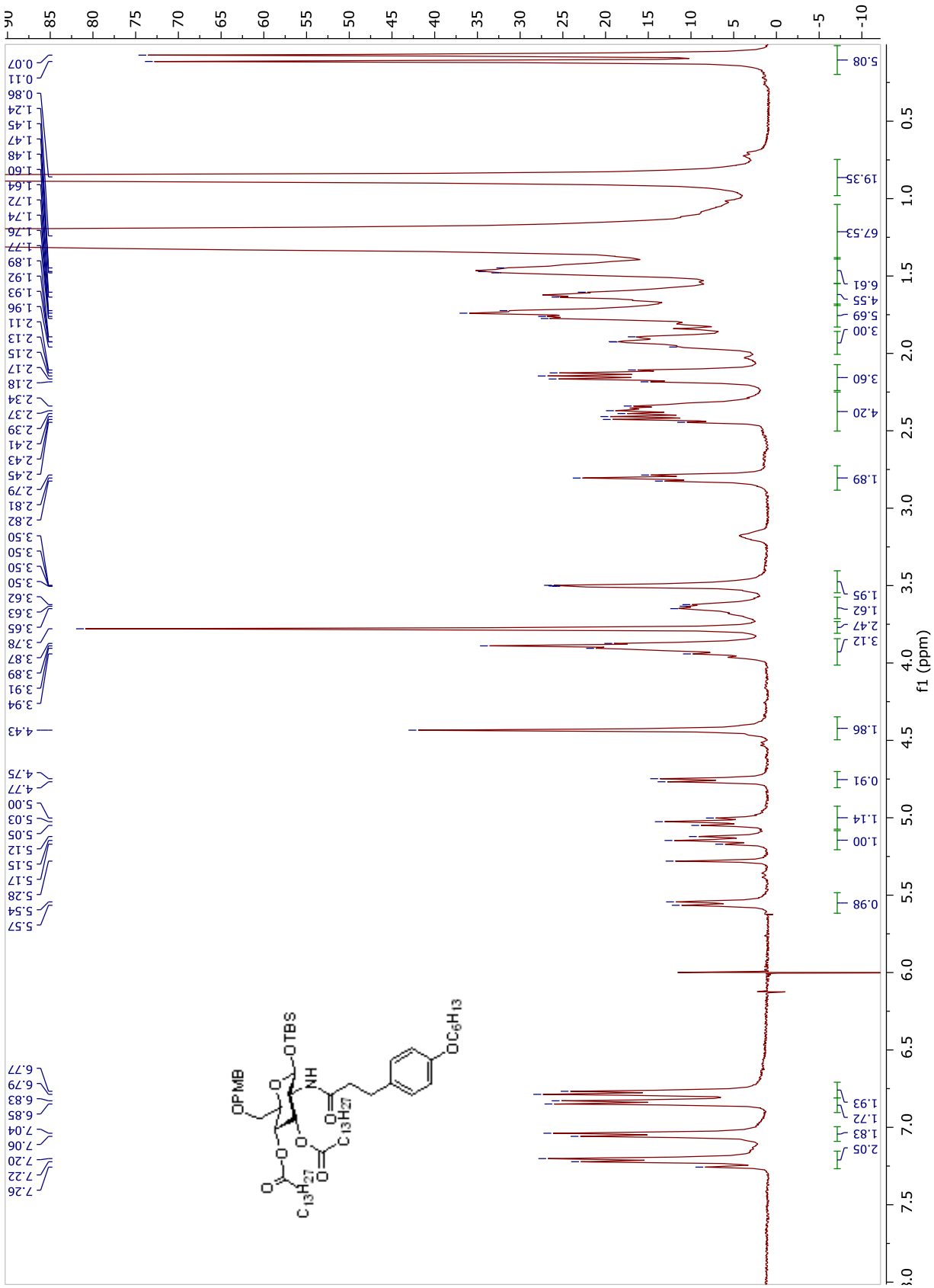

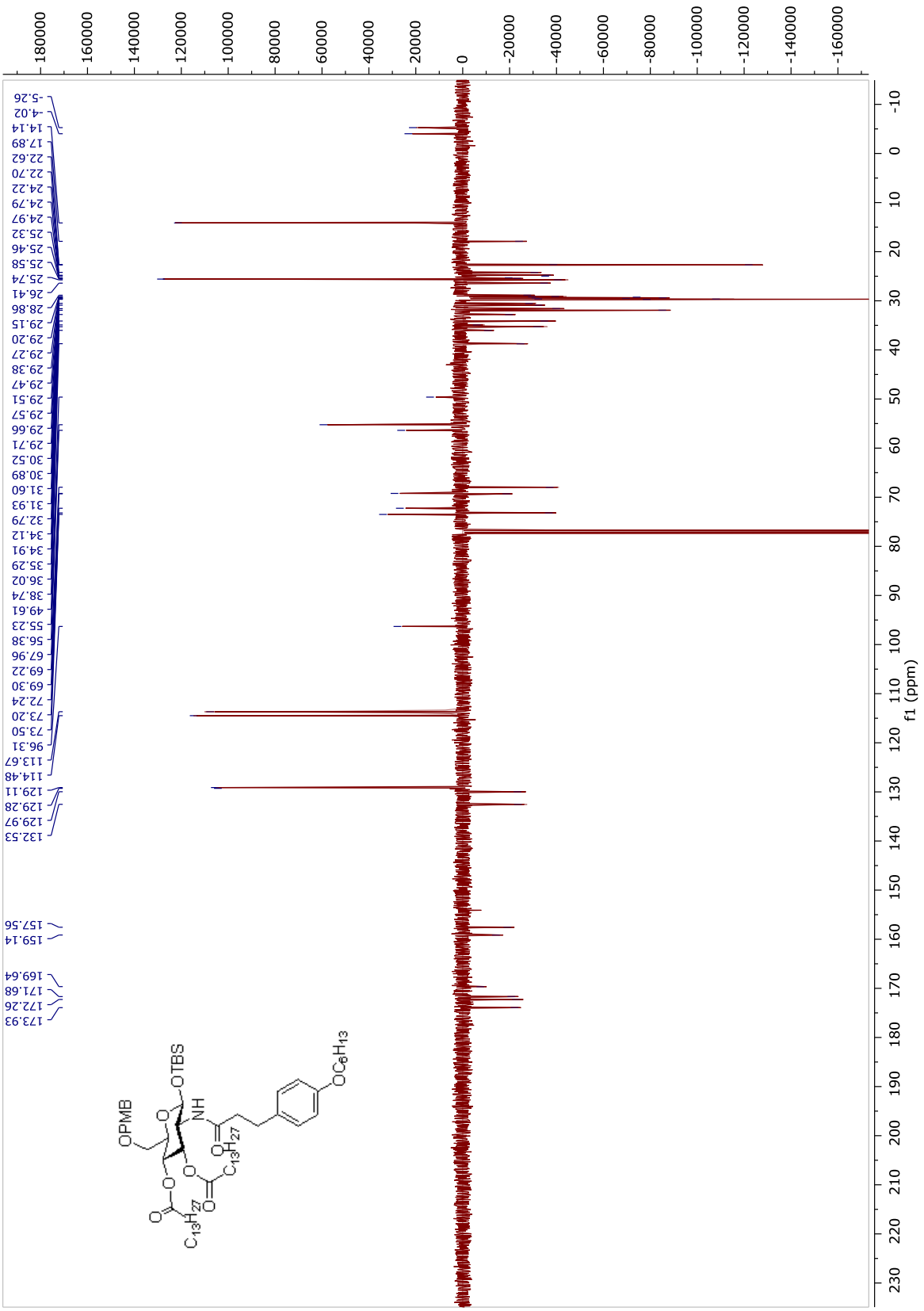
f1 (ppm)
OPMB
OTBS
NH
OC6H13
C13H27
C13H27

Compound 18. ^{1}H NMR and ^{13}C APT NMR spectra in $CDCl_3$

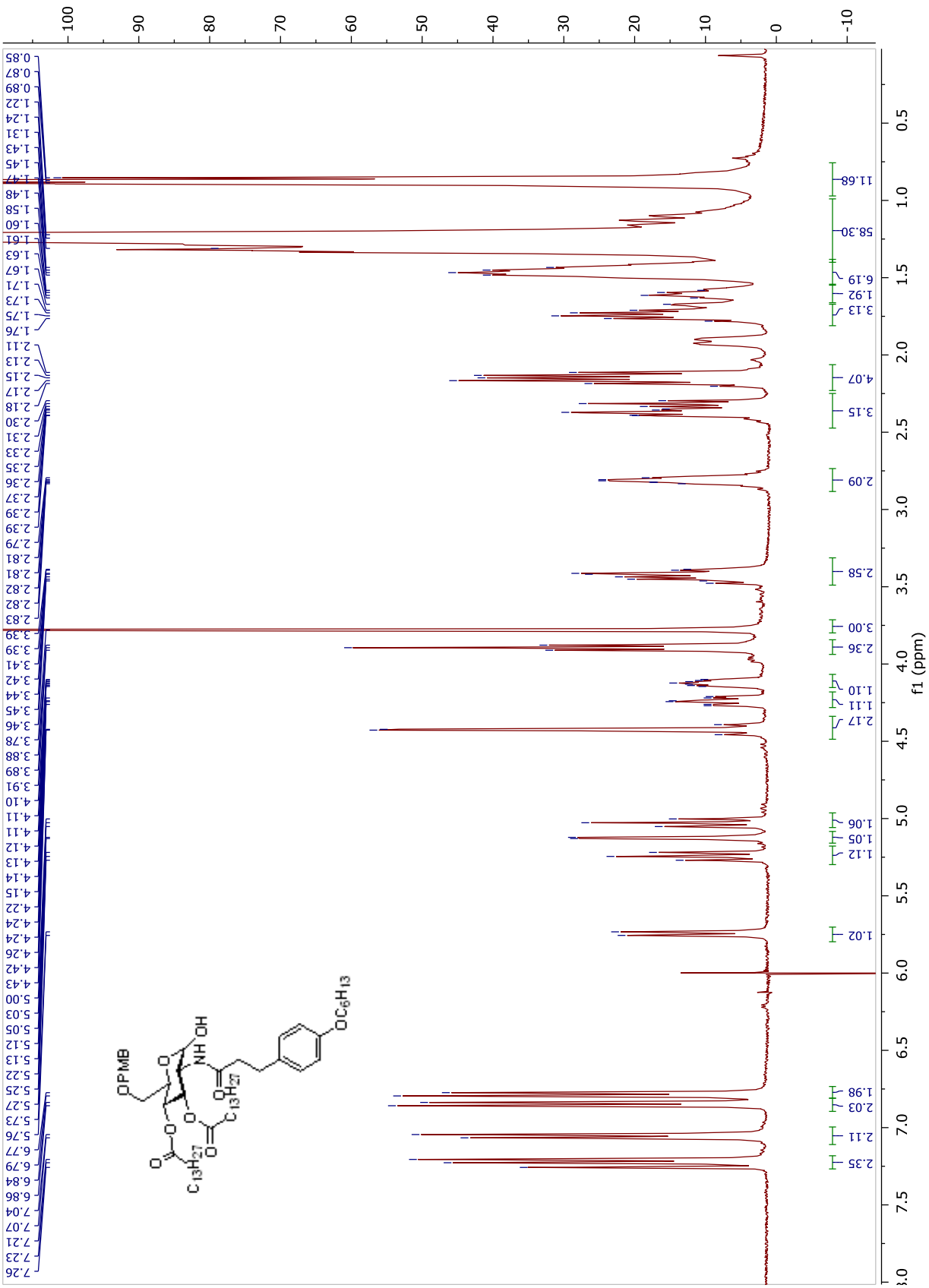

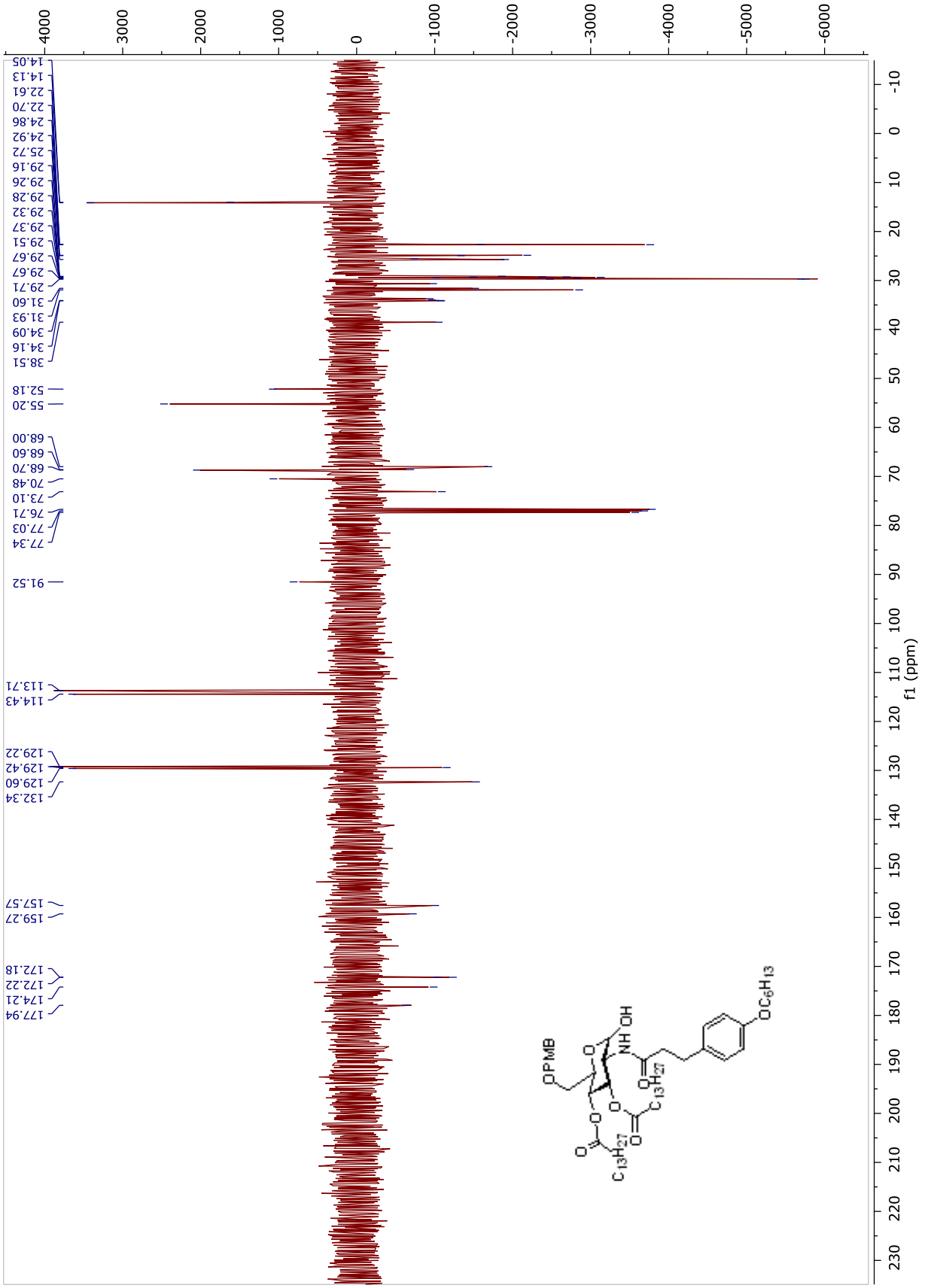
14.05
14.13
22.61
22.70
24.86
24.92
25.72
29.16
29.26
29.28
29.32
29.37
29.51
29.67
29.67
29.71
31.60
31.93
34.09
34.16
38.51
52.18
55.20
68.00
68.60
68.70
70.48
73.10
76.71
77.03
77.34
91.52
113.71
114.43
129.22
129.42
129.60
132.34
157.57
159.27
172.18
172.22
174.21
177.94
OPMB
NH
OH
O
$C_{13}H_{27}$
OC_6H_{13}
f1 (ppm)

Compound 19. ^{1}H NMR and ^{13}C APT NMR spectra in $CDCl_3$

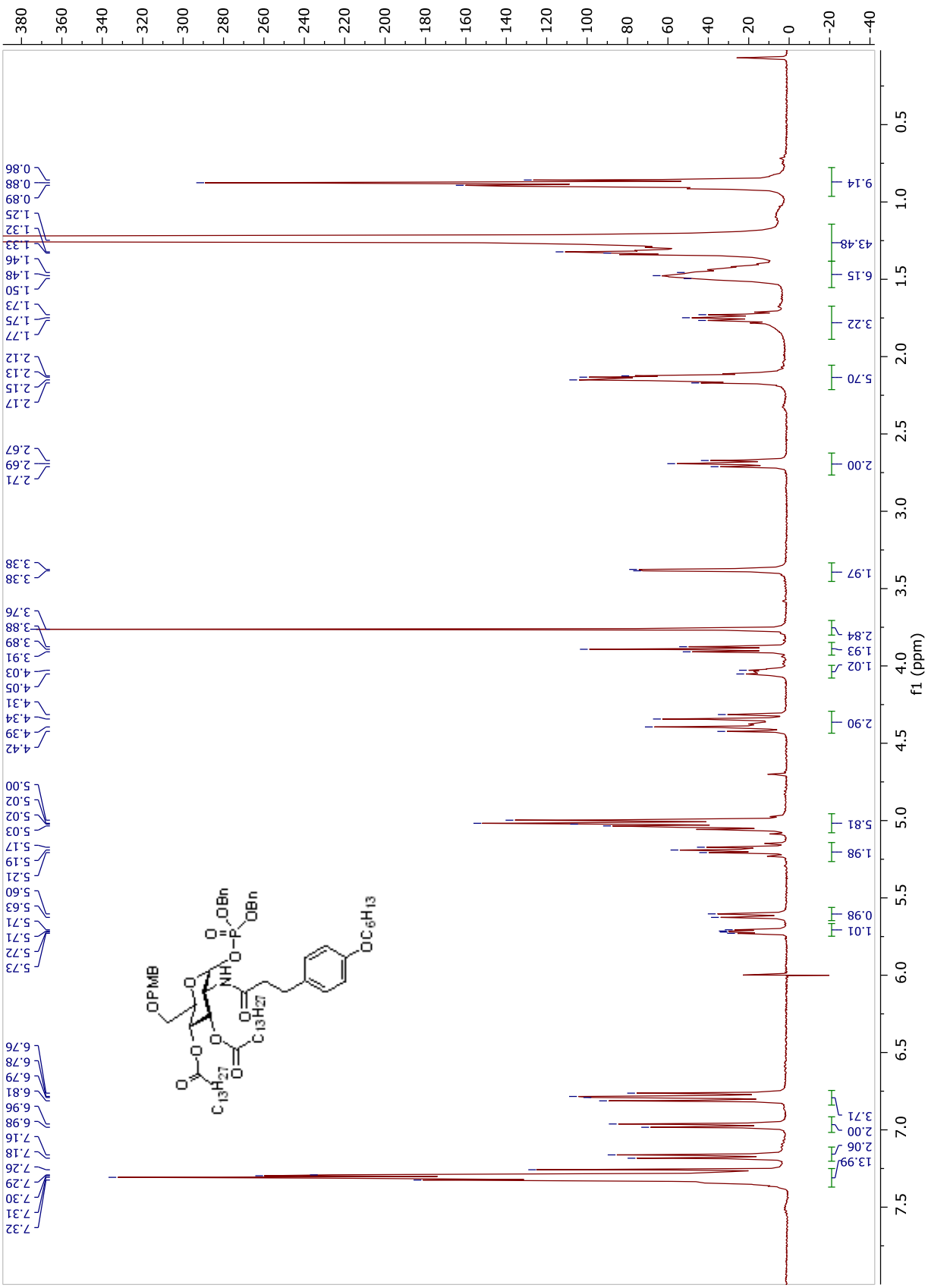

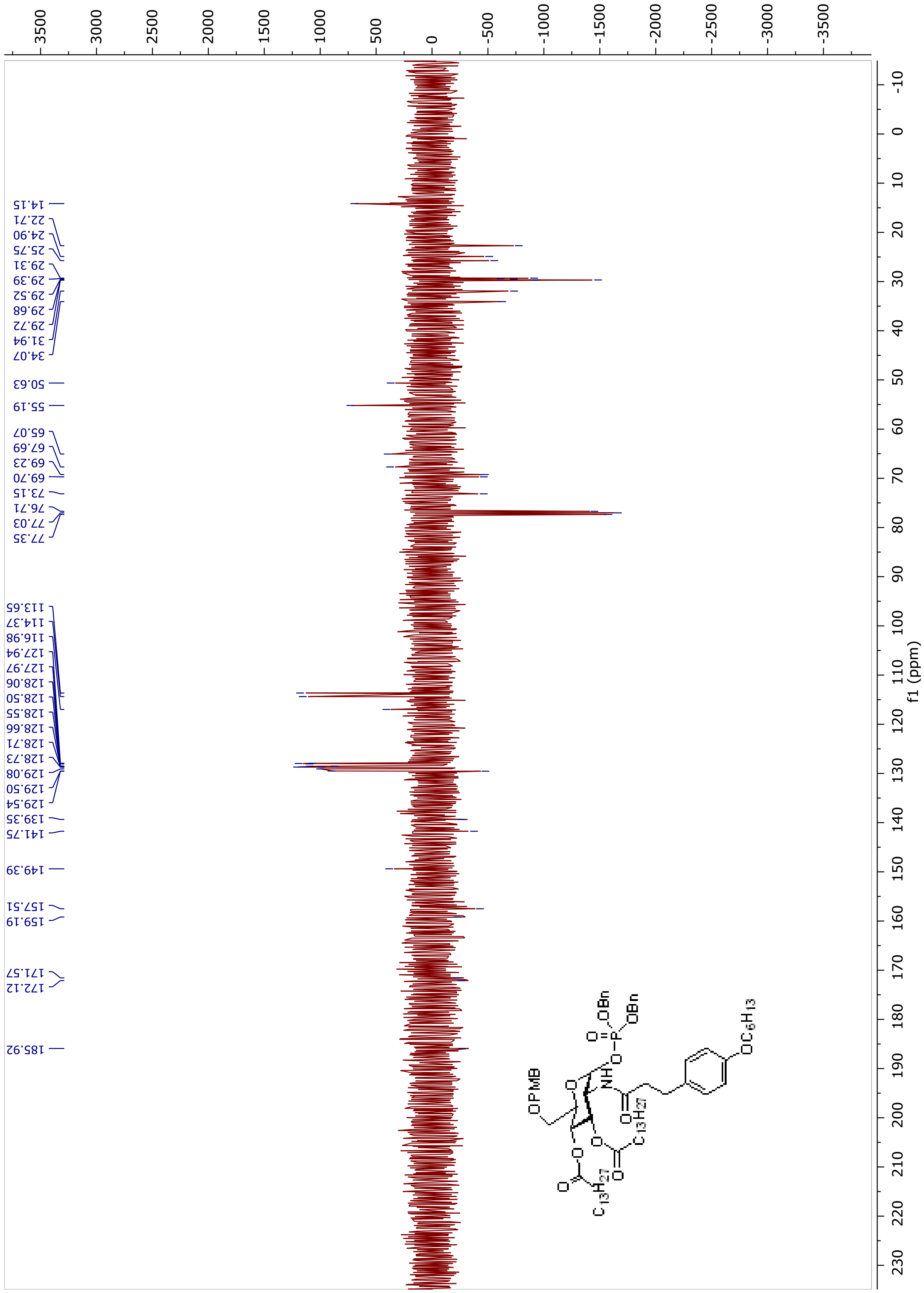
14.15
22.71
24.90
25.75
29.31
29.39
29.52
29.68
29.72
31.94
34.07
50.63
55.19
65.07
67.69
69.23
69.70
73.15
76.71
77.03
77.35
113.65
114.37
116.98
127.94
127.97
128.06
128.50
128.55
128.66
128.71
128.73
129.08
129.50
129.54
139.35
141.75
149.39
157.51
159.19
171.57
172.12
185.92
f1 (ppm)

Compound AM158. ^{1}H NMR and ^{13}C APT NMR spectra in CD_3OD

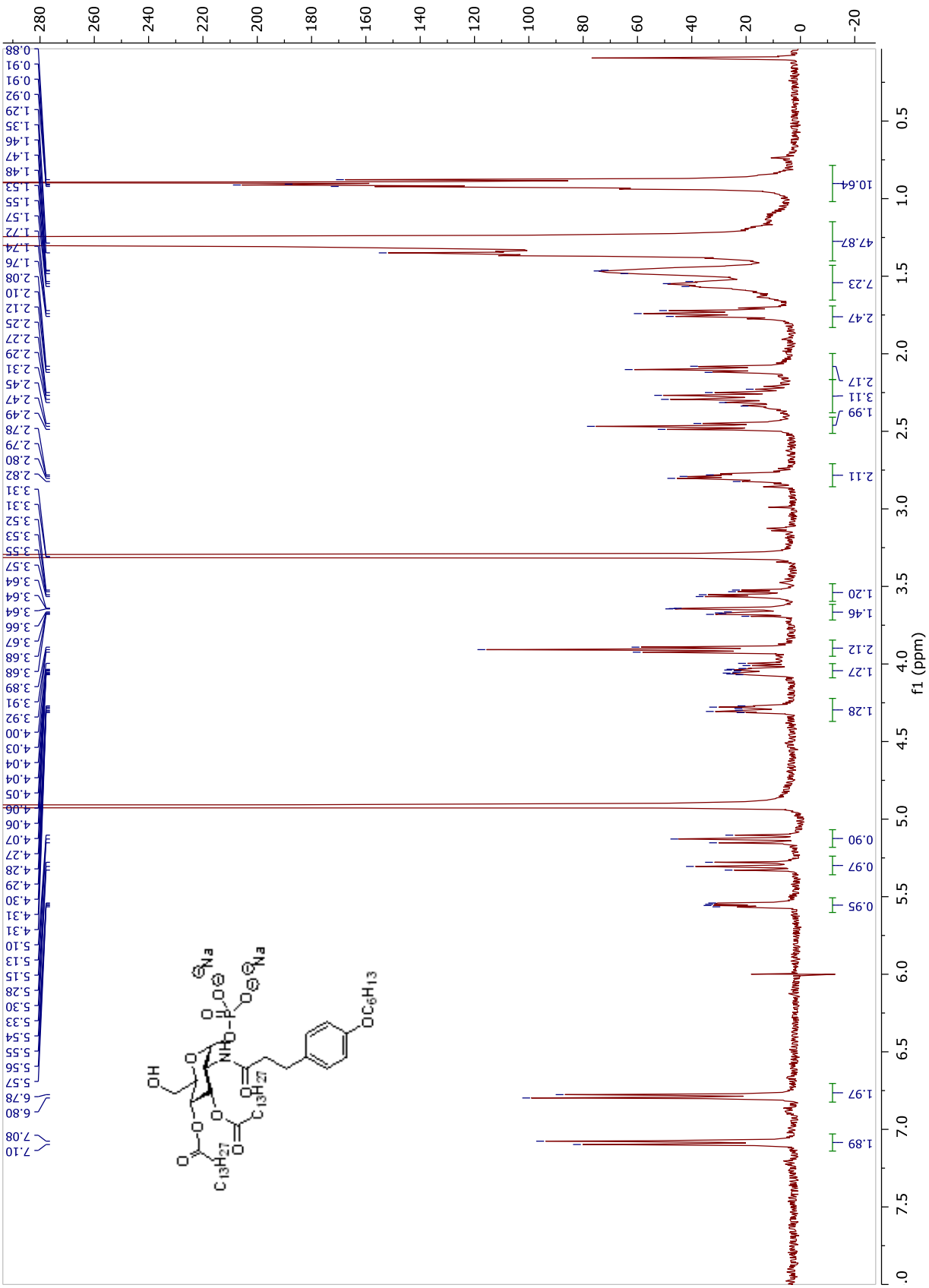

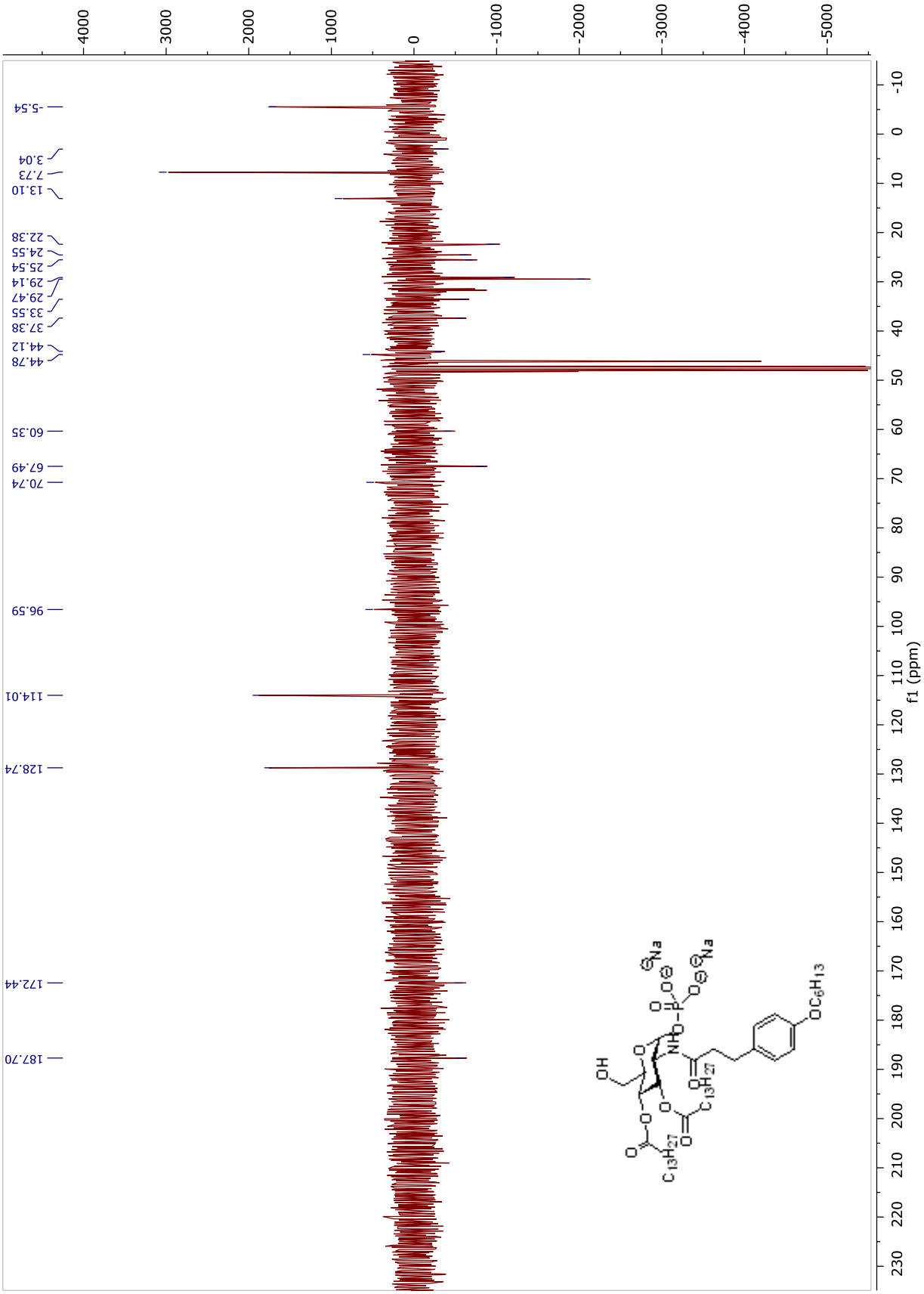
-5.54
3.04
7.73
13.10
22.38
24.55
25.54
29.14
29.47
33.55
37.38
44.12
44.78
60.35
67.49
70.74
96.59
114.01
128.74
172.44
187.70
f1 (ppm)

Chain B2 Synthesis: ^{1}H NMR and ^{13}C-APT NMR spectra

Compound 20. ^{1}H NMR and ^{13}C APT NMR spectra in $CDCl_3$

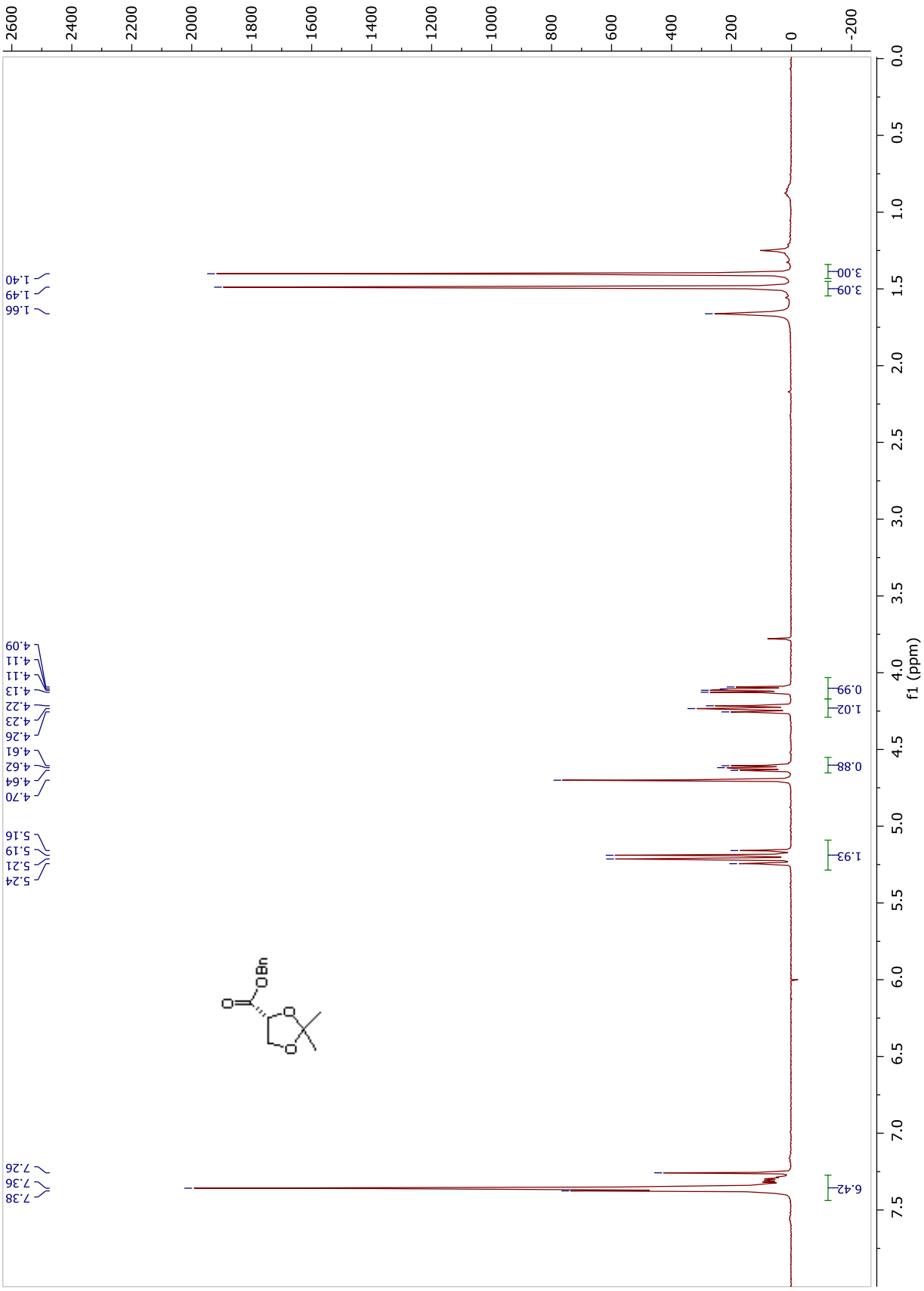

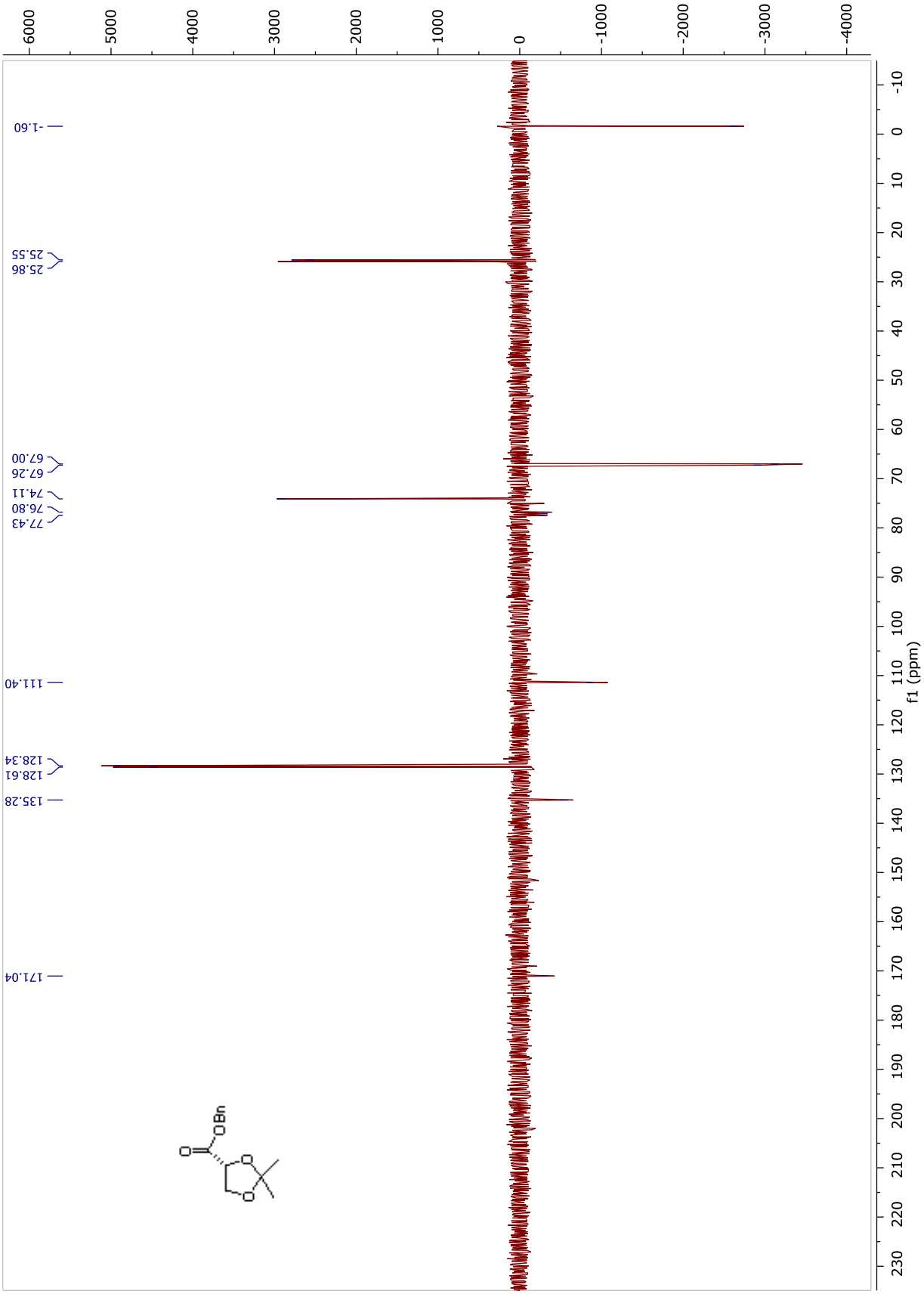
-1.60
25.86
25.55
67.26
67.00
74.11
76.80
77.43
111.40
128.61
128.34
135.28
171.04
f1 (ppm)

Compound 21. ^{1}H NMR and ^{13}C-APT NMR spectra in $CDCl_3$

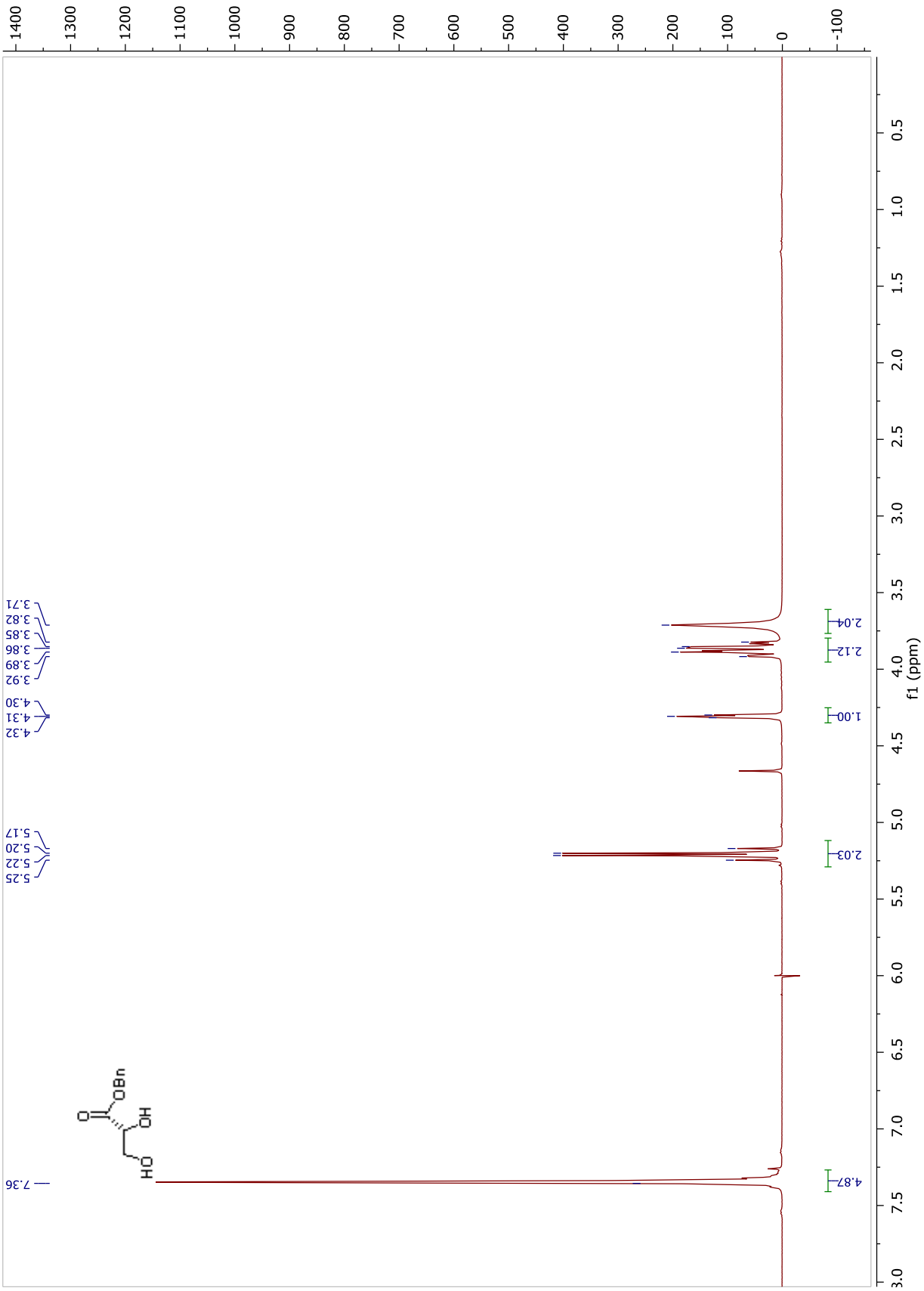

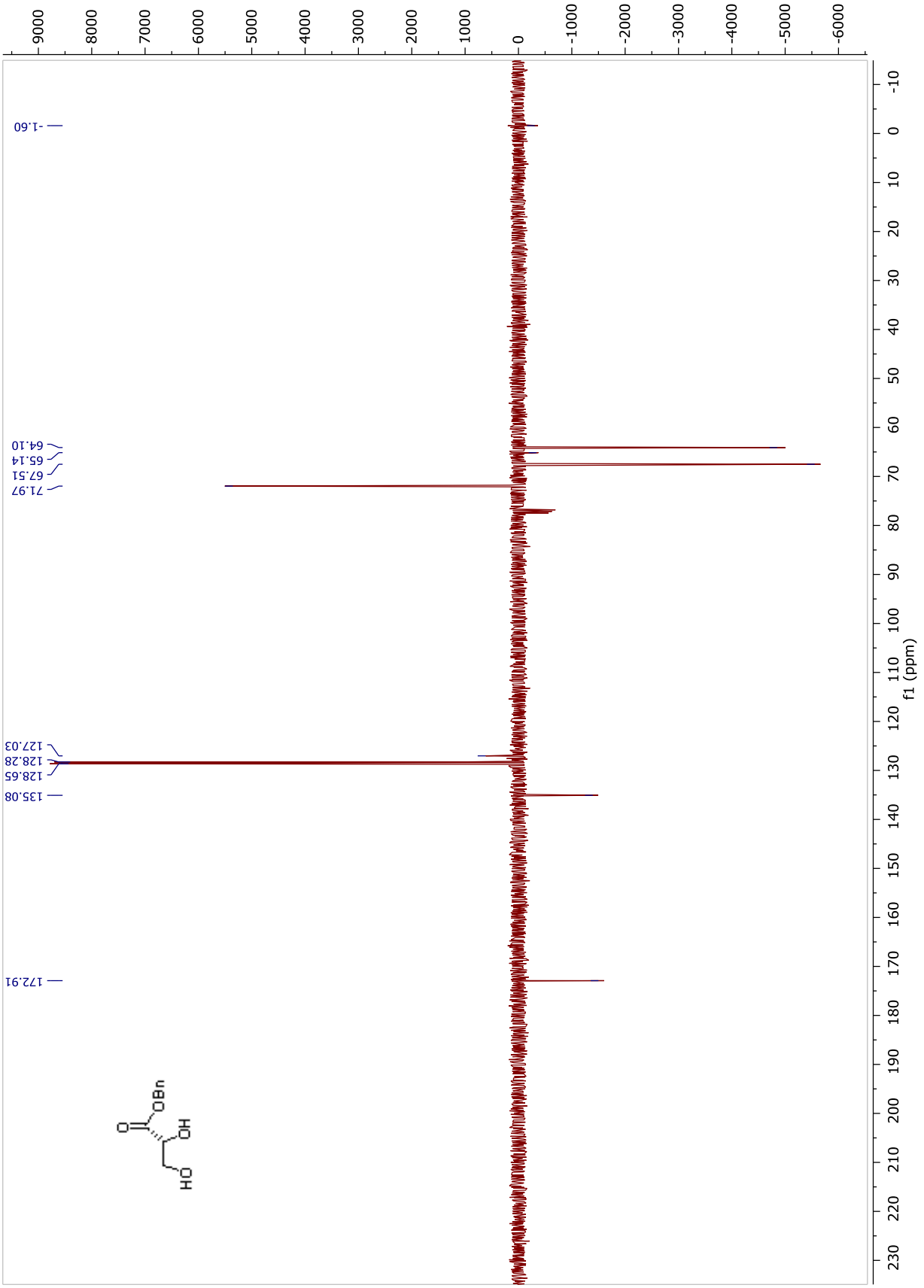
-1.60
64.10
65.14
67.51
71.97
127.03
128.28
128.65
135.08
172.91
f1 (ppm)

Compound 22. ^{1}H NMR and ^{13}C APT NMR spectra in $CDCl_3$

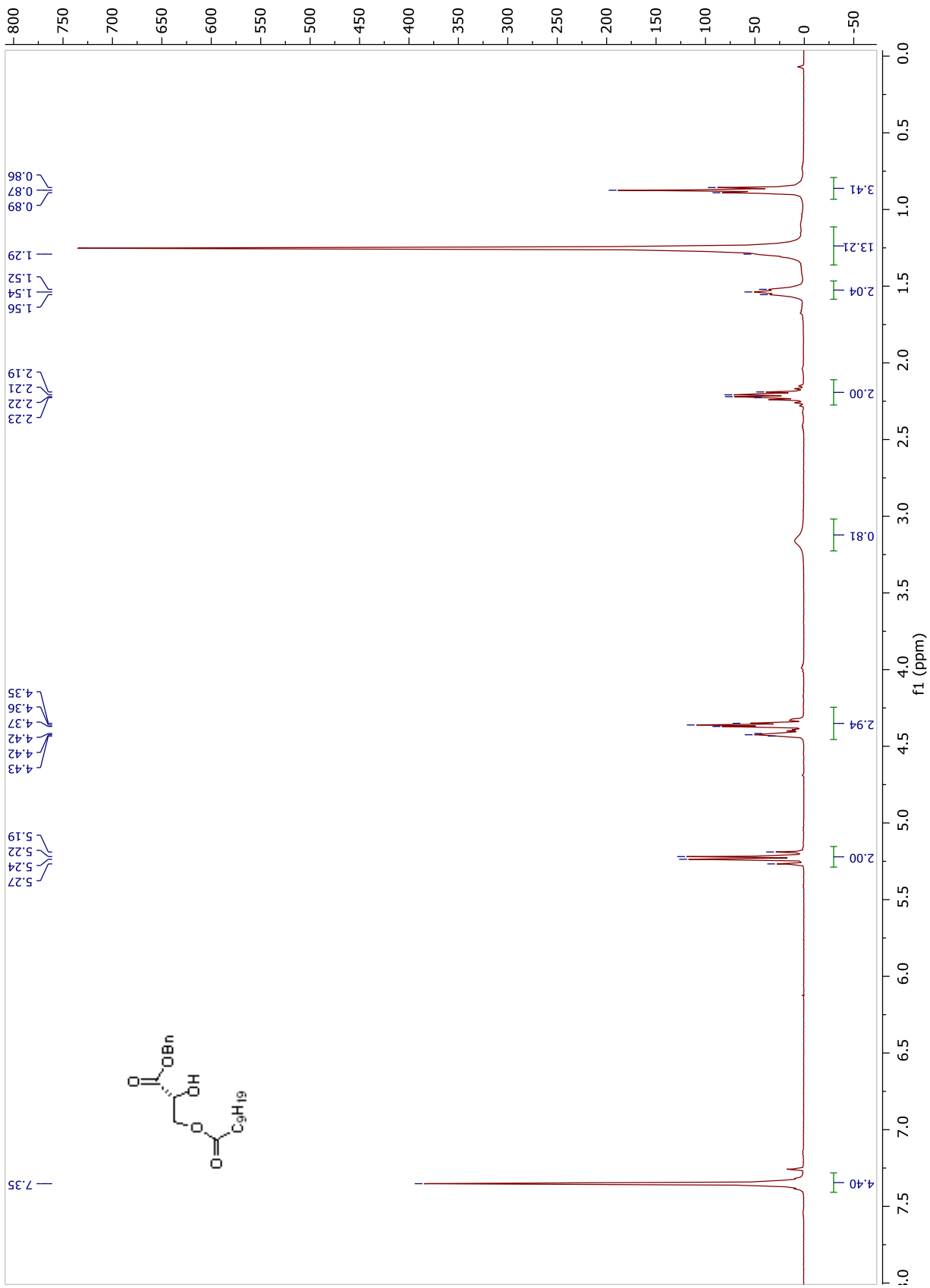

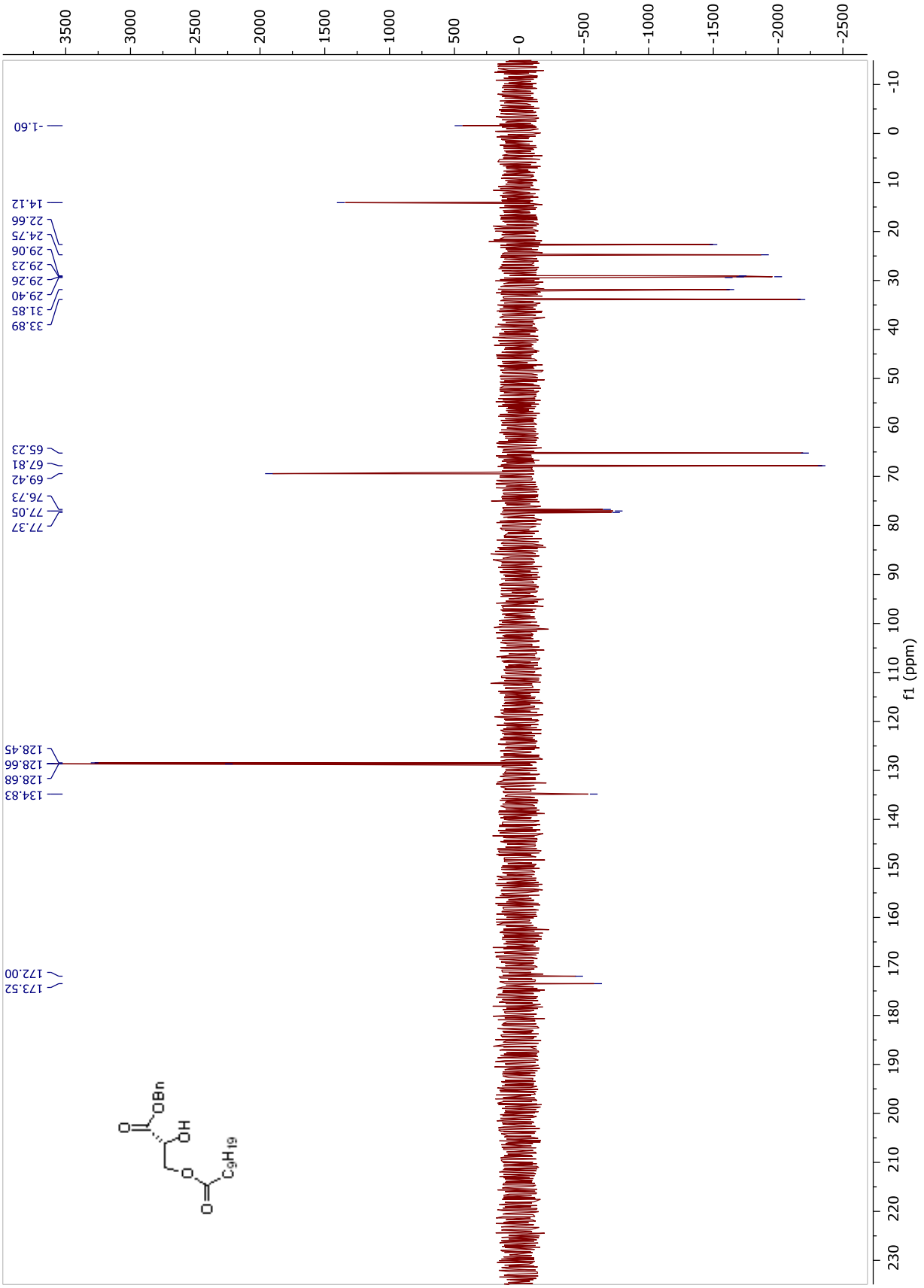
-1.60
14.12
22.66
24.75
29.06
29.23
29.26
29.40
31.85
33.89
65.23
67.81
69.42
76.73
77.05
77.37
128.45
128.66
128.68
134.83
172.00
173.52
f1 (ppm)

Compound 23. ^{1}H NMR and ^{13}C APT NMR spectra in $CDCl_3$

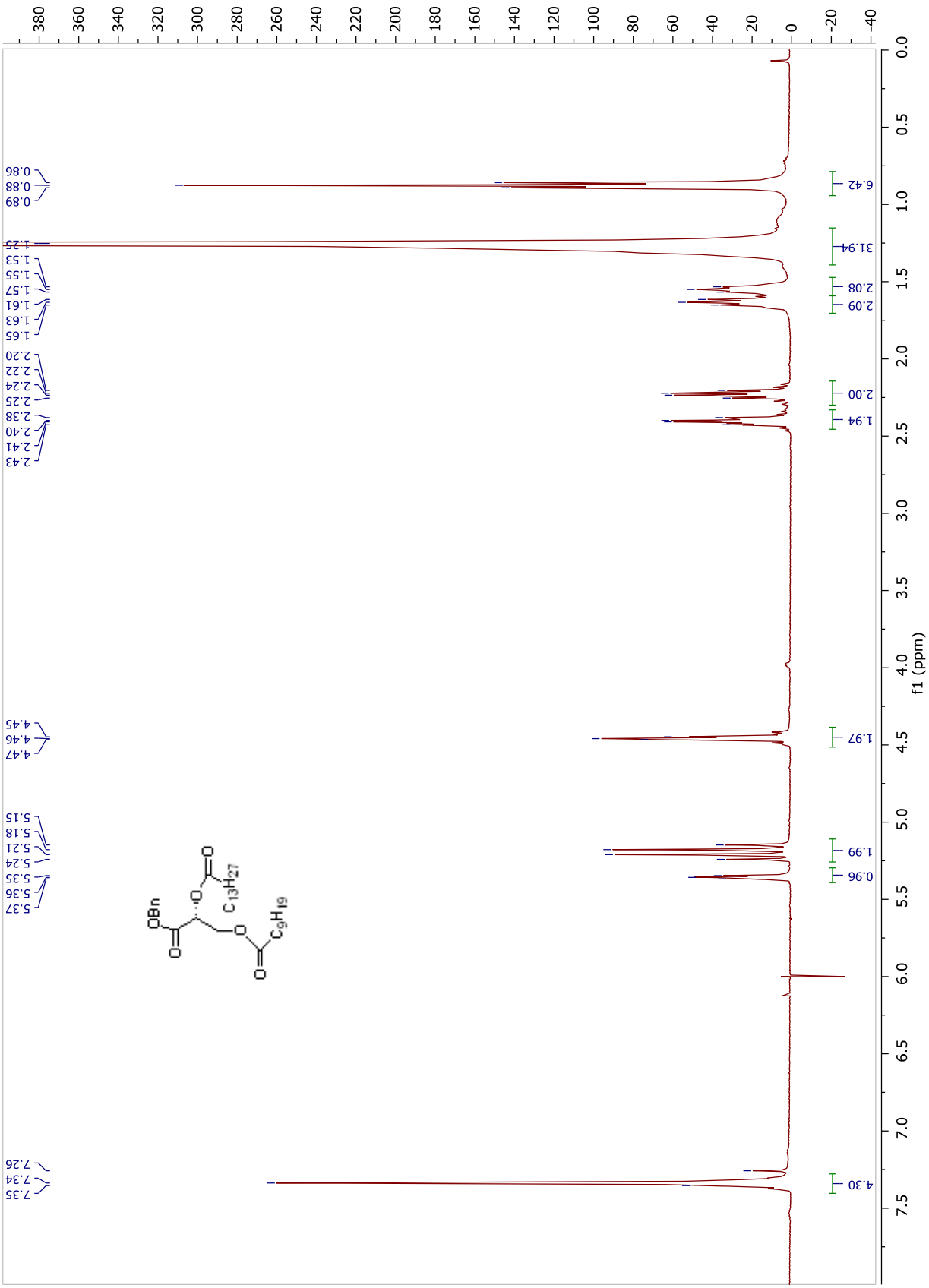

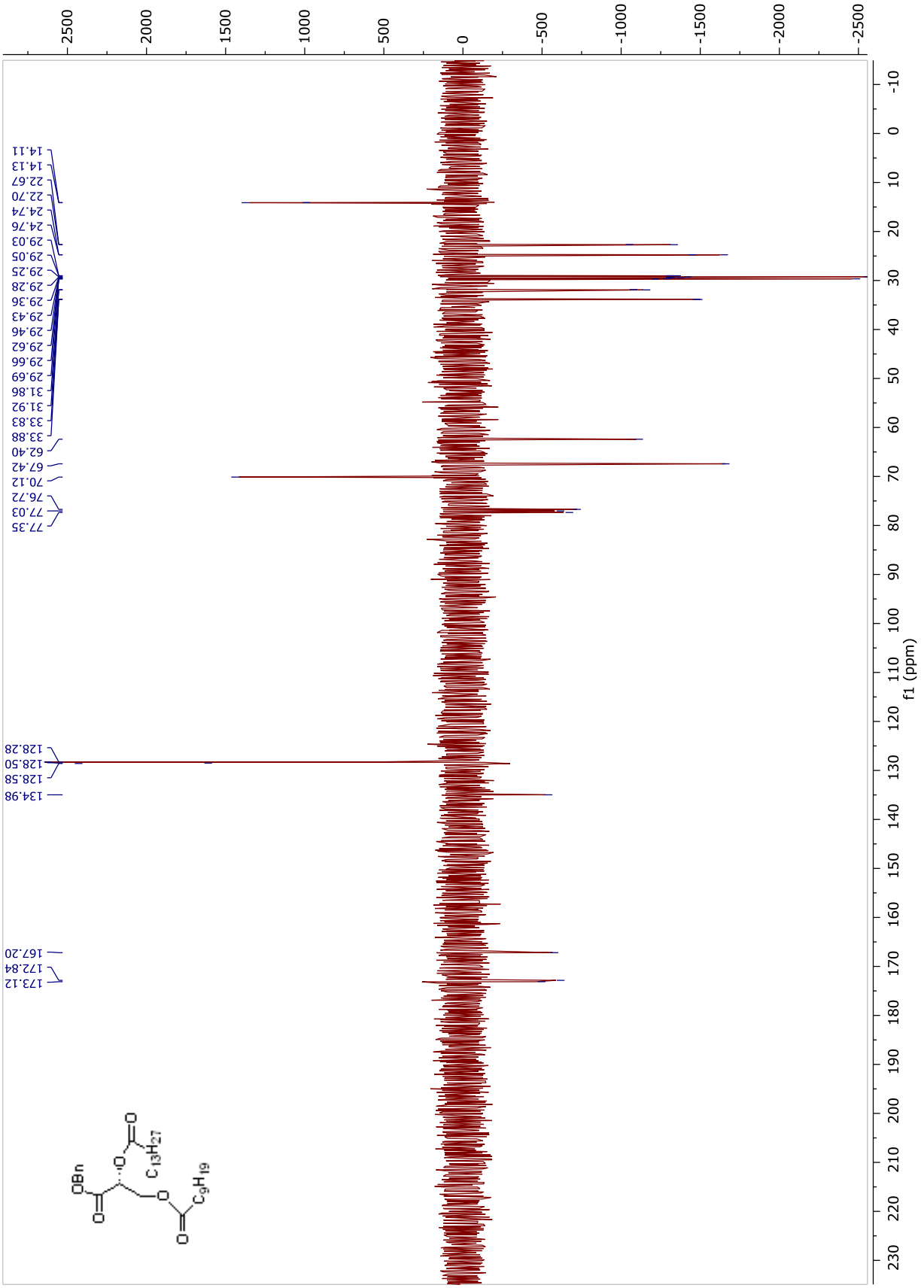
14.11
14.13
22.67
22.70
24.74
24.76
29.03
29.05
29.25
29.28
29.36
29.43
29.46
29.62
29.66
29.69
31.86
31.92
33.83
33.88
62.40
67.42
70.12
76.72
77.03
77.35
128.28
128.50
128.58
134.98
167.20
172.84
173.12
OBn
$C_{13}H_{27}$
C_9H_{19}
f1 (ppm)

Compound B2. ^{1}H NMR and ^{13}C APT NMR spectra in $CDCl_3$

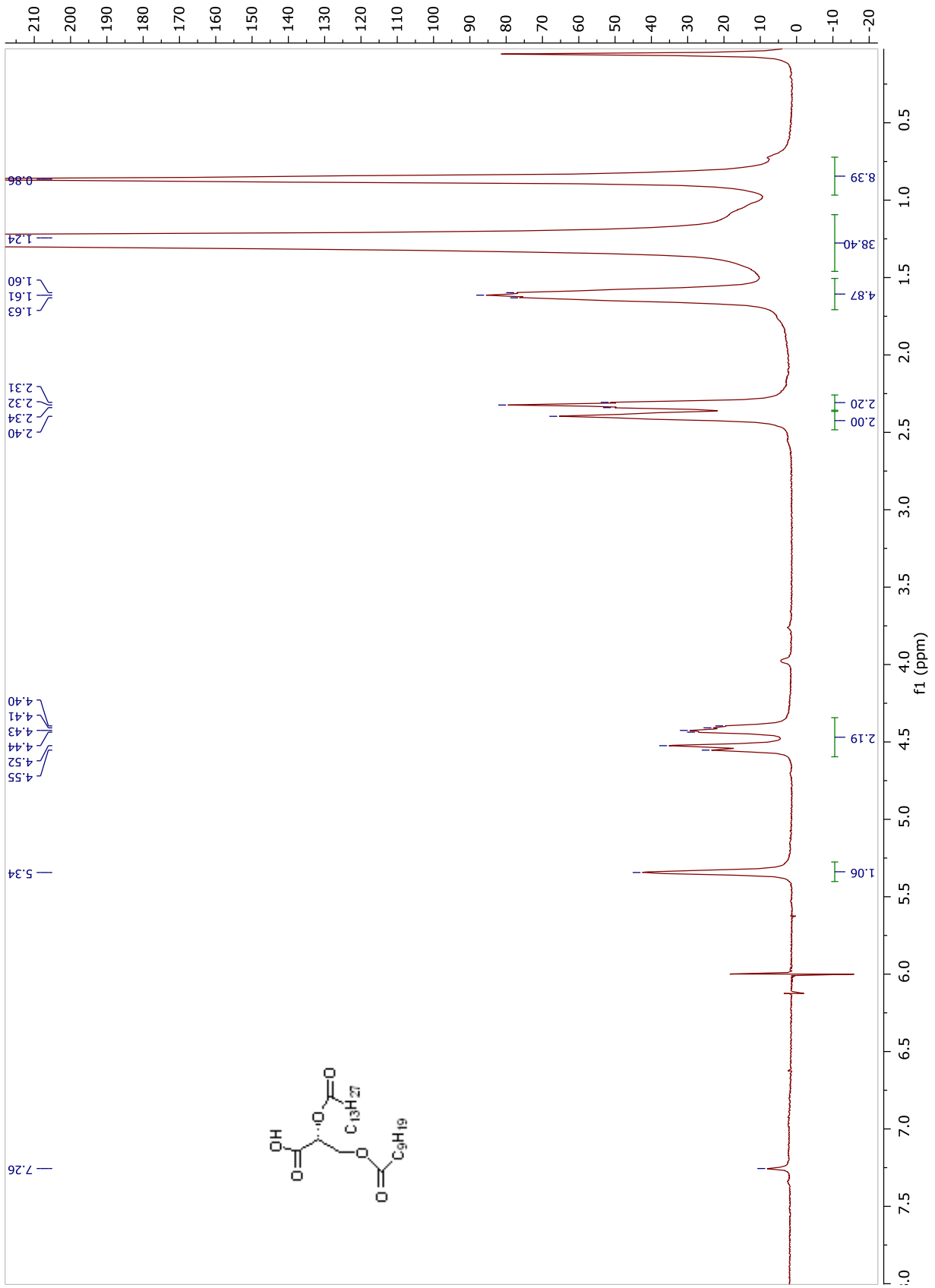

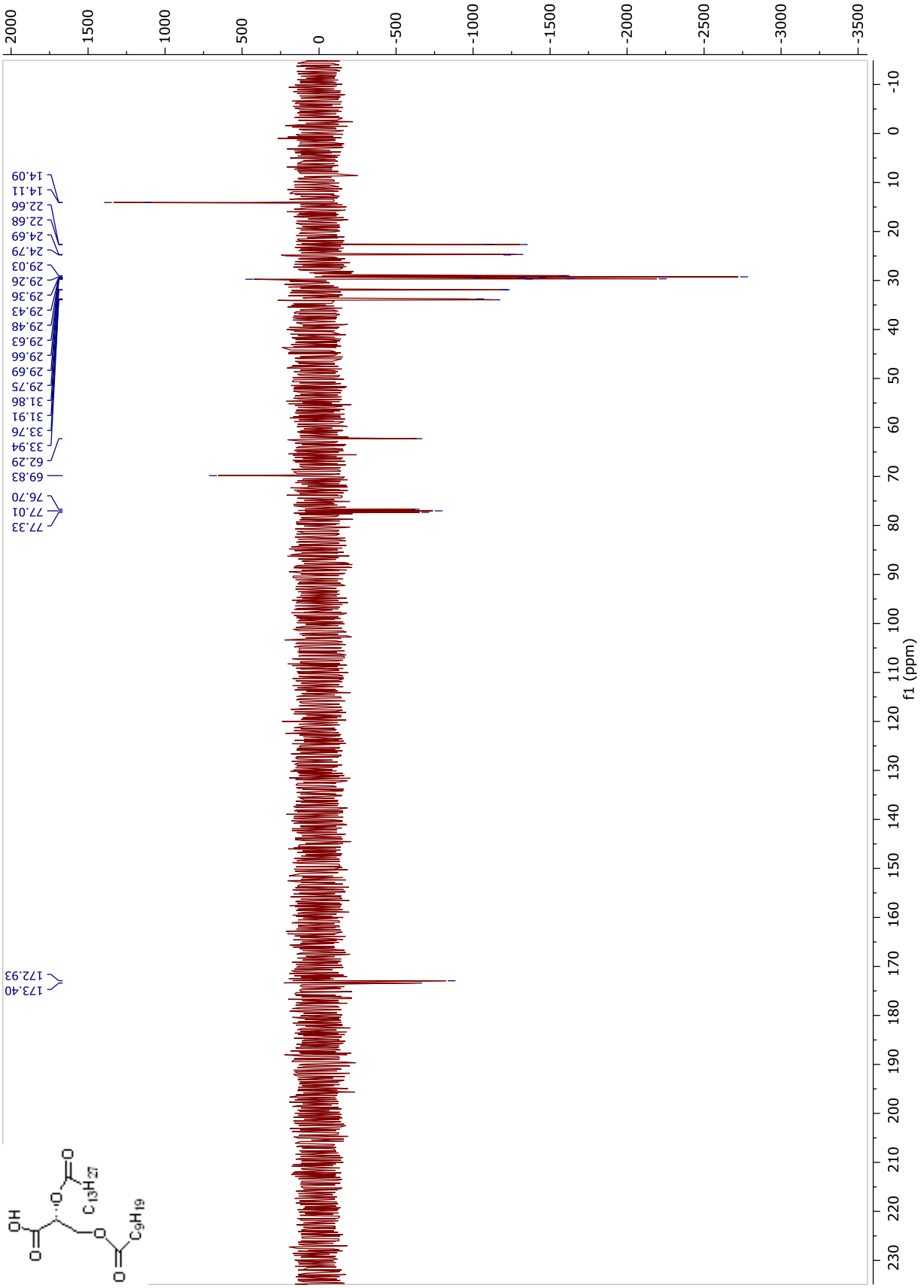
14.09
14.11
22.66
22.68
24.69
24.79
29.03
29.26
29.36
29.43
29.48
29.63
29.66
29.69
29.75
31.86
31.91
33.76
33.94
62.29
69.83
76.70
77.01
77.33
172.93
173.40
f1 (ppm)

AM173 Synthesis: ^{1}H NMR and ^{13}C-APT NMR spectra

Compound 25. ^{1}H NMR and ^{13}C APT NMR spectra in $CDCl_3$

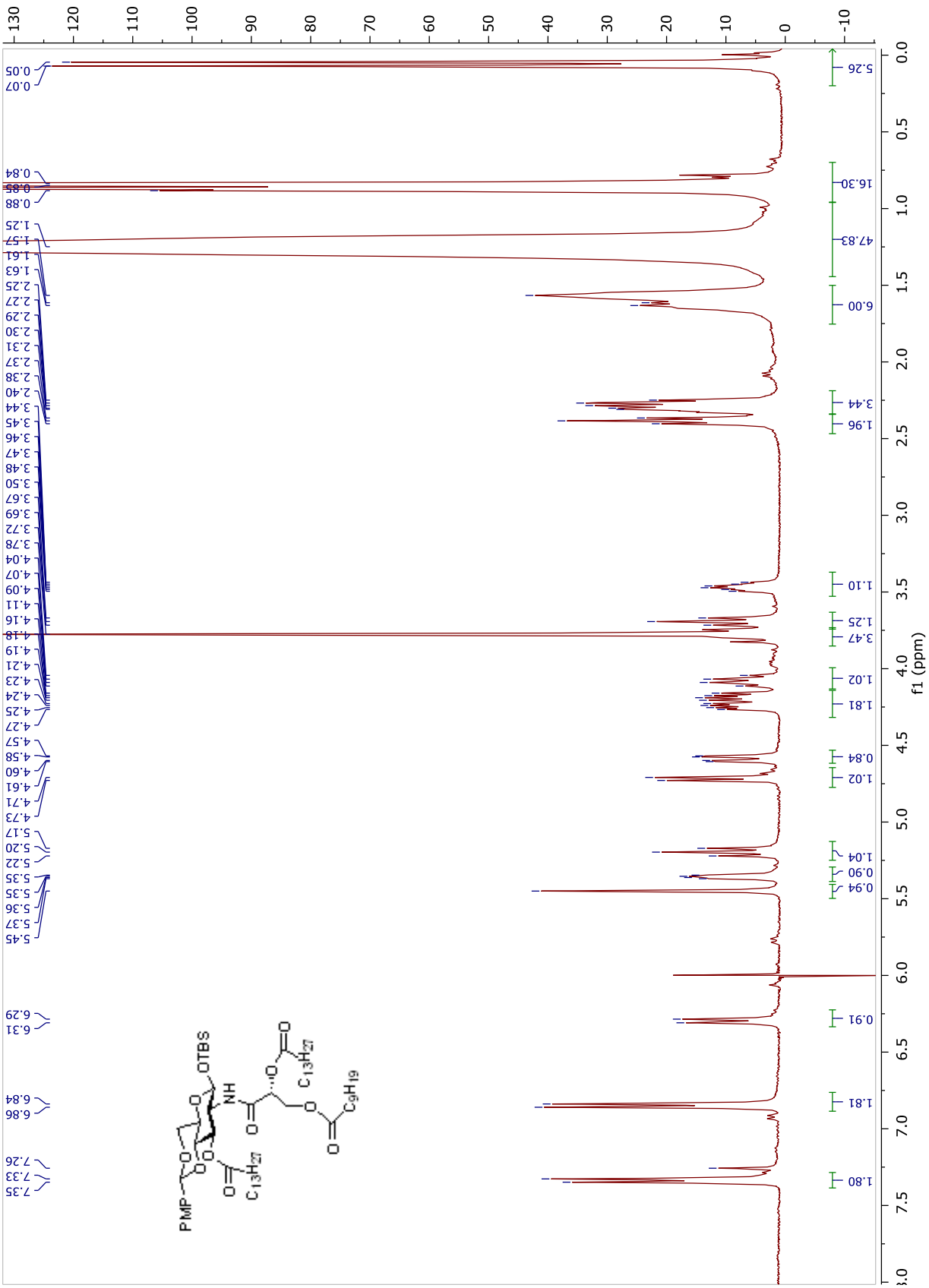

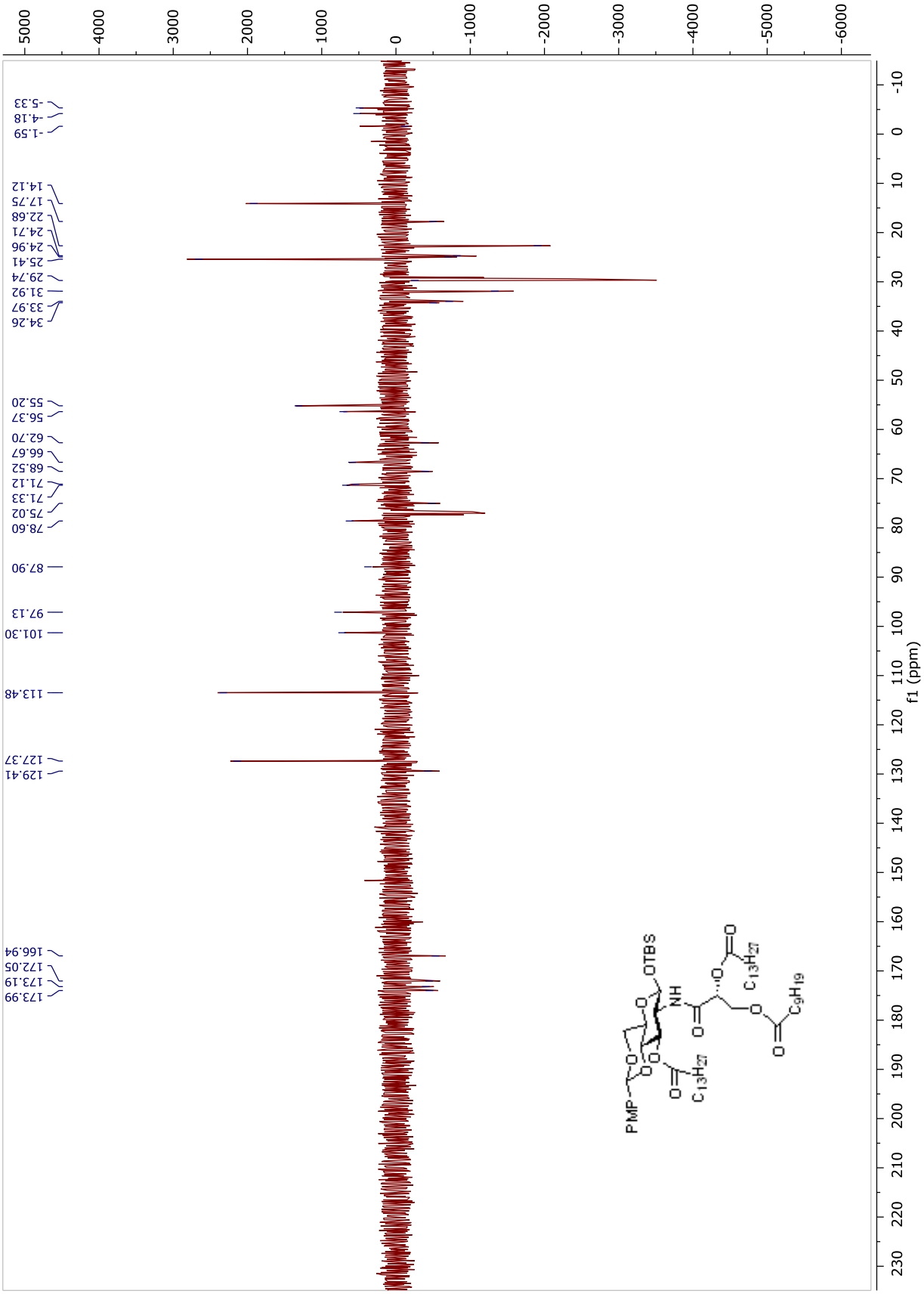
-5.33
-4.18
-1.59
14.12
17.75
22.68
24.71
24.96
25.41
29.74
31.92
33.97
34.26
55.20
56.37
62.70
66.67
68.52
71.12
71.33
75.02
78.60
87.90
97.13
101.30
113.48
127.37
129.41
166.94
172.05
173.19
173.99
OTBS
NH
PMP
C13H27
C13H27
C9H19
f1 (ppm)

Compound 26. ^{1}H NMR and ^{13}C APT NMR spectra in $CDCl_3$

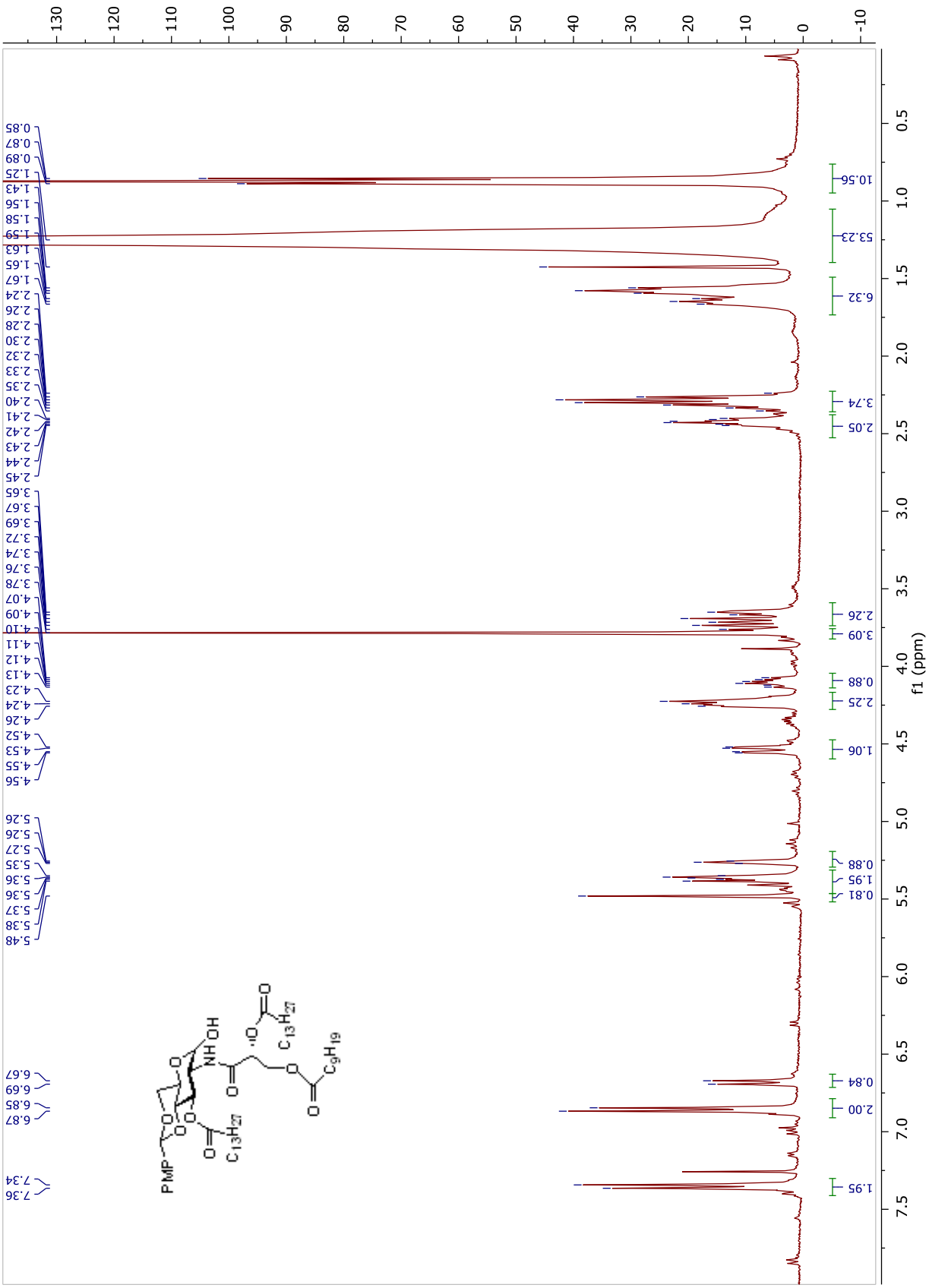

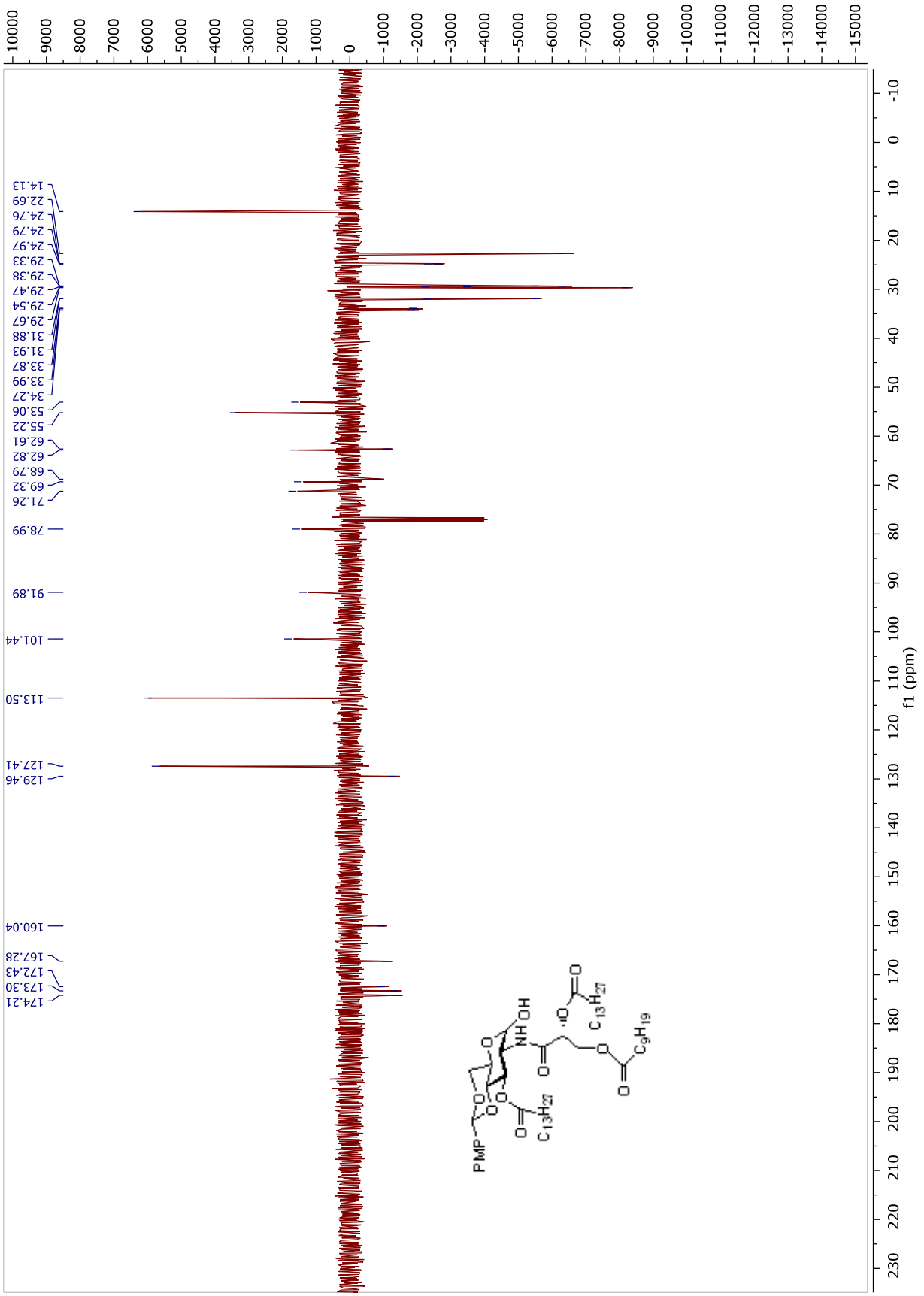
14.13
22.69
24.76
24.79
24.97
29.33
29.38
29.47
29.54
29.67
31.88
31.93
33.87
33.99
34.27
53.06
55.22
62.61
62.82
68.79
69.32
71.26
78.99
91.89
101.44
113.50
127.41
129.46
160.04
167.28
172.43
173.30
174.21
f1 (ppm)
PMP
NH
OH
$C_{13}H_{27}$
$C_{13}H_{27}$
C_9H_{19}

Compound 27. ^{1}H NMR and ^{13}C APT NMR spectra in $CDCl_3$

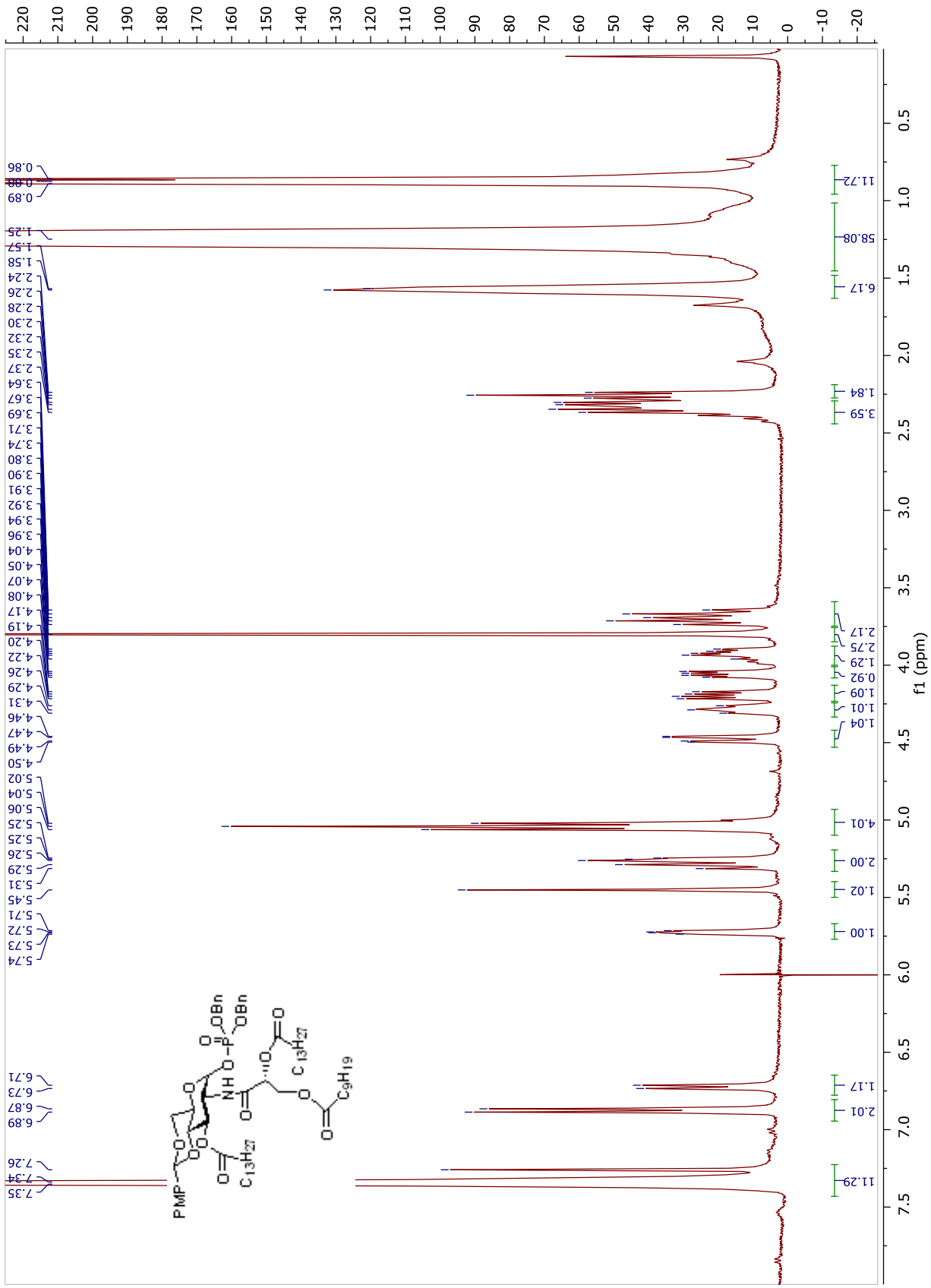

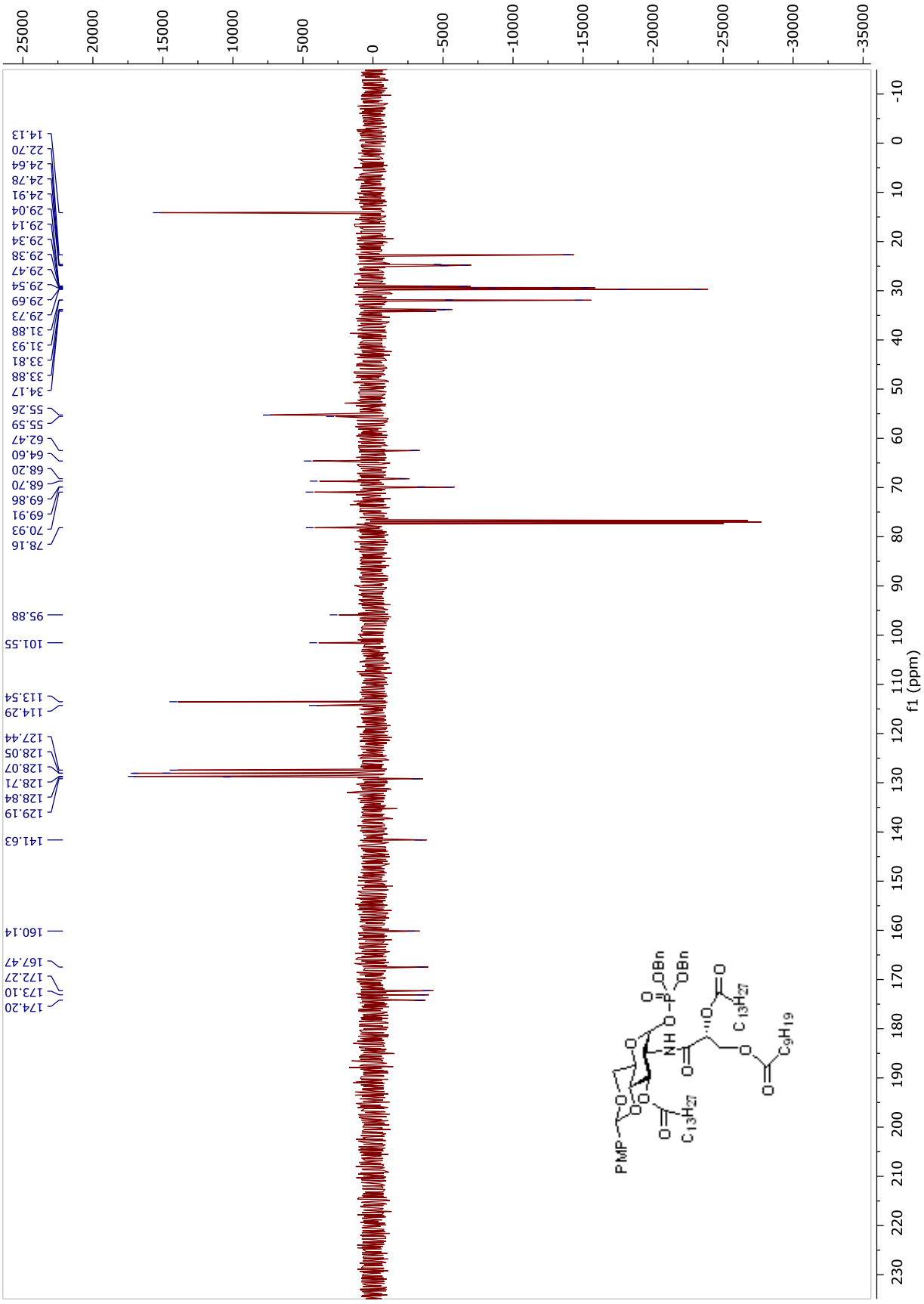
14.13
22.70
24.64
24.78
24.91
29.04
29.14
29.34
29.38
29.47
29.54
29.69
29.73
31.88
31.93
33.81
33.88
34.17
55.26
55.59
62.47
64.60
68.20
68.70
69.86
69.91
70.93
78.16
95.88
101.55
113.54
114.29
127.44
128.05
128.07
128.71
128.84
129.19
141.63
160.14
167.47
172.27
173.10
174.20
PMP
OBn
OBn
NH
C13H27
C13H27
C9H19
f1 (ppm)

Compound AM173. ^{1}H NMR and ^{13}C APT NMR spectra in CD_3OD

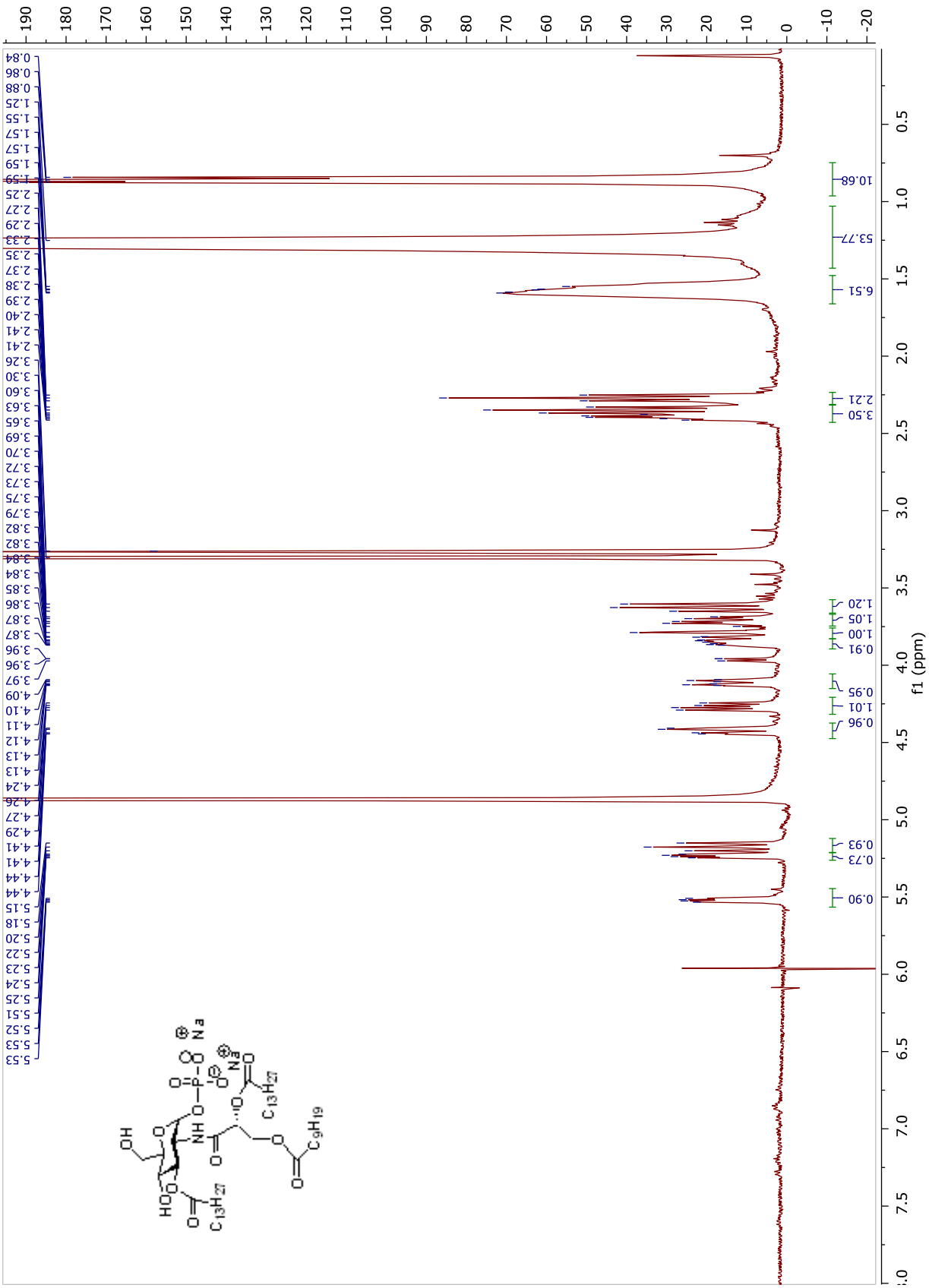

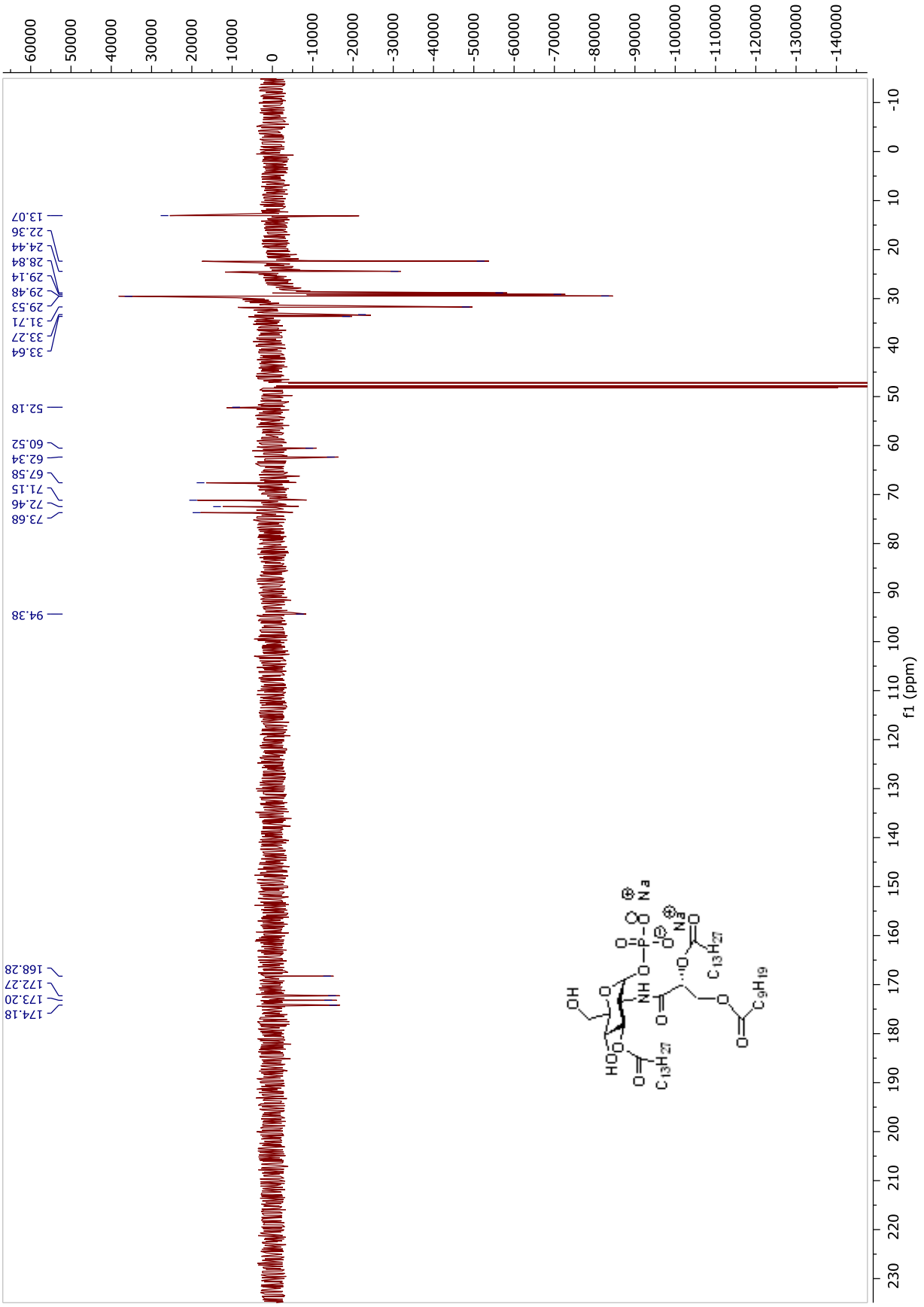
13.07
22.36
24.44
28.84
29.14
29.48
29.53
31.71
33.27
33.64
52.18
60.52
62.34
67.58
71.15
72.46
73.68
94.38
168.28
172.27
173.20
174.18
f1 (ppm)

Chain B3 Synthesis: ^{1}H NMR and ^{13}C-APT NMR spectra

Compound 28. ^{1}H NMR spectrum in $CDCl_3$

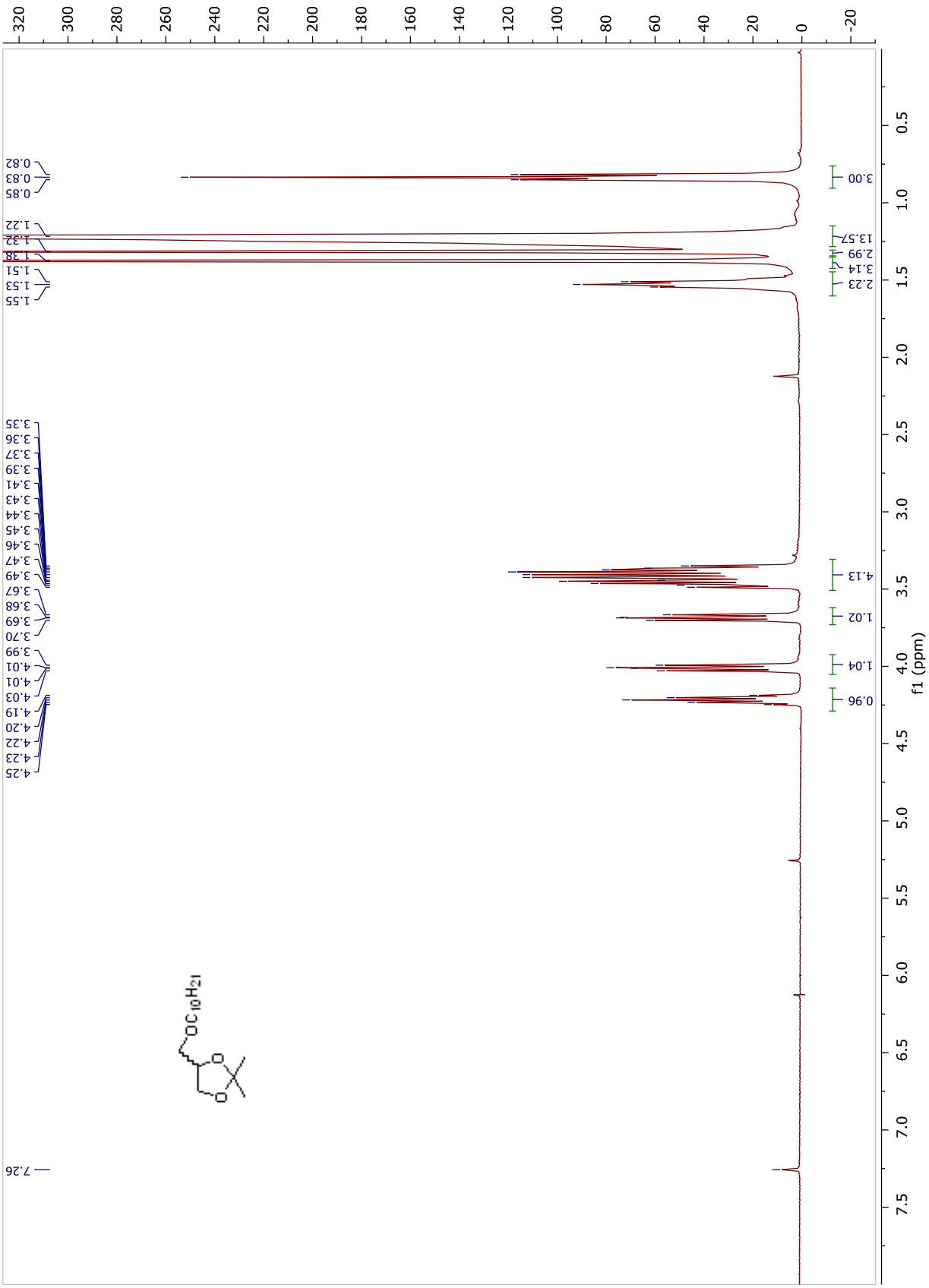

Compound 29. ^{1}H NMR and ^{13}C APT NMR spectra in $CDCl_3$

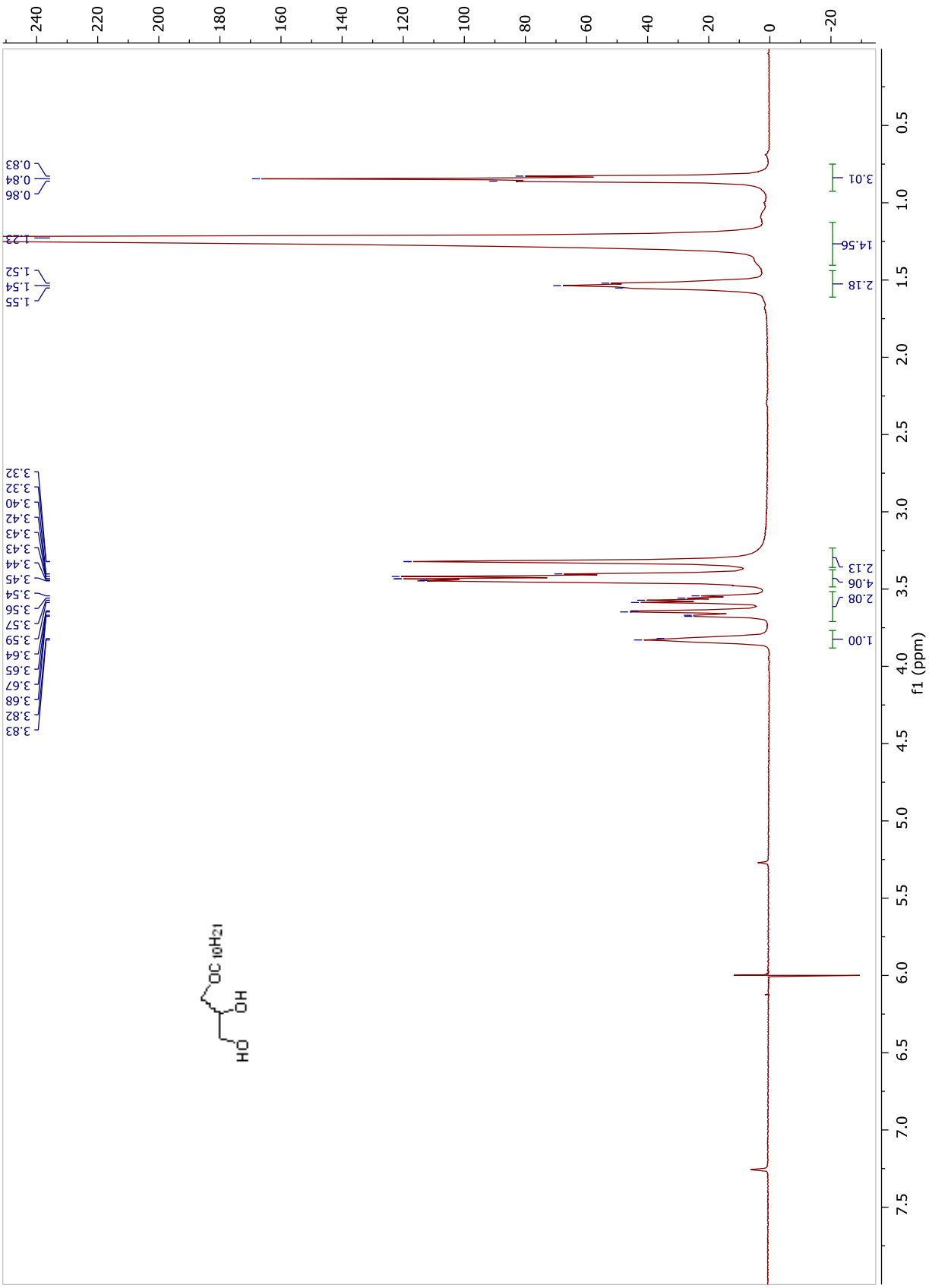

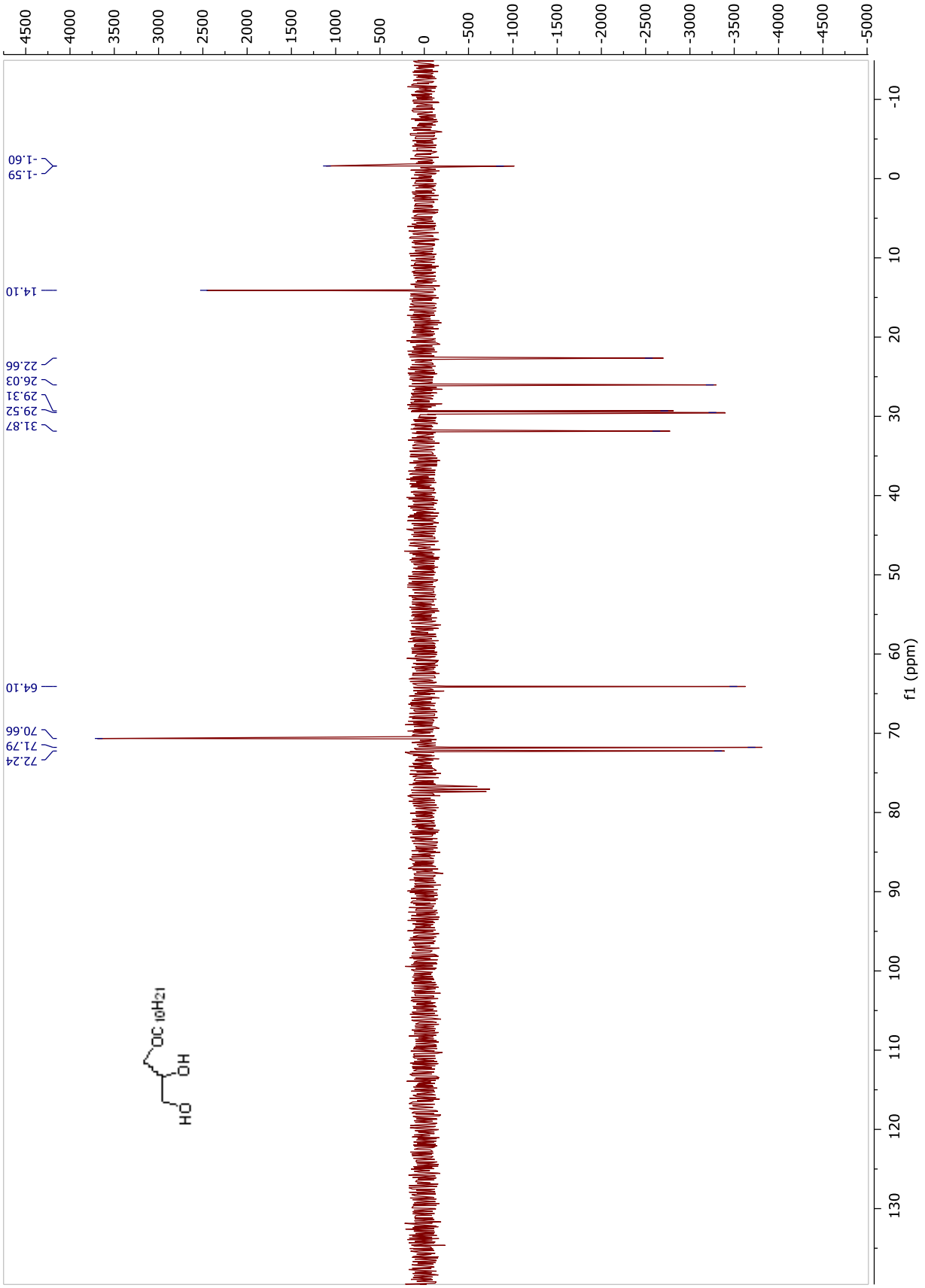
-1.59
-1.60
14.10
22.66
26.03
29.31
29.52
31.87
64.10
70.66
71.79
72.24
f1 (ppm)

Compound 30. ^{1}H NMR and ^{13}C-APT NMR spectra in $CDCl_3$

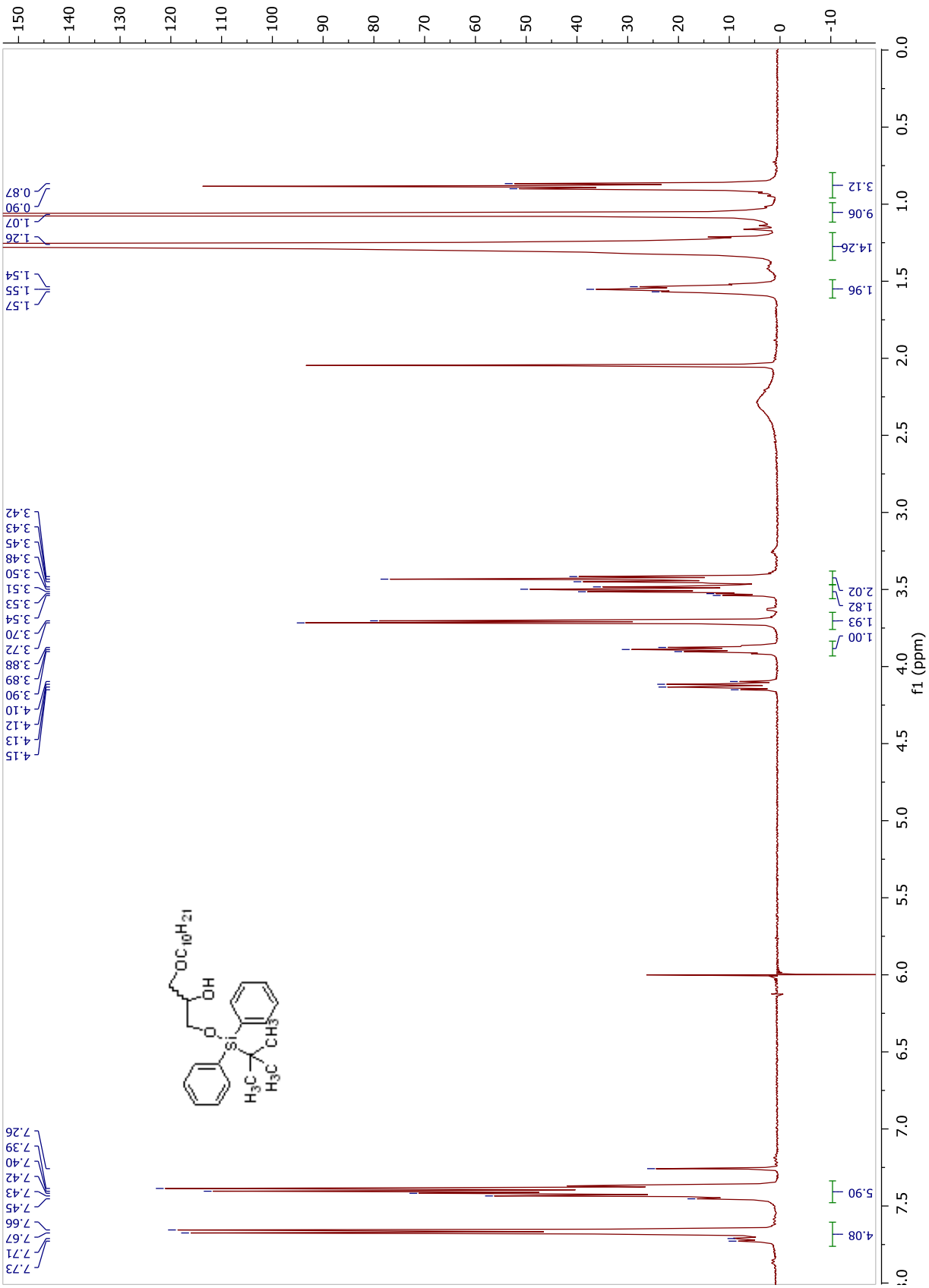

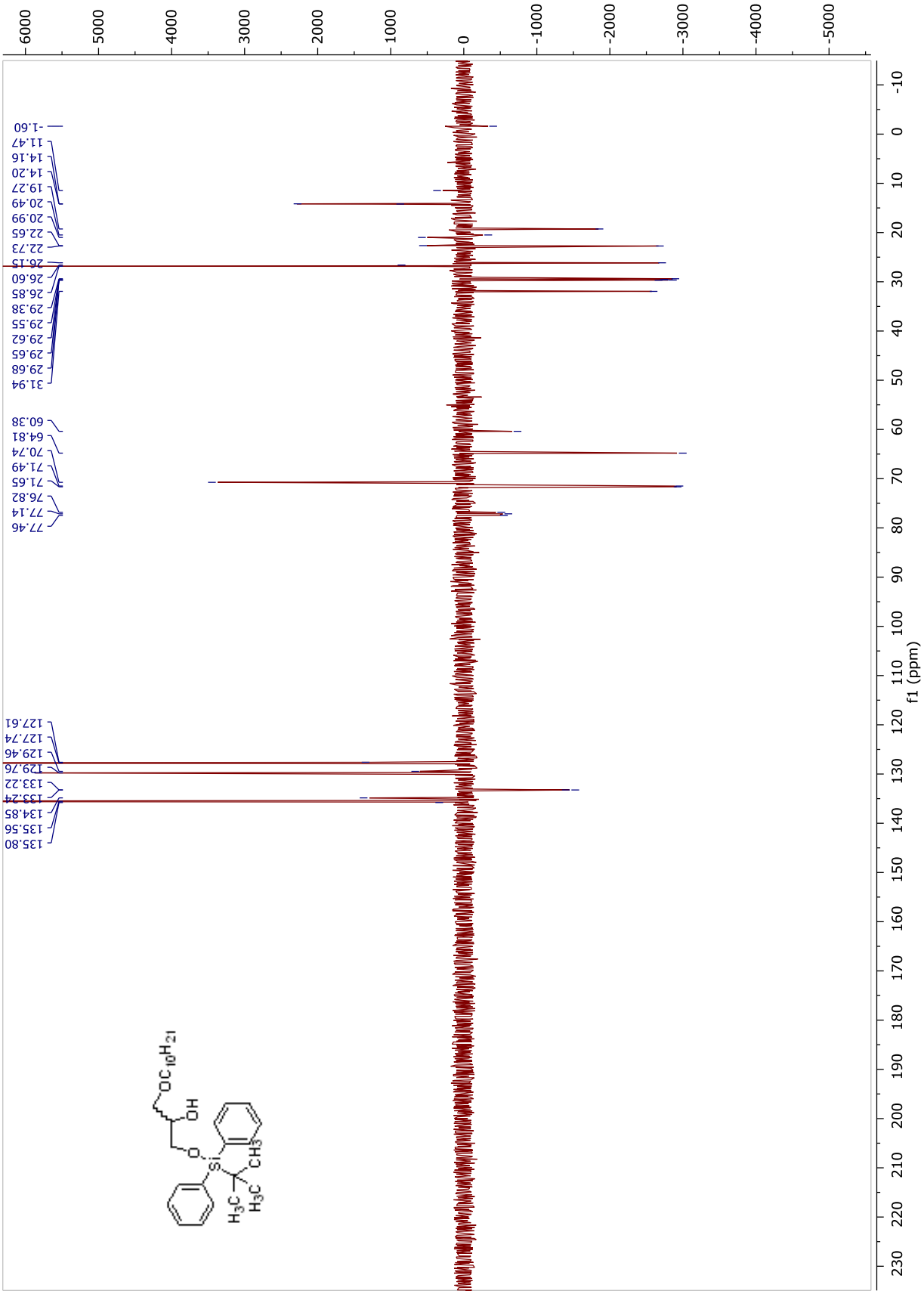
-1.60
11.47
14.16
14.20
19.27
20.49
20.99
22.65
22.73
26.15
26.60
26.85
29.38
29.55
29.62
29.65
29.68
31.94
60.38
64.81
70.74
71.49
71.65
76.82
77.14
77.46
127.61
127.74
129.46
129.76
133.22
133.24
134.85
135.56
135.80
f1 (ppm)

Compound 31. ^{1}H NMR and ^{13}C APT NMR spectra in $CDCl_3$

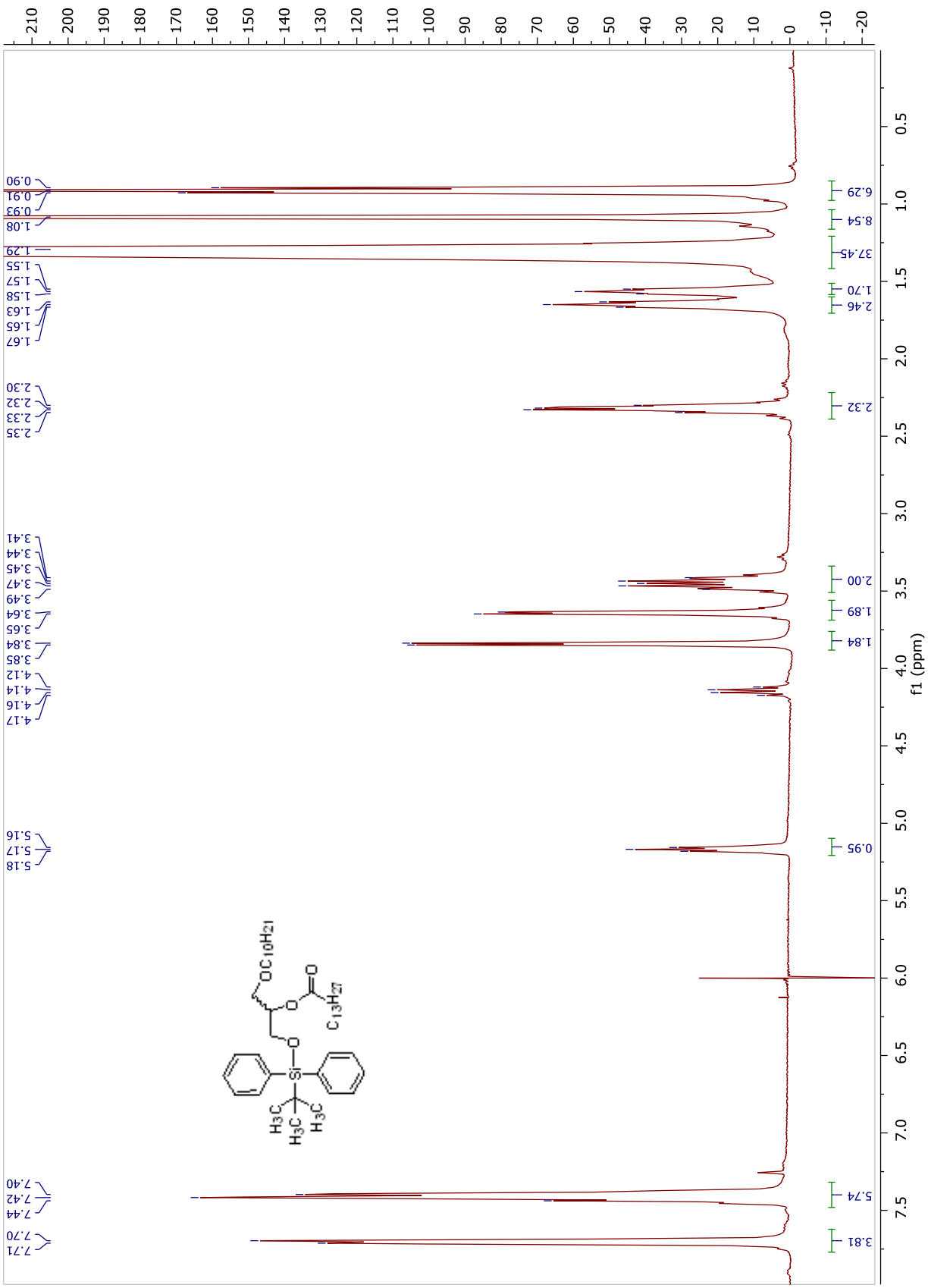

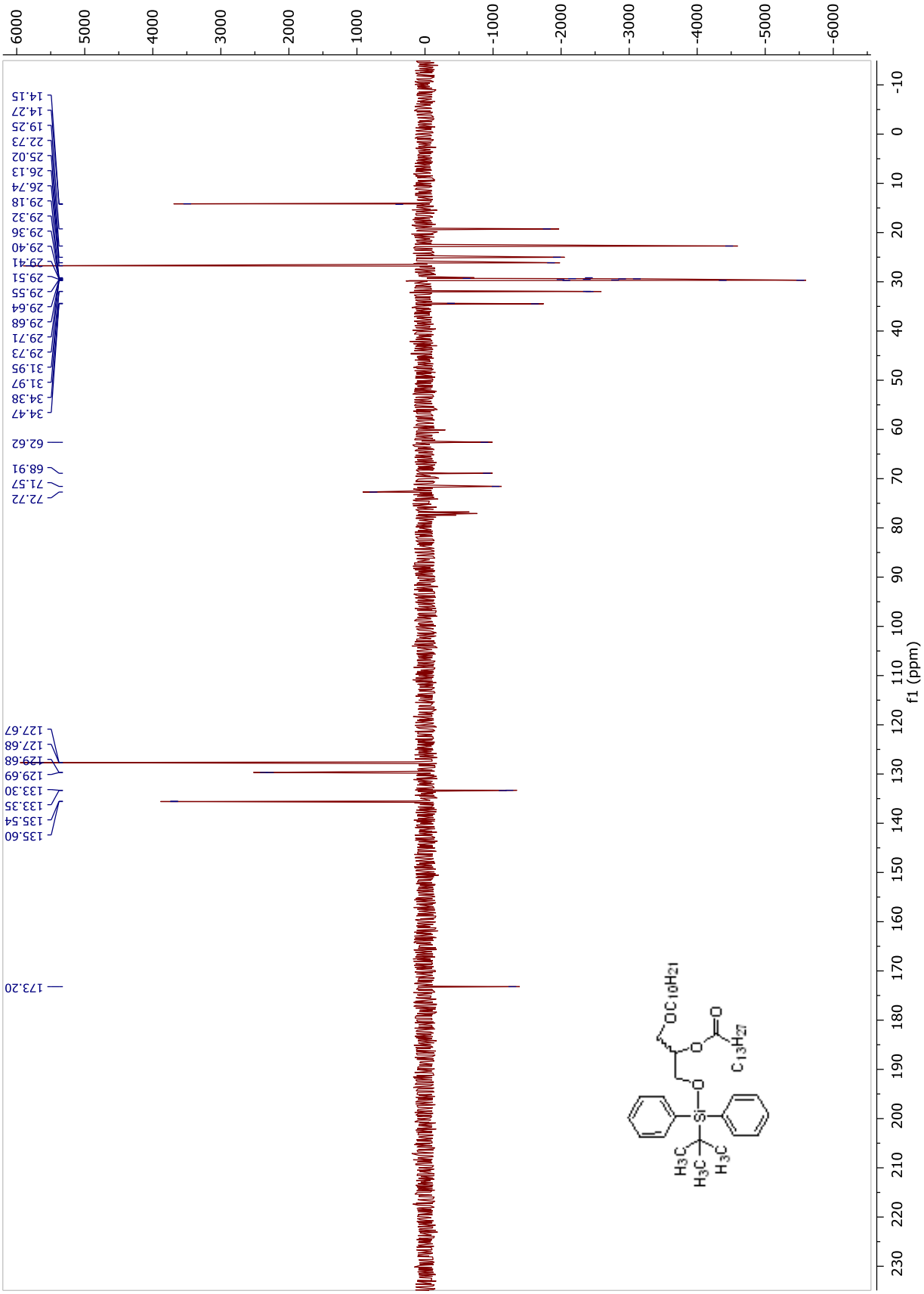
14.15
14.27
19.25
22.73
25.02
26.13
26.74
29.18
29.32
29.36
29.40
29.41
29.51
29.55
29.64
29.68
29.71
29.73
31.95
31.97
34.38
34.47
62.62
68.91
71.57
72.72
127.67
127.68
129.68
129.69
133.30
133.35
135.54
135.60
173.20
f1 (ppm)

Compound 32. ^{1}H NMR and ^{13}C APT NMR spectra in $CDCl_3$

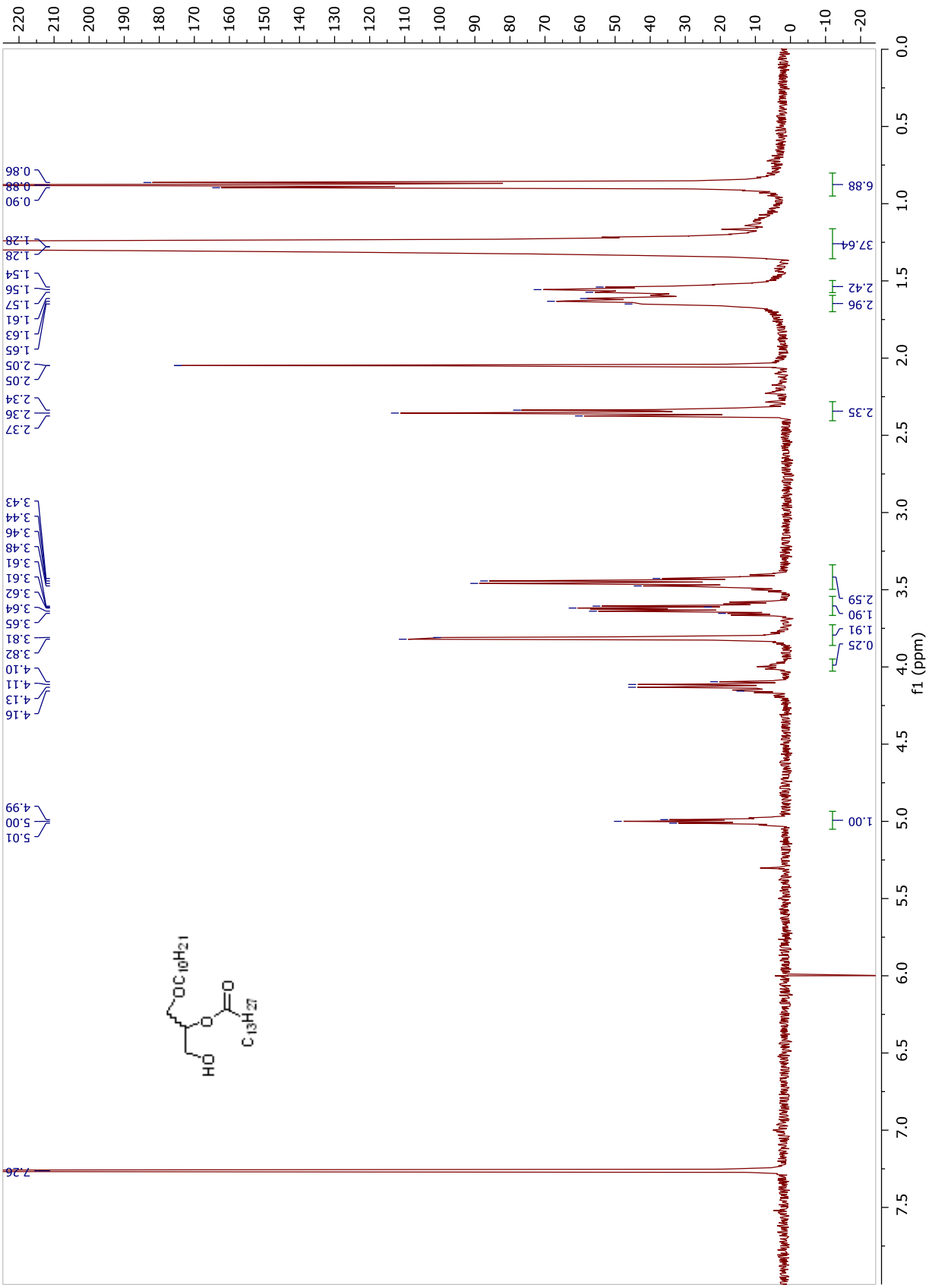

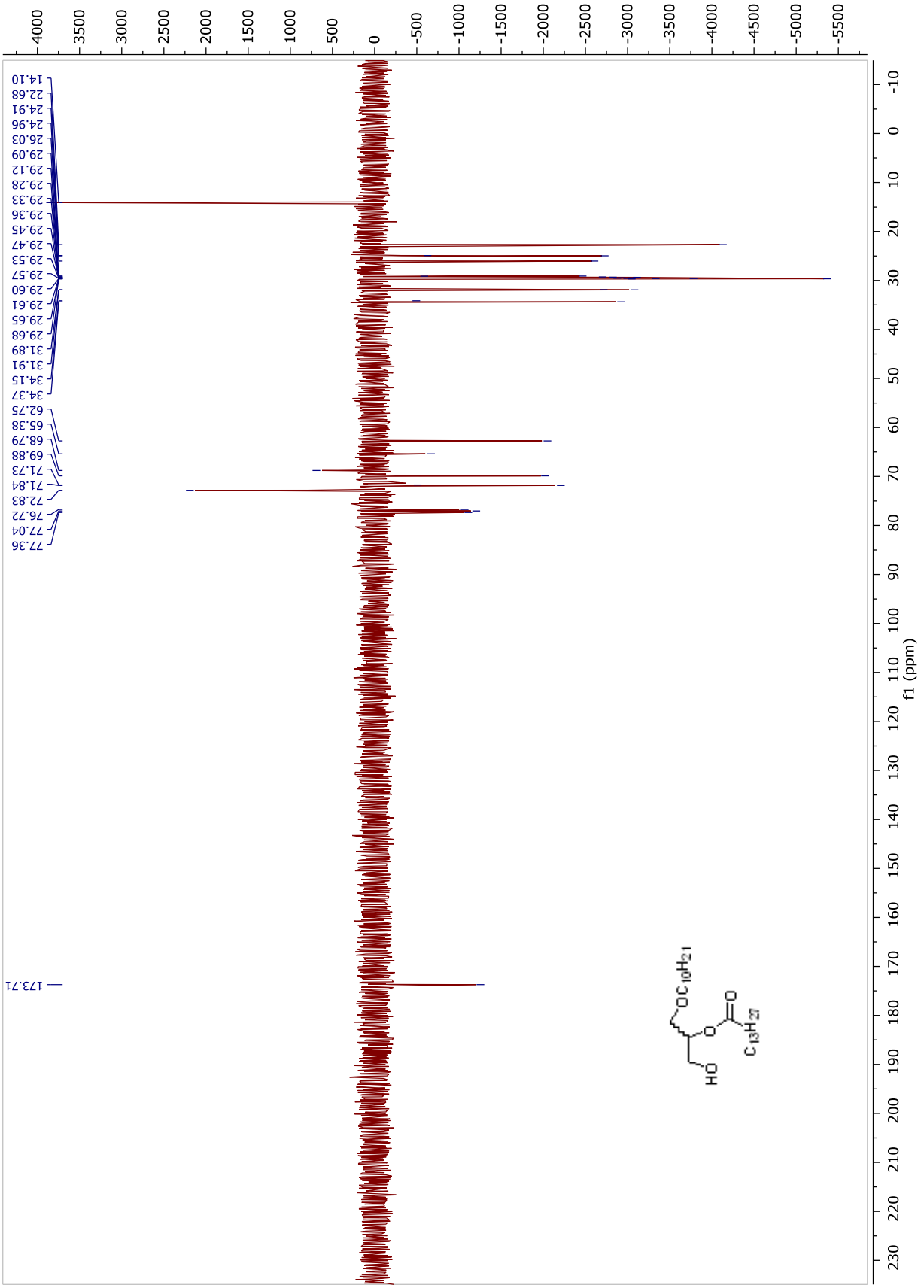
14.10
22.68
24.91
24.96
26.03
29.09
29.12
29.28
29.33
29.36
29.45
29.47
29.53
29.57
29.60
29.61
29.65
29.68
31.89
31.91
34.15
34.37
62.75
65.38
68.79
69.88
71.73
71.84
72.83
76.72
77.04
77.36
173.71
f1 (ppm)
HO
O
O
C10H21
C13H27

Compound B3. ^{1}H NMR and ^{13}C APT NMR spectra in $CDCl_3$

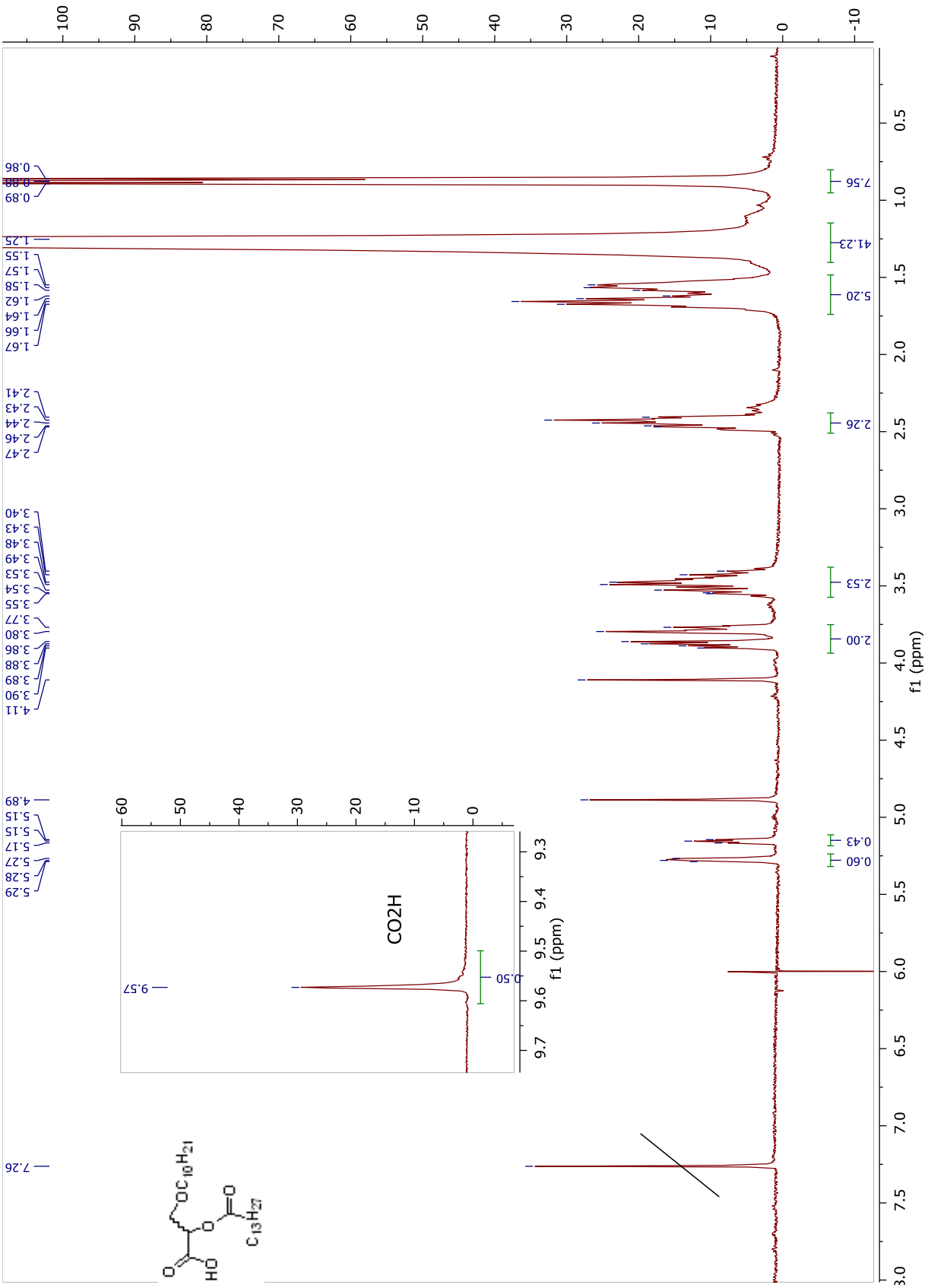

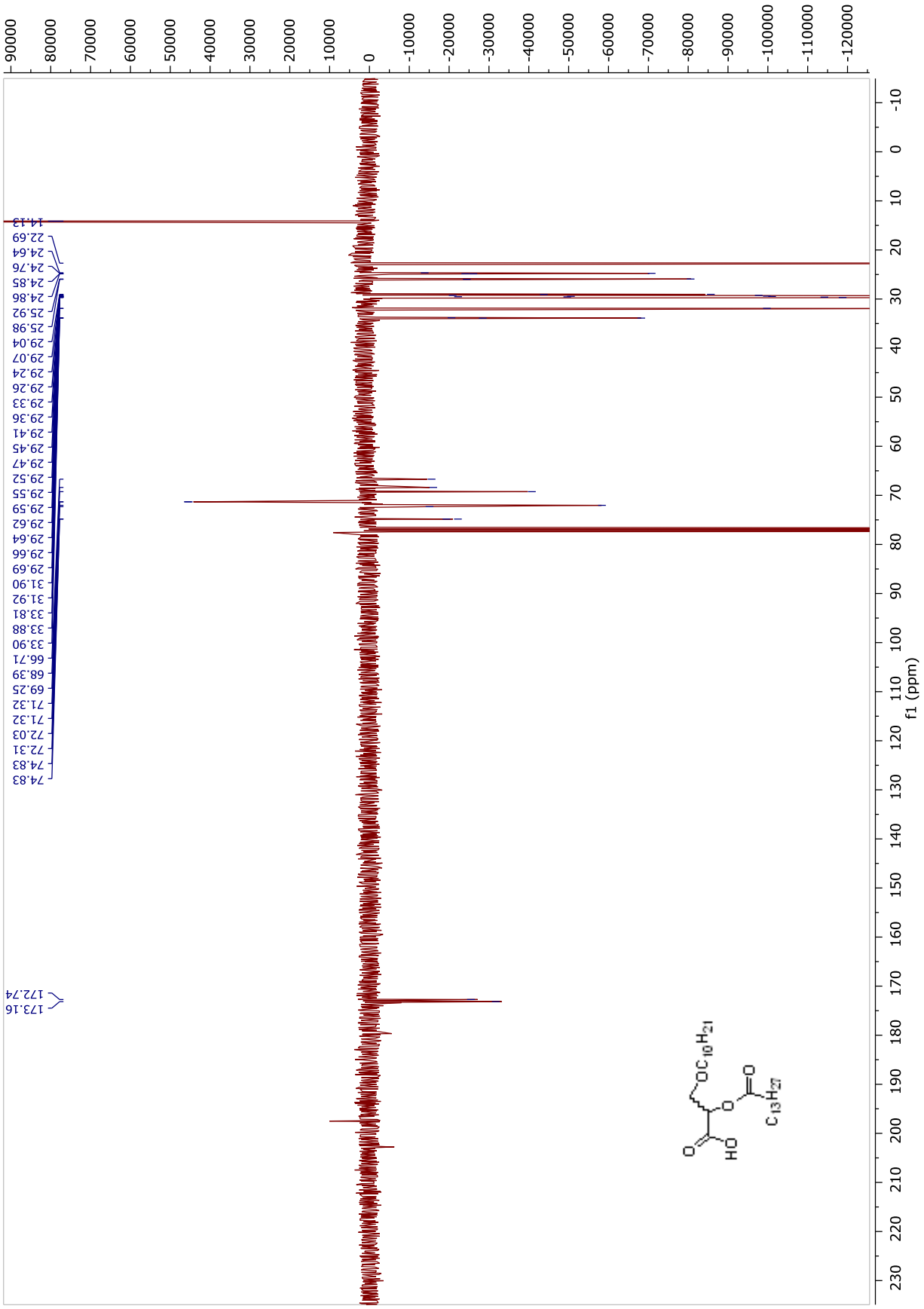
14.13
22.69
24.64
24.76
24.85
24.86
25.92
25.98
29.04
29.07
29.24
29.26
29.33
29.36
29.41
29.45
29.47
29.52
29.55
29.59
29.62
29.64
29.66
29.69
31.90
31.92
33.81
33.88
33.90
66.71
68.39
69.25
71.32
72.03
72.31
74.83
74.83
172.74
173.16
f1 (ppm)

Chain B1 Synthesis: ^{1}H NMR and ^{13}C-APT NMR spectra

Compound 33. ^{1}H NMR and ^{13}C APT NMR spectra in $CDCl_3$

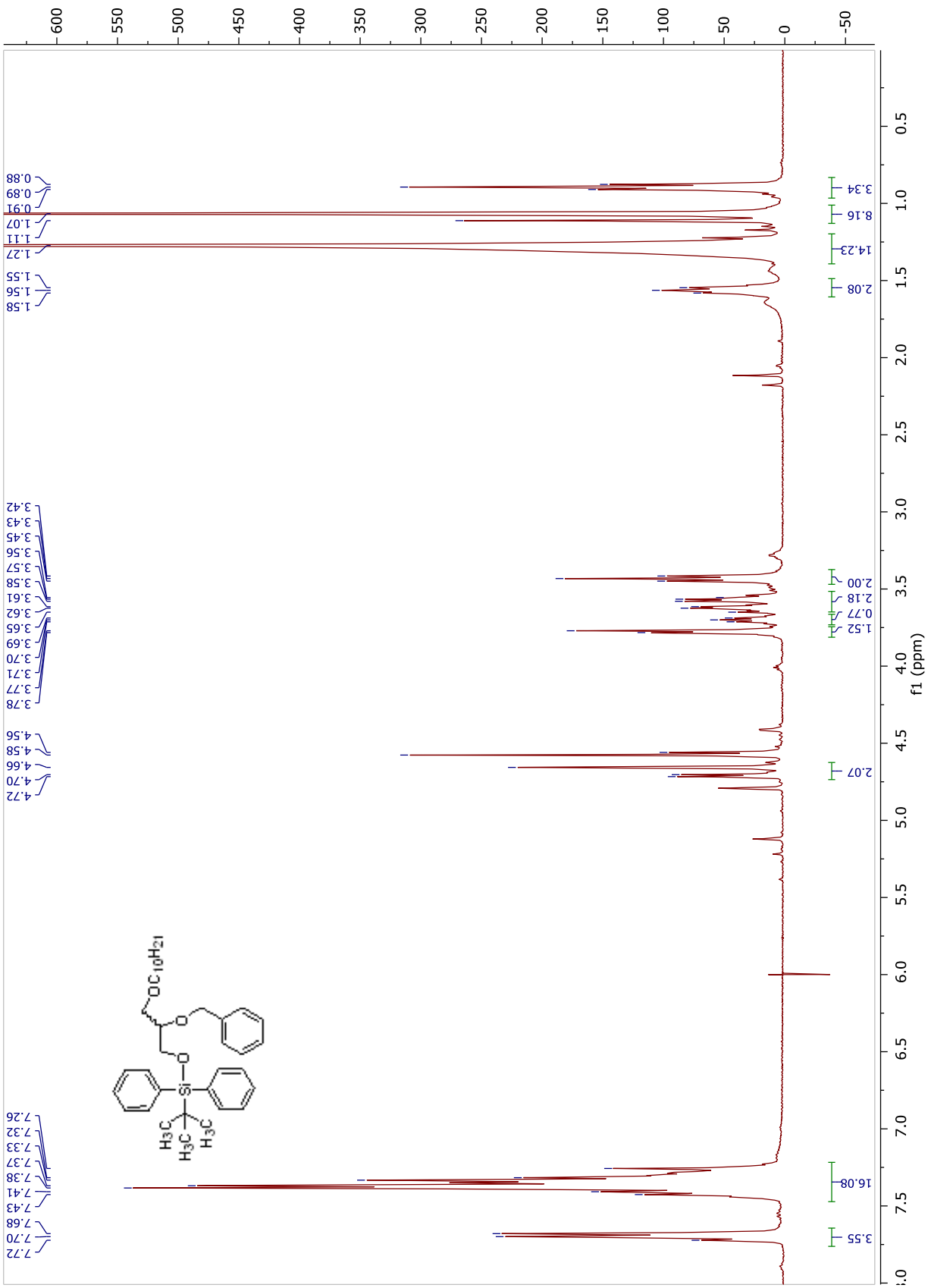

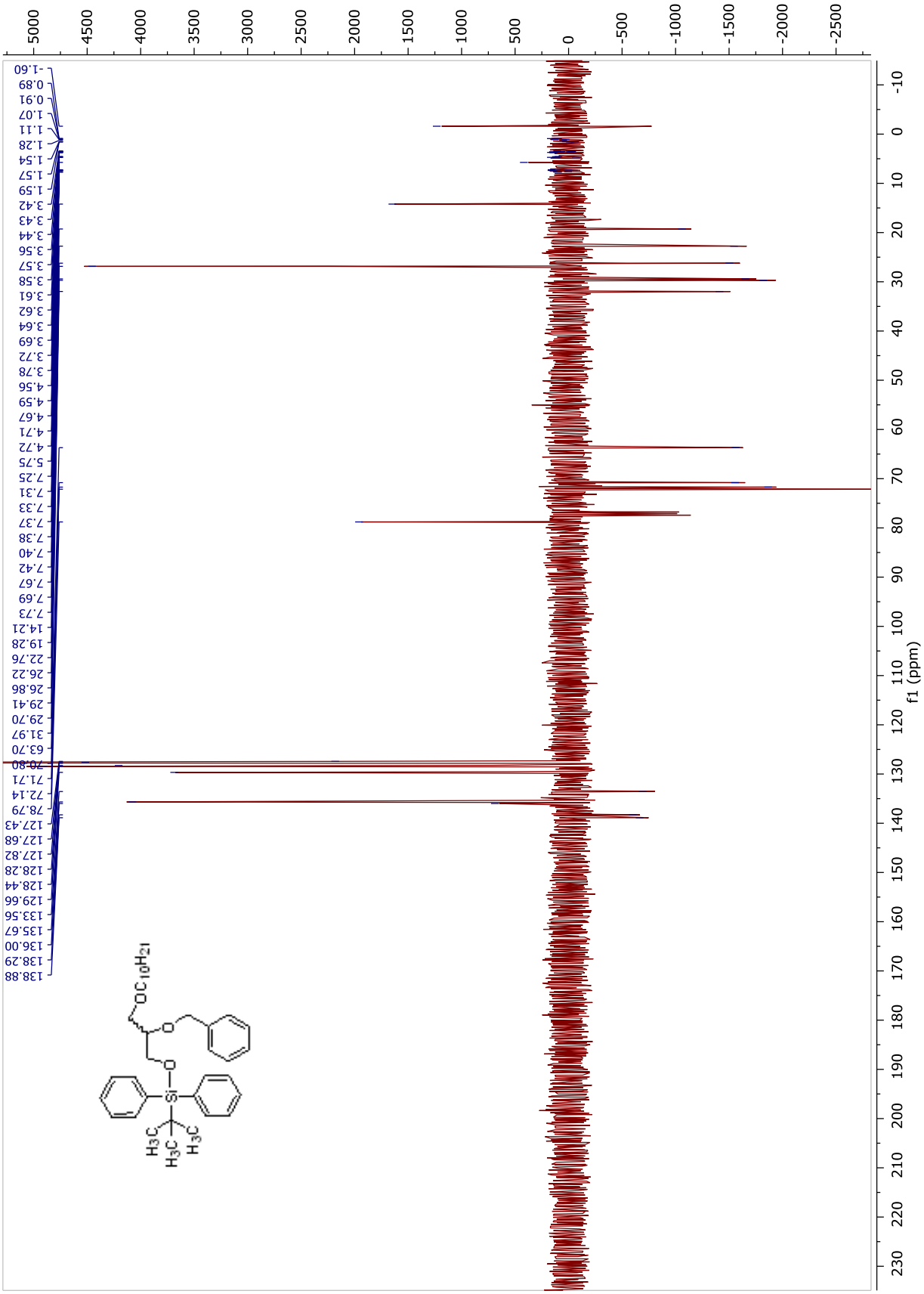
f1 (ppm)
OC10H21
O
O
Si
H3C
H3C
H3C

Compound 34. ^{1}H NMR and ^{13}C APT NMR spectra in $CDCl_3$

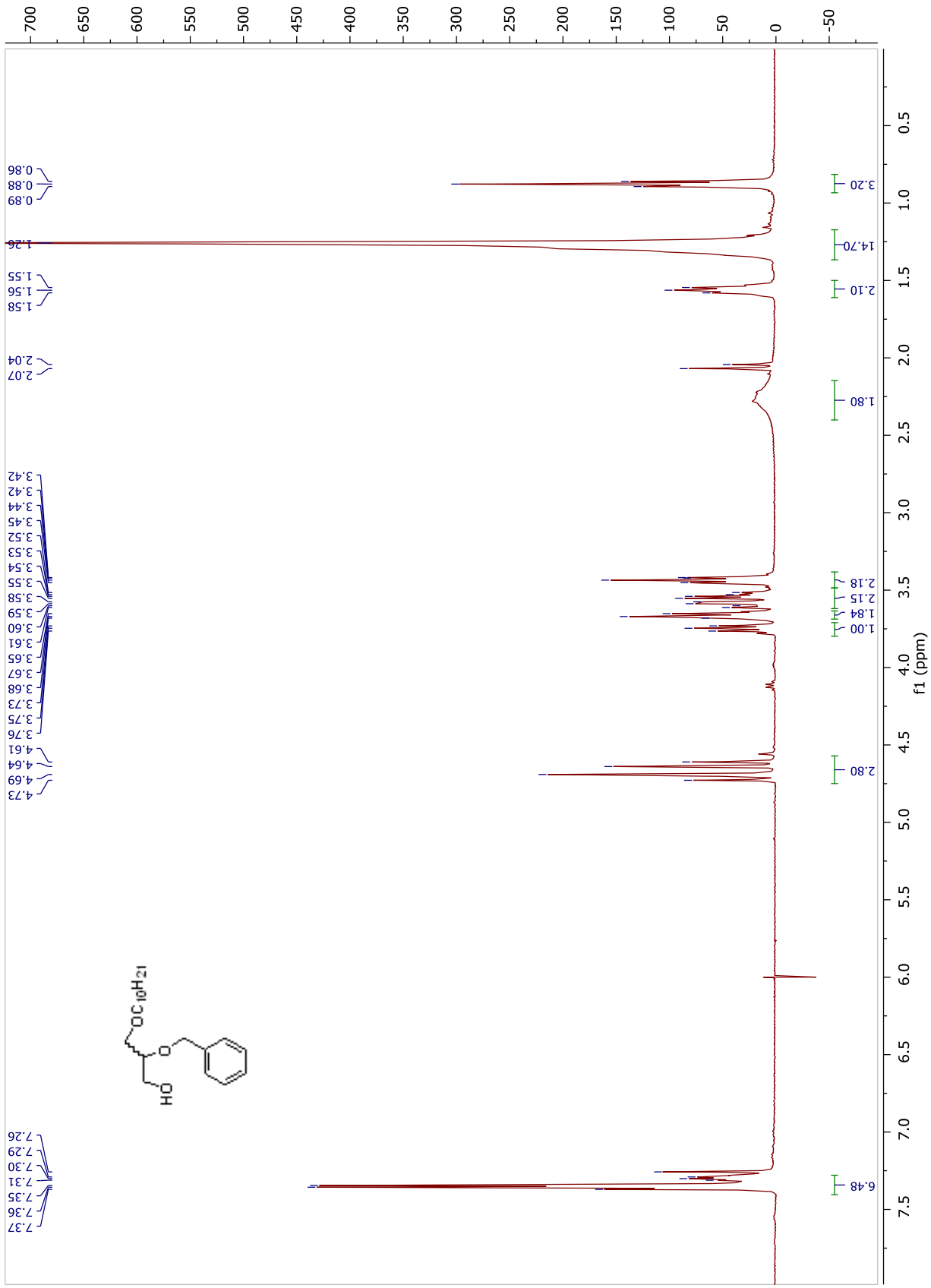

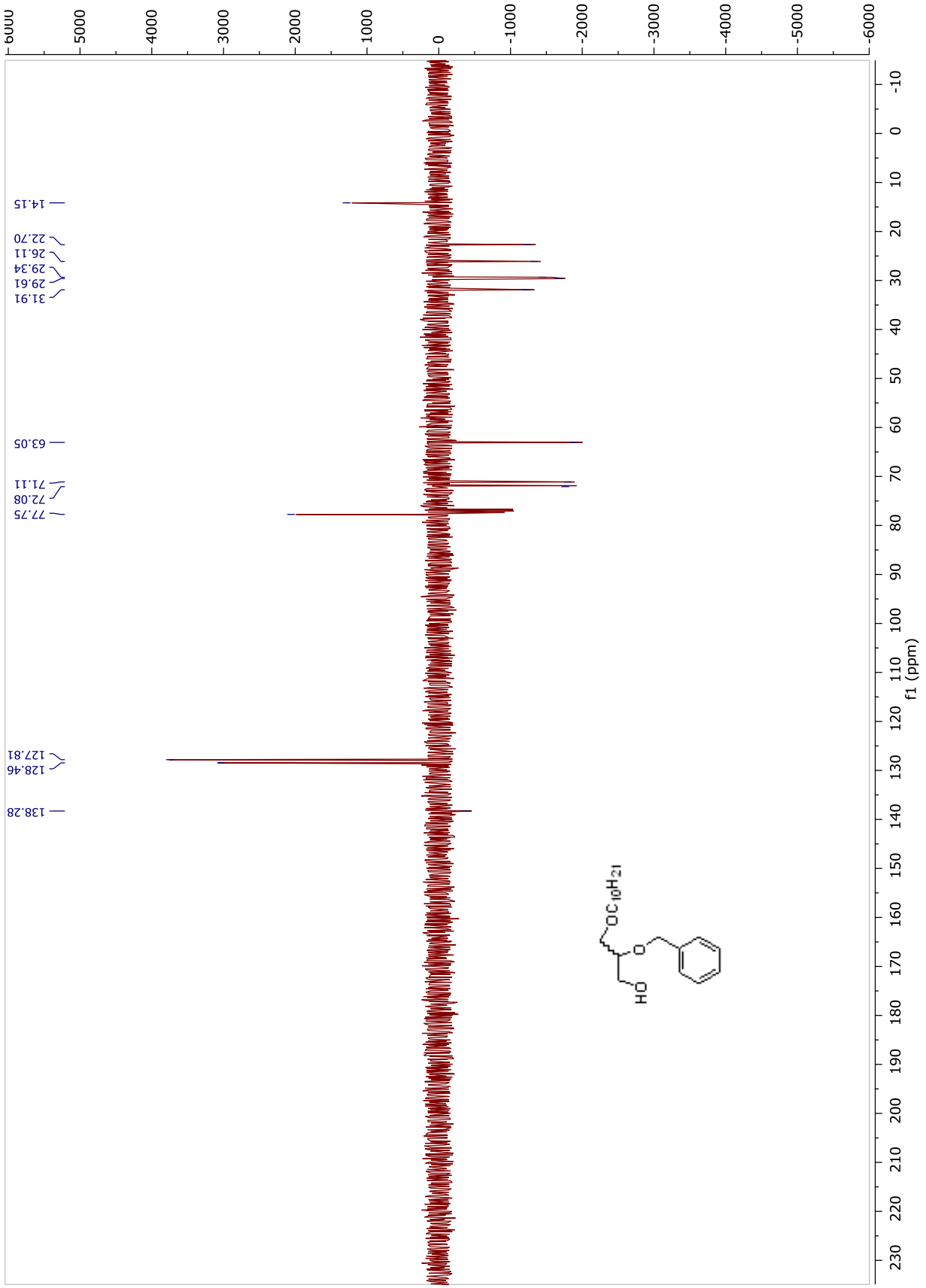
14.15
22.70
26.11
29.34
29.61
31.91
63.05
71.11
72.08
77.75
127.81
128.46
138.28
OC10H21
O
HO
f1 (ppm)

Compound B1. ^{1}H NMR and ^{13}C APT NMR spectra in $CDCl_3$

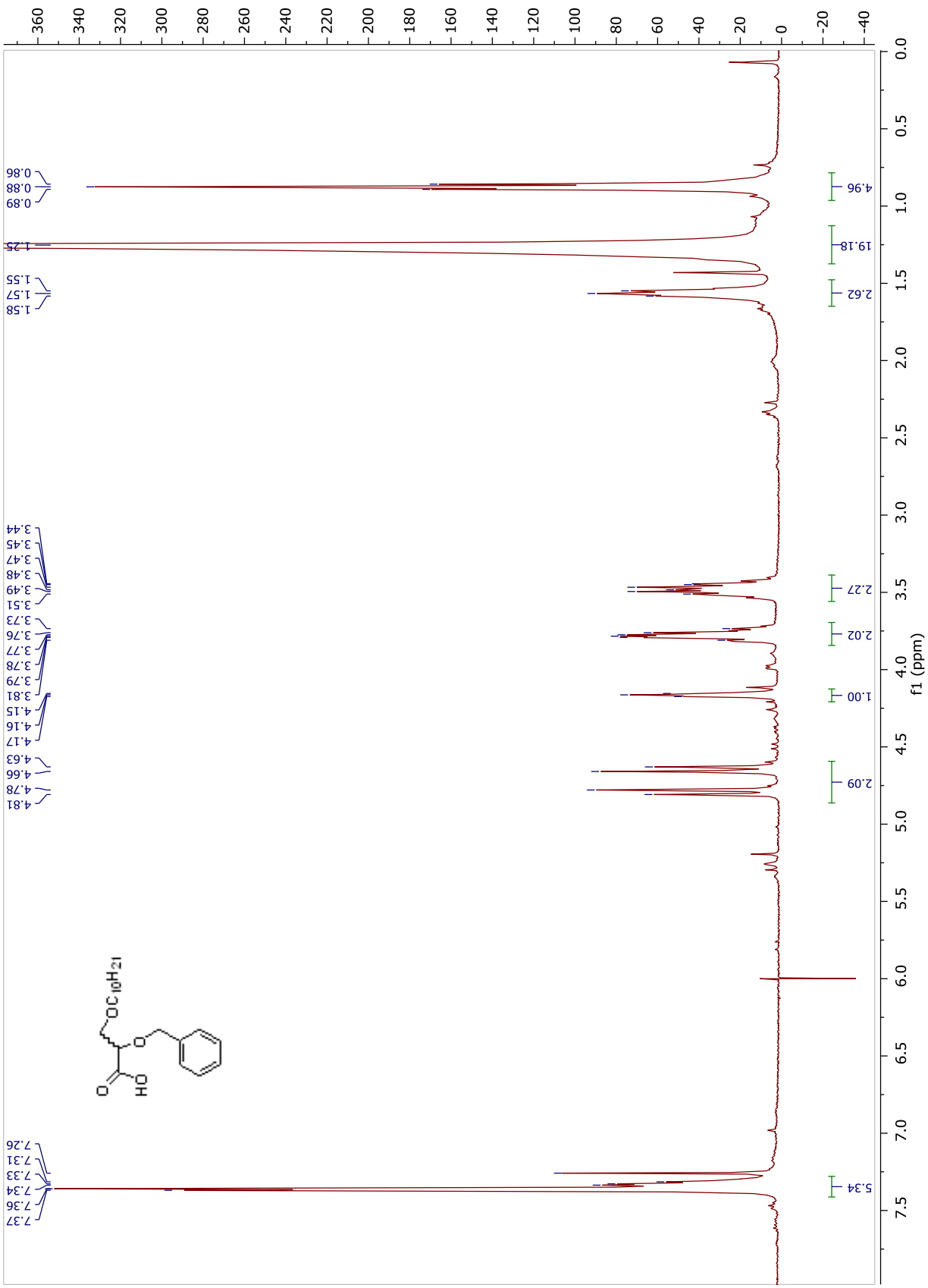

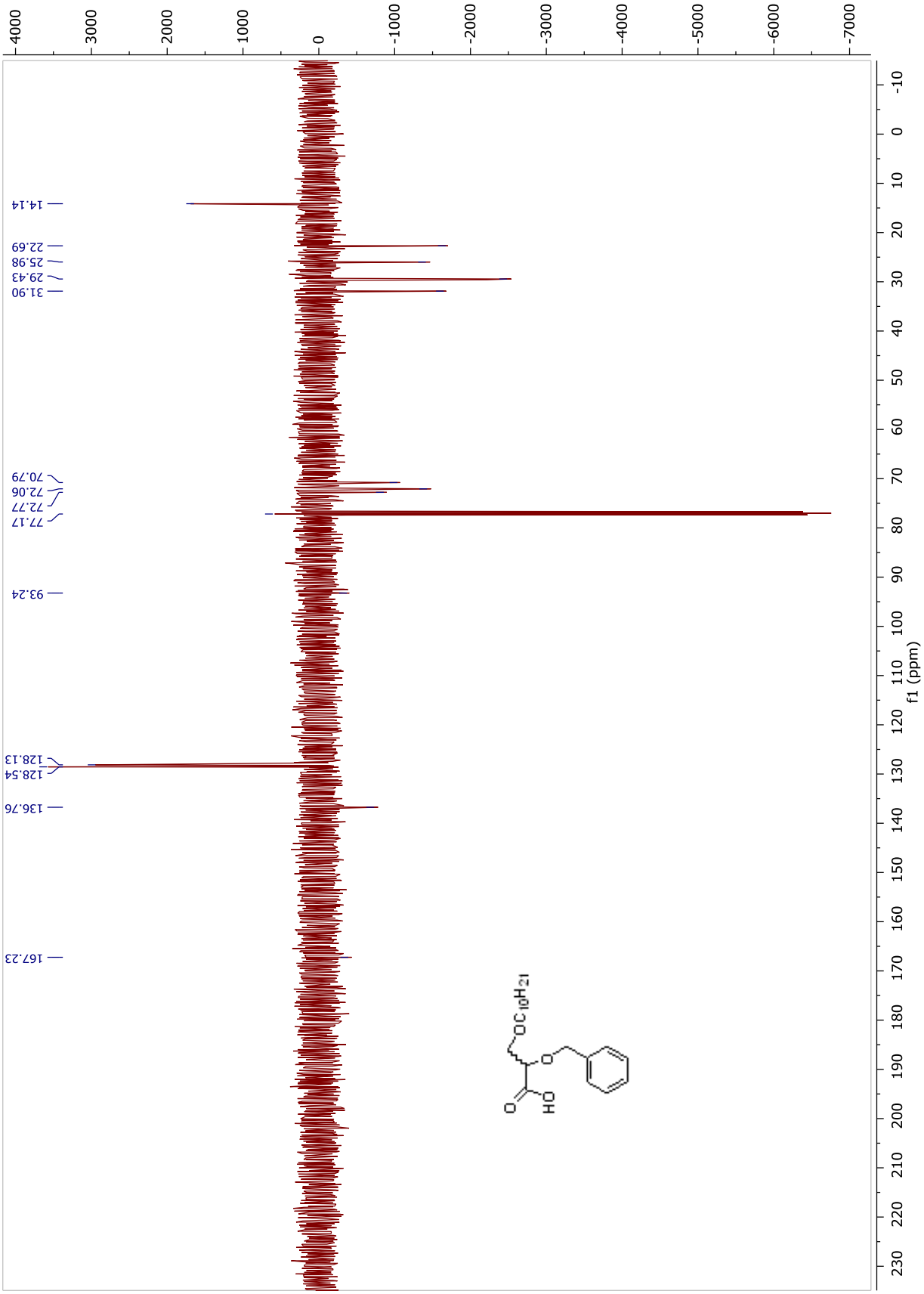
14.14
22.69
25.98
29.43
31.90
70.79
72.06
72.77
77.17
93.24
128.13
128.54
136.76
167.23
f1 (ppm)

AMX1 Partial Synthesis: ^{1}H NMR and ^{13}C-APT NMR spectra

Compound 35. ^{1}H NMR and ^{13}C APT NMR spectra in $CDCl_3$

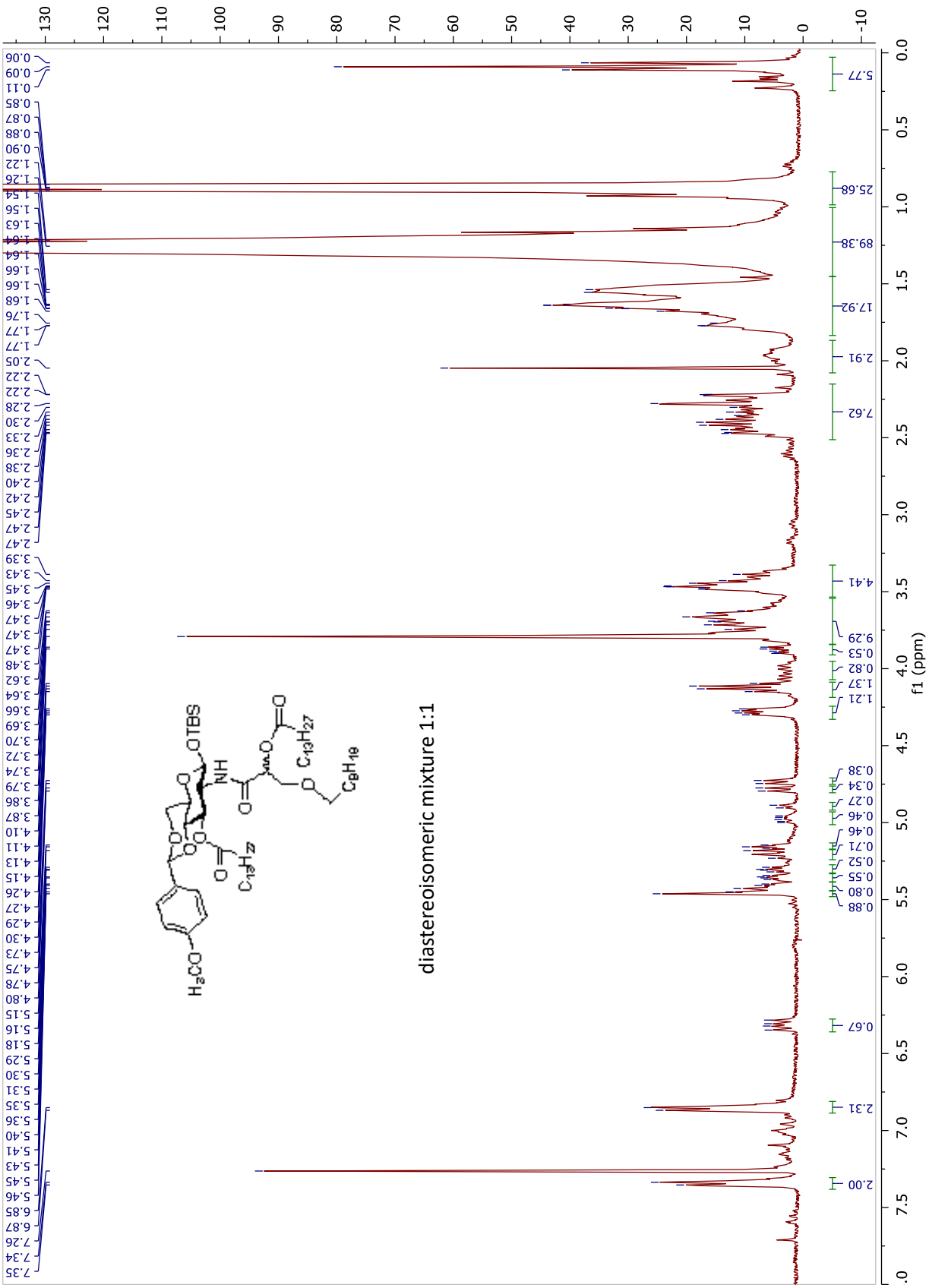

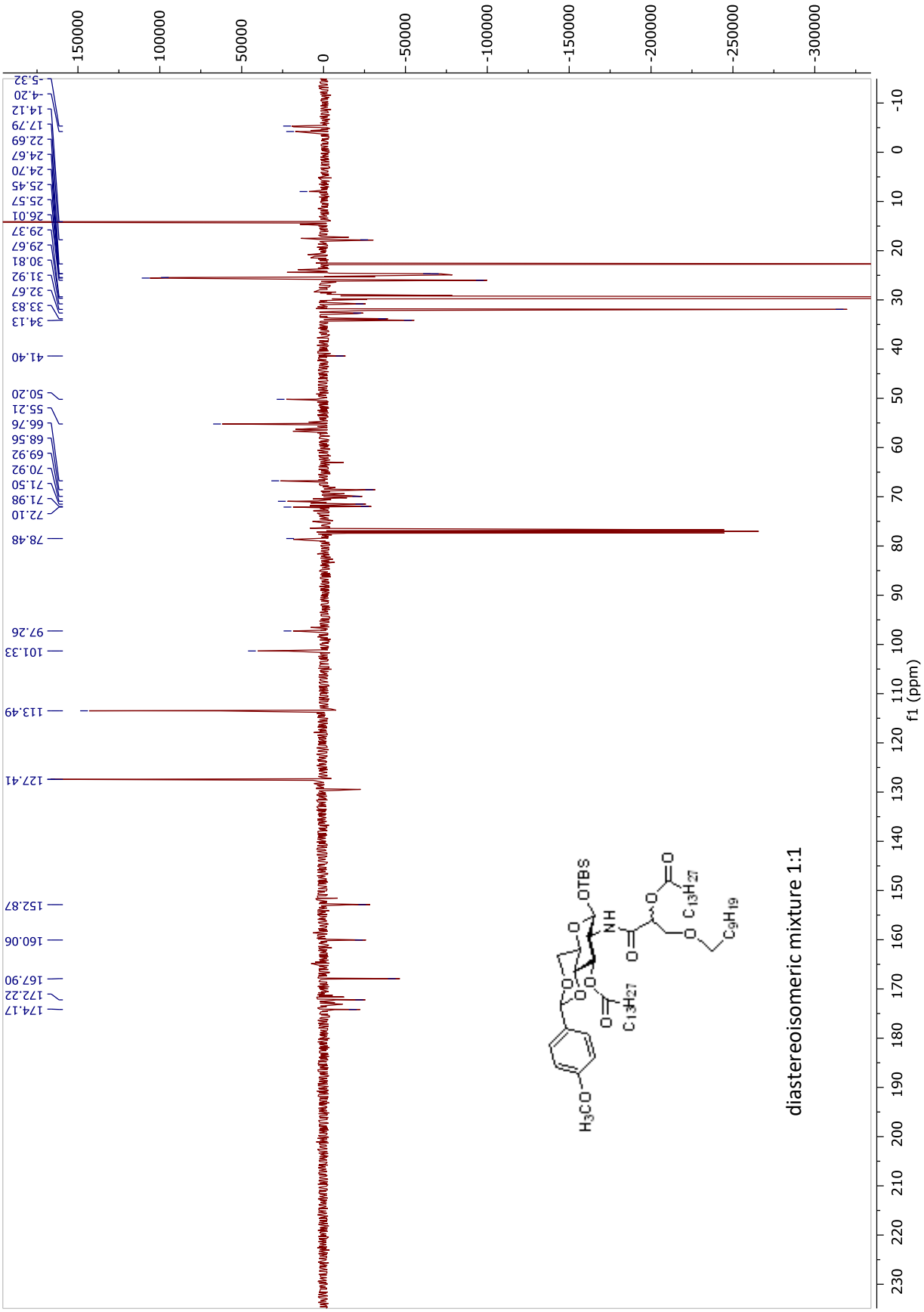
-5.32
-4.20
14.12
17.79
22.69
24.67
24.70
25.45
25.57
26.01
29.37
29.67
30.81
31.92
32.67
33.83
34.13
41.40
50.20
55.21
66.76
68.56
69.92
70.92
71.50
71.98
72.10
78.48
97.26
101.33
113.49
127.41
152.87
160.06
167.90
172.22
174.17
150000
100000
50000
0
-50000
-100000
-150000
-200000
-250000
-300000
-10
0
10
20
30
40
50
60
70
80
90
100
110
120
130
140
150
160
170
180
190
200
210
220
230
f1 (ppm)
OTBS
NH
$C_{13}H_{27}$
C_9H_{19}
H_3CO
diastereoisomeric mixture 1:1

Compound 36. ^{1}H NMR and ^{13}C APT NMR spectra in $CDCl_3$

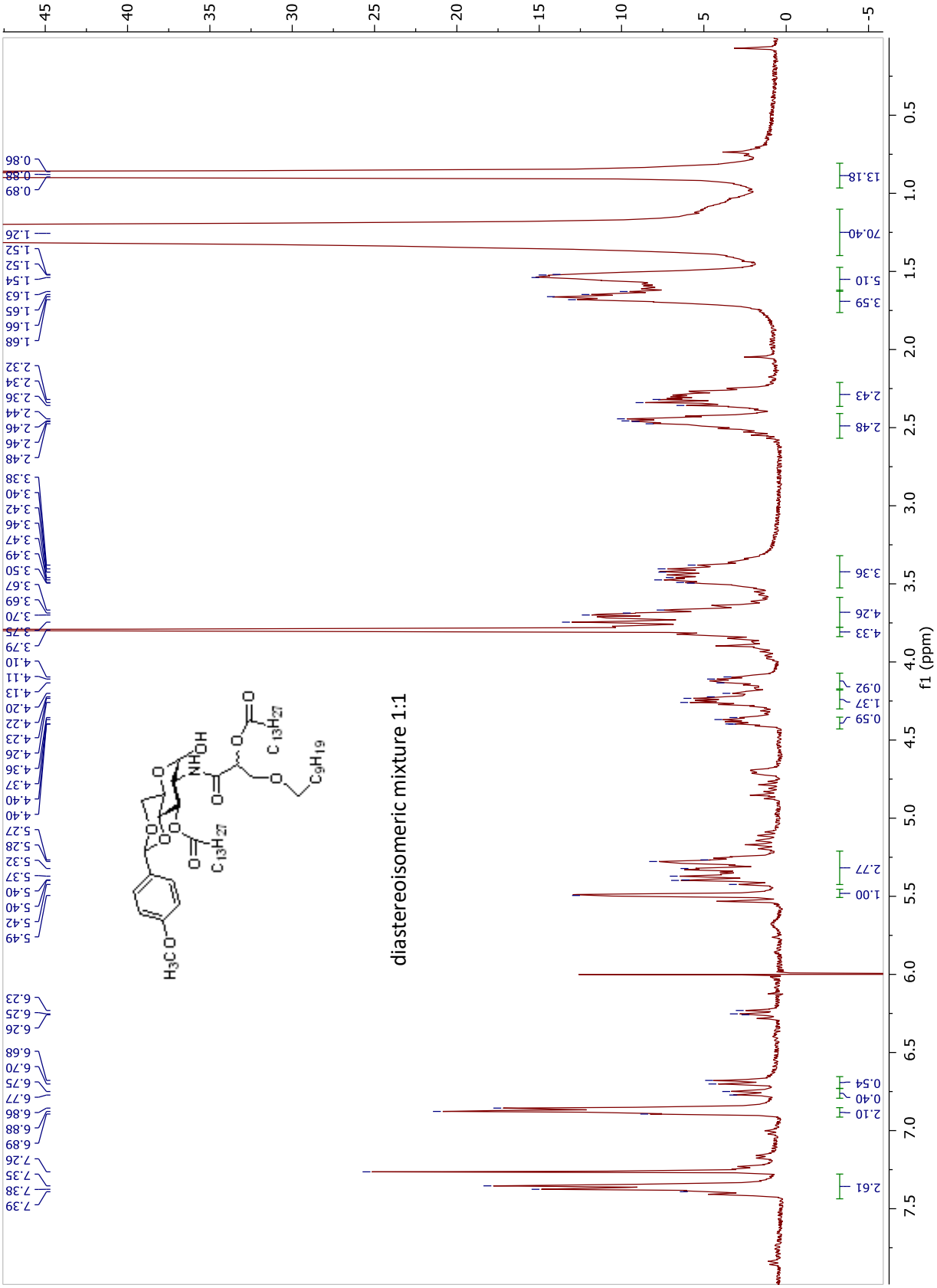

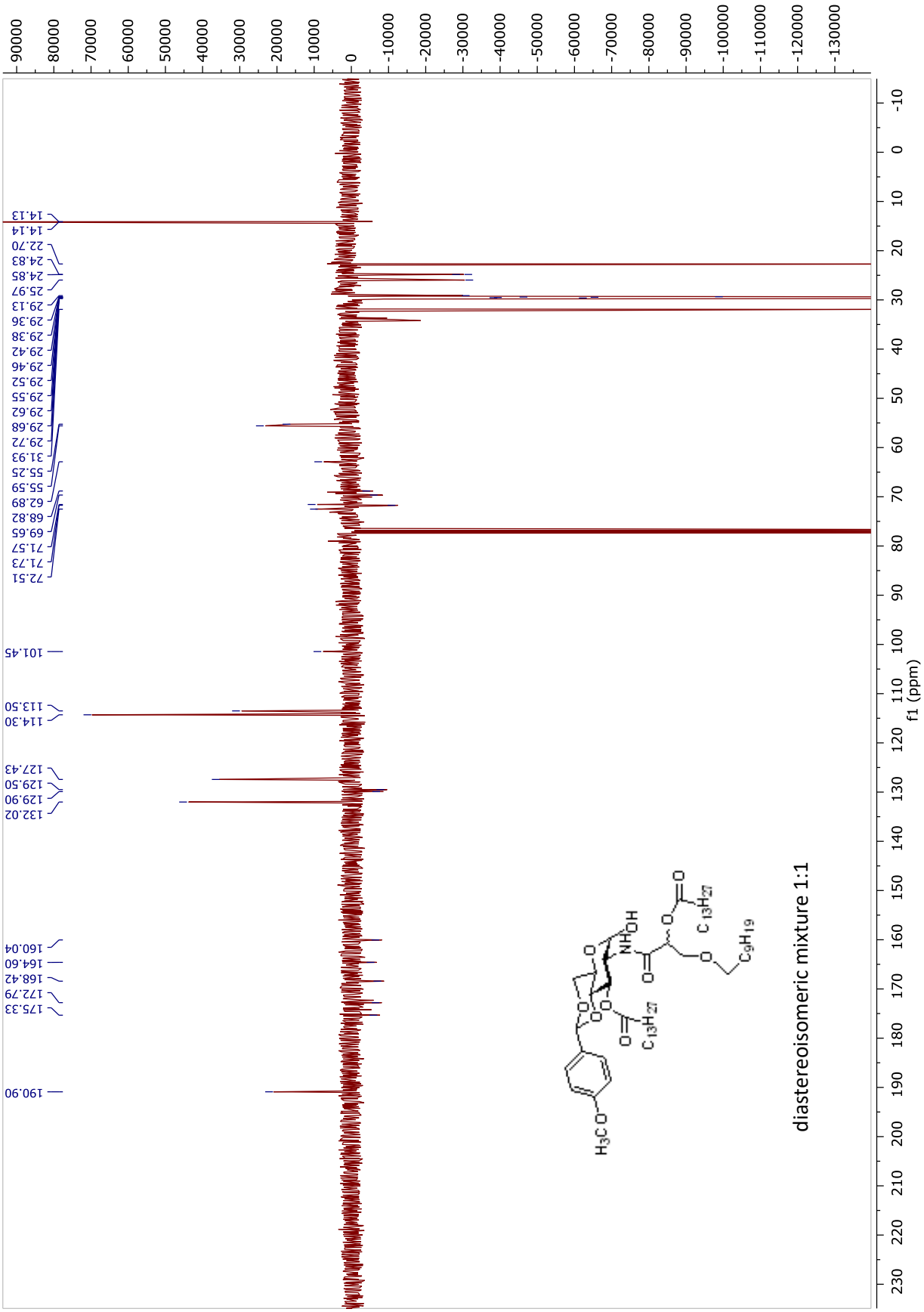
14.13
14.14
22.70
24.83
24.85
25.97
29.13
29.36
29.38
29.42
29.46
29.52
29.55
29.62
29.68
29.72
31.93
55.25
55.59
62.89
68.82
69.65
71.57
71.73
72.51
101.45
113.50
114.30
127.43
129.50
129.90
132.02
160.04
164.60
168.42
172.79
175.33
190.90
f1 (ppm)
diastereoisomeric mixture 1:1

AM241 Synthesis: ^{1}H NMR and ^{13}C-APT NMR spectra

Compound 44. ^{1}H NMR and ^{13}C APT NMR spectra in $CDCl_3$

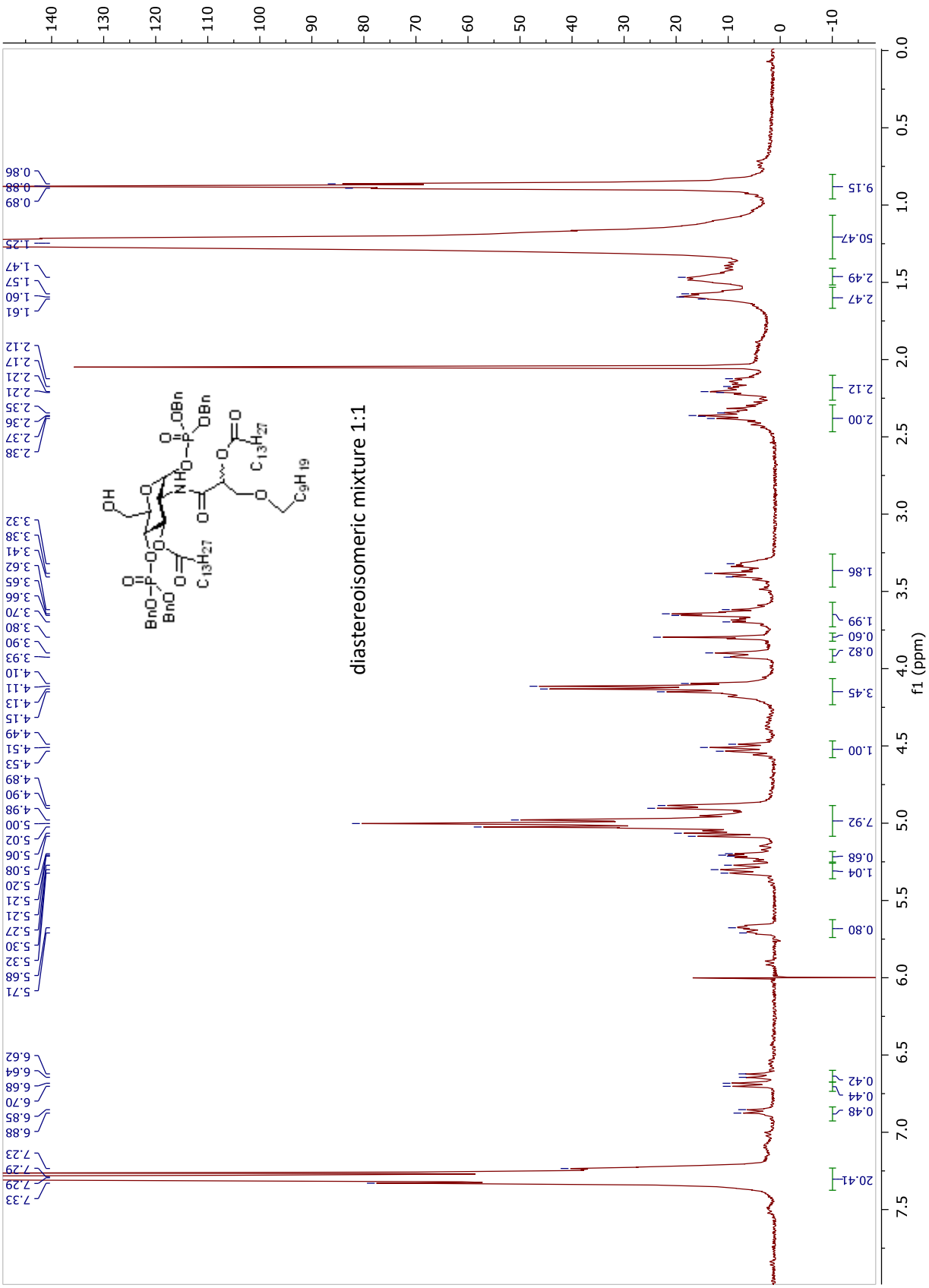

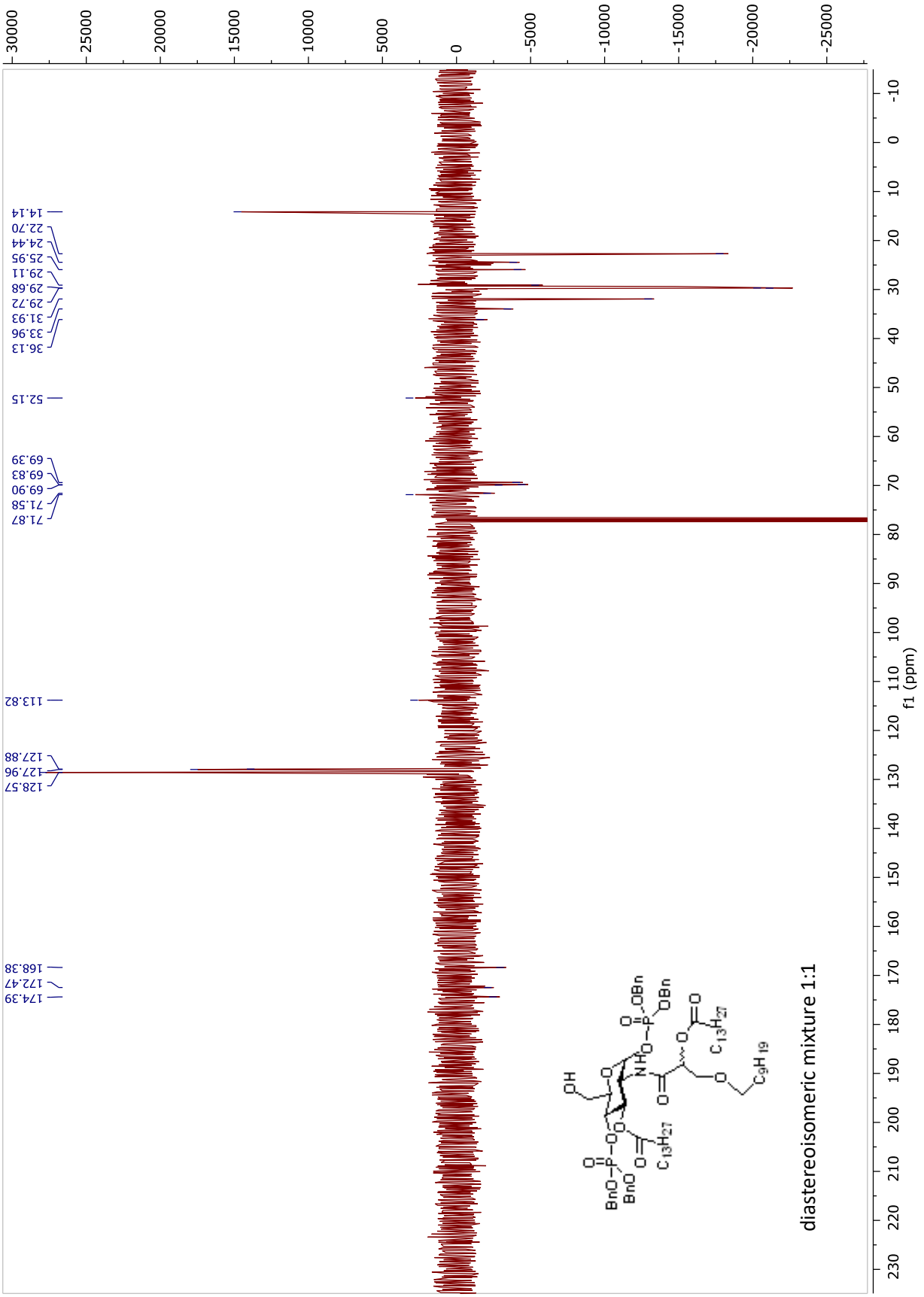
14.14
22.70
24.44
25.95
29.11
29.68
29.72
31.93
33.96
36.13
52.15
69.39
69.83
69.90
71.58
71.87
113.82
127.88
127.96
128.57
168.38
172.47
174.39
diastereoisomeric mixture 1:1
f1 (ppm)

Compound AM241. ^{1}H NMR and ^{13}C APT NMR spectra in CD_3OD

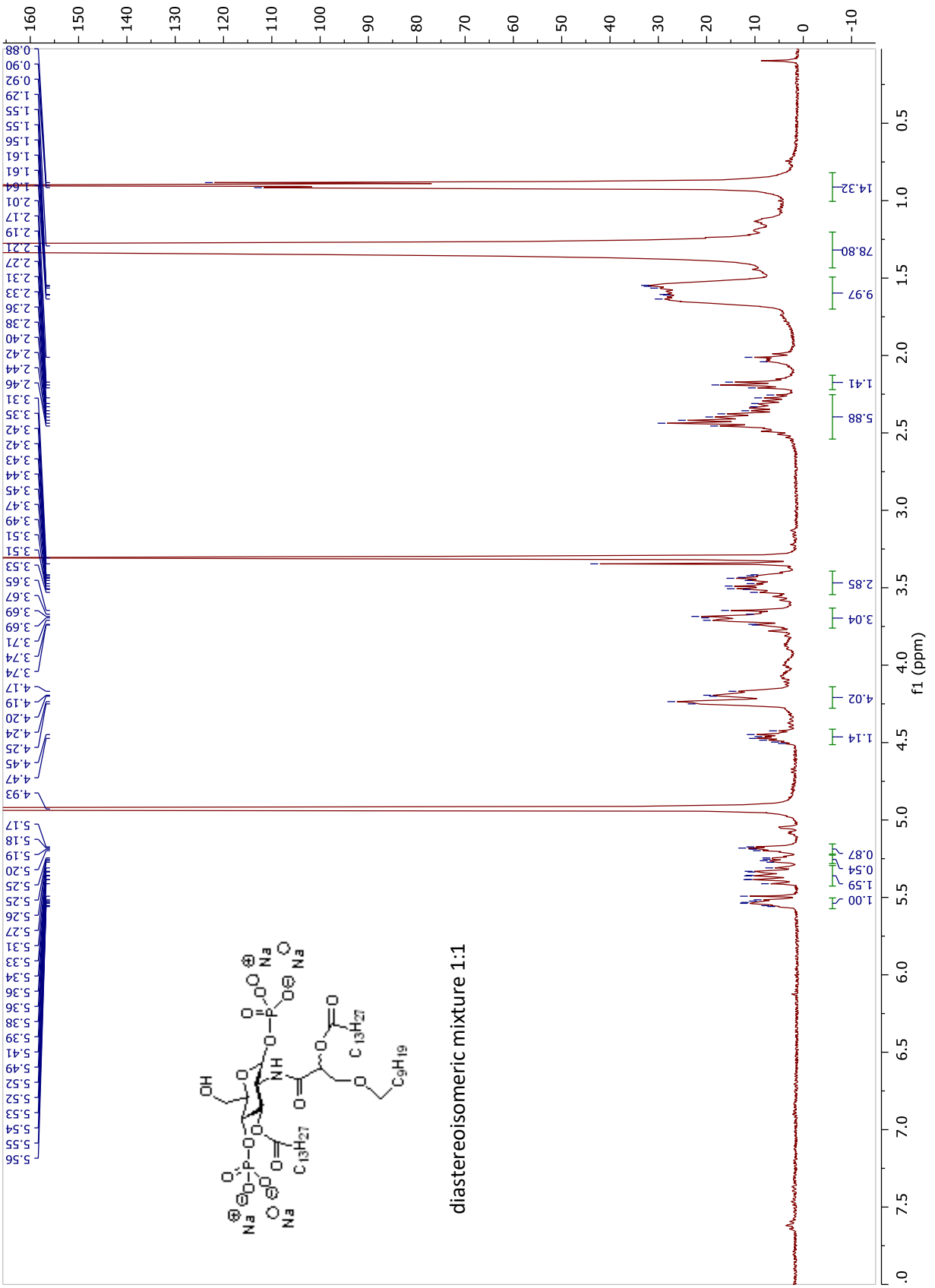

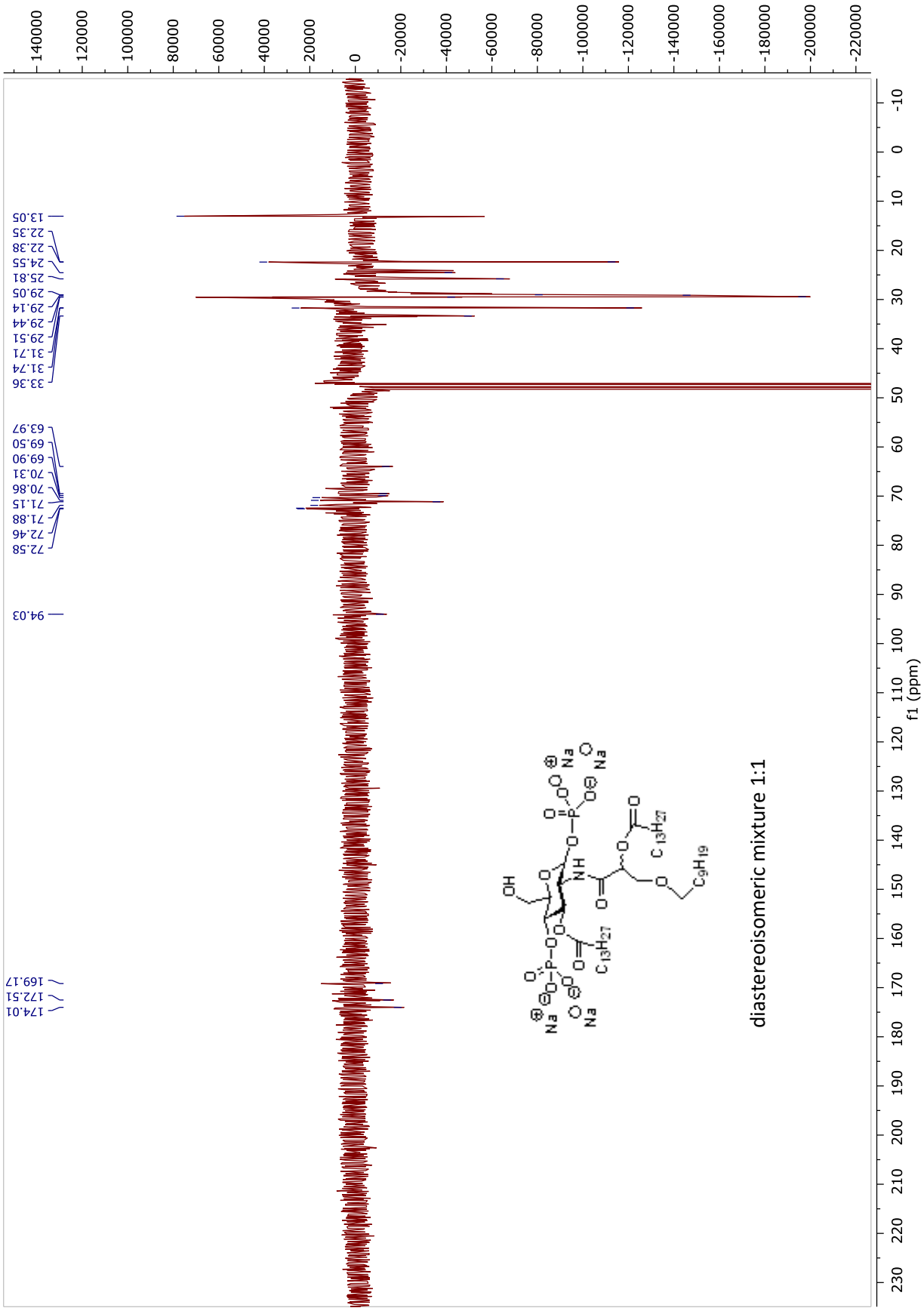
13.05
22.35
22.38
24.55
25.81
29.05
29.14
29.44
29.51
31.71
31.74
33.36
63.97
69.50
69.90
70.31
70.86
71.15
71.88
72.46
72.58
94.03
169.17
172.51
174.01
diastereoisomeric mixture 1:1
f1 (ppm)

AM246248 Synthesis: ^{1}H NMR and ^{13}C-APT NMR spectra

Compound 37-diastereosiomer1. ^{1}H NMR and ^{13}C APT NMR spectra in $CDCl_3$

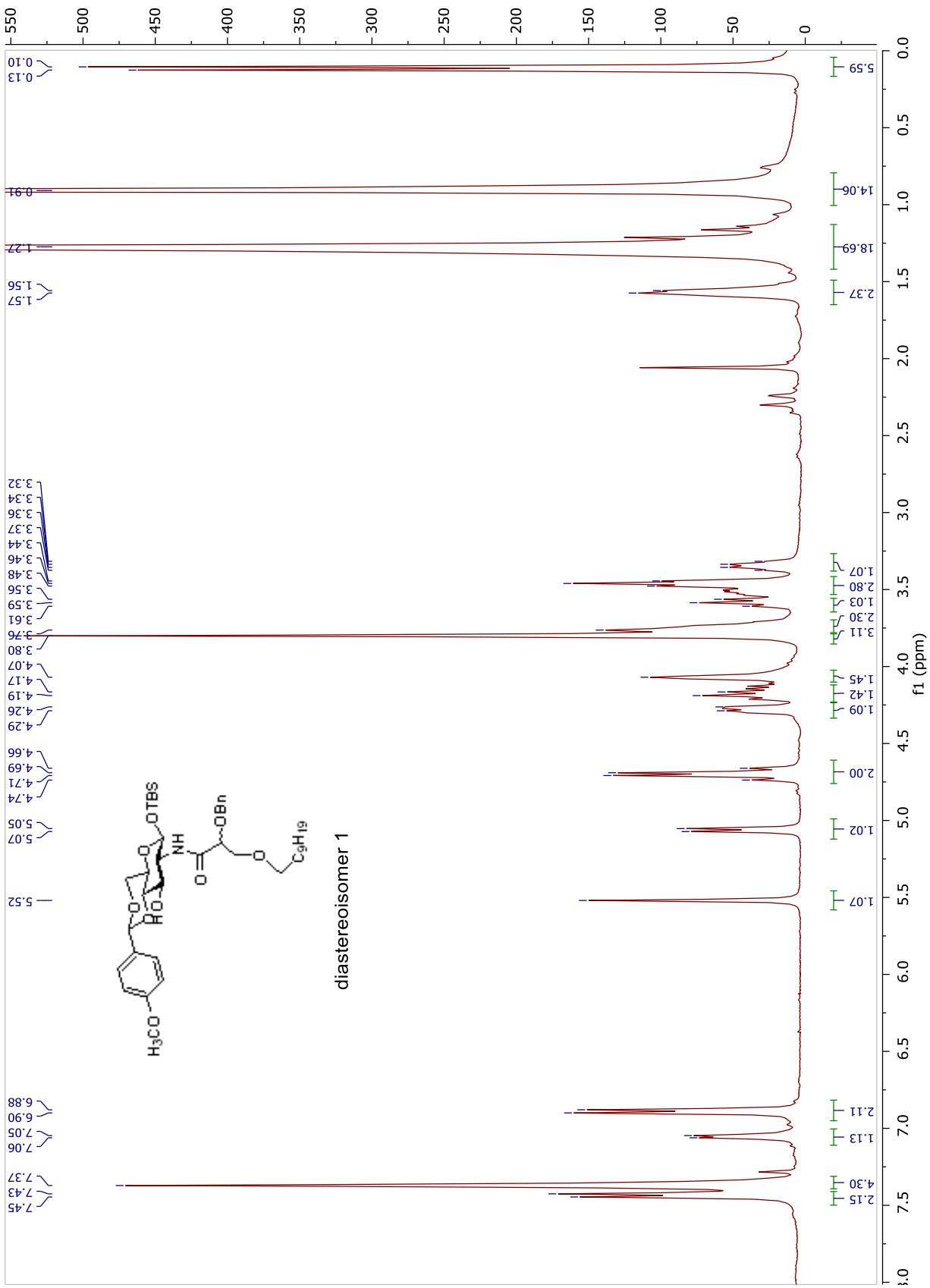

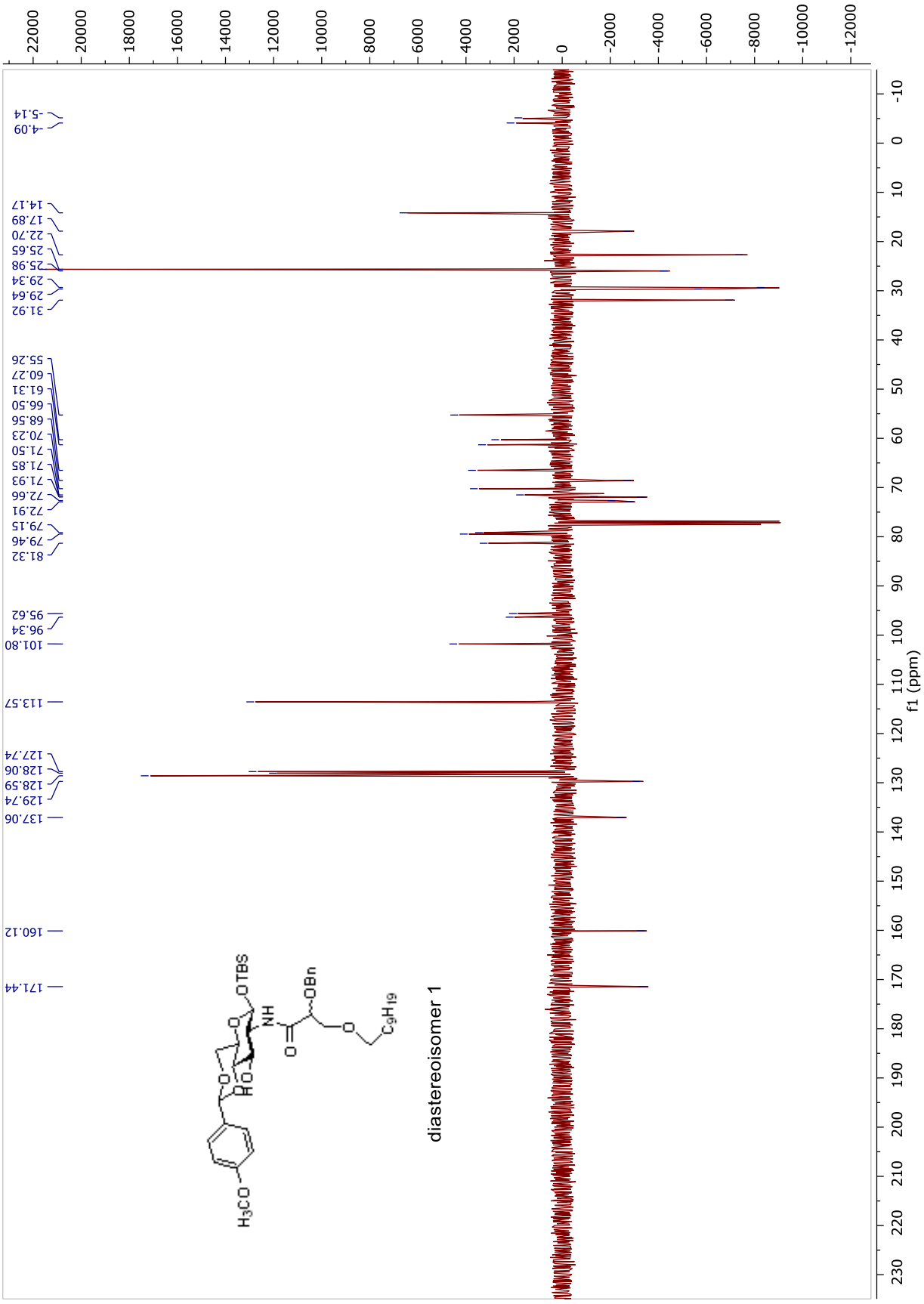
-5.14
-4.09
14.17
17.89
22.70
25.65
25.98
29.34
29.64
31.92
55.26
60.27
61.31
66.50
68.56
70.23
71.50
71.85
71.93
72.66
72.91
79.15
79.46
81.32
95.62
96.34
101.80
113.57
127.74
128.06
128.59
129.74
137.06
160.12
171.44
OTBS
NH
OBn
O
C_9H_{19}
H_3CO
diastereoisomer 1
f1 (ppm)

Compound 37-diastereosiomer2. ^{1}H NMR and ^{13}C APT NMR spectra in $CDCl_3$

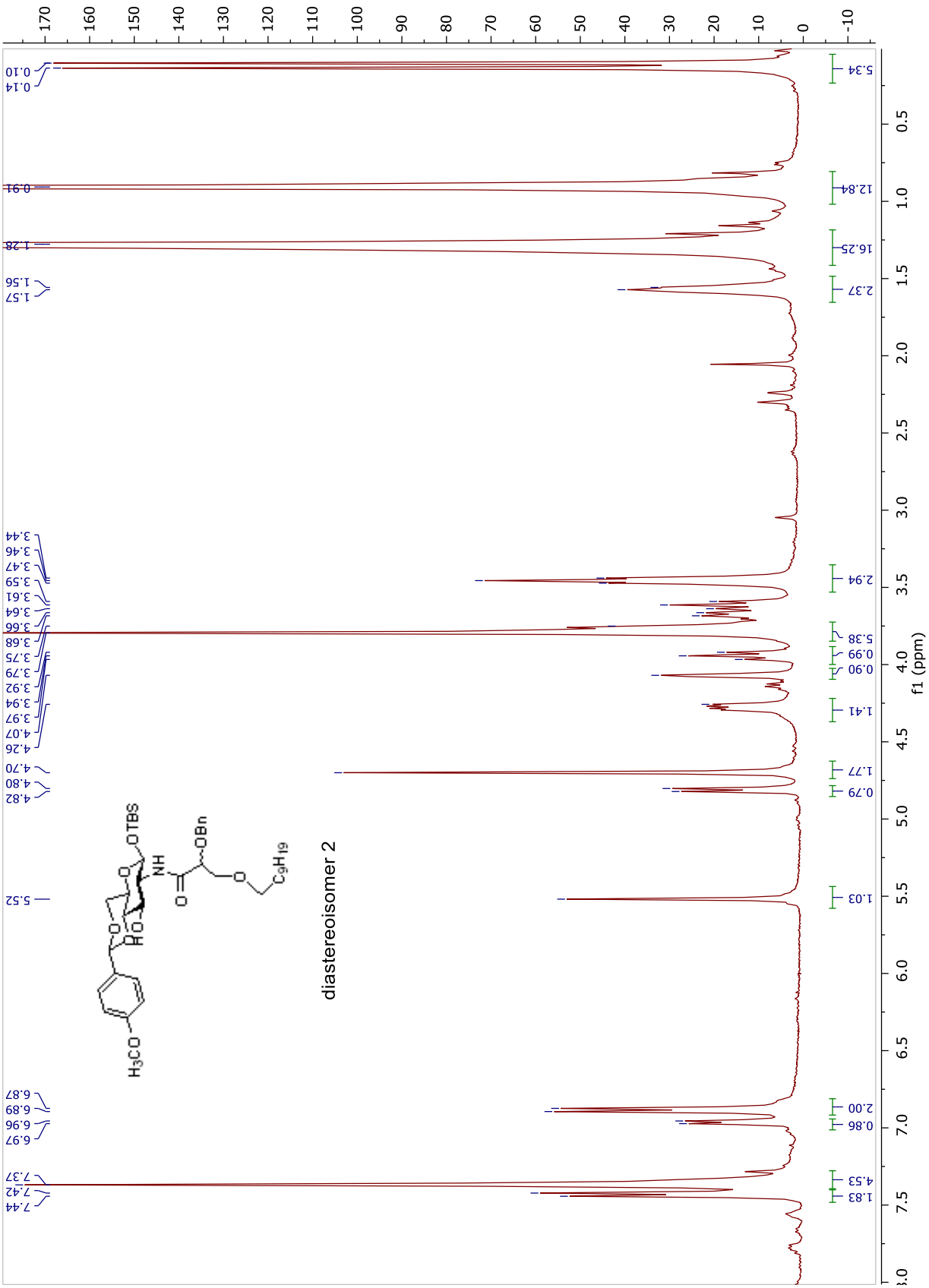

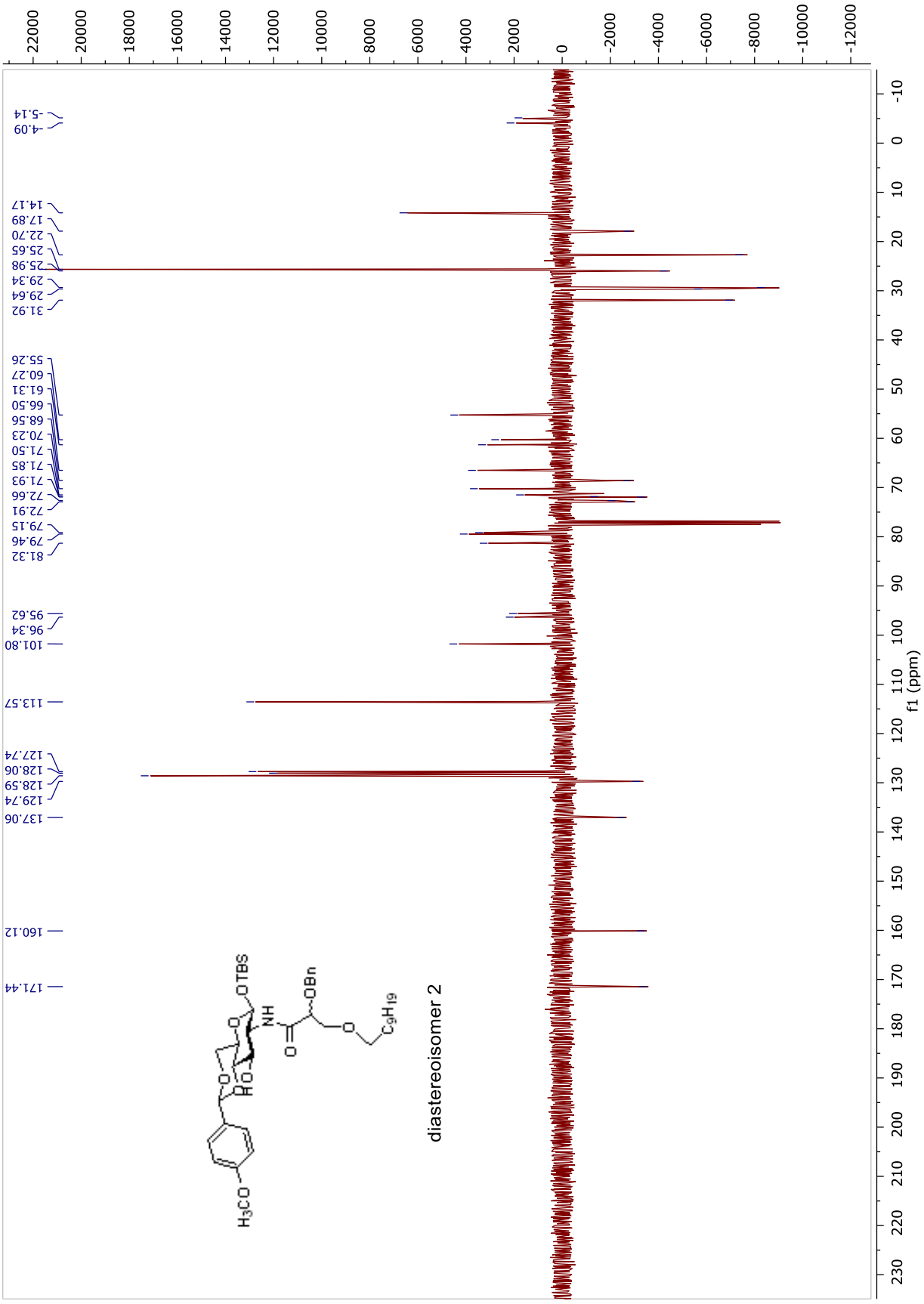
-5.14
-4.09
14.17
17.89
22.70
25.65
25.98
29.34
29.64
31.92
55.26
60.27
61.31
66.50
68.56
70.23
71.50
71.85
71.93
72.66
72.91
79.15
79.46
81.32
95.62
96.34
101.80
113.57
127.74
128.06
128.59
129.74
137.06
160.12
171.44
OTBS
NH
OBn
O
C_9H_{19}
H_3CO
diastereoisomer 2
f1 (ppm)

Compound 38. ^{1}H NMR and ^{13}C APT NMR spectra in $CDCl_3$

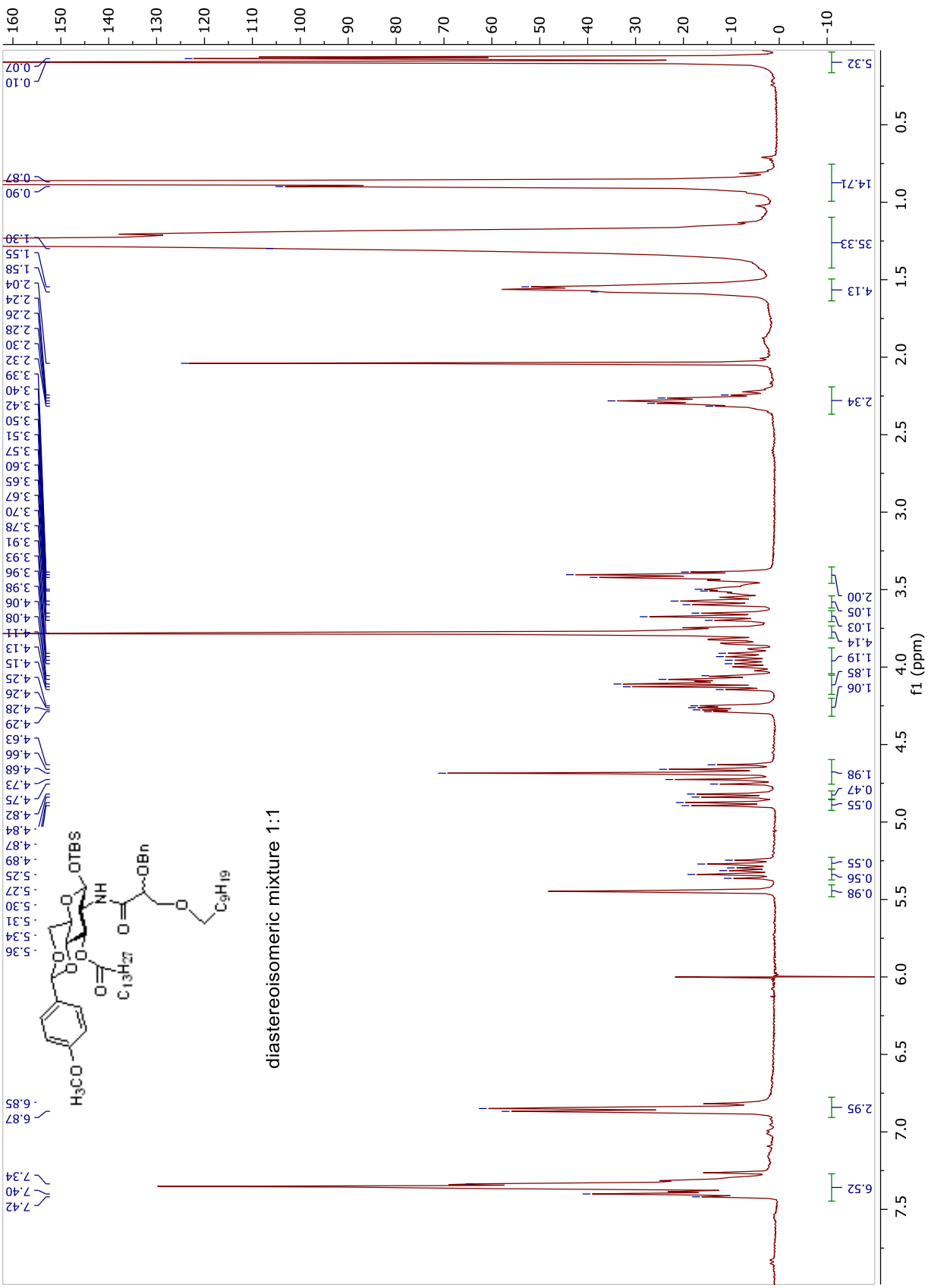

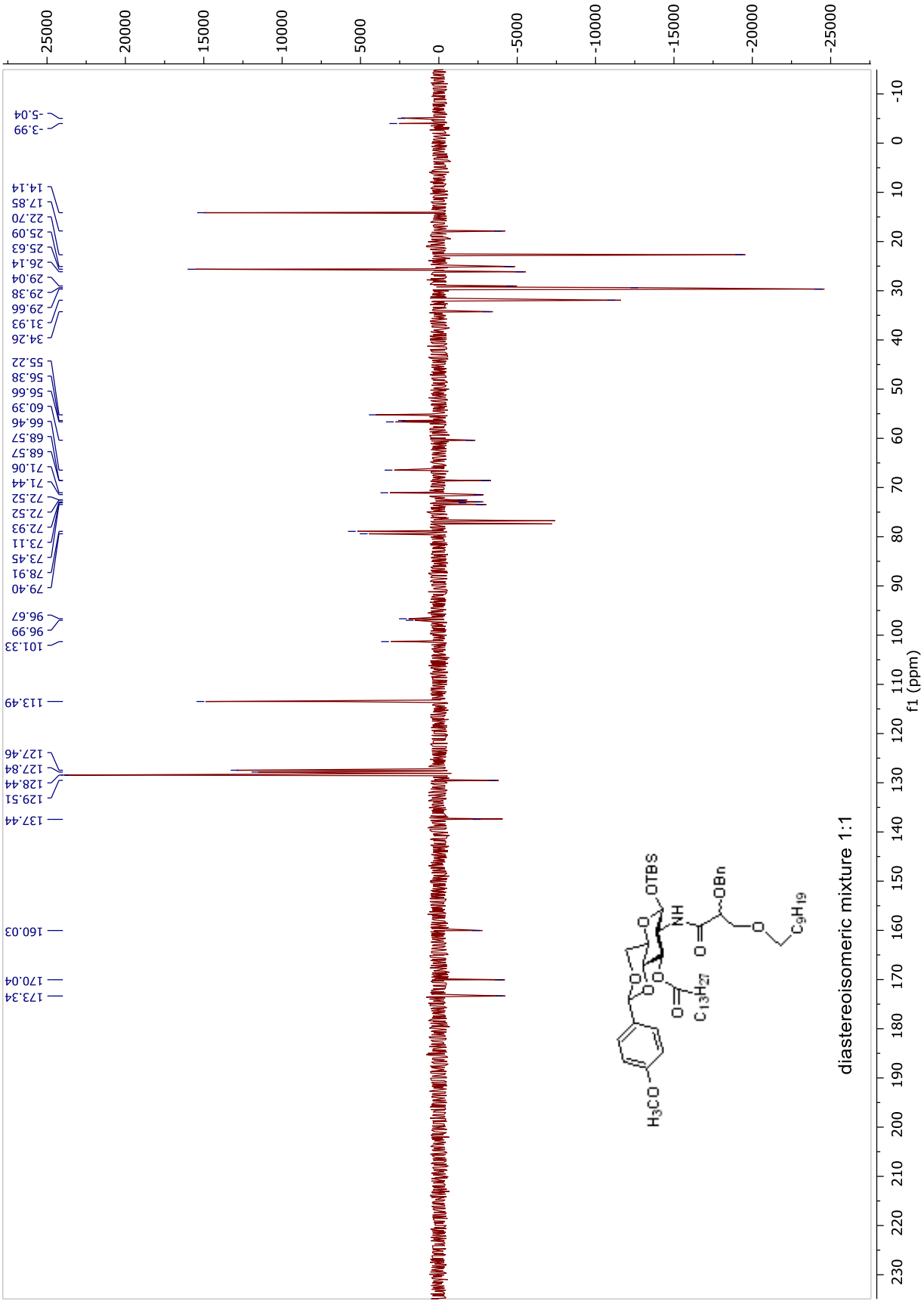
-5.04
-3.99
14.14
17.85
22.70
25.09
25.63
26.14
29.04
29.38
29.66
31.93
34.26
55.22
56.38
56.66
60.39
66.46
68.57
68.57
71.06
71.44
72.52
72.52
72.93
73.11
73.45
78.91
79.40
96.67
96.99
101.33
113.49
127.46
127.84
128.44
129.51
137.44
160.03
170.04
173.34
f1 (ppm)
diastereoisomeric mixture 1:1
OTBS
NH
OBn
O
$C_{13}H_{27}$
C_9H_{19}
H_3CO

Compound 39. ^{1}H NMR and ^{13}C APT NMR spectra in $CDCl_3$

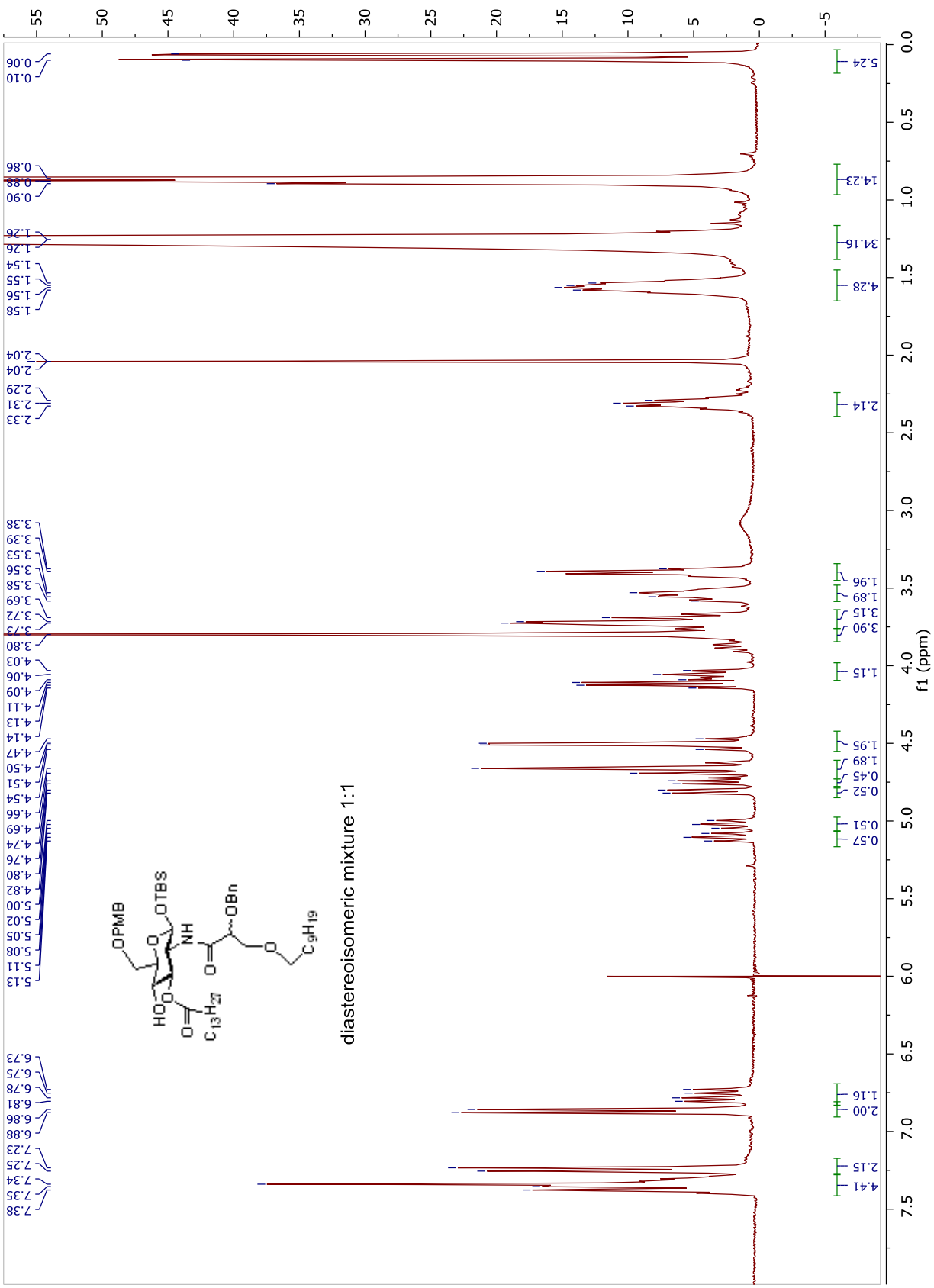

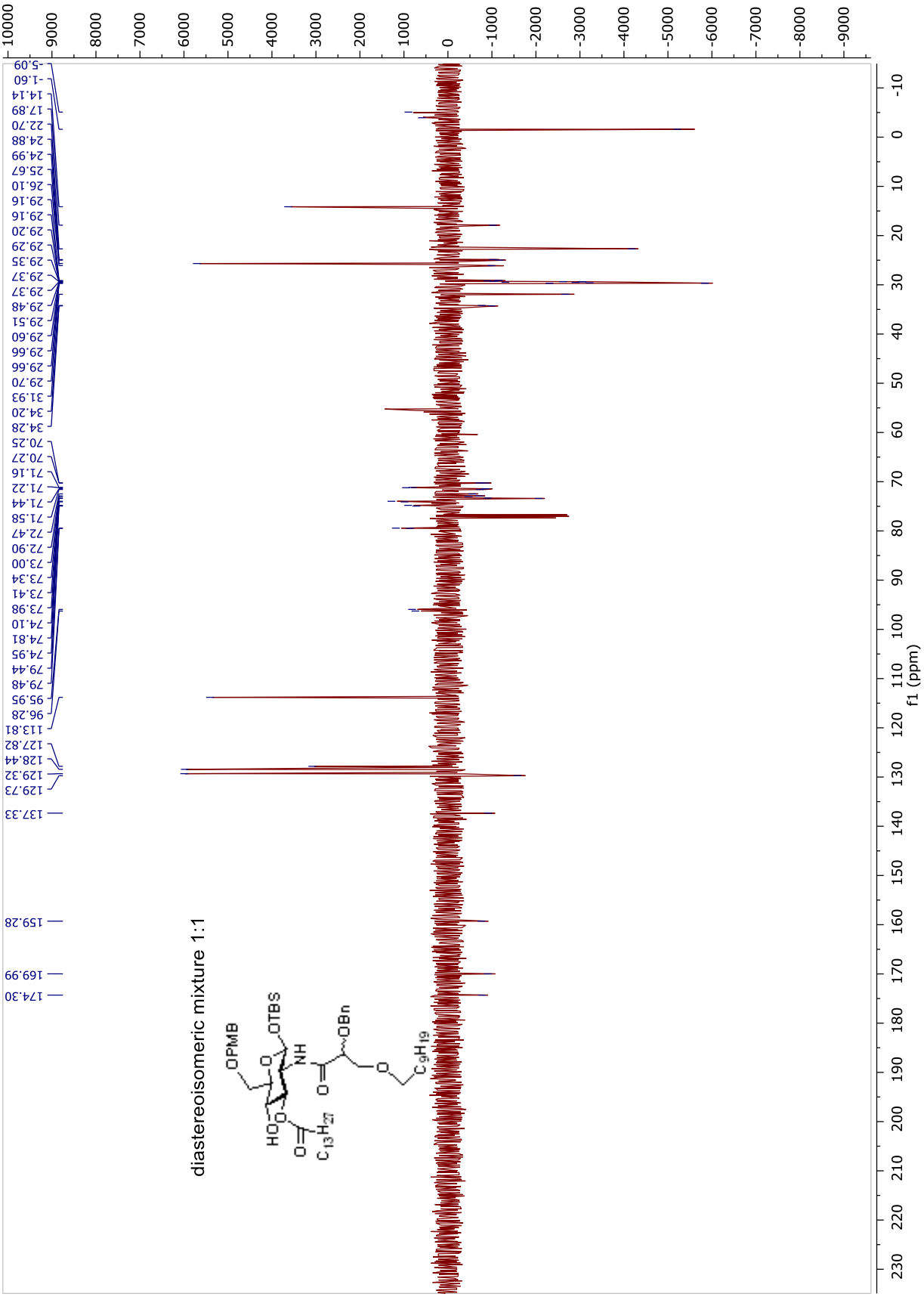
diastereoisomeric mixture 1:1
OPMB
OTBS
NH
OBn
HO
O
$C_{13}H_{27}$
C_9H_{19}
f1 (ppm)

Compound 40. ^{1}H NMR and ^{13}C APT NMR spectra in $CDCl_3$

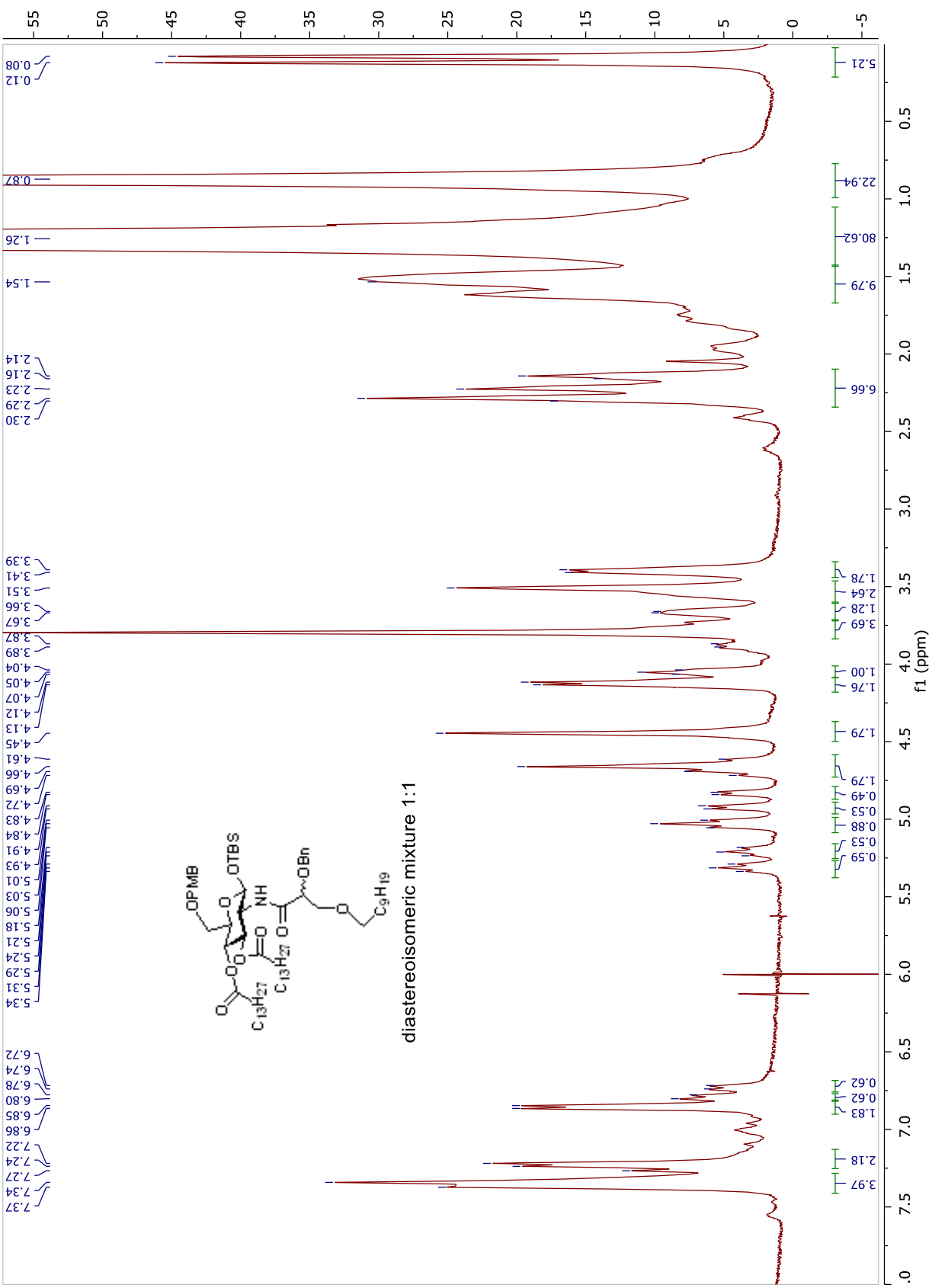

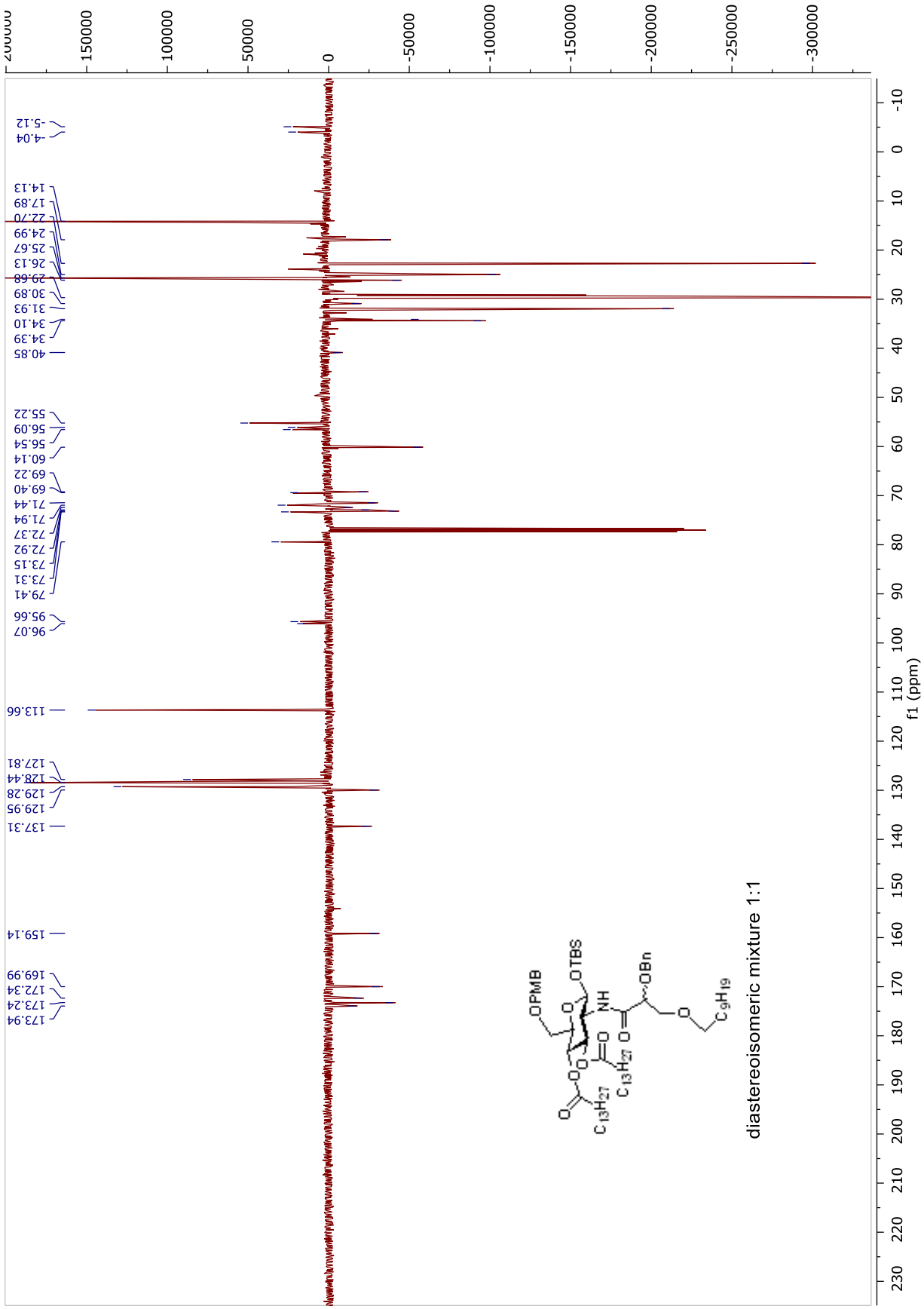
-5.12
-4.04
14.13
17.89
22.70
24.99
25.67
26.13
29.68
30.89
31.93
34.10
34.39
40.85
55.22
56.09
56.54
60.14
69.22
69.40
71.44
71.94
72.37
72.92
73.15
73.31
79.41
95.66
96.07
113.66
127.81
128.44
129.28
129.95
137.31
159.14
169.99
172.34
173.24
173.94
OPMB
OTBS
NH
OBn
$C_{13}H_{27}$
$C_{13}H_{27}$
C_9H_{19}
diastereoisomeric mixture 1:1
f1 (ppm)

Compound 41-diastereosiomer1. ^{1}H NMR and ^{13}C APT NMR spectra in $CDCl_3$

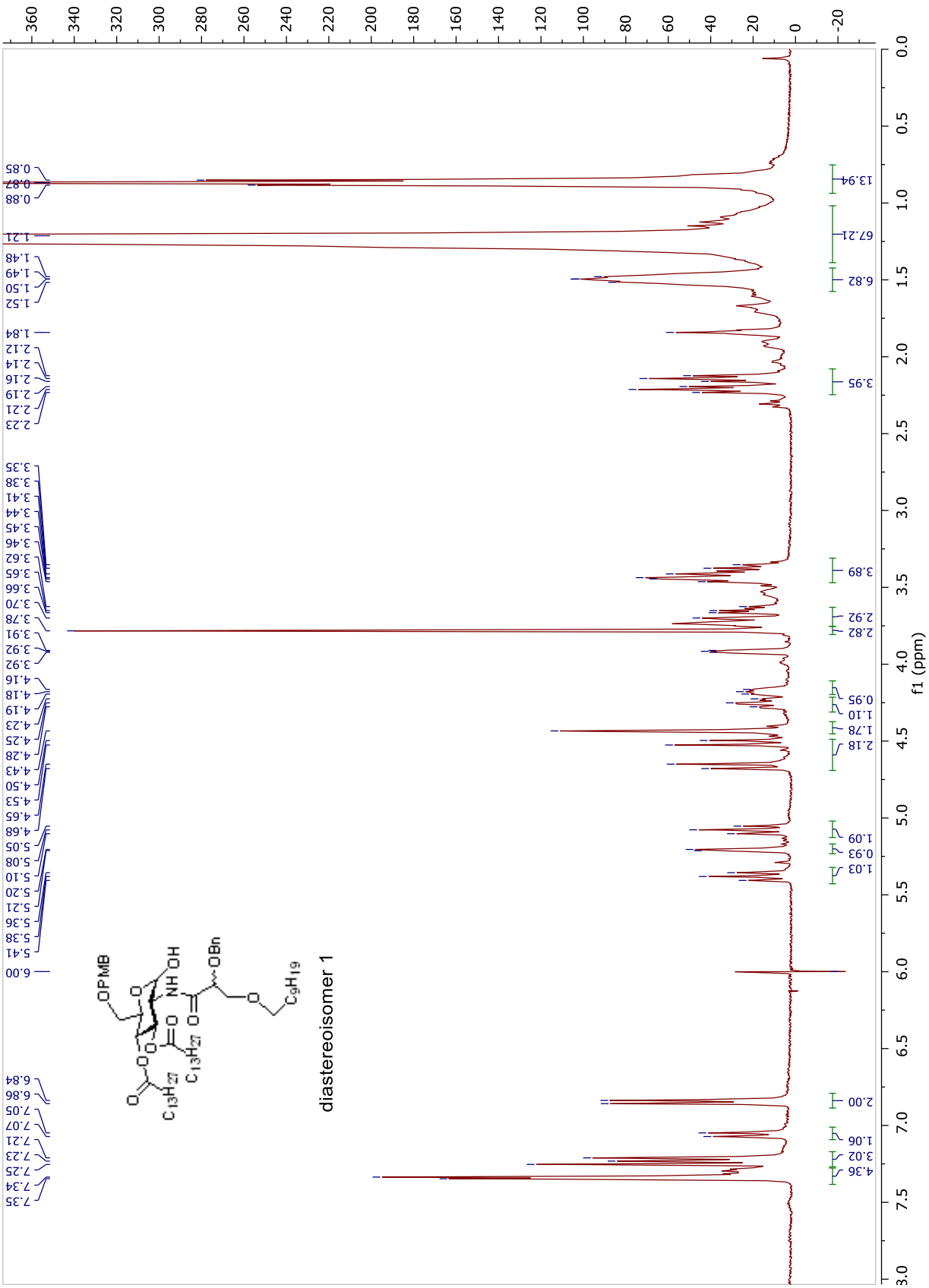

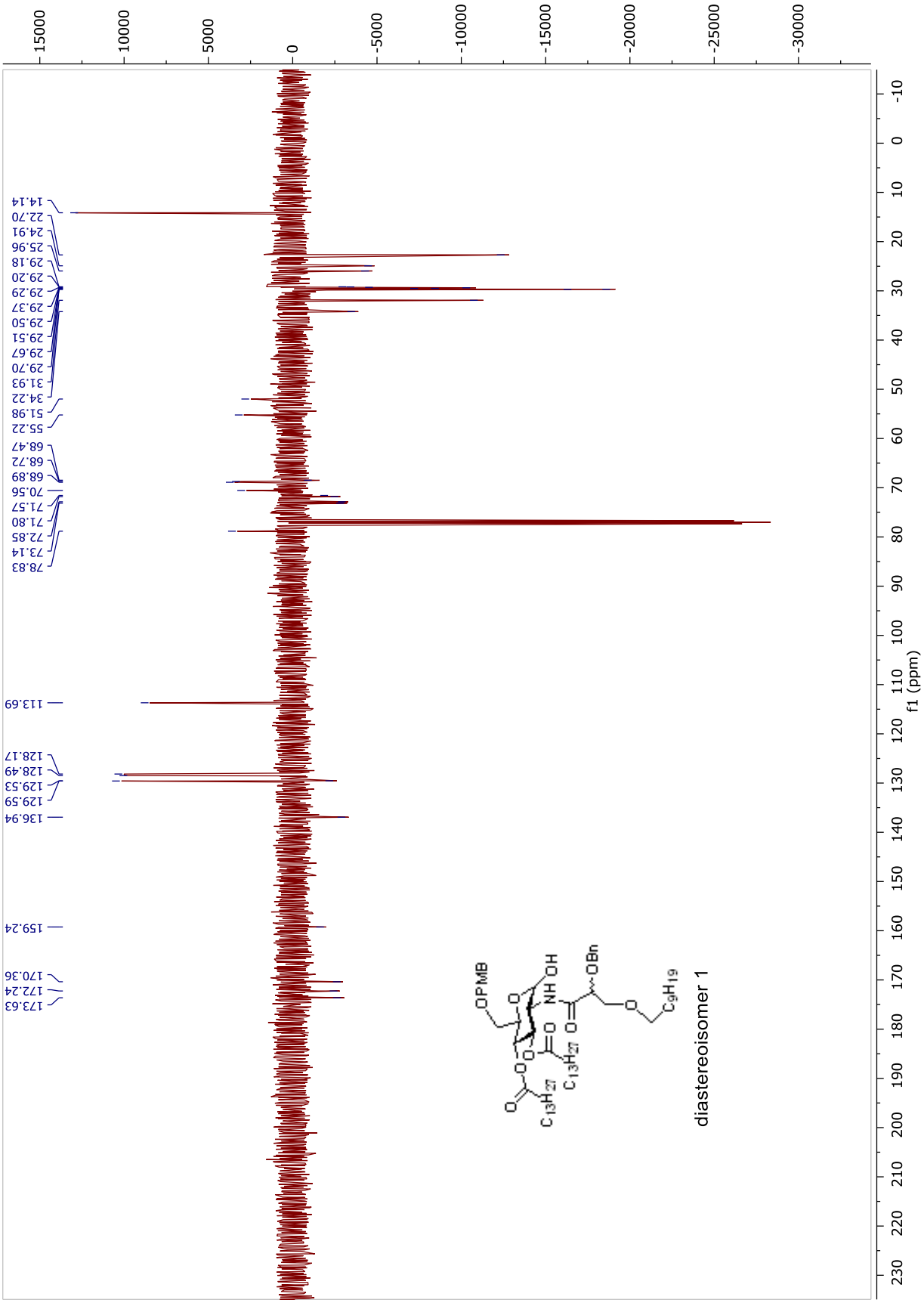
15000
10000
5000
0
-5000
-10000
-15000
-20000
-25000
-30000
14.14
22.70
24.91
25.96
29.18
29.20
29.29
29.37
29.50
29.51
29.67
29.70
31.93
34.22
51.98
55.22
68.47
68.72
68.89
70.56
71.57
71.80
72.85
73.14
78.83
113.69
128.17
128.49
129.53
129.59
136.94
159.24
170.36
172.24
173.63
OPMB
OBn
NH
OH
O
$C_{13}H_{27}$
$C_{13}H_{27}$
C_9H_{19}
diastereoisomer 1
-10
0
10
20
30
40
50
60
70
80
90
100
110
120
130
140
150
160
170
180
190
200
210
220
230
f1 (ppm)

Compound 41-diastereosiomer2. ^{1}H NMR and ^{13}C APT NMR spectra in $CDCl_3$

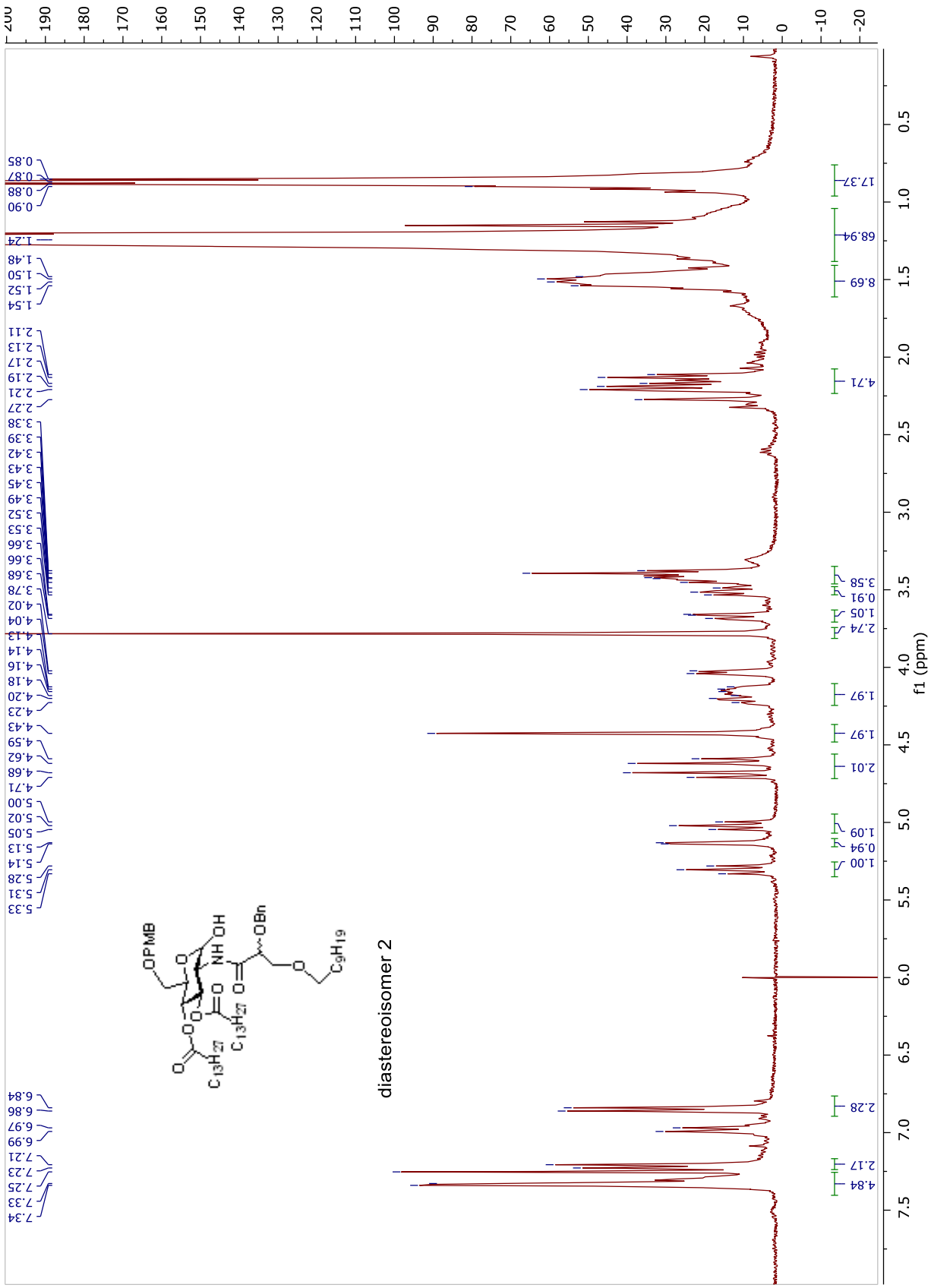

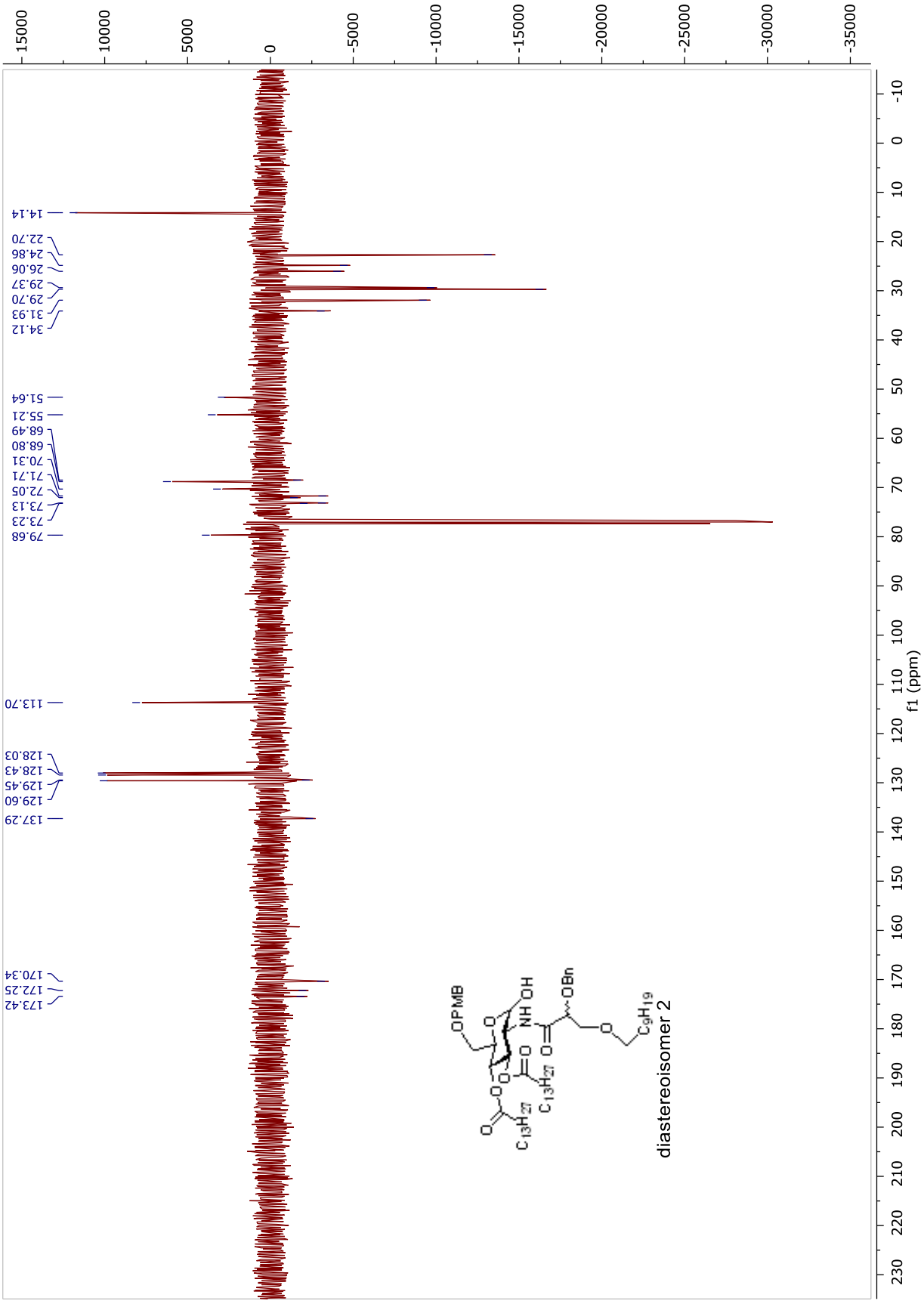
14.14
22.70
24.86
26.06
29.37
29.70
31.93
34.12
51.64
55.21
68.49
68.80
70.31
71.71
72.05
73.13
73.23
79.68
113.70
128.03
128.43
129.45
129.60
137.29
170.34
172.25
173.42
f1 (ppm)
OPMB
OBn
NH
OH
$C_{13}H_{27}$
$C_{13}H_{27}$
C_9H_{19}
diastereoisomer 2

Compound 42-diastereosiomer1. ^{1}H NMR and ^{13}C APT NMR spectra in $CDCl_3$

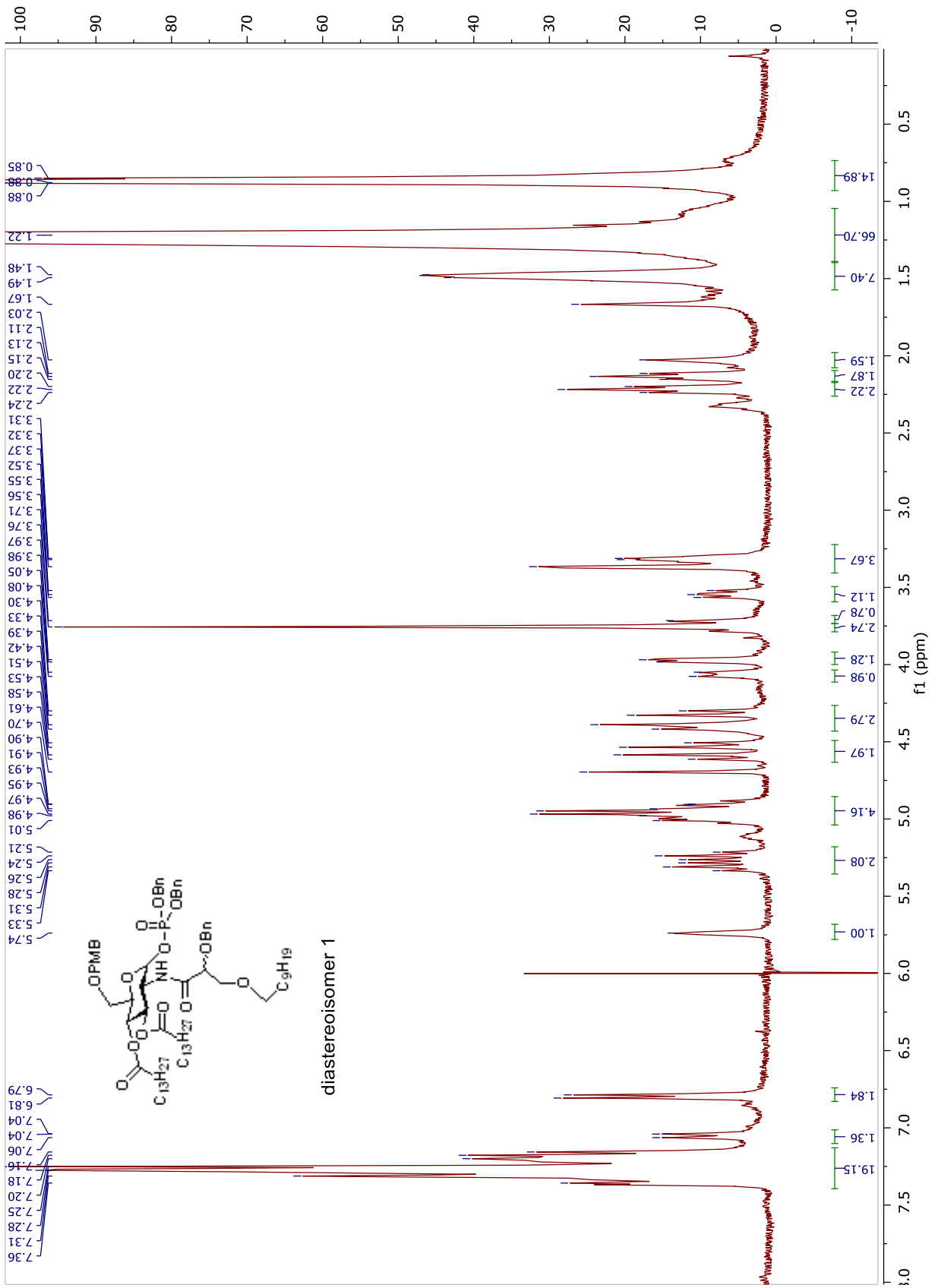

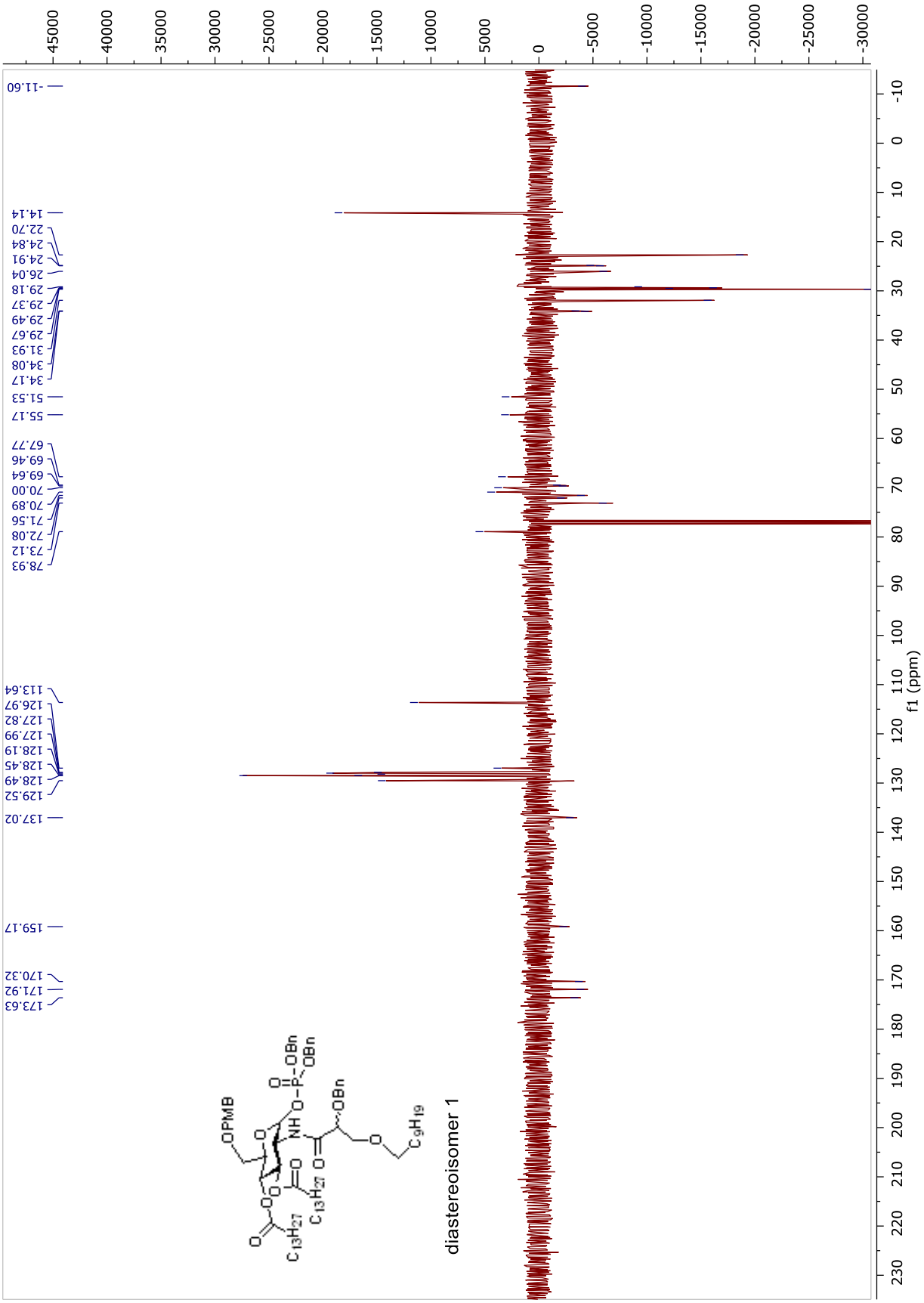
diastereoisomer 1
f1 (ppm)

Compound 42-diastereosiomer2. ^{1}H NMR and ^{13}C APT NMR spectra in $CDCl_3$

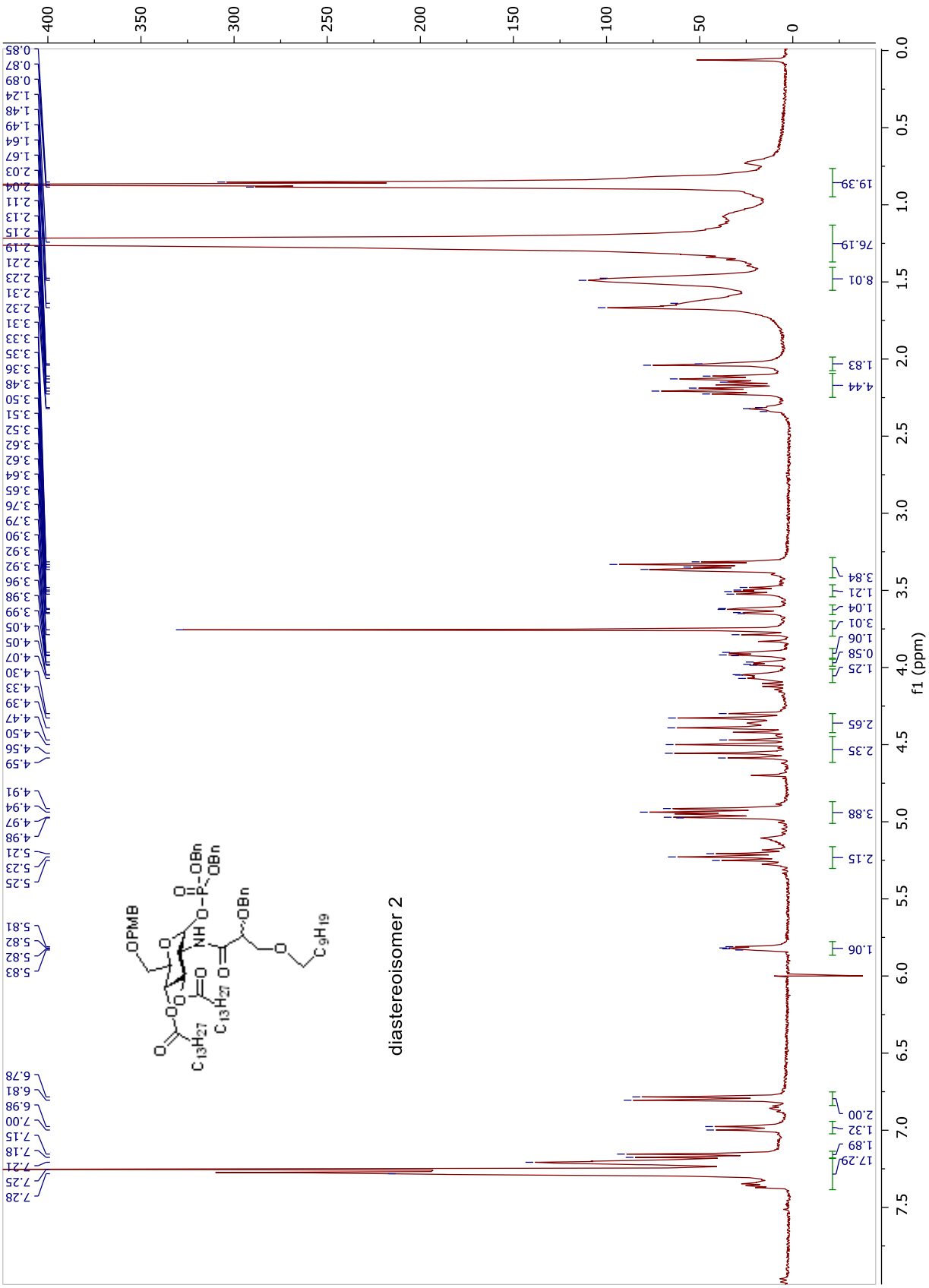

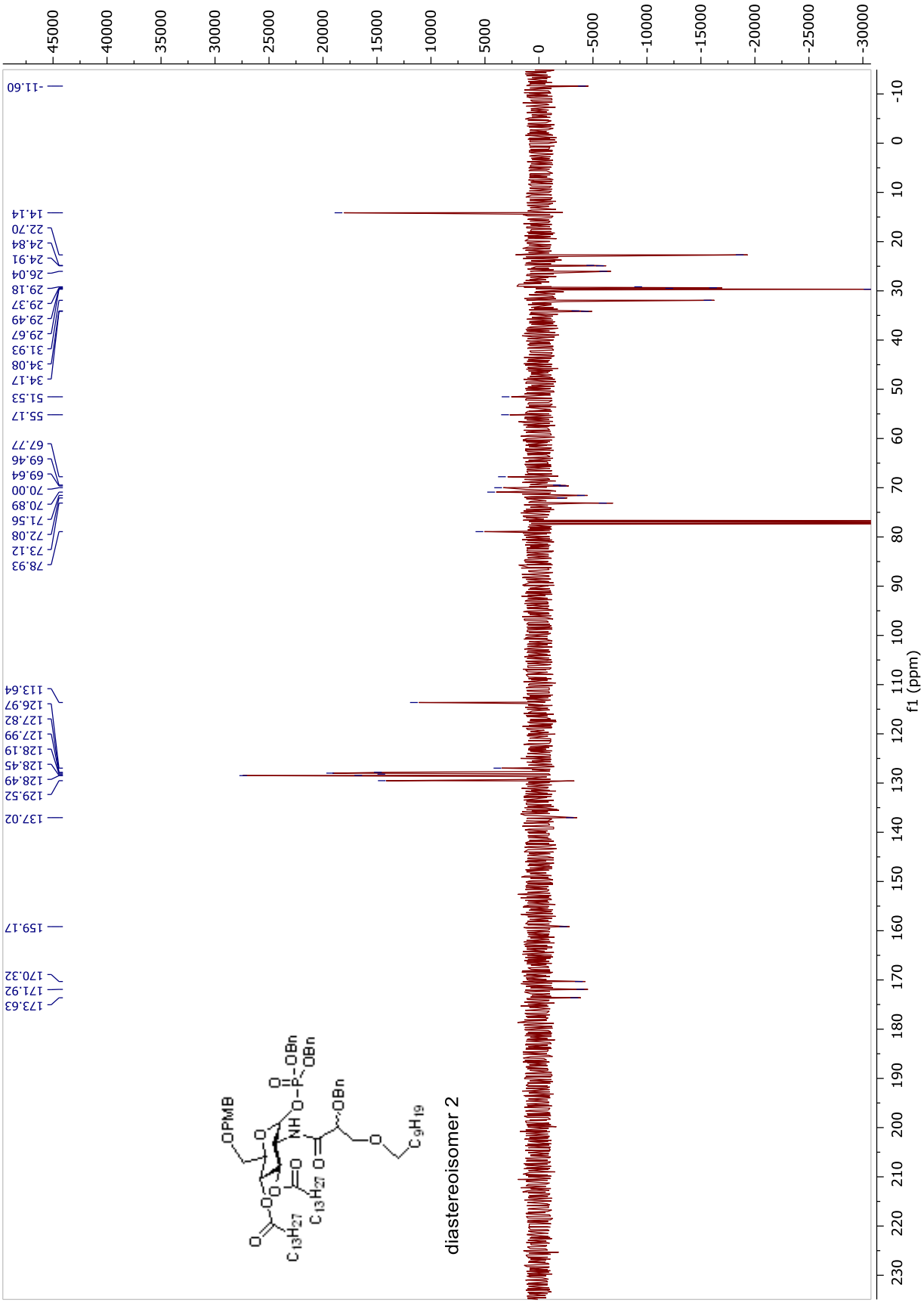
diastereoisomer 2
f1 (ppm)

Compound AM246248-diastereosiomer1. ^{1}H NMR spectrum in CD_3OD

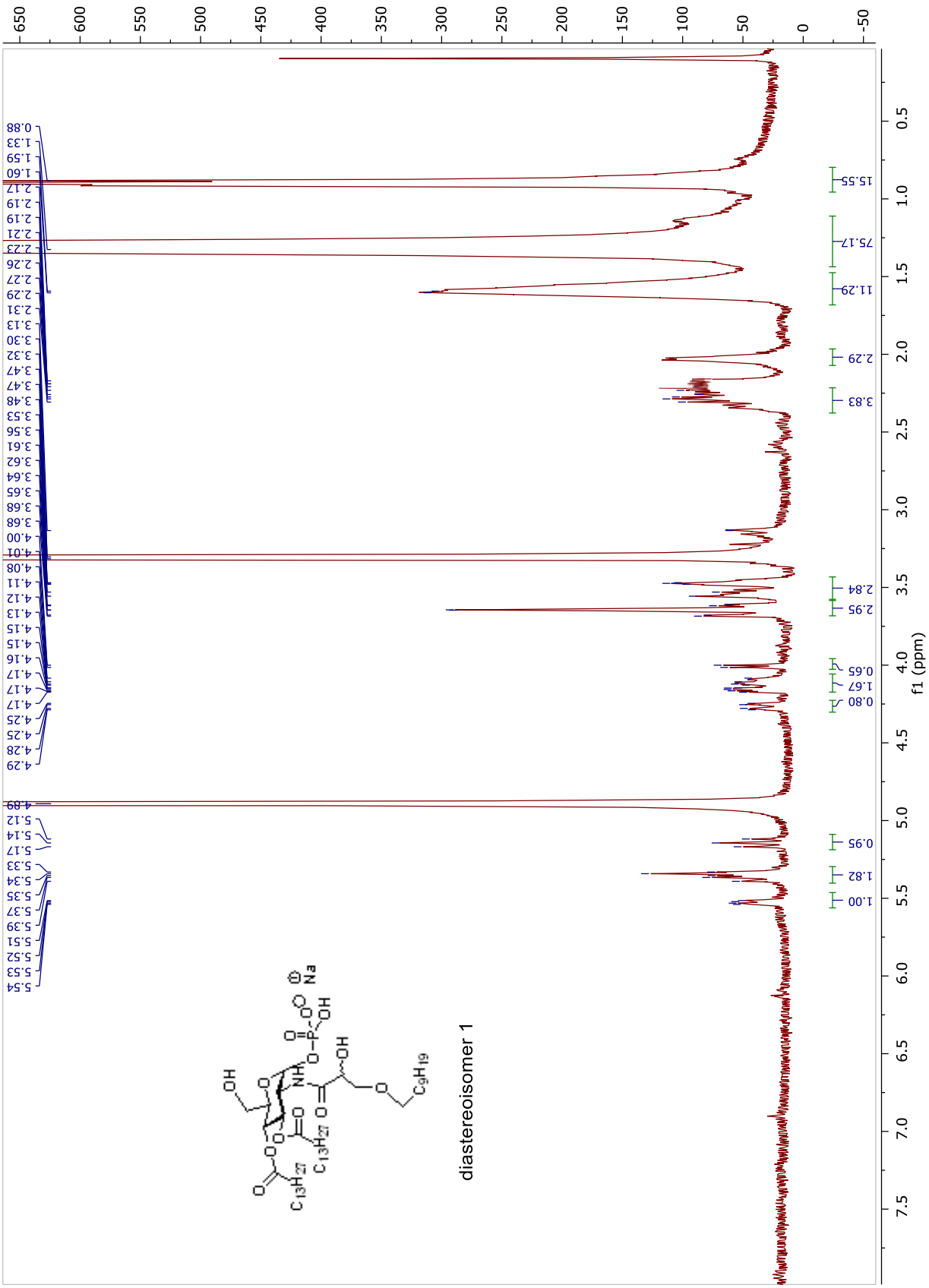

Compound AM246248-diastereoisomer2. ^{1}H NMR spectrum in CD_3OD

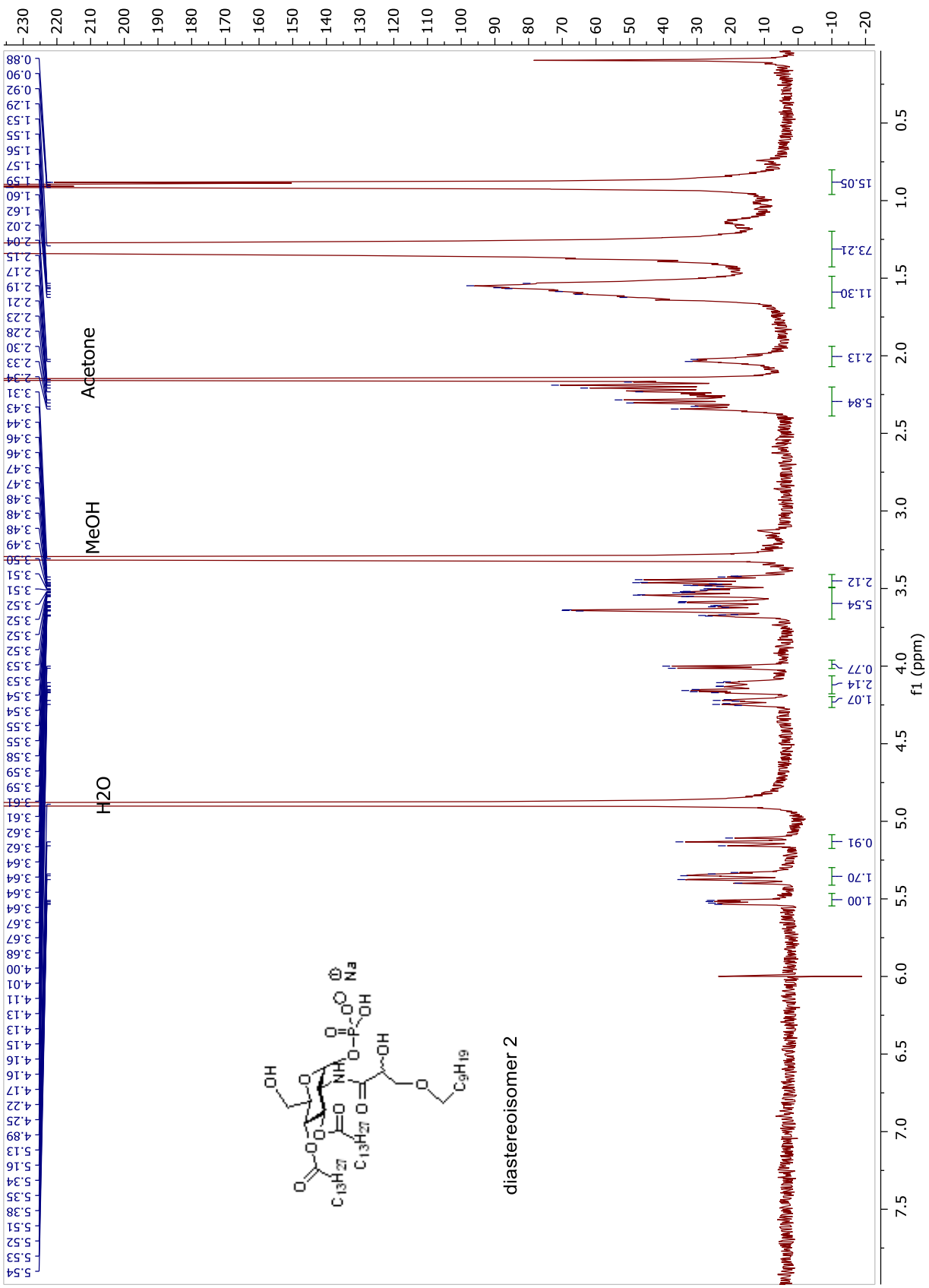

AM30 Synthesis: ^{1}H NMR and ^{13}C-APT NMR spectra

Compound 45. ^{1}H NMR and ^{13}C APT NMR spectra in $CDCl_3$

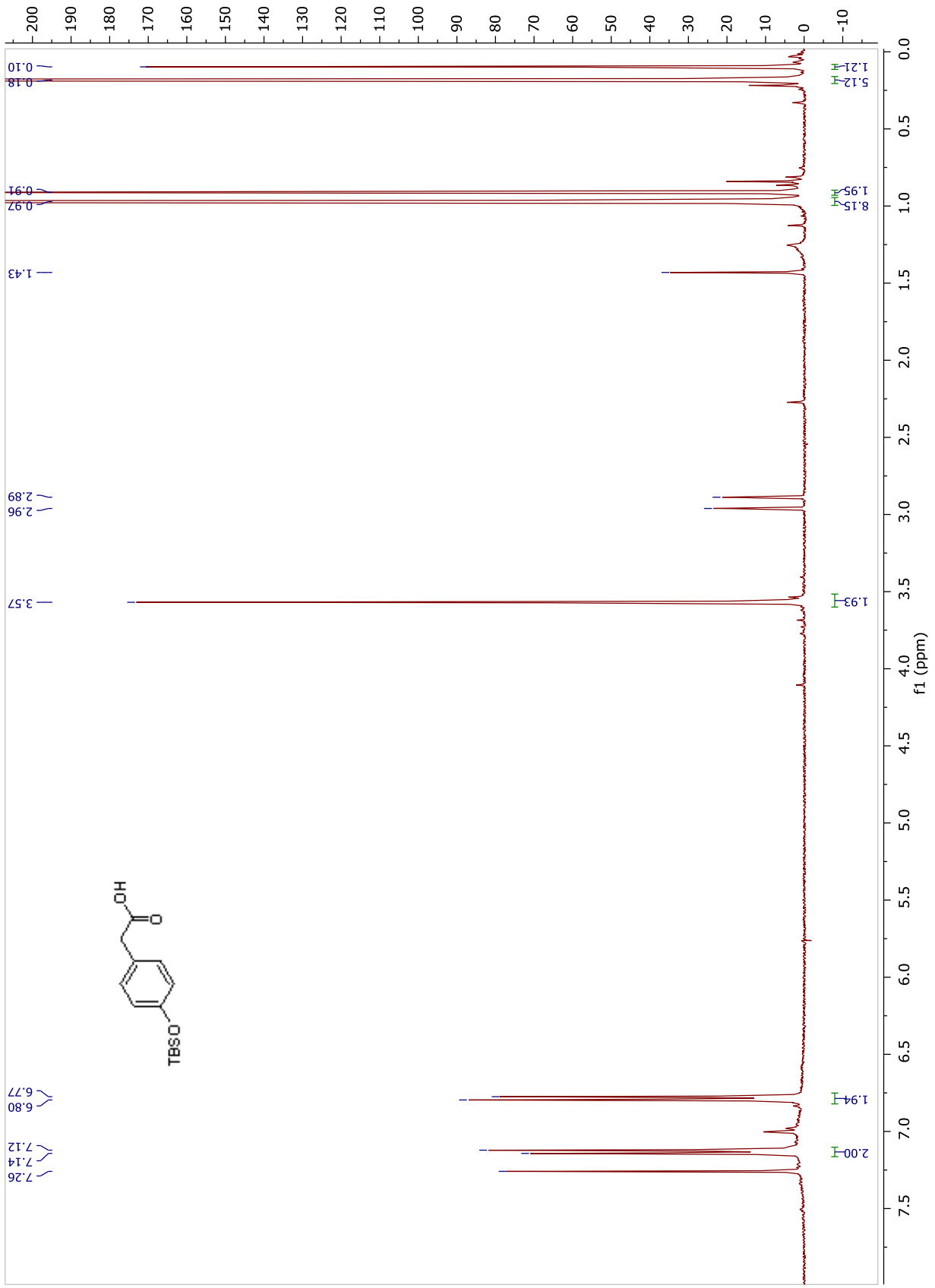

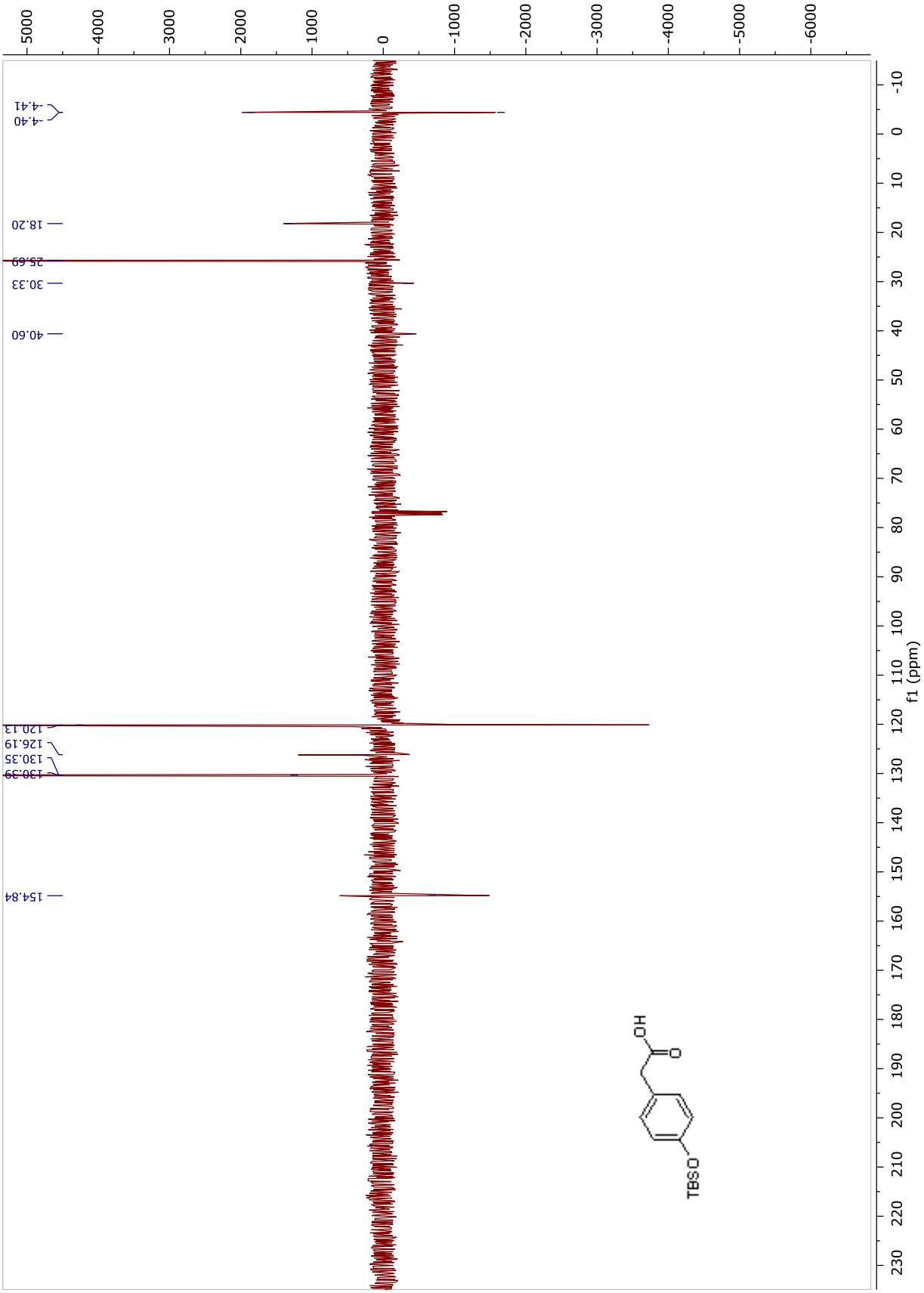
-4.41
-4.40
18.20
25.69
30.33
40.60
120.13
126.19
130.35
130.39
154.84
HO
O
TBSO
f1 (ppm)

Compound 46. ^{1}H NMR and ^{13}C APT NMR spectra in $CDCl_3$

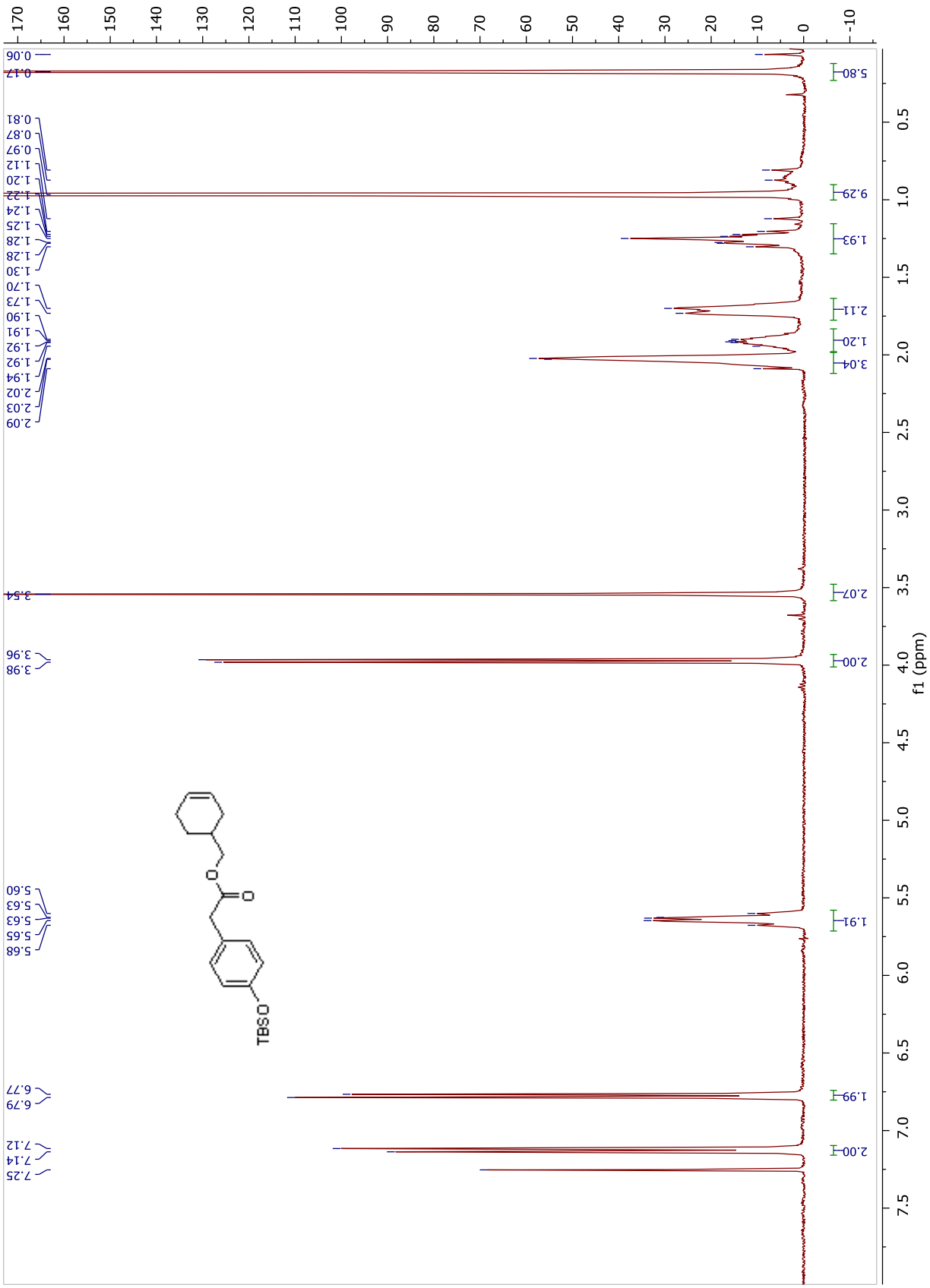

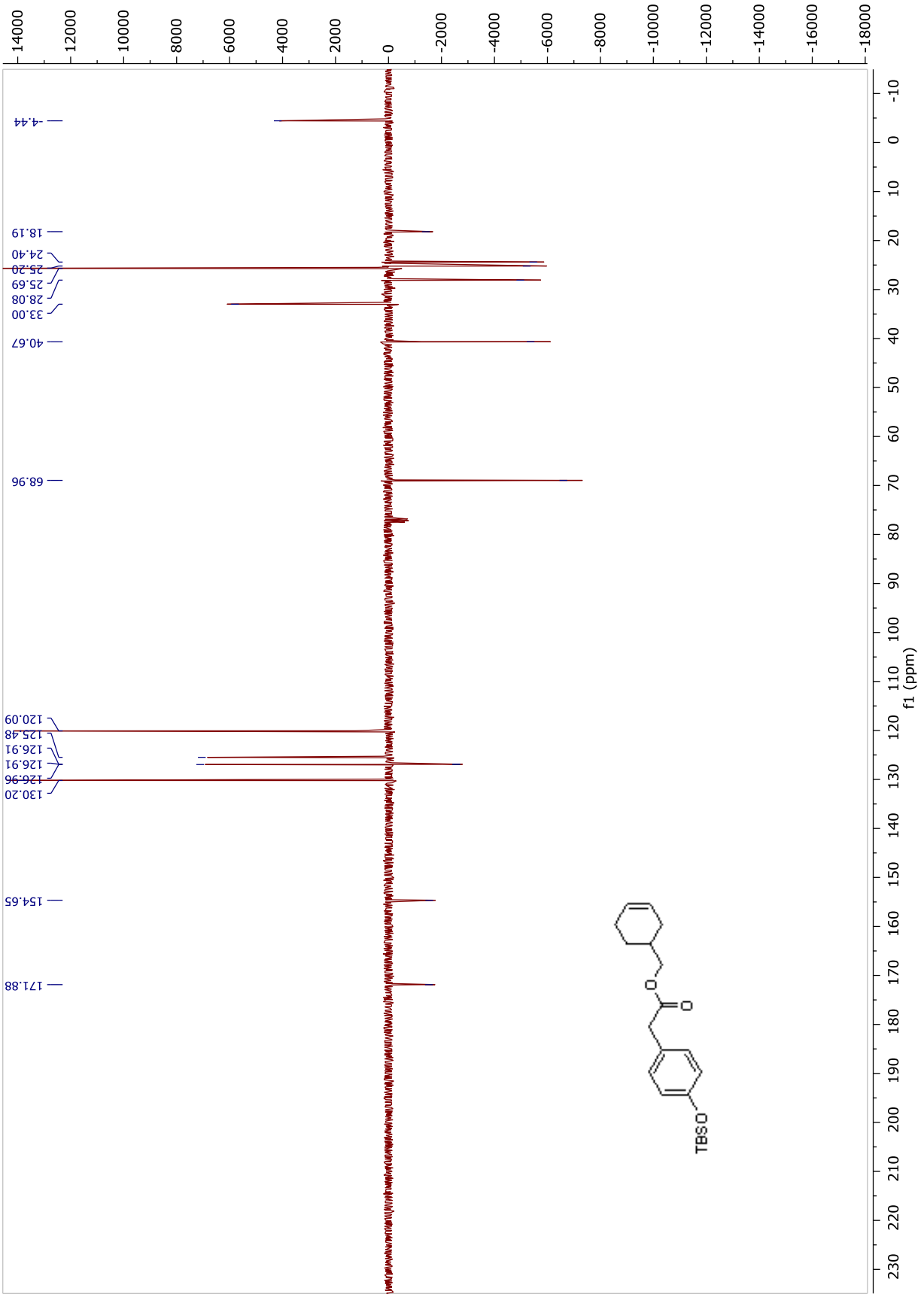
-4.44
18.19
24.40
25.20
25.69
28.08
33.00
40.67
68.96
120.09
125.48
126.91
126.96
130.20
154.65
171.88
f1 (ppm)
TBSO
O
O

Compound 47. ^{1}H NMR and ^{13}C APT NMR spectra in $CDCl_3$

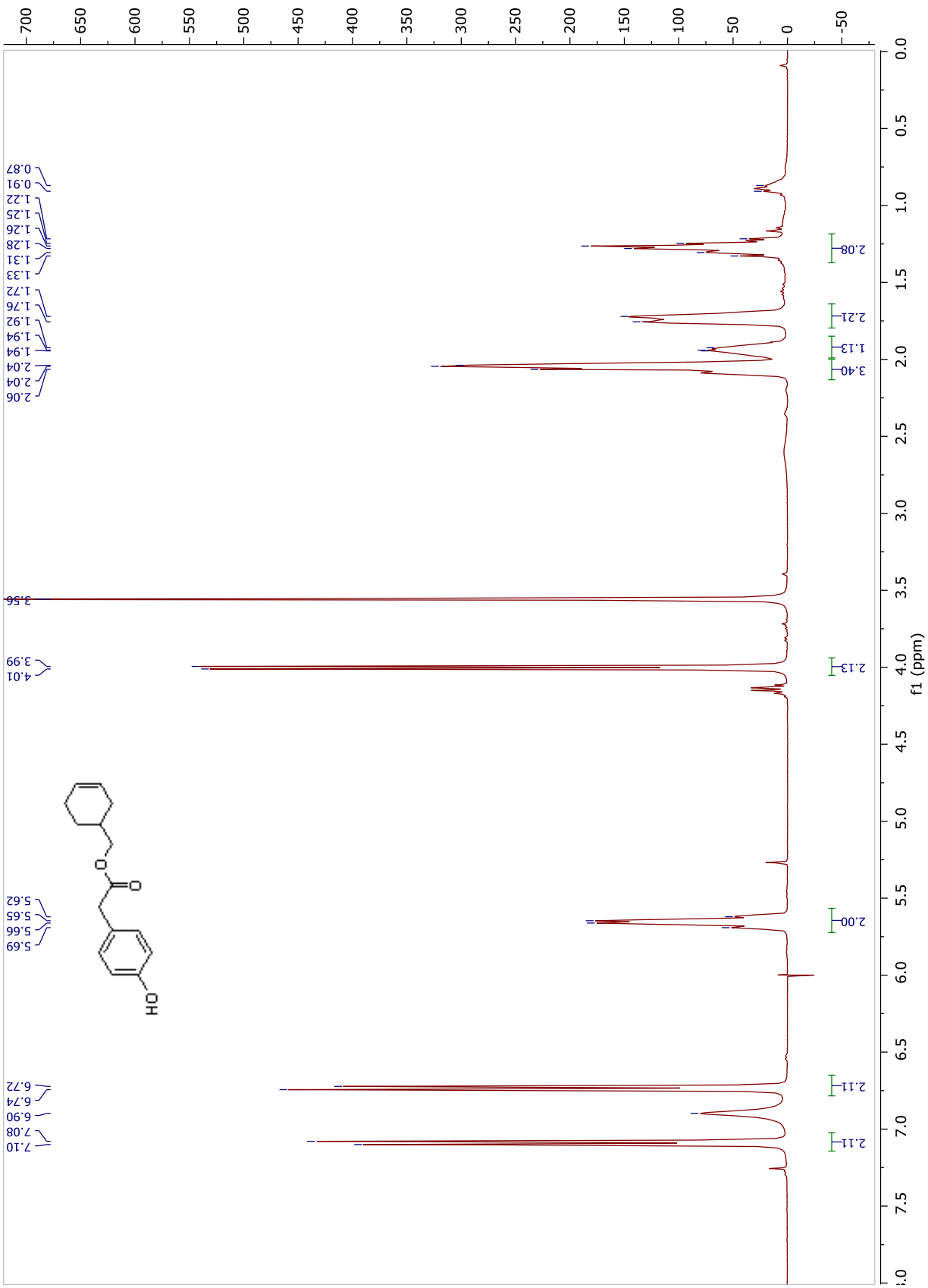

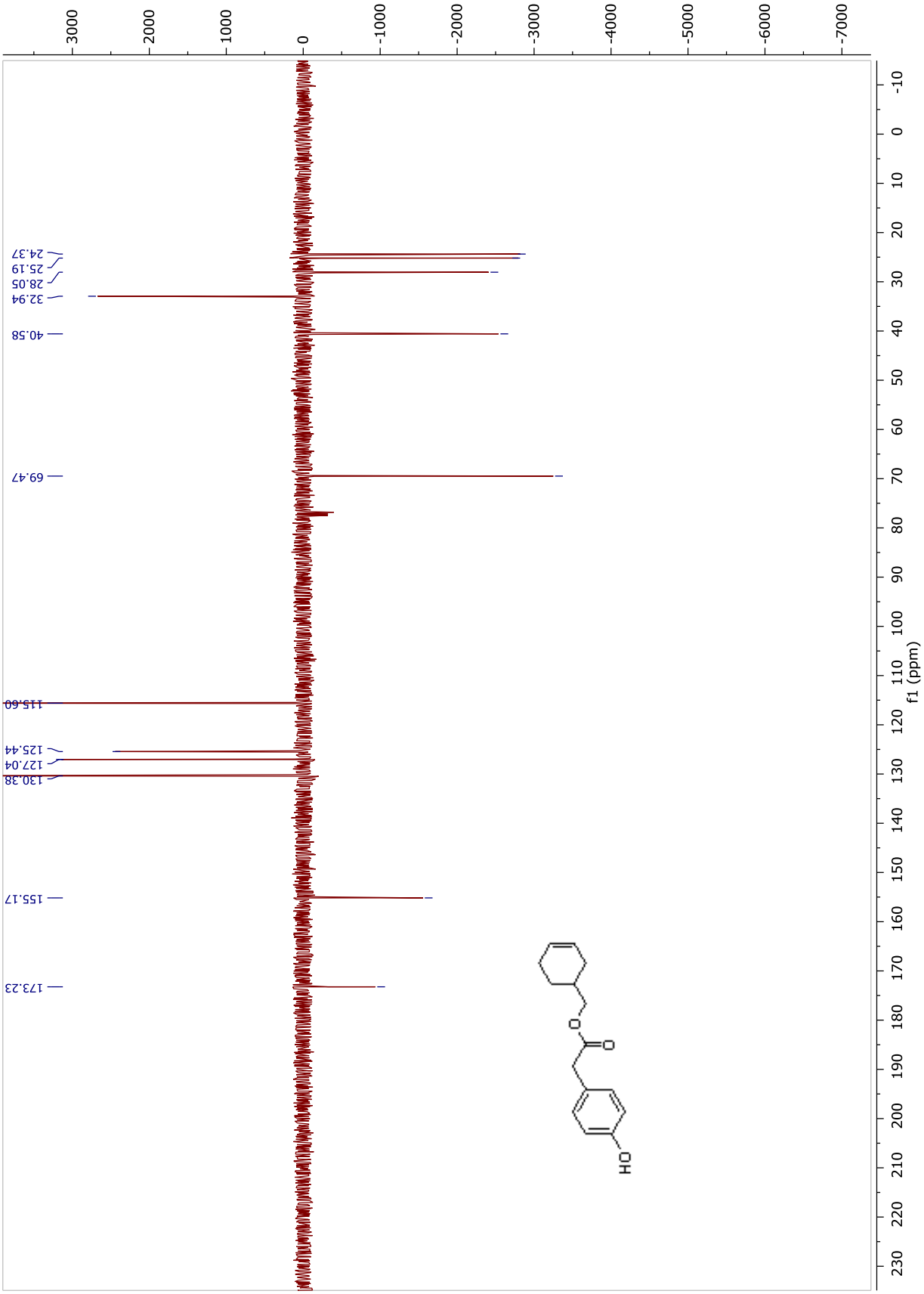
24.37
25.19
28.05
32.94
40.58
69.47
115.60
125.44
127.04
130.38
155.17
173.23
f1 (ppm)
O
O
OH

Compound 48. ^{1}H NMR and ^{13}C APT NMR spectra in CD_3OD

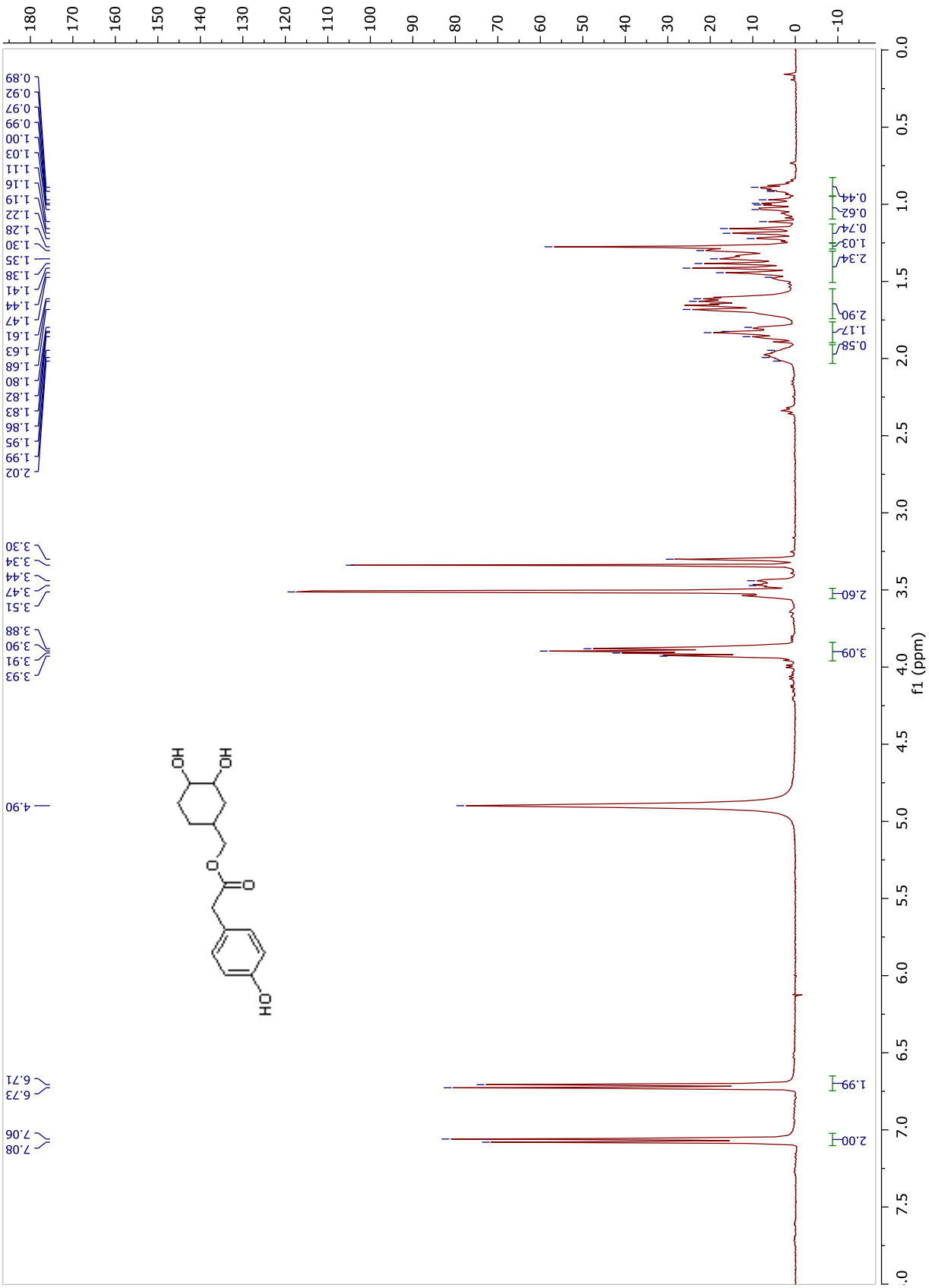

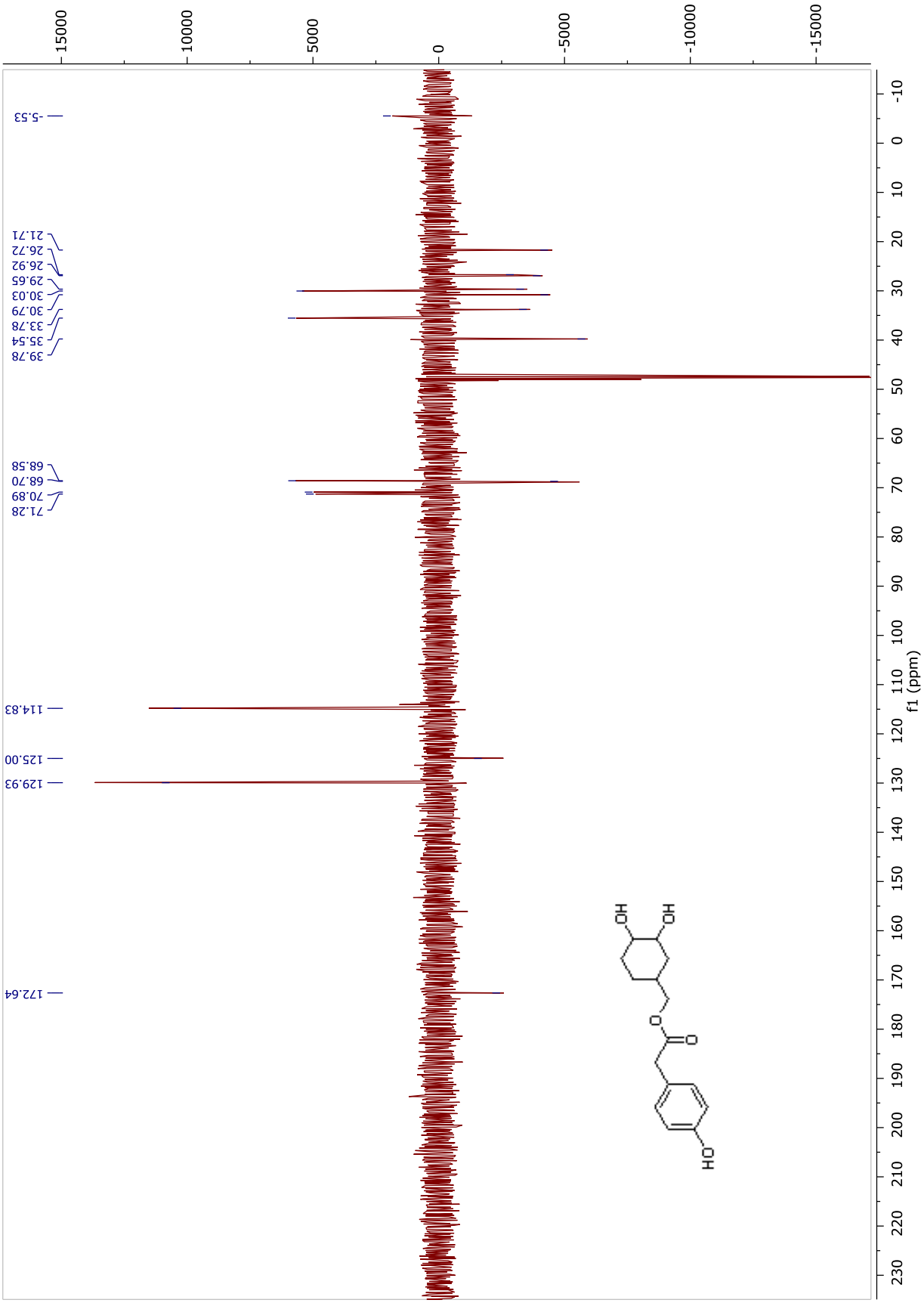
15000
10000
5000
0
-5000
-10000
-15000
-5.53
21.71
26.72
26.92
29.65
30.03
30.79
33.78
35.54
39.78
68.58
68.70
70.89
71.28
114.83
125.00
129.93
172.64
f1 (ppm)
HO
HO
O
O
HO

Compound AM30. ^{1}H NMR and ^{13}C APT NMR spectra in DMSO-d_6

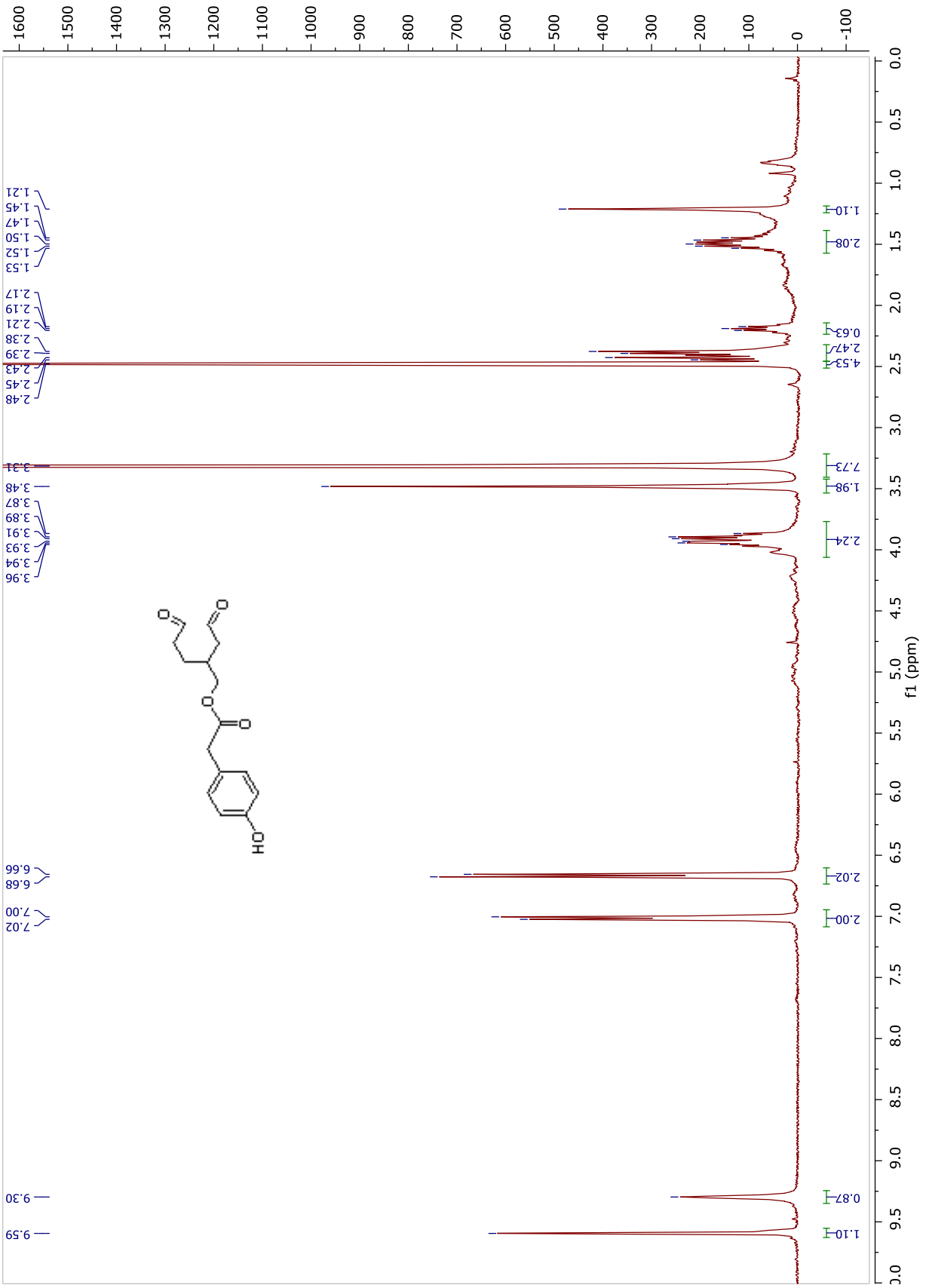

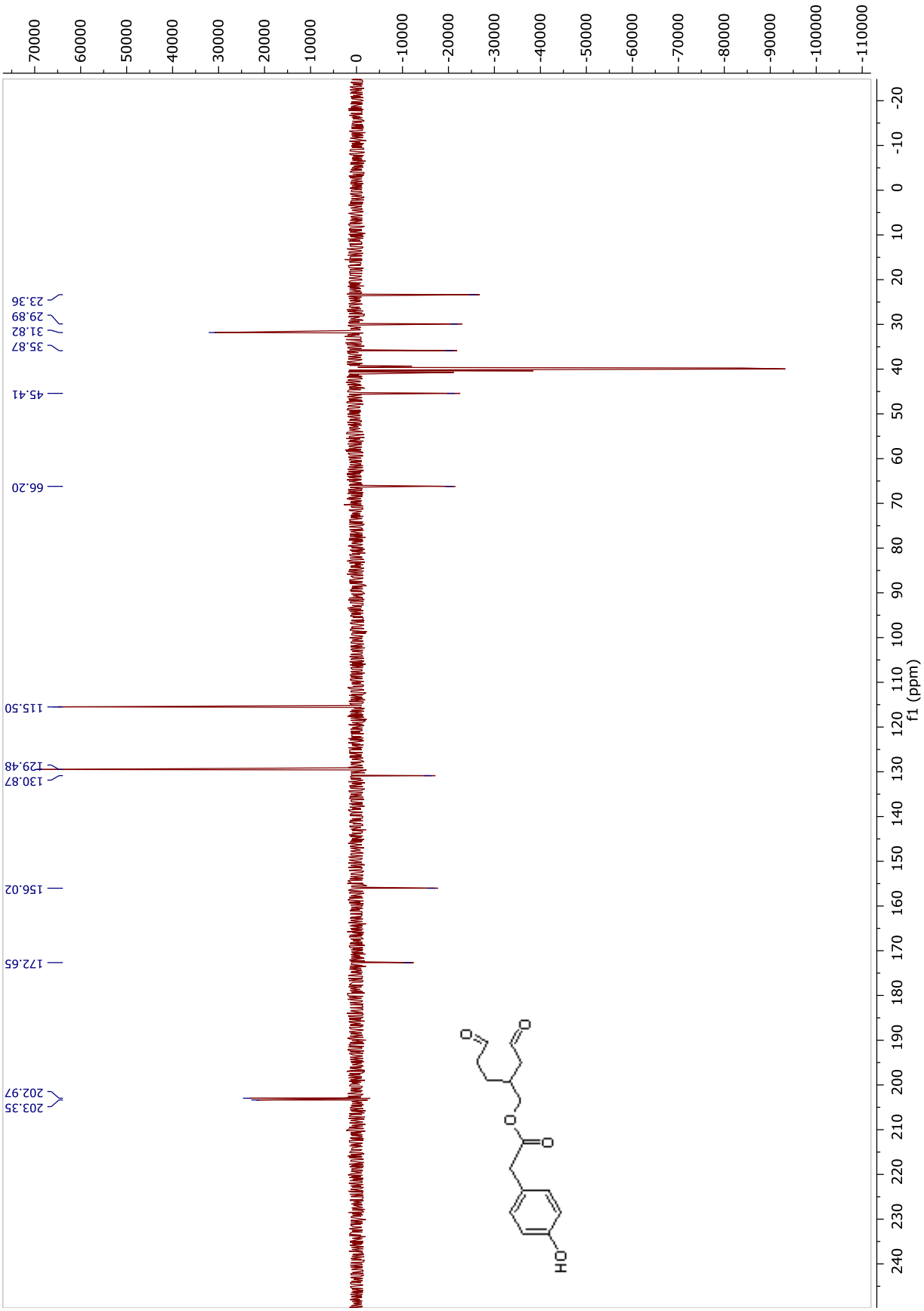
23.36
29.89
31.82
35.87
45.41
66.20
115.50
129.48
130.87
156.02
172.65
202.97
203.35
f1 (ppm)
OH

References

1. Beutler, B. Toll-like receptors: how they work and what they do. *Curr. Opin. Hematol.* **9,** 2–10 (2002).

2. Medzhitov, R. Toll-like receptors and innate immunity. *Nat. Rev. Immunol.* **1,** 135–145 (2001).

3. Leon, C. G., Tory, R., Jia, J., Sivak, O. & Wasan, K. M. Discovery and development of toll-like receptor 4 (TLR4) antagonists: A new paradigm for treating sepsis and other diseases. *Pharm. Res.* **25,** 1751–1761 (2008).

4. Hashimoto, C., Hudson, K. L. & Anderson, K. V. The Toll gene of drosophila, required for dorsal-ventral embryonic polarity, appears to encode a transmembrane protein. *Cell* **52,** 269–279 (1988).

5. Gay, J. N. & Fionna, J. F. Drosophila Toli and IL-1 receptor. *Nature* **351,** 355–356 (1991).

6. Schneider, D. S., Hudson, K. L., Lin, T. Y. & Anderson, K. V. Dominant and recessive mutations define functional domains of Toll, a transmembrane protein required for dorsal-ventral polarity in the Drosophila embryo. *Genes Dev.* **5,** 797–807 (1991).

7. Morisato, D. & Anderson, K. V. The spätzle gene encodes a component of the extracellular signaling pathway establishing the dorsal-ventral pattern of the Drosophila embryo. *Cell* **76,** 677–688 (1994).

8. Lemaitre, B., Nicolas, E., Michaut, L., Reichhart, J. M. & Hoffmann, J. A. The dorsoventral regulatory gene cassette spätzle/Toll/Cactus controls the potent antifungal response in Drosophila adults. *Cell* **86,** 973–983 (1996).

9. Michel, T., Reichhart, J.-M., Hoffmann, J. A. & Royet, J. Drosophila Toll is activated by Gram-positive bacteria through a circulating peptidoglycan recognition protein. *Nature* **414,** 756–759 (2001).

10. Lemaitre, B. *et al.* A recessive mutation, immune deficiency (imd), defines two distinct control pathways in the Drosophila host defense. *Proc Natl Acad Sci U S A* **92,** 9465–9469 (1995).

11. Medzhitov, R., Preston-Hurlburt, P. & Janeway, C. A. J. A human homologue of the Drosophila Toll protein signals activation of adaptive immunity. *Nature* **388,** 394–397 (1997).

12. Rock, F. L., Hardiman, G., Timans, J. C., Kastelein, R. a & Bazan, J. F. A family of human receptors structurally related to Drosophila Toll. *Proc. Natl. Acad. Sci. U. S. A.* **95,** 588–593 (1998).

13. Poltorak, A. Defective LPS Signaling in C3H/HeJ and C57BL/10ScCr Mice: Mutations in Tlr4 Gene.

Science. **282,** 2085–2088 (1998).

14. Hoshino, K. *et al.* Cutting edge: Toll-like receptor 4 (TLR4)-deficient mice are hyporesponsive to lipopolysaccharide: evidence for TLR4 as the Lps gene product. *J. Immunol.* **162,** 3749–52 (1999).

15. Qureshi, B. S. T. *et al.* Endotoxin-tolerant mice have mutations in Toll-like receptor 4 (TLR4). *J. Exp. Med.* **189,** 615–625 (1999).

16. Lucas, K. & Maes, M. Role of the toll like receptor (TLR) radical cycle in chronic inflammation: Possible treatments targeting the TLR4 pathway. *Mol. Neurobiol.* **48,** 190–204 (2013).

17. Kirschning, C. J., Wesche, H., Merrill Ayres, T. & Rothe, M. Human toll-like receptor 2 confers responsiveness to bacterial lipopolysaccharide. *J. Exp. Med.* **188,** 2091–2097 (1998).

18. Wright, S. D. Toll, A New Piece in the Puzzle of Innate Immunity. *J. Exp. Med.* **189,** 605–609 (1999).

19. Shimazu, R. *et al.* MD-2, a molecule that confers lipopolysaccharide responsiveness on Toll-like receptor 4. *J. Exp. Med.* **189,** 1777–82 (1999).

20. Nagai, Y. *et al.* Essential role of MD-2 in LPS responsiveness and TLR4 distribution. *Nat. Immunol.* **3,** 667–672 (2002).

21. Schromm, A. B. *et al.* Molecular genetic analysis of an endotoxin nonresponder mutant cell line: a point mutation in a conserved region of MD-2 abolishes endotoxin-induced signaling. *J. Exp. Med.* **194,** 79–88 (2001).

22. Kim, H. M. *et al.* Crystal Structure of the TLR4-MD-2 Complex with Bound Endotoxin Antagonist Eritoran. *Cell* **130,** 906–917 (2007).

23. Park, B. S. *et al.* The structural basis of lipopolysaccharide recognition by the TLR4-MD-2 complex. *Nature* **458,** 1191–5 (2009).

24. Alexander, C. & Rietschel, E. T. Bacterial lipopolysaccharides and innate immunity. *J. Endotoxin Res.* **7,** 167–202 (2001).

25. Pridmore, A. C. *et al.* A lipopolysaccharide-deficient mutant of Neisseria meningitidis elicits attenuated cytokine release by human macrophages and signals via toll-like receptor (TLR) 2 but not via TLR4/MD2. *J. Infect. Dis.* **183,** 89–96 (2001).

26. Erridge, C., Bennett-guerrero, E. & Poxton, I. R. Structure and function of lipopolysaccharides. *Microbes Infect.* **4,** 837–851 (2002).

27. Tobias, P. S., Soldau, K. & Ulevitch, R. J. Isolation of a Lipopolysaccharide-binding acute phase reactant from rabbit serum. *J. Exp. Med* **164,** 777–793 (1986).

28. Wright, S. D., Tobias, P. S., Ulevitch, R. J. & Ramos, R. A. Lipopolysaccharide (LPS) binding protein opsonizes LPS-bearing particles for recognition by a novel receptor on macrophages. *J. Exp. Med.* **170,** 1231–41 (1989).

29. Schumann, R. *et al.* Structure and function of lipopolysaccharide binding protein. *Science.* **249,** 1429–1431 (1990).

30. Wright, S. D., Ramos, R. A., Tobias, P. S., Ulevitch, R. J. & Mathison, J. C. CD14, a receptor for complexes of lipopolysaccharide (LPS) and LPS binding protein. *Science.* **249,** 1431–1433 (1990).

31. Theofan, G. *et al.* An amino-terminal fragment of human lipopolysaccharide-binding protein retains Lipid-a binding but not CD14-stimulatory activity. *J. Immunol.* **152,** 3623–3629 (1994).

32. Wurfel, M. M., Hailman, E. & Wright, S. D. Soluble CD14 acts as a shuttle in the neutralization of lipopolysaccharide (LPS) by LPS-binding protein and reconstituted high density lipoprotein. *J. Exp. Med.* **181,** 1743–1754 (1995).

33. Yu, B. & Wright, S. D. Catalytic properties of lipopolysaccharide (LPS) binding protein. Transfer of LPS to soluble CD14. *J. Biol. Chem.* **271,** 4100–4105 (1996).

34. Calabrese, V., Cighetti, R. & Peri, F. Molecular simplification of lipid A structure: TLR4-modulating cationic and anionic amphiphiles. *Mol. Immunol.* **63,** 153–161 (2015).

35. Jerala, R. Structural biology of the LPS recognition. *Int. J. Med. Microbiol.* **297,** 353–363 (2007).

36. Jiang, Z. *et al.* CD14 is required for MyD88-independent LPS signaling. *Nat. Immunol.* **6,** 565–570 (2005).

37. Gioannini, T. L., Zhang, D. S., Teghanemt, A. & Weiss, J. P. An essential role for albumin in the interaction of endotoxin with lipopolysaccharide-binding protein and sCD14 and resultant cell activation. *J. Biol. Chem.* **277,** 47818–47825 (2002).

38. Gioannini, T. L. *et al.* Isolation of an endotoxin-MD-2 complex that produces Toll-like receptor 4-dependent cell activation at picomolar concentrations. *Proc. Natl. Acad. Sci.* **101,** 4186–4191 (2004).

39. Saitoh, S. *et al.* Ligand-dependent Toll-like receptor 4 (TLR4)-oligomerization is directly linked with TLR4-signaling. *J. Endotoxin Res.* **10,** 257–60 (2004).

40. O'Neill, L. A. & Bowie, A. G. The family of five: TIR-domain-containing adaptors in Toll-like receptor signalling. *Nat. Rev. Immunol.* **7,** 353–364 (2007).

41. Lu, Y. C., Yeh, W. C. & Ohashi, P. S. LPS/TLR4 signal transduction pathway. *Cytokine* **42,** 145–151 (2008).

42. Detmers, P. A. *et al.* Potential role of membrane internalization and vesicle fusion in adhesion of neutrophils in response to lipopolysaccharide and TNF. *J. Immunol.* **157,** 5589 LP-5596 (1996).

43. Thiéblemont, N. & Wright, S. D. Mice genetically hyporesponsive to lipopolysaccharide (LPS) exhibit a defect in endocytic uptake of LPS and ceramide. *J. Exp. Med.* **185,** 2095–2100 (1997).

44. Thieblemont, N., Thieringer, R. & Wright, S. D. Innate immune recognition of bacterial lipopolysaccharide: Dependence on interactions with membrane lipids and endocytic movement. *Immunity* **8,** 771–777 (1998).

45. Hornef, M. W., Frisan, T., Vandewalle, A., Normark, S. & Richter-Dahlfors, A. Toll-like receptor 4 resides in the Golgi apparatus and colocalizes with internalized lipopolysaccharide in intestinal epithelial cells. *J. Exp. Med.* **195,** 559–70 (2002).

46. Latz, E. *et al.* Lipopolysaccharide rapidly traffics to and from the golgi apparatus with the toll-like receptor 4-MD-2-CD14 complex in a process that is distinct from the initiation of signal transduction. *J. Biol. Chem.* **277,** 47834–47843 (2002).

47. Triantafilou, M., Miyake, K., Golenbock, D. T. & Triantafilou, K. Mediators of innate immune recognition of bacteria concentrate in lipid rafts and facilitate lipopolysaccharide-induced cell activation. *J Cell Sci* **115,** 2603–2611 (2002).

48. Kagan, J. C. *et al.* TRAM couples endocytosis of Toll-like receptor 4 to the induction of interferon-β. *Nat. Immunol.* **9,** 361–368 (2008).

49. Tobias, P. S., Soldau, K., Gegner, J. A., Mintz, D. & Ulevitch, R. J. Lipopolysaccharide binding protein-mediated complexation of lipopolysaccharide with soluble CD14. *J. Biol. Chem.* **270,** 10482–10488 (1995).

50. Beamer, L. J., Carroll, S. F. & Eisenberg, D. Crystal structure of human BPI and two bound phospholipids at 2.4 angstrom resolution. *Science* **276,** 1861–1864 (1997).

51. Beamer, L. J., Carroll, S. F. & Eisenberg, D. The BPI/LBP family of proteins: a structural analysis of conserved regions. *Protein Sci.* **7,** 906–914 (1998).

52. Lamping, N. *et al.* Effects of site-directed mutagenesis of basic residues (Arg 94, Lys 95, Lys 99) of lipopolysaccharide (LPS)-binding protein on binding and transfer of LPS and subsequent immune cell activation. *J. Immunol.* **157,** 4648–56 (1996).

53. Bosshart, H. & Heinzelmann, M. Arginine-rich cationic polypeptides amplify lipopolysaccharide-induced monocyte activation. *Infect. Immun.* **70,** 6904–6910 (2002).

54. Gutsmann, T. *et al.* Dual Role of Lipopolysaccharide (LPS)-Binding Protein in Neutralization of LPS and Enhancement of LPS-Induced Activation of Mononuclear Cells. *Infect. Immun.* **69,** 6942–6950 (2001).

55. Kohara, J., Tsuneyoshi, N., Gauchat, J.-F., Kimoto, M. & Fukudome, K. Preparation and characterization of truncated human lipopolysaccharide-binding protein in Escherichia coli. *Protein Expr. Purif.* **49,** 276–283 (2006).

56. Abrahamson, S. L. *et al.* Biochemical characterization of recombinant fusions of lipopolysaccharide binding protein and bactericidal/permeability-increasing protein. Implications in biological activity. *J. Biol. Chem.* **272,** 2149–2155 (1997).

57. Gegner, J. A., Ulevitch, R. J. & Tobias, P. S. Lipopolysaccharide (LPS) signal transduction and clearance. Dual roles for LPS binding protein and membrane CD14. *J. Biol. Chem.* **270,** 5320–5325 (1995).

58. Ferrero, E. & Goyert, S. M. Nucleotide sequence of the gene encoding the monocyte differentiation antigen, CD14. *Nucleic Acids Res.* **16,** 10003 (1988).

59. Kim, J. I. *et al.* Crystal structure of CD14 and its implications for lipopolysaccharide signaling. *J. Biol. Chem.* **280,** 11347–11351 (2005).

60. Stelter, F. *et al.* Mutation of Amino Acids 39–44 of Human CD14 abrogates Binding of Lipopolysaccharide and Escherichia coli. *Eur. J. Biochem.* **243,** 100–109 (1997).

61. Zanoni, I. *et al.* CD14 Controls the LPS-Induced Endocytosis of Toll-like Receptor 4. *Cell* **147,** 868–880 (2011).

62. Da Silva Correia, J., Soldau, K., Christen, U., Tobias, P. S. & Ulevitch, R. J. Lipopolysaccharide is in close proximity to each of the proteins in its membrane receptor complex. Transfer from CD14 to TLR4 and MD-2. *J. Biol. Chem.* **276,** 21129–21135 (2001).

63. Akashi, S. *et al.* Cutting Edge: Cell Surface Expression and Lipopolysaccharide Signaling Via the Toll-

Like Receptor 4-MD-2 Complex on Mouse Peritoneal Macrophages. *J. Immunol.* **164,** 3471–3475 (2000).

64. Viriyakosol, S., Tobias, P. S. & Kirkland, T. N. Mutational analysis of membrane and soluble forms of human MD-2. *J. Biol. Chem.* **281,** 11955–64 (2006).

65. Ohto, U., Fukase, K., Miyake, K. & Satow, Y. Crystal Structures of Human MD-2 and Its Complex with Antiendotoxic Lipid IVa. *Science.* **316,** 1632–1634 (2007).

66. Yu, L. *et al.* NMR studies of hexaacylated endotoxin bound to wild-type and F126A mutant MD-2 and MD-2·TLR4 ectodomain complexes. *J. Biol. Chem.* **287,** 16346–16355 (2012).

67. Hotchkiss, R. S. & Karl, I. E. The Pathophysiology and Treatment of Sepsis. *New Engl. J. Med.* **348,** 138–150 (2003).

68. Opal, S. M. *et al.* Effect of Eritoran, an Antagonist of MD2-TLR4, on Mortality in Patients With Severe Sepsis. *Jama* **309,** 1154 (2013).

69. Guha, M. & Mackman, N. LPS induction of gene expression in human monocytes. *Cell. Signal.* **13,** 85–94 (2001).

70. Edfeldt, K., Swedenborg, J., Hansson, G. K. & Yan, Z. Expression of toll-like receptors in human atherosclerotic lesions: a possible pathway for plaque activation. *Circulation* **105,** 1158–1161 (2002).

71. Watari, M., Watari, H., Nachamkin, I. & Strauss, J. F. Lipopolysaccharide induces expression of genes encoding pro- inflammatory cytokines and the elastin-degrading enzyme, cathepsin S, in human cervical smooth-muscle cells. *J. Soc. Gynecol. Investig.* **7,** 190–8. (2000).

72. Sasu, S., LaVerda, D., Qureshi, N., Golenbock, D. T. & Beasley, D. Chlamydia pneumoniae and Chlamydial Heat Shock Protein 60 Stimulate Proliferation of Human Vascular Smooth Muscle Cells via Toll-Like Receptor 4 and p44/p42 Mitogen-Activated Protein Kinase Activation. *Circ. Res.* **89,** 244–250 (2001).

73. Grenier, D. & Grignon, L. Response of human macrophage-like cells to stimulation by Fusobacterium nucleatum ssp. nucleatum lipopolysaccharide. *Oral Microbiol. Immunol.* **21,** 190–196 (2006).

74. Ferraiuolo, L., Kirby, J., Grierson, A. J., Sendtner, M. & Shaw, P. J. Molecular pathways of motor neuron injury in amyotrophic lateral sclerosis. *Nat. Rev. Neurol.* **7,** 616–630 (2011).

75. Cleveland, D. W. & Rothstein, J. D. From Charcot to Lou Gehrig: deciphering selective motor neuron death in ALS. *Nat. Rev. Neurosci.* **2,** 806–819 (2001).

76. Chiu, I. M. *et al.* Activation of innate and humoral immunity in the peripheral nervous system of ALS transgenic mice. *Proc. Natl. Acad. Sci. U. S. A.* **106,** 20960–20965 (2009).

77. Appel, S. H., Beers, D. R. & Henkel, J. S. T cell-microglial dialogue in Parkinson's disease and amyotrophic lateral sclerosis: are we listening? *Trends Immunol.* **31,** 7–17 (2010).

78. Barbeito, A. G., Mesci, P. & Boillée, S. Motorneuron-immune interactions: The vicious circle of ALS. *J. Neural Transm.* **117,** 981–1000 (2010).

79. Butovsky, O. *et al.* Identification of a unique TGF-β-dependent molecular and functional signature in microglia. *Nat. Neurosci.* **17,** 131–143 (2014).

80. Mantovani, S. *et al.* Immune system alterations in sporadic amyotrophic lateral sclerosis patients suggest an ongoing neuroinflammatory process. *J. Neuroimmunol.* **210,** 73–79 (2009).

81. Letiembre, M. *et al.* Screening of innate immune receptors in neurodegenerative diseases: A similar pattern. *Neurobiol. Aging* **30,** 759–768 (2009).

82. Casula, M. *et al.* Toll-like receptor signaling in amyotrophic lateral sclerosis spinal cord tissue. *Neuroscience* **179,** 233–243 (2011).

83. Zhao, W. *et al.* Extracellular mutant SOD1 induces microglial-mediated motoneuron injury. *Glia* **58,** 231–243 (2010).

84. Liu, Y., Hao, W., Dawson, A., Liu, S. & Fassbender, K. Expression of amyotrophic lateral sclerosis-linked SOD1 mutant increases the neurotoxic potential of microglia via TLR2. *J. Biol. Chem.* **284,** 3691–3699 (2009).

85. Henkel, J. S. *et al.* Presence of Dendritic Cells, MCP-1, and Activated Microglia/Macrophages in Amyotrophic Lateral Sclerosis Spinal Cord Tissue. *Ann. Neurol.* **55,** 221–235 (2004).

86. Henkel, J. S., Beers, D. R., Siklós, L. & Appel, S. H. The chemokine MCP-1 and the dendritic and myeloid cells it attracts are increased in the mSOD1 mouse model of ALS. *Mol. Cell. Neurosci.* **31,** 427–437 (2006).

87. Nguyen, M. D. Exacerbation of Motor Neuron Disease by Chronic Stimulation of Innate Immunity in a Mouse Model of Amyotrophic Lateral Sclerosis. *J. Neurosci.* **24,** 1340–1349 (2004).

88. Lo Coco, D., Veglianese, P., Allievi, E. & Bendotti, C. Distribution and cellular localization of high mobility group box protein 1 (HMGB1) in the spinal cord of a transgenic mouse model of ALS. *Neurosci. Lett.* **412,** 73–77 (2007).

89. Lee, J. Y., Lee, J. D., Phipps, S., Noakes, P. G. & Woodruff, T. M. Absence of toll-like receptor 4 (TLR4) extends survival in the hSOD1G93A mouse model of amyotrophic lateral sclerosis. *J. Neuroinflammation* **12,** 90 (2015).

90. DePaola, M. & Mariani, A. Neuroprotective Effects of Toll-Like Receptor 4 Antagonism in Spinal Cord Cultures and in a Mouse Model of Motor Neuron Degeneration. *Mol. Med.* **18,** 1 (2012).

91. Kerkhof, M. *et al.* Toll-like receptor 2 and 4 genes influence susceptibility to adverse effects of traffic-related air pollution on childhood asthma. *Thorax* **65,** 690–7 (2010).

92. MacNee, W. Oxidative stress and lung inflammation in airways disease. *Eur. J. Pharmacol.* **429,** 195–207 (2001).

93. Becker, S., Fenton, M. J. & Soukup, J. M. Involvement of microbial components and toll-like receptors 2 and 4 in cytokine responses to air pollution particles. *Am. J. Respir. Cell Mol. Biol.* **27,** 611–618 (2002).

94. Becker, S., Dailey, L., Soukup, J. M., Silbajoris, R. & Devlin, R. B. TLR-2 is involved in airway epithelial cell response to air pollution particles. *Toxicol. Appl. Pharmacol.* **203,** 45–52 (2005).

95. Hollingsworth, J. W. *et al.* Ambient Ozone Primes Pulmonary Innate Immunity in Mice. *J. Immunol.* **179,** 4367–4375 (2007).

96. Brunekreef, B. & Holgate, S. T. Air pollution and health. *Lancet* **360,** 1233–42 (2002).

97. Kleeberger, S. R., Reddy, S., Zhang, L. Y. & Jedlicka, A. E. Genetic susceptibility to ozone-induced lung hyperpermeability. Role of Toll-like receptor 4. *Am. J. Respir. Cell Mol. Biol.* **22,** 620–627 (2000).

98. De Jager, P. L. *et al.* The role of the Toll receptor pathway in susceptibility to inflammatory bowel diseases. *Genes Immun.* **8,** 387–397 (2007).

99. Araki, A. *et al.* MyD88-deficient mice develop severe intestinal inflammation in dextran sodium sulfate colitis. *J. Gastroenterol.* **40,** 16–23 (2005).

100. Fort, M. M. *et al.* A synthetic TLR4 antagonist has anti-inflammatory effects in two murine models of inflammatory bowel disease. *J. Immunol.* **174,** 6416–6423 (2005).

101. Peri, F. & Piazza, M. Therapeutic targeting of innate immunity with Toll-like receptor 4 (TLR4) antagonists. *Biotechnol. Adv.* **30,** 251–260 (2012).

102. David, S. A. Towards a rational development of anti-endotoxin agents: Novel approaches to

sequestration of bacterial endotoxins with small molecules. *J. Mol. Recognit.* **14,** 370–387 (2001).

103. Piazza, M. *et al.* Glycolipids and benzylammonium lipids as novel antisepsis agents: Synthesis and biological characterization. *J. Med. Chem.* **52,** 1209–1213 (2009).

104. Ireton, G. & Reed, S. Adjuvants containing natural and synthetic Toll-like receptor 4 ligands. *Expert Rev Vaccines* **12,** 793–807 (2013).

105. Johnson, A. G., Gains, S. & Landy, M. Studies on the O antigen of salmonella typhosa. *J. Exp. Med.* **103,** 225–246 (1956).

106. Myers, J. *et al.* A critical determinant of lipid A endotoxic activity. *Int. Congr. Ser.* **923,** 145–156 (1990).

107. Coler, R. N. *et al.* A synthetic adjuvant to enhance and expand immune responses to influenza vaccines. *PLoS One* **5,** (2010).

108. Cameron, D. J. & Stromberg, B. V. The ability of macrophages from head and neck cancer patients to kill tumor cells: Effect of prostaglandin inhibitors on cytotoxicity. *Cancer* **54,** 2403–2408 (1984).

109. Yang, D., Satoh, M., Ueda, H., Tsukagoshi, S. & Yamazaki, M. Activation of tumor-infiltrating macrophages by a synthetic lipid A analog (ONO-4007) and its implication in antitumor effects. *Cancer Immunol Immunother* **38,** 287–293 (1994).

110. Peri, F. & Calabrese, V. Toll-like Receptor 4 (TLR4) modulation by synthetic and natural compounds : an update. *J. Med. Chem.* **57,** 3612–3622 (2014).

111. Imoto, M., Yoshimura, H., Sakaguchi, N., Kusumoto, S. & Shiba, T. Total synthesis of lipid A. *Tetrahedron Lett.* **26,** 1545–1548 (1985).

112. Imoto, M. *et al.* Total synthesis of Escherichia coli lipid A, the endotoxically active principle of cell-surface lipopolysaccharide. *Bull. Chem. Soc. Jpn* **60,** 2205–2214 (1987).

113. Ohto, U., Fukase, K., Miyake, K. & Shimizu, T. Structural basis of species-specific endotoxin sensing by innate immune receptor TLR4/MD-2. *Proc. Natl. Acad. Sci. U. S. A.* **109,** 7421–6 (2012).

114. Wang, X. & Quinn, P. J. Endotoxins: lipopolysaccharides of gram-negative bacteria. *Sub-cell. Biochem.* **53,** 3–25 (2010).

115. Mueller, M. *et al.* Aggregates are the biologically active units of endotoxin. *J. Biol. Chem.* **279,** 26307–26313 (2004).

116. Gutsmann, T., Schromm, A. B. & Brandenburg, K. The physicochemistry of endotoxins in relation to bioactivity. *Int. J. Med. Microbiol.* **297,** 341–352 (2007).

117. Brandenburg, K. & Wiese, A. Endotoxins : Relationships between Structure , Function , and Activity. *Curr. Top. Med. Chem.* 1127–1146 (2004).

118. Seydel, U., Oikawa, M., Fukase, K., Kusumoto, S. & Brandenburg, K. Intrinsic conformation of lipid A is responsible for agonistic and antagonistic activity. *Eur. J. Biochem.* **267,** 3032–3039 (2000).

119. Seydel, U., Scheel, O., Müller, M., Brandenburg, K. & Blunck, R. A K+ channel is involved in LPS signaling. *J. Endotoxin Res.* **7,** 243–247 (2001).

120. Papavlassopoulos, M. *et al.* MaxiK Blockade Selectively Inhibits the Lipopolysaccharide-Induced I κB-α/NF-κB Signaling Pathway in Macrophages. *J. Immunol.* **177,** 4086–4093 (2006).

121. Mueller, M., Lindner, B., Dedrick, R., Schromm, a B. & Seydel, U. Endotoxin: physical requirements for cell activation. *J. Endotoxin Res.* **11,** 299–303 (2005).

122. Müller, M., Scheel, O., Lindner, B., Gutsmann, T. & Seydel, U. The role of membrane-bound LBP, endotoxin aggregates, and the MaxiK channel in LPS-induced cell activation. *J. Endotoxin Res.* **9,** 181–6 (2003).

123. Blunck, R. *et al.* New Insights Into Endotoxin-Induced Activation of Macrophages: Involvement of a K+ Channel in Transmembrane Signaling. *J. Immunol.* **166,** 1009–1015 (2001).

124. Li, L., Wang, H., Li, D., Zhang, L. & Lei, W. Roles of lipopolysaccharide receptor cluster and large-conductance Ca2+-activated potassium channel in the lipopolysaccharide recognition. *Guoji Maz. Yu Fusu Zazhi* **33,** 327–329 (2012).

125. Schromm, A. B. *et al.* Biological activities of lipopolysaccharides are determined by the shape of their lipid A portion. *Eur. J. Biochem.* **267,** 2008–2013 (2000).

126. Rietschel, E. T. *et al.* Bacterial endotoxin: molecular relationships of structure to activity and function. *FASEB J.* **8,** 217–225 (1994).

127. Johnson, D. A., Sowell, C. G., Keegan, D. S. & Livesay, M. T. Chemical Synthesis of the Major Constituents of Salmonella Minnesota Monophosphoryl Lipid A. *J. Carbohydr. Chem.* **17,** 1421–1426 (1998).

128. Johnson, D. A. *et al.* 3-O-desacyl monophosphoryl lipid A derivatives: Synthesis and immunostimulant activities. *J. Med. Chem.* **42,** 4640–4649 (1999).

129. Takayama, K., Qureshi, N., Beutler, B. & Kirkland, T. N. Diphosphoryl lipid A from Rhodopseudomonas sphaeroides ATCC 17023 blocks induction of cachectin in macrophages by lipopolysaccharide. *Infect. Immun.* **57,** 1336–1338 (1989).

130. Qureshi, N., Honovich, J. P., Hara, H., Cotter, R. J. & Takayama, K. Location of fatty acids in lipid A obtained from lipopolysaccharide of Rhodopseudomons sphaeroides ATCC 17023. *J. Biol. Chem.* **263,** 5502–5504 (1988).

131. Qureshi, N. *et al.* Chemical reduction of 3-oxo and unsaturated groups in fatty acids of diphosphoryl lipid A from the lipopolysaccharide of Rhodopseudomonas sphaeroides: Comparison of biological properties before and after reduction. *J. Biol. Chem.* **266,** 6532–6538 (1991).

132. Kaltashov, I. a, Doroshenko, V., Cotter, R. J., Takayama, K. & Qureshi, N. Confirmation of the structure of lipid A derived from the lipopolysaccharide of Rhodobacter sphaeroides by a combination of MALDI, LSIMS, and tandem mass spectrometry. *Anal. Chem.* **69,** 2317–22 (1997).

133. Qureshi, N., Takayama, K. & Kurtz, R. Diphosphoryl lipid A obtained from the nontoxic lipopolysaccharide of Rhodopseudomonas sphaeroides is an endotoxin antagonist in mice. *Infect. Immun.* **59,** 441–444 (1991).

134. Manthey, C. L., Qureshi, N., Stütz, P. L. & Vogel, S. N. Lipopolysaccharide Antagonists Block Taxol-induced Signaling in Murine Macrophages. *J. Exp. Med* **178,** (1993).

135. Henricson, B. E., Perera, P. Y., Qureshi, N., Takayama, K. & Vogel, S. N. Rhodopseudomonas-Sphaeroides Lipid-a Derivatives Block Invitro Induction of Tumor-Necrosis-Factor and Endotoxin Tolerance by Smooth Lipopolysaccharide and Monophosphoryl Lipid-A. *Infect. Immun.* **60,** 4285–4290 (1992).

136. Kirkland, T. N., Qureshi, N. & Takayama, K. Diphosphoryl Lipid A Derived from Lipopolysaccharide (Lps) of Rhodopseudomonas-Sphaeroides Inhibits Activation of 70z/3 Cells by Lps. *Infect. Immun.* **59,** 131–136 (1991).

137. Lynn, W. A., Raetz, C. R., Qureshi, N. & Golenbock, D. T. Lipopolysaccharide-induced stimulation of CD11b/CD18 expression on neutrophils. Evidence of specific receptor-based response and inhibition by lipid A-based antagonists. *J. Immunol.* **147,** 3072–3079 (1991).

138. Christ, W. J. *et al.* Total Synthesis of the Proposed Structure of Rhodobacter spheroides Lipid A Resulting in the Synthesis of New Potent Lipopolysaccharide Antagonists. *J. Am. Chem. Soc* 3637–3638 (1994).

139. Rose, J. R., Christ, W. J., Bristol, J. R., Kawata, T. & Rossignol, D. P. Agonistic and antagonistic activities of bacterially derived Rhodobacter sphaeroides lipid A: Comparison with activities of synthetic material of the proposed structure and analogs. *Infect. Immun.* **63,** 833–839 (1995).

140. Loppnow, H. *et al.* Cytokine induction by lipopolysaccharide (LPS) corresponds to lethal toxicity and is inhibited by nontoxic Rhodobacter capsulatus LPS. *Infect. Immun.* **58,** 3743–3750 (1990).

141. Coler, R. N. *et al.* Development and characterization of synthetic glucopyranosyl lipid adjuvant system as a vaccine adjuvant. *PLoS One* **6,** 1–12 (2011).

142. Imoto, M. *et al.* Chemical synthesis of phosphorylated tetraacyl disaccharide corresponding to a biosynthetic precursor of lipid A. *Tetrahedron Lett.* **25,** 2667–2670 (1984).

143. Imoto, M. chemical synthesis of a biosynthetic precursor of Lipid A.pdf. *Bull. Chem. Soc. Jpn* (1987).

144. Meng, J., Lien, E. & Golenbock, D. T. MD-2-mediated ionic interactions between lipid A and TLR4 are essential for receptor activation. *J. Biol. Chem.* **285,** 8695–8702 (2010).

145. Christ, W. J., Rossignol, D. P., Kobayashi, S. & Kawata, T. US 5935938A 19990810 Substituted liposaccharides useful in the treatment and prevention of endotoxemia. (1999).

146. Mullarkey, M. *et al.* Inhibition of Endotoxin Response by E5564, a Novel Toll-Like Receptor 4-Directed Endotoxin Antagonist. *J. Pharmacol. Exp. Ther.* **304,** 1093–1102 (2002).

147. Brandenburg, K. *et al.* Physicochemical characteristics of triacyl lipid A partial structure OM- 174 in relation to biological activity. *Eur. J. Biochem.* **267,** 3370–3377 (2000).

148. Nishijima, M. *et al.* Macrophage Activation by Monosaccharide Precursors of Escherichia-Coli Lipid-A. *Proc. Natl. Acad. Sci. U. S. A.* **82,** 282–286 (1985).

149. Kusumoto, S., Yamamoto, M. & Shiba, T. Chemical Synthesis of Lipid X and Lipid Y, acyl glucosamine 1-phosphates isolated from Escherichia coli mutants. *Tetrahedron Lett.* **25,** 3727–3730 (1984).

150. Aschauer, H., Grob, A., Hildebrandt, J., Schuetze, E. & Stuetz, P. Highly Purified Lipid X Is Devoid of Immunostimulatory Activity. Isolation and characterization of immunostimulating contaminants in a batch of synthetic Lipid X. *J. Biol. Chem.* **265,** 9159–9164 (1990).

151. Van Dervort, A. L., Doerfler, M. E., Danner, R. L., Stuetz, P. & Danner, R. L. Antagonism of lipopolysaccharide-induced priming of human neutrophils by lipid A analogs. *J Immunol* **149,** 359–366 (1992).

152. Danner, R. L., Van Dervort, A. L., Doerfler, M. E., Stuetz, P. & Parrillo, J. E. Antiendotoxin activity of lipid A analogues: Requirements of Chemical Structure. *Pharm. Res.* **7,** (1990).

153. Macher, I. A convenient synthesis of 2-deoxy-2-[(R)-3-hydroxytetradecanamido]-3-O-[(R)-3-hydroxytetradecanoyl]-α-D-glucopyranose 1-phosphate (Lipid X). *Carbohydr. Res.* **162,** 79–84 (1987).

154. Perera, P. Y., Manthey, C. L., Stutz, P. L., Hildebrandt, J. & Vogel, S. N. Induction of early gene expression in murine macrophages by synthetic lipid A analogs with differing endotoxic potentials. *Infect. Immun.* **61,** 2015–2023 (1993).

155. Lam, C. *et al.* SDZ MRL 953, a novel immunostimulatory monosaccharidic lipid A analog with an improved therapeutic window in experimental sepsis. *Antimicrob. Agents Chemother.* **35,** 500–505 (1991).

156. Knopf, H. P. *et al.* Discordant adaptation of human peritoneal macrophages to stimulation by lipopolysaccharide and the synthetic lipid A analogue SDZ MRL 953. Down-regulation of TNF-alpha and IL-6 is paralleled by an up-regulation of IL-1 beta and granulocyte colony-stimulat. *J. Immunol.* **153,** 287–299 (1994).

157. Kiani, A. *et al.* Downregulation of the proinflammatory cytokine response to endotoxin by pretreatment with the nontoxic lipid A analog SDZ MRL 953 in cancer patients. *Blood* **90,** 1673–83 (1997).

158. Stern, A. *et al.* SDZ MRL 953, a lipid A analog as selective cytokine inducer. *Prog. Clin. Biol. Res.* **392,** 594 (1994).

159. Matsuura, M., Kiso, M. & Hasegawa, A. Activity of monosaccharide lipid A analogues in human monocytic cells as agonists or antagonists of bacterial lipopolysaccharide. *Infect. Immun.* **67,** 6286–6292 (1999).

160. Kiso, M., Ishida, H. & Hasegawa, A. Synthesis of Biologically Active, Novel Monosaccharide Analogs of Lipid A. *Agric. Biol. Chem.* **48,** 251–252 (1984).

161. Matsuura, M., Kojima, Y. & Homma, J. Y. Biological activities of chemically synthesized analogues of the nonreducing sugar moiety of lipid A. *FEBS Lett.* **167,** 226–230 (1984).

162. Funatogawa, K., Matsuura, M., Nakano, M., Kiso, M. & Hasegawa, A. Relationship of structure and biological activity of monosaccharide lipid A analogues to induction of nitric oxide production by murine macrophage RAW264.7 cells. *Infect. Immun.* **66,** 5792–8 (1998).

163. Brandenburg, K. *et al.* Biophysical characterization of triacyl monosaccharide lipid a partial structures in relation to bioactivity. *Biophys. J.* **83,** 322–33 (2002).

164. Tamai, R. *et al.* Cell activation by monosaccharide lipid A analogues utilizing Toll-like receptor 4. *Immunology* **110,** 66–72 (2003).

165. Toda, M., Katsuichi, S. & Yutaro, S. Eur. Pat. Appl. EP 226381 A2 19870624 Preparation of glucosamine derivatives as immunostimulants and antitumor agents. (1987).

166. Shimizu, T. *et al.* Mitogenic activity and lethal toxicity of Lipid A Analogs, Glucosamine-phopshate carrying aromatic alkyl groups, in mice. *Biol. Pharm. Bull.* **16,** 932–934 (1993).

167. Johnson, D. A. *et al.* Synthesis and biological evaluation of a new class of vaccine adjuvants: Aminoalkyl glucosaminide 4-phosphates (AGPs). *Bioorganic Med. Chem. Lett.* **9,** 2273–2278 (1999).

168. Johnson, D. A. Synthetic TLR4-active glycolipids as vaccine adjuvants and stand-alone immunotherapeutics. *Curr. Top. Med. Chem.* **8,** 64–79 (2008).

169. Lewicky, J. D., Ulanova, M. & Jiang, Z. H. Improving the immunostimulatory potency of diethanolamine-containing lipid A mimics. *Bioorganic Med. Chem.* **21,** 2199–2209 (2013).

170. Akamatsu, M. *et al.* Synthesis of lipid A monosaccharide analogues containing acidic amino acid: Exploring the structural basis for the endotoxic and antagonistic activities. *Bioorganic Med. Chem.* **14,** 6759–6777 (2006).

171. Cluff, C. W. *et al.* Synthetic toll-like receptor 4 agonists stimulate innate resistance to infectious challenge. *Infect. Immun.* **73,** 3044–3052 (2005).

172. Lewicky, J. D., Ulanova, M. & Jiang, Z. H. Synthesis of a dimeric monosaccharide lipid A mimic and its synergistic effect on the immunostimulatory activity of lipopolysaccharide. *Carbohydr. Res.* **346,** 1705–1713 (2011).

173. Piazza, M. *et al.* A Synthetic Lipid A Mimetic Modulates Human TLR4 Activity. *ChemMedChem* **7,** 213–217 (2012).

174. Cighetti, R. *et al.* Modulation of CD14 and TLR4.MD-2 activities by a synthetic lipid A mimetic. *ChemBioChem* **15,** 250–258 (2014).

175. Hawkins, L. D. *et al.* A Novel Class of Endotoxin Receptor Agonists with Simplified Structure , Toll-Like Receptor 4-Dependent Immunostimulatory Action , and Adjuvant Activity. *J. Pharmacol. Exp. Therpeutics* **300,** 655–661 (2002).

176. Ishizaka, S. T. & Hawkins, L. D. E6020: a synthetic Toll-like receptor 4 agonist as a vaccine adjuvant. *Expert Rev. Vaccines* **6,** 773–784 (2007).

177. Martin, O. R. *et al.* Synthesis and immunobiological activity of an original series of acyclic lipid A mimics based on a pseudodipeptide backbone. *J. Med. Chem.* **49,** 6000–6014 (2006).

178. Mancek-Keber, M. & Jerala, R. Structural similarity between the hydrophobic fluorescent probe and lipid A as a ligand of MD-2. *FASEB J.* **20,** 1836–42 (2006).

179. Yamada, M. *et al.* Discovery of novel and potent small-molecule inhibitors of NO and cytokine production as antisepsis agents: Synthesis and biological activity of alkyl 6-(N-substituted sulfamoyl)cyclohex-1-ene-1-carboxylate. *J. Med. Chem.* **48,** 7457–7467 (2005).

180. Preedy, V. R. & Watson, R. R. *Chemical Synthesis of Diverse Phenolic Compounds Isolated From Olive Oils*. *Olives and Olive Oil in Health and Disease Prevention* (Elsevier Inc., 2010). doi:10.1016/B978-0-12-374420-3.00160-1

181. Cicerale, S., Conlan, X. A., Sinclair, A. J. & Keast, R. S. J. Chemistry and health of olive oil phenolics. *Crit. Rev. Food Sci. Nutr.* **49,** 218–236 (2009).

182. Visioli, F., Poli, A. & Gall, C. Antioxidant and other biological activities of phenols from olives and olive oil. *Med. Res. Rev.* **22,** 65–75 (2002).

183. Maiuri, M. C. *et al.* Hydroxytyrosol, a phenolic compound from virgin olive oil, prevents macrophage activation. *Naunyn. Schmiedebergs. Arch. Pharmacol.* **371,** 457–465 (2005).

184. Iacono, A. *et al.* Effect of oleocanthal and its derivatives on inflammatory response induced by lipopolysaccharide in a murine chondrocyte cell line. *Arthritis Rheum.* **62,** 1675–1682 (2010).

185. Beauchamp, G. K. *et al.* Phytochemistry: Ibuprofen-like activity in extra-virgin olive oil. *Nature* **437,** 45–46 (2005).

186. Xagorari, A., Roussos, C. & Papapetropoulos, A. Inhibition of LPS-stimulated pathways in macrophages by the flavonoid luteolin. *Br. J. Pharmacol.* **136,** 1058–64 (2002).

187. Xagorari, A. *et al.* Luteolin inhibits an endotoxin-stimulated phosphorylation cascade and proinflammatory cytokine production in macrophages. *J. Pharmacol. Exp. Ther.* **296,** 181–7 (2001).

188. Fang, H.-L., Lai, J.-T. & Lin, W.-C. Inhibitory effect of olive oil on fibrosis induced by carbon tetrachloride in rat liver. *Clin. Nutr.* **27,** 900–7 (2008).

189. Morrison, D. C. & Jacobs, D. M. Binding of polymyxin B to the lipid A portion of bacterial lipopolysaccharides. *Immunochemistry* **13,** 813–818 (1976).

190. Miller, K. A. *et al.* Lipopolysaccharide sequestrants: Structural correlates of activity and toxicity in novel acylhomospermines. *J. Med. Chem.* **48,** 2589–2599 (2005).

191. Burns, M. R. *et al.* Polycationic sulfonamides for the sequestration of endotoxin. *J. Med. Chem.* **50,** 877–888 (2007).

192. Chen, W., Yan, W. & Huang, L. A simple but effective cancer vaccine consisting of an antigen and a cationic lipid. *Cancer Immunol. Immunother.* **57,** 517–530 (2008).

193. Tanaka, T. *et al.* DiC14-amidine cationic liposomes stimulate myeloid dendritic cells through toll-like receptor 4. *Eur. J. Immunol.* **38,** 1351–1357 (2008).

194. Chen, X. *et al.* Topomimetics of amphipathic beta-sheet and helix-forming bactericidal peptides neutralize lipopolysaccharide endotoxins. *J. Med. Chem.* **49,** 7754–7765 (2006).

195. Sestito, S. E. *et al.* Amphiphilic Guanidinocalixarenes Inhibit Lipopolysaccharide (LPS)-and Lectin-Stimulated Toll-like Receptor 4 (TLR4) Signaling. *J. Med. Chem.* **60,** 4882–4892 (2017).

196. Cighetti, R. *et al.* Modulation of CD14 and TLR4.MD-2 activities by a synthetic lipid A mimetic. *ChemBioChem* **15,** 250–258 (2014).

197. Perrin-Cocon, L. *et al.* TLR4 antagonist FP7 inhibits LPS-induced cytokine production and glycolytic reprogramming in dendritic cells, and protects mice from lethal influenza infection. *Sci. Rep.* **7,** 1–13 (2017).

198. Imai, Y. *et al.* Identification of Oxidative Stress and Toll-like Receptor 4 Signaling as a Key Pathway of Acute Lung Injury. *Cell* **133,** 235–249 (2008).

199. Shirey, K. A. *et al.* Novel strategies for targeting innate immune responses to influenza. *Mucosal Immunol.* **9,** 1–10 (2016).

200. Shirey, K. A. *et al.* The TLR4 antagonist Eritoran protects mice from lethal influenza infection. *Nature* **497,** 498–502 (2013).

201. De Paola, M. *et al.* Synthetic and natural small molecule TLR4 antagonists inhibit motoneuron death in cultures from ALS mouse model. *Pharmacol. Res.* **103,** 180–187 (2016).

202. Matsuura, M. *et al.* Biological activities of chemically synthesized partial structure analogs of lipid A.

J. Biochem. **98,** 1229–1237 (1985).

203. Kumazawa, Y. *et al.* Structural requirements for inducing in vitro B lymphocyte activation by chemically synthesized derivatives related to the nonreducing D-glucosamine subunit of lipid A. *Eur. J. Immunol.* **16,** 1099–1103 (1986).

204. Stahelin, R. V. Surface plasmon resonance: a useful technique for cell biologists to characterize biomolecular interactions. *Mol. Biol. Cell* **24,** 883–886 (2013).

205. Wang, Y. *et al.* MD-2 as the target of a novel small molecule, L6H21, in the attenuation of LPS-induced inflammatory response and sepsis. *Br. J. Pharmacol.* **172,** 4391–4405 (2015).

206. Zhang, Y. *et al.* Discovery of new MD2 inhibitor from chalcone derivatives with anti-inflammatory effects in LPS-induced acute lung injury. *Sci. Rep.* **6,** 25130 (2016).

207. Wang, Y. *et al.* Curcumin Analog L48H37 Prevents Lipopolysaccharide-Induced TLR4 Signaling Pathway Activation and Sepsis via Targeting MD2. *J. Pharmacol. Exp. Ther.* **353,** 539–550 (2015).

208. Viriyakosol, S. *et al.* Characterization of monoclonal antibodies to human soluble MD-2 protein. *Hybridoma* **25,** 349–357 (2006).

209. Resman, N. *et al.* Taxanes inhibit human TLR4 signaling by binding to MD-2. *FEBS Lett.* **582,** 3929–3934 (2008).

210. Ogawa, Y., Wakida, M., Ishida, H., Kiso, M. & Hasegawa, A. Syntheses of novel nonreducing-sugar subunit analogs of lipid a carrying 2-acyloxytetradecanoyl and 2- hydroxyacyl groups of different carbon chain length. *J. Carbohydr. Chem.* **13,** 433–446 (1994).

211. Ogawa, Y., Fujishima, Y., Konishi, I., Kiso, M. & Hasegawa, A. The Chemical Modification of the C-1 Substituent of A 4-O-Phosphono-O-Glucosamine Derivative (GLA-27) Related to Bacterial Lipid A. *J. Carbohydr. Chem.* **6,** 399–410 (1987).

212. Kumazawa, Y. *et al.* Effect of chemical modification at C1 of the glucosamine backbone of lipid A-subunit analog GLA-27 on manifestation of immunopharmacological activity. *FEBS Lett.* **239,** 117–120 (1988).

213. Smith, A. B., Sperry, J. B. & Han, Q. Syntheses of (-)-Oleocanthal, a Natural NSAID Found in Extra Virgin Olive Oil, the (-)-Deacetoxy-Oleuropein Aglycone, and Related Analogues. *J. Org. Chem.* **72,** 6891–6900 (2007).

Chapter V

Appendix

Collaborations

MD-2 binding studies: National Institute of Chemistry (KI) of Lubiana (thanks to Lenny Zaffaroni[a])

In vivo studies of agonistic activity of FP11 in murine (ongoing): LOFARMA[b]

FT-IR, FRET and SAXS studies on aggregates shape (ongoing): Prof. Andra Schromm[c]

[a] Università degli Studi di Milano Bicocca, Milan, Italy

[b] LOFARMA S.P.A., Milan, Italy

[c] Research Center for Medicine and Biosciences (Forschungszentrum Borstel FG Immunbiophysik) Borstel, Germany

Communications

1. A. Minotti, S. E. Sestito, C. U. Santi, F. Peri, Synthesis of a lipid A mimetic with an alkyne moiety for stimulated Raman scattering imaging in cells and tissues, poster contribution, XXXX "Attilio Corbella" International Summer School on Organic Synthesis, Gargnano (BS), Italy, June 2015.

2. A. Minotti , V. Calabrese, M. Zappa, F. Facchini, L. Zaffaroni, F. Peri, Synthesis of new lipid A and lipid X derivatives as agonists or antagonists of human toll-like receptor-4, oral and poster contribution, XV Convegno Scuola sulla Chimica dei Carboidrati, Certosa di Pontignano, Siena, Italy, June 2016. **Awarded as the best contribution to the Congress by the organizing committee.**

3. A. Minotti, M. Zappa, L. Mazzola, S. Rapisarda, F. Peri, Synthesis of new TLR4 modulators, Unimib Biotechnology and Biosciences Department day - BtBs Day, University of Milan Bicocca, Milano, Italy, December 2016.

4. A. Minotti, M. Zappa, L. Mazzola, F. Peri, Synthesis of new TLR4 modulators based on a monosaccharide scaffold, oral contribution, 19th European Carbohydrate Symposium EUROCARB, Barcellona, Spain, July 2017.

5. F. Cochet, A. Minotti, F. Facchini, L. Zaffaroni, A. Luraghi, J.-M. Billod, S. Martin-Santamaria,T.-C. Wang, T. Huser, H. Coelho, J. Jimenez Barbero, F. Peri, Synthesis and preclinical evaluation of glycolipid-based TLR4 modulators: new therapeutics for inflammatory and autoimmune diseases, poster contribution, 19th European Carbohydrate Symposium EUROCARB, Barcellona, Spain, July 2017.

6. A. Minotti, L. Zaffaroni, F. Facchini, F. Cochet, M. Zappa, L. Mazzola, F. Peri, TLR4: innovative modulators, structure-activity requirements exploration and binding studies, Unimib Biotechnology and Biosciences Department day - BtBs Day, University of Milan Bicocca, Milano, Italy, December 2017.

Acknowledgements

Innanzitutto ringrazio il prof. Peri che mi ha permesso di fare ricerca nel suo gruppo dove ho iniziato e concluso il mio percorso di dottorato.

Seguire tale percorso è stato intenso e ha richiesto tutto me stesso ed ora, guardandomi alle spalle e vedendo ciò di cui ho fatto esperienza, mi sento arricchito e felice di averlo percorso sino alla fine.

Durante questi tre anni ho avuto modo di imparare molto, sia dal punto di vista scientifico che personale.

Ho fatto studi e lavorato su progetti in cui ho convogliato tutta la mia passione per la chimica e la scienza e con dedizione e determinazione ho raggiunto i difficili obiettivi.

Ho inoltre fatto incontri e avuto scambi professionali con numerosi studiosi, ricercatori e professori operanti nel mio campo, in campi affini o in settori notevolmente diversi, e ciò non solo ha contribuito ad accrescere la mia passione per la chimica, ma mi ha altresì aperto a punti di vista più ampi e diversi dal mio semplice sguardo.

Gli incontri personali in università, le lezioni, i seminari, la comune strada fatta con gli altri dottorandi e ancor più il lavoro quotidiano di laboratorio mi hanno inoltre permesso di conoscere persone stupende, con le quali ho passato momenti che porterò sempre con me.

Molto più importante, sono nate amicizie che hanno portato frutto al di fuori dell'ambiente lavorativo e che ancora oggi arricchiscono la mia vita.

I nomi di queste persone sono scritti nel mio cuore.

La fatica, la stanchezza e i momenti negativi non sono mancati in questi tre anni, ma anche nei momenti peggiori ho sempre avuto al mio fianco qualcuno a sostenermi e ad aiutarmi a guardare nella giusta direzione e a guardare a me stesso nel modo giusto.

Di questo devo ringraziare la mia famiglia, mia moglie, i miei amici. Sono loro che, conoscendo i miei limiti e i miei pregi e volendo il bene per il mio destino, mi hanno aiutato nelle difficoltà, così come non mi hanno risparmiato le critiche necessarie quando ho raggiunto i successi. Essi mi hanno ricordato dove sta il vero tesoro della vita al di là degli idoli di questo mondo.

Sono loro la mia vera ricchezza.

Ringrazio inoltre i miei maestri di arti marziali, Enzo e Mauro, e gli altri miei compagni di dojo, per avermi educato alla disciplina, alla determinazione ferrea, alla costanza, alla grandezza di pensiero, all'umiltà di imparare, al senso dell'onore, al non arrendersi mai, perché è in questo modo che sono riuscito a far fronte alle tante sfide incontrate durante questi tre anni per uscirne vincitore.

Ringrazio inoltre don Lino, don Andrea e don Carlo, per i loro consigli e per il loro affetto, ma soprattutto per il loro sguardo su di me e sulla vita. Uno sguardo che non poggia sul successo o sull'efficienza, né sulle false certezze e le false promesse del mondo. Uno sguardo che nessuno può rubare. Uno sguardo proteso a chi dà consistenza alla nostra vita ed ha scritto le leggi della scienza prima che l'uomo le conoscesse.

…ed ora che un capitolo della mia vita si è chiuso… sono pronto ad iniziare il prossimo!!